Genetic Variation Within the IL-18 System and its Association With Cardiovascular Disease and Obesity

Simon R. Thompson
rmhasrt@ucl.ac.uk

2008

A thesis submitted in accordance with the regulations of the University of London for the degree of Doctor of Philosophy

Centre for Cardiovascular Genetics
Department of Medicine
University College London

ProQuest LLC
789 East Eisenhower Parkway
P.O. Box 1346
Ann Arbor, MI 48106-1346

To my parents

Declaration

I confirm that the work presented in this thesis is my own, or has been carried out as part of a collaboration in which I played a major part. Where information or data has been derived from other sources and collaborators, I confirm that this has been indicated in the text.

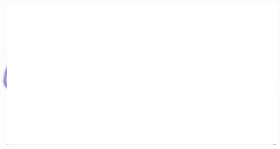

Simon R. Thompson.

Acknowledgements

There is a long list of people who I would like to thank for their role in this thesis, and I am indebted to all of them for their comments, contributions, and support.

First and foremost, this thesis was funded by a BHF studentship, and I am extremely grateful for their generous financial support. They are also key to the funding of the UCL Centre for Cardiovascular Genetics where this thesis was carried out. CVG has been extremely kind to me for the last four years and I would like to thank all past and present members. I'd particularly like to thank Jay Acharya who is a brilliant lab manager with a spectacular gift for making a small amount of money go a long way, and was always my first port of call for any question. The answer was generally provided by Jutta Palmen, Ros Whittall, Tina Hubbart, KaWah Li, or Wendy Putt – thanks to you all for your help, patience, and support. Finally I'd like to thank all the inhabitants of the little PhD office and the larger post-Doc office who, over the years, have consoled, contributed and, just occasionally, congratulated. Of these Pete Wootton, Dino Konstatoulas, Birgit Dorfmeister, Angus Dike and Andy Thompson deserve particular mention, for always fancying a drink and a chat on Friday.

As noted throughout this thesis, I am indebted to many collaborators from all over the world for their contributions. Daniella Novick in Israel has been extremely generous with her time and allowed me to send her numerous samples for her to measure IL-18 and IL-18BP in. Carmel Stock was kind enough to allow me to use her *IL18BP* tSNP set, whilst her supervisor, Pat Woo, often gave advice and constructive criticism on my work – many thanks to both of you. Jon Beilby invited me to Perth, Australia, and gave me access to the CUDAS and CUPID cohorts. Many thanks to his lab for being so welcoming and helpful. On returning home much of my contact was with his statistician – Pam McCaskie – who generously carried out the analysis despite a very heavy workload. A little closer to home, a collaboration with the UCL Centre for Genetic Anthropology allowed me to study the nature of *IL18* genetic variation in Africa. Neil Bradman, Mark Thomas, Chris Plaster, and particularly Krishna Veeramah were very helpful and patient, and I look forward to finishing off this part of my project with them.

The QPCR work presented here would have been very difficult to do without the collaboration with Cauldwell Xtreme Everest. Particularly I'd like to thank Hugh Mont-

gomery, Jim Pate, Iqbal Toor, and Denny Levett, for their help. I wish them good results and small p values for the remainder of the Xtreme Everest project. The SCARF cohort was kindly provided by Per Eriksson, and I'm thankful to him for allowing me access to the samples and database. Jeff Stephens, Julie Sanders, David Brull, and George Miller, established UDACS, CABG, and NPHSII, and deserve acknowledgement here, despite not directly contributing to this thesis. Finally I'd like to thank all of the individuals (in total ~ 6500) who volunteered to take part in the studies used here, without them there is no data, no results, no discussion.

My friends have always been good at reminding me that there is a life away from the desk/bench/laptop, and thank you to you all – you've made my years in London very enjoyable. A very special thanks must go to the other 'London to Monaco 2006' team members – Francesca Achilli, Marie O'Shea, and Paresh Shah. As fellow (medical) PhD students they were the first place to go when in need of advice or consolation, and I've learnt huge amounts from our shared experiences. Another fellow PhD student (in Economics), Emma Tominey, has not only helped to bring me from statsphobe to statsphile, but also proved to be a great sounding board during our numerous tea-breaks.

I owe my family a great deal, their unwavering interest, support and enthusiasm have been a constant throughout my life, and no amount of thanks can repay the debt I owe them. However, a special mention must go to my little brother, Jamie, who encouraged me to write this thesis in the typesetting program, LaTeX. This simple, transparent, and reliable program has been a joy to use, and a welcome change from the mysteries of Microsoft Word.

Finally, my supervisors, Steve Humphries and Philippa Talmud. As I mentioned, my years at CVG have been happy ones and much of this is due to their management of the unit. Both have been instrumental in everything within this thesis and their open and collaborative outlook on science has enabled me to meet many other researchers, and produce a thesis more complete than if it were carried out in a closed, limited atmosphere. Each has always been generous in time and attention, and I would like to wholeheartedly thank both of them for giving me an excellent education in all aspects of research science. They, along with UCL, have made my PhD experience a very happy and satisfying one.

Contents

List of Figures

List of Tables

List of Output

List of Acronyms

5'RACE rapid amplification of 5' complementary DNA ends

ACE angiotensin-converting enzyme

AcPL accessory protein like

AIDS acquired immunodeficiency syndrome

AMOVA analysis of molecular variance

ANOVA analysis of variance

AP-1 activator protein 1

APC antigen presenting cell

apo apolipoprotein

apoe murine apolipoprotein E gene

APS ammonium persulphate

ARIC Atherosclerosis Risk in Communities Study

ASMR age-standardized mortality rate

AST aspartate transaminase

ATP adenosine triphosphate

BACT human BACT gene

BEST Best Enumeration of SNP Tags

β-ME β-mercaptoethanol

BMI body mass index

BP blood pressure

BSA body surface area

CABG coronary artery bypass graft (study)

CAC coronary artery calcification

CBVD cerebrovascular disease

CCU coronary care unit

CD cluster of differentiation

cDNA complementary DNA

CEBPβ CCAAT/enhancer binding protein β

CEPH Centre d'Etude du Polymorphisme Humain

CHB Han Chinese HapMap population

CHD coronary heart disease

CI confidence interval

CK-MB creatine kinase-MB

CPB cardiopulmonary bypass

CRP C-reactive protein

Ct fractional RT-PCR cycle at which threshold is crossed

CTP cytidine triphosphate

CUDAS Carotid Ultrasound Disease Assessment Study

CUPID Carotid Ultrasound in Patients with Ischaemic Heart Disease Study

CV coefficient of variation

CVC cross-validation consistency

CVD cardiovascular disease

DALY disability-adjusted life years

DBP diastolic blood pressure

dbSNP SNP database

DEPC diethylpyrocarbonate

DEXA dual energy X-ray absorbitometry

df degrees of freedom

DMSO dimethyl sulfoxide

DNA deoxyribonucleic acid

DTT dithiothreitol

ECM extracellular matrix

EDTA ethylenediaminetetraacetic acid

EHH extended haplotype homozygosity

ELISA enzyme-linked immunosorbent assay

EM expectation-maximization (algorithm)

EMSA electromobility shift assay

eNOS endothelial nitric oxide synthase

EPIC European Prospective Investigation of Cancer

EtBr ethidium bromide

FCAS familial cold autoinflammatory syndrome

fIL-18 free IL-18

GAPDH human GAPDH gene

GAS gamma-interferon activated site

GTP guanosine triphosphate

GUI graphical user interface

GWA genome-wide association

HapMap human haplotype-mapping project

HDI human development index

HDL high-density lipoprotein

HIV human immunodeficiency virus

HLA human leukocyte antigen

HOMA-IR homeostasis model assessment of insulin resistance index

HR hazard ratio

HT hypertension

HWE Hardy-Weinberg equilibrium

ICAM-1 intracellular adhesion molecule-1

ICSHIB International Collaborative Study of Hypertension in Blacks

ICU intensive care unit

IFN interferon

IFNγ interferon-γ

ifng murine IFNγ gene

IFNγ human IFNγ gene

Ig immunoglobulin

IGT impaired glucose tolerance

IHD ischaemic heart disease

iHS integrated haplotype score

IIPGA Innate Immunity - Programs for Genomics Applications

IkB inhibitor of NF-κB

IKK IκB kinase

IL-1 interleukin 1

IL-12 interleukin 12

IL-12Rβ2 IL-12 receptor β-2

IL-13 interleukin-13

IL-17 interleukin-17

IL18 human IL-18 gene

il18 murine il-18 gene

IL-18 interleukin 18

il-18 murine IL-18

IL18BP human IL-18BP gene

il18bp murine IL-18BP gene

IL-18BP interleukin 18 binding protein

il-18bp murine IL-18BP

IL-18R IL-18 receptor

IL18Rα human IL-18Rα gene

il18rα murine IL-18Rα gene

IL-18Rα IL-18 receptor subunit α

IL18Rβ human IL-18Rβ gene

IL-18Rβ IL-18 receptor subunit β

IL-1α interleukin 1 α

IL-1β interleukin 1β

IL-1F7 IL-1 family, member 7

IL-1R IL-1 receptor

IL-1Ra IL-1 receptor antagonist

IL-1RAcP IL-1 receptor accessory protein

IL-1RII IL-1 decoy receptor

IL-1Rrp IL-1 receptor related protein

IL2 human IL-2 gene

IL-2 interleukin 2

il23 murine IL-23 gene

IL-23 interleukin 23

IL-4 interleukin 4

IL-6 interleukin 6

IMT intima-media thickness

Indel insertion/deletion variation

iNOS inducible nitric oxide synthase

IRAK IL-1 receptor associated kinase

IRF IFN regulatory factor

JIA juvenile idiopathic arthritis

JNK c-Jun N-terminal kinase

JPT Japanese HapMap population

LD linkage disequilibrium

LDH lactate dehydrogenase

LDL low-density lipoprotein

LDLR LDL receptor

ldlr murine LDLR gene

LOD logarithm of odds

LPL lipoprotein lipase

LPS lipopolysaccharide

LR likelihood ratio

LRT likelihood ratio test

mAb monoclonal antibody

MADGE microtitre array diagonal gel electrophoresis

MAF minor allele frequency

MAPK mitogen-activated protein kinase

MCP-1 monocyte chemoattractant protein-1

MDR multifactor dimensionality reduction

MHC major histocompatibility complex

MI myocardial infarction

MM-LDL minimally modified LDL

MMP matrix metalloproteinase

mRNA messenger RNA

MyD88 myeloid differentiation primary response gene 88

myd88 murine myd88 gene

NCBI National Centre for Biotechnology Information

NCEP-ATPIII National Cholesterol Education Program Third Adult Treatment Panel

NF-κB nuclear factor κB

NFQ non-fluorescent quencher

NK natural killer

NLR NOD-like receptor

NLRP3 NLR family, pyrin-domain containing 3

NMR nuclear magnetic resonance

NO nitric oxide

NPHSII second Northwick Park Heart Study

NTC non-template control

OR odds ratio

oxLDL oxidized LDL

PBMC peripheral blood mononuclear cell

PBS phosphate buffered saline

PCO principal co-ordinate analysis

PCR polymerase chain reaction

PDGF platelet-derived growth factor

pI isoelectric point

PRIME Prospective Epidemiological Study of Myocardial Infarction

PU.1 haematopoietic transcription factor PU.1

PYCARD PYR and CARD domain containing protein

QPCR quantitative PCR

RA rheumatoid arthritis

RE restriction enzyme

RER relative expression ratio

REST Relative Expression Software Tool

RFLP restriction fragment length polymorphism

RNA ribonucleic acid

RR relative risk

SBP systolic blood pressure

SCARF Stockholm Coronary Artery Risk Factor Study

SD standard deviation

SE standard error

SEM stochastic version of EM (algorithm)

SES socioeconomic status

SIGIRR single Ig domain-containing IL-1R-related protein

SMC smooth muscle cell

SNP single nucleotide polymorphism

sPLA$_2$ secretory typeII phospholipase A_2

SR scavenger receptor

SSCP single strand conformational polymorphism

STAT signal transducer and activator of transcription

TBA testing balanced accuracy

T_C cytotoxic T

TCR T cell receptor

TEM transmission electron micrograph

TEMED tetramethylethylenediamine

TEX12 testis-expressed gene 12

TF tissue factor

TGFβ transforming growth factor β

T_H1 T helper 1

T_H17 T helper 17

T_H2 T helper 2

THP-1 human acute monocytic leukaemia cell line

TIDM type I diabetes

TIIDM type II diabetes mellitus

TIR Toll-IL-1 receptor

TLR Toll-like receptor

TNFα tumor necrosis factor α

TRAF6 TNF-receptor associated factor 6

TRAIL TNF-related apoptosis-inducing ligand

tSNP tagging SNP

TTP thymidine triphosphate

U937 human leukaemic monocyte lymphoma cell line

UBC human UBC gene

UCSC University of California, Santa Cruz

UDACS University College London Diabetes and Cardiovascular Study

UK United Kingdom

UNDP United Nations Development Program

US United States

UTR untranslated region

VCAM-1 vascular cell adhesion molecule-1

VLDL very low-density lipoprotein

WHO World Health Organization

WTCCC Wellcome Trust Case Control Consortium

WTHR waist to hip ratio

YRI Yoruban HapMap population

Abstract

Background and Aims The interleukin 18 (IL-18) system consists of a pro-inflammatory cytokine (IL-18), a naturally occurring inhibitor (IL-18BP), and a dimeric receptor. IL-18 has been implicated in many autoimmune conditions, with elevated plasma levels predicting future risk of heart disease in healthy individuals. IL-18 also appears to have metabolic consequences, with $il18^{-/-}$ mice having higher bodyweight, attributable to increased feeding. The central hypothesis of this work was that genetic variation within both *IL18* and *IL18BP*, that influenced their circulating levels, would be associated with individual risk for both heart disease and obesity. This was tested by measuring IL-18 levels in several study groups and accessing their correlation with numerous single nucleotide polymorphisms (SNPs) (chosen using a tagging SNP (tSNP) methodology) within both genes. Any effects (either single SNP or haplotypic) were then assessed directly using quantitative PCR (QPCR).

Results For both *IL18* and *IL18BP*, tSNP sets were chosen that captured greater than 90% of the common genetic variation seen in a representative European Caucasian sample. Their association with levels of IL-18 and interleukin 18 binding protein (IL-18BP) were assessed in healthy and diseased individuals; genetic variation in *IL18* only was associated with differences in plasma IL-18 (and free IL-18 (fIL-18)) levels in all cohorts. Carriage of the rare allele of *IL18*-5848 T>C was associated with, on average across all study groups, 44% higher IL-18 levels than TT homozygotes. There was also a haplotypic effect, with a common haplotype – hGTATA (frequency of ~20%) – being associated with 30% lower IL-18 levels. The effect was consistently of greater magnitude in diseased than healthy individuals. Despite IL-18 levels being elevated in those individuals who went on to suffer an myocardial infarction (MI) over 15 yr of follow-up (277.6 pg/ml vs. 239.6 pg/ml, p=0.05), there was no significant difference in genotype, or haplotype, frequencies in those who had heart disease compared to those who did not. No consistent association between BMI/obesity and IL-18 levels was observed, however, in two of the study groups genetic variation in *IL18* was associated with significant differences in body mass index (BMI). Overall, hGTATA was associated with a 9% higher BMI, equating to a 7 kg greater body weight for an average male. In *in vitro* studies of *IL18* expression in healthy, male hGTATA carriers, no significant differ-

ence in *IL18* messenger RNA (mRNA) concentrations were observed when compared to hGCATA controls.

Conclusion The data presented here disagrees with previously published results, showing no role for variation within *IL18* in establishing heart disease risk. However there are novel findings that suggest it may play a role in weight control. Given that these effects appear not to be mediated through plasma IL-18 levels, the identification of individuals through genetic testing may be especially relevant.

Total thesis word count – ~61 000

Chapter 1

Introduction

Despite advances in lifestyle and medical management, coronary heart disease (CHD) is the leading cause of death in the United Kingdom (UK) and United States (US) [Anderson and Smith, 2003; Breslow, 1997], and one of the most important causes of years of life lost before the age of 65 yr [Liu et al., 2002; British Heart Foundation, 1999]. At the age of 40 yr, lifetime risk for developing CHD in the West is 49% in men and 32% in women [Lloyd-Jones et al., 1999]. In the UK, the total annual cost of all CHD related burdens was £7.06 billion in 1999, the highest of all diseases for which comparable analyses have been done [Liu et al., 2002], whilst the direct cost of cardiovascular disease in the US in 1996 was estimated at $259 billion [Braunwald, 1997].

As the 20th century began, CHD was the fourth most common disease in the US [National Center for Health Statistics, 1995]. By 1910 CHD had reached first place, and has remained the most common cause of death in the US since. Following a concerted effort to understand and treat CHD, the age-standardized mortality rate (ASMR) from CHD actually declined from its peak in 1963. The ASMR from cerebrovascular disease (CBVD) has also declined impressively, falling by 70%. In fact, 85% of the reduction in ASMR from all causes between 1963 and 1994 can be ascribed to the decline in deaths from cardiovascular disease (CVD) and stroke [Braunwald, 1997].

However, despite these remarkable improvements in treatment and prevention, the war against CVD is far from over. The "epidemiologic transition" has led to a shift in the predominance of nutritional deficiencies and infectious diseases, to those classified as degenerative (chronic diseases such as CVD, cancer, and diabetes mellitus) leading to dramatic improvements in health and so significant increases in life-expectancy over the past century [Yusuf et al., 2001b] (life expectancy at birth has increased from a global average of 46 yr in 1950 to 66 yr in 1998 [Sen and Bonita, 2000]). This, coupled with increases in population size, has meant the absolute number of deaths from cardiovascular disease in the US has remained nearly constant at 750000 per year over the last 25 yr.

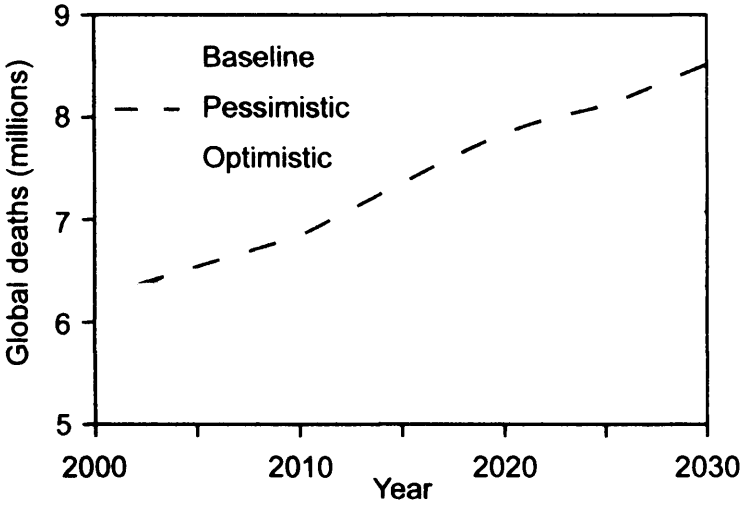

Figure 1.1: Projected increase in CVD deaths, 2000–2030, in those under 70 yr (Adapted from Mathers and Loncar [2006]).

Predictions of future growth in CVD prevalence are complicated due to the complex systems that underlie the disease and the geographical heterogeneity that is often observed. However, recent predictions that use separate models across age and sex groups predict that both ischaemic heart disease (IHD) and CBVD will remain as the top two global causes of death in 2030, together accounting for 24% of all deaths. In total, the predictions showed an 11% increase in CVD death for those under 70 yr and a 34% increase in CVD death when the over 70 yr age group were included (Mathers and Loncar [2006], see figure 1.1). Therefore the need to elucidate and understand the factors that predict CHD risk is of ever-growing importance.

1.1 Ethnic and Geographical Differences in CHD Susceptibility

Due to the numerous environmental and physiological factors that contribute to CVD risk, the prevalence and manner of disease varies greatly across the globe; the CVD death rate in men living within the Russian Federation is almost seven times that of Japan, and 7.5 times higher for women (see figure 1.2 on the next page).

1.1.1 European Origin

People of European origin include those who originate from diverse backgrounds in Northern Europe (eg. Sweden and Norway), Western Europe (eg. UK and France),

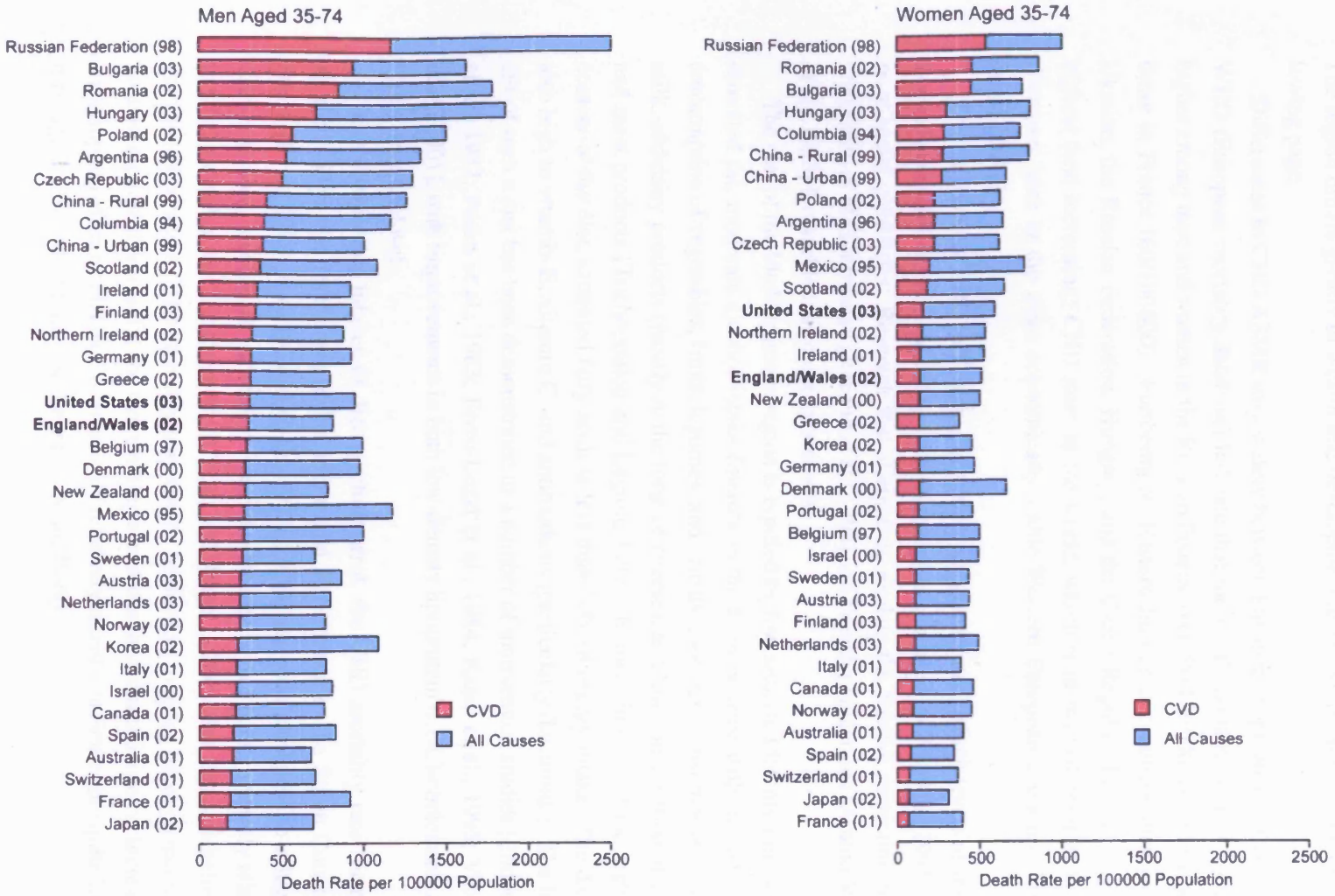

(a) Men 35–74 yr

(b) Women 35–74 yr

Figure 1.2: International CVD statistics (adapted from Callow [2006])

Southern Europe (eg. Spain and Italy), and Eastern Europe (eg. Poland and Ukraine). The region differs greatly in wealth and development as shown in table 1.1 on the following page.

Differences in CHD ASMR vary widely between European populations. Data from WHO (European mortality database) indicate that the CHD mortality rate is six-fold higher among men and women in the Russian Federation (390/100000) compared with those in France (60/100000). Furthermore, Eastern European countries such as the Ukraine, the Russian Federation, Hungary, and the Czech Republic have among the highest (and increasing) CHD rates in the world, which is in marked contrast to the decreases seen in the more economically stable Western European countries [Yusuf et al., 2001a].

The epidemic of CHD in Eastern Europeans is partly related to high levels of smoking and excessive alcohol use, along with diets high in saturated fat [Marmot, 1995] and poor social conditions. Research that attempts to explain the relative protection from CHD seen in Mediterranean [Renaud et al., 1995] and French populations [Artaud-Wild et al., 1993] has yielded different hypotheses.

The diet of the Mediterranean region is typified by low saturated fat, high monounsaturated fat, moderate alcohol intake (mainly in the form of wine with meals), high consumption of vegetables, fruits, legumes, and cereals, moderate consumption of fish, milk, and dairy products (mostly in the form of cheese), and low consumption of meat and meat products [Trichopoulou and Lagiou, 1997]. In total, in spite of the high fat content of the diet, saturated fatty acids is less than 10% of energy intake. The diet is also high in vitamin E, vitamin C, and antioxidants (particularly flavonoids). The benefit of such a diet has been demonstrated in a number of intervention studies [Ehnholm et al., 1982; Puska et al., 1983; Ferro-Luzzi et al., 1984; Katan et al., 1995; Vissers et al., 2001], with improvements in both low-density lipoprotein (LDL)-cholesterol and blood pressure levels.

With comparable intakes of dietary cholesterol, the CHD mortality rate for men aged 55–59 yr was four times higher in Finland than France in the Seven Countries Study [Keys, 1980; Artaud-Wild et al., 1993]. This has been attributed to a higher consumption of alcohol, in particular wine; wine ethanol is, to a point, inversely related to CHD mortality, but not longevity [Criqui and Ringel, 1994]. But it is also believed that the lower rate of CHD mortality may simply be due to a time-lag between increases in consumption of animal fat and the resulting elevations in serum cholesterol; increased consumption of animal fat has occurred only relatively recently in France but quite some time ago in Finland and the UK [Law and Wald, 1999].

Table 1.1: Wealth and development statistics for countries within Europe 2001 data; taken from WHO European Health For All Database, accessed March 2007.

Country	UK	France	Italy	Norway	Poland	Russian Federation	Spain	Sweden	Ukraine
Population (million)	59.1	59.2	57.0	4.5	38.6	144.4	40.6	8.9	48.8
% of population aged 65+ yr	15.9	16.2	18.4	15.0	12.4	12.8	17.0	17.2	14.1
% urban population	89.5	75.5	67.1	75.0	62.6	72.9	77.8	83.3	68.0
Gross domestic product, US$ per capita	24437	22534	19440	37610	4862	2141	14906	24902	766
Literacy rate (%) in population aged 15+ yr	-	-	98.5	-	99.7	99.6	97.7	-	99.6
United Nations Development Program (UNDP) HDI[1]	0.930	0.925	0.916	0.944	0.841	0.779	0.918	0.941	0.766
Life expectancy at birth, yr	78.3	79.4	80.1	79.1	74.4	65.3	79.8	80.0	68.1
Hospitals per 100000	-	5.94	2.29	-	2.15	6.86	1.89	0.87	6.05

[1]The human development index (HDI) is a comparative worldwide measure of life expectancy, literacy, education and standard of living. It is a standard means of measuring well-being.

1.1.2 Chinese Origin

Deaths from CHD have been increasing in China in recent decades [Woo and Donnan, 1989]. Although the CVD mortality rate in China is approximately the same as that in the US, the CHD mortality rate is approximately 50% lower than the rates observed in most Western European countries, with the difference complimented by an increased CBVD rate. A case-control study from Hong Kong indicated that the traditional risk factors (eg. smoking, hypertension (HT), or diabetes mellitus) are important [Donnan et al., 1994]. Also, despite mean serum cholesterol being relatively low in the Chinese population by Western standards ($\sim$4.2 mmol/l), it was still directly related to CHD mortality [Chen et al., 1991]. Cigarette smoking is highly prevalent among Chinese males (over 60%) and increasing [Yang et al., 1999].

Within China there are differences in CHD mortality rates, with rates in northern China (Beijing) higher than in southern China (Shanghai and Guangzhou), and a similar disparity between urban and rural areas [Tao et al., 1989; USCEPR and PRC, 1992]. The prevalence of HT, mean levels of serum cholesterol and BMI were all lower in the South compared to the North and in rural compared to urban areas.

1.1.3 South Asian Origin

South Asia refers to people who originate from India, Sri Lanka, Bangladesh, Nepal, and Pakistan. There are relatively few mortality studies from India, as there is no uniform completion of death certificates and no centralized registry of CVD deaths. However, the WHO and the World Bank estimate that deaths attributable to CVD have increased in parallel with India's expanding population, and now accounts for a large proportion of life years lost [Murray and Lopez, 1996]. Of all deaths in 1990, approximately 25% were attributable to CVD. South Asian migrants to UK, South Africa, Singapore, and the US experienced 1.5 to 4.0 times higher CHD mortality compared to indigenous populations [Enas et al., 1992].

Compared to Europeans, South Asians (in the UK and Canada) do not display higher levels of smoking, HT, or elevated cholesterol, yet still have higher rates of CHD [Sheth et al., 1999; Anand et al., 2000; McKeigue et al., 1993]. However, smoking, HT, and diabetes remain associated with CHD in South Asians [Pais et al., 1996]. Furthermore, South Asian migrants resident in the UK and Canada suffer a high prevalence of impaired glucose tolerance (IGT), central obesity, and experience type II diabetes mellitus (TIIDM) at rates four to five times higher than Europeans (19% versus 4% by age 55 yr) [Anand et al., 2000; McKeigue et al., 1993, 1991]. In contrast, the prevalence of diabetes in rural India is 2-3%, and approximately 8% in urban areas. This geographical variation of diabetes within India is matched by the incidence of CHD, with, over two decades, a nine-fold increase in CHD rates in Indian urban centres, but

only a two-fold increase in rural populations [Gupta and Gupta, 1996]. Taken together, the available data strongly suggests a genetic predisposition to CVD in South Asians.

1.1.4 Blacks of African Origin

Before 1970, CHD was virtually unknown in black people in Africa, in stark contrast with the high rates of CHD in people of African descent living in typically westernized settings [Yusuf et al., 2001a].

1.1.4.1 Blacks in Africa

Collecting CVD mortality data from Sub-Saharan Africa is difficult as only 1.1% of deaths are registered with a central agency [Murray and Lopez, 1996], therefore the range of analysis is limited. However, data from other sources, such as small population studies, indicate that the burden from CHD in 1990 was 4.5 million disability-adjusted life years (DALY), with CHD mortality around 41/100000 [Murray and Lopez, 1996], levels around four to five times lower than those seen in western countries, but still representing a significant proportion of all deaths (CVD–10%; CHD–3%). The prevalence of most conventional CHD risk factors is lower among blacks than other groups within Africa, and the world [Seedat, 1996; Berrios et al., 1997a]. Furthermore, the prevalence of multiple risk factors is strikingly lower, with 65% of the population having no identifiable risk factors, 30% having only one risk factors, and only 5% having two risk factors, compared to 50%, 40%, and 10%, respectively, in the US [Berrios et al., 1997b]. However, the significance of CVD is increased due to limited access to health care.

The INTERHEART study is an international, standardized, case-control study conducted in 52 countries, designed to assess the association of CVD risk factors with MI [Yusuf et al., 2004; Rosengren et al., 2004]. Participants for INTERHEART Africa were recruited from nine countries (>80% from South Africa), constituting 578 cases and 785 controls, with a mix of black African people (36.3%), coloured African people (46.7%), and European and other African people (17%). Overall, African cases presented 3.8 yr earlier than the average INTERHEART study cases, with the risk factors associated with MI not differing between the African sample and the global study. However the association between history of HT and MI was significantly stronger in the African sample than the global sample [Steyn et al., 2005]. This could be of great importance given that the International Collaborative Study of Hypertension in Blacks (ICSHIB) found the age-adjusted prevalence of HT in Nigeria (the largest black nation in the world, with a population of >120 million) was 14.5% [Cooper et al., 1997].

In 2006, a study of over 400 black South Africans (male and female) suggested that the prevalence of risk factors is increasing across the continent. Furthermore, around

80% of the cases in this study were younger than 65 yr and fell within the working-age group; most came from low socio-economic background and had limited education, a finding that questions the common belief that CHD occurs predominantly in the wealthier section of society [Loock et al., 2006]. A recent publication showed that in people of working age (35–64 yr), CVD mortality rates in South Africa in 2000 had already increased to levels higher than those found in US and Portugal. It also reported that the projected CVD mortality in South Africa for this age group will increase by 41% between 2000 and 2030 [Leeder et al., 2004].

The INTERHEART Africa study showed heterogeneity in relation to the magnitude of the risk for MI among the three ethnic groups, suggesting that the three ethnic groups are at different points of the epidemiological transition, and therefore the development of the CVD epidemic [Gillum, 1996]. Burdens of disease estimates adjusted for underregistration and misclassification of cause, show that the black African group in South Africa had CHD mortality rates of 70/100000. For the coloured African group, this estimate was 171/100000, whilst the estimate was 230/100000 for the white South African group [Steyn et al., 2005].

This data suggests that an epidemic of CHD and other atherosclerosis-related CVD could become manifest within Africa in the first half of the 21st century, and will strike a generation already under the spectre of the human immunodeficiency virus (HIV)/acquired immunodeficiency syndrome (AIDS) pandemic.

1.1.4.2 African-Americans

African-Americans are the largest non-white population in the US, representing 12.1% of the population (~35 million) [US Census Bureau, 2005].

Life expectancy is shorter, and mortality rates greater, for black than for whites in America [Cooper, 1993] (see table 1.2 on the next page), and these discrepancies are continuing to widen [Mason, 1993]. CVD, the leading cause of death for all Americans, is thought to be an important determinant of these disturbing trends [Cooper et al., 2000; Geronimus et al., 1996]. For most of the last century, CHD mortality rates were lower in black men than white men. However, although initially the decline in CHD mortality happened in parallel across all ethnic groups, the rates of CHD mortality throughout the 20th century and into the 21st, have declined more slowly in black men and women than white men and women (see figure 1.3 on the following page), such that the ASMR (1999–2003) for CVD in blacks and African Americans was 19% higher than American whites (see table 1.2 on the next page); in 1980 it was estimated that black men living in Harlem had less chance of surviving to the age of 65 than men in Bangladesh [McCord and Freeman, 1990].

In a study based upon death certificate information across eight persistently poor ge-

Table 1.2: 1999–2003 ASMR for US, by ethnicity and sex. Data is expressed as mortality per 100 000 population and are based on rates age-adjusted to the 2000 standard. Data source: US Department of Health and Human Services, National Center for Health Statistics, CDC WONDER On-line (http://wonder.cdc.gov), accessed March 2007.

Race		% of Total Population	ASMR per 100 000 All Cause	ASMR per 100 000 CVD[2]
Black or African American	Male	6.8	911.8	108.8
	Female	6.2	1372.9	164.5
Other Race	Male	2.7	439.7	52.4
	Female	2.6	638.0	87.2
White	Male	41.3	706.4	86.6
	Female	40.3	1007.5	142.4

[2]Classified as ICD-10.I25, and all subsets

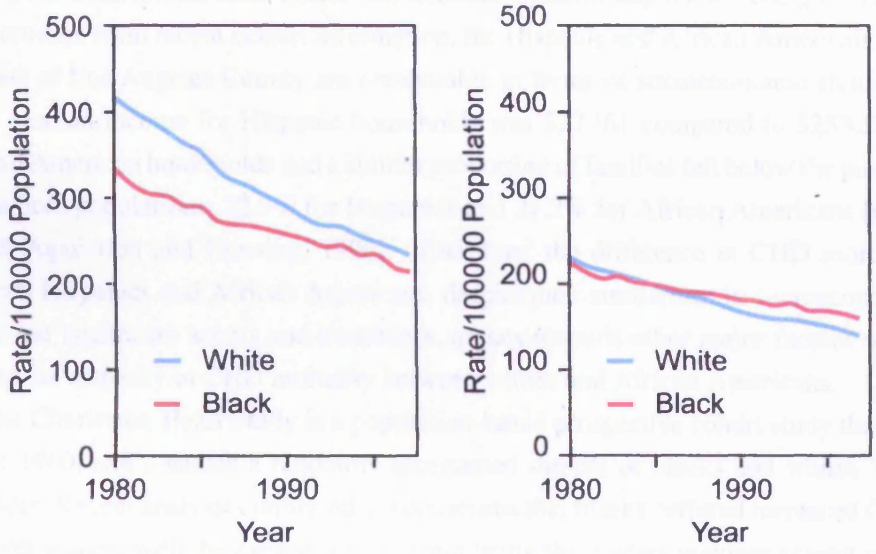

Figure 1.3: ASMR for CHD by sex and race in US from 1980–1997. Rates are age-adjusted to 2000 standard (adapted from Cooper et al. [2000]).

ographic areas and eight geographically proximate, but more advantaged areas, matched for race, diseases of the circulatory system were important to excess mortality in every group, and in most cases they were the leading cause [Geronimus et al., 1996] (see table 1.3 on the following page). There were substantial differences in the excess mortality rates due to CHD between reasonably well-matched (by geographic location and wealth) white and black groups, adjustment for poverty rate accounted for more than half of the racial differences in mortality [Geronimus et al., 1996]. This would suggest that although the inequality in wealth, along with other socioeconomic status (SES) factors [Marmot, 2003], account for a large proportion of the differences in CHD mortality, there still remains a significant proportion that is yet to be explained.

In a separate study that investigated ASMR in Hispanics, blacks and whites in Los Angeles County, California, it was found that deaths from CVD constitute the largest category of deaths among each ethnic group, and that there were large differences in ASMR between the different groups (see table 1.4 on page 12). In all categories, relative risks (RRs) for African Americans were higher than that of the white and Hispanic populations, with the greatest excess observed in hypertensive disease, CBVD, and cardiomyopathy [Henderson et al., 2000]. Hispanics in Los Angeles share with African Americans important lifestyle disadvantages associated with premature mortality, such as inadequate access to medical care and inadequate knowledge of healthful behaviours (data from Behavioural Risk Factor Surveillance System, http://www.cdc.gov/brfss/). Furthermore, from recent census information, the Hispanic and African American populations of Los Angeles County are comparable in terms of socioeconomic status. In 1989, median income for Hispanic households was $27361 compared to $25827 for African American households and a similar proportion of families fell below the poverty line in both populations; 22.9% for Hispanics and 21.2% for African Americans [Census of Population and Housing, 1990]. Therefore, the difference in CHD mortality between Hispanics and African Americans, despite their similarities in socioeconomic status and healthcare access and awareness, argues towards other major factors determining the disparity in CHD mortality between whites and African Americans.

The Charleston Heart Study is a population-based prospective cohort study that began in 1960, and contains a randomly ascertained sample of blacks and whites 35 yr and older. Recent analysis confirmed the consensus that blacks suffered increased CHD risk over whites, with the median age at death being three years younger among black men than white men and five years younger for black women than white women [Nietert et al., 2006]. In a model that included SES (based on education and occupation), there was no significant difference in survival between white men and black men. However, this was not the case for women. In a survival model incorporating SES, survival rates for white women were significantly higher than black women, although the ethnicity effect was attenuated following adjustment for traditional risk factors. In both

Table 1.3: The contribution of CVD to excess mortality among poor blacks and whites 15–64 yr, according to sex and area, 1989–1991 [Geronimus et al., 1996].

Area	Race	Mean Family Income ($)	% Families Below Poverty Level	No. of Excess Deaths per 100 000			
				CVD		Total	
				Men	Women	Men	Women
New York City	Black	24174	33.1	205	137	1296	535
	White	34208	21.3	15	20	208	26
Detroit	Black	19841	44.3	192	146	746	355
	White	29334	22.0	138	93	421	203
Alabama	Black	17222	48.7	114	118	338	201
	White	30480	13.6	64	41	127	58

Table 1.4: ASMR and RR for CVD mortality in African American and Hispanic versus white men in Los Angeles County, 1988–1992 [Henderson et al., 2000].

Disease and Race		RR (95% CI)	ASMR
HT	White	1.00	22.0
	Hispanic	0.98 (0.82 – 1.17)	23.2
	African American	4.50 (3.98 – 5.08)	97.5
MI	White	1.00	163.6
	Hispanic	0.85 (0.79 – 0.92)	142.5
	African American	1.19 (1.10 – 1.28)	190.6
IHD	White	1.00	183.5
	Hispanic	0.75 (0.70 – 0.81)	145.0
	African American	1.29 (1.20 – 1.38)	231.1
CBVD	White	1.00	67.3
	Hispanic	1.21 (1.09 – 1.33)	80.7
	African American	2.33 (2.13 – 2.54)	153.0
Congestive Heart Failure	White	1.00	7.6
	Hispanic	1.12 (0.83 – 1.53)	8.7
	African American	2.24 (1.72 – 2.92)	16.6
Cardiomyopathy	White	1.00	29.1
	Hispanic	0.98 (0.84 – 1.14)	30.2
	African American	2.56 (2.25 – 2.90)	72.1
CVD - Other	White	1.00	221.1
	Hispanic	0.84 (0.79 – 0.90)	190.2
	African American	1.86 (1.76 – 1.96)	404.8
Total	White	1.00	694.5
	Hispanic	0.87 (0.84 – 0.90)	620.6
	African American	1.72 (1.67 – 1.77)	1165.7

sexes, models adjusting for traditional risk factors, showed no significant difference in survival between races [Nietert et al., 2006].

These findings are consistent with a number of other reports from the Charleston Heart Study (South Carolina) [Keil et al., 1993, 1992], and also data from the Evans County, Georgia, Heart Study that again showed a difference in black:white CHD survival between the sexes [Hames et al., 1993]. When both studies were combined and following adjustment for traditional risk factors, black men experienced around 20–30% less CHD mortality than white men, and were largely influenced by the same risk factors [Keil et al., 1995]. Both South Carolina and Georgia are notable for their low CHD mortality (in both white and black populations) so application of these findings to the whole of US is problematic.

With respect to risk factor distributions, blacks have a largely similar profile to whites. Lipid levels in black men and women were found to be largely similar, and in the Atherosclerosis Risk in Communities Study (ARIC) LDL-Cholesterol levels were similarly predictive of CHD risk [Jones et al., 2002]. The prevalence of obesity is high in both sexes and across ethnic and racial groups [Francis, 1997; American Heart Association, 2002], as is smoking [American Heart Association, 2002].

HT however has a remarkably high prevalence in blacks, with blacks developing HT earlier, and having higher average blood pressure than whites [Joint National Committee, 1997]. Inevitably this translates into increased CHD risk, for example in ARIC the CHD incidence rate in black women without HT was 1.6 per 1000 person-years, compared with 7.6 per 1000 person-years for black women with HT. Furthermore, as shown in table 1.4 on the preceding page, the greatest disparity in CHD ASMR in black men is due to HT. The underlying causes of HT, and thus of HT-associated disease mortality, remain obscure. What does seem clear is that rural native Africans seem to be normotensive [Cooper and Rotimi, 1994] and only develop HT upon migration to an urban environment [Kaufman et al., 1996]. Therefore it seems likely that although SES accounts for much of the differences seen in CHD rates, HT is also a significant factor. It is entirely possible that the predisposition to HT among those of African origin is due to a genetic susceptibility and only comes to the fore upon interaction with some environmental factor, be it smoking or diet (which appear to differ little between races).

1.1.4.3 Blacks in the UK

In the UK, blacks (black African, Caribbean, and others) are the second largest non-white population, accounting for around 2% of the population ($\sim$ 1.1 million) [Office for National Statistics, 2001]. In similarity to US blacks, UK blacks (both Caribbeans and West Africans) have a high incidence of stroke, whereas CHD is less common [Balarajan et al., 1989; Balarajan, 1991; Wild and McKeigue, 1997] – ASMR of 62 and

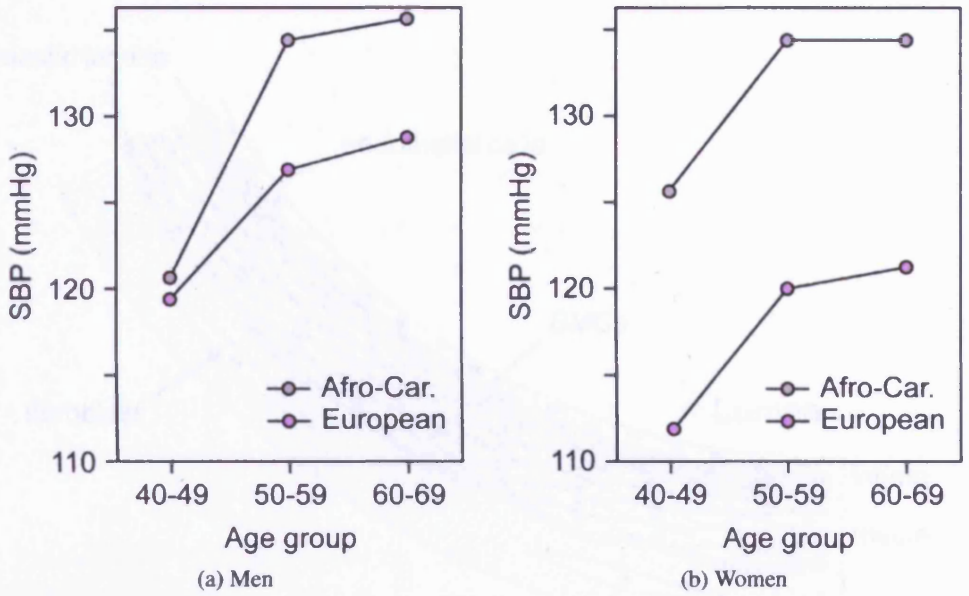

Figure 1.4: Median SBP by age and ethnic group in UK (adapted from Chaturvedi et al. [1993]).

100 per 100000 in black men and white European men respectively, and 86 and 100 in black women and European women respectively [Lip et al., 2007]. Furthermore, the major risk factor to differ consistently between UK blacks and white Europeans again seems to be HT.

In a study of over 1000 subjects, age-standardized prevalence of HT (>140 mmHg systolic blood pressure (SBP), >90 mmHg diastolic blood pressure (DBP), or on HT-treatment) was 35% in blacks and 14% in whites, with age-standardized median SBP 6 mmHg higher in black men than white men; in women this difference was 17 mmHg (see figure 1.4). No difference in median blood pressure (BP) were observed between black subjects born in the Caribbean and those born in West Africa [Chaturvedi et al., 1993].

Therefore it appears that present day UK may reflect the US some 20 yr ago. CHD mortality rates are lower for blacks than whites, however as time progresses we may see the gap narrowing, as shown in figure 1.3 on page 9.

Although the data for CVD susceptibility in blacks resident in Africa and western populations is confusing, it appears that those of African origin have a distinct predisposition to HT. Therefore, as HT is a particularly strong risk factor for CHD in these populations, it seems likely that as a greater proportion of the population is exposed to a western lifestyle this will lead to an overall increase in CHD incidence. Therefore a greater understanding of CHD in Africans will lead to improvements in identifying and

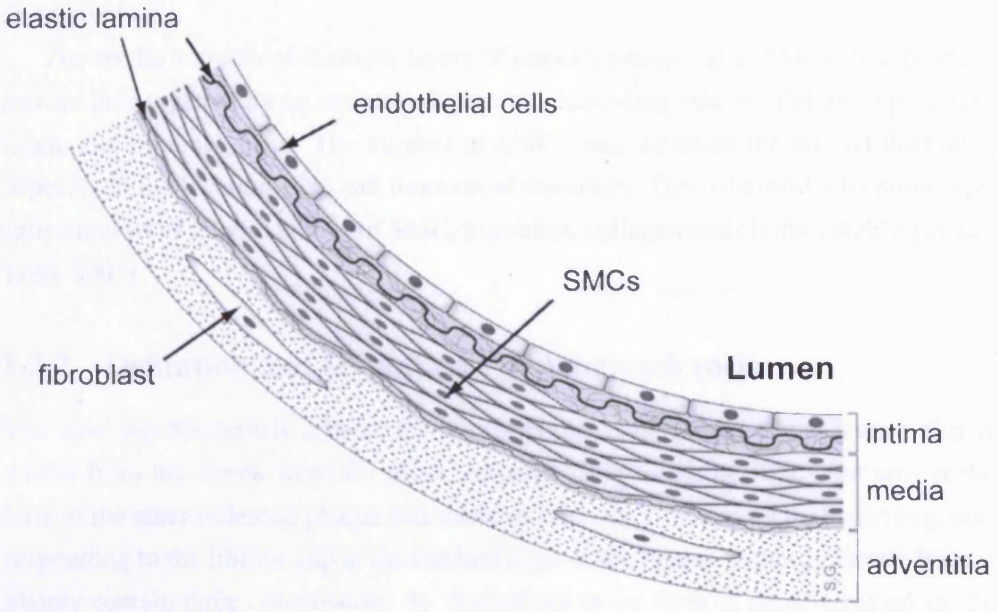

Figure 1.5: Morphology of the healthy arterial wall

treating a population in which CHD is set to increase drastically.

1.2 Pathology of Atherosclerosis

Atherosclerosis can be defined as a chronic vascular disease of medium and large arteries, and includes thickening and remodelling of the vessel wall leading to reduction or obstruction of blood flow, through plaque formation and thrombosis [Stuhlinger and Tsao, 2003].

1.2.1 Morphology of Normal Artery

The wall of the normal artery consists of three concentric cellular layers: the innermost intima, the media, and the outermost adventitia. The layers are separated by rings of elastin: the internal elastic lamina, separating the intima from the media, and the external elastic lamina, separating the media from the adventitia (see figure 1.5).

The luminal surface of the artery is lined by a single layer of endothelial cells on a basement membrane of extracellular matrix. Junctional complexes connect neighbouring endothelial cells. The endothelium forms a barrier between the blood and the arterial wall, and although originally thought to be fairly inert, is now seen as a dynamic cellu-

lar layer regulating a number of functions including vascular tone, leukocyte adhesion, and thrombosis.

The media consists of multiple layers of smooth muscle cells (SMCs) that produce and are held together by an extracellular matrix, consisting mainly of elastic fibres, collagen, and proteoglycans. The number of SMCs, and therefore the arterial thickness, depends on the location, size and function of the artery. The outermost adventitia typically consists of a loose matrix of SMC, fibroblast, collagen and elastin [Stuhlinger and Tsao, 2003].

1.2.2 Definition and Hypotheses of Atherosclerosis

The term atherosclerosis reflects the two principal components of the lesion; that is *athero* from the Greek word for gruel, corresponding to the necrotic core area at the base of the atherosclerotic plaque and *sclerosis* from the Greek word for hardening, corresponding to the fibrous cap at the luminal edge of the plaque. Atherosclerotic lesions mainly contain three components: 1). cholesterol in the form of cholesterol esters; 2). cells consisting mainly of SMCs, macrophages and other cell types; 3). connective tissue composed of collagen, elastin and glycosaminoglycans [Tegos et al., 2001; Woolf, 1990; Davies and Woolf, 1993].

A number of credible hypotheses for atherogenesis have been postulated to explain the cell types, behaviours and products observed within the plaque.

1.2.2.1 The Lipid Theory

It is now well established that the early lesions in atherosclerosis, the type I and type II lesions (according to the Stary classification [Stary et al., 1995]) are characterized by the accumulation of intracellular cholesterol esters within macrophage 'foam cells' [McGill Jr, 1968]. It has also been shown that the type III lesion is characterized by cholesterol ester accumulation in the extracellular space [Stary et al., 1995].

Studies of human arteries and animals fed on cholesterol-rich diets have shown that lipids accumulate in the intima [Smith and Slater, 1972]. This accumulation of cholesterol, and more precisely LDL-cholesterol, in the intima might be the result of: 1). increased plasma LDL concentrations [Smith, 1990]; 2). alteration of the permeability of the arterial intima to LDL [Zhang et al., 1993]; 3). increased retention of LDL in the intima [Bondjers et al., 1990]; and 4). impeded transport of LDL from the intima to the media [Smith, 1990].

1.2.2.2 The Oxidation theory

Cholesterol-loaded foam cells are present in the earliest detectable lesions. Normally, receptor-mediated uptake of LDL, the major carrier of plasma cholesterol, is suppressed by down-regulation of LDL receptor (LDLR) in response to increases in cholesterol concentrations. Therefore, it was thought LDL may undergo modifications, causing it to be internalized via receptors that are not under the control of cholesterol concentrations [Jessup et al., 2004].

The relevance of this hypothesis was increased following the observation that pre-incubation of LDL particles with endothelial cells, increased its subsequent uptake by macrophages, causing cholesterol loading [Henriksen et al., 1981]. The modified LDL includes oxidized LDL (oxLDL), consisting of both lipid and protein component oxidation, that can be formed via incubation with a number of cell types, including SMCs and macrophages [Steinberg, 1997a]. A less modified, but still biologically active, form of LDL – minimally modified LDL (MM-LDL) – is formed at the early stages of LDL oxidation, however this maintains its ability to bind LDLR and does not result in foam cell formation [Jessup et al., 2004].

1.2.2.3 The Hemodynamic Theory

The Hemodynamic theory was first proposed in 1950 and attempts to explain the focal nature of atherosclerosis, and suggested that hydrostatic and shear stresses were most important in lesion development. The theory drew on evidence that HT predisposes to atheroma development, and that the lesions have a predilection for arterial bifurcations and other locations where turbulent or relatively stagnant flow, and thus low shear stress, is usually detected. The lack of shear stress may delay the clearance of blood and its components, allowing prolonged contact of potentially toxic substances with the intima, which in turn could potentiate endothelial injury. In addition, altered hemodynamics may modify the endothelial permeability to LDL, facilitating their transport into the intima [Glagov et al., 1988].

1.2.2.4 The Fibrin Incrustation Theory

First proposed by Rokitansky in the nineteenth century, the theory postulated that fibrinogen is converted into fibrin on the luminal surface of the artery thereby forming a thrombus, which in turn becomes organized and tissue-like. It was demonstrated by two independent investigators that thrombus formation can take place on the surface of a plaque and subsequently can be incorporated into its mass and become fibrous, thus increasing its size [Duguid, 1946; Hand and Chandler, 1962]. Additionally it was proposed that phagocytosis of cholesterol-rich platelets by macrophages will produce the lipid-rich foam cells. On the whole, the layered appearance of the atheroma is

more easily explained by SMC hyperplasia and connective tissue deposition rather than thrombus organization. Despite these inadequacies, this theory focused attention on the crucial role of thrombogenesis, and proposed the idea of thrombus formation in the complicated plaque, leading to its instability [Tegos et al., 2001].

1.2.2.5 The Nonspecific Mesenchymal Hypothesis

Atherosclerosis consists of degenerative and regenerative processes. One such regenerative event is the proliferation of SMC and the subsequent connective tissue production by these cells. The main components of this connective tissue in such settings are proteoglycans and collagen, the principal space-filling agent of the complicated, advanced atherosclerotic plaque [Berenson et al., 1984]. This hypothesis proposes that a wide range of stimuli at the arterial wall – whether physical such as shear stress or chemicals such as vasoactive agents – induce a migration of SMC (mesenchymal cells) from the media to the intima, which subsequently proliferate and produce connective tissue [Hauss et al., 1962]. The processes described in this hypothesis resemble the healing process.

1.2.2.6 The Response to Injury Hypothesis

This hypothesis is a refinement of the previous theory. A wide array of stimuli (physical or chemical) to the arterial wall induce endothelial denudation with subsequent platelet adherence to the area. Platelets then release platelet-derived growth factor (PDGF) which in turn induces the migration of SMC from the media to the intima. SMC then proliferate and produce connective tissue. This theory is particularly pertinent when the endothelium has been mechanically removed, such as in angioplasty [Ross and Glomset, 1976a,b], however the unequivocal demonstration of intact endothelium during atherogenesis [Davies et al., 1976] required an evolution of the theory. Subsequent studies have stressed the role of other factors involved in this process, such as paracrine or local cell-derived inflammatory factors, and the most recent version emphasizes endothelial dysfunction rather than denudation [Ross, 1986, 1999].

1.2.3 The Sequence of Events in Plaque Development

In reality, the above hypotheses are not mutually exclusive but rather emphasize different concepts as the necessary events to support the development of the atherosclerotic lesion (see figure 1.6 on the following page). The exact nature of plaque development will likely differ between individuals, incorporating aspects from each of the hypotheses described above. The exact time-frame and order of the following steps remains a matter of contention, as each of the systems involved often interact with the others,

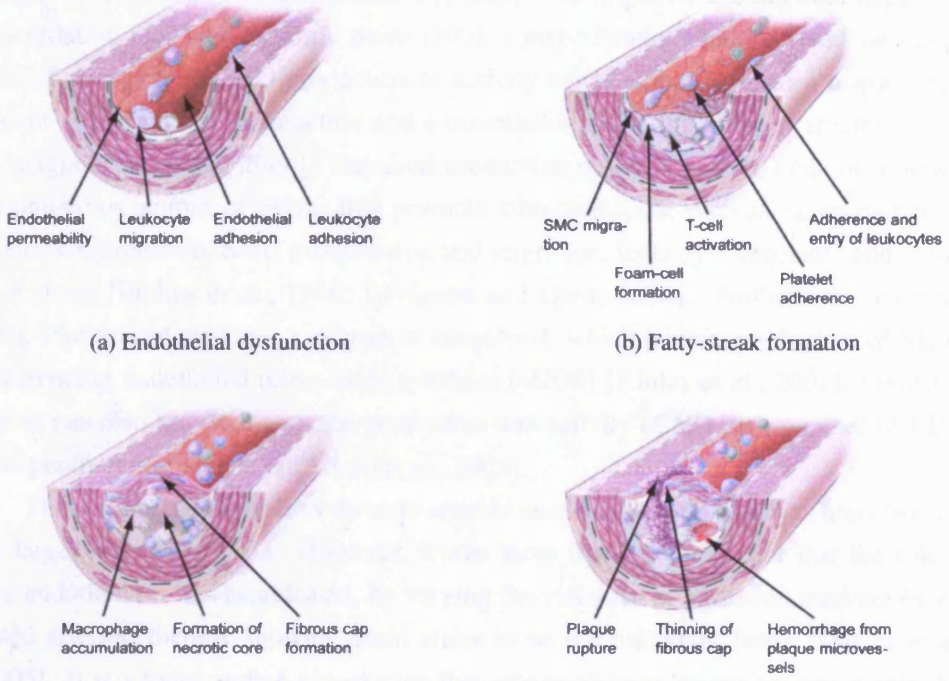

(a) Endothelial dysfunction

(b) Fatty-streak formation

(c) Formation of an advanced complicated lesion

(d) Unstable fibrous plaque

Figure 1.6: The stepwise progression of the atherosclerotic plaque (adapted from Ross [1999]).

causing a vicious circle, the beginning of which is difficult to pinpoint.

1.2.3.1 Plaque Initiation

Although the endothelium represents only a single layer of cells, the total volume of the endothelial cells of the human body is comparable to that of the liver [Huttner and Gabbiani, 1983]. As the major regulator of vascular homeostasis, the endothelium maintains the balance between vasodilation and vasoconstriction, inhibition and stimulation of SMC proliferation and migration (through direct endothelium-SMC myoendothelial gap junctions), and thrombogenesis and fibrinolysis [Luscher and Barton, 1997; Kinlay et al., 2001]. Damage to the endothelium upsets the balance between vasoconstriction and vasodilation and initiates a number of processes that promote and exacerbate atherosclerosis. Endothelial dysfunction is considered an early marker of atherosclerosis, preceding angiographic or ultrasonic evidence of atherosclerosis [Luscher and Barton, 1997].

The vessel wall reacts to many chemical and mechanical stimuli in the flowing

blood. The hallmark of endothelial dysfunction is impaired endothelium-dependent vasodilation mediated by nitric oxide (NO), a pivotal endothelium-derived substance. Therefore a defect in NO production or activity has been proposed as a major mechanism of endothelial dysfunction and a contributor to the initiation of atherosclerosis [Davignon and Ganz, 2004]. Impaired production or activity of NO has been linked to numerous actions or events that promote atherosclerosis, such as vasoconstriction, platelet aggregation, SMC proliferation and migration, leukocyte adhesion, and oxidative stress [Endres et al., 1998; Davignon and Ganz, 2004]. Furthermore, oxidized LDL-cholesterol increases synthesis of caveolin-1, which inhibits production of NO by inactivating endothelial nitric oxide synthase (eNOS) [Kinlay et al., 2001]. Oxidative stress can also interfere with the production and activity of NO by a number of LDL-independent mechanisms [d'Uscio et al., 2003].

That increasing blood flow through arteries results in vasodilation was first observed in larger arteries in 1933. However, it was more than 50 years later that the role of the endothelium was established, by varying the viscosity of perfusion medium in isolated arteries, thereby showing shear stress to be the important factor [Davies et al., 2005]. It is a longstanding observation that atherosclerotic lesions are not evenly distributed through the arterial system, and, as detailed in section 1.2.2.3 on page 17, the hemodynamic theory of atherosclerosis was postulated to address this observation. Evidence that low shear stress is a plaque-modulating factor has accumulated, although the complex flow characteristics in these regions may be as important as the average magnitude of the stress per se [Davies et al., 2005]. As yet, the method by which shear stress and turbulence acts on the endothelial and influences atherogenesis (potentially LDL-infiltration [Worth Longest and Kleinstreuer, 2003], shear-dependent accumulation of inflammatory cells [Hsiai et al., 2003], and shear stress dependent gene expression [Resnick et al., 1997]) is not clear.

The exact nature of endothelial dysfunction, and precisely the relationship between inflammation, LDL, and endothelial dysfunction, is still poorly understood, however a number of major risk factors are associated with an increase in oxidative stress and endothelial dysfunction (eg. dyslipidemia, smoking, aging, diabetes etc.) and therefore it poses an attractive therapeutic intervention. To date a number of interventions have been shown to be effective in restoring endothelium-dependent vasodilation (eg. statins, angiotensin-converting enzyme (ACE) inhibitors, antioxidants, reducing hyperglycemia, diet, and exercise [Davignon and Ganz, 2004]). As we gain a greater understanding of the role and pathology of endothelial dysfunction, further agents that act on endothelial dysfunction may yield therapies that prevent atherosclerosis initiation.

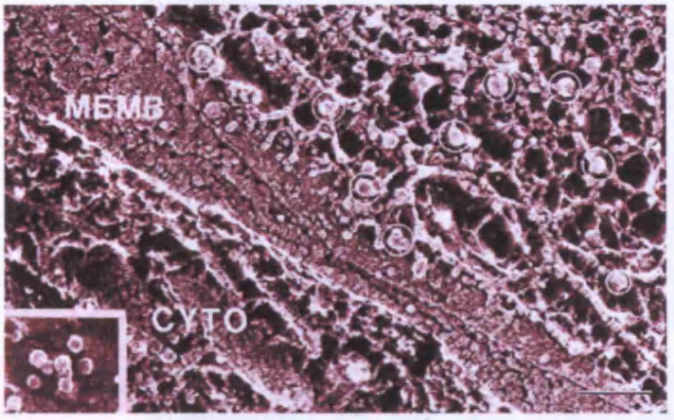

(a) A freeze-etch micrograph showing the accumulation of 23 nm LDL particles (circled) in the matrix of a rabbit atrial-ventricular valve following incubation with LDL. An endothelial cell at lower left shows the plasma membrane (MEMB) and cytoplasm (CYTO). Magnification x141 732, scale bar 0.1 μm.

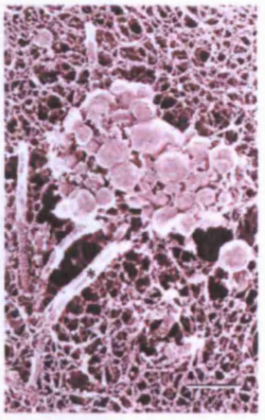

(b) Lipoprotein aggregation in a rabbit intima following administration of a bolus of LDL. Magnification x57 876, scale bar 0.2 μm.

Figure 1.7: Electron micrographs showing LDL accumulation and aggregation [Lusis, 2000]).

1.2.3.2 LDL Accumulation and Leukocyte Adhesion

The bulk of circulating cholesterol that circulates in the blood is in LDL particles. Any excess of LDL particles not taken up by the cells is rapidly removed by the lymphatic system. A striking morphological difference of the arterial intima from other tissues is the lack of lymphatic vessels [Groszek and Grundy, 1980]. Therefore to reach the lymphatic vessels in the media, LDL must pass through the intima. However, the elastic lamina presents a major barrier to its passage. Thus the passage of LDL particles can be slow, with more LDL particles entering the intimal fluid than are removed from it. This leads to a progressive increase in the concentration of LDL that sees LDL in the intimal fluid rise to 10-fold that seen in the interstitial fluids of other tissues [Smith, 1990]. This high concentration downregulates LDL receptors and so closes the physiological exit of LDL particles into cells [Pentikainen et al., 2000]. Following this accumulation, the initial LDL modification occurs, namely LDL aggregation and, often perifibrous, lipid droplet formation [Guyton et al., 1985; Guyton and Klemp, 1992] (see figure 1.7).

It is well recognized that leukocytes continually interact with the endothelium as part of immune surveillance. However, the endothelial monolayer of the healthy blood vessel resists firm adhesion of leukocytes, and the initial tethering of the leukocyte is reversible [Butcher, 1991]. It has been reported that monocytes from patients with hypercholesterolemia display increased adhesion to endothelial cells [Weber et al., 1997].

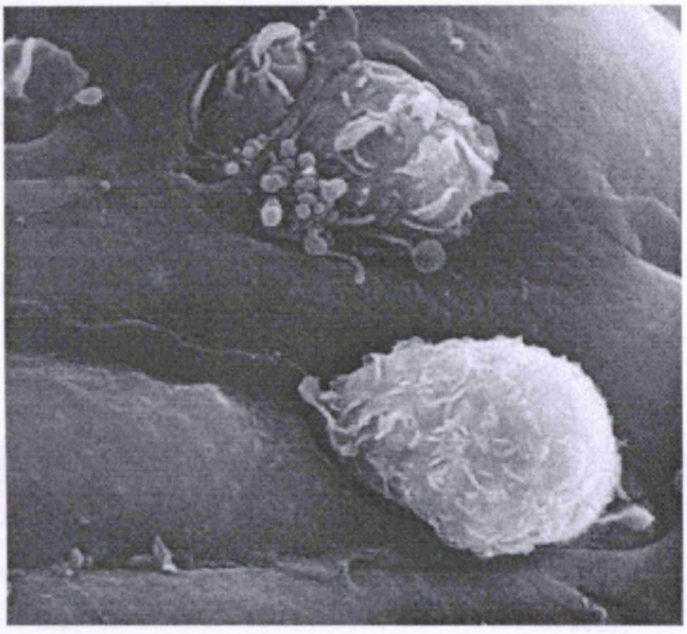

Figure 1.8: Scanning electron micrographs of the intimal surface of the aorta in a hyperlipidemic rabbit showing two macrophages. One is adherent to the plasma membrane of the endothelium; the other appears to have in part gained entry to the subendothelial space and is transversed by a 'bridge' of endothelial cytoplasm, magnification x4900 [Woolf, 1990].

Circulating LDL is known to damage endothelial cells and cause endothelial dysfunction [Anderson et al., 1995], as is bacterial or viral infection [Albert, 2000]. Increased adhesion to endothelial cells was also seen in human monocytes exposed to LDL *ex vivo*, suggesting that in addition to their effect on endothelial cells, lipoproteins also induce changes in circulating monocytes that may be pertinent to the recruitment process [Quehenberger, 2005].

The strong attachment of the monocyte to the endothelium is mediated by the interaction of integrins with ligands belonging to the immunoglobulin superfamily, most notably intracellular adhesion molecule-1 (ICAM-1) and vascular cell adhesion molecule-1 (VCAM-1). Normally the integrins are in a low-affinity state, and it has become apparent that they must undergo activation by a chemokine (small, secreted, chemotactic proteins) signal to mediate firm adhesion [Chan et al., 2003]. Chemokines also play a role in guiding the adherent macrophage across the endothelium [Johnston and Butcher, 2002], particularly monocyte chemoattractant protein-1 (MCP-1) [Gu et al., 1999] (see figure 1.8). Once resident in the arterial lamina, the monocytes undergo morphological changes and differentiate into macrophages. Locally produced cytokines and growth factors not only serve to attract and retain the monocytes but also to govern the differ-

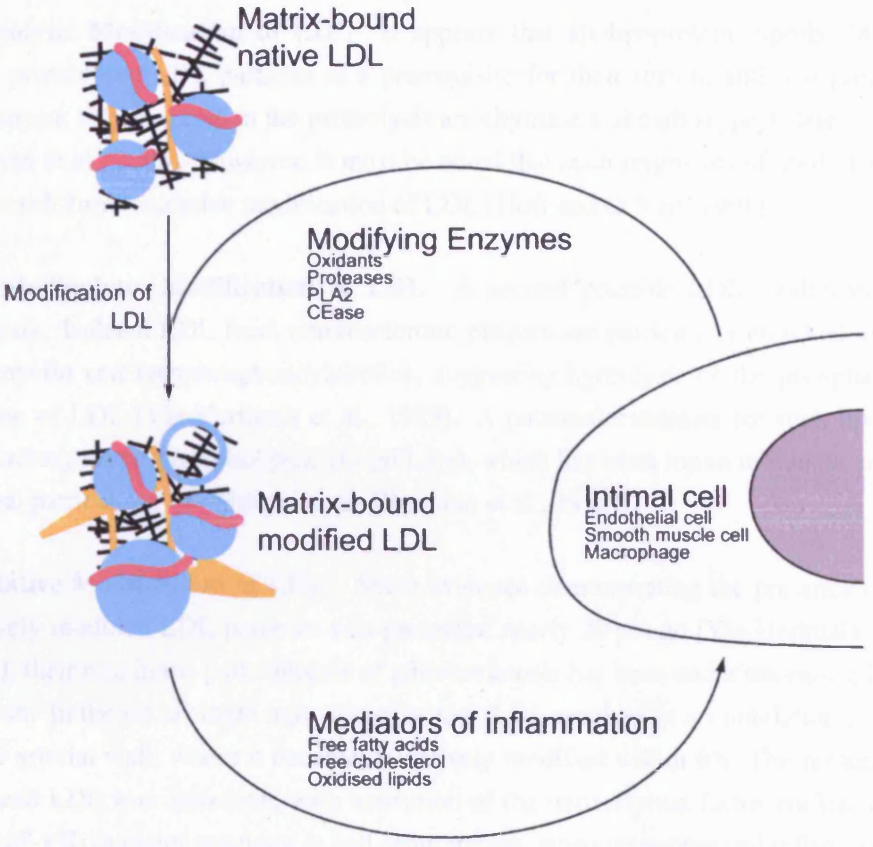

Figure 1.9: A schematic demonstrating the vicious cycle caused by LDL modification in the arterial intima. Taken from Pentikainen et al. [2000].

entiation of the monocytes into mature macrophages [Hansson, 2001; Linton and Fazio, 2003].

1.2.3.3 LDL Modification

The initial morphological sign of atherosclerosis is the appearance of enlarged LDL particles in the sub-endothelial space [Tamminen et al., 1999], and it is of particular interest that modified LDL has been observed in aortic samples from human foetuses even before signs of inflammation were visible [Napoli et al., 1997] suggesting that LDL modification is a very early event in atherogenesis. There are two major effects of LDL modification: 1). increased proteoglycan binding causing LDL retardation; and 2). interactions with intimal cells and upregulation of inflammatory and modifying processes. Thus LDL modification is part of a vicious cycle that causes only to exacerbate atherogenesis (see figure 1.9).

Proteolytic Modification of LDL It appears that apolipoprotein (apo)B-100 loss from proteolysed LDL particles is a prerequisite for their fusion, and two proteases that appear to play a role in the proteolysis are chymase and carboxypeptidase A [Pentikainen et al., 2000]. However, it must be noted that such fragments of apoB-100 can also result from oxidative modification of LDL [Hoff and O'Neil, 1991].

Phospholipolytic Modification of LDL A second possible LDL modification is lipolysis. Isolated LDL from atherosclerotic plaques are particularly enriched in sphingomyelin and lysophosphatidylcholine, suggesting hydrolysis of the phosphatidylcholine of LDL [Yla-Herttuala et al., 1989]. A potential candidate for such lipolysis is secretory typeII phospholipase A_2 ($sPLA_2$), which has been found in human arterial intima, particularly in inflamed areas [Romano et al., 1998].

Oxidative Modification of LDL Since evidence demonstrating the presence of oxidatively modified LDL particles was presented nearly 20 yr ago [Yla-Herttuala et al., 1989], their role in the pathogenesis of atherosclerosis has been under unceasing investigation. In the rat, a single injection of human LDL resulted in accumulation of LDL in the arterial wall, where it became oxidatively modified within 6 h. The presence of oxidized LDL was associated with activation of the transcription factor nuclear factor κB (NF-κB) (a major regulator in cell proliferation, stress responses and inflammation) in the endothelium as well as endothelial expression of ICAM-1 [Calara et al., 1998].

1.2.3.4 Foam Cell Formation and Immune Potentiation

When circulating monocytes migrate from the vasculature into the extravascular compartment, a process of maturation into macrophages is concomitantly launched. The process renders the cells ready for active participation in the inflammatory responses. This process is complex, with a role for NF-κB seemingly being central [Takashiba et al., 1999; Osterud and Bjorklid, 2003]. Macrophage sensitivity and reactivity is seemingly substantially higher than monocytes, so that although oxidized LDL may fail to induce monocyte activation in whole blood [Brand et al., 1994], modified LDL within the intima is likely to have a largely different effect [Osterud and Bjorklid, 2003]. One such effect is the uptake of modified LDL by monocyte-derived macrophages, turning them into fat-laden foam cells that remain in the vessel wall, furthering the local inflammatory response (see figure 1.10 on the next page). The mechanisms underlying such foam cell generation have been the focus of intensive research for some years [Berliner et al., 1995; Brown and Goldstein, 1986; Chisolm III et al., 1999; Steinberg, 1997b; Witztum and Steinberg, 1991].

Macrophages are normally protected from the accumulation of toxic cholesterol loads, primarily by the downregulation of surface LDL receptor molecules in response

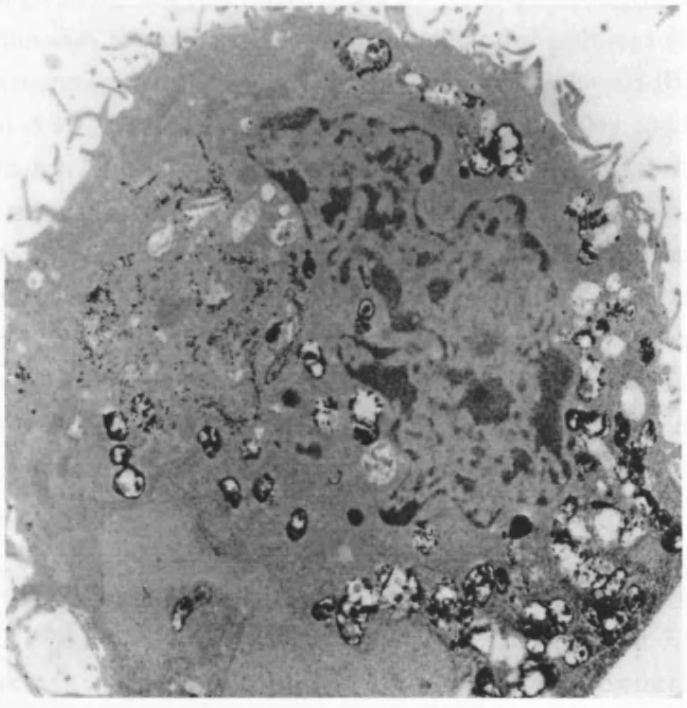

Figure 1.10: TEM of stained macrophage foam cell with numerous intracellular lipid droplets (Vanderbilt Cel Imaging Shared Resource, www.mc.vanderbilt.edu).

to replete intracellular cholesterol stores [Brown and Goldstein, 1986]. However, modified LDL is taken up by alternate scavenger receptors (SRs) that are not similarly down-regulated [Berliner et al., 1995; Chisolm III et al., 1999; Steinberg, 1997b; Witztum and Steinberg, 1991]. A number of different such scavenger receptors have been identified, comprising several transmembrane receptors that all share a common affinity for negatively charged macromolecules or particles, such as modified LDL [Osterud and Bjorklid, 2003].

The presence of activated T cells within human atherosclerotic plaques has been known for some time [Hansson et al., 1989]. Following this, interferon-γ (IFNγ) and major histocompatibility complex (MHC) class II were found in atherosclerotic lesions along with antibodies to oxidized LDL, demonstrating that pathways of the adaptive arm of the immune system were also established in atherosclerosis [Hansson et al., 1989; Palinski et al., 1989]. Both cluster of differentiation (CD)4+ and CD8+ T cells are found in human lesions but CD4+ generally dominate in number [Frostegard et al., 1999]. Furthermore these processes contribute to the overall pathogenesis of the lesion, as demonstrated by various animal models enriched or depleted for the numerous T cell subsets [Robertson and Hansson, 2006]. The activation of T cells and other antigen presenting cells (APCs) involve not only contact dependent mechanisms but also the secretion of soluble mediators, important in the development of atherosclerosis [Daugherty et al., 2005; Tedgui and Mallat, 2006]. Just such a cytokine, IFNγ, is produced by most T cells in human atherosclerotic plaques and is the principal T helper 1 (T_H1) cytokine [Hansson et al., 1989; Harvey and Ramji, 2005].

Role of IFNγ in Atherosclerosis The interferon (IFN) family of cytokines is divided into type I and type II IFNs. Type I IFNs, including IFNα, β, ω, and θ, share notable sequence homology and are synthesized by most cell types. On the other hand, IFNγ is at present the only type II interferon identified and binds to a distinct type II receptor [Harvey and Ramji, 2005]. IFNγ itself is secreted mainly by natural killer (NK) cells and activated CD4+ T_H1 cells, but recent evidence indicates that it can also be produced by monocytes/macrophages and B cells [Schroder et al., 2004]. IFNγ has a multitude of functions, displaying direct antiviral activity as well as a variety of immunomodulatory and inflammatory roles [Schroder et al., 2004; Boehm et al., 1997]. Immunohistochemical studies have shown IFNγ within the atherosclerotic lesion [Young et al., 2002], where it is known to have a range of influences on disease progression, acting on all the major cell types of the plaque. Due to the large number of genes affected by IFNγ, approximately 25% of the macrophage transcriptome is under IFNγ control [Ehrt et al., 2001], the overall effect of IFNγ is complex with it assigned both pro- and anti-atherogenic effects.

Potentiation of Immune Response The lesions of $apoe^{-/-}$ or $ldlr^{-/-}$ mice deficient in IFNγ have a dramatically reduced content of the key cells in atherogenesis – macrophages, T-lymphocytes, and SMCs, and therefore reduced atherosclerosis, indicating a key role for IFNγ in their recruitment [Gupta et al., 1997; Buono et al., 2003].

IFNγ is responsible for the upregulation of a number of key chemokines and chemokine receptors [Charo and Taubman, 2004], most notably being the dramatic induction of MCP-1 by IFNγ [Valente et al., 1998]. IFNγ also appears to be an important mediator of both VCAM-1 and ICAM-1 expression on SMC and endothelial cells [Li et al., 1993; Chung et al., 2002], and is able to increase expression of integrins (such as α-5-β-1 integrin) on the surface of vascular SMCs [Barillari et al., 2001]. Therefore IFNγ plays a role in attracting monocytes, and increasing the available adhesion molecules to ensure more monocytes enter the sub-endothelial space. Once there, it is well known that IFNγ is able to stimulate both the differentiation of monocytes to macrophages and the activation of macrophages and T-lymphocytes [Schroder et al., 2004; Boehm et al., 1997; Harvey and Ramji, 2005].

Foam Cell Formation IFNγ regulates the expression of a number of genes known to be important in cholesterol metabolism [Harvey and Ramji, 2005]. Overall, incubation of foam cells with IFNγ results in reduced cholesterol efflux, with an increase in cholesterol ester accumulation [Panousis and Zuckerman, 2000]. More recently, IFNγ has been shown to impede reverse cholesterol transport and so promote foam cell formation in a human acute monocytic leukaemia cell line (THP-1) [Reiss et al., 2004]. More specifically IFNγ decreases production of apoE (a protein component of lipoproteins that is responsible for the transport of cholesterol from the peripheral tissues to the liver – reverse cholesterol transport) in both monocytes and macrophages, and increases its intracellular degradation. Because of apoE's pivotal role in atherosclerosis, this action of IFNγ is likely to be an important factor in IFNγ's overall atherogenic effect [Harvey and Ramji, 2005].

IFNγ – Pro- or Anti-Atherogenic? As well as the potent pro-atherogenic functions of IFNγ detailed above, IFNγ also has a number of protective functions. Transplantation of IFNγ-deficient bone marrow in *LDLR* -/- mice increases the extent of atherosclerosis development [Niwa et al., 2004], suggesting that IFNγ has an atheroprotective effect.

IFNγ has been shown to inhibit two scavenger receptors – SR-A and CD36 – specifically in macrophages [Geng and Hansson, 1992], thereby reducing foam cell formation. IFNγ is also known to reduce the expression of lipoprotein lipase (LPL) in macrophages at the transcriptional level [Hughes et al., 2002]. LPL's main physiological role is to catalyse the hydrolysis of triacylglycerol to non-esterified fatty acids for tissue utiliza-

tion. Macrophage derived LPL is believed to be atherogenic, as demonstrated by animal models, with LPL-null macrophages showing decreased atherogenesis [Mead and Ramji, 2002].

IFNγ has beneficial effects on oxidative stress within the vascular wall, inhibiting macrophage-mediated LDL oxidation [Fong et al., 1994; Folcik et al., 1997]. In particular, signalling by IFNγ has been shown to upregulate inducible nitric oxide synthase (iNOS) gene expression in a wide variety of cell types, including endothelial cells, SMCs and macrophages [Yokoyama et al., 1996]. IFNγ also regulates the expression of other genes implicated in the control of oxidative stress, however a consensus on the action of such gene regulation has not been reached [Harvey and Ramji, 2005].

Thus the majority of evidence from numerous animal studies has identified IFNγ as a pro-atherogenic cytokine, although it undeniably has some atheroprotective effects. The exact role of IFNγ may well differ depending on the exact stage of the disease and the presence of other factors.

1.2.3.5 Plaque Maturation and Remodelling

Most atherosclerosis is clinically silent, and the consequences of atherosclerosis rarely occur before the development of advanced lesions [Clarke and Bennett, 2006]. Segments of an angiographically-normal coronary artery can harbour many asymptomatic plaques that do not encroach on the lumen, termed compensatory enlargement [Varnava, 1998]. The remodelling that occurs is plaque specific rather than patient specific [Varnava, 1998]. The exact mechanisms involved in the degree and type of remodelling are not well understood, however there appears to be a positive correlation between core size and history of remodelling, that suggests hemodynamic forces may be important in this process [Davies, 2000].

An important determinant of plaque stability is the nature of the fibrous cap. Many advanced lesions comprise a SMC-rich fibrous cap overlying a lipid- and macrophage-rich necrotic core, and it is the relative proportion of these two elements that determine the clinical manifestation of the plaque; unstable plaques that are particularly prone to rupture contain a higher proportion of inflammatory cells and lipid, and a lower proportion of SMCs [Davies et al., 1993]. In advanced lesions, fibrous cap thinning is due to loss of SMCs, and it is these such thin-capped atheromas that are prone to rupture [Virmani et al., 2000]. The impact of SMC apoptosis was elegantly shown in an $apoe^{-/-}$ transgenic mouse model who's SMCs could undergo inducible apoptosis. Such SMC apoptosis induced marked fibrous cap thinning, loss of collagen and extracellular matrix (ECM), and intense intimal inflammation [Clarke et al., 2006].

Role of IFNγ in Plaque Maturation Increased expression of pro-inflammatory cytokines has been shown in vulnerable plaques, and IFNγ-secreting T_H1 cells frequently accumulate at the sites of plaque rupture [Harvey and Ramji, 2005]. The increased cellularity of the plaque caused by IFNγ has already been discussed, but IFNγ can also act to weaken the fibrous cap by inhibiting the expression of collagen genes, SMC proliferation and matrix synthesis [Amento et al., 1991; Yuan et al., 1999].

The ECM is broken down by matrix metalloproteinases (MMPs), a group of enzymes that therefore contribute to plaque instability, and have been localized to the shoulder regions of plaques that are particularly prone to rupture [Galis et al., 1994]. IFNγ is known to stimulate increased production of MMPs by macrophages and SMCs [Schonbeck et al., 1997], and therefore potentially contribute to plaque instability.

1.2.3.6 Necrotic Core Formation and Plaque Rupture

The intensive aggregation of foam cells leads to the formation of an atheromatous core. In the centre of the core the destruction of foam cells leads to the extracellular accumulation of lipids and cellular debris [Lusis, 2000; Lusis et al., 2004].

Thrombus formation is triggered by vascular injury secondary to atherosclerotic pathology. Such sudden rupture may occur spontaneously without obvious triggers, however it may follow a particular event such as extreme physical activity, emotional trauma, sexual activity, exposure to narcotics, cold or acute infection [Shah, 2003]. Platelets play a central role in this process by adhering to the exposed subendothelium, and initiating a cascade of platelet recruitment [Hennerici, 2004]. Pathological studies have identified tissue factor (TF), present in cells and in the extracellular debris of the atheroma, as a candidate molecule responsible for the thrombogenicity associated with plaque rupture [Tremoli et al., 1999]. In some instances, thrombus formation may result in growth of a plaque through resolution and incorporation of the thrombus. Alternatively, formation of a major thrombus can occlude the vessel and lead to an atherothrombotic event, such as stroke, MI or vascular death.

Role of IFNγ in Necrotic Core Formation The function of IFNγ in apoptosis is complex, however it has been shown that IFNγ will stimulate foam cell apoptosis *in vitro* [Inagaki et al., 2002], through activation of various pro-apoptopic pathways.

1.3 IL-18 – An IFNγ-Inducing Factor

In vitro secretion of IFNγ from T_H1 cells is induced by stimulation with antigen or antibodies against CD3, however Wada et al. [1985] found IFNγ induction by antigen in mice pre-treated by *Propionibacterium acnes* was significantly greater. Furthermore,

P. acnes-primed animals were, unusually for mice, susceptible to lipopolysaccharide (LPS) injection. It was believed unlikely that LPS stimulated T_H1 cells directly, and most probably an intermediate molecule was involved [Ushio et al., 1996].

That sera from *P. acnes*-primed mice was able to induce IFNγ production from anti-CD3 stimulated T cells above that achieved with interleukin 12 (IL-12) alone, suggested that an IFNγ-inducing factor was present within the sera [Okamura et al., 1995a]. The factor was purified from the sera of mice that had been sequentially treated with *P. acnes* and LPS, and found to be a single peptide [Okamura et al., 1995b]. Human IFNγ-inducing factor complementary DNA (cDNA) was isolated using murine IFNγ-inducing factor cDNA as a probe from a normal human liver cDNA library. The amino acid sequence included an interleukin 1 (IL-1) signature-like sequence. Subsequently, the cloned cDNA was expressed in *Escherichia coli* and was able to induce IFNγ production from human peripheral blood mononuclear cells (PBMCs). The factor was designated IL-18 [Ushio et al., 1996].

1.3.1 The IL-18 System

Since the discovery of IL-18 a number of other affiliate proteins have been identified, all of which play a role in IL-18 function. Analogous to the IL-1 system, the IL-18 system constitutes the ligand (IL-18), a dimeric receptor (constituting IL-18 receptor subunit α (IL-18Rα) and IL-18 receptor subunit β (IL-18Rβ)), and an intrinsic inhibitor protein (IL-18BP) that binds strongly to IL-18 and prevents it engaging it's receptor.

1.3.1.1 IL-18

Protein Structure IL-18 is a single peptide with a molecular weight of around 18000, and an isoelectric point (pI) of 4.8. Both mouse and human IL-18 lack the usual leader sequence necessary for secretion, but instead have an unusual N-terminal leader sequence of 35 amino acids [Okamura et al., 1995b]. The protein also lacks any N-glycosylation sites or putative hydrophobic signal peptide [Okamura et al., 1995b]. It's tertiary structure was solved by nuclear magnetic resonance (NMR) spectroscopy by Kato et al. [2003] and found to consist of three twisted four-stranded β-sheets, one short α-helix and one 3_{10} helix. The β-sheets form the distinctive β-trefoil structure (see figure 1.11 on the following page).

IL-18 has only moderate sequence identity to IL-1 (17%) but when the protein sequence was threaded through protein fold databases it consistently drew top matches to the interleukin 1β (IL-1β) structure, particularly the β-trefoil structure detailed above [Kato et al., 2003]. That the two proteins matched so well suggested that the unusual leader sequence is analogous to the IL-1β pro-domain which must be enzymatically cleaved, by caspase-1, for optimal secretion and biological activity.

Figure 1.11: IL-18 protein structure as determined by NMR spectroscopy [Kato et al., 2003].

IL-18-Producing Tissues and It's Post-Translational Processing IL-18 is widely expressed in both immune system cells and non-immune cells. Human PBMCs secrete proIL-18 under normal conditions suggesting that it may be cleaved extracellularly, yet dendritic cells constitutively express IL-18 mRNA and produce mature IL-18. Epidermal cells, particularly keratinocytes, can secrete IL-18, along with IL-12, in response to stimulation with contact allergens. However, under normal circumstances, keratinocytes do not produce caspase-1 suggesting that IL-18 secretion by keratinocytes might be via a caspase-1-independent manner [Nakanishi et al., 2001a].

Intestinal, along with airway, epithelial cells express IL-18, as do osteoblastic stromal cells. IL-18 secretion occurs in the central nervous system and endocrine system, moreover IL-18 and IL-18 receptor (IL-18R) can be detected in the brains of adult rats, suggesting IL-18 may play an important role in connecting the immune system to the endocrine and nervous systems [Nakanishi et al., 2001a].

ProIL-18 processing is via the IL-1β/IL-18 inflammosome, the initiation of which is the binding of pathogen to one of the intracellular pathogen-sensing NOD-like receptors (NLRs). The NLRs are a family of proteins that share similar structural features with Toll-like receptor (TLR) and IL-1 receptor (IL-1R) and are involved in the regulation of apoptosis, inflammation, and host defence; their ability to activate or inhibit caspases is at the basis of these functions. They contain an N-terminal effector-binding domain and a C-terminal ligand-recognition domain, mostly a leucine-rich repeat similar to that seen in TLR [Boraschi and Dinarello, 2006] (see figure 1.12 on the next page).

Mutations in NLR family, pyrin-domain containing 3 (NLRP3), are involved in a series of autosomal dominant, severe pathologies characterized by persistent and gener-

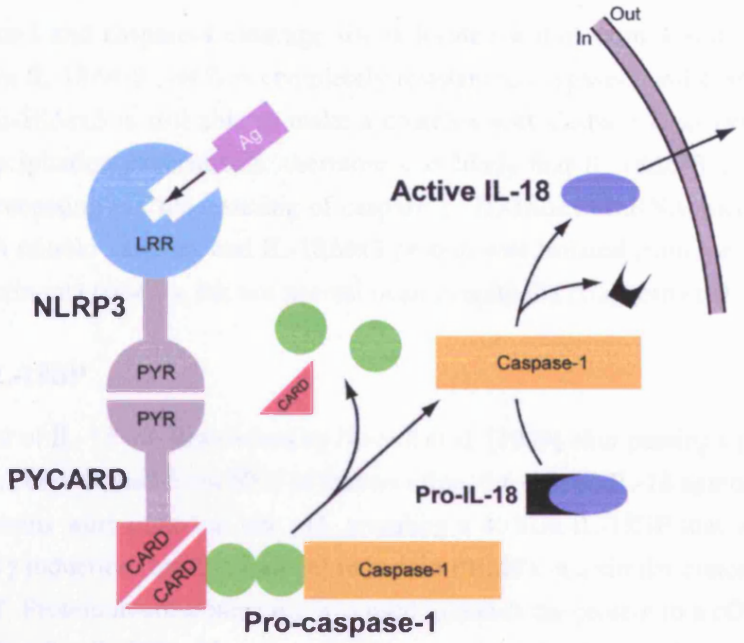

Figure 1.12: The IL-18/IL-1β inflammosome. Activation of an intracellular NLR (here NLRP3) via the LRR domain causes the inflammosome to form, ultimately resulting in maturation of caspase-1 via sequential cleavages by active caspase-1 molecules. Active caspase-1 then cleaves pro-IL-18 allowing it to leave the cell.

alized inflammation and is therefore a good candidate for caspase-1 activation in IL-18 processing. NLRP3 contains an N-terminal PYR effector binding domain which interacts with the PYR domain of the adapter protein, PYR and CARD domain containing protein (PYCARD), which in turn activates caspase-1 maturation by sequential cleavages by active enzyme molecules. Activated caspase-1 is then able to cleave proIL-18 (and IL-1β) and so allows it's extracellular export [Boraschi and Dinarello, 2006].

IL-18 Isoforms IL-18 is expressed in a number of ovarian carcinoma cell lines and fresh tumour samples, but the expression of caspase-1 is more variable. Nevertheless, in those ovarian carcinoma cells that expressed both IL-18 and caspase-1, no mature IL-18 was detectable in the cell culture supernatants, yet in normal ovarian epithelial cells mature IL-18 is produced [Wang et al., 2002]. Recombinant caspase-1 digestion of lysates from two ovarian cell lines, IGROV-1 (negative for caspase-1 expression) and OVCAR-3 (positive for caspase-1 production), resulted in mature IL-18 and a band of unprocessed pro-IL-18 that did not disappear at higher concentrations of caspase-1. By QPCR on OVCAR-3 total ribonucleic acid (RNA), two different IL-18 cDNAs were revealed – one with exon 3, and one without (Δex3). Exon 3 consists of 12 nucleotides, therefore the Δex3 cDNA translates into a protein that lacks four amino acids – AEDD.

The caspase-1 and caspase-4 cleavage site is located within exon 4 and is therefore preserved in IL-18Δex3, yet it is completely resistant to caspase-1 and caspase-4 processing. IL-18Δex3 is still able to make a complex with caspase-1, as evidenced by immunoprecipitation experiments, therefore it is likely that IL-18Δex3 could inhibit classical processing via sequestering of caspase-1. IL-18Δex3 mRNA was detectable in 3/3 fresh tumour samples and IL-18Δex3 protein was isolated from ascitic fluid of ovarian carcinoma patients, but not normal ovarian epithelia [Gaggero et al., 2004].

1.3.1.2 IL-18BP

An inhibitor of IL-18 was discovered by Novick et al. [1999] after passing a preparation of proteins, concentrated from 500 l of human urine, through an IL-18 agarose column. Bound proteins were eluted at low pH, revealing a 40 kDa IL-18BP that was able to inhibit IFNγ induction (by IL-18 alone) in human PBMCs at a similar concentration to IL-18 itself. Protein microsequencing was used to match the protein to a cDNA from a human Jurkat T cell cDNA library, coding for a protein of unknown function. Further examination of other cDNA libraries revealed four splice variants – a,b,c, and d [Novick et al., 1999]. The protein was constitutively expressed by the spleen and had no obvious homology to other human proteins, but did have homology (up to 47% homology) with various poxvirus proteins.

Structure The amino acid sequence of IL-18BP suggested that the polypeptide belonged to the immunoglobulin (Ig) super-family, and had an Ig domain homologous to that found in IL-1 decoy receptor (IL-1RII) along with numerous potential N-glycosylation sites [Novick et al., 1999].

IL-18BP-Producing Tissues IL-18BP is highly expressed in the spleen and intestinal tract [Boraschi and Dinarello, 2006], is constitutively expressed by PBMCs [Hurgin et al., 2002], and circulates at plasma concentrations of around 2.5 ng/ml [Novick et al., 2001]. There is evidence to suggest that IL-18BP gene expression is under the regulation of IFNγ. In a colon carcinoma/epithelial cell line – DLD-1 – IFNγ induced IL-18BPa mRNA upregulation in parallel with an increase in IL-18BPa protein secretion, this was also the case in a keratinocyte cell line (HaCaT). The histone deacetylase inhibitor, sodium butyrate, suppressed the upregulation [Paulukat et al., 2001]. Similar experiments in the liver carcinoma cell line, HepG2, and in human PBMCs supported these observations [Hurgin et al., 2002], indicating that *de novo* protein synthesis is required for IFNγ-mediated IL-18BP upregulation.

IL-18BP Isoforms The *IL18BP* gene encodes for at least four distinct isoforms derived from mRNA splice variants, isolated from several cDNA libraries. They differ

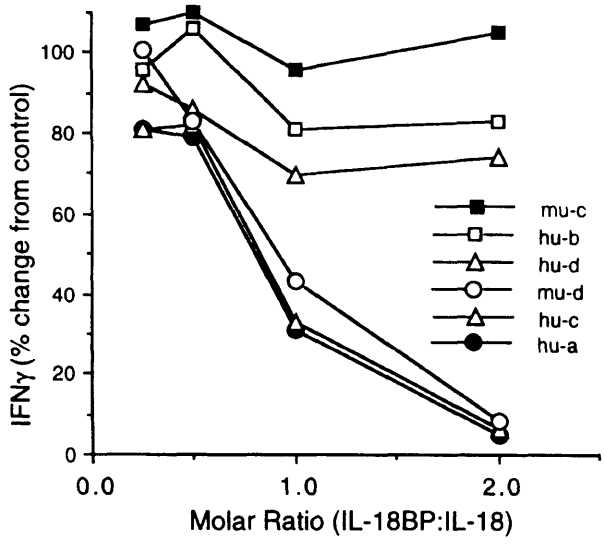

Figure 1.13: Titration of human and murine IL-18BP isoforms on IL-18 activity [Kim et al., 2000].

primarily in their carboxyl termini whereas the N-terminal is largely identical [Novick et al., 1999; Kim et al., 2000]. Using COS cells transiently transfected for six different IL-18BP isoforms (two murine and four human), Kim et al. [2000] assessed the ability of each isoform to bind IL-18 and prevent IFNγ induction. As shown in figure 1.13, complete inhibition of IL-18 was achieved with a two-fold molar excess of both IL-18BPa and c, in contrast there was no inhibition by IL-18BPb or d (even at six-fold molar excess). Such binding is remarkably strong, given that IL-1RII requires a molar excess of five for inhibition of IL-1β [Arend et al., 1994].

1.3.1.3 The IL-18 Receptor

An IL-18R was purified from a Hodgkin's disease cell line, with ^{125}I-labelled IL-18 showing a single class of binding site for IL-18 [Torigoe et al., 1997]. That addition of IL-1β did not inhibit the binding demonstrated that the IL-18R was distinct from IL-1R. IL-18R was purified from membrane extracts using a monoclonal antibody (mAb) clone that inhibited IL-18:IL-18R formation. N-term sequencing showed that the purified protein matched a previously identified member of the IL-1R family that failed to bind interleukin 1 α (IL-1α), IL-1β or IL-1 receptor antagonist (IL-1Ra) – IL-1 receptor related protein (IL-1Rrp) [Parnet et al., 1996]. Expression of IL-1Rrp in COS cells and subsequent addition of IL-18 (but not IL-1β) caused activation of NF-κB deoxyribonucleic acid (DNA)-binding ability [Torigoe et al., 1997], and was therefore a good candidate for IL-18R despite a relatively weak affinity for IL-18. Further proof

was provided by studies in *il18rα*$^{-/-}$ mice, showing that they were not responsive to, and did not bind, IL-18 [Hoshino et al., 1999].

Upon identification of a novel member of the IL-1R family (accessory protein like (AcPL)) that had no role in IL-1 induced activation of NF-κB, Born et al. [1998] examined whether AcPL might function in a similar way to IL-1 receptor accessory protein (IL-1RAcP), namely recruit intracellular signalling molecules following IL-1R:IL-1 formation, for IL-1Rrp. They were able to show that both IL-1Rrp and AcPL were needed for both NF-κB and c-Jun N-terminal kinase (JNK) activation in response to IL-18. Further immunoprecipitation studies showed AcPL was unable to bind IL-18 itself, yet a dominant-negative version (lacking the cytoplasmic domain required for signalling) of AcPL specifically inhibited IL-18 signalling. It was therefore proposed that both IL-1Rrp and AcPL were needed for a functional IL-18R [Born et al., 1998], as such IL-1Rrp and AcPL were renamed IL-18Rα and IL-18Rβ, respectively. The synergy of IL-12 and IL-18 is mediated via induction of IL-18Rα on naïve T cells and NK cells, and then subsequent up-regulation of IL-12 receptor β-2 (IL-12Rβ2) by IL-18 [Yoshimoto et al., 1998]. In the human NK cell line – NKO – both IL-18Rα and IL-18Rβ mRNA levels were up-regulated by IL-12 [Kim et al., 2001].

Downstream Signalling That both IL-18Rα and IL-18Rβ are required for signalling, was further illustrated by COS-1 cells that do not respond to IL-18 despite abundant expression of IL-18Rα. Yet transient transfection with IL-18Rβ and a luciferase reporter, gave IL-18 responsiveness [Kim et al., 2001].

Following IL-18's binding to IL-18Rα, IL-18Rβ is recruited into a signalling complex. Signal transduction is initiated by the approximation of of the Toll-IL-1 receptor (TIR) domains present in the intracellular portions of both receptor chains. The signalling pathway, shared with other receptors of the TLR/IL-1R family, involves recruitment of the adaptor molecule, myeloid differentiation primary response gene 88 (MyD88) and of IL-1 receptor associated kinase (IRAK), followed by interaction with TNF-receptor associated factor 6 (TRAF6). The resultant activation of IκB kinase (IKK) causes degradation of inhibitor of NF-κB (IkB) and subsequent activation of NF-κB [Boraschi and Dinarello, 2006; Bowie and O'Neill, 2000] (see figure 1.14 on the next page). An additional signalling pathway has been described that involves the activation of mitogen-activated protein kinase (MAPK) p38 [Wyman et al., 2002].

There also appears the potential for IL-18-independent engagement of IL-18R in autoimmune inflammation. *Il18*$^{-/-}$ mice were susceptible to autoimmune encephalomyelitis, yet *il18rα*$^{-/-}$ were resistant, suggesting that IL-18Rα may have an, as yet unknown (mice do not express IL-1 family, member 7 (IL-1F7)), natural ligand other than IL-18.

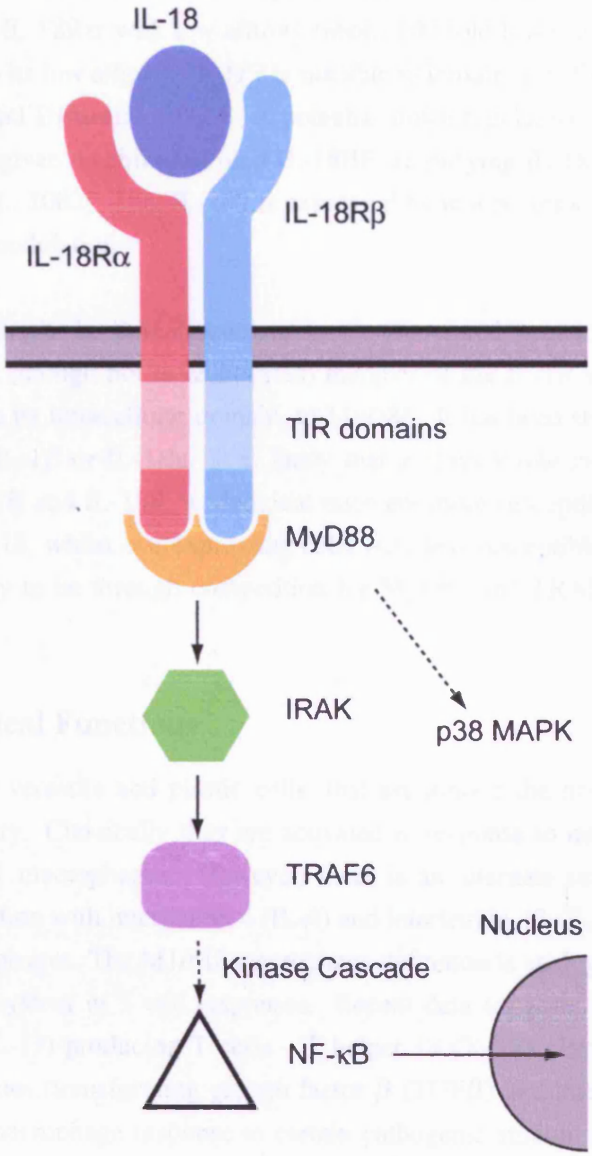

Figure 1.14: The IL-18R signalling cascade. Upon binding of IL-18 to IL-18Rα, IL-18Rβ is recruited. Through approximation of the TIR domains MyD88 is recruited, initiating a signalling cascade that ultimately leads to NF-κB entering the nucleus and changes in gene expression.

1.3.1.4 IL-1F7 and SIGIRR

IL-1F7 The IL-1 homologue IL-1F7 was discovered from expressed sequence tag database searches. One of a number of splice variants is matured by caspase-1 and is then able to bind IL-18Rα with low affinity (about 100-fold lower than IL-18). However, likely due to its low affinity, IL-1F7 is not able to initiate signalling [Kumar et al., 2002; Boraschi and Dinarello, 2006]. A potential down-regulatory role has been assigned to IL-1F7 given its ability to bind IL-18BP, amplifying IL-18 inhibition by IL-18BP [Bufler et al., 2002]. That IL-1F7 is expressed by monocytes suggests a real role for it in immunomodulation.

SIGIRR The single Ig domain-containing IL-1R-related protein (SIGIRR) is a widely-expressed (though not in leukocytes) member of the IL-1R super-family with high similarity, in its intracellular domain, to MyD88. It has been shown not to interact with IL-1α, IL-1β or IL-1Ra. It is likely that it plays a role in down-regulating signalling by IL-1R and IL-18R, as deficient mice are more susceptible to stimulation with IL-1 and IL-18, whilst overexpressing cells were less susceptible. The method of inhibition is likely to be through competition for MyD88 and TRAF6 [Boraschi and Dinarello, 2006].

1.3.2 Biological Functions

Macrophages are versatile and plastic cells, that are among the first to be recruited to the site of injury. Classically they are activated in response to microbial products, giving rise to M1 macrophages. However, there is an alternate activation pathway, following stimulation with interleukin 4 (IL-4) and interleukin-13 (IL-13), which gives rise to M2 macrophages. The M1/M2 macrophage definition is analogous to the T_H1/T helper 2 (T_H2) system in T cell responses. Recent data suggests a pivotal role for interleukin-17 (IL-17)-producing T cells – T helper 17 (T_H17). Production of T_H17 polarizing cytokines (transforming growth factor β (TGFβ) and interleukin 6 (IL-6)) depends on the macrophage response to certain pathogenic stimuli, and it is possible there is an M17 macrophage subtype [Boraschi and Dinarello, 2006]. IL-18 is able to cause differentiation of naïve T cells into T_H1, T_H2, or T_H17, dependent on the cytokine milieu (see figure 1.15 on the following page).

1.3.2.1 IL-18 in T_H1 Responses

Generally, IFNγ production by T cells requires T cell receptor (TCR)-mediated T cell activation. However, IL-18 and IL-12 synergistically induce IFNγ production by T cells without TCR engagement. Such induction is not enhanced by additional anti-CD3 (i.e.

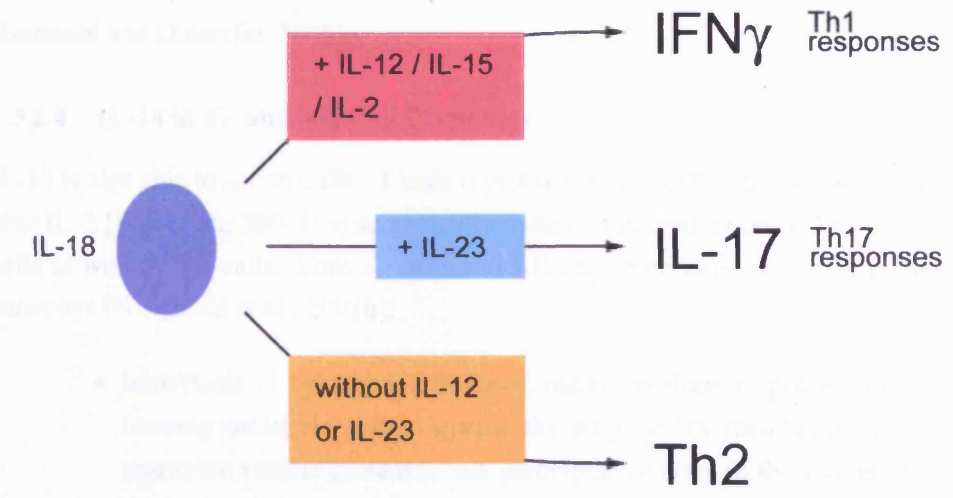

Figure 1.15: IL-18 is able to activate T_H1, T_H2, or T_H17 responses dependant on the cytokine milieu (adapted from Boraschi and Dinarello [2006]).

TCR engagement), nor inhibition of TCR signalling (with cyclosporin A). However, TCR signalling is required for differentiation from naïve T cells to T_H1 cells – in T cells stimulated with IL-18 and IL-12, and with, or without, anti-CD3, only those stimulated with anti-CD3 developed into T_H1 cells [Nakanishi et al., 2001a].

1.3.2.2 IL-18 in T_H2 Responses

IL-18 entirely fails to act on mature T_H2 cells. Naïve T cells express a low level of IL-18Rα, and recently naïve T cells cultured with interleukin 2 (IL-2) and IL-18 for four days, even without antigen, produce modest amounts of IL-4 (a major T_H2 cytokine). While IL-4 production is markedly enhanced with antigen co-stimulation, co-culture with anti-IL-4 causes naïve T cells to produce trace amounts of IL-4, but large amounts of IFNγ. Therefore, IL-18 has the ability to induce T_H2 differentiation in an IL-4-dependent manner [Nakanishi et al., 2001b].

1.3.2.3 IL-18 in T_H17 Responses

T_H17 cells have been recently classified as a new effector T cell subset, distinct from T_H1 and T_H2 cells. They have been linked to interleukin 23 (IL-23), as $il23^{-/-}$ mice have very few T_H17 cells, and are protected from autoimmune diseases. It also appears that TGFβ and IL-6 are factors responsible for the differentiation of this subset from naïve T cells [Stockinger and Veldhoen, 2007]. The role of IL-18 appears to be to amplify/activate IL-17 production in already polarized T_H17 cells, in a TCR-independent manner, similar to its role in TCR-independent activation of T_H1 in synergy with IL-12

[Boraschi and Dinarello, 2006].

1.3.2.4 IL-18 in T_C and NK Cell Responses

IL-18 is also able to act on CD8+ T cells (cytotoxic T (T_C) cells). IL-18 and IL-12 (but also IL-2 [Son et al., 2001]) synergistically induced the production of IFNγ from T_C cells as well as NK cells. Both T_C cells and NK cells exert cytotoxicity by numerous pathways [Nakanishi et al., 2001b]:

- Exocytosis of cytocidal substances, mainly perforin (a potent pore-forming molecule acting against the target cell's membrane) and granzyme (serine proteases that participate directly in the killing of the target cell)
- Expressing FAS ligand thereby inducing apoptosis in FAS-expressing target cells
- TNF-related apoptosis-inducing ligand (TRAIL) expression causing apoptopic death in a wide variety of tumour cell lines

IL-18 up-regulates perforin-mediated and FAS ligand-mediated cell death by NK cells, but not TRAIL-mediated pathways. No IL-18/IL-12 synergy is required for these actions suggesting different pathways from those used by T_H1 cells, are responsible [Nakanishi et al., 2001b].

1.3.3 The IL-18 System Genes

1.3.3.1 *IL18*

As shown in figure 1.16 on the next page, *IL18* consists of six exons on chr11 (q23.1), totalling 21 kbp.

IL18 gene expression is unlike many other cytokines. Firstly, cytokine gene expression is often tightly controlled by TATA-type promoters, however *IL18*'s promoter is TATA-less allowing more widespread expression [Tone et al., 1997]. That IL-18 protein production remains specific despite extensive gene expression could be reconciled by tight caspase-1 regulation, yet IL-1β is also caspase-1 dependent but is still controlled by a TATA-type promoter [Hunninghake et al., 1992]. Secondly, the structure of *IL18* mRNA is unusual. To ensure tight control of cytokine expression it is generally considered advantageous to have mRNA with a short half-life. Therefore, many cytokine mRNAs contain RNA-destabilizing elements in the 3'untranslated region (UTR), namely multiple AUUUA sequences and overall AU rich mRNA. However, *IL18* has no AUUUA sequences and the 3'UTR is not particularly AU rich [Tone et al., 1997].

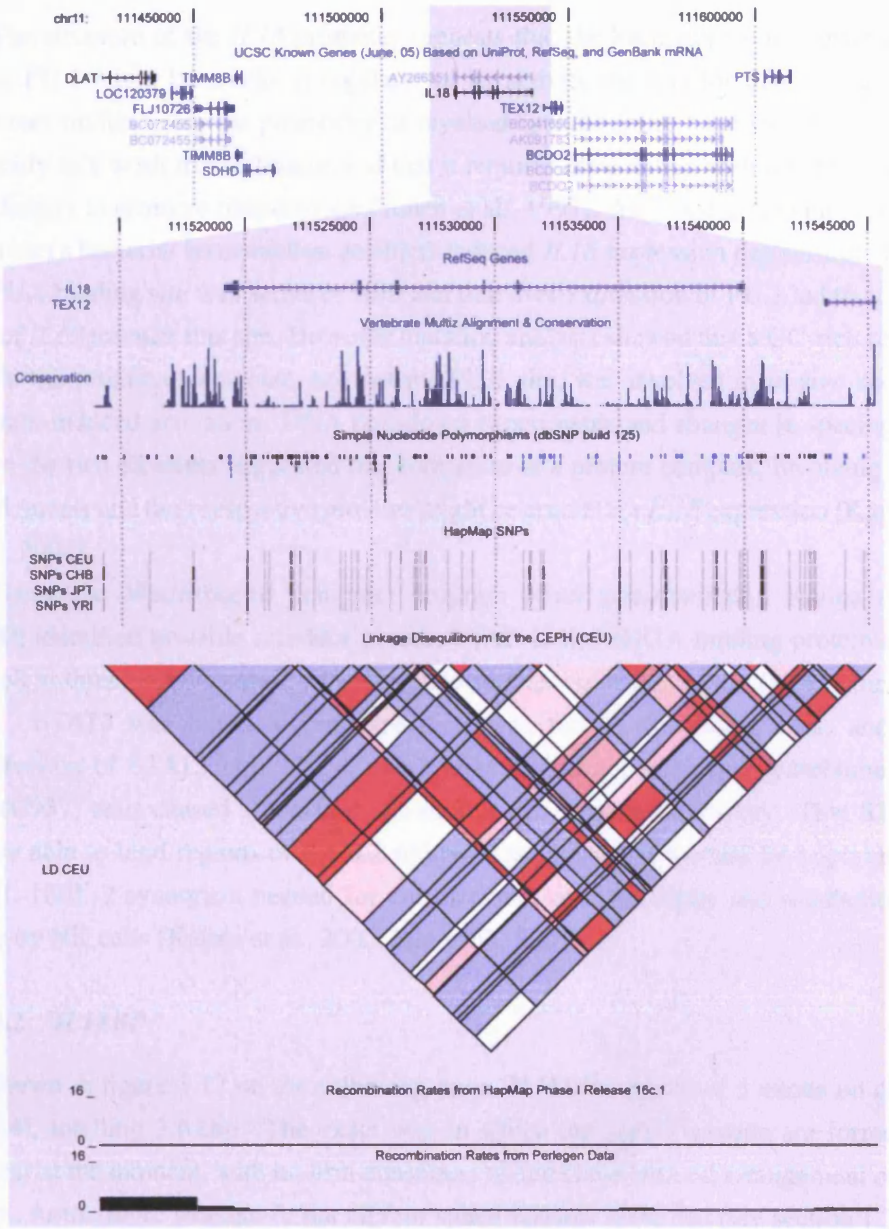

Figure 1.16: The genomic context of *IL18* taken from UCSC Genome Browser (May 2004 assembly), accessed July 2007[3].

[3]The known genes track shows known protein-coding genes taken from the National Centre for Biotechnology Information (NCBI) mRNA RefSeq collection. The level of shading indicates the level of review the RefSeq record has undergone (predicted–light, provisional–medium, reviewed–dark). The conservation track displays vertebrate sequence conservation between human and mouse, rat, rabbit, dog, armadillo, elephant, opossum, and chicken. The SNP database (dbSNP) track shows data from dbSNP build 125. Untranslated SNPs are shown in blue, SNPs of unknown function are in black, whilst synonymous coding SNPs are shown in green. The human haplotype-mapping project (HapMap) tracks show data from HapMap phase II release 21a. The SNPs are displayed in grey using a color gradient based on allele frequency (a higher allele frequency has a darker color). The HapMap linkage disequilibrium (LD) plot uses the standard colour scheme used elsewhere in this thesis (see section 2.4.2 on page 90). The recombination rates track shows recombination rates in cM per Mbp, calculated from HapMap phase I, release 16a and Perlegen data.

The structure of the *IL18* promoter suggests that the haematopoietic transcription factor PU.1 might be a critical regulator of its activity (as it is for *il18*'s promoter). However studies using the promoters of myeloid specific genes have shown that PU.1 acts only as a weak transactivator, and that it requires cooperation with other transcription factors to promote transcription [Tenen et al., 1997]. An investigation into sodium butyrate (a bacterial fermentation product)-induced *IL18* expression demonstrated that the PU.1 binding site was active *in vitro* and that over-expression of PU.1 led to activation of *IL18* through this site. However mutation analysis showed that a GC-rich region within the proximal promoter, and not the PU.1 site, was involved in *in vivo* sodium butyrate-induced activation. DNA pull-down experiments and changes in spacing between the two elements suggested that formation of a protein complex, involving both cis-elements and their respective proteins might be crucial for *IL18* expression [Koyama et al., 2004].

Using the MatInspector computer program (www.genomatix.de), Kalina et al. [2000] identified possible activator protein 1 (AP-1) and GATA-binding protein sites, as well as three specific signal transducer and activator of transcription (STAT)-binding sites. STAT5 was found to bind specifically to the STAT-binding sites, and co-transfection of STAT5 into THP-1 and human leukaemic monocyte lymphoma cell line (U937) cells caused a two-fold elevation in *IL18* promoter activity. That STAT5 is also able to bind regions of the *IL2* promoter suggests that it could be important in the IL-18/IL-2 synergism needed for enhancement of cytotoxicity and production of IFNγ by NK cells [Kalina et al., 2000; Son et al., 2001].

1.3.3.2 *IL18BP*

As shown in figure 1.17 on the following page, *IL18BP* consists of 5 exons on chr11 (q13.4), totalling 3.6 kbp. The exact way in which the splice variants are formed is unclear at the moment, with no firm consensus on the chromosomal arrangement of the exons, furthermore whether or not all four splice variants identified (see section 1.3.1.2 on page 33) are translated *in vivo* is also unclear.

The *IL18BP* promoter, was mapped by Hurgin et al. [2002] using rapid amplification of 5' complementary DNA ends (5'RACE). A 1.6 kbp fragment, constituting the proximal promoter, was shown to have basal promoter activity when cloned into luciferase reporter vectors. The promoter lacks a TATA-box but has several GC-rich regions near to the transcriptional start site. Analysis of the promoter using a transcription factor search algorithm, found a gamma-interferon activated site (GAS), an IFN regulatory factor (IRF) element, and two CCAAT/enhancer binding protein β (CEBPβ) sites. Mutating these sites completely abolished basal activity. Studying the IFNγ induction of IL-18BP production, it appeared that the IRF element and GAS were crucial, but that

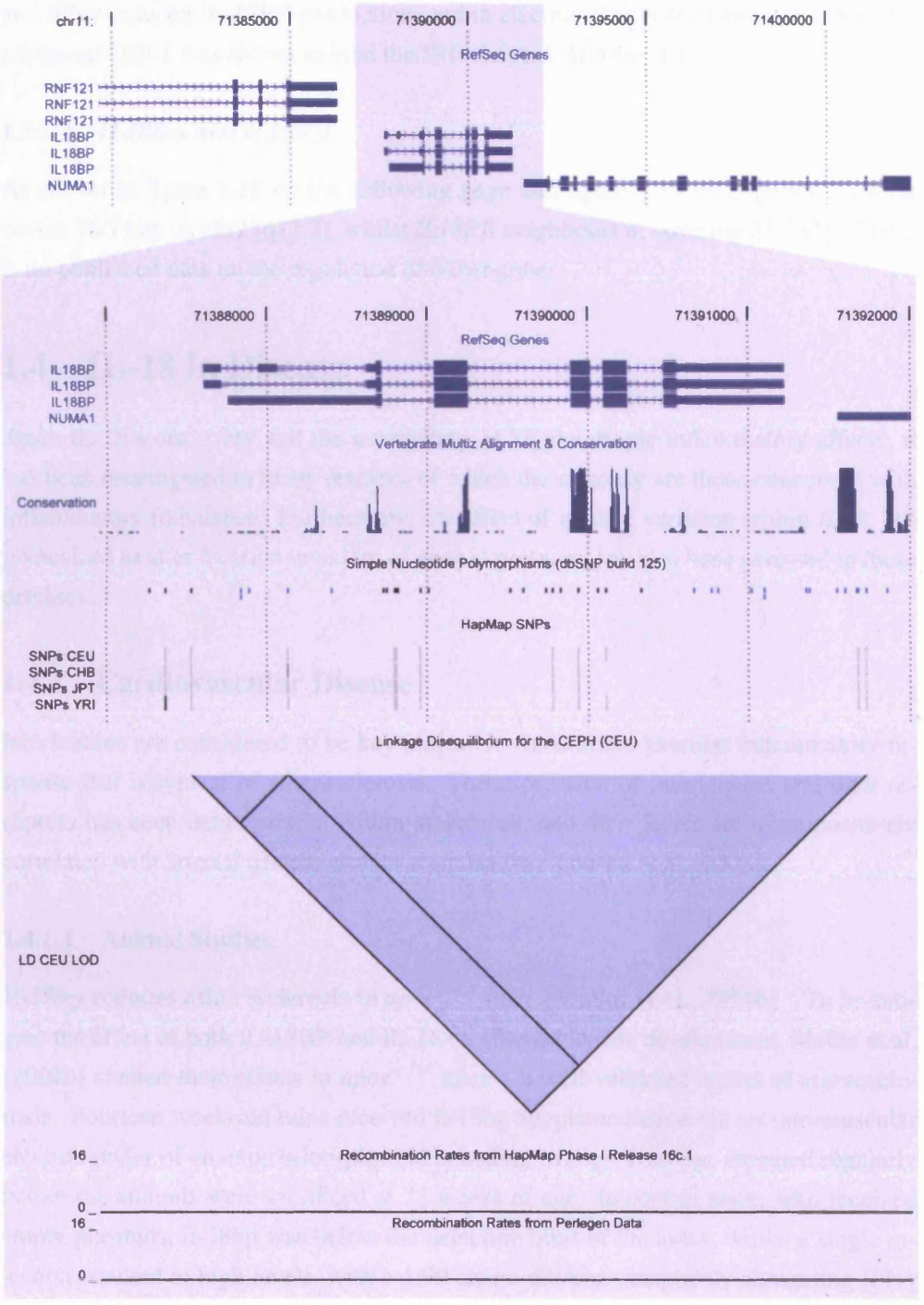

Figure 1.17: The genomic context of *IL18BP* taken from UCSC Genome Browser (May 2004 assembly), accessed July 2007[3].

the CEBPβ pair increased the induction. Sera from IRF-1 deficient mice lacked basal and IFNγ-induced IL-18BP production, and in electromobility shift assay (EMSA) experiments IRF-1 was shown to bind the IRF element [Hurgin et al., 2002].

1.3.3.3 *IL18Rα* and *IL18Rβ*

As shown in figure 1.18 on the following page and figure 1.19 on page 45, *IL18Rα* covers 36.1 kbp on chr2 (q11.2), whilst *IL18Rβ* neighbours it, covering 33.7 kbp. There is no published data on the regulation of either gene.

1.4 IL-18 in Disease

Since IL-18's discovery and the unravelling of its pleiotropic inflammatory affects, it has been investigated in many diseases of which the majority are those concerned with inflammatory imbalance. Furthermore, the effect of genetic variation within *IL18*, hypothesized to alter location or extent of gene expression, has also been assessed in these diseases.

1.4.1 Cardiovascular Disease

Interleukins are considered to be key players in the chronic vascular inflammatory response that is typical of atherosclerosis. The expression of interleukins and their receptors has been demonstrated within atheromas, and their levels are often positively correlated with arterial disease and its sequelae [der Thusen et al., 2003].

1.4.1.1 Animal Studies

Il-18bp reduces atherosclerosis in *apoe*$^{-/-}$ mice [Mallat et al., 2001b] To investigate the effect of both IL-18BP and IL-18 on atherosclerosis development, Mallat et al. [2001b] studied their effects in *apoe*$^{-/-}$ mice – a well-validated model of atherosclerosis. Fourteen week-old mice received il-18bp supplementation via an intramuscular electrotransfer of an expression-plasmid encoding *il18bp*. This was repeated regularly before the animals were sacrificed at 23 weeks of age. In control mice, who received empty plasmids, il-18bp was below the detection limit of the assay, whilst a single injection resulted in high levels, with a 1:90 serum dilution completely abrogating IFNγ induction in a murine spleen cell bioassay. Interestingly there was a modest, but significant, increase in mean animal weight in the *il18bp* plasmid group compared with the control group (31.8 g vs. 28.6 g, $p<0.05$).

Examination of the thoracic aorta showed a marked reduction in lipid deposition in those mice treated with *il18bp* plasmid compared to controls. Quantitative computer-

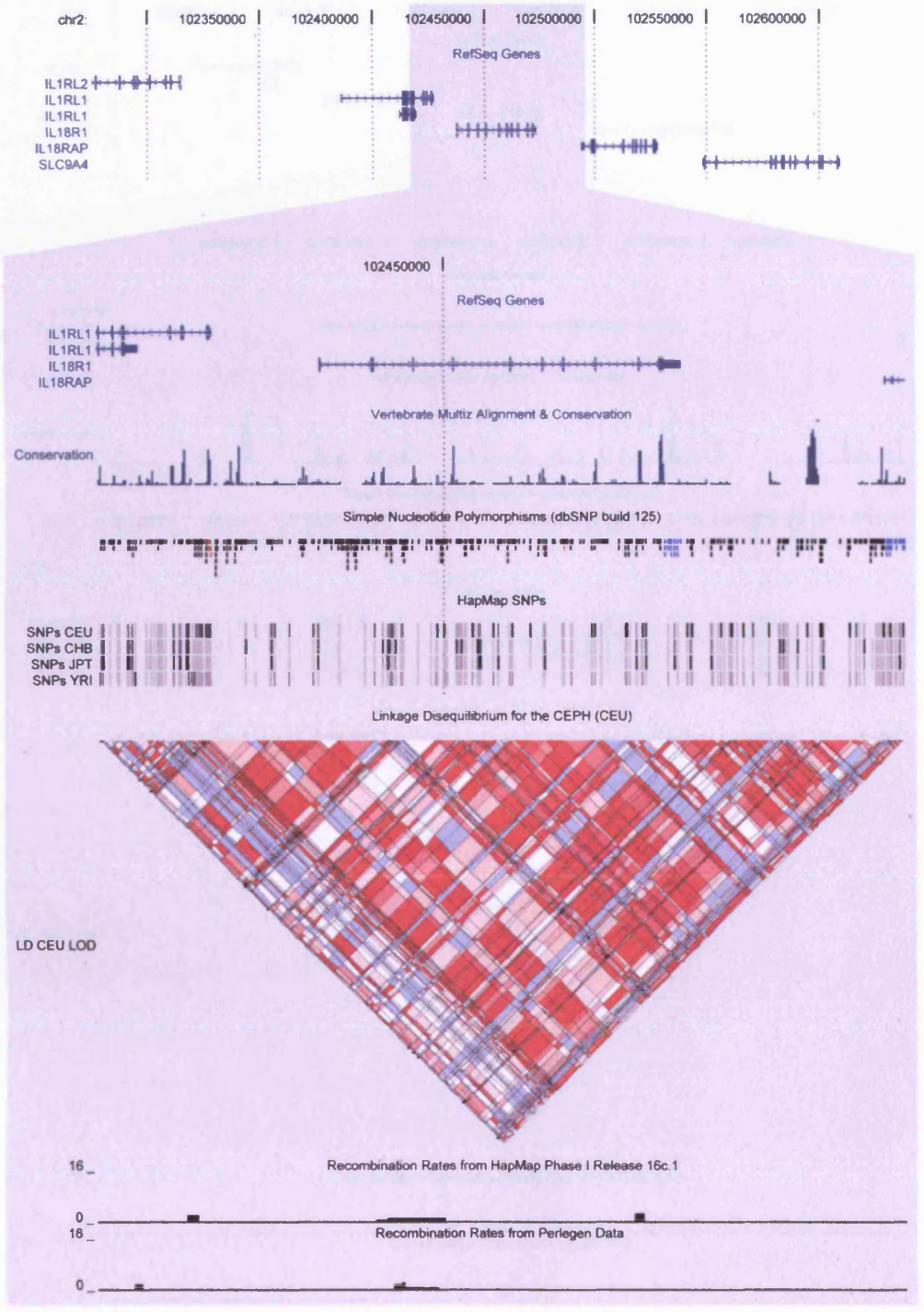

Figure 1.18: The genomic context of *IL18Rα* taken from UCSC Genome Browser (May 2004 assembly), accessed July 2007[3].

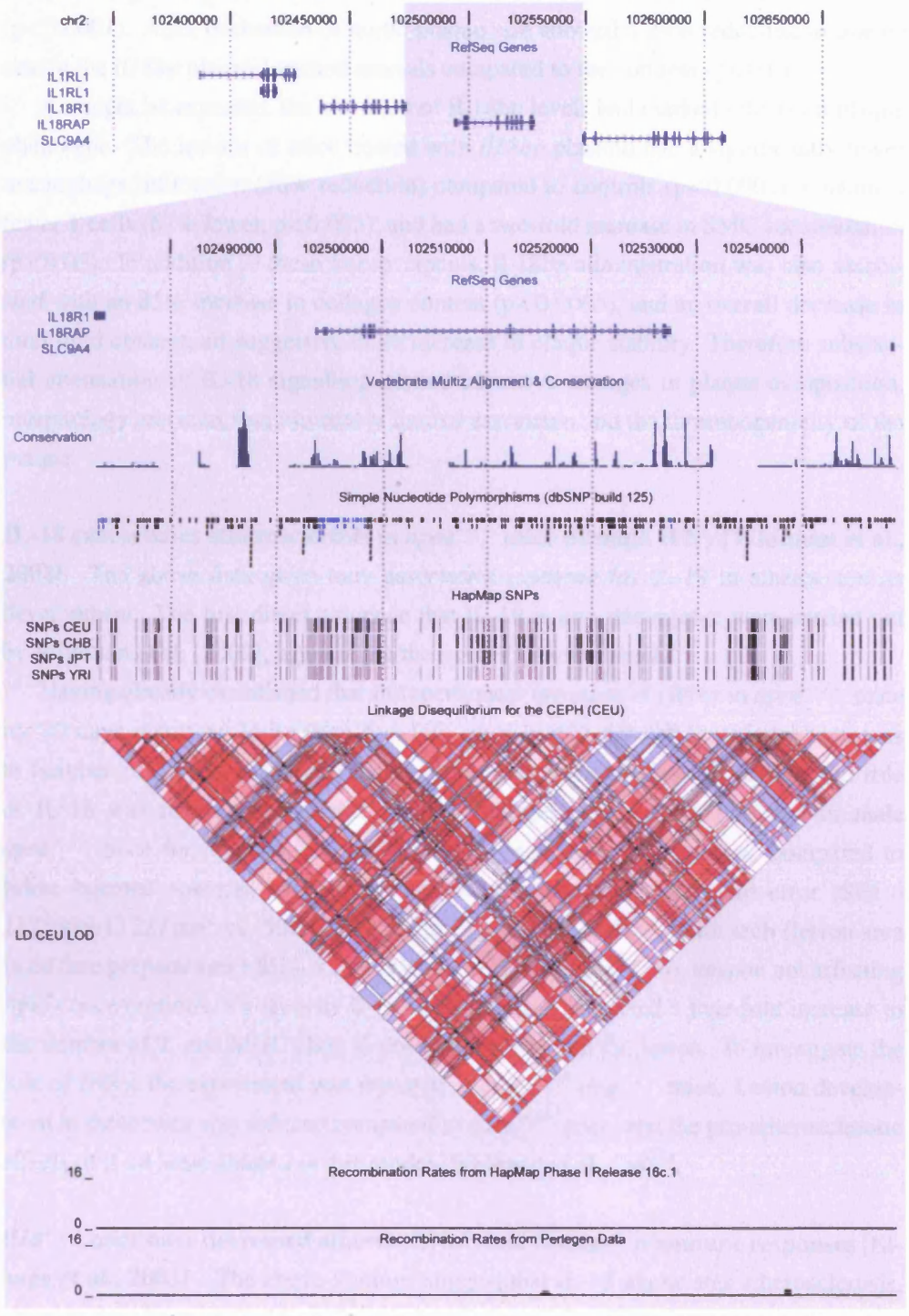

Figure 1.19: The genomic context of *IL18Rβ* taken from UCSC Genome Browser (May 2004 assembly), accessed July 2007[3].

assisted image analysis showed a 69% reduction in the extent of atherosclerotic lesions ($p<0.0001$). Also, evaluation of aortic plaque size showed a 24% reduction in plaque size in the *il18bp* plasmid-treated animals compared to the controls ($p<0.01$).

As might be expected, the elevation of il-18bp levels had marked effects on plaque phenotype. The lesions of mice treated with *il18bp* plasmid had a significantly lower macrophage infiltration (50% reduction) compared to controls ($p<0.0001$), contained fewer T cells (67% fewer, $p<0.005$), and had a two-fold increase in SMC accumulation ($p<0.05$). In addition to these improvements, il-18bp administration was also associated with an 85% increase in collagen content ($p<0.0005$), and an overall decrease in total lipid content, all suggestive of an increase in plaque stability. Therefore substantial attenuation of IL-18 signalling caused extensive changes in plaque composition, morphology and size, that ultimately limited expansion and the thrombogenicity of the plaque.

IL-18 exacerbates atherosclerosis in *apoe*$^{-/-}$ mice through IFNγ [Whitman et al., 2002] The above data gives only associative evidence for IL-18 in atherosclerosis development. The first direct evidence that IL-18 is pro-atherogenic were carried out by Whitman et al. [2002], again using the *apoe*$^{-/-}$ mouse model.

Having already established that intraperitoneal injection of rIFNγ in *apoe*$^{-/-}$ mice for 30 days increased lesion size two-fold, presumably through significant increases in number of T, and MHC class II-positive, cells [Whitman et al., 2000], the role of IL-18 was investigated in this model. Intraperitoneal ril-18 injection in male *apoe*$^{-/-}$ mice for 30 days, caused a two-fold increase in plaque area, compared to saline injected controls, in both the ascending aorta (mean±standard error (SE) – 112399±13227 μm^2 vs. 50642±12515 μm^2, p=0.004) and the aortic arch (lesion area in en face preparations±SE – 6.2±0.9% vs. 3.1±0.3%, p=0.006), despite not affecting lipid concentrations. Exogenous il-18 administration promoted a four-fold increase in the number of T, and MHC class II-positive, cells within the lesion. To investigate the role of IFNγ, the experiment was repeated in *apoe*$^{-/-}$ *ifng*$^{-/-}$ mice. Lesion development in these mice was reduced compared to *apoe*$^{-/-}$ mice, and the pro-atherosclerotic effects of il-18 were ablated in this model [Whitman et al., 2002].

***Il18*$^{-/-}$ mice have decreased atherosclerosis and changes in immune responses [Elhage et al., 2003]** The above findings suggest that IL-18 aggravates atherosclerosis, however the effects of IL-18 on disease development was unclear since the studies were limited by the time frame during which the plasmid or recombinant protein was administered. The crossing of *apoe*$^{-/-}$ mice with *il18*$^{-/-}$ mice produced the first model for studying IL-18's role in early disease development. 24-week old *apoe*$^{-/-}$*il18*$^{-/-}$ mice exhibited substantially reduced mean±SE lesion size, compared to *apoe*$^{-/-}$ mice, in

the aortic root (93866±11273 μm^2 vs. 144019±9667 μm^2, p=0.005).

In immunohistochemical analysis, lesions of *apoe*$^{-/-}$*il18*$^{-/-}$ mice had significantly lower expression of the IFNγ inducible gene I-A^b (p<0.001). Furthermore, in studies to estimate the degree to which IL-18 loss affected T cell phenotypes, analyses of the IgG isotypes produced by each mouse in response to modified LDL were conducted. A 50% reduction in the IgG2a/IgG1 ratio suggested a switch from the T_H1 to T_H2 response to the auto-antigen. In agreement with previous data, *apoe*$^{-/-}$*il18*$^{-/-}$ had a significantly higher mean body weight than their *apoe*$^{-/-}$ counterparts (33.3 g vs. 28.1 g, p=0.0035).

***Myd88*$^{-/-}$ mice linked cholesterol level to innate immunity [Bjorkbacka et al., 2004]** To establish whether macrophage innate immunity signalling pathways, normally activated by pathogens, could also be activated in response to hyperlipidemia, Bjorkbacka et al. [2004] fed *apoe*$^{-/-}$*myd88*$^{-/-}$ mice a western-type diet. *Apoe*$^{-/-}$*myd88*$^{-/-}$ mice had serum cholesterol modestly above those of *apoe*$^{-/-}$ (although not statistically significant), with changes in LDL and very low-density lipoprotein (VLDL), but not high-density lipoprotein (HDL), responsible. This would be expected to result in increased atherosclerosis, but *apoe*$^{-/-}$*myd88*$^{-/-}$ mice had marked reductions in lesion size, with males having a 65% reduction in lesion size compared to *apoe*$^{-/-}$ (40% in females). Lesion pathology showed fewer foams cells in *apoe*$^{-/-}$*myd88*$^{-/-}$ mice, with macrophages from these mice having impaired chemokine expression in response to both IL-1β and IL-18.

1.4.1.2 Human Studies – IL-18 Protein

A number of studies have attempted to establish the role of IL-18 in human atherosclerosis.

Increased IL-18 in patients with acute MI correlates with severity of myocardial damage [Seta et al., 2000] To elucidate the changes in the release of IL-18 in patients with advanced disease, Seta et al. [2000] examined the correlation between IL-18 concentrations and serum activities of myocardial enzymes – creatine kinase-MB (CK-MB), aspartate transaminase (AST), and lactate dehydrogenase (LDH), with the hope that measurement of IL-18 could be used as a new indicator of myocardial damage in patients with acute MI.

The study comprised 24 male and female patients with acute MI (all aged 39-79 yr), and a control group of 12 age- and sex-matched patients with no coronary stenosis observed on angiography. A blood sample was taken immediately following patient admission, and then at 1 h, 2 h, 3 h, 6 h, and 9 h after admission, followed by samples every 12 h until five days after admission. Baseline serum IL-18 (mean±standard deviation

(SD)) was significantly higher in patients with acute MI than controls (46±16 pg/ml vs. 26±10 pg/ml, $p<0.05$). The peak level of IL-18 correlated significantly with serum activities of CK-MB ($r=0.54$, $p<0.05$), AST ($r=0.48$, $p<0.01$), and LDH ($r=0.55$, $p<0.05$). Therefore suggesting that IL-18 may be useful as a novel marker of cardiac damage in acute MI.

IL-18 is found in atherosclerotic plaques and is related to plaque instability [Mallat et al., 2001a] Following on from their animal studies that had suggested that IL-18 is an important factor in plaque development (see section 1.4.1.1 on page 43), Mallat et al. [2001a] investigated the expression and cellular localization of IL-18 in human carotid atherosclerotic plaques, and attempted to relate its expression to plaque vulnerability and stability.

A total of 40 human plaques were taken from 35 patients undergoing carotid endarterectomy. As controls, two carotid and three internal mammary arteries, free from atherosclerosis, were obtained at autopsy or during coronary artery bypass graft (CABG) surgery. Western blots were performed on protein extracts, showing that both pro- and mature forms of IL-18 were highly expressed in most atherosclerotic plaques, whilst little or no expression were seen in normal arteries. Detection of the active form of IL-18 seemed to correlate with expression of caspase-1. Furthermore, IL-18Rα expression was detected in all atherosclerotic plaques whilst its expression in normal arteries was low.

Immunohistochemical analysis showed IL-18 expression was mainly in macrophages, but also in some intimal (but not medial) SMCs and the occasional endothelial cell. IL-18Rα was highly expressed in both plaque macrophages and endothelial cells. Semi-quantitative polymerase chain reaction (PCR) showed IL-18 mRNA expression in all atherosclerotic plaques although the degree of expression was fairly heterogenous. When the plaques were characterized clinically and pathologically as either symptomatic (stable, n=13) or asymptomatic (unstable, n=9), the amount of IL-18 mRNA was greater than three-fold higher in symptomatic over asymptomatic plaques ($p<0.007$). These results suggested that IL-18 might play a major role in atherosclerotic plaque destabilization, and that its upregulation could lead to acute disease.

IL-18 is predictive of future cardiovascular events, independent of other serum inflammatory factors [Blankenberg et al., 2002] To evaluate whether baseline serum levels of IL-18 might be predictive of future fatal cardiovascular events in patients with angiographically-proven CHD, Blankenberg et al. [2002] measured IL-18 levels in the Atherogene cohort.

The Atherogene cohort recruited from November 1996 to June 2000, selecting pa-

tients undergoing coronary angiography who had at least one stenosis of greater than 30% [Blankenberg et al., 2001]. The cohort of 1229 individuals had an average age of 62 yr, with 75% being male. These patients were followed up for a median of 3.9 yr, during which a number of individuals suffered a fatal event (n=95), non-fatal MI (n=43), or died from other causes (n=18).

Median serum concentrations of IL-18 were significantly higher in those who had a fatal CHD event during follow-up than those who did not (68.4 pg/ml vs. 58.7 pg/ml, $p<0.0001$). Each quartile increase in baseline IL-18 was associated with a 1.46 (95% CI 1.21 to 1.76, $p<0.0001$) increase in risk for future CVD death. Adjustment for C-reactive protein (CRP), IL-6, or fibrinogen had no effect on this association. In a final model that included all the inflammatory variables and other classical risk factors (eg. age, sex, smoking status, BMI etc.), the upper quartile of IL-18 still showed a 3.3-fold increase in risk compared to the lowest quartile.

This study was the first to show a strong and independent association between serum IL-18 and future CVD events in patients with a broad spectrum of CVD, thereby suggesting, along with the results from Mallat et al. [2001a], that IL-18 might be a novel therapeutic strategy for plaque stabilization.

IL-18 levels associate with carotid IMT in an asymptomatic cohort [Yamagami et al., 2005] For this study, 366 (equally comprising men and women) patients without history of any cardiovascular events were recruited form those undergoing carotid ultrasound examination at Osaka University, Japan.

Mean (SD) IL-18 levels were significantly higher in men than women (208 ± 85 pg/ml vs. 180 ± 74 pg/ml, $p<0.001$), in those with hypertension than those without ($p<0.001$), and in smokers than non-smokers ($p=0.008$). Furthermore, IL-18 positively correlated with age ($r=0.17$, $p=0.001$), and BMI ($r=0.11$, $p=0.041$), and inversely correlated with HDL ($r=-0.17$, $p=0.001$). Of note, a strong correlation for IL-18 was observed with both IL-6 ($r=0.23$, $p<0.001$) and CRP ($r=0.29$, $p<0.001$), but there were no statistically significant correlations between IL-18 and common CHD medication (aspirin, statin, or ACE inhibitors).

IL-18 was very strongly correlated with mean carotid max-intima-media thickness (IMT) ($r=0.36$, $p<0.001$), which remained significant following adjustment for age, sex, and other traditional risk factors (including IL-6 and CRP). Conversely, correlations between both IL-6 and CRP, and max-IMT, were lost when adjusted for IL-18. Analysis by tertiles of IL-18 showed mean max-IMT was around 0.2 mm higher in the top tertile than the lowest tertile ($p<0.001$, see figure 1.20 on the next page). These associations did not differ greatly in men and women.

These results suggest that IL-18, independent of other known pro-inflammatory cytokines, is associated with early asymptomatic atherosclerosis.

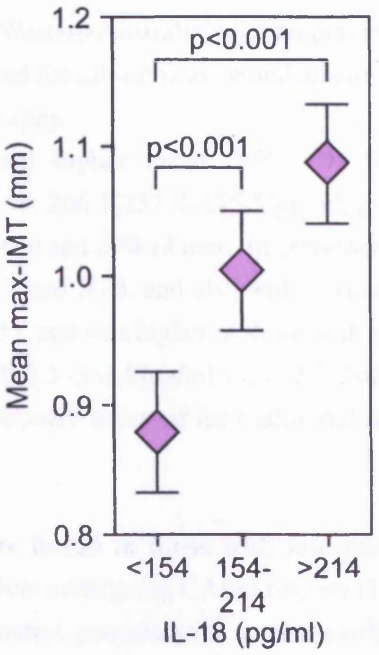

Figure 1.20: Mean max-IMT by to tertiles of IL-18. Error bars are 95% CI [Yamagami et al., 2005].

IL-18 levels are higher in those with advanced CHD and are independently related to disease severity [Hulthe et al., 2006] Hulthe et al. [2006] studied a cohort of 387 first-MI survivors, all less than 60 years, from the northern region of Sweden. For each case, a sex- and age-matched control was also recruited from the general population. Three months after the index event, blood was taken and a patient interview undertaken.

IL-18 levels were positively correlated with IFNγ in the whole cohort ($r=0.34$, $p<0.001$), and mean (SD) IL-18 levels were higher in the post-infarct patients than controls (309.6 ± 138.6 pg/ml vs. 285.4 ± 115.7 pg/ml, $p=0.014$). No significant difference in IL-18 levels were observed by lipid-lowering or ACE inhibitor treatment. Plaque area, assessed by quantitative coronary angiography ($n=236$), was positively correlated with IL-18 ($r=0.17$, $p=0.009$), a correlation that remained significant following adjustment for IL-6 and CRP. No other quantitative angiography measures correlated with IL-18.

This study suggests an independent role for IL-18 in determining disease severity, and also illustrates its close relationship with IFNγ production.

In a population-based sample, IL-18 levels do not independently associate with subclinical carotid atherosclerosis [Chapman et al., 2006] The Carotid Ultrasound Disease Assessment Study (CUDAS) is a random electoral roll sample of 1111 subjects

aged 22–77 yr from Perth, Western Australia, with no previous CHD events or surgery. Each participant was assessed for sub-clinical carotid atherosclerosis by high-resolution B-mode carotid ultrasonography.

In this study, men had higher mean (95% CI) IL-18 levels than women (340.4[329.1–352.0]pg/ml vs. 266.1[257.0–275.5]pg/ml, $p<0.0001$), with plaque being observed in 22% of women and 29% of men. In agreement with past data, IL-18 was correlated weakly with CRP and IL-6, and also with fibrinogen. IL-18 was correlated with IMT ($r=0.17$, $p<0.001$), and was higher in those with evidence of carotid plaques than those without (322.1[306.3–338.8]pg/ml vs. 292.7[284.3–301.2]pg/ml, $p=0.001$). However, once IL-18 levels were adjusted for traditional risk factors this association was ablated.

Higher levels of IL-18 are found in those with late restenosis [Kawasaki et al., 2003] A group of 21 patients undergoing CABG surgery (12 men, and 9 women) were recruited, along with 10 control patients with normal cardiac function, to investigate whether IL-18 concentrations were associated with restenosis after angioplasty. Blood samples were drawn immediately after admission, and at four hours, twenty-four hours, three days, one week, and six months following admission. Restenosis was defined as greater than 50% reduction in percent diameter stenosis (percent diameter stenosis = 1-(minimal luminal diameter/reference diameter) x100) at the target lesion.

There was no significant difference in age, BMI, stenting procedure, or traditional risk factors between the no-restenosis and restenosis groups. There was no significant difference in reference vessel diameter, but minimal luminal diameter was significantly greater, and percent diameter stenosis significantly smaller, in the restenosis group than the no-restenosis group.

Mean (SD) plasma levels of IL-18 at admission were significantly higher in the patient group than control group (231.5 ± 98.4 pg/ml vs. 59.3 ± 40.0 pg/ml, $p<0.001$). IL-18 levels in the intervention group decreased at four hours (immediately after angioplasty) and reached their peak at three days. Levels of IL-18 were significantly higher at all time-points, except 24 hours, in the restenosis group than the no-restenosis group (see figure 1.21 on the following page). This data suggests that IL-18 can act as in independent predictor of future restenosis.

IL-18 levels predict future coronary events in healthy men, independent of other risk factors [Blankenberg et al., 2003] This study assessed the impact of circulating IL-18 in a study concerned with primary prevention. The Prospective Epidemiological Study of Myocardial Infarction (PRIME) study recruited 10600 men aged 50–69 yr living in Lille, Strasbourg, Toulouse, and Belfast. A five-year follow-up was accomplished on more than 98% of all subjects. The outcome was a combined endpoint that included

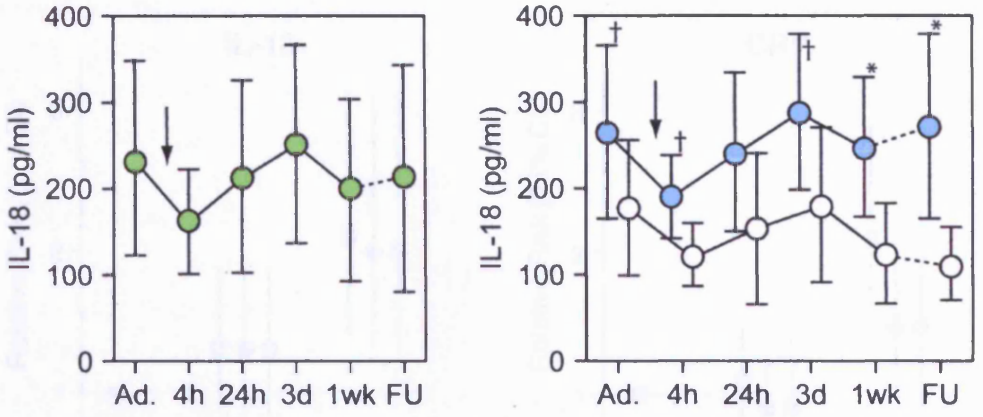

(a) Time course of circulating plasma IL-18 in patient group

(b) Time course of circulating plasma IL-18 in patients with restenosis (closed circles) and those without restenosis (open circles)

Figure 1.21: Circulating IL-18 levels in the patient groups. All data are expressed as mean±SD. * – $p<0.01$ vs. patient without restenosis; † – $p<0.05$ vs. patients without restenosis. Arrows denotes time of percutaneous coronary intervention; Ad. – admission; FU – follow-up.

non-fatal MI, coronary deaths and angina.

The baseline characteristics of cases compared to controls were as expected with cases having a higher incidence of traditional CHD risk factors. Baseline measures of IL-18 did not differ by smoking, hypertension, diabetes status, age or sex (unlike IL-6 or CRP). IL-18 was not correlated with fibrinogen, but did modestly correlate with both IL-6 and CRP. Furthermore, IL-18 was not associated with statin, ACE inhibitor, or β-blocker use, all suggesting a degree of independence for IL-18.

Baseline IL-18 was significantly higher in those who had an event during follow-up than those who did not (225.1 pg/ml vs. 203.9 pg/ml, p=0.005). The RR (95% CI) for the combined endpoint was 1.32 (0.90–1.93, p=0.16) for second vs. first tertile, and 2.07 (1.40–3.05, $p<0.001$) for the third vs. first tertile. These were similar risks as those found for both IL-6, CRP, and fibrinogen, however these were significantly attenuated when adjusted for coronary risk factors (see figure 1.22 on the next page). Conversely, the association with IL-18 was not lost when adjusted for coronary risk factors, or for CRP (as a representative of the acute phase reactants). The association between IL-18 and risk was strongest in Northern Ireland, however this is likely due to the increased levels of IL-18 and increased incidence of CHD seen, compared to the French participants. Importantly, IL-18 added to the predictive ability of the common risk factors, as demonstrated by an increase in risk when elevation of IL-18 was associated with another risk factor.

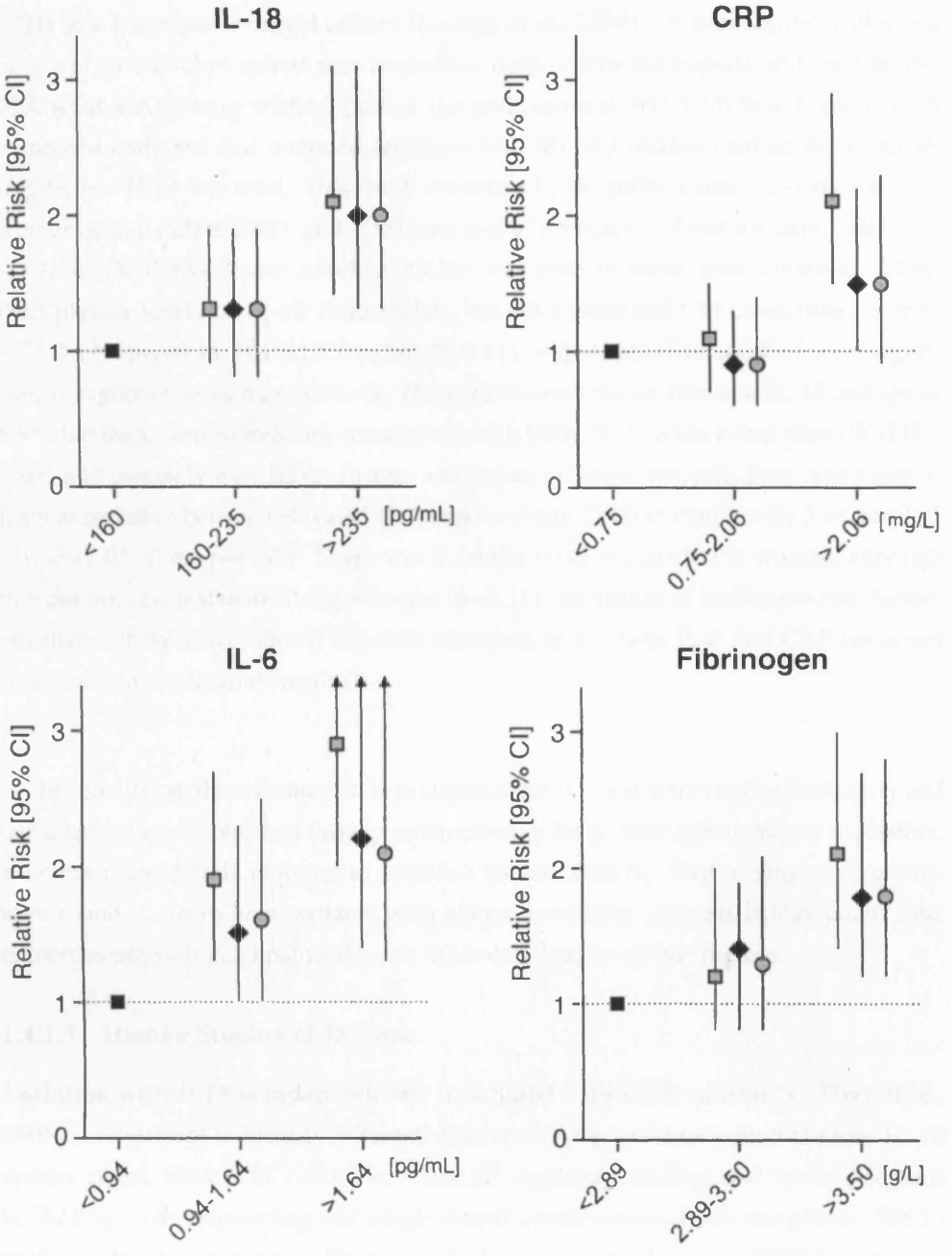

Figure 1.22: RRs for combined coronary events according to tertiles of IL-18, IL-6, CRP and fibrinogen. Tertiles were derived from control distribution, lowest tertile as reference group. ■ indicates crude RRs; ♦ indicate RRs adjusted for BMI, smoking status, diabetes, hypertension, total cholesterol, HDL, and triglycerides; • indicate RRs further adjusted for CRP (in case of IL-18) or IL-18 (in other cases) [Blankenberg et al., 2003].

Elevated CRP and IL-6, but not IL-18, were independently associated with risk of CHD in a large case-control cohort [Koenig et al., 2006] A prospective (follow-up of 11 yr) case-control cohort was assembled from within the population-based MONICA/KORA Augsburg studies, part of the multinational WHO MONICA project. A combined endpoint that included fatal/non-fatal MI and sudden cardiac death occurring before 75 yr was used. This study considered 2362 participants – 295 men and 87 women with incident CHD, and 1009 men and 971 women without incident CHD.

A standard risk factor baseline profile was seen in cases over controls. Mean (SE) plasma levels of IL-18 were higher, but not significantly, in cases than controls (172.4±1.0 pg/ml vs. 161.3±1.0 pg/ml, p=0.11), whilst both CRP and IL-6 were significantly higher in cases than controls. There was no correlation between IL-18 and age or BMI, but there were significant correlations with CRP, IL-6, waist to hip ratio (WTHR), DBP, and inversely with HDL. In age- and survey-adjusted analysis, there was a significant association between elevated IL-18 and incident CHD in men (tertile 3 vs. tertile 1 – 1.43 (1.05–1.96) p=0.02). There was a similar sized association in women, although this did not reach statistical significance (p=0.11). Inclusion of traditional risk factors attenuated these associations, however associations for both IL-6 and CRP remained significant in multivariate analysis.

In conclusion, there is much data to suggest that IL-18 is active during both early and late atherosclerosis and acts largely independently from other inflammatory mediators, although more data is required to establish its true effects. That a number of groups have found IL-18 to be associated with plaque instability suggests it may control the numerous physiological pathways that ultimately lead to plaque rupture.

1.4.1.3 Human Studies–*IL18* Gene

Variation with *IL18* is independently associated with CHD mortality [Tiret et al., 2005] To attempt to identify potential disease-causing variation within the four IL-18 system genes, Tiret et al. [2005] screened all regulatory, coding, and intronic regions in *IL18* by both sequencing and single strand conformational polymorphism (SSCP) analysis. Innate Immunity - Programs for Genomics Applications (IIPGA) data was used for the three other genes – *IL18BP*, *IL18Rα*, and *IL18Rβ*.

Within *IL18*, 11 polymorphisms were found and confirmed in IIPGA. Taking common SNPs and those that marked areas of LD, five SNPs were eventually carried forward for genotyping. These five SNPs were in relatively strong LD and together defined six major haplotypes. For *IL18Rα*, nine SNPs were chosen that together defined seven haplotypes, whilst for *IL18Rβ* eight SNPs were genotyped giving eight haplotypes. Only one SNP was found in *IL18BP*, but as it was of relatively low frequency (<2%),

it was excluded.

In the Atherogene cohort, there was a significant global association between *IL18* haplotypes and age- and sex-adjusted IL-18 levels ($p<0.001$). One *IL18* haplotype (hGCAGT) was associated with 9% lower IL-18 levels when compared to the most common ($p<0.001$). Further adjustment for variables that were correlated with IL-18 (smoking, HDL, and triglycerides), did not attenuate this association. In total, haplotypes explained 1.8% of the variance in IL-18 levels, which was more than each of the single SNPs. None of the *IL18Rα* haplotypes or single SNPs were associated with IL-18 levels, however *IL18Rβ* haplotypes were globally associated with IL-18 levels ($p=0.04$) although none of the individual haplotypes reached significance.

The Atherogene cohort had continued follow-up with the number of CHD events increasing to 142. IL-18 remained predictive as detailed above. *IL18* single SNPs were not associated with CHD mortality, although *IL18* haplotypes were globally associated with mortality ($p=0.045$). Adjustment for traditional risk factors strengthened the association ($p=0.006$), whilst adjustment for IL-18 attenuated it. Both hGCAGT and one other haplotype (hGCCAT) were associated with CHD risk (95% CI) but in opposite directions – 0.57 (0.36–0.92, $p=0.021$) and 3.01 (1.27–7.13, $p=0.012$) respectively. Adjustment for IL-18 levels attenuated that association of hGCAGT, but not that of hGCCAT. Neither *IL18Rα* nor *IL18Rβ* were associated with CHD mortality.

hGCAGT under-expresses *IL18* mRNA compared to the reference haplotype [Barbaux et al., 2007] To further investigate the associations found by Tiret et al. [2005], Barbaux et al. [2007] examined *IL18* expression levels in lymphoblastoid cell lines with known haplotypes. The haplotypes were reduced to just two SNPs – C-105T and A+183G (the second and third SNPs in the haplotypes above) – as they were located in functional regions (5'UTR and 3'UTR, respectively). An allelic imbalance method was used to investigate differential allelic expression. It was found that hCG (equivalent to hGCAGT) significantly under-expresses ($p=0.005$) compared to hCA (equivalent to hGCAAC, the reference haplotype). In homozygous cells, using standard QPCR protocols, the results were repeated. In further studies, there appeared no difference in promoter activity or mRNA stability between the haplotype.

Therefore both Tiret et al. [2005] and Barbaux et al. [2007] have provided compelling evidence that variation within *IL18* is associated with CHD risk. Allied with the information concerning levels of IL-18 and risk of CHD, it suggests that IL-18 is causative in heart disease, and that common variation within *IL18* predisposes to CHD.

1.4.2 The Metabolic Syndrome

The metabolic syndrome represents a combination of CHD risk determinants that contrasts it to isolated cigarette smoking, hypertension, hypercholesterolemia, or diabetes. Its components include atherogenic dyslipidemia, high blood pressure, elevated glucose, a prothrombotic and proinflammatory state. In an advanced state, TIIDM is present. As a multiple component condition, the metabolic syndrome can be called a multiplex CHD risk factor. Even without diabetes, the metabolic syndrome imparts a doubling of risk for CHD, with diabetes the risk is even greater [Grundy, 2007]. Several cross-sectional studies show acute phase reactants such as CRP, and cytokines such as IL-6 and tumor necrosis factor α (TNFα), associate with features of the metabolic syndrome and may be the link between the metabolic syndrome, diabetes and atherosclerosis [Grundy, 2007].

1.4.2.1 Obesity

A number of studies have suggested IL-18 has a role in maintaining caloric control, thereby giving it a potential role in the interaction between obesity and CHD.

The *il18*$^{-/-}$ mouse has a markedly increased body weight [Netea et al., 2006] Up to three months of age the bodyweights of *il18*$^{-/-}$ and wild-type mice did not differ significantly. However, at six months *il18*$^{-/-}$ mice were 18.5% heavier, at twelve months they were 38.1% heavier, and 24 months they were 27.6% heavier. In dual energy X-ray absorbitometry (DEXA) analysis the *il18*$^{-/-}$ animals had significantly higher percent fat mass. The knockout mice ate significantly more, although there was no significant difference in metabolic rates, and both *il18*$^{-/-}$ and wild-type animals had similar body temperatures.

Leptin (an adipocytokine that regulates food intake and energy expenditure) concentrations were significantly higher in knockout animals and strongly correlated with body weight (r^2=0.72), however leptin:body weight ratios did not differ between the *il18*$^{-/-}$ and wild-type animals. Such results were suggestive of leptin resistance, however injection of leptin decreased food intake similarly in both knockout and wild-type animals. IL-18 injection also decreased food intake in both *il18*$^{-/-}$ and wild-type animals, however only intracerebral (not intravenous) injection had an effect. Histological analysis of the aorta of *il18*$^{-/-}$ animals showed increased lipid deposition.

At three months, there was no difference in fasting plasma glucose, however at six months fasting plasma glucose was significantly higher in *il18*$^{-/-}$ than wild-type mice. Furthermore, these mice had severely impaired glucose tolerance and insulin resistance, although this resistance appeared to be at the muscle and adipose, not liver, level.

The *il18r*$\alpha^{-/-}$ mice were phenocopies of *il18*$^{-/-}$, being significantly heavier from

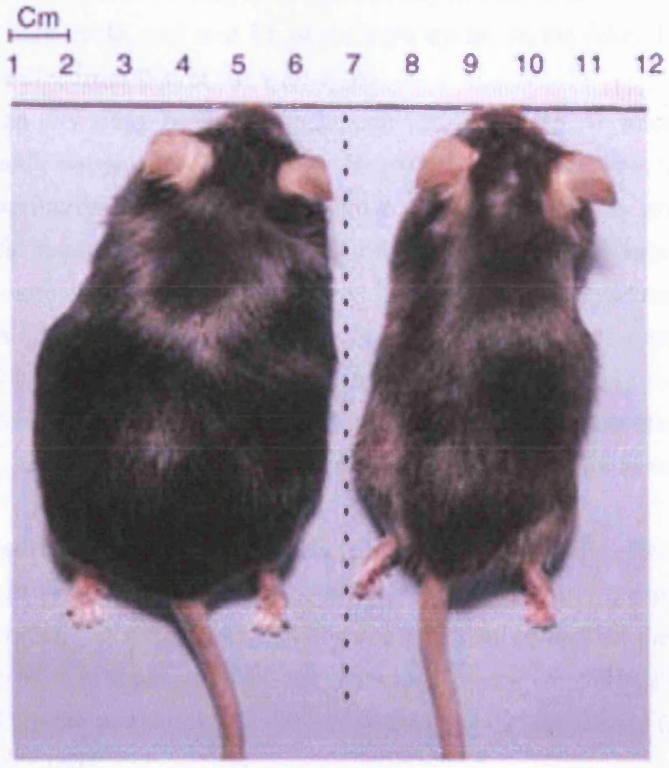

Figure 1.23: Obesity in an $il18^{-/-}$ (left) mouse compared to a wild-type (right) mouse, photographed at 1 yr [Netea et al., 2006].

six months onwards, and showing abnormal glucose and insulin tolerance. Transgenic *il18bp* mice were obese and also developed insulin resistance.

***Il18* suppresses appetite and feed efficiency [Zorrilla et al., 2007]** Both male and female $il18^{-/-}$ mice ate more chow over a one week study period, than wild-type mice. This hyperphagia predated the body weight differences detailed above, occurring at 15 weeks, and increased into adulthood in both males and females. Normalizing for body weight, $il18^{-/-}$ animals still ate more than wild-type animals. This hyperphagia in il-18-deficient mice varied according to the time of day in both sexes, being greater in the last 6 h of the dark cycle, and first 3 h of the light cycle. In the other 15 h, their food intake did not differ from that of the wild-types.

Across a ten day study period, both female and male $il18^{-/-}$ mice gained 2- to 3-fold more body weight per unit energy consumed of purified low-fat, or high-fat diet, suggesting increased feed efficiency and decreased whole-body energy expenditure. Brown fat mass did not differ between the animals, whilst white fat mass was greater, in absolute and relative terms, in $il18^{-/-}$ mice than wild-type mice. Collective white fat mass was 2- to 3-fold greater in $il18^{-/-}$ mice than wild-type mice. Intraperitoneal and intra-cerebral injection of mature IL-18 reduced body weight gain and chow intake after food deprivation in $il18^{-/-}$ mice, whilst injection of pro-IL-18 did not have an effect, suggesting the effect was pharmacologically specific to mature IL-18.

Weight loss reduces plasma IL-18 levels [Esposito et al., 2002c, 2003b; Vilarrasa et al., 2007] In a study comprising 40 obese, and 40 age-matched, normal weight, premenopausal women (aged 25–40 yr) undergoing a calorie controlled diet, bodyweight was reduced to 90% of their baseline. All participants were free from a history of diabetes and CHD, were non-smokers, and had normal insulin sensitivity (as shown by a glucose tolerance test).

Median (25th to 75th percentile) IL-18 levels were high in obese women than controls (247[204–309]pg/ml vs. 127[98–170]pg/ml, $p<0.01$) and IL-18 levels were positively correlated with bodyweight. Weight loss significantly reduced IL-18 levels (247[204–309]pg/ml vs. 147[111–210]pg/ml, $p<0.01$, Esposito et al. [2002c]).

A subsequent study recruited 60 obese women, using the same criteria as above, into either a control (advice on exercise at baseline, and at monthly visits) or intervention (personal tailored information on how to reduce weight by 10%) groups. After two years of follow-up, both the control and intervention group showed weight loss, and improvements in BMI, WTHR, BP, fasting glucose and insulin, homeostasis model assessment of insulin resistance index (HOMA-IR), triglyceride levels, and free fatty acid levels. The change in mean (SD) BMI was larger in the intervention group ($35\pm2.3\,kg/m^2 \Rightarrow 30\pm2.1\,kg/m^2$, p (for mean decrease) <0.001) than the control

group ($34\pm2.4\,kg/m^2 \Rightarrow 34\pm2.4\,kg/m^2$, p (for mean decrease) =0.04). Median (25th to 75th percentile) IL-18 at two years were significantly lower in the intervention group compared to the control group (157[112–212]pg/ml vs. 206[165–274]pg/ml, p=0.02, Esposito et al. [2003b]).

In 65 morbidly obese white subjects (5 men, 60 women), who underwent gastric bypass to reduce stomach volume to 20 ml, BMI (SD) was decreased massively ($49.2\pm7.7\,kg/m^2 \Rightarrow 31.9\pm4.8\,kg/m^2$). Fasting glucose, insulin and HOMA-IR decreased significantly following this weight loss. Median (75th percentile) IL-18 levels decreased significantly 12 months post-operative (229.8[346.8]pg/ml⇒168.9[240.1]pg/ml, $p<0.01$), whilst levels of adiponectin increased [Vilarrasa et al., 2007].

This data strengthens the evidence for assigning a metabolic role to IL-18. That IL-18 is reactive to weight changes suggests it is linked to adipose tissue mass.

IL-18 is associated with CHD risk factors and factors associated with the metabolic syndrome, but does not add to current risk prediction [Zirlik et al., 2007] The Dallas Heart Study is a multiethnic population-based probability sample of Dallas County, with intentional over-sampling of self-identified African-Americans so that they comprise ~50% of the final cohort. For analyses with IL-18, patients with sufficient plasma volume (n=2331) were included. Their median age was 44 yr, and median BMI was $30\,kg/m^2$, 39% were white. A coronary artery calcification (CAC) score greater than 10 was present in 21% of the cohort and aortic plaque was present in 38% of the sample.

Subjects with high IL-18 were more frequently older, Caucasian, and obese. Also they more frequently had a history of diabetes and hypertension, were smokers, had low HDL, high triglycerides (all $p<0.001$), or a history of previous MIs (p=0.036). Subjects with highest IL-18 also more frequently took aspirin, however there was no difference in statin use. These differences were largely similar in males and females.

IL-18 levels were correlated with a number of metabolic syndrome factors and geometric means of IL-18 rose progressively with the number of metabolic syndrome factors present (see figure 1.24 on page 61). IL-18 was significantly higher in those with CAC>10 (561 pg/ml vs. 503 pg/ml, p=0.005) and those with prevalent aortic plaque (536 pg/ml vs. 478 pg/ml, p not given). However, adjustment for traditional risk factors attenuated these associations. As shown in table 1.5 on the next page, a number of markers of obesity and insulin resistance correlated with IL-18.

This well-powered study shows that IL-18, although associated with markers of atherosclerosis, is not independently so. However, IL-18 is shown to correlate well with a number of factors involved in the metabolic syndrome.

Table 1.5: Correlation of IL-18 plasma levels with markers of obesity and insulin resistance [Zirlik et al., 2007].

		BMI	Total Fat Mass	Lean Mass	% Fat Mass	WTHR	Waist Circ.	HOMA-IR	Glucose
	r	0.11	0.06	0.12	0.0016	0.2	0.18	0.17	0.13
All patients	p	<0.0001	0.007	<0.0001	0.95	<0.0001	<0.0001	<0.0001	<0.0001
	n	1920	1863	1863	1863	1919	1920	1878	2231
	r	0.15	0.12	0.08	0.12	0.21	0.21	0.21	0.14
Females	p	<0.0001	<0.0001	0.005	<0.0001	<0.0001	<0.0001	<0.0001	<0.0001
	n	1176	1144	1144	1144	1175	1176	1154	1378
	r	0.09	0.12	0.05	0.13	0.12	0.11	0.14	0.08
Males	p	0.01	0.002	0.21	0.0005	0.0008	0.002	0.0003	0.03
	n	744	719	719	719	744	744	724	853
	r	0.1	0.05	0.12	-0.01	0.2	0.17	0.13	0.07
No TIIDM	p	<0.0001	0.048	<0.0001	0.62	<0.0001	<0.0001	<0.0001	0.002
	n	1680	1645	1645	1645	1679	1680	1649	1960
	r	0.01	0.03	-0.004	0.05	0.04	0.04	0.25	0.1
TIIDM	p	0.9	0.69	0.95	0.46	0.57	0.56	<0.0001	0.1
	n	240	218	218	218	240	240	229	271

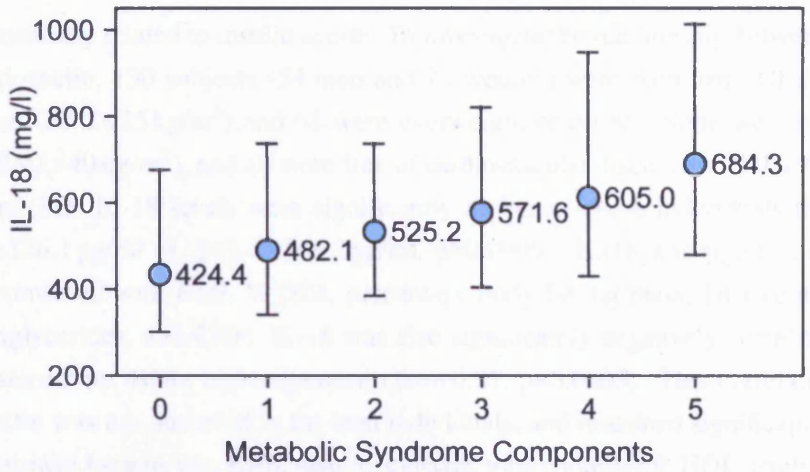

Figure 1.24: IL-18 plasma levels with increasing number of components of the metabolic syndrome. Box is median and whiskers are 25th and 75th percentile. Taken from Zirlik et al. [2007].

IL-18 is secreted by adipocytes [Skurk et al., 2005; Wood et al., 2005] To assess whether IL-18 was produced by adipocytes, adipose tissue samples were obtained from mammary adipose tissue of lean to slightly overweight adult females, undergoing elective mammary reduction. The cells were cultured for 12 days, allowing differentiation from preadipocytes to mature adipocytes. These cells secreted IL-18 protein spontaneously and without any significant change over a 16 day period [Skurk et al., 2005].

In conditions that favoured adipocyte maturation, IL-18 secretion was significantly elevated. Production was also observed in male donors and did not differ depending on which fat depot was used. Mean (SD) IL-18 production from obese donors (BMI$\geq$30 kg/m^2) was greater than non-obese donors (5.5$\pm$4.2 pg/ml vs. 1.8$\pm$0.9 pg/ml) although this was not significant (p=0.09). QPCR analysis showed that IL-18 expression was evident during adipocyte maturation, and immunohistochemical studies showed strongest staining in cells with lipid droplets, demonstrating that it is not the stromal-vascular fraction that is responsible for this expression.

Further studies from other groups [Wood et al., 2005] also showed, by QPCR analysis, that IL-18 is expressed in subcutaneous and omental adipose tissue (in both the mature adipocyte and the stromal-vascular fraction). The same pattern of expression was also seen for IL-18BP, IL-18Rα, and IL-18Rβ.

IL-18 is associated with hypoadiponectinemia and obesity [Straczkowski et al., 2007; Vilarrasa et al., 2006] Adiponectin is a protein secreted by adipose tissue which has insulin-sensitizing, antiatherogenic, and anti-inflammatory effects. Circulating adiponectin is decreased in obesity, TIIDM, and lean offspring of TIIDM subjects,

and is positively related to insulin action. To investigate the relationship between IL-18 and adiponectin, 130 subjects (54 men and 76 women) were recruited. Of these, 62 were lean (BMI<25 kg/m^2) and 68 were overweight or obese. None were morbidly obese (BMI>40 kg/m^2), and all were free of cardiovascular disease and TIIDM.

Mean (SD) IL-18 levels were significantly higher in obese individuals than lean (308.0±126.1 pg/ml vs. 240.4±106.2 pg/ml, p=0.0006). IL-18 was significantly positively correlated with BMI, WTHR, percentage body fat, fat mass, fat-free mass, insulin, triglycerides, and CRP. IL-18 was also significantly negatively correlated with insulin sensitivity, HDL, and adiponectin (r=−0.31, p=0.0003). This correlation with adiponectin was not observed in the lean individuals, and remained significant following adjustment for age, sex, BMI, insulin, glucose, total cholesterol, HDL, triglycerides, IL-6, and CRP (r=−0.38, p=0.005).

To investigate the distribution of plasma IL-18 levels across the sexes and decades of adult life, Vilarrasa et al. [2006] recruited 134 healthy men and 127 healthy women. There were no significant differences in IL-18 distribution between the sexes or across decades of life, but IL-18 levels were significantly higher in obese than normal weight men and women. IL-18 was also higher in those with hypertension than those without. IL-18 was significantly correlated with WTHR, but this association, not surprisingly, lost significance following adjustment for age, sex, and BMI.

Both obesity and insulin resistance are associated with increased adipose tissue *IL18* expression [Leick et al., 2007] To test whether *IL18* mRNA expression was related to obesity and insulin resistance, a cohort of obese (n=13) and non-obese (BMI<30 kg/m^2, n=29) men and women were recruited. Adipose tissue biopsies were taken from all subjects, and *IL18* mRNA levels were 80% higher in obese men ($p<0.05$) and 130% higher in obese women ($p<0.05$), compared to the non-obese. Both *IL18* mRNA, and plasma IL-18, were significantly positively correlated with HOMA-IR in men and women ($p<0.05$), and importantly mRNA levels correlated with IL-18 plasma levels (men – $r^2=0.46$, $p<0.05$; women – $r^2=0.28$, $p<0.05$).

1.4.2.2 Type II Diabetes

TIIDM is associated with an increased risk of premature atherosclerosis, and both prospective studies and clinical trials of intensive glucose control have found a link between high glucose levels and cardiovascular disease, without any apparent threshold [Laakso, 1999].

IL-18 is reactive to hyperglycemia through oxidative stress [Esposito et al., 2002a] In investigating the effect of hyperglycemia on IL-18 expression, Esposito et al. [2002a] recruited 20 control subjects and 12 subjects with impaired glucose tolerance. During

Figure 1.25: Circulating IL-18 levels after consecutive glucose pulses in 20 control subjects (•) and in 12 subjects with impaired glucose tolerance (○) [Esposito et al., 2002a]

a hyperglycemic clamp (with glucose stabilized to 15 mmol/l for 5 h) IL-18 levels (SD) rose in controls from a basal value of 116±28 pg/ml to a peak of 140±31 pg/ml at 2 h ($p<0.01$), before returning to basal levels by 3 h. Those subjects with impaired glucose tolerance had similar glucose and insulin levels during the clamp, and the levels of IL-18 observed were not significantly different from control subjects. In further studies using glucose pulses, rises in IL-18 appeared to correlate with glucose pulses (see figure 1.25). When glutathione, an antioxidant, was administered the glucose pulses remained unchanged but IL-18 lost its reactivity, suggesting the effect was mediated by an oxidative mechanism.

IL-18 levels are modulated by familiar foodstuffs in humans [Esposito et al., 2003a] Mean (SD) IL-18 levels were significantly higher in 30 TIIDM patients (15 men and 15 women) than in 30 age- sex- and bodyweight-matched control subjects (205±39 pg/ml vs. 120±25 pg/ml, $p<0.01$), whilst serum adiponectin levels were significantly lower. In the diabetic patients, serum IL-18 increased significantly 4 h after ingestion of a high fat meal ($p<0.05$), but decreased significantly after a high carbohydrate high fibre meal ($p<0.05$). IL-18 was significantly correlated with triglycerides following the high fat meal ($r=0.29$, $p<0.05$). In the control subjects, changes in IL-18 mirrored that of the diabetic patients, but were significantly lower ($p<0.05$).

IL-18 is an independent predictor of HOMA-IR in diabetic patients [Fischer et al., 2005] To establish whether IL-18 is associated with insulin resistance, Fischer et al.

[2005] measured IL-18 levels in 97 patients with TIIDM and 84 healthy age-matched controls. The diabetic patients had higher weight, BMI, SBP, plasma glucose, insulin, and HOMA-IR than the controls. As with other inflammatory mediators measured (CRP, IL-6, and TNFα), mean (95% CI) levels of IL-18 were significantly higher in the diabetic patients than the controls (307[286–329]pg/ml vs. 258[240–278]pg/ml, p=0.001). IL-18 was linearly associated with HOMA-IR quartiles, as was CRP, but not IL-6. The linear association of IL-18 remained significant following adjustment for age, sex, BMI, and smoking, whereas CRP did not. After adjustment, a 50% increase in IL-18 was associated with a 26% increase in HOMA-IR in controls (p=0.014) and a 25% increase in diabetics (p=0.003), suggesting an independent role for IL-18 in TIIDM development.

Elevated levels of IL-18 predict the development of TIIDM [Thorand et al., 2005] In the MONICA/KORA Augsburg Study, mean (SE) IL-18 levels were significantly elevated in subjects who went on to develop TIIDM compared to those who did not (188.7±1.0 pg/ml vs. 159.4±1.0 pg/ml, p<0.001), as were levels of IL-6 and CRP. In contrast to IL-6 and CRP, IL-18 was not strongly associated with most of the diabetic risk factors, and only weak correlations (r<0.1) were observed with smoking, hypertension, SBP, DBP, HDL, WTHR, IL-6, and CRP.

Elevated concentrations of IL-18 were strongly associated with an increased risk of TIIDM, with crude hazard ratios (HRs) (95% CI) for the fourth quartile being 1.96[1.49–2.58] and for the third quartile being 1.57[1.18–2.09] (see table 1.6 on the next page). Adjustment for age, sex and survey had no influence on the HRs, whilst fuller adjustment slightly attenuated the associations but they remained highly significant, even with adjustment for IL-6 and CRP, again suggesting IL-18 may independently contribute to TIIDM disease risk.

Therefore, taken together, the data suggests IL-18 is associated with both obesity and TIIDM development. Furthermore there is evidence to suggest that this role is independent from other inflammatory markers. It seems likely that functional genetic variation within *IL18* could be of use in TIIDM or obesity risk prediction.

1.4.3 Other Diseases

Because of its potent proinflammatory properties, IL-18 has been implicated in a number of other diseases, particularly those associated with autoimmunity [Boraschi and Dinarello, 2006]. As such there has also been a great number of studies concerned with estimating the effect of genetic variation in *IL18*, on disease susceptibility. A summary of this data is provided in table 1.7 on page 66.

Table 1.6: HRs (95% CI) of developing diabetes comparing quartiles of IL-18 in the MONICA/KORA Augsburg Study [Thorand et al., 2005]. Model 1 – crude; model 2 – adjusted for age, sex, and survey; model 3 – model 2 + BMI, SBP, ratio of total cholesterol to HDL, physical activity, alcohol intake, smoking status, an parental history of diabetes; model 4 – model 3 + CRP and IL-6.

	Quartile of IL-18				
	1	2	3	4	
Median (lower, upper limit) (pg/ml)	80.09 (4.9, 116.7)	145.18 (116.8, 173.5)	205.04 (173.6, 244.6)	322.08 (244.7, 8792.4)	p for trend
n (nondiabetic/diabetic)	424/95	429/108	417/146	428/178	
Model 1	1	1.13[0.84–1.52]	1.57[1.18–2.09]	1.96[1.49–2.58]	<0.001
Model 2	1	1.18[0.87–1.60]	1.64[1.22–2.20]	1.93[1.45–2.56]	<0.001
Model 3	1	1.10[0.78–1.57]	1.62[1.16–2.25]	1.73[1.25–2.40]	<0.001
Model 4	1	1.10[0.78–1.57]	1.61[1.16–2.24]	1.73[1.25–2.40]	<0.001

Table 1.7: Summary of current *IL18* gene association data for autoimmune disease. NS – non-significant.

Disease	Population	SNP	Test	Genotype	Effect	P value	Reference
Asthma	221 asthmatic children, 276 asthmatic adults, 85 adult controls	+105	IL-18 serum levels (±SD, pg/ml)	AA AC	220±148 224±102	NS	Higa et al. [2003]
			Minor allele odds ratio (OR) (95% CI)		1.83[1.37–2.26]	0.0062	
	228 asthmatic children, 270 controls	-607, -137, +113, +127, -133	Armitage trend test			All NS	Heinzmann et al. [2004]
	435 Korean asthmatics, 140 controls	-607, -137, +105	Allele frequency (%) vs. control			All NS	Shin et al. [2005]
	SAPALDIA – 268 atopic asthmatics, 5204 controls	-137	Allele frequency (%) vs. control	G C	77.6 vs. 73.2 22.4 vs. 26.8	0.012	Imboden et al. [2006]
Type I diabetes (TIDM)	201 TIDM patients, 194 healthy controls	-607	Allele frequency (%) vs. control	C A	67.9 vs. 66.0 32.1 vs. 34.0	0.564	Kretowski et al. [2002]
		-137		G C	62.4 vs. 72.7 37.6 vs. 27.3	0.002	
	116 Japanese TIDM patients, 114 healthy controls	-607	Allele frequency (%) vs. control	C A	53.4 vs. 44.7 46.6 vs. 55.3	0.062	Ide et al. [2004]
		-137		G C	87.9 vs. 88.6 12.1 vs. 11.4	0.825	
	1560 cases, 1715 controls	-607	Minor Allele OR (95% CI)		1.06[0.95–1.19]	0.27	Szeszko et al. [2006]
		-137			1.00[0.93–1.07]	0.94	
	53 late onset Iranian TIDM patients, 194 controls	-607	Allele frequency (%) vs. control	C A	51.9 vs. 58.8 48.1 vs. 41.2	NS	Mojtahedi et al. [2006]
		-137		G C	66 vs. 76 34 vs. 24	0.038	
Multiple sclerosis	208 cases, 139 controls	-607	Allele frequency (%) vs. control	C A	59 vs. 62 41 vs. 38	0.64	Giedraitis et al. [2001]
		-137		G C	70 vs. 75 30 vs. 25	0.17	
Rheumatoid arthritis (RA)	106 cases, 273 controls	-607	Allele frequency (%) vs. control	C A	63 vs. 55 37 vs. 45	NS	Sivalingam et al. [2003]
		-137		G C	86 vs. 87 14 vs. 13	NS	
	309 Polish RA patients, 305 controls	-607	Genotype OR (95% CI)	CC AC	1.27[0.92–1.77] 0.95[0.71–1.57]	0.146 0.754	Pawlik et al. [2006]
		-607		AA GG	0.71[0.45–1.10] 1.07[0.78–1.46]	0.126 0.695	
				GC CC	1.14[0.82–1.58] 0.51[0.28–0.95]	0.432 0.045	
Juvenile idiopathic arthritis (JIA)	33 JIA patients, 173 controls	Haplotypes of 13 SNPs	IL-18 serum levels (SD, pg/ml)	S01/S01 Others	78683±22778 10122±28210	0.017	Sugiura et al. [2006]
			Haplotype frequency (%) vs. controls	S01	54.5 vs. 37.9	0.011	
CD	134 cases, 110 controls	+105	Minor allele OR (95% CI)		2.19[1.24–3.87]	0.006	Tamura et al. [2002]
	210 CD patients, 265 controls	-607, -137, +105	Allele frequency (%) vs. control			All NS	Glas et al. [2005]
Graft-versus-host disease	157 patient-donor pairs	Haplotypes of -656, -607, -137	Cox regression non-relapse survival (95% CI)	No GCG haplotype	2.09[1.24–3.51]	<0.01	Cardoso et al. [2004]

1.4.4 Potential For Therapy

That IL-18 appears involved in a number of diseases makes it an attractive therapeutic strategy. Therapeutic options under investigation to inhibit IL-18 include the use of neutralizing antibodies to IL-18, and IL-18R, IL-18BP, and caspase-1 inhibitors.

With regard to IL-18BP, a human IL-18BP:IgG1 Fc fusion protein binds and neutralizes IL-18. Using *E. coli*-derived endotoxin, administration of IL-18BP:IgG1 10 min prior to the endotoxin significantly reduced mortality. Furthermore, IL-18BP:IgG1 has a long plasma half-life, being effective when injected 6 d prior to challenge.

A number of caspase-1 inhibitors have been into clinical trials for their efficacy. VX-765 is currently in trials for the treatment of psoriasis and is reported to be effective in blocking the hyperreactivity to inflammatory stimulation of monocytes from familial cold autoinflammatory syndrome (FCAS) patients.

Although promising, each potential approach has their drawbacks and must be carefully optimized to obtain a reduction, not an abolishment, of IL-18. In fact, as IL-18 plays a key role in balancing T_H1 and T_H2 responses, complete down-regulation could lead to immunosuppression with severe consequences.

1.5 Study Aims

Hypothesis Common genetic variants within *IL18* or *IL18BP* cause inter-individual differences in serum fIL-18 concentrations, therefore contributing to individual risk for CHD and obesity.

Aims

1. Identify tSNP sets that capture whole gene variation within both *IL18* and *IL18BP*.

2. Assess causality for the IL-18 system in both obesity and CHD, by applying a Mendelian randomization approach in numerous study groups.

3. Investigate the impact of any potentially functional genetic variants on *IL18* or *IL18BP* mRNA production.

Chapter 2

Materials and Methods

Detailed below are the reagents and protocols used throughout this study. Care has been taken to standardize methods throughout, however deviations from the given protocol are noted in the relevant results sections.

2.1 Genotyping Methods

A variety of genotyping methods were used in this study, all of which were high-throughput and designed to offer the greatest efficiency whilst maintaining accuracy.

2.1.1 DNA Extraction, the 'Salting Out' Method

Reagents

Sucrose Lysis Buffer 0.32 mol/l sucrose; 5 mmol/l $MgCl_2$; 10 mmol/l Tris-HCl pH 7.5; 1% Triton-X-100.

Nuclei Lysis Buffer 10 mmol/l Tris-HCl pH 8.2; 0.4 mol/l NaCl; 2 mmol/l Na_2ethylenediaminetetraacetic acid (EDTA) pH 8.0; 1% SDS.

TE Buffer 10 mmol/l Tris; 1 mmol/l EDTA; pH to 7.6 with HCl.

Protocol Genomic DNA was isolated from potassium-EDTA-anti-coagulated whole blood (stored at −20 °C) by an adaptation of the 'salting out' method, described by Miller et al. [1988]. The salting out protocol involves cellular lysis using a sucrose lysis buffer, and nuclear lysis using a lysis buffer containing 10% (w/v) SDS. The DNA is finally ethanol-precipitated following a deproteinisation step.

Blood was thawed (at room temperature) and transferred to a 30 ml centrifuge tube containing 12 ml cold (4 °C) sucrose lysis buffer and mixed several times by inversion.

After centrifugation at 1300 G, 4 °C for 10 min (Sorvall RC5C centrifuge, rotor SA-600), the supernatant was discarded and the pellet resuspended in 12 ml cold (4 °C) sucrose lysis buffer, then re-centrifuged at 1300 G.

Following centrifugation, the supernatant was discarded and 2 ml nuclei buffer was added then mixed thoroughly with a pipette (or by incubation at 37 °C). 5 mol/l sodium perchlorate (1 ml) was added and the tube mixed by inversion before addition of 2 ml ice-cold chloroform. The sample was then mixed by inversion and centrifuged at 1300 G for 3 min at room temperature. The upper aqueous phase was transferred to a fresh 30 ml centrifuge tube without disturbing the organic phase, and 10 ml ice-cold 100% ethanol gently added to it. The precipitated DNA, apparent on the interface between the two phases as a fine wooly network, was spooled off with a Pasteur pipette and washed in 70% ethanol. It was then transferred to a sterile microtube containing 1 ml TE buffer. To allow the DNA to fully dissolve, it was incubated at 37 °C overnight.

2.1.2 Standardization of DNA Arrays

All DNA samples were standardized to 15 ng/µl. Initially a 1/10 dilution (to 100 µl) of each sample was made into a 96-well Costar UV plate with dH_2O, and briefly centrifuged at 200 G. The plate was then loaded into the Tecan GENios plate reader and the absorption of each sample read at both 260 nm (for dsDNA) and 280 nm (for protein). Given that 1 O.D. at 260 nm for dsDNA equates to 50 ng/µl, the volume of sample required for an end concentration of 15 ng/µl could be calculated. Dilutions were made to 750 µl with dH_2O into 96-well arrays (Matrix Technologies Corp., NH, US). All DNA samples were stored at −20 °C.

2.1.3 PCR

The technique of PCR relies on double stranded DNA being denatured into single strands by heat, consequent annealing with oligonucleotides (primers), and, via the addition of DNA polymerase and nucleotide bases, the synthesis of a double strand upon cooling [Mullis et al., 1986]. This cycle leads to binary (base 2) replication, generating large quantities of specific DNA in a short period of time.

The first step is a period of high temperature (normally 95 °C) to denature or 'melt' the double-stranded 'template' DNA to single strands. This is followed by cooling to a primer-pair-specific temperature, allowing short oligonucleotides (typically 20–30 bp), complementary to sequences either side of the area of interest, to anneal to the template strands. The temperature is then increased to 72 °C and a DNA polymerase then adds nucleotides, complimentary to the template sequence, replicating the DNA base by base. The polymerase used is derived from the bacterium *Thermus aquaticus*, it

is heat stable and therefore does not need replenishing following each cycle of heating and cooling.

Reagents

10x Polmix Buffer 500 mmol/l KCl; 100 mmol/l Tris-HCl pH 8.3; 0.01% gelatine; 2 mmol/l dATP; 2 mmol/l dTTP; 2 mmol/l dGTP; 2 mmol/l dCTP.

10x NH_4 Polmix Buffer 16 mmol/l $[NH_4]_2SO_4$; 67 mmol/l Tris-HCl pH 8.4; 0.01% Tween 20; 2 mmol/l dATP; 2 mmol/l dTTP; 2 mmol/l dGTP; 2 mmol/l dCTP.

Protocol Following extraction and arrangement into 96-well arrays, DNA samples were prepared for PCR by centrifuging the working array at 1000 G for 1 min. This ensures the collection of DNA samples at the bottom of their respective wells, reducing the possibility of cross-well contamination. Typically, around 20 ng of DNA was removed for each PCR reaction using a Finnpipette multichannel dispenser (Life Sciences, Basingstoke, Hants, UK) and placed into a corresponding position in a standard 96-well PCR plate (Corning Inc., Hemel Hempstead, UK). Extreme care was taken to ensure the accurate transfer of DNA from the working array to the PCR plate. Negative and, where necessary, positive controls were utilized to ensure accuracy. Loaded plates were then centrifuged at 200 G for 1 min to ensure that the DNA was collected at the bottom of each well, reducing the possibility of cross-contamination during the dispensing of the PCR mix.

The PCR mix was made up freshly for each separate PCR reaction. PCRs were performed in a total volume of 20 µl, with each reaction containing either 1x Polmix or 1x NH_4 Polmix, the optimum concentration of $MgCl_2$, 8 pmol of each primer, and 0.6 U of *T. aquaticus* polymerase. The PCR mix was added to each well of the PCR plate using an automatic Biohit repeating dispenser (Alpha Laboratories, UK). Each sample was overlaid with 20 µl mineral oil to prevent evaporation. The microtitre plate was then sealed with a clear sticky plastic lid and carefully labelled. Plates were centrifuged at 200 G for 1 min to ensure correct placement of the reaction components before cycling. Thermal cycling was performed on an MJ Tetrad DNA Engine Thermocycler with the following protocol:

95 °C	5 min	
95 °C	30 s	x30–40 cycles
xx °C	45 s	
72 °C	45 s	
75 °C	5 min	

The PCR was cycled between 30–40 cycles, depending on the individual PCR efficiency. The final polymerization step, ensured all partial DNA products were fully extended by *T. aquaticus* polymerase.

Upon receipt of new primer pairs, or prior to the genotyping of whole studies, an optimization procedure was conducted; $MgCl_2$ concentration and annealing temperature were altered in a gradient across the plate, and the most effective combination of both was assessed for each primer pair. A higher annealing temperature increases the specificity of the primer, while a higher $MgCl_2$ concentration (in the order of 2.5 mmol/l) lowers the specificity. If the above measures failed to produce a cleanly and correctly amplified PCR product, the optimization was repeated with a different PCR buffer – NH_4 Polmix, and with the addition of 5% dimethyl sulfoxide (DMSO)[1]. Oligonucleotides were designed using Primer3 software [Rozen and Skaletsky, 2000], freely available at http://frodo.wi.mit.edu. Primer3 chooses primer pairs taking into consideration primer melting temperature, length, GC content, 3' stability, estimated secondary structure, the likelihood of primer-dimer formation between two copies of the same primer, and the accuracy of the source sequence.

If primer pairs failed to amplify cleanly and correctly, they were redesigned. If this was not possible a ready-made PCR mix – MegaMix Blue (Microzone Ltd. Haywards Heath, UK) – was used that required only the addition of both primers and template DNA. This mix uses a set $MgCl_2$ concentration and *T. aquaticus* polymerase, and also offers an accompanying clean-up mix – *micro*CLEAN (Microzone Ltd., Haywards Heath, UK) – that can be used in place of the methods detailed in section 2.1.7 on page 81. Simply, an equal volume of *micro*CLEAN is added and mixed with the complete PCR reaction. The mixture is spun for 7 min at 13 000 r/min in a microfuge and the supernatant removed. The tubes are re-spun and any remaining dregs removed, before resuspension of the pellet in the appropriate volume of dH_2O.

2.1.4 RFLP Genotyping

Derived from bacteria, restriction enzymes (REs) function to destroy foreign DNA (such as bacteriophages). They are a widely used tool in molecular biology as they recognize and cut at specific short sequences. Numerous such enzymes have been identified and the list of recognition sites is long, so that it is often possible that a genetic variant of interest occurs within an RE site. The enzymes are sensitive enough that a single base change within the recognition site will prevent its recognition, and therefore they represent a reliable and efficient method for genetic variant identification and genotyping.

[1] DMSO facilitates strand separation, thereby preventing non-specific binding of primers.

Protocol Primer pairs were designed to flank the restriction enzyme site and PCR performed as detailed in section 2.1.3 on page 69. If the sequence variant did not occur within a recognition site, one of the primers was designed to anneal exactly adjacent to the sequence change and certain bases altered to introduce a recognition site through purposeful sequence mismatch (via a 'forcing' primer).

An RE digest mix with the recommended buffer for the enzyme being used, was made up in a 1.5 ml Eppendorf tube on each occasion. Typical quantities per well were 3.3 µl dH_2O, 1.5 µl buffer, and 2 U enzyme (~0.2 µl) per sample. 5 µl of digestion mix was added to 8 µl of PCR product in a 96-well microtitre plate with lid (Bibby-Sterilin, Staffordshire, UK). Each plate was centrifuged at 200 G for 1 min to collect the reactants, before being incubated at 37 °C overnight in a box sitting on moistened paper towel to prevent excessive evaporation. For those enzymes requiring higher temperatures, the reaction was prepared in a PCR plate, overlayed with 10 µl mineral oil and sealed with a sticky lid, before incubation on a heated PCR block at the specified temperature overnight.

Primer pairs and PCR conditions for the commonly used *IL18* genotyping assays are shown in table 2.1 on the next page, and RE digest details are given in table 2.2 on page 74.

2.1.5 DNA Separation and Visualization

PCR products were visualized using both agarose and microtitre array diagonal gel electrophoresis (MADGE) gels.

Reagents

MADGE Loading Dye 0.0015% bromophenol blue; 0.015% xylene cyanol; 10% glycerol; 10 mmol/l EDTA

Sticky Silane 0.5% v/v γ methacryloxy-propyl-trimethoxysilane

10x TBE Buffer 0.04 mol/l tris-borate; 1 mmol/l EDTA pH 7.4

TE Buffer 10 mmol/l tris-HCl; 1 mmol/l EDTA pH 7.6

7.5% MADGE Mix 25 ml 10x TBE buffer; 62.5 ml 19:1 acrylamide:N,N'-methylenebenebisacrylamide; 162.5 ml distilled water; 900 µl tetramethylethylenediamine (TEMED)

Protocol

Table 2.1: Primer pairs and PCR conditions for commonly used *IL18* genotyping assays.

SNP	Forward Primer	Reverse Primer	$MgCl_2$ (mmol/l)	Annealing Temp. (°C))	Cycles	Product Size (bp)
IL18-9731 G>T	GCC CTC TTA CCT GAA TTT TGG AA[2]	AGC CAC ACG GAT ACC ATC ATT	1.5	56	38	104
IL18-5848 T>C	GAG GAA TGG GGA TGA GAA CA	AAA CTT TCC CTC CAC CTG AAA	1.5	58	35	239
IL18+105 A>C	TGT TTA TTG TAG AAA ACC TGG AAT T[3]	CCT CTA CAG TCA GAA TCA GT	1.5	52	40	148
IL18+8855 T>A	CCC TTA TGT GCT CAC CTT TCA	CCC AAG TGC ACT GGA AAG TC	1.5	60	35	203
IL18+11015 A>C	CTT GAG CAA ATG TGG ACA CC	CAG CAG TAC TGA CCT CCT CTC C	1.5	55	40	153
IL18-11238 C>A	TAG CCT AGA TAA CTA TGG CGA AG	TTT TCC CTT CAT TTT ACC ACA GA	1.0	60	38	102

[2]Primer forces a *HinfI* site – GATAC→GATTC
[3]Primer forces a *TaqI* site – CCGA→TCGA

Table 2.2: RE digest details for commonly used RFLP assays; NEB – New England Biolabs UK Ltd., Hertfordshire, UK.

SNP	Enzyme	Supplier	Buffer	Temp. (°C)	Fragment sizes (bp)
IL18-9731 G>T	*HinfI*	NEB	NEB 2	37	83, 21
IL18-5848 T>C	*RsaI*	NEB	NEB 1	37	195, 44
IL18+105 A>C	*TaqI*	NEB	*TaqI* Buffer	65	123, 25
IL18+8855 T>A	*HinfI*	NEB	NEB 2	37	113, 90
IL18+11015 A>C	*BfaI*	NEB	NEB 4	37	84, 69
IL18-11238 C>A	*BsmAI*	NEB	NEB 3	55	31, 71

Agarose gels Where determining the size and relative intensities of PCR products, agarose gels were used. For a 2% (effective visualization range – 80–200 bp) gel, 2 g of agarose (Helena Biosciences, Sunderland, UK) was mixed with 100 ml of 1x TBE. The agarose was dissolved by heating the mix in a microwave oven at full power for 2 min. 10 µl of 10 µg/ml ethidium bromide (EtBr) was added as the mix cooled to stain DNA within the gel. When the mix had cooled but remained molten it was poured into a gel tray (10x14 cm) with combs, and allowed to set for 1 h. For separation of larger PCR products, the percentage agarose used was adjusted correspondingly (1% – 500 bp–1 kbp; 0.5% – 1–30 kbp).

Solid gels were placed into an electrophoresis tank containing 1x TBE. Typically 2 µl of MADGE loading dye was added to 5 µl of PCR product and the entire volume was mixed and placed in the separate submerged wells of the gel. 1 µl of 1 kbp ladder (Invitrogen, Paisley, UK) was added to the two outer wells as a size standard. Gels were typically electrophoresed at 100 V for 30 min.

MADGE To visualize a full 96-well PCR plate or products from an RE digest, DNA fragments were also separated on a non-denaturing polyacrylamide gel using MADGE [Day and Humphries, 1994]. This technique allows all 96 wells to be run on a single gel slab by loading the samples at an angle, thus running them diagonally between their neighbours. The technique allows the 96-well format to be retained throughout the genotyping process and improves throughput and accuracy.

MADGE consists of an open arrangement of 8x12 wells each 2 mm deep. The wells are arranged at an angle of 71.6 °to the array. With this arrangement the maximum track length is 26.5 mm, allowing sufficient travel for genotype resolution (see figure 2.1 on the next page).

Glass plates of appropriate size (160x120x2 mm) were cleaned and dried rigourously. Five drops of sticky silane were spread across the plates and left to air-dry

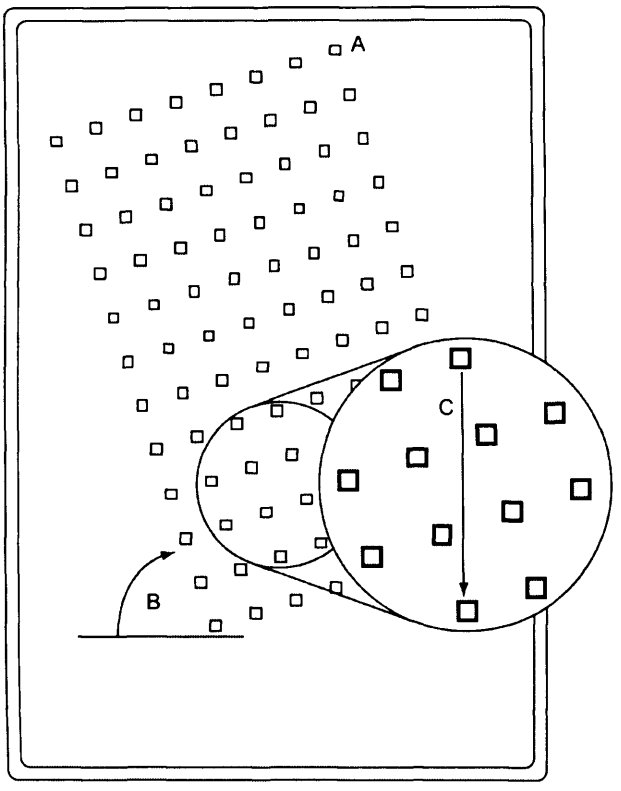

Figure 2.1: Schematic showing the arrangements of wells (A) on a MADGE gel, tilted at 71.2° (B) allowing a 26.5 mm track length (C) for the DNA fragments.

briefly in a fume-hood. Sticky silane ensures that the acrylamide mix would adhere to the glass plate. Polymerization of the acrylamide was initiated by the addition of 150 µl 25% w/v ammonium persulphate (APS) per 40 ml MADGE mix, quickly mixed, then poured into the MADGE former. A glass plate was then placed upon the former (sticky silane side adjacent to the MADGE mix), taking care not to trap any air bubbles and that the plate is in-line with the former. This was then left to set for around 10 min with a small weight upon it. When set, excess polyacrylamide was trimmed from the former, and the glass plate (with gel attached) was then prized from the former. MADGE gels were stored in a foil-wrapped plastic tupperware box containing 1x TBE, and 0.5 µg/ml EtBr.

Upon use, an individual MADGE gel was placed into an electrophoresis tank containing 1x TBE. Typically 5 µl of sample was mixed with 2 µl MADGE loading dye and loaded into the gel wells using a multichannel pipette, ensuring to maintain the particular arrangement of the 96-well plate. The gel was then electrophoresed at 100 V for 30 min.

Gel Visualization Following electrophoresis the gel was viewed and photographed under ultraviolet light using the Syngene Gel Documentation System, and Genesnap v6.04 software. Care was once more taken to ensure the correct orientation of the gel

Genotyping Gel Control All genotyping was performed using negative controls. MADGE results were read by two independent observers blinded to clinical details, and entered onto the computer database under observation. Any genotype dropouts or discrepancies were resolved by repeat PCR if possible.

2.1.6 TaqMan Genotyping

The TaqMan method involves the inclusion of two fluorescent, dye-labelled probes for each allele of the specific variant being investigated. The allele specific probes each contain a short sequence complementary to the allele and surrounding sequence being investigated, a fluorescent reporter dye (labelled either VIC or FAM for each allele) at the 5' end, and a non-fluorescent quencher (NFQ) at the 3' end that prevents the 5' dye from fluorescing. During the PCR cycle, the forward/reverse primer pair anneals to the template DNA, along with the respective allelic probe. Amplitaq Gold DNA polymerase replicates the single strand of DNA up to the allele-specific probe. If the probe is entirely complementary to the target sequence (ie. the correct allele probe), the 5' to 3' exonuclease activity of the enzyme releases the 5' fluorescent dye. Therefore as PCR cycle increases so does the level of VIC or FAM fluorescence dependant on the

sample genotype (see figure 2.2 on the following page). A 7900HT Sequence Detection machine (Applied Biosystems, California, US) is able to read each sample following PCR and determine the levels of both VIC and FAM, so determining the genotype of each sample.

Protocol

Sample Preparation In contrast to the other genotyping methods detailed here, the TaqMan system enables high-throughput genotyping in a 384-well format. Typically DNA was standardized to 1.25 ng/µl as detailed in section 2.1.2 on page 69, and an aliquot of 5 ng used in each reaction. A Biomek 2000 robot (Beckman-Coulter, High Wycombe, UK) transferred DNA from four 96-well plates to one Thermofast 384-well PCR plate (ABgene, Surrey, UK) thereby reducing pipetting error. A data sheet detailing the plate layout and the unique plate identifier was prepared and the plate left to dry out overnight, or until further use, at room temperature in a sterile paper bag.

TaqMan Master Mix Forward and reverse oligonucleotides and their respective labelled probe pairs were ordered using the 'Assay by Design' service from Applied Biosystems Online (www.appliedbiosystems.com). A master mix comprising 2.5 µl TaqMan Absolute QPCR Rox Mix (ABgene, Surrey, UK), 0.125 µl 40x Assay, 2.375 µl Sigma dH_2O per well was prepared and a 5 µl aliquot was added to each well using an 8-channel pipette. A clear plastic lid (ABgene, Surrey, UK) was applied to seal the plate and prevent excess evaporation, then each plate was centrifuged at 200 G for 30 s. Each plate then underwent the following standard PCR program on a Thermohybaid (Basingstoke, UK) 384-well heated block:

95 °C	10 min	
95 °C	15 s	} x 40 cycles
60 °C	1 min	} x 40 cycles

All plates were then read on a 7900HT Sequence Detection machine, and SDS v2.1 (Applied Biosystems) was used to differentiate the different genotypes. SDS v2.1 produces an allelic discrimination plot (see figure 2.3 on page 79) as well as assigning genotypes automatically to plate coordinate in a text output file. The file was then converted from 384-well to four 96-well plates in Microsoft Excel, and merged with the study database. To ensure no incorrect data input, a second researcher validated the entire process.

The *IL18* and *IL18BP* primer and probe sets used in this study are detailed in table 2.3 on page 80.

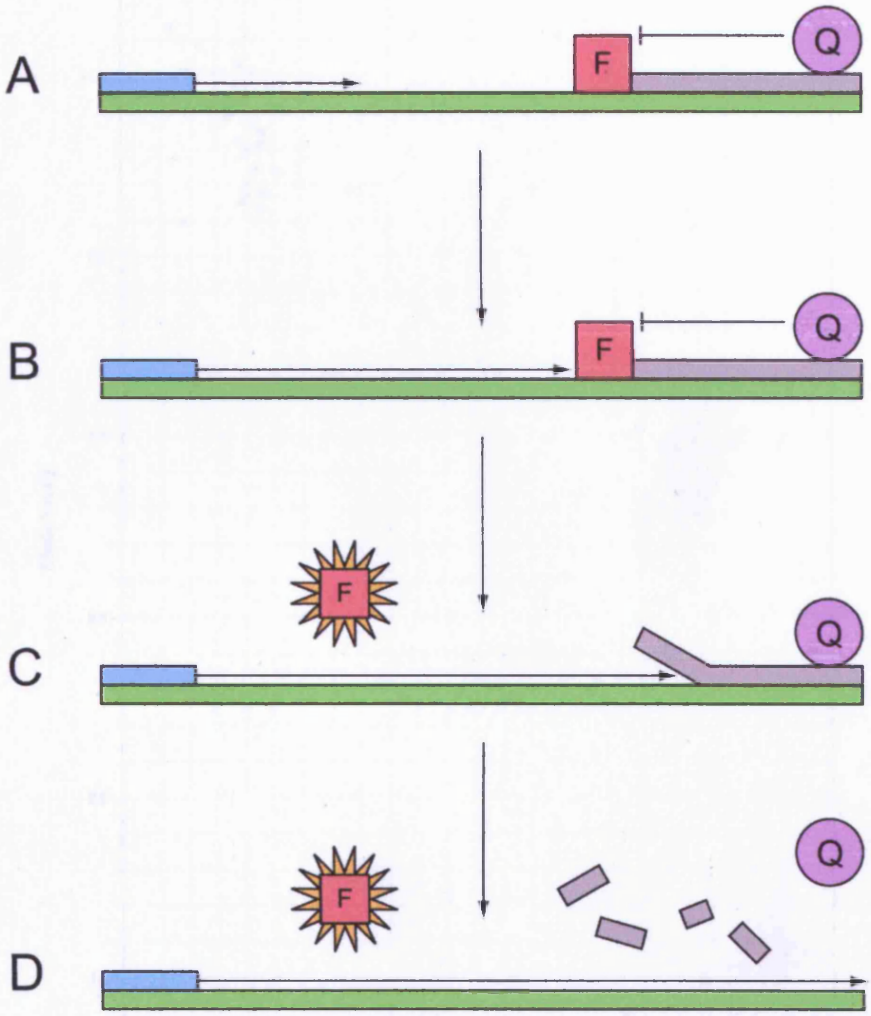

Figure 2.2: Schematic of the TaqMan assay system. The Probe containing allele specific 5' fluorescent dye (F) and 3' quencher (Q) anneals to the target sequence, and primer elongation begins (A). As the *T. aquaticus* polymerase meets the fluorescent dye (B) its exonuclease activity cleaves the dye from the probe, freeing it from the quencher and therefore allowing it to fluoresce (C). The rest of the probe is digested and elongation can continue (D).

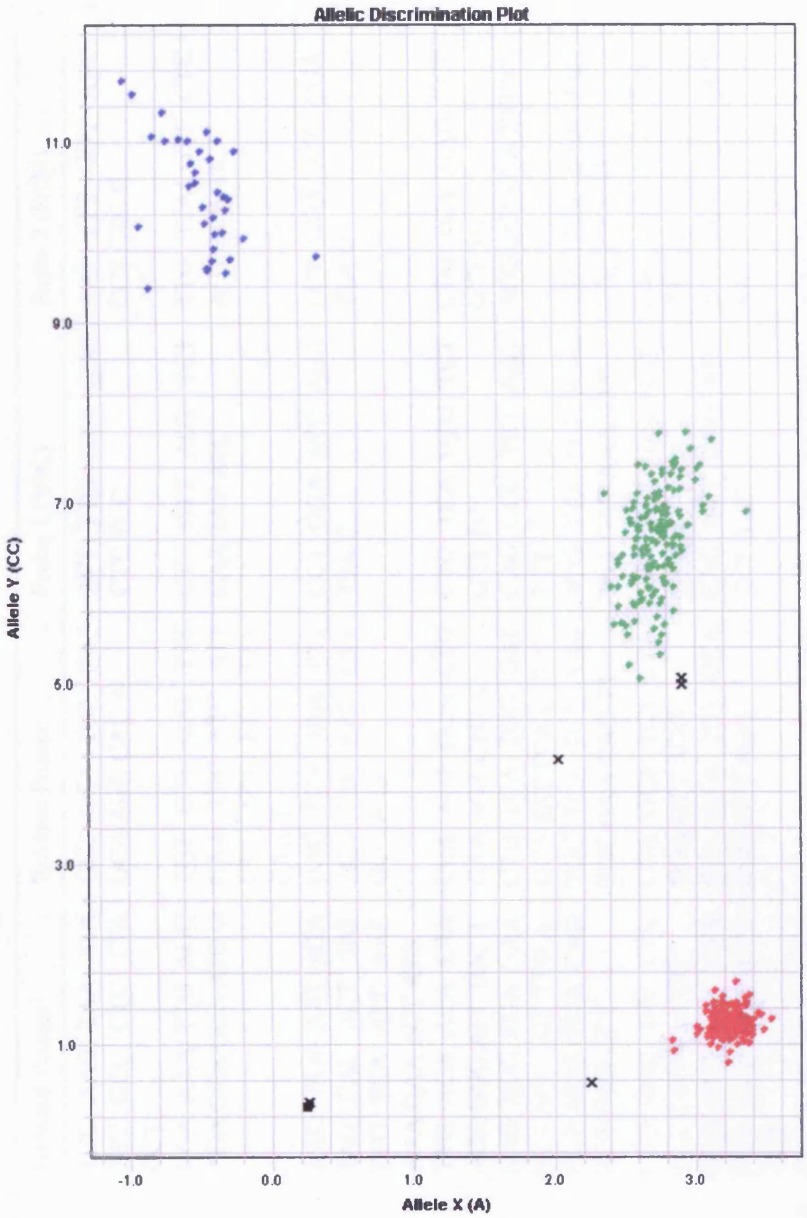

Figure 2.3: Screen capture from SDS v2.1, showing a typical allelic discrimination plot, with successful separation of the three genotype groups – homozygotes (• & •) and heterozygotes (•) – and the NTCs (■). Unassigned genotypes were those that did not cluster with other samples (×).

Table 2.3: *IL18* and *IL18BP* TaqMan primer and probe pairs used. The interrogated base change is underlined.

SNP	Forward Primer	Reverse Primer	Probe 1 (VIC)	Probe 2 (FAM)
IL18-9731 G>T	TGC AAG TAA ATA TTT GCC CTC TTA CCT	GCT GTA TCA GAT GCA AGC CAC A	ATT TTG GTA GCC CTC TCC	AAT TTT GGT ATC CCT CTC C
IL18-5848 T>C	GGA AAA TTG AGG AGA GGA GGA ATG G	TGT GTT GAT TTT GAA TTC TTC ATT CTT ATT TTC TTA CAA T	CTT GTT AGT TCT CAA TAC ATC	TTG TTA GTT CTC AGT ACA TC
IL18+105 A>C	AAC TAA AAT ATA TAG CAT ACT TAT TTG TCA ATT AAC AAA GAA ACT ATG	GAC TGA TAA TTT AGA TTC AAG CTT GCC AAA	CCT GGA ATC AGA TTA C	CCT GGA ATC CGA TTA C
IL18+8855 T>A	TTG ACA ACA CTA AGA GGG ATT TGC T	CCA AGT GCA CTG GAA AGT CTG A	CTG TCA GTG TCT GTT TC	CTG TCA GAG TCT GTT TC
IL18+11015 A>C	GAG AGG AGA GAA GTA AGC TGT TTG A	CTG TCA TGG GAT GCA TAT TCA GTT C	CAG GCC TCT AGT TTT	AGG CCT CTA TTT TT
IL18-1368 A>G	CCT GGG TGA CAG AGT GAG ACT	TGC TCA TCT AAG TGC GAA CAG TT	ATG TTA TCT AAA TAA GAT AAA TTT	TTA TCT AAA TAA GGT AAA TTT
IL18BP-1765 T>C	CTG GAC TGT CTC TCT CAG AAA CC	CCA GCA TCT CCA GGA GTT AGG	CAG CCT TGC CTC CTG A	CAG CCT TGC TTC CTG A
IL18BP-559 T>G	GAG ACT CAT CTA GTT CAT ACC CTA GGT	CCA GCA TCT CCA GGA GTT AGG	CAG ACT GGG ATC TCT AAT	ACT GGG ATC GCT AAT
IL18BP+3041 C>T	CCC CAA CCC CAC TCC TG	CAC CTG CCA GAG GAT GCT	ATG GGC CCT GTG TCT	ATG GGC CCT ATG TCT

2.1.7 Sequencing

Sequencing was carried out using a modification of the dimethylsulfoxide chain terminator method [Sanger and Coulson, 1975] in which chain terminating nucleotides are labelled with fluorescent dyes for automated detection. The DYEnamic ET Terminator kit (Amersham Biosciences UK Ltd., Buckinghamshire, UK) uses two dyes to label each dideoxy terminator; fluorescein and one of four different rhodamine dyes (rhodamine 110, rhodamine-6-G, tetramethyl rhodamine, and rhodamine X). Fluorescein absorbs energy from the incident laser light and transfers it to the rhodamine acceptor dye on the same terminator molecule. Each acceptor dye then emits light at its characteristic wavelength for detection, so identifying the nucleotide that terminated extension of the DNA fragment.

Protocol

Sample PCR Preparation Sequencing primer pairs were designed to flank the region of interest. Generally acceptable sequencing read-length tended to be around 500 bp. Therefore if the area of interest extended over 500 bp, overlapping primer pairs were designed to cover the entire region. A summary of the primer pairs used in this project are detailed in table 2.4 on the following page. Separate PCR product was generated for each primer pair as detailed in section 2.1.3 on page 69. The product was then visualized on an agarose gel to ensure that the product was of correct size and high enough quality to proceed. High stringency was placed on PCR quality as any 'shadow-bands' present would likely interfere with sequencing accuracy. If it proved impossible to produce a single product band for a particular primer pair, the band of interest was gel purified using the QIAquick Gel Extraction kit (Qiagen Inc., US) according to the manufacturer's instructions.

Sequencing Reaction The DYEnamic ET Dye Terminator kit contains all dNTPs and ddNTPs needed, along with Thermo Sequenase DNA polymerase, and therefore simply requires the addition of template PCR, and sequencing primer. Typically the sequencing reaction comprised:

Template PCR	5 µl
10 µmol/l F or R primer	0.5 µl
dH_20	8.5 µl
	14 µl

Table 2.4: *IL18* sequencing primers used.

Primer	Forward	Reverse	$MgCl_2$ (mmol/l)	Annealing Temp (°C)	Cycles	Product Size (bp)
IL18-9731 seq	GGT CAG TCT TTG CTA TCA TTC CA	TTC AGT GGA ACA GGA GTC CA	1.5	58	40	226
IL18-5848 seq	TTA AAG CAA AGA AAC ACG GAT G	CTA ATG TCT TCT CCA TTT TTC CCT A	1.5	58	40	200
IL18+105 seq	CAA GAA ATT GAG TGT GCC TTT G	ATA GAG GCC GAT TTC CTT GG	1.5	58	40	284
IL18+8855 seq	TAG GCT GCA GTG AGC TGA GA	CTG GCC AAG CCT GGA TAT AG	1.5	63	38	267
IL18+11015 seq	AGA GCG AGA CCC TGT CTC AA	CTC CCT GTC ATG GGA TGC	1.5	58	38	270

Based on the agarose gel, the proportions of template PCR:dH_2O was adjusted to ensure that roughly equal amounts of PCR product was included in each reaction. Two separate sequencing reactions were carried out for each sample – forward and reverse, so the target region is sequenced in both directions to improve accuracy. The mix was then placed in a thermal cycler and the following program run:

95 °C	20 s	} x 25 cycles
50 °C	15 s	
60 °C	60 s	

Clean-Up – Magnetic Separation The sequencing reaction is not cycled until completion, and therefore there remains a surplus of unincorporated fluorescent nucleotides (along with excess primers and enzyme) that must be removed prior to electrophoresis. The AMPure PCR Purification system (Agencourt Bioscience Corporation, Massachusetts, US) utilizes an optimized buffer to selectively bind PCR amplicons 100 bp and larger to small microparticles. The paramagnetic beads are then captured by magnet, whilst all contaminants are washed from the sample. The beads are small and do not interfere with subsequent electrophoresis.

Initially 36 µl of AMPure bead mixture was added to the sample, and mixed thoroughly. The sample is then placed upon the SPRIPlate 96R magnet for 10 min to separate the beads from the sample and bring them out of solution. Whilst the sample remains upon the magnet, the cleared solution was aspirated and discarded. 200 µl of 70% ethanol was added to the sample and incubated at room temperature for 30 s, this wash step was repeated twice more. Once washed the sample was taken from the magnet and left to air-dry for 1 h. To elute the sample from the beads, 10 µl of MegaBACE loading solution was added and the sample thoroughly mixed.

Electrophoresis The MegaBACE 1000 DNA Analysis System (Amersham Biosciences UK Ltd., Buckinghamshire, UK) is a high-throughput, fluorescence-based DNA system utilizing capillary-based electrophoresis in a 96-well plate arrangement – 6 arrays of 16 capillaries. The system uses high-pressure nitrogen gas to inject the capillaries with linear polyacrylamide (MegaBACE Long Read Matrix – Amersham Biosciences UK Ltd., Buckinghamshire, UK), excreting the used acrylamide simultaneously. To load samples, a current is set up at the tip of the capillaries where it contacts the sample. DNA (and other charged particles in the sample) are electro-kinetically 'injected' into the gel. Both ends of the capillary are then placed in buffer (MegaBACE LPA Buffer), and a voltage applied across the capillary, moving the charged DNA fragments through the matrix. Analogous to an agarose gel, the chain terminator fragments separate by size, effectively reading base by base along the target sequence. Typical run conditions for the sequencing protocol was 3 kV injection potential for 45 s, followed

by 100 min electrophoresis. Should the first run fail, a second run could be done with the same samples with a 3 kV, 100 s injection protocol.

As the fragments pass a window in the capillary a laser excites the fluorescein dye, which then passes energy to the rhodamine dye, causing it to emit at its particular frequency. Therefore as the fragments pass, the typical ladder pattern forms from which the sequence can be read. The electrophoretogram from each dye is overlayed and interpreted by Sequence Analyser (Amersham Biosciences UK Ltd.), with Cimarron 3.12 base calling. Traces reading for the forward and reverse strands were compared manually to improve sequence accuracy and confirm any potential polymorphisms found.

2.2 QPCR

Reverse transcription followed by PCR (QPCR) is the most suitable method for the detection and quantification of mRNA. It offers high sensitivity, good reproducibility and a wide quantification range. Below are detailed the laboratory methods and statistical tests used in this study.

2.2.1 PBMC Isolation

A common technique for separating PBMCs from whole blood is to mix the blood with a compound (Lymphoprep, Axis-Shield, Norway) that aggregates the erythrocytes, thereby increasing their sedimentation rate. The sedimentation of PBMCs is only slightly affected and can be easily removed from the upper phase of the tube. RNAlater (Ambion, US) was then used to stabilize and protect cellular RNA.

Approximately 16 ml of blood was drawn into two tubes (BD Vacutainer, NJ, US; K3E, 0.12 ml EDTA) and mixed with 8 ml phosphate buffered saline (PBS) (at 37 °C). 6 ml of this mix was then carefully layered onto 3 ml of Lymphoprep in four separate 15 ml Falcon tubes. This was then centrifuged at 2000 r/min for 30 min at room temperature. Following centrifugation the PBMCs form a distinct band at the sample/medium interface, and these cells were carefully removed using a Pasteur pipette into two 15 ml Falcon tubes. An equal volume of PBS was added to both tubes before they were centrifuged at 1100 r/min for 10 min at room temperature. Following this centrifugation all steps were performed on ice to minimize RNA degradation. The supernatant was removed from each tube before the PBMC pellets were resuspended in 100 µl PBS. 1 ml of RNAlater was added to each tube, and mixed before being transferred to a 1.5 ml Eppendorf tube. This mix was stored at 4 °C overnight. The PBMCs were then pelleted by spinning at maximum speed for 1 min in a microfuge, before removing the majority of the supernatant, leaving around 100 µl in which the pellet was resuspended. This was then stored at −80 °C until further use.

2.2.2 mRNA Extraction

Reagents

DEPC-Treated Water 1 ml diethylpyrocarbonate (DEPC)[4] was added to 1 l dH_2O, and shaken vigorously to bring it into solution. The solution was then incubated for 12 h at 37 °C, before autoclaving to remove any traces of DEPC.

Protocol All materials were handled with gloves, and surfaces and pipettes cleaned thoroughly with RNase Zap (Ambion Inc., Austin, US), a detergent that completely removes RNase contamination from glass and pipette. mRNA was isolated using the RNeasy kit (Qiagen, Crawley, UK) spin protocol. This uses a high-salt buffer system which allows up to 100 µg of RNA, longer than 200 bp, to bind to a silica-gel based membrane within a mini column.

The PBMC:RNAlater mix was thawed before spinning for 1 min at maximum speed to pellet the cells. The supernatant was removed and the pellet resuspended in 350 µl of lysis buffer (RLT buffer)-β-mercaptoethanol (β-ME) mix (10 µl β-ME:1 ml RLT buffer). 350 µl of 70% ethanol was added to the sample and the entire mix pipetted onto an RNeasy column. The column was placed in a 2 ml collection tube and spun in a microfuge at 10000 r/min for 15 s. All flow through was discarded, and 700 µl of the first wash buffer (RW1 buffer) added to the column and spun through at 10000 r/min for 15 s. The column was placed in a fresh collection tube and 500 µl of the second wash buffer (RPE buffer) was added and spun through at 10000 r/min for 15 s. Flow through was discarded and the RPE wash repeated at 10000 r/min for 2 min. The column was dried by spinning at maximum speed for 1 min, before being placed in a fresh 1.5 ml collection tube. The RNA was eluted by addition of 50 µl of DEPC-treated water, and spinning at 10000 r/min for 1 min. To improve yield and increase RNA concentration, the flow through was added back on to the column and spun again. The resulting sample was immediately divided into 5 µl aliquots, and stored at −80 °C until use.

2.2.3 cDNA Synthesis

Protocol The concentration of mRNA was determined using a NanoDrop ND-1000 Spectrophotometer. The NanoDrop ND-1000 has a unique sample retention system that requires only 1 µl of sample to be loaded for reading, allowing direct determination of RNA concentration. Therefore error due to dilution preparation is eliminated giving a more reliable and accurate measure than that given by cuvette-type spectrophotometers.

[4]DEPC is a strong but not absolute inhibitor of RNases that inactivates by covalent modification of the enzyme. Any traces must be completely removed as DEPC will also modify purine residues by carboxymethylation

RNA absorbs at 260 nm, whilst protein at 280 nm, and salts, solvents, and other impurities (eg. carbohydrate) absorbs at 230 nm. Therefore 260:280 nm and 260:230 nm ratios give an idea of the overall purity of the sample, with values in the order of 2 considered highly pure. Ensuring that equal quantities of RNA enter the cDNA synthesis and subsequent processes is important, therefore NanoDrop measurements were made in triplicate to increase accuracy.

cDNA was generated for each RNA sample using the SuperScript II Reverse Transcriptase (Invitrogen, Paisley, UK), and all components were kept on ice during initial preparation. An aliquot of each sample was diluted appropriately in DEPC-treated water to 10 µl, to be of equal quantity as all others. 2 µl of random hexamer primers (pd[N]$_6$ – 100 ng/µl) were added to the sample along with 1 µl dNTP mix (10 mmol/l). The sample was then heated to 65 °C for 5 min, and cooled briefly (10 s) on ice, before adding 4 µl First-Strand buffer and 2 µl 0.1 mol/l dithiothreitol (DTT)[5]. The sample was then heated to 42 °C for 2 min and then 1 µl of SuperScript II reverse transcriptase added, before further incubation at 42 °C for 2 h. The enzyme was then heat-inactivated by heating to 70 °C for 15 min.

2.2.4 RNA Quantification

TaqMan QPCR uses the same chemistry and principles as TaqMan genotyping (see section 2.1.6 on page 76), with the exception that QPCR uses just a single FAM-labelled probe. To distinguish between remaining genomic DNA contaminants and cDNA copies of mature mRNA species, the probe for each gene of interest was designed to span across introns and therefore will anneal only to the cDNA of interest. Forward and reverse oligonucleotides and the probe sequences were ordered and supplied through the Applied Biosystems 'Assay on Demand' service (www.allgenes.com). All gene expression assays used are detailed in table 2.5 on the next page. As the PCR reaction continues, the relative quantities of the target gene between samples is conserved. More FAM is released as cycle number increases, the level of fluorescence eventually reaching a threshold and rising above the background. Once established the relationship between cycle number (C) and fluorescence (Rn) describes a sigmoidal curve. The fractional PCR cycle at which the sample fluorescence crosses a particular threshold (Ct), is directly related to the initial concentration of the mRNA species. The fluorescence threshold was set automatically as the point at which all samples being measured for that target gene went into logarithmic growth. Using endogenous controls (housekeeping genes) whose levels remain stable between samples, it was possible to control for differing amounts of starting material, and its quality. Therefore comparisons between Ct's generated from different samples and experiments can be made.

[5]DTT is used in this instance to stabilize the reverse transcriptase

Table 2.5: Commonly used TaqMan QPCR probes and Assay ID's.

Gene	Assay ID	Probe Sequence
IL18	Hs00155517_m1	ATT TCC TTT AAG GAA ATG AAT CCT C
*IL18*Δex3	Hs01038787_m1	AAT ACG CTT TAC TTT ATA GAA AAC C
IFNγ	Hs99999041_m1	AAT TAT TCG GTA ACT GAC TTG AAT G
UBC	Hs00824723_m1	GTG ATC GTC ACT TGA CAA TGC AGA T
GAPDH	Hs99999905_m1	TTG GGC GCC TGG TCA CCA GGG CTG C
BACT	Hs99999903_m1	TCG CCT TTG CCG ATC CGC CGC CGC CCG T

Protocol Freshly made cDNA product was used as a template for QPCR, with the following mix made for each well of a 384-well plate:

TaqMan Absolute QPCR ROX Mix	2.5 µl
cDNA	1 µl
Assay	0.25 µl
Sigma dH_2O	1.25 µl
	5 µl

Each cDNA sample was run in triplicate for each probe and each experiment triplicated on sequential days, thereby improving accuracy and decreasing any differences caused by pipetting or experimental error. Once assembled the plate was sealed with a clear plastic lid (ABgene, Surrey, UK), and spun briefly to collect all reagents. Data was collected by the ABI 7900HT TaqMan machine and recorded by SDS v2.1 software, as the sample underwent the following PCR protocol:

50 °C	2 min	
95 °C	10 min	
95 °C	15 s	x 40 cycles
60 °C	1 min	

2.3 Measurement of IL-18 and IL-18BP

Both IL-18 and IL-18BP were measured by Daniella Novick at The Weizmann Institute of Science, in Rehovot, Israel, using enzyme-linked immunosorbent assay (ELISA) methods.

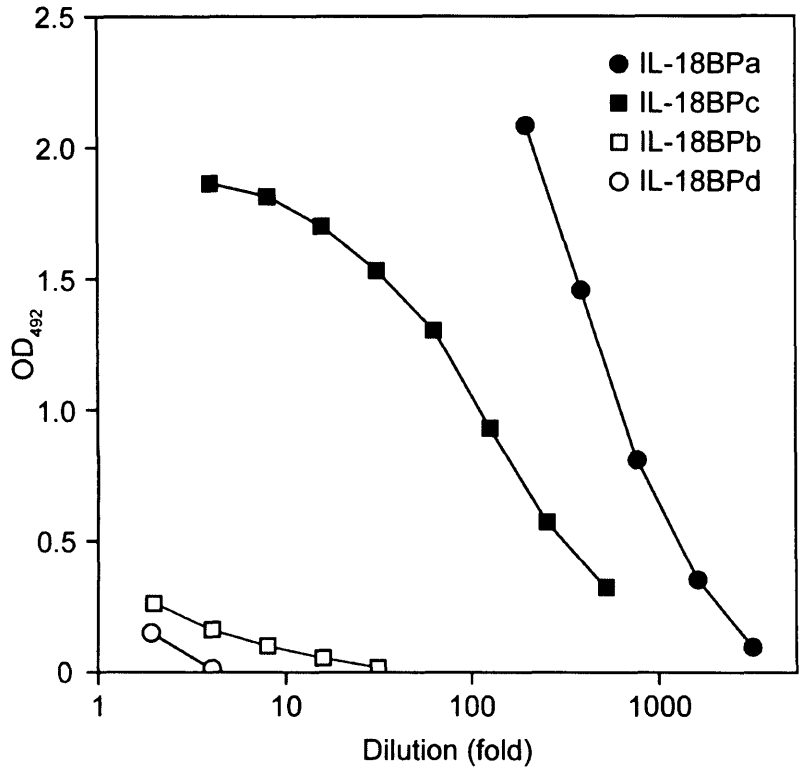

Figure 2.4: Cross-reactivity of IL-18BP isoforms with the IL-18BPa ELISA, taken from Novick et al. [2001].

2.3.1 IL-18

Total IL-18 was measured by a commercially available ELISA kit (MBL, Naka-Ku Nagoya, Japan), according to the manufacturer's instructions.

2.3.2 IL-18BP

A sandwich ELISA for IL-18BPa (the most abundant isoform of IL-18BP [Novick et al., 1999; Kim et al., 2000]) was developed by Novick et al. [2001], using two anti-rIL-18BP-His_6 antibodies for capture and detection. There was no effect of IL-18 on the IL-18BP ELISA, at those concentrations seen in sera. The IL-18BP ELISA was tested with the three other IL-18BP splice variants, IL-18BPc gave a 10-fold lower signal compared with IL-18BPa, whereas isoforms b and d gave very low signal (see figure 2.4).

2.3.3 Calculation of fIL-18

The formation of the IL-18:IL-18BP complex can be thought of as a reaction between a receptor, R, and it's ligand, L, with a 1:1 stoichiometry:

$$R + L \rightleftharpoons R:L \tag{2.1}$$

At equilibrium the concentrations of free ligand, free receptor and the complex is given by the law of mass action:

$$K_D = \frac{[R] \cdot [L]}{[R:L]} \tag{2.2}$$

With the dissociation constant being a constant for this reaction. However, in this case we only know the original concentration of R, $[R]_0$, and L, $[L]_0$. The concentrations of free R and L are given by:

$$[R] = [R]_0 - [R:L] \tag{2.3}$$

and:

$$[L] = [L]_0 - [R:L] \tag{2.4}$$

From this the concentration of complex R:L can be calculated by:

$$[R:L] = \frac{[R]_0 + [L]_0 + K_D}{2} + \sqrt{\frac{([R]_0 + [L]_0 + K_D)^2}{4} - [R]_0 \cdot [L]_0} \tag{2.5}$$

Therefore the concentration of free ligand (fIL-18) can be calculated by:

$$[L] = [L]_0 - [R:L] = \frac{[L]_0 - [R]_0 - K_D}{2} + \sqrt{\frac{([R]_0 + [L]_0 + K_D)^2}{4} - [R]_0 \cdot [L]_0} \tag{2.6}$$

2.4 Data Analysis Software and Resources

Detailed below are the numerous packages, tools, and resources used throughout this study.

2.4.1 Haplotype Inference

Haplotype information is an essential ingredient of data analysis when multiple loci are being used in a population genetics approach. Routine genotypes do not provide genotype phase (haplotype) information. This can be obtained to some degree, at increased expense, via genotyping of additional family members [Sobel and Lange, 1996]. Alternatively, a statistical method can be used to infer phase from genotype of linked loci.

PHASE v2.1 One method for inferring genotype phase is via an implementation of maximum likelihood using the expectation-maximization (EM) algorithm [Excoffier and Slatkin, 1995; Hawley and Kidd, 1995; Long et al., 1995], however PHASE uses a Bayesian-based statistical method for reconstructing haplotypes from population genotype data. In direct comparisons [Stephens et al., 2001] PHASE has been shown to be more accurate than the EM algorithm, correctly reconstructing $\geq$80% of the sample with a reduction in error rate of >50%.

Implementation PHASE is able to accept input genotypes in a variety of different formats, and is also able to accept missing data. As output it generates many different files with the main output file showing the haplotypes inferred and their counts, as well as suggesting the most likely haplotype pair for each individual.

Availability The latest version of PHASE is available from http://www.stat.washington.edu/stephens/software.html.

2.4.2 tSNP Selection

The pattern of LD varies across the genome [Reich et al., 2001], and studies suggests that discrete regions of high LD, haplotype blocks, exist that are characterized by restricted haplotype diversity [Alper et al., 2006; Cardon and Abecasis, 2003]. In regions of high LD within these blocks, a reduced set of tSNPs may be selected to efficiently identify the common haplotypes [Johnson et al., 2001].

STRAM Given the haplotype structure of a population, STRAM optimizes the predictability of the common haplotypes by selecting potential tSNPs based on a statistic analogous to the usual coefficient of determination, R^2. For a given set of true haplotypes, a formal calculation of the squared correlation, R_h^2, between the estimate haplotypes (those inferred using the tSNPs being tested) and the true haplotypes can be made. The set of tSNPs that gives sufficiently high R_h^2 (typically >0.95) across all common haplotypes is then selected and can be assumed to accurately 'tag' >95% of the genetic variation present in the haplotypes.

Implementation Input data for STRAM can be either population genotype or haplotype data, as the program can also utilize an EM algorithm to estimate haplotype frequencies. However, as detailed in section 2.4.1 on the previous page, the accuracy of PHASE is greater than the EM algorithm so routinely STRAM input was haplotypes from PHASE and not population genotype data.

The input file format in this case is a simple listing of binary haplotypes and their relative frequencies. An optional 'rsq force in' command allows the user to specify which SNPs must be included in the first tSNP set. The output file lists the tSNP set tested and the R_h^2 values for each haplotype for that test. The number of SNPs being tested rises incrementally and the most suitable (best improvement in R_h^2) SNP is chosen at each round.

The selection of the most suitable tSNP set is a decision taking into account a minimum R_h^2 threshold, and the balance of increases in R_h^2 via increases in number of tSNPs (and the consequent decrease in genotyping efficiency). The exact sigmoidal relationship between R_h^2 and number of tSNPs differs greatly between genes and populations since it is derived from the nature of LD and population structure. Therefore, although tSNPs do appear to translate well between ethnic groups [Tenesa and Dunlop, 2006], it is considered best practice to derive ethnic group-specific tSNP sets; otherwise a specific tSNP set can be derived for cross-populational analysis [Howie et al., 2006].

Availability STRAM is freely available at http://www-rcf.usc.edu/~stram/.

BEST

Background Best Enumeration of SNP Tags (BEST) implements a different strategy to tSNP identification than STRAM, using an exact algorithm-based method over the statistical approach used by the latter [Sebastiani et al., 2003].

The initial step is to convert the haplotype set into a binary form. SNPs that share the same binary representation, are termed binary equivalents. After the initial binary conversion only one of the binary equivalents is taken forward in the algorithm. The algorithm then searches for SNP subsets that together show within-set redundancy ('derivable' SNPs). From each set, set-tSNPs are taken forward and then superset-SNPs can then be derived. Using this method ensures minimal tSNP numbers and no loss of information.

Implementation BEST runs through a graphical user interface (GUI), that requires only one input file describing the allelic structure of the haplotypes identified. The results of the algorithm are presented in a schematic format showing the haplotypes being interrogated and the result of the algorithm for each SNP. A SNP labelled with an 'X' is a derivable SNP, whilst a numbered label designates the first SNP in the haplotype to which that SNP is a binary equivalent. No label shown designates a tSNP.

Availability BEST is freely available at http://genomethods.org/best/.

Haploview

Background Haploview [Barrett et al., 2005] is designed to provide a comprehensive suite of tools for haplotype analysis, providing marker quality statistics, LD information, haplotype blocks, population haplotype frequencies and single marker association statistics in a relatively user-friendly format. Haploview also directly accepts genotype data 'dumped' from the HapMap website (see section 2.4.3).

Implementation Haploview accepts data in a variety of formats. Pedigree data can be loaded as either partially or fully phased chromosomes or as unphased diplotypes. The majority of the Haploview analysis in this study concentrated on LD calculations and therefore data input was in the form of unphased diplotypes.

The Haploview LD plot summarizes the extent and pattern of LD between the markers. Data is presented as D' with the background colour denoting a scale of logarithm of odds (LOD) score.

Availability Haploview is available for download from http://www.broad.mit.edu/mpg/haploview/.

2.4.3 Online Genomic Resources

UCSC Genome Browser The UCSC Genome Browser [Kent et al., 2002] provides an online portal to reference sequence and working draft assemblies for a large collection of genomes. The Genome Browser zooms and scrolls over chromosomes, showing a browser window that can be changed to display a number of different 'tracks' and annotations. Once a region or gene is selected annotated genomic sequence can be downloaded in a variety of formats.

Availability UCSC Genome Browser can be accessed at http://genome.ucsc.edu/.

The HapMap Project The goal of the HapMap project [HapMap, 2003] was to determine the common patterns of DNA sequence variation in the human genome. The project is a collaboration between scientists and funding agencies from Japan, US, Canada, Nigeria, China and UK, with all of the information generated by the project being released into the public domain.

The project has genotyped over six million SNPs in a total of 270 samples: 90 (30 trios of two parents and an adult child) Centre d'Etude du Polymorphisme Humain (CEPH) samples; 90 Yoruban (West African) samples (YRI); 45 Japanese samples

(JPT); and 45 Chinese samples (CHB). A high density of SNPs is needed to describe adequately the genetic variation across the entire genome. Initially the project genotyped 600000 SNPs spaced at approximately 5 kbp intervals with a minor allele frequency (MAF) of at least 5%. The LD was then analysed, and a hierarchical approach taken to ensure that regions of low LD were genotyped to a greater density (up to 1 kbp per SNP).

All data is now available online and can be downloaded either to a text file or can be downloaded to Haploview. The data browser is a searchable resource that shows genotyped SNPs and basic genome architecture, as well as a number of other possible tracks including dbSNP SNP, LD, and recombination rates, amongst others.

Availability The HapMap data can be accessed at http://www.hapmap.org/.

IIPGA The goal of the IIPGA is to discover and model the associations between nucleotide sequence variations, primarily SNPs and insertion/deletion variations (Indels), in the genes of the innate immunity pathway in humans. The program has two phases, initially the candidate genes are re-sequenced in both European American and African American populations to gather allele frequencies and haplotypes. Second to this, the variants are then used in case:control association studies of airways disease. Therefore IIPGA is a useful resource for identifying the extent of genetic variation in a number of different inflammation-related genes. An extensive array of genotype data ranging from individual genotypes to PHASE-derived haplotypes or LD plots are freely available within the site.

Availability IIPGA data is freely available at http://innateimmunity.net/.

2.4.4 Comparative Genomics

VISTA Alignment of genomic sequence from different organisms is an increasingly powerful method in biology and has been used for many purposes. Comparative sequence analysis has enabled identification of regulatory regions [Dubchak et al., 2000; Loots et al., 2000], and coding exons [Batzoglou et al., 2000], using purely computational methods.

VISTA [Frazer et al., 2004] is a comprehensive suite of programs and databases for comparative analysis of genomic sequences, using the VISTA curve-based visual front-end to present multiple alignments. The program mVISTA uses three separate alignment programs to align up to 100 different sequences:

AVID works by recursively finding strong anchors from the collection of maximal matches in the sequences [Bray et al., 2003]

LAGAN performs progressive pairwise alignments, guided by a phylogenetic tree [Brudno et al., 2003a]

Shuffle-LAGAN is able to find rearrangements (inversions, transpositions and some duplications) that are then aligned using LAGAN [Brudno et al., 2003b]

The results of these alignments are then visualized with VISTA.

Implementation Sequences are prepared in FASTA format with an annotation file that details the presence of genes, direction of their transcription and presence of exons. Once complete, the results of the alignment are presented as percentage identity against sequence position. The example shown in figure 2.5 on the next page shows a 70 kbp alignment of four sequences: human/mouse in the upper pane, human/rat in the middle pane, and human/chimp in the lower pane. Those regions with greater than 75% sequence identity (arbitrarily considered to be of significance) within a sliding 100 bp window are highlighted in light pink. In this example there is near complete sequence identity between human and chimp, whilst little identity with mouse and rat, and human (although there are similar patterns of identity between them).

Availability Various generations of VISTA are available for use at http://genome.lbl.gov/vista.

2.4.5 Quantitative Data Analysis

Thesias Thesias is a statistical program that performs haplotype-based association analysis in unrelated individuals [Tregouet et al., 2004]. The program is based on a maximum likelihood model [Tregouet et al., 2002], and is linked to a stochastic version of the EM algorithm (SEM) [Tregouet et al., 2004]. Thesias, therefore allows the simultaneous estimation of haplotype frequencies and of their associated effects on the phenotype of interest. Quantitative, qualitative and survival analysis can be carried-out as well as covariate-adjusted effects and interactions.

Implementation The input file is prepared with genotypes coded as '11', '12', '22' and '0' for missing genotypes. The phenotype and covariates must have no missing data. The initial Thesias run must be a null run, allowing the algorithm to generate haplotypes, this information is stored in the 'para.txt' file which must be edited by the user to select which haplotype effects are to be tested.

The next run is then the analysis run, during which the phenotype and covariate variables are defined and specific analyses (homogeneity of allelic effects, additivity

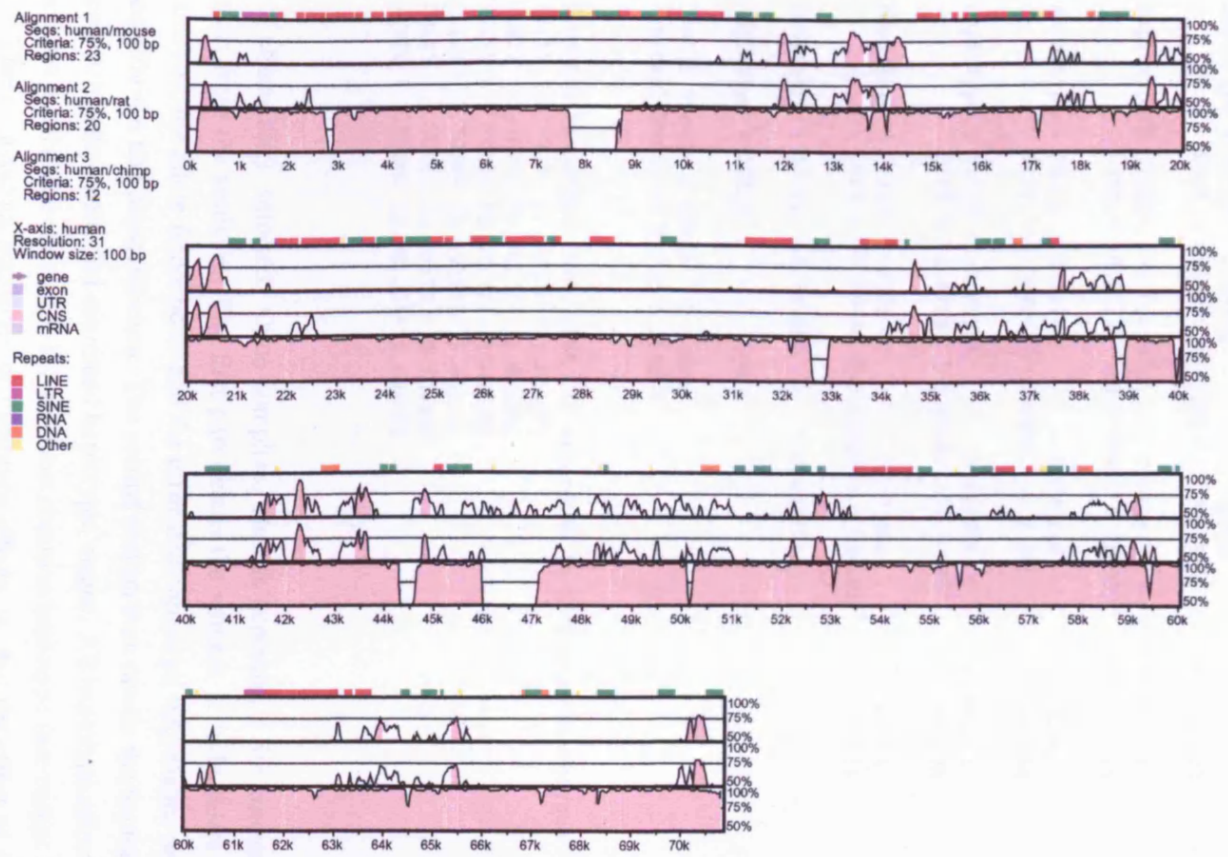

Figure 2.5: Example of VISTA output showing three alignments (mouse, rat and chimp) against a 70 kbp human reference sequence. Those sections with greater than 75% identity are shown in light pink ( ).

Output 2.1: Example of Thesias output.

```
Haplotype Effects
(Haplotypic effect by comparison to the reference with its 95% CI)

                    Estimation      StError         T-Test
Haplotype 4 21112   0.03232         0.042593        0.758888
            Diff = 0.03232 [-0.05116 - 0.11581]     p=0.447920

Haplotype 2 21222   -0.00728        0.033473        -0.217506
            Diff = -0.00728 [-0.07289 - 0.05833]    p=0.827814

Haplotype 5 22111   0.00704         0.493146        0.014284
            Diff = 0.00704 [-0.95952 - 0.97361]     p=0.988604

Haplotype 6 11112   -0.07791        0.196738        -0.396000
            Diff = -0.07791 [-0.46352 - 0.30770]    p=0.692105

Haplotype 3 11111   -0.05036        0.039056        -1.289473
            Diff = -0.05036 [-0.12691 - 0.02619]    p=0.197234

Intercept 1 12111   1.760565        0.063524

Haplotype 7 12222       0.00000

Global Standard Error   0.168511
Residual Standard Error 0.151306
...

Expected Phenotypic Mean [95% CI] According to Estimated Haplotypes
12111   1.76057 [1.63606 - 1.88507]
21222   1.75328 [1.64173 - 1.86484]
11111   1.71020 [1.57112 - 1.84928]
21112   1.79289 [1.65210 - 1.93368]
22111   1.76761 [0.79573 - 2.73949]
11112   1.68266 [1.28125 - 2.08406]
...
```

of effects etc.) selected. Once complete, Thesias generates a file containing the results from the analysis. The first part details the number of individuals used in the analysis, the allele frequencies and the estimated haplotype frequencies under linkage equilibrium and disequilibrium. The second section then details the haplotype effects, covariate adjustment and estimated haplotypic means. All haplotype effects are tested against a reference (Intercept 1) – the most common haplotype (see output 2.1).

Thesias assumes additivity of haplotype effects, ie. that the effect of a haplotypic pair $h_a h_b$ compared to the reference $h_0 h_0$ is equal to the sum of their haplotype effects, $b_{(h_a)} + b_{(h_b)}$. This assumption can be tested in Thesias and allows a greater understanding of the nature of the haplotype effect. Thesias also provides the log-likelihood which allows the overall impact of haplotypes on the phenotype of interest, to be tested using the likelihood ratio test (LRT). The input for LRT is the log-likelihood provided by

thesias without estimating haplotype effects ($\ln L_1$), and with haplotype effects ($\ln L_2$):

$$LR = 2(lnL_1 - lnL_2) \tag{2.7}$$

The likelihood ratio (LR) approximately follows a χ^2 distribution, with the degrees of freedom (df) being the number of haplotypes studied. It is also possible to assess the degree of variation in the phenotype, explained by the haplotypes (R^2). Using the residual standard error with (SE_1), and without (SE_2) estimating haplotype effects, R^2 can be calculated:

$$R^2 = 1 - \left(\frac{SE_1}{SE_2}\right)^2 \tag{2.8}$$

Availability Thesias is freely available at http://genecanvas.ecgene.net/downloads.php?cat_id=1.

Arlequin Arlequin is a complete package of methods and statistical tests for extracting information on genetic and demographic features of a collection of population samples. In this study, Arlequin was used mainly to calculate the F statistic in multi-populational analysis.

Founder effects acting on different demes generally lead to subpopulations with allele frequencies that are different from the population as a whole. Furthermore these demes are smaller in size than the larger population; since allele frequency in each generation represents a sample of the previous generation's allele frequency, there will be greater sampling error in these small populations. Therefore, genetic drift will push these smaller demes towards differing allele frequencies.

The decline in heterozygosity due to subdivision within a population (see table 2.6 on the next page) can be quantified using an index known as Wright's F statistic (also known as the fixation index). The F statistic is a measure of the difference between the mean heterozygosity among the subdivisions (H_{Sub}) in a population, and the potential frequency of heterozygotes if all members of the population mixed freely (H_{Total}) and takes the form:

$$F = \frac{H_{Total} - H_{Sub}}{H_{Total}} \tag{2.9}$$

F ranges from 0 (indicating no differentiation between the overall population and its subpopulations) to a theoretical maximum 1, though observed F's tend to be much less than 1 in highly differentiated populations. Both inbreeding and subdivision both lead to an apparent deficiency of heterozygotes over Hardy-Weinberg expectations, thus nothing can be said about the cause of an observed deficiency without more information.

Table 2.6: An example of the loss of heterozygosity of a single SNP in a divided population.

	p	pp	pq	qq
Freq. in subpop. 1	$\frac{1}{4}$	$\frac{1}{16}$	$\frac{3}{8}$	$\frac{9}{16}$
Freq. in subpop. 2	$\frac{3}{4}$	$\frac{9}{16}$	$\frac{3}{8}$	$\frac{1}{16}$
Freq. in species	$\frac{1}{2}$	$\frac{5}{16}$	$\frac{3}{8}$	$\frac{5}{16}$
HWE freqs	$\frac{1}{2}$	$\frac{1}{4}$	$\frac{1}{2}$	$\frac{1}{4}$

Implementation Arlequin is able to support a broad range of input data types, including simple genotypes, DNA sequences, microsatellite data, and RFLP data. The result file describes the pair-wise F across all populations and its p value. The significance of F is tested using a non-parametric permutation approach [Excoffier et al., 1992], whereby individuals are permuted among populations or groups of populations. After each round, all statistics are re-computed to establish a null distribution (after 1000+ permutations).

Availability Arlequin is freely available at http://lgb.unige.ch/arlequin/.

MDR Analysis The multifactor dimensionality reduction (MDR) approach is a non-parametric alternative to logistic regression for detecting non-linear interactions among genetic and environmental factors. Essentially MDR is a data-mining tool that assesses the impact of grouping numerous genetic variables to produce high-risk or low-risk attributes. The effectiveness of this grouping is tested against a permuted null distribution.

Implementation For each MDR run the testing balanced accuracy (TBA) and cross-validation consistency (CVC) was recorded for the top-performing SNP combination. Only 1–5 order interactions were considered. For each analysis, 10 separate runs were conducted on the same dataset using random seeds generated by www.random.org (a random number generator that uses atmospheric noise as its random source). To assess the significance of each analysis, the program MDRperm was used to produce a null distribution of TBA and CVC by permuting individuals between classes. The average TBA from the 10 runs was then used to generate a p-value for each order of interaction.

Availability MDR and MDRperm are freely available from www.epistasis.org/mdr.html.

SPSS All data management and statistical analysis was study carried out using SPSS v15 (SPSS Inc.).

Chapter 3

tSNP Selection

The aim of this chapter is to assemble tSNP sets for both *IL18* and *IL18BP*, that mark gene-wide variation identified by IIPGA. Also, computational techniques will be used to identify important variation away from the immediate gene region that could be of importance in gene regulation.

3.1 Introduction

Traditionally, disease-causing genetic variations have been identified using family-based linkage analysis. However, it is now well-recognized that there are limitations to this approach when applied to complex diseases. For assessing the effect of risk factors on overall risk, a large study cohort is required. This allied with the observation that many complex diseases are late-onset, means there is great difficulty in collecting pedigrees with sufficient cases for linkage analysis. Therefore, studies are carried out in completely unrelated individuals, large numbers of parent-offspring trios, or case-siblings pairs.

Such studies rely upon LD to identify genes or regions involved in disease susceptibility. They are also heavily reliant on the large-scale genotyping resources that have mapped LD and common SNP haplotypes across the genome (eg. HapMap). Such approaches operate under four primary assumptions:

1. An important fraction of susceptibility to disease may be explained by relatively modest effects of a small number of relatively common variants.
2. Much of the causal variants are SNPs themselves, or are thought to arise or mutate at rates no greater than that at which SNPs tend to appear.
3. The rate at which SNPs or other variants arise and become common

within the population are low enough that carriers today of a given common variant inherited this variant from a single ancestor.

4. Recombination rates are low enough that carriers of a common disease-related variant will also tend to carry a pattern of surrounding SNPs that reflects the SNPs that appeared on the ancestral chromosome locus surrounding the causal variant.

The most controversial of these assumptions is point 1; the common-disease common-variant hypothesis. It is possible that common disease could also be caused by there being many rare mutations that have large effects. However, the current knowledge of patterns of common variation across the genome has tended to motivate studies along the earlier hypothesis.

Recombination adds to the number of haplotypes that exist in the population in a particular chromosomal region, and will also add to the uncertainty when genotyped SNPs are reassembled into haplotypes – haplotype inference. However it is now becoming clear that recombination does not occur equally and randomly across the genome, and that there is considerable local variation. Indeed it has been estimated that 50% of recombination occurs in less than 10% of the sequence [McVean et al., 2004]. This phenomenon gives the genome a 'haplotype block' structure, with large regions (haplotype blocks) of little recombination (and consequently few haplotypes), interspersed with areas undergoing high rates of recombination – recombination hotspots (see figure 3.1 on the following page).

Denser and denser genotyping of a haplotype block tends to reveal fewer and fewer SNPs that split haplotypes. Almost always the observed maximum number of haplotypes is considerably smaller than the theoretical maximum of non-recombinant haplotypes. Such an observation is consistent with population genetics theory, in that, without recombination, only a fraction of haplotypes appearing as new mutations are expected to avoid random drift towards extinction.

Given this, and the assumption described in point 4, to test whether certain genetic variants within a region are associated with disease risk there is no need to genotype the actual causal variant, as other variants on the ancestral haplotype will act as a marker for the causal variant. To extend this further, there is no need to genotype all SNPs within a region to capture its total genetic variation, as many will prove redundant. Therefore, the redundancy in genetic variation at the candidate gene level, allows efficient (in time and cost) capturing of genetic variation using informative SNPs – tSNPs. The methods used to select tSNP sets fall under two separate groups – haplotype-tagging SNP selection and SNP-tagging SNP selection. As detailed in section 2.4.2 on page 90, the two programs used here exploit either one of these approaches.

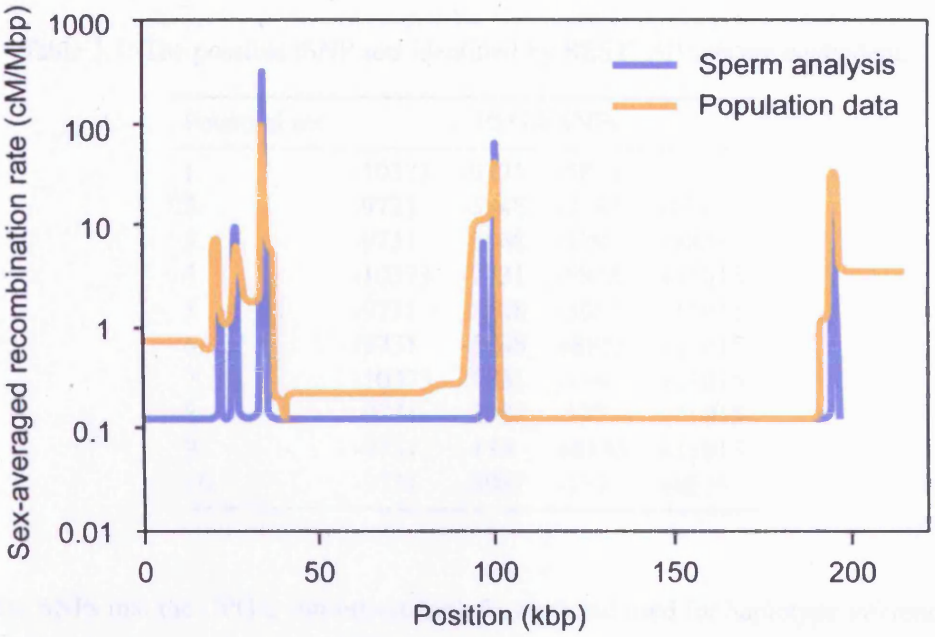

Figure 3.1: Local recombination rates from population genetic data and sperm analysis in the HLA region (adapted from McVean et al. [2004]).

3.2 tSNP Selection in *IL18*

As detailed in table 1.7 on page 66, a number of SNPs had been discovered at the time of this analysis, with the most commonly studied being *IL18*-607 C>A, *IL18*-137 G>C, and *IL18*+105 A>C. The resequencing consortium, IIPGA had also resequenced the *IL18* region – a total of 23.5 kbp from 2 kbp upstream to 1 kbp downstream. The IIPGA numbering is relative to the start of translation, and as such +105≡+4860, -607≡-9682, and -137≡-9212.

3.2.1 IIPGA - The Ascertainment Panel

IL18 resequencing was carried out in Coriell DNA Samples from 23 CEPH individuals as well as an African-American sample, using standard PCR-based sequencing methods. The data was then freely available online as raw genotypes, and also as phased haplotypes (the data used here). As expected, the genetic variation within the African-American sample exceeded that of the European sample, and as the majority of the study groups upon which the tSNPs would be used were of European origin, this analysis was concerned with the European samples alone.

A total of 56 variants were found in *IL18*. When selecting for SNPs that had a MAF of >10% in the European samples, 31 SNPs were found within the *IL18* region, and it is

Table 3.1: The possible tSNP sets identified by BEST. All sets are equivalent.

Potential set	IIPGA SNPs			
1.	-10373	-9731	-5848	-139
2.	-9731	-5848	-3987	-139
3.	-9731	-5848	-139	+8855
4.	-10373	-9731	-5848	+11015
5.	-9731	-5848	-3987	+11015
6.	-9731	-5848	+8855	+11015
7.	-10373	-9731	-139	+11015
8.	-9731	-3987	-139	+11015
9.	-9731	-139	+8855	+11015
10.	-9731	-3987	-139	+8855

these SNPs that the IIPGA consortium took forward and used for haplotype inference, therefore forming the basis for tSNP selection here.

As can be seen from figure 3.2 on the next page, LD was extremely strong between many of the SNPs, and consequently the number of haplotypes was low (n=13), see figure 3.3 on page 105. Of the 13 haplotypes inferred, six were rare (estimated to occur only once in 46 chromosomes). Such rare haplotypes were excluded from analyses, and therefore seven haplotypes were taken forward as the data-set for tSNP analysis.

3.2.2 BEST and STRAM Analysis

BEST Analysis BEST was run with common (frequency >2%) haplotypes inferred from resequencing data, using SNPs found in European individuals with MAF exceeding 10%. The BEST output is shown in figure 3.4 on page 106. Analysis revealed that the minimum number of SNPs required to tag the haplotypes was four. The possible SNP combinations are shown in table 3.1.

It must be noted that, using the BEST analysis *IL18*+105 (SNP23 in figure 3.4) is equivalent to tSNP2, as is *IL18*-137 (SNP5). Therefore by genotyping *IL18*+105, *IL18*-137 is 'captured', and, according to BEST only a further three SNPs are needed to capture all common genetic variation within *IL18*. Furthermore, *IL18*-607 (SNP4 in figure 3.4) is equivalent to tSNP3.

STRAM Analysis The results from analysis using STRAM can be seen in output 3.1 on page 107. STRAM found that to mark all the genetic variation within the haplotypes, five SNPs were required, with four SNPs performing well but only marking 88.6% of the variation in one of the haplotypes (see figure 3.5 on page 108).

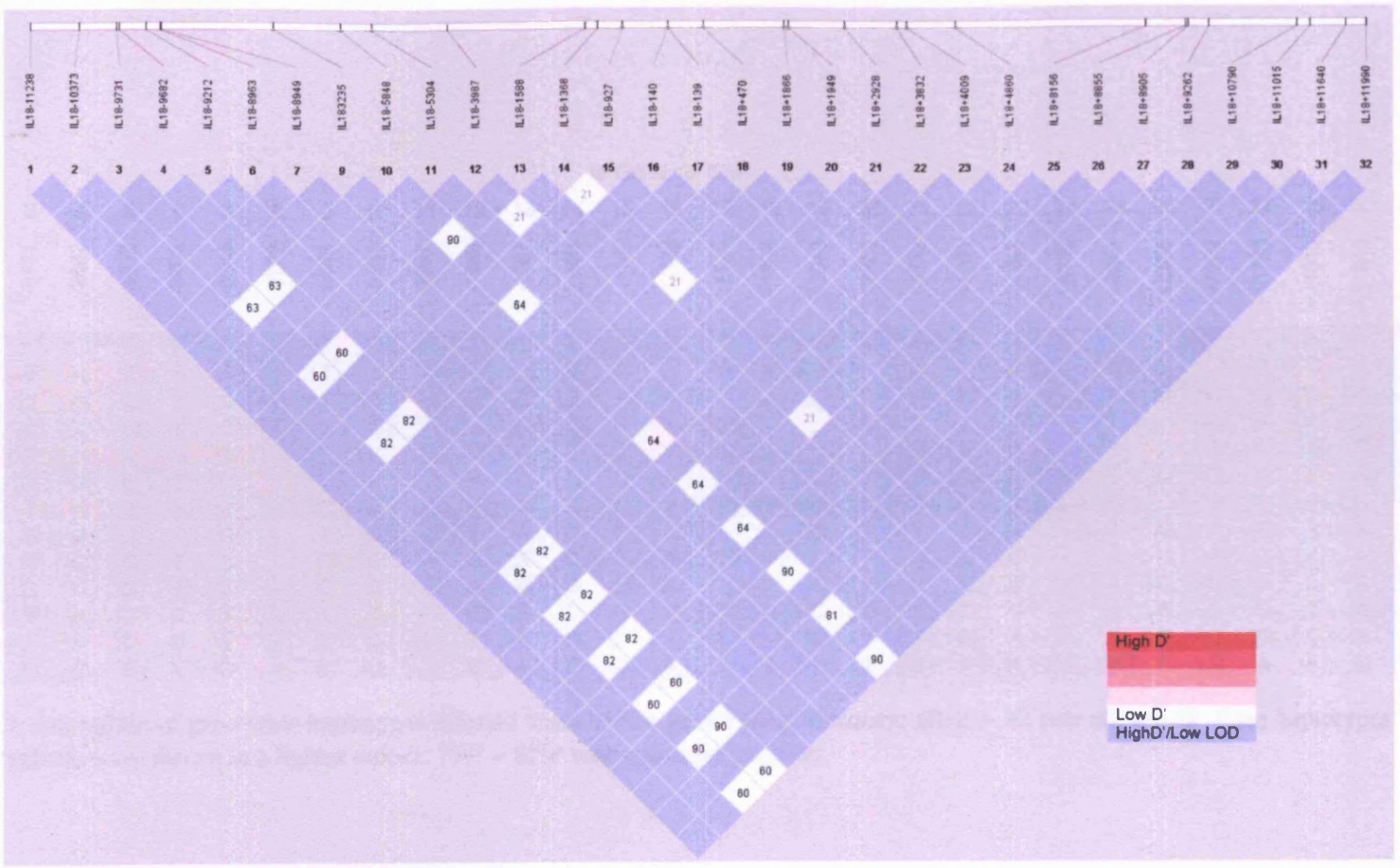

Figure 3.2: Haploview LD plot of common (MAF>10%) SNPs found in the *IL18* region by IIPGA resequencing.

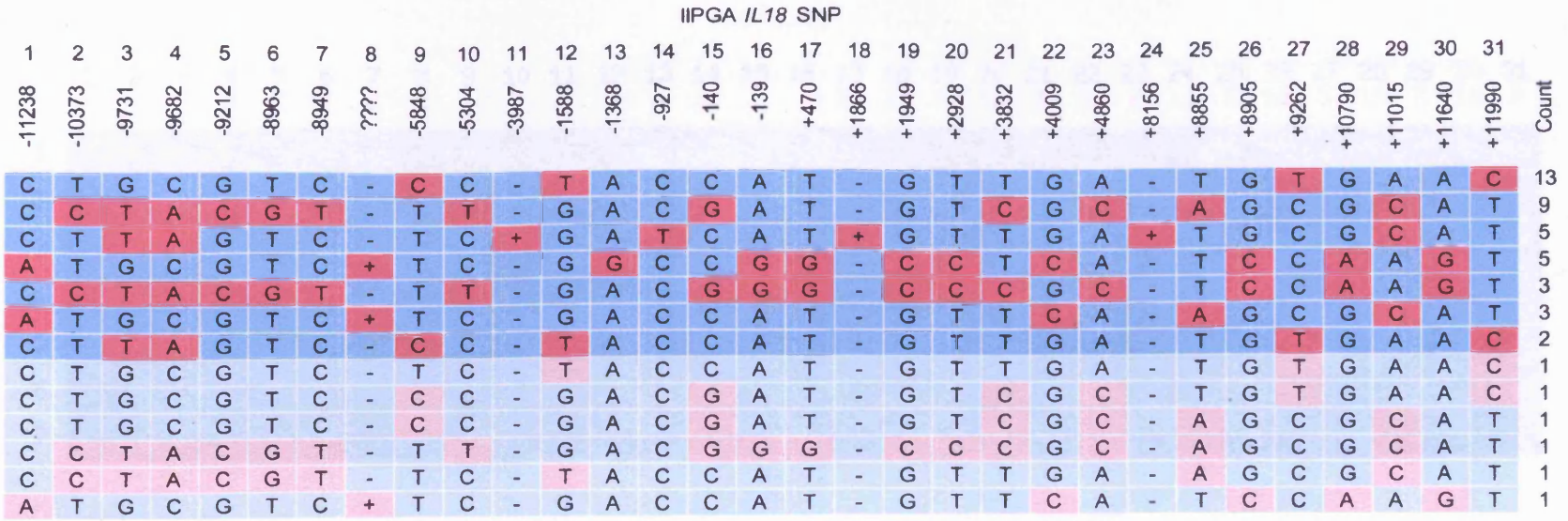

Figure 3.3: Schematic of gene-wide haplotypes inferred from IIPGA genotyping. Common allele – ■; rare allele – ■. Rare haplotypes not used for tSNP selection are shown in a lighter colour. ???? – SNP with unknown position.

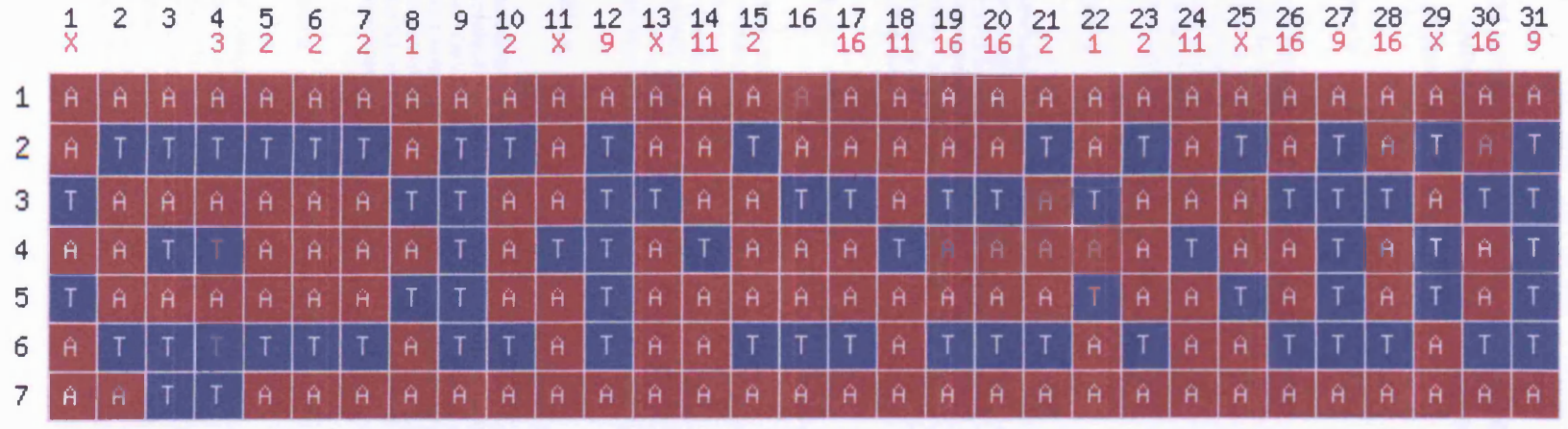

Figure 3.4: Result from BEST analysis using common European haplotypes from IIPGA resequencing.

Output 3.1: STRAM output from IIPGA European samples, using common haplotypes inferred by IIPGA. SNPs are coded so that alleles present on the most common haplotype are 0, and the alternative alleles are 1.

```
Best choice of  1  SNPS= 3
Hnum  Haplotype                          Prob    CumProb Var(Haplo) Var(E(H|G)) R2
        *
    1 00000000000000000000000000000000 0.3250 0.3250  0.43875    0.19113     0.4356
    2 01111110110100100000101010101010 0.2250 0.5500  0.34875    0.11191     0.3209
    3 10000001100110011011010001110l1 0.1250 0.6750  0.21875    0.02827     0.1293
    4 00110000101101000100000010010101 0.1250 0.8000  0.21875    0.03454     0.1579
    5 10000001100100000000001001010101 0.0750 0.8750  0.13875    0.01018     0.0734
    6 01111110110100111011101001110l1 0.0750 0.9500  0.13875    0.01243     0.0896
    7 00110000000000000000000000000000 0.0500 1.0000  0.09500    0.00553     0.0582
 min RSQ= 0.0582

Best choice of  2  SNPS= 3   29
Hnum  Haplotype                          Prob    CumProb Var(Haplo) Var(E(H|G)) R2
        *                          *
    1 00000000000000000000000000000000 0.3250 0.3250  0.43875    0.24896     0.5674
    2 01111110110100100000101010101010 0.2250 0.5500  0.34875    0.18072     0.5182
    3 10000001100110011011010001110l1 0.1250 0.6750  0.21875    0.03683     0.1684
    4 00110000101101000100000010010101 0.1250 0.8000  0.21875    0.05578     0.2550
    5 10000001100100000000001001010101 0.0750 0.8750  0.13875    0.12105     0.8725
    6 01111110110100111011101001110l1 0.0750 0.9500  0.13875    0.07238     0.5217
    7 00110000000000000000000000000000 0.0500 1.0000  0.09500    0.03217     0.3386
 min RSQ= 0.1684

Best choice of  3  SNPS= 1   3   29
Hnum  Haplotype                          Prob    CumProb Var(Haplo) Var(E(H|G)) R2
      * *                          *
    1 00000000000000000000000000000000 0.3250 0.3250  0.43875    0.43875     1.0000
    2 01111110110100100000101010101010 0.2250 0.5500  0.34875    0.18165     0.5209
    3 10000001100110011011010001110l1 0.1250 0.6750  0.21875    0.20331     0.9294
    4 00110000101101000100000010010101 0.1250 0.8000  0.21875    0.05607     0.2563
    5 10000001100100000000001001010101 0.0750 0.8750  0.13875    0.12331     0.8887
    6 01111110110100111011101001110l1 0.0750 0.9500  0.13875    0.07319     0.5275
    7 00110000000000000000000000000000 0.0500 1.0000  0.09500    0.03253     0.3424
 min RSQ= 0.2563

Best choice of  4  SNPS= 2   3   9   25
Hnum  Haplotype                          Prob    CumProb Var(Haplo) Var(E(H|G)) R2
       **     *               *
    1 00000000000000000000000000000000 0.3250 0.3250  0.43875    0.42792     0.9753
    2 01111110110100100000101010101010 0.2250 0.5500  0.34875    0.33938     0.9731
    3 10000001100110011011010001110l1 0.1250 0.6750  0.21875    0.19854     0.9076
    4 00110000101101000100000010010101 0.1250 0.8000  0.21875    0.20792     0.9505
    5 10000001100100000000001001010101 0.0750 0.8750  0.13875    0.12937     0.9324
    6 01111110110100111011101001110l1 0.0750 0.9500  0.13875    0.12937     0.9324
    7 00110000000000000000000000000000 0.0500 1.0000  0.09500    0.08417     0.8860
 min RSQ= 0.8860

Best choice of  5  SNPS= 2   3   9   13  25
Hnum  Haplotype                          Prob    CumProb Var(Haplo) Var(E(H|G)) R2
       **     *   *           *
    1 00000000000000000000000000000000 0.3250 0.3250  0.43875    0.43875     1.0000
    2 01111110110100100000101010101010 0.2250 0.5500  0.34875    0.34875     1.0000
    3 10000001100110011011010001110l1 0.1250 0.6750  0.21875    0.21875     1.0000
    4 00110000101101000100000010010101 0.1250 0.8000  0.21875    0.21875     1.0000
    5 10000001100100000000001001010101 0.0750 0.8750  0.13875    0.13875     1.0000
    6 01111110110100111011101001110l1 0.0750 0.9500  0.13875    0.13875     1.0000
    7 00110000000000000000000000000000 0.0500 1.0000  0.09500    0.09500     1.0000
 min RSQ= 1.0000
```

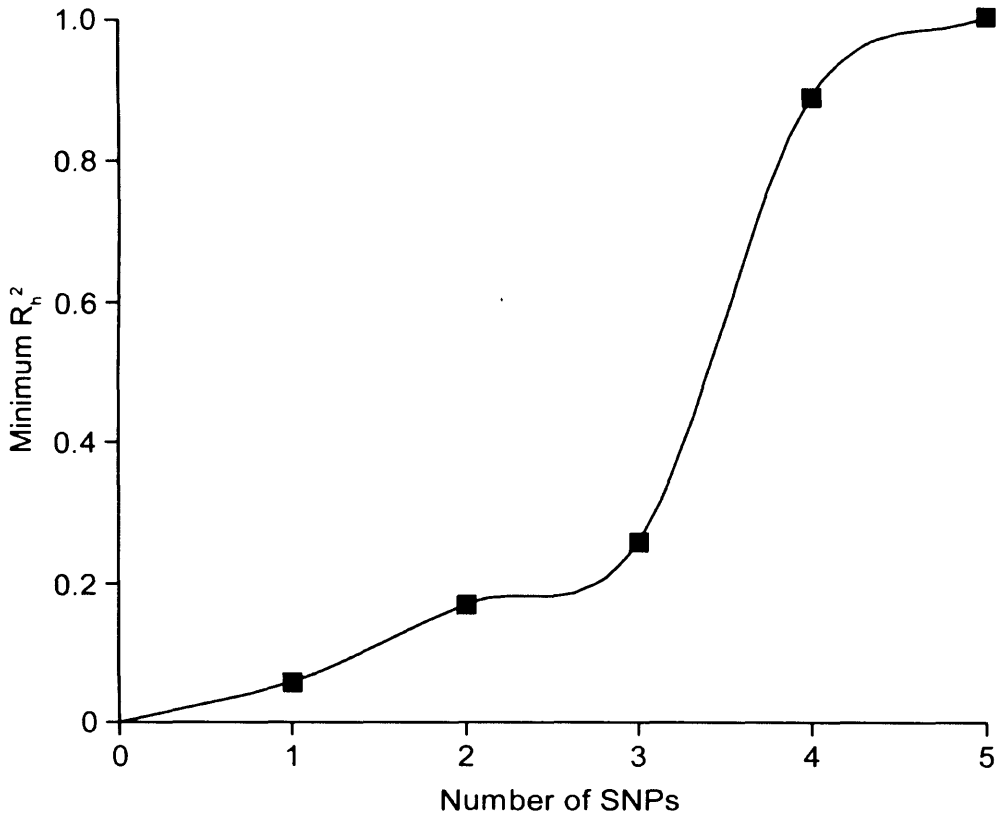

Figure 3.5: STRAM analysis on common European IIPGA haplotypes, showing an increase in minimum R_h^2 with the number of SNPs entered into the tSNP set.

Output 3.2: STRAM output from IIPGA European common haplotypes, forcing in *IL18*-9731, -5848, +105, +8855, and +11015.

```
Hnum  Haplotype                          Prob   CumProb Var(Haplo) Var(E(H|G)) R2
        *     *              * *   *
    1 00000000000000000000000000000000 0.3250 0.3250  0.43875    0.43875     1.0000
    2 01111110110100100000101010101010 0.2250 0.5500  0.34875    0.33938     0.9731
    3 10000001100110011011010000111011 0.1250 0.6750  0.21875    0.20937     0.9571
    4 00110000101101000100000010010101 0.1250 0.8000  0.21875    0.21875     1.0000
    5 10000001100100000000001001010101 0.0750 0.8750  0.13875    0.12937     0.9324
    6 01111110110100111011101001110111 0.0750 0.9500  0.13875    0.12937     0.9324
    7 00110000000000000000000000000000 0.0500 1.0000  0.09500    0.09500     1.0000
 min RSQ= 0.9324
```

Set Selection Neither BEST nor STRAM were in agreement over a single tSNP set to select, though each assigned importance to particular SNPs; SNPs 2 (-10373), 3(-9731), 9 (-5848), 25 (+8855), and 29 (+11015) were repeatedly chosen by each program. Indeed, BEST identified *IL18*-9731, -5848, +8855, and +11015 as a potential tSNP set. However, with this particular set neither *IL18*-137 nor +105 (equivalent SNPs previously genotyped and potentially functional) are directly marked. Therefore, STRAM was used to 'force in' -9731, -5848, +105, +8855, and +11015 and assess how well they performed as a set. The results of this analysis are shown in output 3.2. With these five SNPs, over 90% of the common genetic variation in *IL18* is captured, and it is this tSNP set that was used as the core *IL18* tSNP set throughout the remainder of this work:

-9731 G>T	rs1946519
-5848 T>C	rs2043055
+105 A>C	rs549908
+8855 T>A	rs360729
+11015 A>C	rs3882891

3.2.3 tSNP Validation

Without genotyping all 31 SNPs from which the tSNP set is derived, there is no way to directly test how well the tSNPs mark variation within the study populations used here. However, if haplotype architecture and allele and haplotype frequencies match well, then it is reasonable to assume that the IIPGA sample and the study populations are fairly genetically homogenous. Therefore the tSNP set will mark genetic variation as efficiently as it did in the IIPGA sample set.

Table 3.2: tSNP genotype data comparing 100 European CABG study subjects to 23 European IIPGA samples. Comparison between MAFs carried out in Thesias.

SNP		Count n (%) CABG	IIPGA	p CABG vs. IIPGA
	GG	36 (36.4)	4 (17.4)	
-9731	GT	48 (48.5)	17 (73.9)	0.087
	TT	15 (15.2)	2 (8.7)	
	MAF (%)	39.4	45.6	0.501
	TT	37 (37.0)	10 (43.5)	
-5848	TC	49 (49.0)	9 (39.1)	0.691
	CC	14 (14.0)	4 (17.4)	
	MAF (%)	38.5	37.0	0.838
	AA	38 (38.0)	8 (34.8)	
+105	AC	47 (47.0)	15 (65.2)	0.094
	CC	15 (15.0)	0 (0.0)	
	MAF (%)	38.5	32.6	0.548
	TT	39 (39.0)	8 (34.8)	
+8855	TA	48 (48.0)	15 (65.2)	0.125
	AA	13 (13.0)	0 (0.0)	
	MAF (%)	37.0	32.6	0.640
	AA	28 (28.0)	5 (21.7)	
+11015	AC	51 (51.0)	16 (69.6)	0.226
	CC	21 (21.0)	2 (8.7)	
	MAF (%)	46.5	43.5	0.742

3.2.3.1 European Populations

To test the tSNP set and its efficiency in European samples, 100 European samples from the CABG study, were genotyped for the tSNP set and compared to IIPGA data. All genotype counts in CABG were in agreement with Hardy-Weinberg equilibrium (HWE) ($p>0.05$).

As can be seen from table 3.2, there were no significant differences in genotype counts, or allele frequency between the two groups. Furthermore, there were no significant differences in haplotype frequencies or architecture between the two samples sets (see table 3.3 on the next page). It can therefore be concluded that the tSNP set selected transfered well, and that with this tSNP set >90% of the common genetic variation within *IL18* can be captured in the study samples of European ancestry used here.

Table 3.3: *IL18* haplotype (ordered -9731;-5848;+105;+8855;+11015) frequencies in 100 European CABG study subjects and the European IIPGA samples. Haplotype frequencies inferred in Thesias, using a binary outcome variable (IIPGA or CABG) to test for differences in frequencies between the two groups.

Haplotype		Frequency (%)		p CABG vs.
		CABG	IIPGA	IIPGA
hGCATA	h12111	28.3	30.3	-
hTTCAC	h21222	26.9	30.3	0.495
hGTATA	h11111	19.0	21.7	0.414
hTTATC	h21112	8.0	10.9	0.363
hTCATA	h22111	2.6	4.5	0.353
hGCCAC	h12222	5.0	2.2	0.579

3.2.3.2 African American Populations

The vast majority of the cohorts used in this thesis specifically recruited participants of Caucasian origin. However, these study groups included a minority of individuals of African origin, therefore an appreciation of how well the tSNP set performs in this population was important. The IIPGA resequenced *IL18* in both Europeans and 24 Coriell Repository African Americans.

Applying the same selection criteria as used when selecting the tSNP set (SNP MAF>10%), 30 SNPs were used to infer 8 common haplotypes (and 8 rare haplotypes) by PHASE. All five tSNPs were common in the African American sample and therefore it was possible to 'force in' these SNPs in STRAM analysis. As shown in output 3.3 on the following page, the tSNP set performed poorly in the African American sample. It successfully distinguished only one haplotype (hTTCAC), whilst R_h^2 for the other seven haplotypes ranged from 0.065 to 0.813. To satisfactorily capture variation in all haplotypes, at least another three SNPs were required – SNP24 (+9262), SNP25 (+9583), SNP26 (IIPGA21446). These results imply that haplotype analysis in African Americans using this tSNP set would be under-powered, due to the great deal of genetic variation present within *IL18* in Africa, to which these tSNPs are naïve.

3.2.4 Identifying Important Variation Outside of the *IL18* Region

The *IL18* region resequenced by IIPGA stretches from 2 kbp upstream to 1 kbp downstream. Although this region covers the proximal promoter, it is possible that there are other elements, further upstream of *IL18*, that are important in determining gene regulation and expression. Because it is likely that these elements are conserved across species, the area further upstream of *IL18* was investigated using Vista, a program that

Output 3.3: STRAM output from IIPGA African Americans haplotypes. The first pass is the five tSNPs alone, the next four passes build on this set until R^2_h=1.

```
Hnum  Haplotype                        Prob   CumProb Var(Haplo) Var(E(H|G)) R2
       *      *           * *   *
    1 00000000100010000000000001000001 0.3998 0.3998  0.47990    0.39036     0.8134
    2 00000011000001101101000000 1000 0.1501 0.5498  0.25508    0.13532     0.5305
    3 00000000000000010010000000101000 0.0996 0.6495  0.17942    0.05966     0.3325
    4 11111100010000010010101000 1000 0.0996 0.7491  0.17942    0.17942     1.0000
    5 01100000001100100100010001 1110 0.0996 0.8487  0.17942    0.07919     0.4413
    6 01100000001100100100000000 1000 0.0504 0.8992  0.09576    0.02028     0.2118
    7 01100000001100100100010010 1000 0.0504 0.9496  0.09576    0.02028     0.2118
    8 00000000100010000000000000000001 0.0504 1.0000  0.09576    0.00621     0.0648
 min RSQ= 0.0648

Best choice of  6  SNPS= 2   9   21  23  24  27
Hnum  Haplotype                        Prob   CumProb Var(Haplo) Var(E(H|G)) R2
       *      *           * **  *
    1 00000000100010000000000001000001 0.3998 0.3998  0.47990    0.47990     1.0000
    2 00000011000001101101000000 1000 0.1501 0.5498  0.25508    0.13532     0.5305
    3 00000000000000010010000000101000 0.0996 0.6495  0.17942    0.05966     0.3325
    4 11111100010000010010101000 1000 0.0996 0.7491  0.17942    0.17942     1.0000
    5 01100000001100100100010001 1110 0.0996 0.8487  0.17942    0.07919     0.4413
    6 01100000001100100100000000 1000 0.0504 0.8992  0.09576    0.02028     0.2118
    7 01100000001100100100010010 1000 0.0504 0.9496  0.09576    0.02028     0.2118
    8 00000000100010000000000000000001 0.0504 1.0000  0.09576    0.09576     1.0000
 min RSQ= 0.2118

Best choice of  7  SNPS= 2   9   21  23  24  26  27
Hnum  Haplotype                        Prob   CumProb Var(Haplo) Var(E(H|G)) R2
       *      *           * ** **
    1 00000000100010000000000001000001 0.3998 0.3998  0.47990    0.47990     1.0000
    2 00000011000001101101000000 1000 0.1501 0.5498  0.25508    0.13532     0.5305
    3 00000000000000010010000000101000 0.0996 0.6495  0.17942    0.05966     0.3325
    4 11111100010000010010101000 1000 0.0996 0.7491  0.17942    0.17942     1.0000
    5 01100000001100100100010001 1110 0.0996 0.8487  0.17942    0.17942     1.0000
    6 01100000001100100100000000 1000 0.0504 0.8992  0.09576    0.04534     0.4735
    7 01100000001100100100010010 1000 0.0504 0.9496  0.09576    0.04534     0.4735
    8 00000000100010000000000000000001 0.0504 1.0000  0.09576    0.09576     1.0000
 min RSQ= 0.3325

Best choice of  8  SNPS= 2   9   21  23  24  25  26  27
Hnum  Haplotype                        Prob   CumProb Var(Haplo) Var(E(H|G)) R2
       *      *           * *****
    1 00000000100010000000000001000001 0.3998 0.3998  0.47990    0.47990     1.0000
    2 00000011000001101101000000 1000 0.1501 0.5498  0.25508    0.24905     0.9763
    3 00000000000000010010000000101000 0.0996 0.6495  0.17942    0.17339     0.9663
    4 11111100010000010010101000 1000 0.0996 0.7491  0.17942    0.17942     1.0000
    5 01100000001100100100010001 1110 0.0996 0.8487  0.17942    0.17942     1.0000
    6 01100000001100100100000000 1000 0.0504 0.8992  0.09576    0.08972     0.9369
    7 01100000001100100100010010 1000 0.0504 0.9496  0.09576    0.08972     0.9369
    8 00000000100010000000000000000001 0.0504 1.0000  0.09576    0.09576     1.0000
 min RSQ= 0.9369

Best choice of  9  SNPS= 2   7   9   21  23  24  25  26  27
Hnum  Haplotype                        Prob   CumProb Var(Haplo) Var(E(H|G)) R2
       *    * *           * *****
    1 00000000100010000000000001000001 0.3998 0.3998  0.47990    0.47990     1.0000
    2 00000011000001101101000000 1000 0.1501 0.5498  0.25508    0.25508     1.0000
    3 00000000000000010010000000101000 0.0996 0.6495  0.17942    0.17942     1.0000
    4 11111100010000010010101000 1000 0.0996 0.7491  0.17942    0.17942     1.0000
    5 01100000001100100100010001 1110 0.0996 0.8487  0.17942    0.17942     1.0000
    6 01100000001100100100000000 1000 0.0504 0.8992  0.09576    0.09576     1.0000
    7 01100000001100100100010010 1000 0.0504 0.9496  0.09576    0.09576     1.0000
    8 00000000100010000000000000000001 0.0504 1.0000  0.09576    0.09576     1.0000
 min RSQ= 1.0000
```

assesses sequence similarity across species.

The genomic sequence 10 kbp upstream of *IL18*, from human and mouse, was submitted to Vista. This region includes testis-expressed gene 12 (*TEX12*), which transcribes away from *IL18* and therefore shares the promoter region. There is currently no literature describing functional polymorphisms within the *TEX12* promoter. The resulting Vista plot for the *IL18* gene and 10 kbp upstream, is shown in figure 3.6 on the next page. The plot shows no areas of significant sequence conservation between mouse and human, other than those in exonic regions and the area already resequenced by IIPGA. Therefore, with the absence of evidence suggesting areas outside of the immediate *IL18* region that may be important in gene regulation, this study deals solely with genetic variation within, and immediately surrounding, the *IL18* gene.

3.2.5 Evolutionary History of *IL18*

Having an understanding of the process of haplotype evolution, ie. the ancestral haplotype and the interrelatedness of the other common haplotypes, can aid later data analysis [Bardel et al., 2005]. With an accurate tree of haplotype evolution haplotypes can be grouped according to common ancestors, and furthermore knowing how haplotypes relate to one another can help to assess likely functional variants for any haplotype differences seen. Therefore, to establish the ancestral *IL18* haplotype, each tSNP's genotype was ascertained in a panel of primate samples. To establish the phylogenetic relationship of the haplotypes, haplotypes present in the CABG study and 95 Ethiopians, were used.

3.2.5.1 Ancestral Haplotype

That polymorphisms found in human samples, are also polymorphic in primate populations is highly unlikely, as it is expected that the forces of genetic drift and selection will cause one or other of the primate alleles to become extinct. However, some forms of selection will protect genetic variation and increase the average lifespan of a polymorphism, possibly indefinitely. Collectively such forces are called 'balancing selection' and can arise by a number of causes [Asthana et al., 2005]:

Overdominance or heterozygote advantage The heterozygous form of the polymorphism has an advantage over either homozygous form. This therefore often maintains a deleterious phenotype in the population.

Frequency dependence An advantage is conferred by a rare feature; for example, mate preference for unique phenotype.

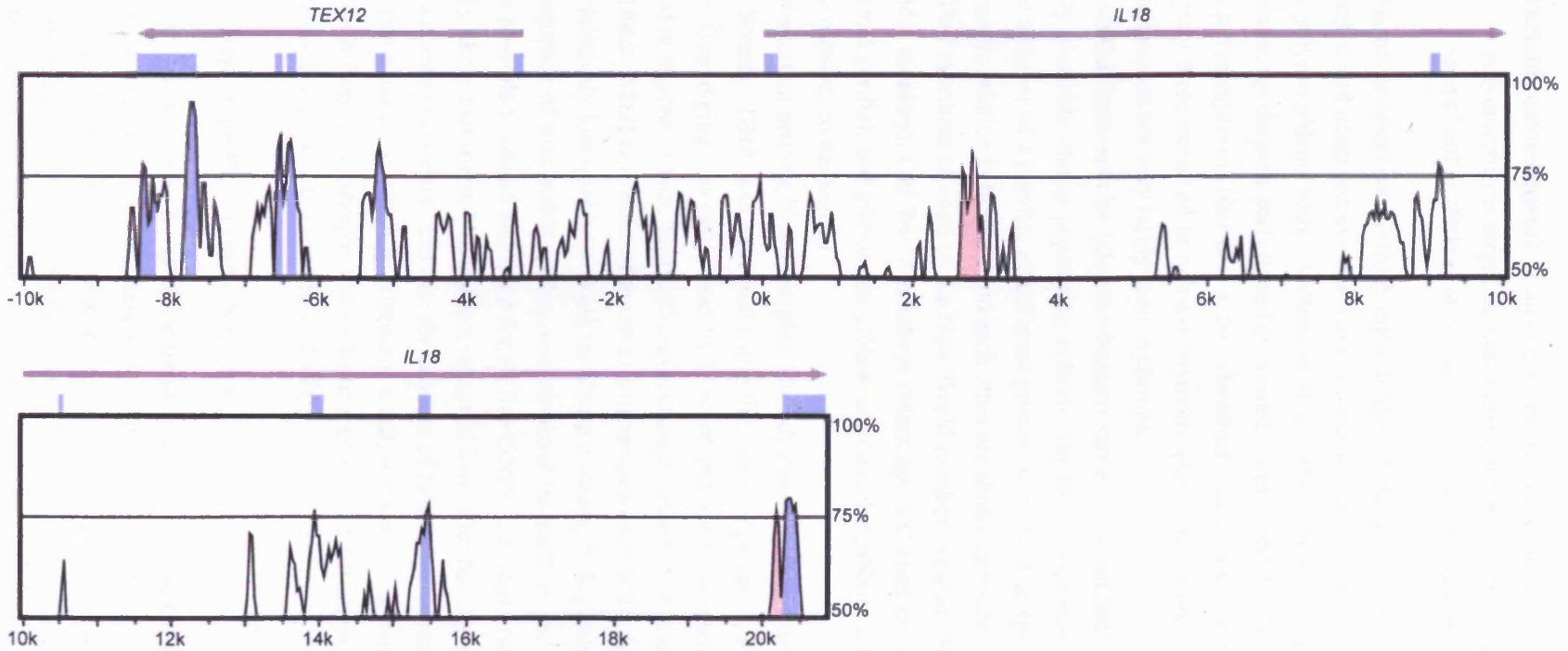

Figure 3.6: Vista plot for *IL18* and the region 10 kbp upstream. The plot compares human to mouse, and shows areas of significant conservation in both exonic (■) and non-exonic (■) regions.

Variable environments If an organism occupies multiple environments, polymorphisms might be maintained in the population if the possession of either allele is advantageous in a different environment.

If balancing selection is strong enough then the lifetime of a polymorphism could be extended and observed in closely related species. To establish how common trans-species polymorphisms were, Asthana et al. [2005] studied variation in several large chimp transcript datasets and aligned the variation onto dbSNP. They found eight trans-species polymorphisms (out of 1×10^4 identified human SNPs within the region), of which only three occurred at non-synonymous sites, suggesting that polymorphisms found in humans are very rarely seen in chimps.

Given that trans-species (chimp⇒human) variation is extremely rare, and the lack of easily available chimp population cohorts, the tSNP sequence was established in a single member of a number of different primate species. The species used, and their phylogenetic relation to humans and each other are shown in figure 3.7 on the following page. Two members of each of the New World monkeys (golden headed lion tamarin and spider monkey), Old World monkeys (black ape and entellus langur), Hominidae (chimp and gorilla), and gibbon (lar gibbon and concolor gibbon) families were chosen as close relatives to the human.

Post-mortem primate blood samples (300 µl) were obtained from the London Zoological Society. DNA was extracted using the standard protocol, adjusted for sample volume. Genotyping was carried out by forward and reverse sequencing, with primers designed in regions of high human:chimp sequence conservation, using a human:chimp BLAT [Kent, 2002] alignment of the areas surrounding each tSNP. In all samples, DNA was of relatively low quality, making obtaining a strong PCR product difficult. However, sequence of reasonable quality was obtained for each of the tSNPs, although it was not possible to obtain sequence for all five tSNPs in a single sample. Given that it is highly likely that the polymorphism occurred long after humans and these primates shared a common ancestor, and that the chances of two independent variants occurring at the same genomic position is extremely small, it is satisfactory to take the genotype information from each sample and so form a composite haplotype. In doing so, the ancestral haplotype was found to be hTTATC.

3.2.5.2 Haplotype Phylogenetic Network

Due to various pressures on haplotype frequencies, the current haplotypes observed in the CABG cohort will not accurately reflect all haplotypes derived from the ancestral one. Therefore, in order to gain greater information on haplotypes derived from the ancestral haplotype, a sample of 95 Ethiopians was selected and analysed in tandem with the CABG samples genotyped above, giving a more accurate picture of the relationship

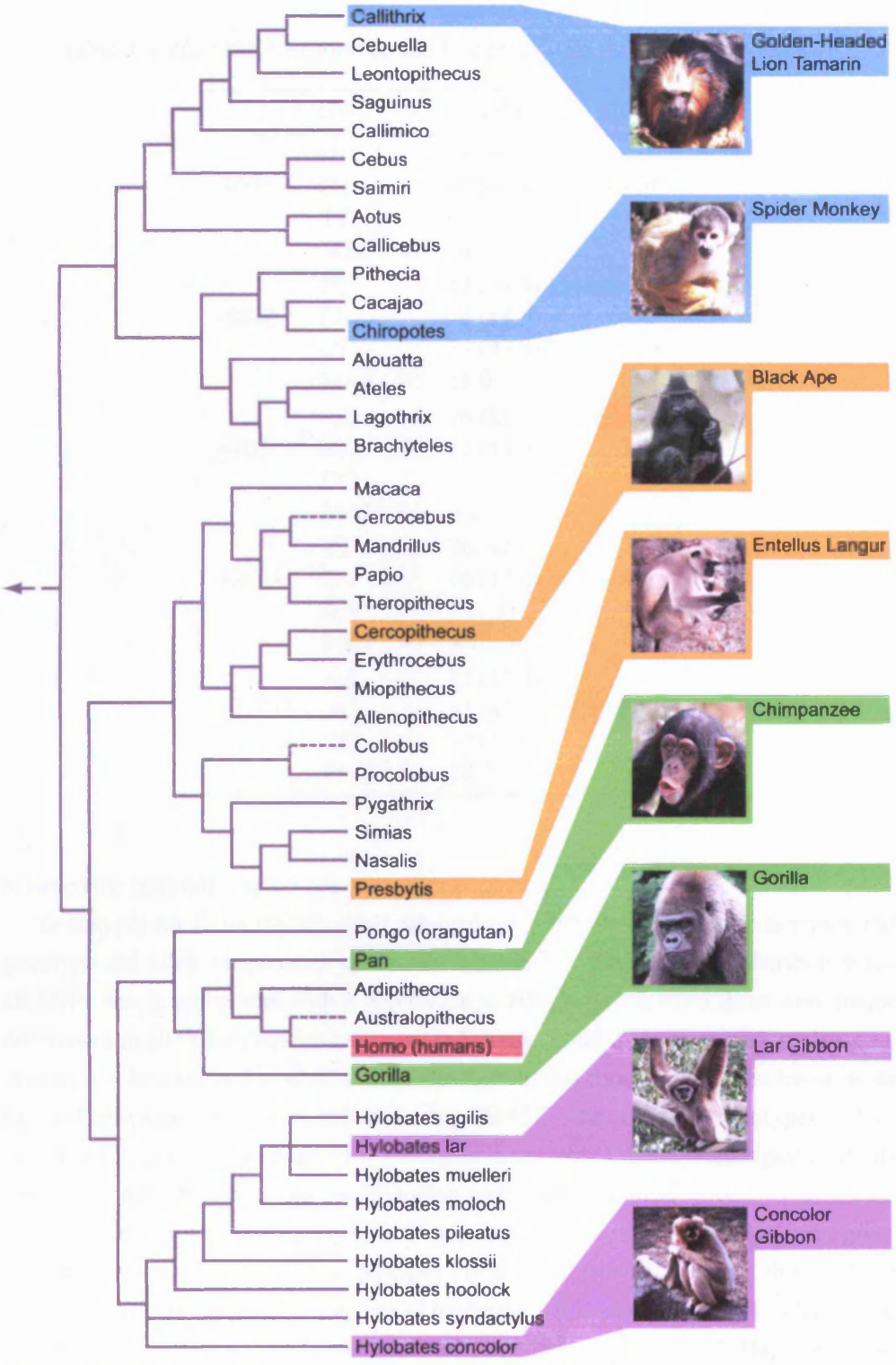

Figure 3.7: Phylogenetic tree of the primate samples used. Two members of the New World monkeys (■), Old World monkeys (■), hominides (■), and gibbons (■) were chosen as close relatives to humans (■).

Table 3.4: *IL18* tSNP genotypes and frequency data for Ethiopian samples.

SNP		Count n (%)	HWE p
	GG	55 (57.9)	
-9731	GT	34 (35.8)	0.809
	TT	6 (6.3)	
	MAF (%)	24.2	
	TT	12 (13.3)	
-5848	TC	39 (43.3)	0.651
	CC	39 (43.3)	
	MAF (%)	35.0	
	AA	76 (81.7)	
+105	AC	17 (18.3)	0.332
	CC	-	
	MAF (%)	9.1	
	TT	76 (81.7)	
+8855	TA	16 (17.2)	0.878
	AA	1 (1.1)	
	MAF (%)	9.7	
	AA	15 (17.4)	
+11015	AC	41 (47.7)	0.878
	CC	30 (34.9)	
	MAF (%)	58.7	

between the common haplotypes.

Genotypes for all five tSNPs were obtained for >90% of the Ethiopian samples, the genotype and allele frequencies are shown in table 3.4. The genotype distribution for all SNPs was in agreement with a population in HWE. As expected there were major differences in allele frequencies between the Ethiopian and CABG samples, such observations will be explored in more detail elsewhere in this thesis. Haplotype frequencies for the Ethiopian sample were inferred using PHASE. The common haplotypes (>1%) are shown in table 3.5 on page 119, and again, as expected, there were significant differences in frequency between the Ethiopian and CABG samples.

Assessing haplotype frequency and architecture in two different population gives a more accurate picture of the haplotypes currently in existence. From this, and the primate data (that identifies the ancestral haplotype), it is possible to infer a haplotype tree that illustrates how each haplotype coalesces back to the ancestral. Haplotypes appear to be derived from two separate clades, with SNPs +8855 and +105 occurring in one clade and -9731, -5848, and +11015 occurring on the other. Two remaining haplotypes, apparently not possibly formed by mutations on haplotypes alone, are seemingly formed by recombination events (see figure 3.8 on the next page). hTCATA appears to

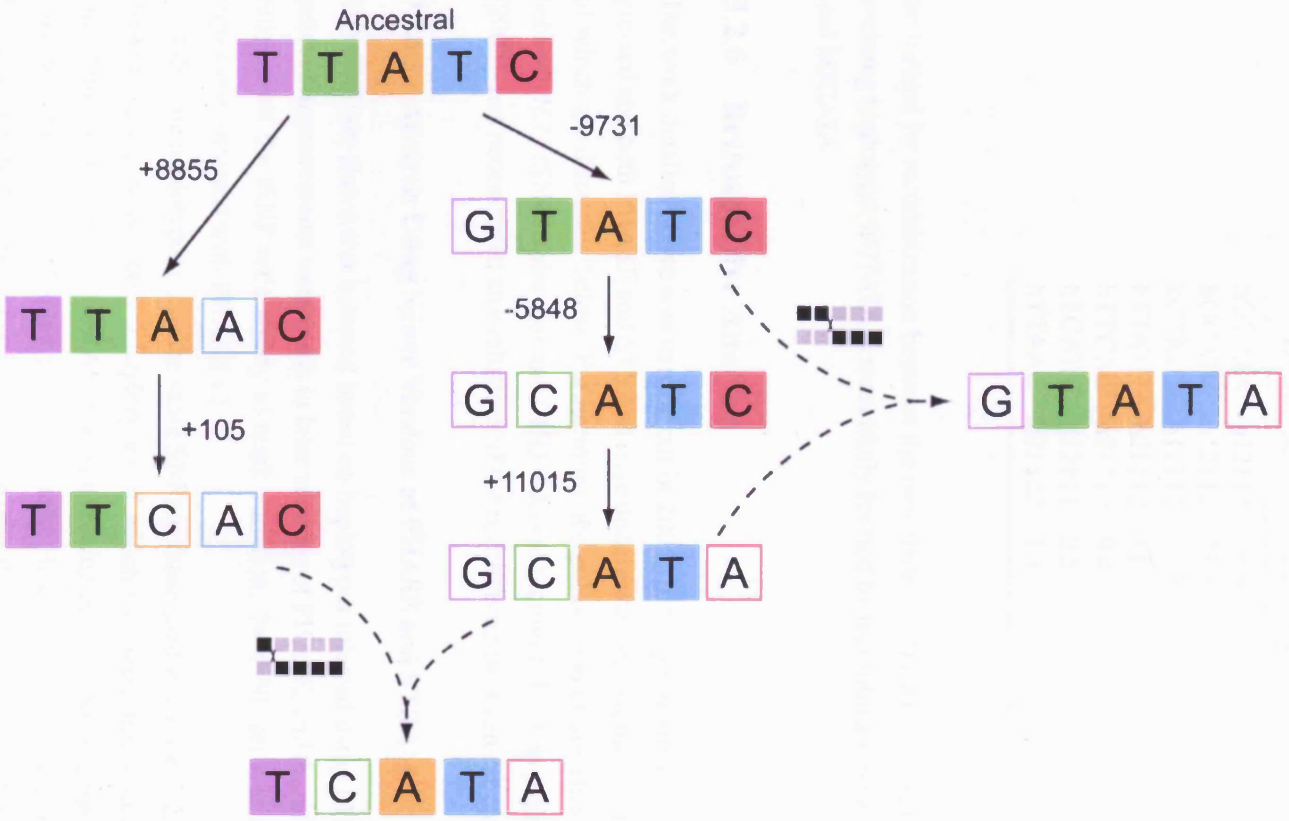

Figure 3.8: An inferred haplotype tree for *IL18* common haplotypes. Structure is derived from common haplotypes in both Ehtiopian and European samples. Closed square (■) indicates same allele as ancestral haplotype, whilst open square (□) indicates variant allele. Haplotypes are ordered -9731 (■); -5848 (■); +105 (■); +8855 (■); +11015 (■), and recombination events are indicated by dotted arrows.

Table 3.5: Common *IL18* haplotype frequencies in an Ethiopian sample. Haplotypes are ordered -9731; -5848; +105; +8855; +11015 with 1/2 designation related to allele frequencies within the European populations.

Haplotype		Frequency (%)
hGCATA	h12111	38.3
hGCATC	h12112	23.8
hGTATC	h11112	13.7
hTTATC	h21112	11.1
hTTCAC	h21222	9.4
hTCATA	h22111	2.5
hTTAAC	h21122	1.1

be formed by recombination between the two clades (hTTCAC and hGCATA). The remaining haplotype, hGTATA is most likely formed by recombination between hGTATC and hGCATA.

3.2.6 Retrospective Analysis

The work detailed above was carried out in 2004. In the years since, the field has progressed and both PHASE and STRAM have undergone improvements, the implications of which are discussed below. Furthermore, the publication of significant associations between *IL18* tSNP haplotypes and CHD risk (see section 1.4.1.3 on page 54, Tiret et al. [2005]) has necessitated an evaluation of the relationship between the two tSNPs set.

3.2.6.1 Analysis Using Newer Versions of PHASE and STRAM

The tSNP set above was selected based on haplotypes inferred using PHASE v.1. Significant improvements were made in later versions of PHASE, and therefore, as a better estimate of the tSNP set's ability to mark variation, the tSNP set was assessed using haplotypes inferred with PHASE v2.1.

Inferring haplotypes using the same SNPs as those used in section 3.2.1 on page 102, PHASE v2.1 reconstructed 8 haplotypes of which two were rare (occurring on only one chromosome). When STRAM was run forcing in the tSNP set, the set performed fairly well marking four haplotypes completely. However, overall the minimum R^2_h was 0.388, whilst another haplotype had an R^2_h of only 0.499 (see output 3.4 on the following page). With the addition of one other SNP, -1368 A>G, all haplotypes reached an R^2_h of 1. Using STRAM v2 had no effect on these results, returning the same results as those with STRAM v1.

Output 3.4: STRAM output from IIPGA European common haplotypes, inferred using PHASE v2.1. The first pass is the result of forcing in the tSNP set, with the second pass building on this.

```
Hnum  Haplotype                          Prob  CumProb Var(Haplo) Var(E(H|G))  R2
        *     *              * *   *
    1 01111110010000100000010101000100  0.3180  0.3180 0.43375    0.43375    1.0000
    2 00000000100100000000000000010001  0.3180  0.6360 0.43375    0.43375    1.0000
    3 10000001000010011011010001010101  0.1140  0.7500 0.20201    0.10080    0.4990
    4 00110000001001000100000010000100  0.1140  0.8640 0.20201    0.20201    1.0000
    5 10000001000000011011010001010101  0.0910  0.9550 0.16544    0.06423    0.3882
    6 00110000100100000000000000010001  0.0450  1.0000 0.08595    0.08595    1.0000
 min RSQ= 0.3882

Best choice of  6  SNPS= 3   9   13  23  25  29

Hnum  Haplotype                          Prob  CumProb Var(Haplo) Var(E(H|G))  R2
        *     *   *          * *   *
    1 01111110010000100000010101000100  0.3180  0.3180 0.43375    0.43375    1.0000
    2 00000000100100000000000000010001  0.3180  0.6360 0.43375    0.43375    1.0000
    3 10000001000010011011010001010101  0.1140  0.7500 0.20201    0.20201    1.0000
    4 00110000001001000100000010000100  0.1140  0.8640 0.20201    0.20201    1.0000
    5 10000001000000011011010001010101  0.0910  0.9550 0.16544    0.16544    1.0000
    6 00110000100100000000000000010001  0.0450  1.0000 0.08595    0.08595    1.0000
 min RSQ= 1.0000
```

3.2.6.2 tSNP Relevance to Tiret et al. [2005]

The only study to have investigated the relevance of *IL18* SNPs in CHD risk, found a significant association between one *IL18* haplotype, hGCAGT, IL-18 levels, and CHD risk [Tiret et al., 2005]. The haplotypes were formed of *IL18*G-887T, C-105T, S35S, A+183G, and T+533C, equivalent to IIPGA SNPs -9731, -8949, +105, +11640, and +11990. When Tiret et al. [2005] SNPs were aligned onto haplotypes inferred (by PHASE v2.1) from IIPGA data, hGCAGT was found to be equivalent to the tSNP haplotype hGTATA (see figure 3.9 on the next page). In this retrospective analysis using PHASE v2.1, hGTATA marked two, common, gene-wide haplotypes, along with one rarer haplotype. Tiret's hGCAGT marked the same two common gene-wide haplotypes as hGTATA, therefore hGTATA marked the very same genetic variation as Tiret's hGCAGT does. In Tiret et al. [2005], hGCAGT was associated with lower production of IL-18 compared to the reference (most common) haplotype, hGCAAC. hGCAAC is equivalent to tSNP haplotype hGCATA, and hGCATA only. Therefore in conclusion, while the tSNP set used here is distinct from that used by Tiret et al. [2005], the haplotypes derived from both sets are closely related and can be easily related to one another.

3.3 tSNP Selection in *IL18BP*

IL18BP tSNP selection was carried out by Carmel Stock at The Department of Immunology and Molecular Pathology, University College London. Genotyping data for

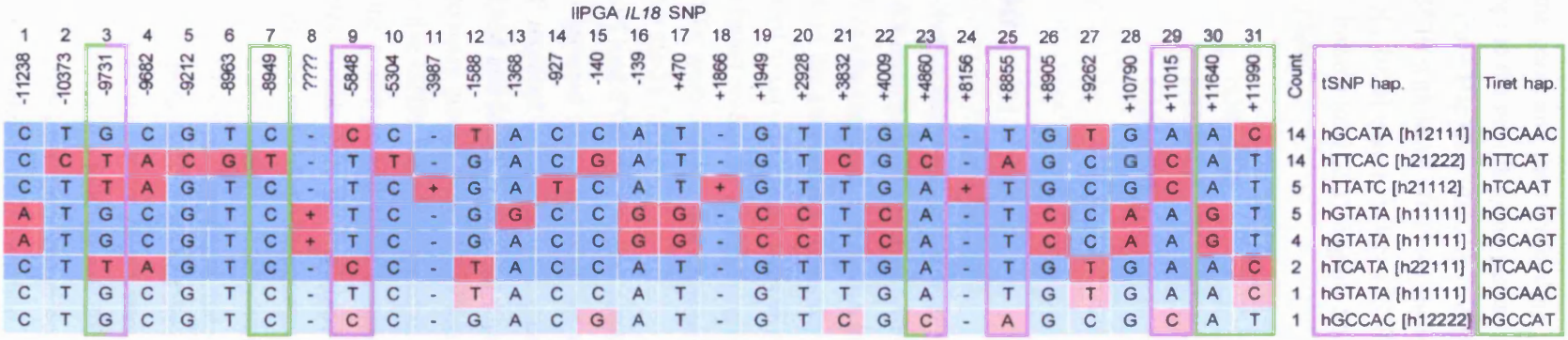

Figure 3.9: The relationship between Tiret et al. [2005] haplotypes (■) and the tSNP haplotypes used here (■). Both -9731 and +105 (+4860) were used by Tiret et al. [2005] and in this thesis. Haplotypes were inferred from IIPGA European samples, using PHASE v2.1.

all the SNPs within the gene, and the surrounding sequence both upstream (1.5 kbp) and downstream (3 kbp) to the next flanking genes (in total 8.8 kbp) were obtained for the CEPH population from HapMap (data release 18/phaseII) and IIPGA. The combined data set for all SNPs with MAF>0.05 was opened in Haploview version 3.0, and Tagger [de Bakker et al., 2005] used to select a tSNP set, using pairwise tagging with a minimum R^2 of 0.8. From a total of 31 eligible SNPs, three SNPs were selected and form the tSNP set used here:

-1765 T>C	rs3814721
-559 T>G	rs2298455
+3041 C>T	rs1541304

3.4 Discussion

The results from this chapter demonstrate that with a panel of only eight SNPs, a substantial proportion of common genetic variation within the immediate genomic area of both *IL18* and *IL18BP*, can be captured. For *IL18*, a total of 31 common European polymorphisms were found in the gene region. Using two subtly different approaches, the number of SNPs required to capture greater than 90% was reduced to just five. A total of 31 SNPs were also found within the *IL18BP* region when including common European SNPs. Three tSNPs were isolated that captured greater than 80% of the genetic variation represented by the 31 SNPs.

For *IL18*, both BEST and STRAM returned results that shared a number of SNPs. The STRAM results suggested that a five-SNP set represented the start of a plateau in the number of SNP required to capture total genetic variation. By combining the results from both STRAM and BEST, a tSNP set was isolated that, when 'forced in' in STRAM, was shown to mark greater than 93% of the common variation in *IL18*.

To test this set, the five tSNPs were genotyped in 100 participants from the CABG study. As expected, the genotype and allele frequencies did not differ significantly from the IIPGA samples, furthermore the haplotype frequencies did not differ either. These results suggest that the individuals resequenced by IIPGA, and those recruited into the study groups used here, were genetically homogenous and therefore the tSNP set should translate well. However, it appears that certain inaccuracies in the initial haplotype inference have significantly weakened the strength of the tSNP set.

Using haplotypes inferred by a more recent version of PHASE, the tSNP set was found to perform poorly, capturing a minimum of 39% of the variation within the common European haplotypes. However, only one more SNP was required to completely distinguish all of the the identified genetic variation – -1368 A>G. The importance of

this in the results presented later will be discussed in the following chapters.

The region of the genome resequenced by IIPGA begins 2 kbp upstream of *IL18* and ends 1 kbp downstream of the gene. It is entirely possible that there are areas of the genome, outside of this region, that have a major effect on *IL18* gene expression. Therefore comparative genomics was used to find regions of the genome, surrounding *IL18*, that have been conserved across species and therefore may contain important regulatory sequences. *TEX12* is located 3 kbp upstream from *IL18*, and the genes transcribe away from each other, therefore sharing immediate promoters. The only regions that appeared to be significantly conserved between humans and mouse, within the 10 kbp region studied, were the exons of *TEX12*. Without any evidence for important sequences in this region, the subject of this thesis relates to genetic variation found only in the immediate gene region.

To gain a greater understanding of the evolutionary relationship between the common tSNP haplotypes, a haplotype network was formed using haplotypes seen in both European and African individuals. The starting point of the haplotype network was the ancestral haplotype, that was established using a number of primate samples. This ancestral haplotype was hTTATC, which was observed at relatively common frequencies ($\sim$10%) in both European and African populations. Given the assumptions that a mutation can only occur once and that recombination events were to be kept to a minimum, a haplotype network connecting each of the common haplotypes was drawn. In this scheme recombination events formed both hGTATA and hTCATA.

The origin of the recombinatory event that formed hGTATA is not clear from this data. That hGTATA is not evident in the Ethiopian sample could suggest that this event may have occurred following human's migration out of Africa, however that one of the haplotypes involved, hGTATC, is not found in European populations could suggest that the event occurred in Africa but that hGTATA was subsequently lost, or that the event occurred outside of Africa but that hGTATC was subsequently lost. Without further study of African and Asian populations, this cannot be resolved.

The only other study to investigate *IL18* whole-gene variation was that by Tiret et al. [2005]. They showed a significant association between a single haplotype and both IL-18 levels and CHD risk. Their tSNP was not identical to that selected here, but using the IIPGA data it was possible to show that there is good correspondence between the haplotypes they identified and those identified here.

In conclusion, in this chapter we have established a set of SNPs that allow whole-gene variation within both *IL18* and *IL18BP* to be studied. The following chapters use this tool to assess the impact of variation within *IL18* on IL-18 levels and individual risk for CHD and obesity.

Chapter 4

Variation Within *IL18*'s Impact on IL-18 Levels

The aim of this chapter is to assess the impact of genetic variation in *IL18* and *IL18BP*, marked by the tSNP sets selected in the previous chapter, on levels of IL-18 and IL-18BP in a number of different studies. Given that in some studies both IL-18 and IL-18BP have been measured, it is possible to calculate the amount of fIL-18. Therefore any genetic variation, associated with differences in either IL-18 or IL-18BP production, may also influence fIL-18 levels and so have pathological consequences.

4.1 Introduction

To fully take advantage of all genetic information held within the tSNP set, a number of new approaches, building on traditional statistical techniques, are needed.

4.1.1 Haplotype Association Analysis

In order to better characterize the role of genetic variation in the etiology of complex traits, full haplotypic information should be exploited. However, without family data, haplotypic information is not readily obtained, except from individuals homozygous at all loci, or heterozygous at only one. Therefore such information must be estimated, or inferred, and there has been a good deal of interest in developing statistical methods and algorithms for performing such analyses. One of the major algorithms used is the EM algorithm. A stochastic version of the EM algorithm, the SEM algorithm, was developed and shown to be computationally less burdensome and more appropriate in coping with missing data [Tregouet et al., 2004].

The SEM algorithm is an iterative procedure. At each iteration, an ambiguous haplotype pair, considered as a type of missing data, is replaced by a simulated value drawn

from a distribution, given the observed data and the parameters estimated from the previous iteration. The starting point for the algorithm is haplotype frequencies assuming linkage equilibrium, and then a stochastic-expectation step is carried out whereby the unobserved haplotypic pair of an ambiguous set of genotypes is set at a single draw from the distribution of compatible haplotype pairs. Following this, the maximization step updates the haplotype frequencies given the pseudo-observed haplotypes, and takes these into another stochastic-expectation step. The result is that, after a sufficiently long 'burn-in' period, the haplotype distribution reaches stationarity, and therefore the estimated haplotype frequency is simply the mean of the frequency in this stationary distribution [Tregouet et al., 2004].

To perform association analysis, the end haplotype distribution is associated with the phenotype, assuming an equal contribution of each haplotype in the haplotype pair (additivity), and a normal distribution to the trait. This therefore yields haplotype ORs, or haplotypic means, for the phenotype. Assessments of significance are carried out using a t-test comparing each haplotype to the reference haplotype (the most common haplotype) [Tregouet et al., 2002].

In simulation studies, the bias of haplotype frequencies was negligible in large samples, whatever the number of polymorphisms involved and the true haplotype frequency. However, rare haplotype ($<2\%$) determination became challenging, especially as the number of polymorphisms increased, since the number of compatible haplotypes associated with the genotypic data also increased. The same conclusions could also be drawn for the estimation of haplotypic effects, with these being most accurate in large samples (n=1000) with common haplotypes, and slightly less accurate in moderate samples (n=400) when the ORs are associated with rare haplotypes. Overall the SEM algorithm performed well and was more trustworthy than alternative approaches [Tregouet et al., 2004].

4.1.2 Searching for Epistasis

It is inevitable that to understand the genetic susceptibility to common human disease, such as CHD, the possibility of gene-gene interactions (epistasis) must be considered. Indeed, epistasis is arguably a ubiquitous component of the genetic architecture of disease susceptibility [Moore, 2003].

Epistasis exists both as a statistical and biological phenomenon. Biological epistasis is the result of interactions between biomolecules within gene regulatory networks in an individual, such that the effect of a gene is dependent on one or more other genes. In contrast, statistical epistasis is a mathematical observation, where the relationship between genotype and phenotype is not predictable solely considering the single genotype. It is the fusion of these two forms of epistasis that is at the basis of systems

Table 4.1: Penetrance values of genotypes for two SNPs exhibiting interactions in the absence of independent main effects.

		SNP1			Margin
		AA (0.25)	Aa (0.50)	aa (0.25)	penetrance
SNP2	BB (0.25)	0	1	0	0.5
	Bb (0.50)	1	0	1	0.5
	bb (0.25)	0	1	0	0.5
	Margin penetrance	0.5	0.5	0.5	

biology, and has much promise for the future.

The importance of statistical epistasis is best illustrated using a simple penetrance function, detailing the probability of disease, given a genotype. The example shown in table 4.1 details an extreme model whereby two SNPs, in linkage equilibrium, interact such that neither SNP alone has a main effect, but when only Aa or Bb, but not both, are present are subjects at high risk of disease (p=1). Otherwise individuals are at low risk (p=0). The margin penetrances show that these do not differ between single SNP genotypes [Moore and Williams, 2005].

4.1.2.1 Assessing Epistasis with MDR

As the evidence for statistical epistasis in complex disease research increases, a number of statistical tools have been developed to characterize this phenomenon. The MDR approach has identified significant epistasis in a number of diseases including hypertension and TIIDM [Moore and Williams, 2005]. MDR is a nonparametric data-mining alternative to logistic regression for identifying nonlinear interactions among discrete genetic variations and environmental factors. With MDR, multilocus genotypes are pooled into high-risk and low-risk combinations, thereby reducing the dimensionality of the genotype predictors (attributes) from n dimensions to one dimension. This new multilocus genotype attribute can then be evaluated to see how well it predicts disease status [Moore et al., 2006].

A schematic of the MDR process is illustrated in figure 4.1 on the next page. The first step is to randomly split the sample into ten, $\frac{9}{10}$ forms the training set and $\frac{1}{10}$ the testing set. The training set is used to classify each genotype combination as either low- or high-risk depending on the ratios of cases and controls that are present in that genotype combination (model), compared to the total ratio of cases to controls. This analysis is repeated ten times to use each possible testing set. For each genotype combination, TBA and CVC are reported. The TBA is the mean of sensitivity and specificity (as shown in equation (4.1) on the following page, where TP is true positives, FN–false

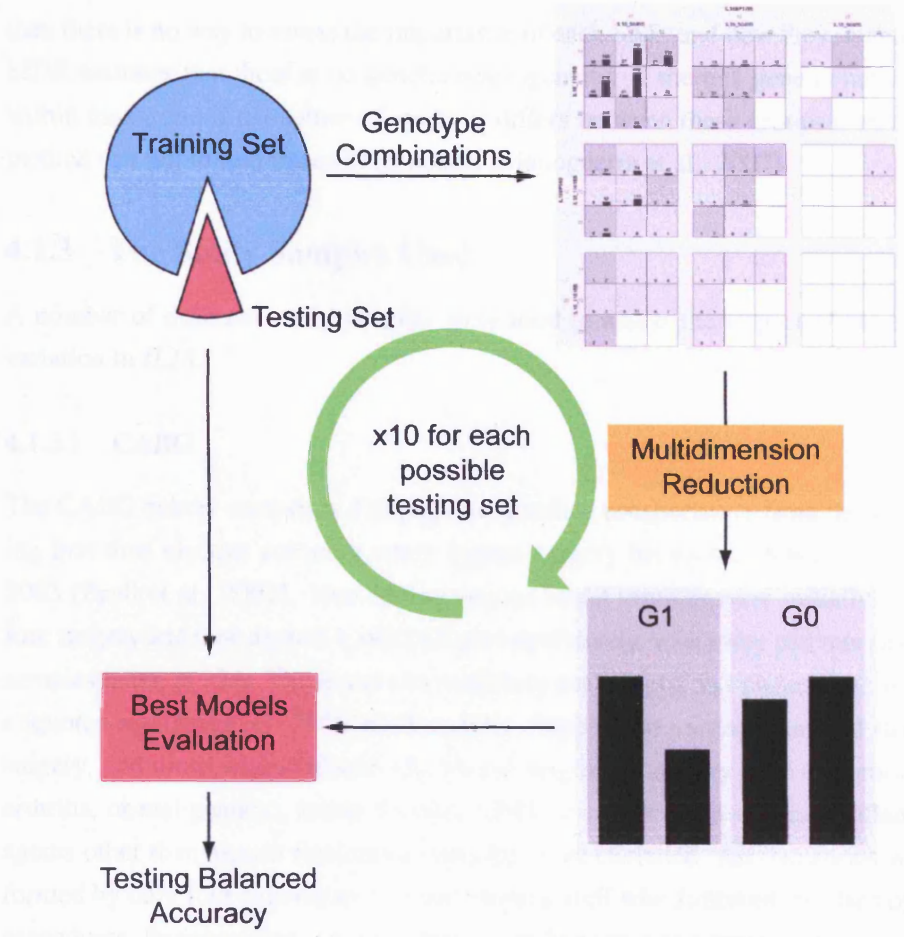

Figure 4.1: A Schematic of the MDR approach in identifying SNP:SNP interactions.

negatives, TN–true negatives). TBA assesses the performance of each model in the testing set, while the CVC is the number of times a particular combination of loci is identified as a high-risk combination in each testing set. The data presented here is of the SNP combination which produces the highest TBA in each run.

$$\begin{aligned} TBA &= \frac{(TP/(TP+FN)+TN/(TN+TP))}{2} \\ &= \frac{\text{sensitivity}+\text{specificity}}{2} \end{aligned} \tag{4.1}$$

To assess the magnitude and significance of TBA, the status of cases and controls in the sample can be permuted 1000 times and therefore a distribution for TBA and CVC for each genotype combination can be formed.

Although, at present the MDR approach appears to be of great promise, the results are difficult to interpret. If a strong main effect is present then it is difficult to understand the contributions of other polymorphisms, and if there are multidimensional interactions

then there is no way to assess the importance of each SNP, and how they interact. Also, MDR assumes that there is no genetic heterogeneity. If there is genetic heterogeneity within cases, and if the nature of epistasis differs between these groups then the MDR method can fail to find the correct models [Manuguerra et al., 2007].

4.1.3 The Study Samples Used

A number of different study samples were used to assess the impact of the identified variation in *IL18*.

4.1.3.1 CABG

The CABG cohort comprises 439 patients recruited prospectively from those undergoing first time elective coronary artery bypass surgery between October 1999 and July 2003 [Brull et al., 2001]. Non-fasting venous blood samples were initially drawn before surgery and then again 6 h and 24 h post-operatively, with some patients also having samples taken at 72 h. These were immediately centrifuged and plasma was separated, aliquoted and frozen at $-20\,^{\circ}C$ until analysis. Aspirin was routinely omitted 10 d before surgery, and those with evidence of a preexisting inflammatory state (infection, active arthritis, or malignancy), active unstable CHD, or concurrent use of anti-inflammatory agents other than aspirin (including steroids), were excluded. All operations were performed by only four experienced senior surgical staff who followed standard operating procedures. Perioperative anticoagulation with heparin was reversed after surgery with the use of protamine sulfate. At recruitment, a 5 ml EDTA sample of peripheral blood was drawn, from which DNA was extracted by use of the salting out method (see section 2.1.1 on page 68). Written informed consent was obtained from all participants. IL-18 and IL-18BP was measured by Daniella Novick (Weizmann Institute of Science, Israel) using a commercially available ELISA (MBL Co. Ltd.) and a novel ELISA method [Novick et al., 2001], respectively (see section 2.3 on page 87). The *IL18* tSNP set was genotyped using RFLP, whilst the *IL18BP* tSNPs was genotyped using TaqMan protocols. IL-6 and CRP were measured by Gordon Lowe, Department of Medicine, University of Glasgow, using a standard commercial assay (R&D Systems) and a BN Prospec (Dade Behring) respectively.

4.1.3.2 NPHSII

The second Northwick Park Heart Study (NPHSII) is a large prospective study of healthy middle-aged (50–61 yr) men from nine UK general practices, totalling 3052 men [Miller et al., 1996]. The study has been ongoing for 15 yr and men were followed-up throughout the study for CHD events. All men with a history of unstable angina, MI,

CBVD, life-threatening malignancy, or regular medication with aspirin or anticoagulants were excluded. A fasting blood sample was taken upon enrollment, and baseline characteristics and demographic information was obtained by means of a questionnaire completed at entry to the study. IL-18 and IL-18BP was again measured by Daniella Novick using the same methods as above. Both *IL18* and *IL18BP* tSNPs were genotyped using TaqMan protocols. CRP was measured using a commercial assay (Cordia High Sensitivity CRP) by Dave Howarth, Wolfson Institute, St. Bartholomew's Hospital, London.

4.1.3.3 CUDAS

The CUDAS cohort was a random electoral roll sample of 1111 subjects (558 men and 553 women) aged 27–77 yr from Perth, Western Australia [McQuillan et al., 1999]. Subjects who had previous carotid artery surgery were excluded. A self-administered questionnaire was used to record a history of smoking, hypertension, hyperlipidemia, diabetes, angina, MI, stroke, or a family history of premature-onset MI or stroke by age 55 yr in first degree relatives. Anthropometric measurements and the lower of two BP measurements recorded. Written informed consent was obtained from all study participants. A fasting blood sample was obtained from each subject, and IL-18 was measured at the University of Western Australia by ELISA (MBL Co. Ltd.). The *IL18* tSNP set was genotyped using TaqMan.

4.1.3.4 CUPID

The Carotid Ultrasound in Patients with Ischaemic Heart Disease Study (CUPID) was collected in Perth, Western Australia, in 1995, and consisted of 556 predominantly male subjects, 26–60 yr, with CHD. All subjects were medically stable at the time of data collection but had a history of angina, unstable angina, or MI and angiographically demonstrated CHD with at least one coronary vessel with >5% stenosis [McCaskie et al., 2006]. IL-18 was measured at the University of Western Australia by ELISA (MBL Co. Ltd.). The *IL18* tSNP set was genotyped using TaqMan protocols.

4.1.3.5 SCARF

The Stockholm Coronary Artery Risk Factor Study (SCARF) is a case-control cohort of survivors of a first MI before 60 yr, who were admitted to the coronary care units (CCUs) of three hospitals in the northern part of Stockholm. Exclusion criteria were TIDM, renal insufficiency, any known chronic inflammatory disease, drug addiction, psychiatric disease, or inability to comply with the protocol. For each postinfarction patient a sex- and age-matched control was recruited from the general population of the same catchment area [Eriksson et al., 2004]. Venous blood samples were drawn

in the morning after a 12 h fasting period, and immediately centrifuged with aliquots of plasma stored at −80 °C until use. IL-18 was measured by Per Eriksson, Atherosclerosis Research Unit, Karolinska Hospital, using a commercially available ELISA (R&D systems Inc.). Both IL-6 and CRP were also measured at the Atherosclerosis Research Unit using a commercially available ELISA (R&D Systems) and the BN system (Dade Behring) respectively. The *IL18* tSNP set was genotyped using TaqMan.

4.2 Results

4.2.1 Study Baseline Characteristics

As can be seen from table 4.2 on the next page, the six studies used here represent, in total, a cross-section of the European population. As expected, the studies using exclusively diseased individuals (CABG and CUPID) have a less favourable risk profile. Both CABG and CUPID participants have higher BMI, more diabetes, and higher triglycerides than the healthy/population-based cohorts (NPHSII and CUDAS), and were also, on the whole, older. Total cholesterol was lower in both CABG and CUPID than either CUDAS and NPHSII, although this is likely due to the pervasive use of cholesterol-lowering medication in these cohorts. The baseline characteristics in SCARF are those of both cases and controls; all variables are in the same range as the other studies, suggesting that comparisons are possible between the studies.

4.2.2 Single SNP Univariate Analysis

Raw IL-18 measurements from all populations used here were not normally distributed, therefore ln-transformation was carried out for both total IL-18 and fIL-18 so that parametric tests could be applied. Raw IL-18BP levels were also non-normally distributed and required a square root transformation for normality.

4.2.2.1 CABG

For measurements of IL-18 and IL-18BP in CABG, only those samples with sufficient plasma still available from baseline, 6 h, and 24 h were used (n=248). For these individuals who also had sufficient plasma from 48 h, measurements were made at this time-point also. The analysis presented in this chapter is based upon this subset.

IL-18 As can be seen from table 4.3 on page 132, all tSNPs were in HWE within the CABG subset and genotypes were ascertained for >99% of all individuals for all tSNPs. IL-18 levels were significantly different by *IL18*-5848T>C only, with levels higher in carriers of the C allele. This effect was observed at both baseline and 6 h, but

Table 4.2: Baseline characteristics of the study groups used. Data is presented as geometric mean[95% CI].

Variable	CABG (491)	NPHSII (3052)	CUDAS (1109)	CUPID (556)	SCARF (774)
Males, %[n]	70.1[344]	100[3052]	50.3[558]	87.6[487]	82.3[637]
Age (yr)	64[63–65]	56[56–56]	53[52–54]	50[50–50]	52[52–53]
BMI (kg/m^2)	28.1[27.6–28.6]	26.2[26.1–26.3]	26.1[25.9–26.3]	28.2[27.9–28.5]	26.4[26.1–26.7]
SBP (mmHg)	ND[1]	137[136–138]	128[127–129]	126[125–127]	128[127–130]
DBP (mmHg)	ND	84[83–84]	80[79–81]	81[80–82]	81[80-82]
Diabetes, %[n]	15.9[78]	2.5[75]	2.1[23]	15.8[88]	ND
Past History of MI %[n]	30.8[151]	0[0]	5.7[63]	61.3[341]	ND
Cholesterol-lowering medication, %[n]	64.0[314]	0[0]	6.8[75]	66.7[371]	ND
Ever smoked, %[n]	64.4[316]	68.9[2104]	6.8[75]	72.8[406]	67.1[520]
Total cholesterol (mmol/l)	4.5[4.4–4.6]	5.6[5.6–5.6]	5.6[5.5–5.7]	5.2[5.1–5.3]	5.2[5.1–5.2]
LDL (mmol/l)	2.5[2.4–2.6]	1.8[1.8–1.9]	3.6[3.5–3.7]	3.2[3.1–3.3]	3.3[3.2–3.4]
HDL (mmol/l)	1.2[1.2–1.3]	0.8[0.8–0.8]	1.3[1.3–1.3]	1.1[1.1–1.1]	1.2[1.2–1.2]
Triglycerides (mmol/l)	ND	1.8[1.8–1.8]	1.3[1.3–1.3]	2.0[1.9–2.1]	1.4[1.4–1.5]

[1]No data

Table 4.3: Geometric mean [95% CI] IL-18 levels by *IL18* genotype, at baseline, 6 h, 24 h, and 48 h. Genotype completeness and frequency data is also provided.

tSNP (% genotypes)		Count, %[n]	HWE p	IL-18[95% CI] (pg/ml) Baseline	p/ R^2 (%)	6 h	p/ R^2	24 h	p/ R^2	Count, %[n]	48 h	p/ R^2
-9731 (99.2)	GG	35.4[87]	0.58	222.5[161.7–306.3]	0.53/ 0.7	461.8[401.3–531.6]	0.30/ 1.1	220.4[165.7–293.2]	0.41/ 0.9	44.1[26]	413.9[272.8–627.9]	0.34/ 3.8
	GT	46.7[115]		183.8[147.8–228.6]		391.5[334.9–457.7]		273.1[223.9–333.2]		42.4[25]	503.7[361.6–701.6]	
	TT	17.9[44]		179.9[123.0–263.2]		443.3[351.2–559.6]		267.7[189.9–377.3]		13.6[8]	692.4[493.3–971.8]	
-5848 (100.0)	TT	35.9[89]	0.07	136.9[105.9–176.8]	0.002/ 6.3	344.8[289.8–410.3]	0.004/ 5.0	235.0[180.9–305.3]	0.77/ 0.3	25.4[15]	674.0[557.9–814.2]	0.14/ 6.7
	TC	52.4[130]		229.0[186.9–280.7]		469.2[413.0–533.0]		262.9[217.4–317.8]		59.3[35]	459.8[335.8–629.5]	
	CC	11.7[29]		312.3[158.9–613.7]		523.7[408.5–671.4]		266.6[159.9–444.4]		15.3[9]	332.5[130.5–847.4]	
+105 (99.6)	AA	47.0[116]	0.91	181.7[138.4–238.5]	0.67/ 0.4	450.5[395.8–512.9]	0.56/ 0.5	230.1[182.6–289.9]	0.36/ 1.0	55.9[33]	430.2[313.9–589.7]	0.54/ 2.2
	AC	42.9[106]		212.8[168.5–268.8]		404.8[342.0–479.1]		285.5[233.8–348.7]		35.6[21]	551.8[357.0–853.1]	
	CC	10.1[25]		200.1[134.4–298.0]		406.2[311.7–529.4]		229.2[129.3–406.5]		8.5[5]	582.4[406.3–834.9]	
+8855 (99.2)	TT	45.1[111]	0.92	197.7[150.9–258.9]	0.91/ 0.1	462.8[405.4–528.3]	0.31/ 1.1	216.5[168.4–278.4]	0.08/ 2.6	51.7[30]	420.0[297.5–592.9]	0.50/ 2.5
	TA	44.3[109]		203.8[160.6–258.7]		401.5[341.0–472.6]		302.3[250.6–364.6]		39.7[23]	535.2[360.2–795.3]	
	AA	10.6[26]		180.4[119.3–272.8]		383.3[289.2–508.2]		210.3[130.1–340.1]		8.6[5]	617.1[423.4–899.6]	
+11015 (99.2)	AA	32.1[79]	0.91	206.4[145.2–293.3]	0.93/ 0.1	486.8[419.6–564.6]	0.11/ 2.0	215.1[157.7–293.3]	0.27/ 1.3	34.5[20]	371.8[225.7–612.4]	0.19/ 5.9
	AC	48.8[120]		199.6[161.6–246.6]		386.4[332.6–448.8]		282.0[233.4–340.7]		50.0[29]	506.1[367.7–696.6]	
	CC	19.1[47]		188.7[131.5–270.7]		445.1[356.4–555.8]		243.8[175.7–338.3]		15.5[9]	694.7[554.1–871.1]	

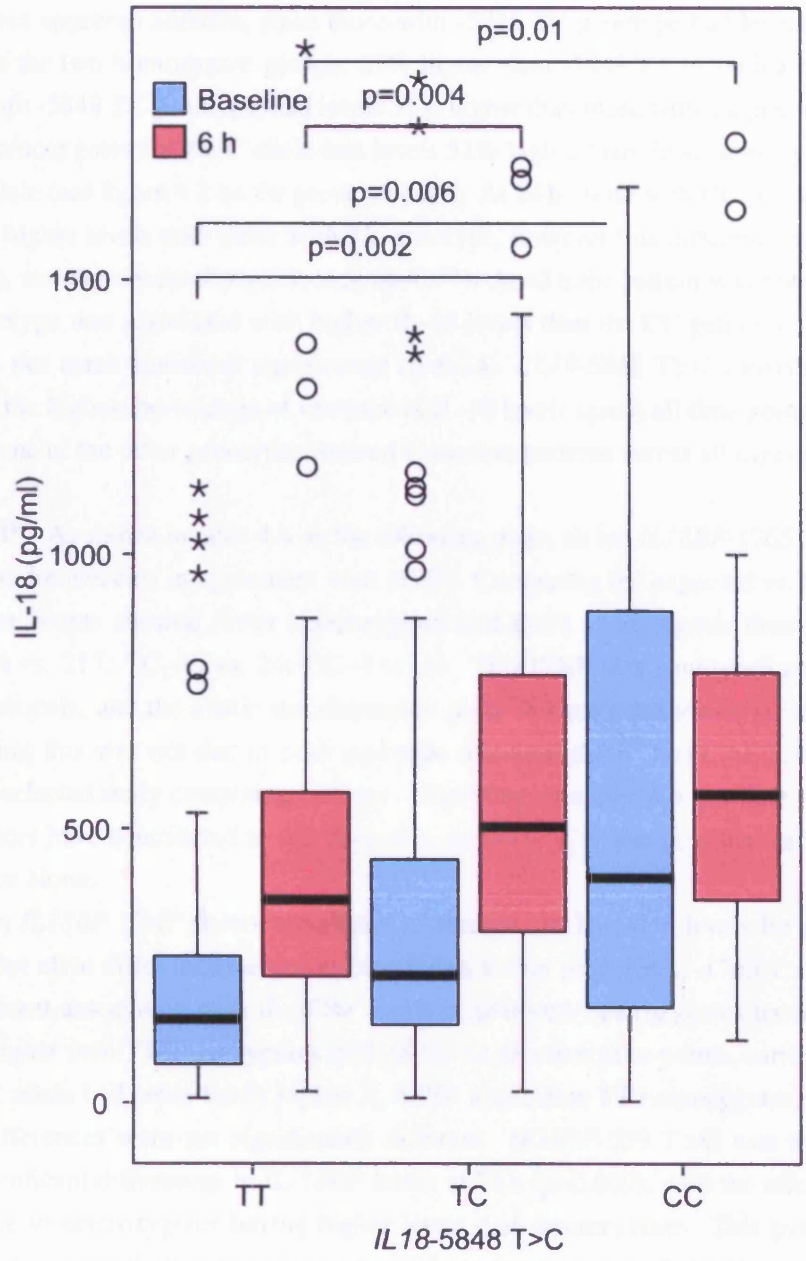

Figure 4.2: A boxplot of raw IL-18 levels by *IL18*-5848 T>C genotypes at both baseline and 6 h in CABG. Line – Median; Box – 75th to 25th percentile; ∘ – outlier (>1.5 box lengths out of box); ⋆ – extreme (>3 box lengths out of box); whisker – last value not an outlier.

not at 24 h or 48 h. The effect at baseline was such that at baseline those with -5848 CC genotype had mean IL-18 levels 128% greater than those with -5848 TT genotype. The effect appeared additive, since those with -5848 TC genotype had levels midway between the two homozygote groups, 67% higher than -5848 TT individuals. At 6 h, those with -5848 TC genotype, had levels 36% higher than those with TT genotype, and those homozygotes for the C allele had levels 52% higher than those homozygotes for the T allele (see figure 4.2 on the previous page). At 24 h, those with CC genotype tend to have higher levels than those with TT genotype, however this difference was slight (13.4%), and did not reach significance (p=0.77). At 48 h the pattern was reversed; the TT genotype was associated with higher IL-18 levels than the CC genotype, however this did not reach statistical significance (p=0.14). *IL18*-5848 T>C consistently explained the highest percentage of variance in IL-18 levels across all time-points, except 24 h. None of the other genotypes showed consistent patterns across all time-points.

IL-18BP As shown in table 4.4 on the following page, all but *IL18BP*-1765 T>C had genotype frequencies in agreement with HWE. Comparing the expected vs. observed genotype counts showed fewer heterozygotes and more homozygotes than expected (TT–214 vs. 217; TC–30 vs. 24; CC–4 vs. 1). This tSNP was genotyped using TaqMan protocols, and the allelic discrimination plots showed good genotype separation suggesting this was not due to poor genotype discrimination. The CABG study is a heavily selected study containing patients of differing ethnicity, it is possible that these two factors have contributed to this deviation, however it is also possible that it is due to chance alone.

Each *IL18BP* tSNP shows significant differences in IL-18BP levels by genotype group, but all at different time-points (see figure 4.3 on page 136). -1765 T>C shows a significant association with IL-18BP levels at 48 h with heterozygotes having levels 201% higher than TT homozygotes (p=0.005). At all other time-points, carriers of the -1765 C allele had consistently higher IL-18BP levels than TT homozygotes, however these differences were not significantly different. *IL18BP*-559 T>G was associated with significant differences in IL-18BP levels at 24 h (p=0.009), with the effect seemingly due to heterozygotes having higher levels than homozygotes. This pattern was consistent across all other time-points but did not reach statistical significance. Those patients heterozygous at *IL18BP*+3041 C>T had 193% higher IL-18BP levels at 48 h than CC homozygotes (p=0.01), a pattern that was again consistent across all other time-points but did not reach statistical significance. On the whole each SNP explains very little of the variation in IL-18BP levels, except at 48 h where both -1765 and +3041 explain >10%.

Table 4.4: Geometric mean [95% CI] IL-18BP levels by *IL18BP* genotype, at baseline, 6 h, 24 h, and 48 h in CABG. Genotype completeness and frequency data is also provided.

tSNP (% genotypes)	geno-	Count, %[n]	HWE p	IL-18BP[95% CI] (pg/ml) Baseline	p/R^2	6 h	p/R^2	24 h	p/R^2	Count, %[n]	48 h	p/R^2
-1765 (98.8)	TT	88.6[217]	0.002	4783[4421–5159]	0.79/ 0.2	2805[2532–3093]	0.92/ 0.1	12943[12336–13565]	0.38/ 0.8	85.0[51]	11480[10116–12931]	0.005/ 13.7
	TC	9.8[24]		5162[4265–6145]		2864[2188–3631]		13712[11974–15569]		15.0[9]	17199[13311–21585]	
	CC	1.6[4]		5142[1762–10289]		3215[1945–4804]		15827[9961–23046]		0[0]	—	
-559 (98.8)	TT	77.9[190]	0.44	4772[4413–5144]	0.75/ 0.2	2748[2466–3045]	0.57/ 0.5	12600[11974–13241]	0.009/ 3.9	81.7[49]	12157[10652–13763]	0.67/ 0.3
	TG	21.3[52]		5069[4195–6026]		3079[2501–3717]		14815[13518–16170]		18.3[11]	12940[9390–17058]	
	GG	0.8[2]		4264[0–56871]		2370[208–6879]		11925[3915–78945]		0[0]	—	
+3041 (98.4)	CC	95.1[233]	0.69	4798[4452–5158]	0.48/ 0.2	2788[2531–3058]	0.76/ <0.1	13004[12417—13604]	0.37/ 0.3	90.2[55]	11709[10390–13106]	0.01/ 10.6
	CT	4.9[12]		5379[4164–6750]		2970[1996–4137]		14279[12076–16666]		9.8[6]	17769[12024–24634]	
	TT	0[0]		—		—		—		0[0]	—	

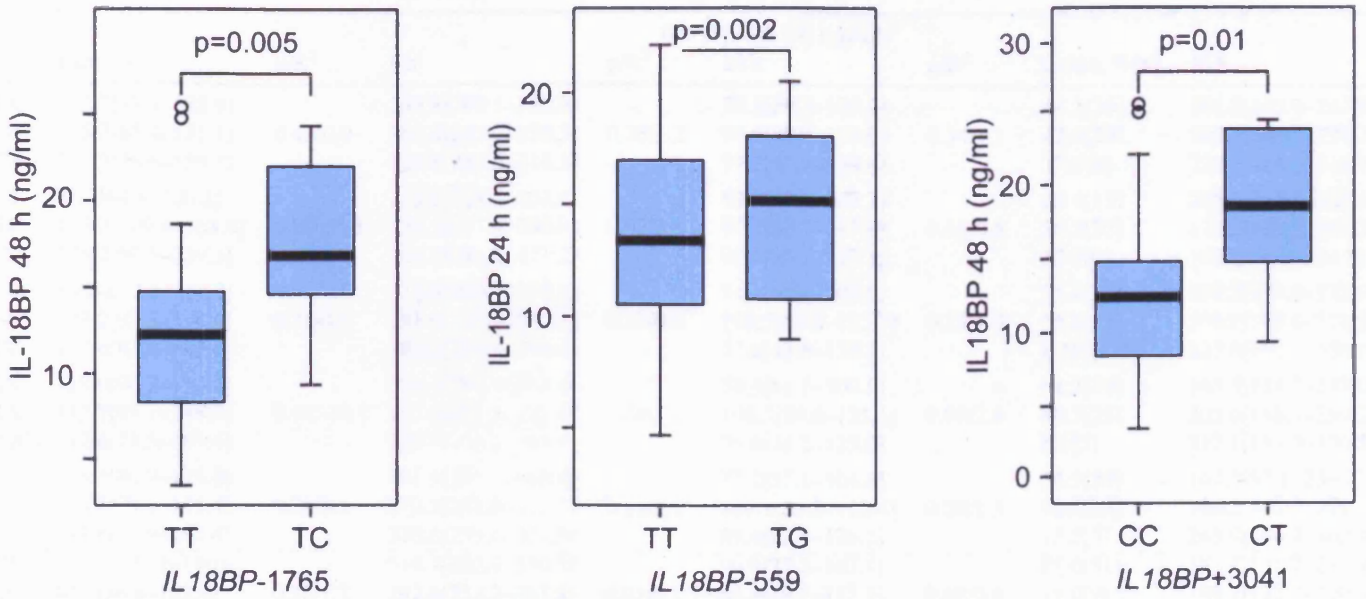

(a) IL-18BP levels at 48 h by *IL18BP*-1765 T>C genotype.

(b) IL-18BP levels at 24 h by *IL18BP*-559 T>G genotype, data for GG homozygotes (n=2) is not shown.

(c) IL-18BP levels at 48 h by *IL18BP*+3041 C>T genotype.

Figure 4.3: Boxplots of the significant associations between *IL18BP* tSNPs and IL-18BP levels in CABG (raw data shown).

Table 4.5: Geometric mean [95% CI] fIL-18 levels by *IL18* and *IL18BP* genotype, at baseline, 6 h, 24 h, and 48 h.

	tSNP		fIL-18[95% CI] (pg/ml) Baseline	p/R^2	6 h	p/R^2	24 h	p/R^2	Count, %[n]	48 h	p/R^2
IL18	-9731	GG	133.7[97.3–183.8]	0.43/0.9	335.8[290.1–388.8]	0.28/1.2	78.2[59.2–103.2]	0.34/1.1	44.1[26]	161.5[105.2–247.9]	0.56/2.1
		GT	105.9[85.4–131.1]		283.5[243.2–330.5]		98.9[80.9–120.9]		42.4[25]	198.5[143.5–274.7]	
		TT	110.3[76.6–159.7]		323.6[251.7–416.1]		97.2[67.9–139.4]		13.6[8]	226.3[162.0–316.1]	
	-5848	TT	83.7[64.8–108.2]	0.005/5.3	255.8[214.8–304.6]	0.02/3.8	82.9[63.7–107.7]	0.63/0.5	25.4[15]	255.3[215.4–302.6]	0.13/7.0
		TC	133.9[109.4–163.9]		339.2[297.4–386.9]		97.2[80.1–117.9]		59.3[35]	178.5[130.9–243.3]	
		CC	175.2[90.5–339.3]		364.1[281.4–471.2]		90.5[55.7–147.1]		15.3[9]	122.2[46.0–324.8]	
	+105	AA	108.4[82.6–142.2]	0.74/0.3	332.8[292.3–378.9]	0.37/0.9	84.1[67.0–105.5]	0.35/1.0	55.9[33]	168.2[121.6–232.6]	0.66/1.5
		AC	123.2[98.2–154.6]		287.0[242.1–340.2]		102.5[83.6–125.7]		35.6[21]	203.9[133.6–311.2]	
		CC	123.6[83.4–183.0]		303.2[227.4–404.4]		77.9[43.6–139.1]		8.5[5]	223.0[152.1–326.9]	
	+8855	TT	118.0[90.2–154.4]	0.98/<0.1	336.4[294.2–384.6]	0.31/1.1	78.3[61.1–100.5]	0.09/2.5	51.7[30]	163.5[114.7–233.0]	0.61/1.1
		TA	117.7[93.1–148.7]		287.2[243.6–338.6]		108.3[89.6–131.1]		39.7[23]	203.4[138.3–299.2]	
		AA	112.4[75.5–167.4]		293.7[218.2–395.4]		75.4[46.2–123.0]		8.6[5]	217.1[154.0–306.3]	
	+11015	AA	123.3[86.9–175.0]	0.93/0.1	351.8[301.7–410.3]	0.11/2.1	77.2[57.1–104.4]	0.28/1.3	34.5[20]	144.3[87.1–239.0]	0.28/4.5
		AC	114.8[93.2–141.4]		279.3[241.0–323.7]		101.1[83.5–122.4]		50.0[29]	196.5[142.5–271.1]	
		CC	117.8[82.9–167.4]		330.6[259.6–421.0]		89.4[63.3–126.2]		15.5[9]	243.9[196.7–302.4]	
IL18BP	-1765	TT	119.3[101.7–140.0]	0.33/1.2	314.7[282.6–350.5]	0.91/0.1	90.9[77.2–107.1]	0.68/0.4	85.0[51]	180.7[136.7–238.9]	0.90/<0.1
		TC	84.1[38.8–182.4]		292.6[232.7–367.9]		83.3[59.1–117.3]		15.0[9]	188.7[122.7–290.0]	
		CC	199.1[5.9–6694.5]		314.8[30.8–3216.8]		164.8[31.0–875.7]		0[0]	—	
	-559	TT	113.6[94.7–136.2]	0.77/0.3	311.3[277.6–349.1]	0.09/2.2	94.0[80.5–109.8]	0.70/0.1	81.7[49]	190.9[144.4–252.6]	0.42/1.2
		TG	129.5[87.5–191.8]		336.8[278.5–407.2]		87.7[60.3–127.6]		18.3[11]	149.3[90.9–245.2]	
		GG	86.2[2.1–3560.0]		107.2[5.7–2010.2]		—		0[0]	—	
	+3041	CC	120.2[103.1–140.2]	0.30/2.0	311.6[281.4–345.1]	0.80/<0.1	91.8[78.7–107.1]	0.82/<0.1	90.2[55]	183.3[141.4–237.6]	0.77/0.2
		CT	60.3[15.0–241.4]		331.1[239.9–456.9]		85.0[51.7–139.9]		9.8[6]	163.5[90.0–297.3]	
		TT	—		—		—		0[0]	—	

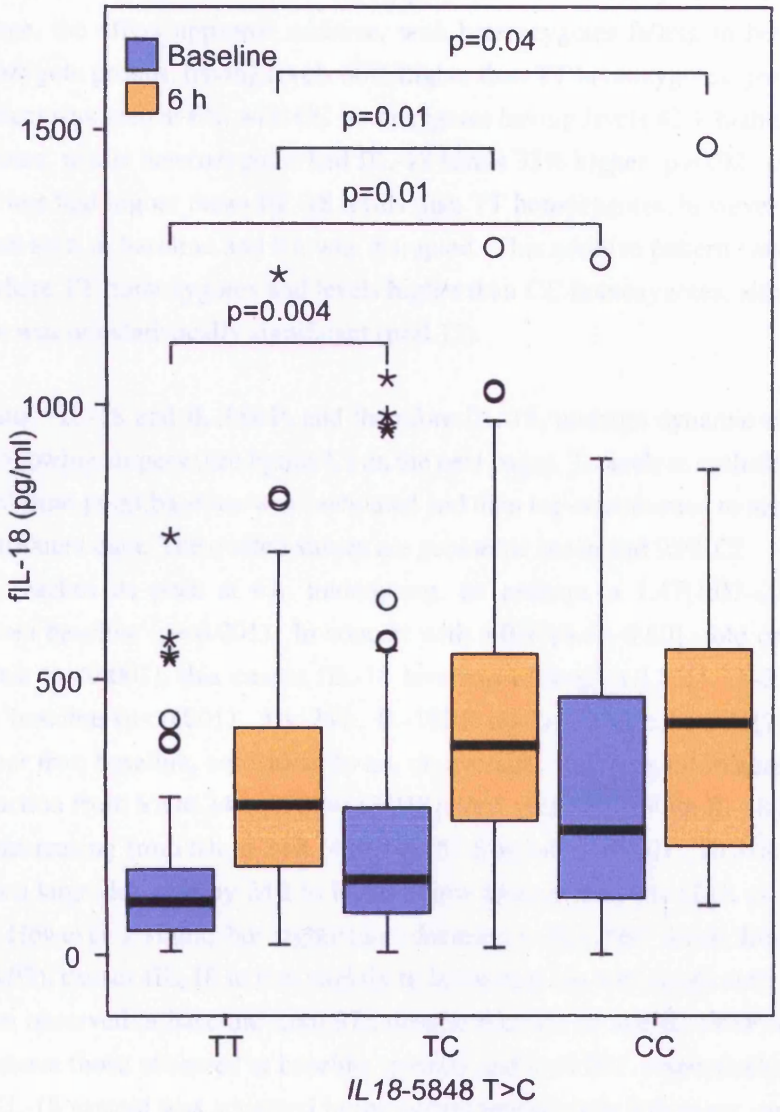

Figure 4.4: A boxplot of raw fIL-18 levels by *IL18*-5848 T>C genotypes at both baseline and 6 h in CABG. Line – Median; Box – 75th to 25th percentile; ∘ – outlier (>1.5 box lengths out of box); ⋆ – extreme (>3 box lengths out of box); whisker – last value not an outlier.

fIL-18 As shown in table 4.5 on page 137 and figure 4.4 on the previous page, only *IL18*-5848 T>C was significantly associated with differences in fIL-18 levels and explained the most of their variation (except at 24 h). At baseline, CC homozygotes had fIL-18 levels 109% higher than TT homozygotes. As shown in figure 4.4 on the preceding page, the effect appeared additive, with heterozygotes falling in between the two homozygote groups, having levels 60% higher than TT homozygotes (p=0.005). A similar effect was seen at 6 h, with CC homozygotes having levels 42% higher than TT homozygotes, whilst heterozygotes had fIL-18 levels 33% higher (p=0.02). At 24 h C allele carriers had higher mean fIL-18 levels than TT homozygotes, however the additive pattern seen at baseline and 6 h was disrupted. This additive pattern was reversed at 48 h, where TT homozygotes had levels higher than CC homozygotes, although this difference was not statistically significant (p=0.13).

Transitions IL-18 and IL-18BP, and therefore fIL-18, undergo dynamic changes in the 48 h following surgery (see figure 4.5 on the next page). To analyse such differences, the ratio of time-point:baseline was calculated and then log-transformed to achieve normally distributed data. The quoted values are geometric mean and 95% CI.

IL-18 reaches its peak at 6 h, undergoing, on average, a 1.47[1.07–2.02] -fold change from baseline ($p<0.001$). In concert with a 0.49[0.40–0.60] -fold drop in IL-18BP levels ($p<0.001$), this causes fIL-18 levels to undergo a 1.83[1.33–2.50] -fold rise from baseline ($p<0.001$). By 24 h, IL-18BP reaches it's peak, 2.71[2.29–3.20] -fold higher than baseline, equivalent to an, on average, 10254 pg/ml increase in protein production from 6 h to 24 h (2784⇒13038 pg/ml, $p<0.001$). With IL-18 levels, on average, decreasing from 6 h to 24 h (460.4⇒251.6 pg/ml, $p<0.001$), fIL-18 therefore undergoes a large decrease by 24 h to levels below those at baseline (24 h vs. baseline, p=0.04). However a slight, but significant, decrease in IL-18BP levels from 24 h to 48 h (p=0.02), causes fIL-18 to rise slightly to levels that are not significantly different from those observed at baseline (p=0.97), despite both IL-18 and IL-18BP remaining at levels above those observed at baseline (p=0.01 and $p<0.001$, respectively). Therefore, the IL-18 system was activated in the period immediately following surgery and reached its peak (in terms of peak fIL-18 levels) at 6 h. However, largely due to a highly significant activation of IL-18BP, levels of fIL-18 returned to baseline levels by 48 h. At 48 h, both IL-18 and IL-18BP levels remained elevated, and only with observations beyond 48 h would it be possible to see how long it took for these two proteins to return to pre-operative levels.

In assessing whether there were significant differences, by genotype, in the changes from baseline to peak for IL-18, IL-18BP, and fIL-18, no significant differences by *IL18* or *IL18BP* tSNP were found (data not shown).

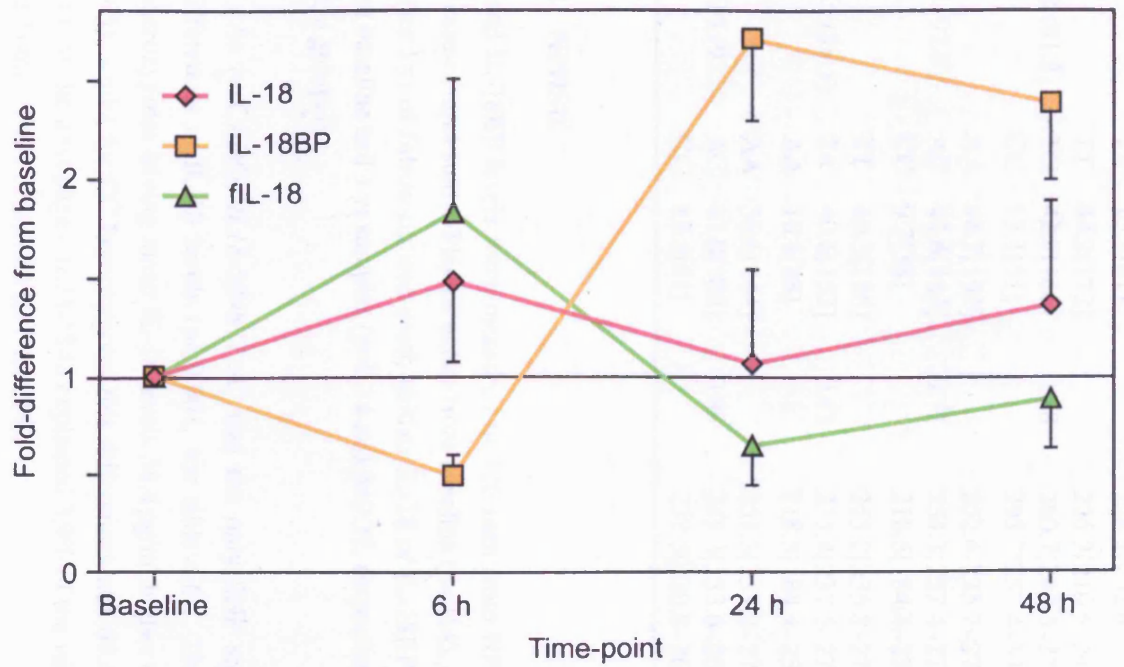

Figure 4.5: Fold-changes in IL-18, IL-18BP, and fIL-18 levels in the period following CABG surgery, relative to baseline[2].

[2]Data presented is geometric mean and 95% CI of $\ln(\text{level}^{time-point}/\text{level}^{baseline})$. Ratios are innately highly skewed and therefore must be log-transformed for analysis.

Table 4.6: Geometric mean [95% CI] IL-18 levels by *IL18* genotype in NPHSII.

tSNP (% genotypes)		Count, %[n]	HWE p	IL-18 [95% CI] (pg/ml)	p	R^2
	GG	42.3[164]		261.6[242.8–281.8]		
-9731 (91.0)	GT	42.0[163]	0.06	246.5[229.1–265.1]	0.15	1.0
	TT	15.7[61]		228.2[202.6–257.1]		
	TT	44.2[172]		226.3[210.5–243.3]		
-5848 (91.3)	TC	42.7[166]	0.28	260.7[243.5–279.0]	<0.001	3.9
	CC	13.1[51]		295.7[257.4–339.8]		
	AA	48.7[191]		252.6[235.7–270.7]		
+105 (92.0)	AC	41.6[163]	0.71	254.3[237.4–272.4]	0.19	0.8
	CC	9.7[38]		218.5[184.4–259.0]		
	TT	49.3[186]		253.2[235.8–271.9]		
+8855 (88.5)	TA	40.6[153]	0.43	255.4[237.5–274.6]	0.19	0.9
	AA	10.1[38]		218.5[184.4–259.0]		
	AA	36.6[144]		251.3[231.2–273.2]		
+11015 (92.3)	AC	47.8[188]	0.98	249.3[233.6–265.9]	0.77	0.1
	CC	15.5[61]		238.5[210.8–269.9]		

4.2.2.2 NPHSII

IL-18 and IL-18BP levels were measured in 426 men from NPHSII, assembled as a nested case-control study. Plasma either from baseline (n=314), or if this was unavailable, after 1 yr of follow-up was used; neither IL-18 or IL-18BP differed significantly between baseline and 1 yr samples (p=0.14 and p=0.32, respectively), therefore the two sets were grouped.

IL-18 As in CABG, *IL18*-5848 T>C was the only SNP significantly associated with differences in IL-18 levels ($p<0.001$, see table 4.6). The effect was additive with heterozygotes having mean IL-18 levels 34.4 pg/ml higher than TT homozygotes (p=0.005), whilst for CC homozygotes this differences was 69.4 pg/ml (p=0.001, see figure 4.6 on the next page). *IL18*-5848 explained 3.9% of the variation in IL-18 levels whilst all other SNPs explained less than 1%.

IL-18BP As can be seen from table 4.7 on the following page, none of the *IL18BP* tSNPs showed significant associations with IL-18BP levels. However the ranking of genotypes by their mean IL-18BP levels is similar to that seen in CABG at baseline, with the heterozygote group consistently being associated with higher mean IL-18BP levels than the homozygote groups.

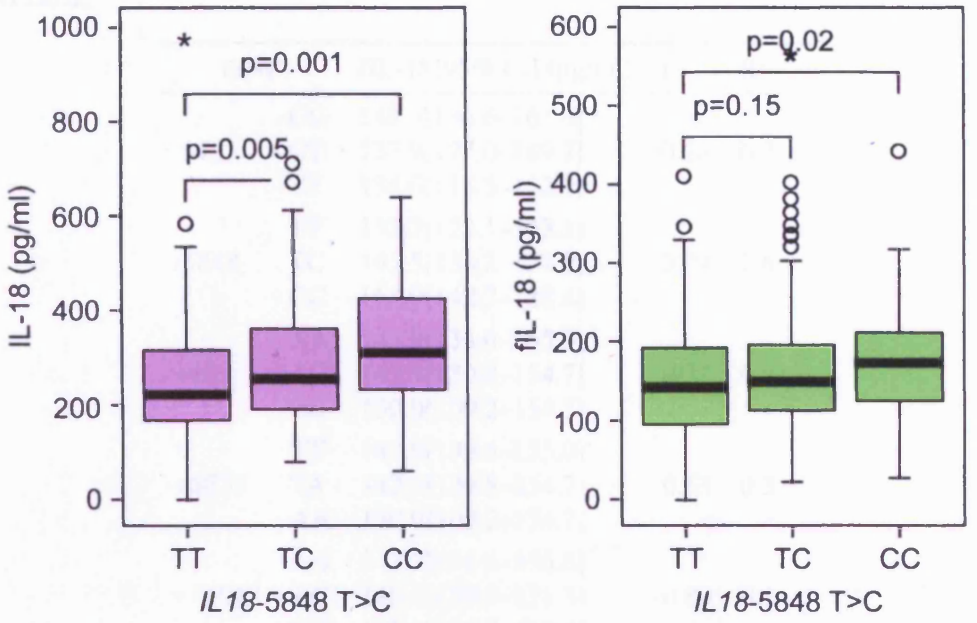

(a) IL-18 levels by *IL18*-5848 T>C genotype.

(b) fIL-18 levels by *IL18*-5848 T>C genotype.

Figure 4.6: Boxplots of significant differences in both IL-18 and fIL-18, by *IL18*-5848T>C genotype in NPHSII (raw data shown).

Table 4.7: Geometric mean [95% CI] IL-18BP levels by *IL18BP* genotype in NPHSII.

tSNP (% genotypes)		Count, %[n]	HWE p	IL-18BP[95% CI] (pg/ml)	p	R^2
	TT	92.9[367]		5620[5165–6096]		
-1765 (92.7)	TC	6.6[26]	0.05	6364[4669–8322]	0.27	0.7
	CC	0.5[2]		2031[416–4863]		
	TT	76.6[301]		5566[5069–6086]		
-559 (92.3)	TG	22.6[89]	0.19	6022[5059–7068]	0.69	0.2
	GG	0.8[3]		4973[594–13612]		
	CC	97.5[384]		5629[5191–6084]		
+3041 (92.5)	CT	2.5[10]	0.80	6821[2552–13147]	0.43	0.2
	TT	0[0]		—		

Table 4.8: Geometric mean [95% CI] fIL-18 levels by *IL18* and *IL18BP* genotype in NPHSII.

tSNP		fIL-18[95% CI] (pg/ml)	p	R^2
	GG	148.3[136.6–161.0]		
-9731	GT	137.9[127.0–149.7]	0.26	0.7
	TT	134.6[118.5–152.9]		
	TT	132.2[122.1–143.1]		
-5848	TC	145.5[134.2–157.9]	0.04	1.6
	CC	164.0[142.7–188.4]		
	AA	143.9[133.6–155.0]		
+105	AC	142.3[130.8–154.7]	0.51	0.3
	CC	130.0[109.2–154.7]		
	TT	143.9[133.6–155.0]		
+8855	TA	142.3[130.8–154.7]	0.53	0.3
	AA	130.0[109.2–154.7]		
	AA	143.7[131.6–156.8]		
+11015	AC	140.1[129.7–151.3]	0.80	0.1
	CC	142.2[124.5–162.4]		
	TT	141.8[134.3–149.8]		
-1765	TC	141.2[115.5–172.8]	0.94	<0.1
	CC	—		
	TT	142.2[133.7–151.3]		
-559	TG	141.6[128.0–156.6]	0.60	0.3
	GG	105.9[19.7–570.3]		
	CC	142.1[134.7–149.8]		
+3041	CT	130.1[82.2–206.0]	0.44	0.2
	TT	—		

fIL-18 *IL18*-5848 T>C was the only SNP associated with fIL-18 levels (see table 4.8). The difference is such that CC homozygotes had levels 24% higher than TT homozygotes, and heterozygotes have levels 10% higher than TT homozygotes (see figure 4.6 on the preceding page). The level of fIL-18 across the genotype groups is in a similar, but blunted, pattern to that seen with IL-18 levels.

4.2.2.3 CUDAS

IL-18 levels and all five *IL18* tSNPs were determined in the whole CUDAS sample. Data analysis was carried out by Pamela McCaskie (Laboratory for Genetic Epidemiology, University of Western Australia) using SimHap. Three of the five *IL18* tSNPs were found to be out of HWE, with consistently fewer heterozygotes observed than expected. That the CUDAS is a random electoral roll samples argues against selection as a cause

Table 4.9: Geometric mean [95% CI] IL-18 levels by *IL18* genotype in CUDAS.

tSNP (% genotypes)		Count, %[n]	HWE p	IL-18[95% CI] (pg/ml)	p	R^2
	GG	36.8[407]		298.7[286.6–311.4]		
-9731 (99.9)	GT	46.2[511]	0.19	299.0[288.0–310.4]	0.65	<0.1
	TT	17.1[189]		308.4[290.2–327.8]		
	TT	41.0[454]		286.5[275.5–298.0]		
-5848 (99.7)	TC	45.7[505]	0.73	306.5[295.4–318.1]	0.003	0.9
	CC	13.3[147]		324.3[302.8–347.3]		
	AA	48.5[537]		296.6[286.0–307.5]		
+105 (99.9)	AC	40.3[447]	0.04	303.5[291.7–315.8]	0.57	<0.1
	CC	11.2[124]		307.4[285.1–331.5]		
	TT	48.8[540]		297.1[286.6–308.0]		
+8855 (99.8)	TA	40.0[443]	0.02	304.1[292.1–316.6]	0.42	<0.1
	AA	11.2[124]		303.7[281.4–327.7]		
	AA	34.8[386]		295.1[282.7–308.0]		
+11015 (99.9)	AC	45.8[508]	0.04	301.7[290.8–313.1]	0.66	<0.1
	CC	19.3[214]		307.8[290.5–326.1]		

of this disequilibrium. That fewer heterozygotes than expected were observed strongly suggests that it is due to poor heterozygote group discrimination, a common problem with TaqMan genotyping. It is likely therefore that the assigned genotypes are accurate, and that of those undetermined samples it is most likely that proportionally more were heterozygotes.

Only *IL18*-5848 T>C was significantly associated with IL-18 levels (p=0.003, see table 4.9), with C allele carriers having higher IL-18 levels than TT homozygotes. The effect appeared additive, with CC homozygotes having levels 13% higher than TT homozygotes (p=0.002), and heterozygotes having levels 7% higher (p=0.01). Overall, none of the SNPs explained large proportions of the variance in IL-18 levels (all SNPs<0.9%), yet -5848 T>C explained more than the other SNPs (0.9% vs. <0.1%).

4.2.2.4 CUPID

This analysis was carried out by Pam McCaskie. As shown in table 4.10 on the following page, both *IL18*-9731 G>T (p=0.02) and +11015 A>C (p=0.01) were significantly associated with differences in IL-18 levels. In both cases the effects had additive patterns, with the rare allele associated with higher IL-18 levels. *IL18*-5848 T>C was not globally associated with differences in IL-18 levels in CUPID, but those heterozygous at -5848 had borderline significantly higher IL-18 levels (p=0.05). As in CUDAS, none

Table 4.10: Geometric mean [95% CI] IL-18 levels by *IL18* genotype in CUPID.

tSNP (% genotypes)		Count, %[n]	HWE p	IL-18[95% CI] (pg/ml)	p	R^2
	GG	32.5[180]		322.5[304.1–342.0]		
-9731 (99.6)	GT	50.9[282]	0.30	335.5[320.1–351.6]	0.02	1.0
	TT	16.6[92]		372.4[342.9–404.5]		
	TT	39.2[216]		324.0[307.0–342.1]		
-5848 (99.1)	TC	48.3[266]	0.35	348.4[331.8–365.8]	0.13	0.4
	CC	12.5[69]		330.1[300.2–363.1]		
	AA	44.6[247]		334.3[317.9–351.7]		
+105 (99.6)	AC	46.9[260]	0.06	338.2[321.8–355.4]	0.89	<0.1
	CC	8.5[47]		343.9[305.9–386.5]		
	TT	44.3[245]		332.4[316.0–349.6]		
+8855 (99.5)	TA	47.2[261]	0.05	339.4[323.1–356.5]	0.79	<0.1
	AA	8.5[47]		343.9[305.9–386.5]		
	AA	31.0[172]		314.4[296.1–333.9]		
+11015 (99.6)	AC	52.5[291]	0.08	343.2[327.6–359.5]	0.01	1.2
	CC	16.4[91]		362.7[333.8–394.1]		

of the SNPs explained a large proportion of the variance in IL-18 levels (all SNPs<1.2).

4.2.2.5 SCARF

The *IL18* tSNP set was genotyped in the SCARF cohort, and only *IL18*-5848 T>C was found to be associated with significantly different IL-18 levels (p<0.001, see table 4.11 on the next page). The association appeared additive, with CC homozygotes having levels 18% higher than TT homozygotes (p<0.001), whilst in heterozygotes the difference was 11% (p=0.001). When the cohort was divided into cases and controls the association was significant in cases only (controls–p=0.13; cases–p<0.001). Although the difference between CC homozygotes and TT homozygotes in controls was borderline significant (p=0.06, see figure 4.7 on page 147).

4.2.3 Single SNP Multivariate Analysis

In selecting covariate sets across each study, care was taken to select appropriate variables that could be used across studies and that were biologically plausible. As such, four models were selected, each building on the previous covariate set:

Model 1 Sex and age

Model 2 Sex, age, smoking and statin use

Table 4.11: Geometric mean [95% CI] IL-18 levels by *IL18* genotype in SCARF.

tSNP (% genotypes)		Total study (n=774) Count, %[n]	HWE p	IL-18[95% CI] (pg/ml)	p/ R^2	Controls (n=387) Count, %[n]	IL-18[95% CI] (pg/ml)	p/ R^2	Cases (n=387) Count, %[n]	IL-18[95% CI] (pg/ml)	p/ R^2
-9731 (98.4)	GG	35.8[273]	0.71	273.7[261.0–287.0]	0.66/ 0.1	35.8[138]	259.3[243.7–275.9]	0.39/ 0.5	35.9[135]	289.3[269.4–310.8]	0.14/ 1.1
	GT	47.5[362]		278.9[267.7–290.6]		49.7[192]	268.5[254.8–283.0]		45.2[170]	291.7[273.5–311.0]	
	TT	16.7[127]		270.2[255.0–286.3]		14.5[56]	280.6[254.4–309.6]		18.9[71]	262.5[244.6–281.8]	
-5848 (98.3)	TT	38.4[292]	0.62	256.8[246.1–268.1]	<0.001/ 2.5	39.5[152]	256.0[241.4–271.4]	0.13/ 1.1	37.2[140]	257.7[241.9–274.6]	<0.001/ 4.5
	TC	47.8[364]		284.0[272.8–295.7]		47.8[184]	270.7[256.9–285.3]		47.9[180]	298.9[281.1–317.9]	
	CC	13.8[105]		302.6[281.7–325.0]		12.7[49]	286.6[256.6–320.1]		14.9[56]	318.1[289.7–349.3]	
+105 (98.6)	AA	44.3[338]	0.97	276.2[264.4–288.4]	0.46/ 0.2	43.8[169]	260.5[246.3–275.6]	0.35/ 0.6	44.8[169]	293.3[274.6–313.2]	0.31/ 0.6
	AC	44.6[340]		278.2[267.2–289.6]		46.6[180]	274.8[260.4–290.0]		42.4[160]	282.0[265.3–299.8]	
	CC	11.1[85]		262.8[244.5–282.5]		9.6[37]	257.8[228.4–291.0]		12.7[48]	266.7[243.4–292.3]	
+8855 (98.6)	TT	44.4[339]	0.90	276.2[264.4–288.4]	0.43/ 0.2	44.0[170]	260.5[246.3–275.6]	0.33/ 0.6	44.8[169]	293.3[274.6–313.2]	0.29/ 0.7
	TA	44.3[338]		278.3[267.3–289.8]		46.4[179]	274.8[260.4–290.0]		42.2[159]	282.3[265.5–300.2]	
	AA	11.3[86]		262.5[244.4–281.9]		9.6[37]	257.8[228.4–291.0]		13.0[49]	266.0[243.2–290.9]	
+11015 (98.7)	AA	33.8[258]	0.20	270.6[257.8–283.9]	0.54/ 0.2	33.3[129]	257.8[241.7–274.9]	0.34/ 0.6	34.2[129]	284.2[264.5–305.4]	0.28/ 0.7
	AC	46.7[357]		279.9[268.4–291.9]		50.4[195]	269.3[255.5–283.8]		43.0[162]	293.7[274.4–314.2]	
	CC	19.5[149]		273.9[259.7–288.8]		16.3[63]	278.7[254.8–304.7]		22.8[86]	270.5[253.1–289.1]	

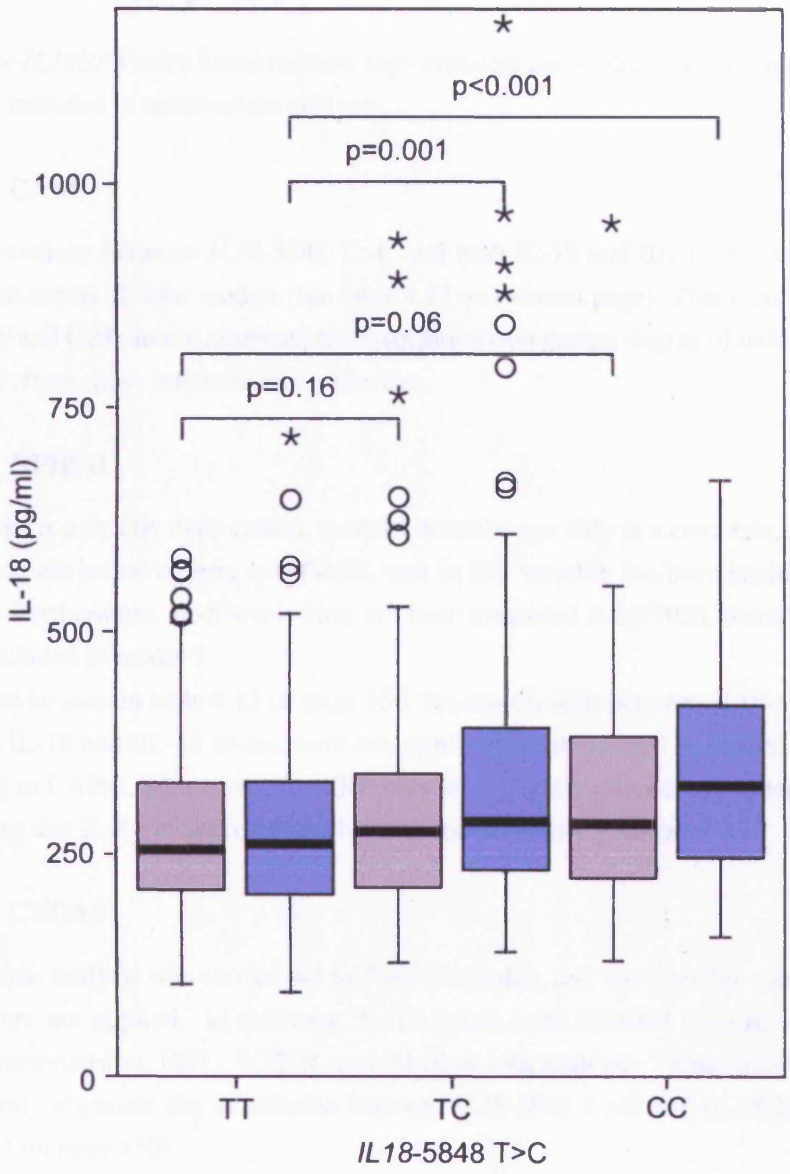

Figure 4.7: A boxplot of raw SCARF IL-18 levels by *IL18*-5848 T>C genotype in both cases and controls. Line – Median; Box – 75th to 25th percentile; ∘ – outlier (>1.5 box lengths out of box); ⋆ – extreme (>3 box lengths out of box); whisker – last value not an outlier.

Model 3 Sex, age, smoking, statin use, IL-6, and CRP

Model 4 Sex, age, smoking, statin use, IL-6, CRP, and IL-18/IL-18BP (where appropriate)

As the *IL18BP* tSNPs failed to show any consistent associations across studies, they were not included in multivariate analysis.

4.2.3.1 CABG

The associations between *IL18*-5848 T>C and both IL-18 and fIL-18 at baseline and 6 h remain across all four models (see table 4.12 on the next page). That adjustment for both IL-6 and CRP do not attenuate the associations suggests a degree of independence for IL-18, from these inflammatory pathways.

4.2.3.2 NPHSII

As NPHSII is a strictly male cohort, model 1 contains age only as a covariate, and statin use was an exclusion criteria in NPHSII, and so this variable has been excluded from model 2. Furthermore, IL-6 levels have not been measured in NPHSII, therefore it can not be included in model 3.

As can be seen in table 4.13 on page 150, the associations between *IL18*-5848 T>C and both IL-18 and fIL-18 levels, were not significantly attenuated by covariate adjustment. As in CABG, adjustment for CRP only very slightly attenuated the association, suggesting that IL-18 is not regulated by such inflammatory pathways.

4.2.3.3 CUDAS

Multivariate analysis was carried out by Pam McCaskie, and therefore the models used above were not applied. In this case, IL-18 levels were adjusted for age, sex, presence of hypertension, HDL, WTHR, and Alcohol consumption. These factors did not significantly attenuate the association between *IL18*-5848 T>C and IL-18 levels (see table 4.14 on page 150).

4.2.3.4 CUPID

Multivariate analysis was carried out by Pam McCaskie, and therefore, as in CUDAS, the models used in the other studies were not applied. In CUPID, IL-18 levels were adjusted for age, sex, BMI, LDL, and triglycerides. As shown in table 4.15 on page 150, the associations between *IL18*-9731 G>T and +11015 A>C were not attenuated by adjustment for traditional CHD risk factors.

Table 4.12: P values from multivariate analysis of IL-18 and fIL-18 levels by *IL18* genotype in CABG.

		Model 1 sex and age			Model 2 Model 1 + smoking, and statin use			Model 3 Model 2 + IL-6[3], and CRP			Model 4 Model 3 + IL-18BP		
	SNP	Baseline	6 h	24 h	Baseline	6 h	24 h	Baseline	6 h	24 h	Baseline	6 h	24 h
IL-18	-9731	0.39	0.15	0.59	0.54	0.14	0.58	0.39	0.26	0.39	0.37	0.26	0.34
	-5848	0.001	0.002	0.72	0.002	0.003	0.70	0.005	0.004	0.54	0.008	0.004	0.54
	+105	0.74	0.40	0.47	0.70	0.25	0.51	0.85	0.17	0.37	0.87	0.12	0.37
	+8855	0.89	0.23	0.09	0.94	0.16	0.14	0.88	0.08	0.30	0.84	0.06	0.30
	+11015	0.82	0.07	0.29	0.86	0.06	0.33	0.66	0.23	0.52	0.73	0.23	0.51
fIL-18	-9731	0.33	0.18	0.60	0.51	0.18	0.63	0.35	0.27	0.29	—[4]	—	—
	-5848	0.004	0.01	0.49	0.005	0.02	0.45	0.009	0.007	0.52	—	—	—
	+105	0.79	0.26	0.59	0.76	0.14	0.66	0.87	0.09	0.36	—	—	—
	+8855	0.96	0.26	0.15	0.95	0.12	0.22	0.83	0.05	0.29	—	—	—
	+11015	0.84	0.08	0.40	0.93	0.06	0.47	0.75	0.25	0.48	—	—	—

[3]For IL-6, CRP and IL-18BP, the covariates match the dependent variable, ie. in baseline IL-18 analysis, baseline IL-6, CRP, and IL-18BP are used, whilst for 6 h analysis, measurements made at 6 h were used as covariates

[4]As fIL-18 is derived from IL-18BP, model 4 was not used in fIL-18 analysis

Table 4.13: P values from multivariate analysis of IL-18 and fIL-18 levels by *IL18* genotype in NPHSII.

	SNP	Model 1 age	Model 2 Model 1 + smoking	Model 3 Model 2 + CRP	Model 4 Model 3 + IL-18BP
IL-18	-9731	0.19	0.22	0.43	0.56
	-5848	0.001	0.001	0.001	0.002
	+105	0.21	0.22	0.43	0.54
	+8855	0.21	0.22	0.46	0.56
	+11015	0.80	0.81	0.85	0.92
fIL-18	-9731	0.24	0.28	0.76	—
	-5848	0.04	0.05	0.05	—
	+105	0.49	0.50	0.77	—
	+8855	0.51	0.52	0.78	—
	+11015	0.81	0.85	0.87	—

Table 4.14: P values from multivariate analysis of IL-18 levels by *IL18* genotype in CUDAS.

SNP	IL-18 multivariate analysis Adjusted for age, sex, presence of hypertension, HDL, WTHR, and Alcohol consumption
-9731	0.82
-5848	0.003
+105	0.71
+8855	0.82
+11015	0.44

Table 4.15: P values from multivariate analysis of IL-18 levels by *IL18* genotype in CUPID.

SNP	IL-18 multivariate analysis Adjusted for age, sex, BMI, LDL, and triglycerides
-9731	0.01
-5848	0.19
+105	0.95
+8855	0.84
+11015	0.03

4.2.3.5 SCARF

No data for statin use or IL-18BP levels were available in SCARF, therefore model 2 was adjusted accordingly and model 4 was not used. The associations previously identified in univariate analysis remained in multivariate analysis (see table 4.16 on the next page), with the association between *IL18*-5848 T>C identified in the total cohort significantly stronger in cases than in controls. Interestingly, the association of -5848 and IL-18 levels in controls was stronger in multivariate analysis (p=0.13⇒0.06).

4.2.4 Haplotype Univariate Analysis

Haplotype analysis was limited to the four most common haplotypes in each study.

4.2.4.1 CABG

To avoid errors in haplotype inference caused by genetic heterogeneity between ethnicities, haplotype analysis in CABG was limited to those of Caucasian origin (n=197).

IL-18 Common *IL18* haplotypes explained 5.2% of the variance in IL-18 levels at baseline, but were only borderline significantly associated with IL-18 levels (p=0.08, see table 4.17 on page 153) possibly due to the reduced sample size. Only one haplotype, hGTATA, was significantly associated with IL-18 levels at baseline (p=0.01). The effect of this haplotype did not significantly deviate from additivity (p=0.73). hGTATA was also significantly associated with lower IL-18 levels at 6 h (p=0.03), but not 24 h (p=0.15), although at 24 h the IL-18 haplotypic mean for hGTATA was lower than that of hGCATA (the reference haplotype). The effect of this haplotype was such that those homozygous for hGTATA would be expected to have baseline IL-18 levels 35% of those for hGCATA homozygotes, whilst at 6 h this was 55% (see figure 4.8 on page 154).

IL-18BP As can be seen in table 4.18 on page 153, *IL18BP* haplotypes explained little of the variation in IL-18BP levels across all time points compared to *IL18* haplotypes, and no haplotype was associated with significantly different levels from that of the reference haplotype.

fIL-18 *IL18* haplotypes consistently explained a greater amount of the variation in fIL-18 levels across all time points, than *IL18BP* haplotypes. The haplotype found to be significantly associated with IL-18 levels, hGTATA, was also associated with significantly lower fIL-18 levels than the reference haplotype (hGCATA) at both baseline and 6 h. The difference was such that those homozygous for hGTATA had an estimated mean level of fIL-18 at baseline, 48% of that of hGCATA homozygotes, at 6 h it was

Table 4.16: Multivariate analysis of IL-18 levels by *IL18* genotype in SCARF.

	Model 1 sex and age			Model 2 Model 1 + smoking			Model 3 Model 2 + IL-6 and CRP		
SNP	Total	Controls	Cases	Total	Controls	Cases	Total	Controls	Cases
-9731	0.55	0.48	0.15	0.57	0.44	0.16	0.50	0.47	0.18
-5848	<0.001	0.07	<0.001	<0.001	0.06	<0.001	<0.001	0.06	0.001
+105	0.38	0.26	0.33	0.38	0.25	0.34	0.30	0.24	0.37
+8855	0.35	0.24	0.31	0.36	0.23	0.32	0.28	0.22	0.35
+11015	0.43	0.40	0.30	0.44	0.37	0.28	0.38	0.36	0.30

Table 4.17: Haplotypic mean [95% CI] lnIL-18 levels by *IL18* haplotype, at baseline, 6 h, and 24 h in CABG.

Haplotype		Frequency (%)	Haplotypic mean lnIL-18[5][95% CI] Baseline	p	6 h	p	24 h	p
hGCATA	h12111	27.3	2.81[2.62–3.00]	Ref	3.18[3.01–3.34]	Ref	2.79[2.60–2.97]	Ref
hTTCAC	h21222	26.8	2.63[2.39–2.88]	0.31	2.97[2.85–3.09]	0.09	2.81[2.51–3.11]	0.90
hGTATA	h11111	20.6	2.29[2.00–2.58]	0.01	2.88[2.71–3.05]	0.03	2.57[2.39–2.76]	0.15
hTTATC	h21112	10.4	2.66[2.24–3.08]	0.55	3.13[2.87–3.40]	0.95	2.81[2.44–3.18]	0.91
	Global p/R^2			0.08/5.2		0.15/4.0		0.67/1.5

Table 4.18: Haplotypic mean [95% CI] sqrtIL-18BP levels by *IL18BP* haplotype, at baseline, 6 h, and 24 h in CABG.

Haplotype		Frequency (%)	Haplotypic mean sqrtIL-18BP[95% CI] Baseline	p	6 h	p	24 h	p
hTTC	h111	85.6	34.1[32.7–35.5]	Ref	25.8[24.3–27.3]	Ref	56.2[54.7–57.7]	Ref
hTGC	h121	9.5	34.6[28.0–41.3]	0.87	26.2[19.6–32.9]	0.90	59.8[53.9–65.8]	0.27
hCTT	h212	1.8	42.9[24.2–61.6]	0.36	26.4[11.2–41.6]	0.94	56.5[27.0–86.0]	0.99
hCTC	h211	1.7	33.5[6.4–60.6]	0.97	24.4[6.5–42.2]	0.88	51.4[35.4–67.3]	0.56
	Global p/R^2			0.57/1.6		0.89/0.7		0.34/2.5

[5]Due to the laws of logarithms, geometric haplotypic means are difficult to interpret and therefore data is presented as transformed data throughout.

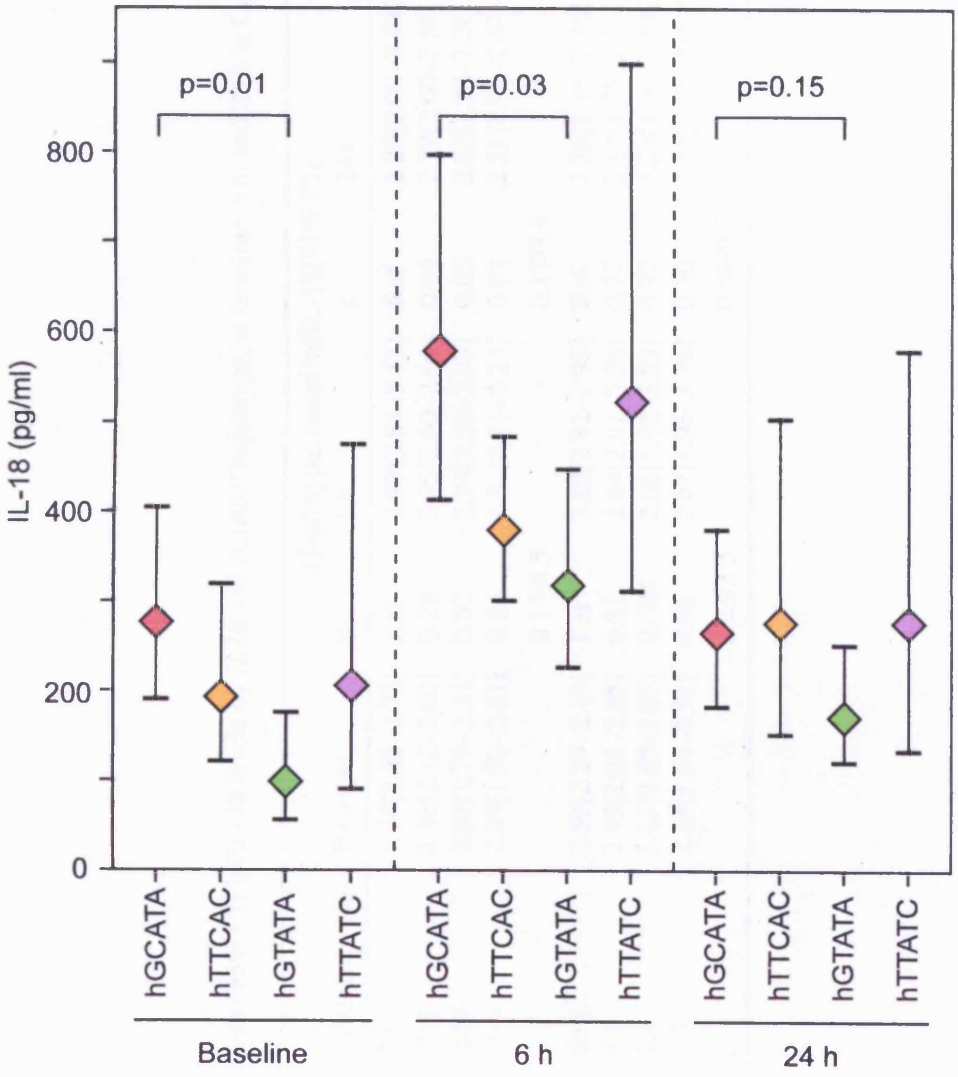

Figure 4.8: Estimated homozygote IL-18 levels for common *IL18* haplotypes in CABG. Data is double the estimated haplotypic mean (◇), with 95% CIs (whiskers), p values are those relating to haplotypic means.

Table 4.19: Haplotypic mean [95% CI] lnfIL-18 levels by *IL18* and *IL18BP* haplotype, at baseline, 6 h, and 24 h in CABG.

	Haplotype		Frequency (%)	Haplotypic mean lnfIL-18[95% CI] Baseline	p	6 h	p	24 h	p
IL18	hGCATA	h12111	27.3	2.54[2.35–2.73]	Ref	2.99[2.84–3.13]	Ref	2.29[2.09–2.49]	Ref
	hTTCAC	h21222	26.8	2.36[2.12–2.60]	0.28	2.75[2.60–2.91]	0.06	2.29[2.00–2.58]	0.99
	hGTATA	h11111	20.6	2.07[1.79–2.35]	0.02	2.74[2.56–2.93]	0.05	2.07[1.88–2.26]	0.15
	hTTATC	h21112	10.4	2.40[1.99–2.81]	0.54	2.97[2.71–3.23]	0.92	2.31[1.94–2.67]	0.95
		Global p/R^2			0.14/4.5		0.17/3.9		0.69/1.5
IL18BP	hTTC	h111	85.6	2.39[2.29–2.49]	Ref	2.88[2.82–2.95]	Ref	2.26[2.16–2.36]	Ref
	hTGC	h121	9.5	2.45[2.04–2.85]	0.81	2.84[2.61–3.08]	0.77	2.13[1.75–2.51]	0.54
	hCTT	h212	1.8	1.43[0.80–2.07]	0.004	2.86[1.88–3.83]	0.97	2.23[1.06–3.39]	0.96
	hCTC	h211	1.7	2.23[1.54–2.93]	0.66	2.67[1.98–3.36]	0.56	2.15[1.28–3.02]	0.81
		Global p/R^2			0.23/3.5		0.94/0.5		0.98/0.5

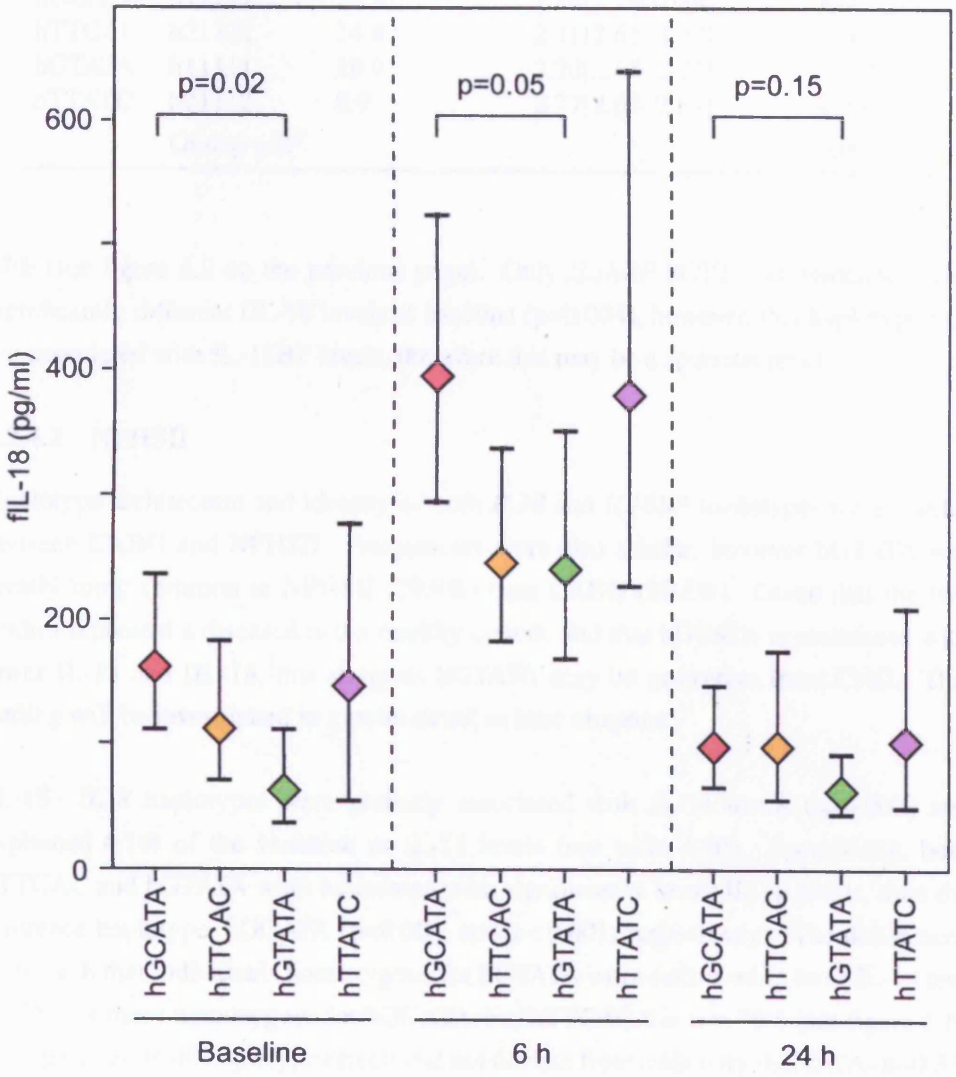

Figure 4.9: Estimated homozygote fIL-18 levels for common *IL18* haplotypes in CABG. Data is double the estimated haplotypic mean (◇), with the 95% CIs (whiskers), p values are those relating to haplotypic means.

Table 4.20: Haplotypic mean [95% CI] lnIL-18 levels by *IL18* haplotype in NPHSII.

Haplotype		Frequency (%)	Haplotypic mean lnIL-18[95% CI	p
hGCATA	h12111	28.2	2.84[2.79–2.89]	Ref
hTTCAC	h21222	24.8	2.71[2.65–2.77]	0.002
hGTATA	h11111	29.9	2.70[2.65–2.75]	<0.001
hTTATC	h21112	8.9	2.77[2.65–2.89]	0.29
	Global p/R^2			0.003/4.1

67% (see figure 4.9 on the previous page). Only *IL18BP* hCTT was associated with significantly different fIL-18 levels at baseline (p=0.004), however, this haplotype was not associated with IL-18BP levels, therefore this may be a spurious result.

4.2.4.2 NPHSII

Haplotype architecture and identity of both *IL18* and *IL18BP* haplotypes were similar between CABG and NPHSII. Frequencies were also similar, however hGTATA was greatly more common in NPHSII (29.9%) than CABG (20.6%). Given that the two studies represent a diseased and a healthy cohort, and that hGTATA is associated with lower IL-18 and fIL-18, this suggests hGTATA may be protective from CHD. This finding will be investigated in greater detail in later chapters.

IL-18 *IL18* haplotypes were globally associated with IL-18 levels (p=0.003) and explained 4.1% of the variation in IL-18 levels (see table 4.20). Specifically, both hTTCAC and hGTATA were associated with significantly lower IL-18 levels, than the reference haplotype, hGCATA (p=0.002, and p<0.001, respectively). The differences were such that individuals homozygous for hGTATA were estimated to have IL-18 levels 75% of those homozygous for hGCATA. For hTTCAC this was 76% (see figure 4.10 on page 160). Both haplotype effects did not deviate from additivity (hGTATA–p=0.37; hTTCAC–p=0.16).

IL-18BP As shown in table 4.21 on the following page, *IL18BP* haplotypes explained only 0.5% of the variation in IL-18BP levels in NPHSII. None of the common *IL18BP* haplotypes were associated with levels significantly different from those of the reference haplotype.

fIL-18 *IL18*, but not *IL18BP*, haplotypes were significantly associated with differences in fIL-18 levels (p=0.04, see table 4.22 on the next page). This was seemingly

Table 4.21: Haplotypic mean [95% CI] sqrtIL-18BP levels by *IL18BP* haplotype in NPHSII.

Haplotype		Frequency (%)	Haplotypic mean sqrtIL-18BP[95% CI]	p
hTTC	h111	85.2	37.3[35.5–39.0]	Ref
hTGC	h121	11.0	39.5[33.2–45.8]	0.53
hCTT	h212	1.3	44.9[31.6–58.1]	0.27
hCTC	h211	1.4	30.3[0–65.7]	0.70
	Global p/R^2			0.77/0.5

Table 4.22: Haplotypic mean [95% CI] lnfIL-18 levels by *IL18* and *IL18BP* haplotype in NPHSII.

	Haplotype		Frequency (%)	Haplotypic mean lnfIL-18[95% CI]	p
IL18	hGCATA	h12111	28.2	2.54[2.48–2.59]	Ref
	hTTCAC	h21222	24.8	2.42[2.35–2.48]	0.01
	hGTATA	h11111	29.9	2.43[2.38–2.48]	0.01
	hTTATC	h21112	8.9	2.53[2.41–2.66]	0.95
		Global p/R^2			0.04/2.6
IL18BP	hTTC	h111	85.2	2.48[2.45–2.51]	Ref
	hTGC	h121	11.0	2.46[2.36–2.57]	0.81
	hCTT	h212	1.3	2.35[2.07–2.64]	0.39
	hCTC	h211	1.4	2.63[2.23–3.02]	0.46
		Global p/R^2			0.65/0.7

Table 4.23: Geometric mean [95% CI] IL-18 levels (pg/ml) by *IL18* haplotype in CUDAS.

Haplotype		Copies	Geometric mean IL-18[95% CI] (pg/ml)	p	R^2
		0	291.4[280.9–302.3]		
hGCATA	h12111	1	305.7[294.2–317.7]	0.04	0.4
		2	322.8[298.1–349.5]		
		0	301.1[290.9–311.6]		
hTTCAC	h21222	1	298.2[286.1–310.8]	0.82	<0.1
		2	307.1[281.5–335.1]		
		0	314.8[304.7–325.2]		
hGTATA	h11111	1	283.6[271.7–296.0]	<0.001	1.7
		2	269.1[245.2–295.3]		
		0	299.2[290.9–307.6]		
hTTATC	h21112	1	309.1[291.6–327.6]	0.35	<0.1
		2	268.8[218.0–331.4]		

due to both hGTATA and hTTCAC being associated with significantly lower fIL-18 levels than the reference haplotype (p=0.01 for both). The effects for these two haplotypes were such that homozygotes for both were estimated to have fIL-18 levels 81% and 79%, respectively, of those estimated for hGCATA homozygotes (see figure 4.10 on the following page).

4.2.4.3 CUDAS

Haplotype analysis in CUDAS was carried out by Pam McCaskie using SimHap, therefore data is presented as estimated geometric means for carriers of 0,1, or 2 copies of each haplotype. In CUDAS, hGCATA was associated with significant differences in IL-18 levels (p=0.04, see table 4.23) with homozygotes having levels, on average, 1.1-fold higher than those without a copy of hGCATA. hGTATA was also significantly associated with differences in IL-18 levels (p<0.001), with those homozygous for the haplotype having average levels 85% of those with no copies (see figure 4.11 on page 161). In both cases the effect appeared additive, with those carrying one copy of the haplotype having mean IL-18 levels midway between the two homozygote groups.

4.2.4.4 CUPID

Haplotype analysis in CUPID was carried out by Pam McCaskie using SimHap, therefore data is presented as estimated geometric means for carriers of 0,1, or 2 copies of each haplotype. In CUPID, both hGTATA and hTTATC were significantly associated

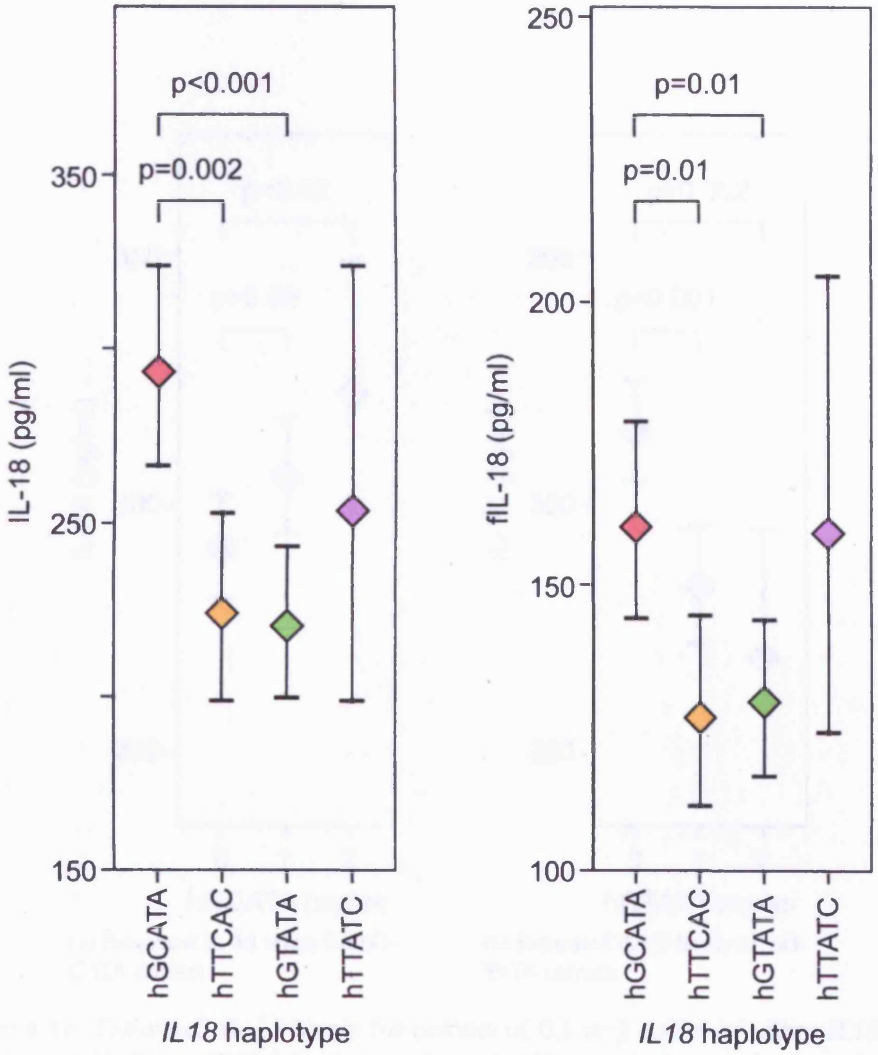

(a) Estimated IL-18 levels for homozygotes of common *IL18* haplotypes

(b) Estimated fIL-18 levels for homozygotes of common *IL18* haplotypes

Figure 4.10: Estimated IL-18 and fIL-18 levels for homozygotes of *IL18* haplotypes in NPHSII. Data is double the estimated haplotypic mean (◇), with 95% CIs (whiskers), p values are those relating to haplotypic means.

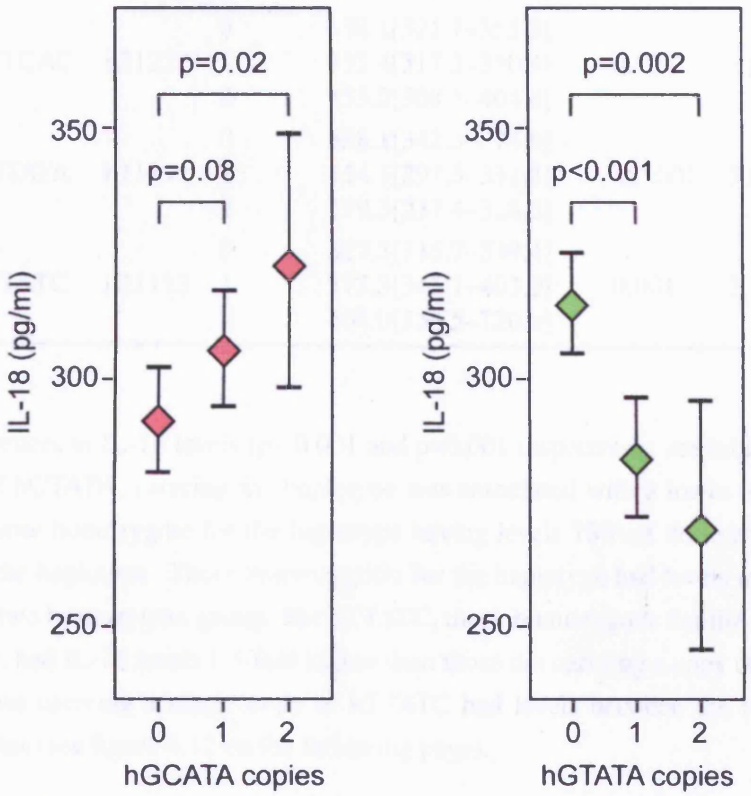

(a) Estimated IL-18 levels for hGCATA carriers

(b) Estimated IL-18 levels for hGTATA carriers

Figure 4.11: Estimated IL-18 levels for carriers of 0,1 or 2 copies of either *IL18* hGCATA or hGTATA in CUDAS. Data is from SimHap analysis and shows estimated mean (◇), with 95% CIs (whiskers).

Table 4.24: Geometric mean [95% CI] IL-18 levels (pg/ml) by *IL18* haplotype in CUPID.

Haplotype		Copies	Geometric mean IL-18[95% CI] (pg/ml)	p	R^2
		0	334.2[319.4–349.6]		
hGCATA	h12111	1	340.4[322.5–359.4]	0.88	<0.1
		2	335.7[301.3–374.1]		
		0	338.1[321.7–355.3]		
hTTCAC	h21222	1	333.4[317.3–350.4]	0.72	<0.1
		2	353.2[308.5–404.4]		
		0	358.1[342.3–374.6]		
hGTATA	h11111	1	314.1[297.5–331.5]	<0.001	3.0
		2	279.3[237.4–328.5]		
		0	327.3[315.7–339.4]		
hTTATC	h21112	1	373.3[345.7–403.0]	0.001	2.1
		2	507.0[356.5–720.9]		

with differences in IL-18 levels ($p<0.001$ and $p=0.001$ respectively, see table 4.24). In the case of hGTATA, carrying the haplotype was associated with a lower level of IL-18, with those homozygote for the haplotype having levels 78% of those not carrying a copy of the haplotype. Those heterozygotic for the haplotype had levels midway between the two homozygote group. For hTTATC, those homozygotic for the haplotype, on average, had IL-18 levels 1.5-fold higher than those not carrying a copy of hTTATC. Again, those carrying a single copy of hTTATC had levels between the two sets of homozygotes (see figure 4.12 on the following page).

4.2.4.5 SCARF

IL18 haplotypes were associated with significant differences in IL-18 levels in the total SCARF cohort ($p<0.001$), and also in cases ($p<0.001$) and controls ($p=0.006$) separately (see table 4.25 on page 165), explaining more of the variation in IL-18 levels in cases (5.9%) than controls (3.8%). Specifically, both hTTCAC and hGTATA were associated with significantly lower IL-18 levels in the total cohort ($p=0.001$ and $p<0.001$, respectively). These associations remained to the same extent when only cases were analysed, however, in controls hTTCAC was no longer associated with differences in IL-18 levels ($p=0.44$), yet hGTATA showed a similar association to that observed in the cases ($p=0.001$). The differences were such that in the total SCARF cohort, those homozygous for hGTATA were estimated to have IL-18 levels 76% of the average for homozygotes of hGCATA (controls–80%, cases–77%), for hTTCAC this was

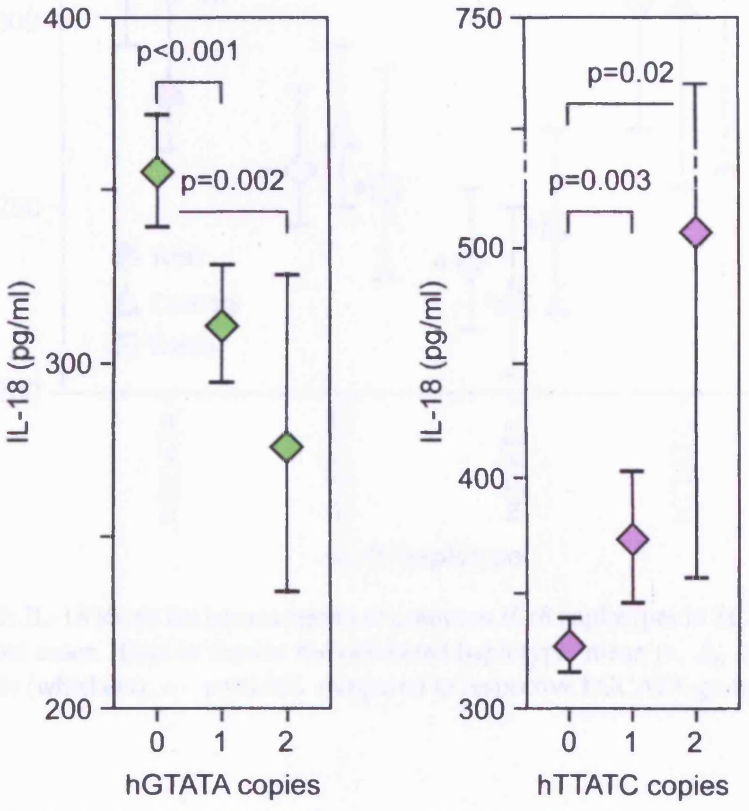

(a) Estimated IL-18 levels for hGTATA carriers

(b) Estimated IL-18 levels for hTTATC carriers

Figure 4.12: Estimated IL-18 levels for carriers of 0,1 or 2 copies of either *IL18* hGTATA or hTTATC in CUPID. Data is from SimHap analysis and shows estimated mean ($\diamond$), with 95% CIs (whiskers).

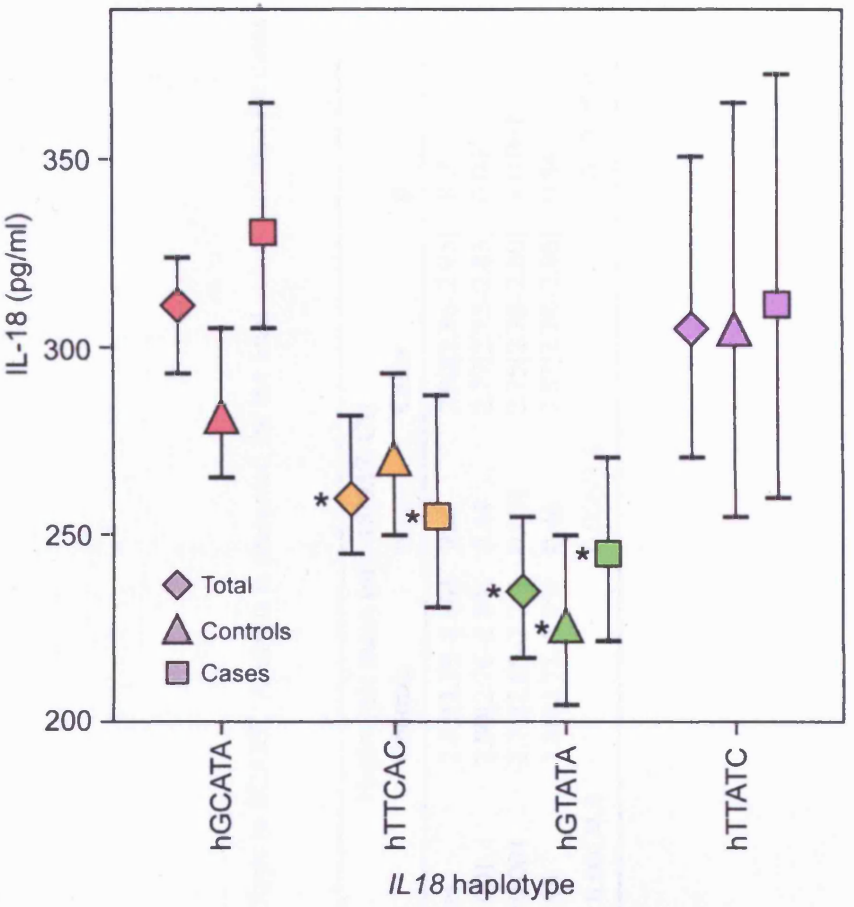

Figure 4.13: IL-18 levels for homozygotes of common *IL18* haplotypes in SCARF total, controls, and cases. Data is double the estimated haplotypic mean (◇, △, or □), with the 95% CIs (whiskers); ⋆ – p≤0.001 compared to respective hGCATA group.

84% (cases–77%, see figure 4.13).

4.2.5 Haplotype Multivariate Analysis

The same four models used in single SNP multivariate analysis (see section 4.2.3 on page 145) were used in haplotype multivariate analysis.

4.2.5.1 CABG

IL-18 In multivariate analysis, the association between hGTATA and IL-18 levels at both baseline and 6 h remained (see table 4.26 on page 167). However, the associations were greatly affected when adjusted for IL-6, CRP (model 3), and IL-18BP (model 4), such that the association with baseline IL-18 levels was only borderline in model 3 and model 4 (p=0.04 and p=0.05, respectively). The association with levels at 6 h

Table 4.25: Haplotypic mean [95% CI] lnIL-18 levels by *IL18* haplotype in SCARF. Analysis is presented for the total cohort and also for cases and controls separately.

Haplotype		Frequency (%)	Haplotypic mean lnIL-18[95% CI] Total	p	Controls	p	Cases	p
hGCATA	h12111	33.2	2.87[2.84–2.89]	Ref	2.82[2.79–2.86]	Ref	2.90[2.86–2.95]	Ref
hTTCAC	h21222	30.0	2.78[2.75–2.82]	0.001	2.80[2.76–2.84]	0.44	2.77[2.72–2.83]	0.001
hGTATA	h11111	22.9	2.73[2.69–2.77]	<0.001	2.71[2.66–2.76]	0.001	2.75[2.70–2.80]	<0.001
hTTATC	h21112	8.9	2.86[2.80–2.93]	0.98	2.86[2.77–2.95]	0.46	2.87[2.78–2.96]	0.54
	Global p/R^2			<0.001/4.4		0.006/3.8		<0.001/5.9

were no longer significant in model 3 or model 4 (p=0.07 and p=0.12, respectively). Interestingly, in both model 3 and model 4, hGTATA was significantly associated with IL-18 levels at 24 h (p=0.04 in both cases), whilst in univariate analysis, despite being associated with lower IL-18 levels, this association was not significant (p=0.15, see table 4.17 on page 153).

IL-18BP As in univariate analysis, *IL18BP* haplotypes did not significantly associate with IL-18BP levels in multivariate analysis (see table 4.27 on page 168).

fIL-18 Similar to those associations seen in IL-18 analysis, the association between hGTATA and fIL-18 levels (when compared to hGCATA) remained in multivariate analysis (see table 4.26 on the next page). In both model 1 and model 2, hGTATA was associated with a significantly lower haplotypic mean fIL-18 level at both baseline and at 6 h, however in model 3, when levels were additionally adjusted for IL-6 and CRP, the association at 6 h was no longer significant (p=0.12). Furthermore, in model 3, hGTATA was associated with a borderline significant association (p=0.05) with differences in fIL-18 levels at 24 h, an association which was not seen in univariate analysis.

For *IL18BP*, hCTT was significantly associated with differences in fIL-18 levels at baseline in all models (see table 4.27 on page 168). However, this haplotype was not significantly associated with differences in IL-18BP levels (p=0.36) therefore interrupting this result is difficult and it seems likely that this is a type I error.

4.2.5.2 NPHSII

IL-18 As shown in table 4.28 on page 169, in multivariate analysis both associations with hTTCAC and hGTATA remained in all four models. Furthermore, haplotypes remained globally associated with IL-18 levels in all models.

IL-18BP Common *IL18BP* haplotypes were not associated with IL-18BP levels in multivariate analysis (see table 4.29 on page 169).

fIL-18 *IL18* haplotypes were globally associated with differences in fIL-18 levels in all multivariate models. Specifically, as in univariate analysis, both hTTCAC and hGTATA were associated with fIL-18 levels. The associations were equally strong in both model 1 and model 2 (p=0.01 for all), however when further adjusted for CRP the association with hTTCAC was significantly attenuated and was only borderline significant (p=0.05), whilst that with hGTATA was made more significant (p=0.003, see table 4.28 on page 169).

No *IL18BP* haplotype was significantly associated with fIL-18 levels in NPHSII (see table 4.29 on page 169).

Table 4.26: P values from multivariate analysis of IL-18 and fIL-18 levels by *IL18* haplotype in CABG.

			Model 1 sex and age			Model 2 Model 1 + smoking, and statin use			Model 3 Model 2 + IL-6, and CRP			Model 4 Model 3 + IL-18BP		
	Haplotype		Base.	6 h	24 h	Base.	6 h	24 h	Base.	6 h	24 h	Base.	6 h	24 h
IL-18	hGCATA	h12111	Ref	Ref	Ref	Ref	Ref	Ref	Ref	Ref	Ref	Ref	Ref	Ref
	hTTCAC	h21222	0.36	0.08	0.98	0.39	0.13	0.97	0.31	0.20	0.98	0.23	0.19	0.97
	hGTATA	h11111	0.01	0.02	0.09	0.007	0.02	0.12	0.04	0.07	0.04	0.05	0.12	0.04
	hTTATC	h21112	0.34	0.75	0.81	0.32	0.82	0.56	0.15	0.88	0.65	0.32	0.95	0.68
		Global p	0.10	0.11	0.61	0.06	0.11	0.61	0.14	0.13	0.33	0.22	0.20	0.34
fIL-18	hGCATA	h12111	Ref	Ref	Ref	Ref	Ref	Ref	Ref	Ref	Ref	—	—	—
	hTTCAC	h21222	0.36	0.05	0.88	0.52	0.09	0.86	0.22	0.14	0.95	—	—	—
	hGTATA	h11111	0.02	0.04	0.08	0.03	0.05	0.14	0.04	0.12	0.05	—	—	—
	hTTATC	h21112	0.43	0.88	0.76	0.29	0.81	0.70	0.32	0.97	0.72	—	—	—
		Global p	0.19	0.07	0.60	0.18	0.13	0.66	0.21	0.16	0.36	—	—	—

Table 4.27: P values from multivariate analysis of IL-18BP and fIL-18 levels by *IL18BP* haplotype in CABG.

	Haplotype		Model 1 sex and age			Model 2 Model 1 + smoking, and statin use			Model 3 Model 2 + IL-6, and CRP			Model 4 Model 3 + IL-18		
			Base.	6 h	24 h	Base.	6 h	24 h	Base.	6 h	24 h	Base.	6 h	24 h
IL-18BP	hTTC	h111	Ref	Ref	Ref	Ref	Ref	Ref	Ref	Ref	Ref	Ref	Ref	Ref
	hTGC	h121	0.90	0.79	0.45	0.91	0.79	0.45	0.69	0.41	0.21	0.75	0.40	0.48
	hCTT	h212	0.49	0.95	0.96	0.52	0.98	0.89	0.50	0.89	0.96	0.46	0.91	0.99
	hCTC	h211	0.99	0.89	0.52	0.99	0.86	0.55	0.99	0.81	0.81	0.69	0.76	0.77
		Global p	0.75	0.95	0.59	0.76	0.89	0.55	0.80	0.84	0.55	0.91	0.94	0.98
fIL-18	hTTC	h111	Ref	Ref	Ref	Ref	Ref	Ref	Ref	Ref	Ref	—	—	—
	hTGC	h121	0.73	0.58	0.61	0.82	0.61	0.61	0.55	0.13	0.91	—	—	—
	hCTT	h212	0.007	0.92	0.87	0.005	0.84	0.81	0.006	0.95	0.98	—	—	—
	hCTC	h211	0.67	0.52	0.80	0.67	0.57	0.83	0.64	0.61	0.99	—	—	—
		Global p	0.37	0.97	0.99	0.30	0.97	0.99	0.27	0.66	0.99	—	—	—

Table 4.28: P values from multivariate analysis of IL-18 and fIL-18 levels by *IL18* haplotype in NPHSII.

	Haplotype		Model 1 age	Model 2 Model 1 + smoking	Model 3 Model 2 + CRP	Model 4 Model 3 + IL-18BP
IL-18	hGCATA	h12111	Ref	Ref	Ref	Ref
	hTTCAC	h21222	0.002	0.002	0.006	0.01
	hGTATA	h11111	<0.001	<0.001	<0.001	<0.001
	hTTATC	h21112	0.28	0.32	0.43	0.63
		Global p	0.003	0.004	0.001	0.003
fIL-18	hGCATA	h12111	Ref	Ref	Ref	—
	hTTCAC	h21222	0.01	0.01	0.05	—
	hGTATA	h11111	0.01	0.01	0.003	—
	hTTATC	h21112	0.98	0.93	0.94	—
		Global p	0.04	0.04	0.03	—

Table 4.29: P values from multivariate analysis of IL-18BP and fIL-18 levels by *IL18BP* haplotype in NPHSII.

	Haplotype		Model 1 age	Model 2 Model 1 + smoking	Model 3 Model 2 + CRP	Model 4 Model 3 + IL-18
IL-18BP	hTTC	h111	Ref	Ref	Ref	Ref
	hTGC	h121	0.60	0.60	0.38	0.38
	hCTT	h212	0.24	0.24	0.26	0.23
	hCTC	h211	0.67	0.68	0.65	0.67
		Global p	0.84	0.84	0.81	0.74
fIL-18	hTTC	h111	Ref	Ref	Ref	—
	hTGC	h121	0.83	0.81	0.65	—
	hCTT	h212	0.38	0.40	0.42	—
	hCTC	h211	0.43	0.46	0.49	—
		Global p	0.71	0.77	0.88	—

Table 4.30: P values from multivariate analysis of IL-18 levels by *IL18* haplotype in CUDAS.

Haplotype		IL-18 multivariate analysis Adjusted for age, sex, presence of hypertension, HDL, WTHR, and Alcohol consumption
hGCATA	h12111	0.04
hTTCAC	h21222	0.81
hGTATA	h11111	<0.001
hTTATC	h21112	0.12

Table 4.31: P values from multivariate analysis of IL-18 levels by *IL18* haplotype in CUPID.

Haplotype		IL-18 multivariate analysis Adjusted for age, sex, BMI, LDL, and triglycerides
hGCATA	h12111	0.80
hTTCAC	h21222	0.70
hGTATA	h11111	<0.001
hTTATC	h21112	<0.001

4.2.5.3 CUDAS

Multivariate haplotype analysis in CUDAS was carried out by Pam McCaskie using SimHap. As such the four models presented above were not used and IL-18 levels were adjusted for age, sex, presence of hypertension, HDL, WTHR, and alcohol consumption.

Adjustment of IL-18 levels for these parameters had no effect on the *IL18* haplotype associations described in section 4.2.3.3 on page 148. Both hGCATA and hGTATA were associated with significant differences in IL-18 levels with the effect of hGTATA being more significant ($p<0.001$) than that of hGCATA ($p=0.04$).

4.2.5.4 CUPID

Multivariate haplotype analysis in CUPID was carried out by Pam McCaskie using SimHap. As such the four models presented above were not used and IL-18 levels were adjusted for age, sex, BMI, LDL, and triglycerides.

As in CUDAS, multivariate analysis had little impact on the associations seen in univariate analysis. Both hGTATA and hTTATC were significantly associated with dif-

ferences in IL-18 levels (both $p<0.001$) when adjusted for numerous factors seen to correlate with IL-18 levels (see table 4.31 on the preceding page).

4.2.5.5 SCARF

Haplotypes remained globally associated with differences in IL-18 levels in both the entire SCARF study, and in cases and controls separately, in all three multivariate models ($p \leq 0.003$ in all analyses, see table 4.32 on the next page). Specifically, both hTTCAC and hGTATA showed significantly different IL-18 levels from those associated with the reference haplotype (hGCATA). However, the level of IL-18 associated with hTTCAC was only significantly different from that associated with hGCATA in cases ($p \leq 0.002$ in all models), not controls ($p \geq 0.28$ in all models). This was not the case for hGTATA, with this haplotype being significantly associated with IL-18 levels in both the total cohort and cases and controls separately ($p<0.001$ in all samples across all models).

4.2.6 MDR Analysis

MDR analysis was carried out in both CABG and NPHSII as these were the only studies that had both *IL18* and *IL18BP* SNPs genotyped. The binary variable used was top tertile of lnIL-18, sqrtIL-18BP, or lnfIL-18, vs. the bottom two tertiles. To ease data interpretation and presentation only five-way interactions were investigated.

4.2.6.1 CABG

Given that, in total, 45 sets of data are presented, two or more results would be expected to exceed p=0.05. In this case there were three, with two of these exceeding p=0.01 (see figure 4.14 on page 173). The four and five SNP combination sets for fIL-18 at 6 h were highly significant (p=0.004, and p=0.002, respectively), and had high average CVC over ten runs (7.8 and 7.1, respectively). The four SNP set was *IL18*-9731;-5848;+105;*IL18BP*-559, whilst the five SNP set built on this adding *IL18BP*-1765, both were identified in each one of the ten runs as the best performing model. The five SNP set was a common combination being identified also in each run for baseline fIL-18 (p=0.44), and IL-18 at 6 h (p=0.04), and all but one run for baseline IL-18 (p=0.60).

4.2.6.2 NPHSII

The same five SNP combination was also identified in each of the ten runs for IL-18 in NPHSII (p=0.49) with an average CVC of 10, and for fIL-18 (p=0.05), again with an average CVC of 10. The only other significant result was the identification of a four SNP set, *IL18*-5848:+11015:*IL18BP*-1765:-559, associated with IL-18BP in NPHSII, which had an average TBA over ten runs that was equivalent to p=0.03, with an average

Table 4.32: P values from multivariate analysis of IL-18 levels by *IL18* haplotype in SCARF.

Haplotype		Model 1 sex and age			Model 2 Model 1 + smoking			Model 3 Model 2 + IL-6 and CRP		
		Total	Controls	Cases	Total	Controls	Cases	Total	Controls	Cases
hGCATA	h12111	Ref	Ref	Ref	Ref	Ref	Ref	Ref	Ref	Ref
hTTCAC	h21222	<0.001	0.28	<0.001	<0.001	0.28	0.001	<0.001	0.30	0.002
hGTATA	h11111	<0.001	<0.001	<0.001	<0.001	<0.001	<0.001	<0.001	<0.001	<0.001
hTTATC	h21112	0.95	0.50	0.54	0.93	0.48	0.56	0.85	0.48	0.48
	Global p	<0.001	0.003	<0.001	<0.001	0.001	<0.001	<0.001	0.002	<0.001

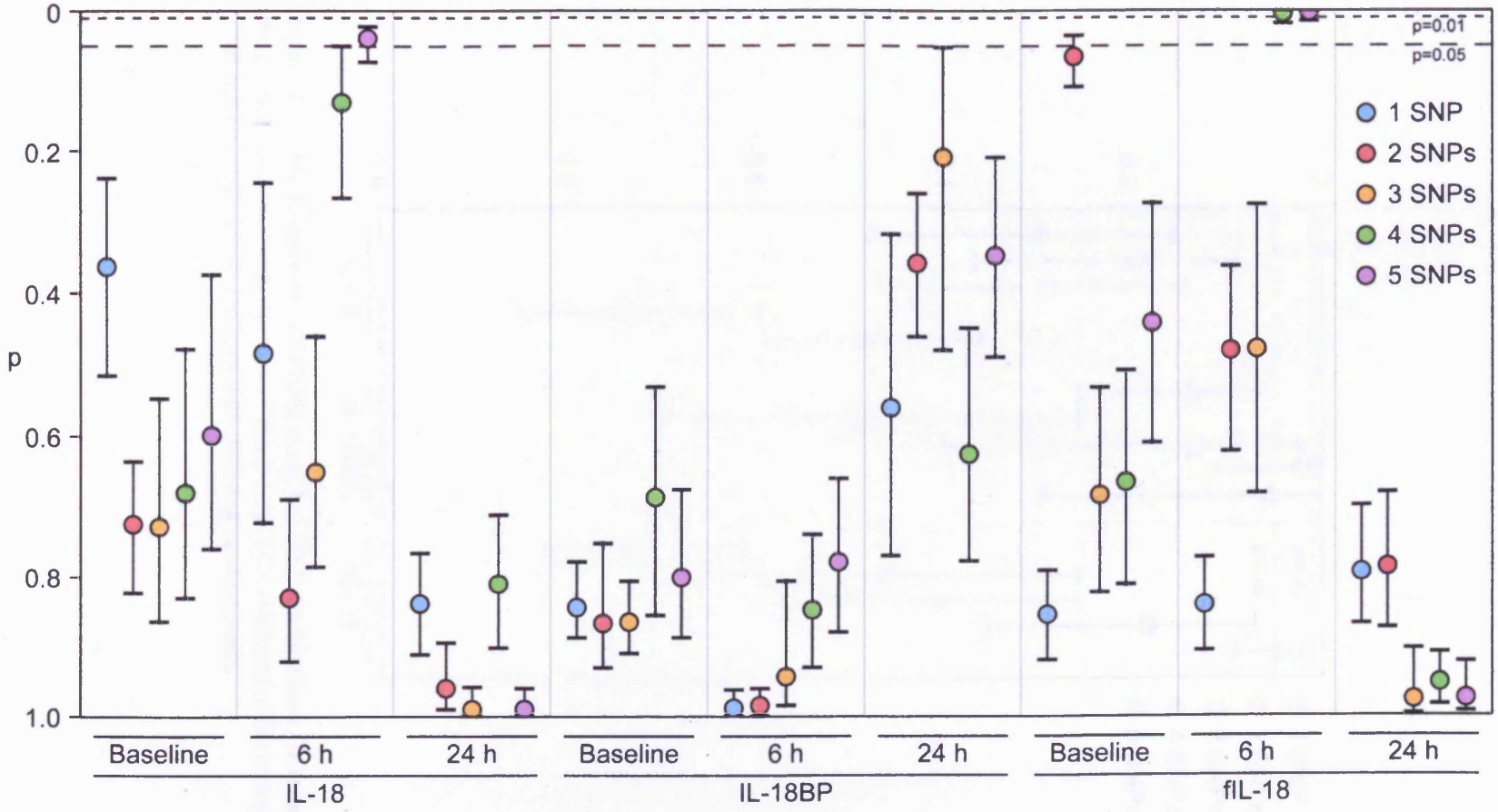

Figure 4.14: MDR analysis in CABG using 1–5 SNP combinations. Data presented is the p value associated with the mean TBA (○) and SD (whiskers) of the best performing SNP combinations across ten runs with differing random seeds.

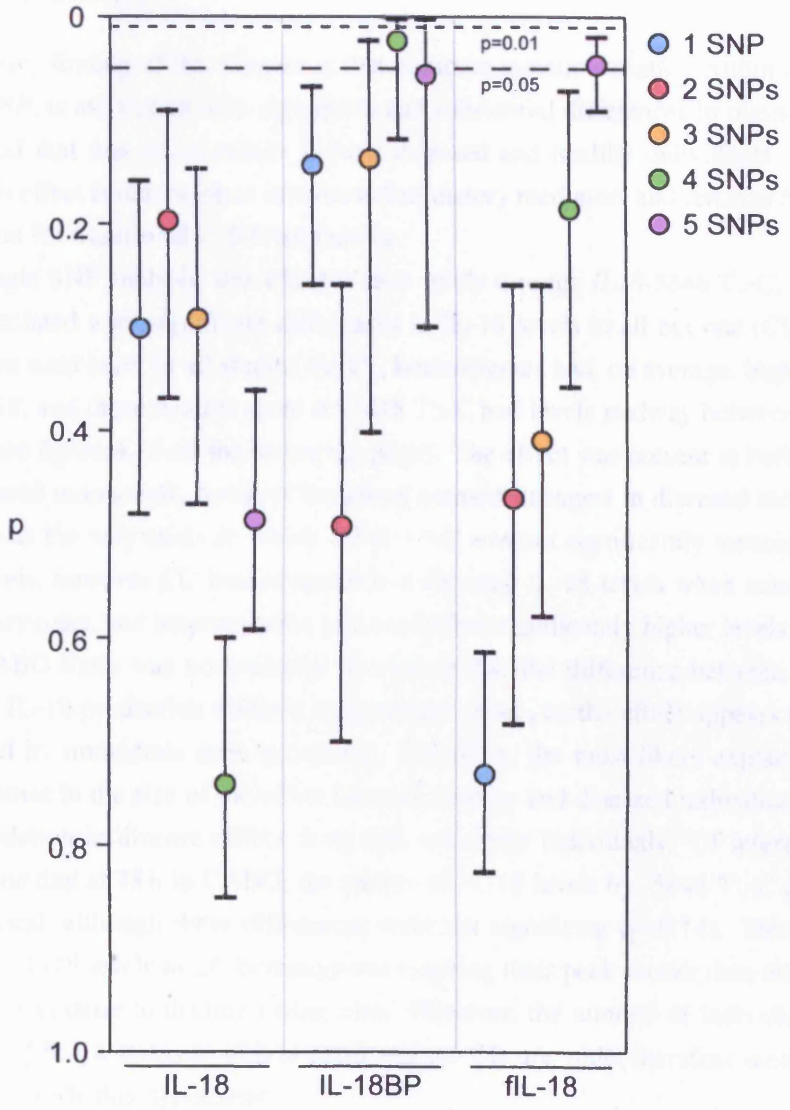

Figure 4.15: MDR analysis in NPHSII using 1–5 SNP combinations. Data presented is the p value associated with the mean TBA (○) and SD (whiskers) of the best performing SNP combinations across ten runs with differing random seeds.

CVC of 6 (see figure 4.15 on the previous page). This set was not identified in any of the CABG IL-18BP runs at any time-point.

4.3 Discussion

The primary finding of this chapter is that common genetic variation within *IL18*, but not *IL18BP*, is associated with significant and substantial differences in plasma fIL-18 levels, and that this effect occurs in both diseased and healthy individuals. Furthermore, this effect is independent of other inflammatory mediators and remains following adjustment for traditional CHD risk factors.

In single SNP analysis, this effect is seen solely through *IL18*-5848 T>C, with this SNP associated with significant differences in IL-18 levels in all but one (CUPID) of the studies used here. In all studies the CC homozygotes had, on average, higher levels than IL-18, and those heterozygote at -5848 T>C had levels midway between the two groups (see figure 4.16 on the following page). The effect was present in both healthy and diseased individuals, however the effect seemed strongest in diseased individuals. CUPID was the only study in which -5848 T>C was not significantly associated with IL-18 levels, however CC homozygotes had elevated IL-18 levels when compared to TT homozygotes, and heterozygotes had borderline significantly higher levels.

In CABG there was no evidence to suggest that the difference between baseline and peak IL-18 production differed by genotype group, so the effect appears not to be influenced by immediate gene activation. Therefore, the most likely explanation for the difference in the size of the effect between healthy and diseased individuals, is that *IL18* regulation in disease differs from that in healthy individuals. Of interest is the observation that at 48 h in CABG, the pattern of IL-18 levels by -5848 T>C genotype was reversed, although these differences were not significant (p=0.14). This may be due to the IL-18 levels in CC homozygotes reaching their peak sooner than others, and therefore beginning to decline earlier also. However, the number of individuals with measures of IL-18 levels at 48 h is small and the CIs are wide, therefore more data is required to study this hypothesis.

In the studies where both IL-18 and IL-18BP measurements were made (CABG and NPHSII) it was possible to calculate, based on known stoichiometry and dissociation constants, the likely amount of IL-18 able to bind IL-18R and have pathophysiological effects–fIL-18. In both studies, -5848 T>C was the only *IL18* tSNP associated with significant differences in fIL-18 levels, showing a similar, but blunted, pattern to that seen with IL-18 levels. Given that the concentration of IL-18BP vastly exceeded that of IL-18 and also appeared to have a greater range during activation (see figure 4.5 on page 140), it was important to ascertain whether the effect of *IL18*-5848 T>C remained in fIL-18 analysis. That the effect was strong enough to remain in fIL-18 analysis

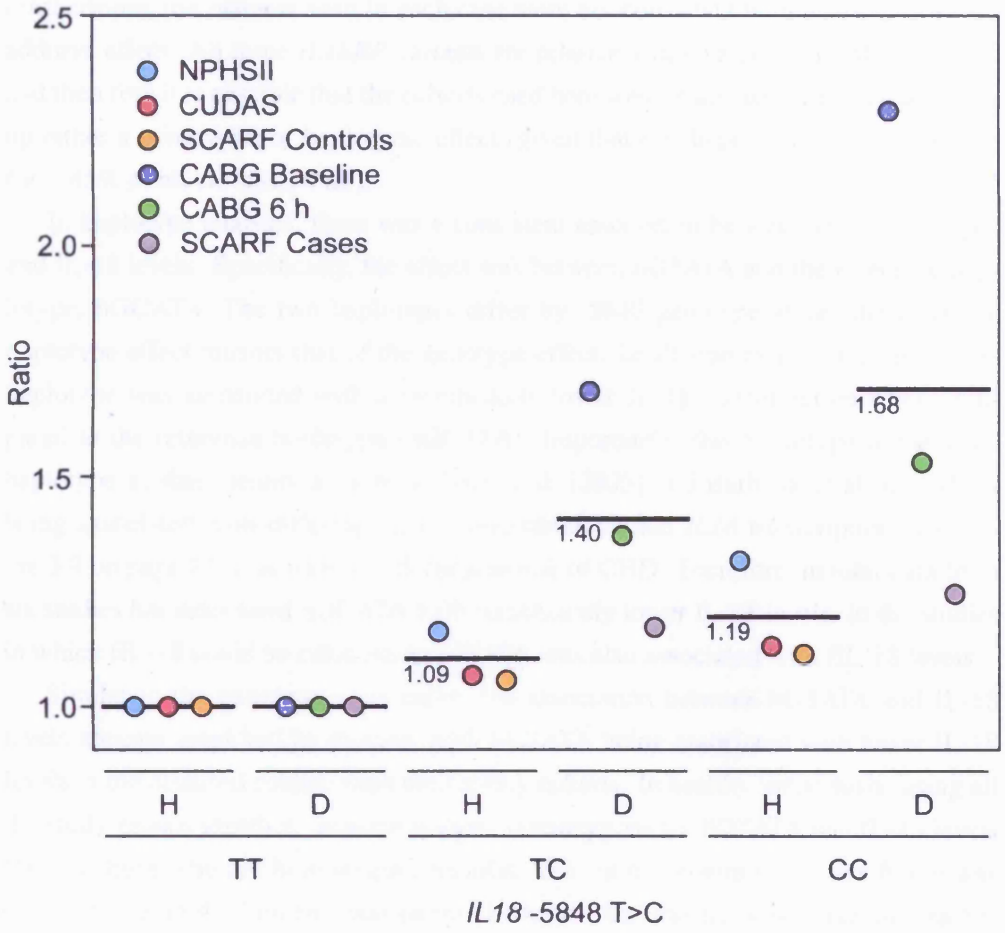

Figure 4.16: Summary of the significant *IL18*-5848 T>C associations. Data presented is ratio of mean IL-18 level compared to TT homozygotes, with bar (—) showing average of cohorts. Studies split into healthy (H) and diseased (D) study groups.

suggests that CC homozygotes might be at greater risk of CHD, as IL-18 is a potentially causal factor in disease. That the effect also remained following adjustment for both IL-6 and CRP shows that it is independent of these inflammatory factors.

Genetic variation within *IL18BP* did not appear to play a significant role in dictating plasma IL-18BP levels. Although there were significant associations for each of the *IL18BP* tSNPs in CABG, these were not consistent across time-points or other studies. Furthermore, the patterns seen in each case were not consistent with a straightforward additive effect. All three *IL18BP* variants are relatively rare variants (all MAF<12%), and therefore it is possible that the cohorts used here were inadequately powered to pick up either a genotypic, or haplotypic effect (given that one haplotype alone accounted for >85% of all chromosomes).

In haplotype analysis, there was a consistent association between *IL18* haplotypes and IL-18 levels. Specifically, the effect was between hGTATA and the reference haplotype, hGCATA. The two haplotypes differ by -5848 genotype alone, therefore the haplotype effect mirrors that of the genotype effect. In all studies presented here, this haplotype was associated with a significantly lower IL-18 concentration when compared to the reference haplotype (hGCATA). Importantly, this haplotype is the same haplotype as that identified by both Tiret et al. [2005] and Barbaux et al. [2007], as being associated with differing IL-18 concentrations and *IL18* transcription (see figure 3.9 on page 121), as well as a decreased risk of CHD. Therefore, in total data from six studies has associated hGCATA with significantly lower IL-18 levels. In the studies in which fIL-18 could be calculated, hGTATA was also associated with fIL-18 levels.

Similar to the genotype association, the association between hGTATA and IL-18 levels appears amplified by disease, with hGTATA being associated with lower IL-18 levels in the diseased cohorts than the healthy cohorts. In healthy individuals, using all the study groups together, on average those homozygous for hGTATA had IL-18 levels 80% of those who are homozygous for hGCATA, in those with CHD this figure was 61% (see figure 4.17 on the next page). However, heterogeneity between the studies means that this estimate may not truly reflect the size of the effect; in CABG the haplotypic effect appears particularly strong, perhaps due to other influences besides underlying disease. In both SCARF, CUDAS and CUPID, diseased and healthy individuals had IL-18 levels measured in tandem. In these two studies the difference (between healthy and diseased individuals) in the effect of hGTATA is modest. However, IL-18 levels are higher in SCARF cases than controls (309.6 vs. 285.4 pg/ml, p=0.01), as they are in CUPID compared to CUDAS (366.2 vs. 327.8 pg/ml), so truly assessing the relative impact of hGTATA in diseased vs. healthy individuals is difficult. This is made more difficult given that hGCATA (the reference haplotype in most analyses) appears to also be associated with differences in IL-18 levels in CUDAS (see figure 4.11 on page 161).

Multivariate analysis had only minor effects on the univariate haplotype results de-

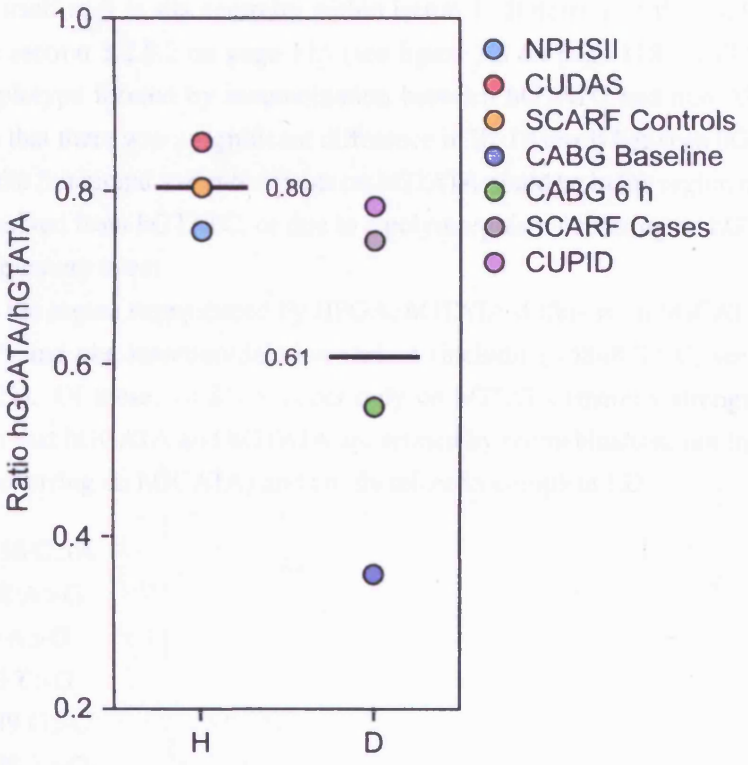

Figure 4.17: Ratio between the estimated serum IL-18 concentration of those homozygote for both *IL18* hGCATA and hGTATA. Studies are separated into healthy (H) and diseased cohorts (D). The mean for each group is also shown (—).

tailed. In most cases the associations remained but were attenuated. As in the genotype associations, these remained following adjustment for other inflammatory factors–IL-6 and CRP (although this was not necessarily the case in CABG), and also when IL-18 levels were adjusted for IL-18BP levels, suggesting that *IL18* transcription is not under the control of IL-18BP.

It is not possible to say exactly where the functional variant/variants are within or around *IL18* since LD is strong across the gene and each of the tSNPs are chosen for their ability to mark other SNPs. However, *IL18*-5848 T>C itself looks unlikely to be functional itself as it is sits centrally within intron 1. Referring to the haplotypic tree inferred in section 3.2.5.2 on page 115 (see figure 3.8 on page 118), hGTATA seems to be a haplotype formed by recombination between hGTATC and hGCATA. Therefore, given that there was a significant difference in IL-18 levels between hGCATA and hGTATA, the functional variant/variants on hGTATA could be in the region of the chromosome derived from hGTATC, or due to a polymorphism occurring on hGTATA after this recombinatory event.

Across the region resequenced by IIPGA, hGTATA differs from hGCATA at a total of 14 SNPs and one insertion/deletion variant (including -5848 T>C, see figure 3.9 on page 121). Of these, 10 SNPs occur only on hGTATA (thereby strengthening the assumption that hGCATA and hGTATA are related by recombination, not by the -5848 mutation occurring on hGCATA) and are therefore in complete LD:

-11238 C>A
-1368 A>G
-139 A>G
+470 T>G
+1949 G>C
+2928 T>C
+4009 G>C
+8905 G>C
+10790 G>A
+11640 A>G

As hGTATA is the only haplotype to be consistently associated with differences in IL-18 levels it would seem that these SNPs, of the ones identified by IIPGA, are the most likely functional changes. However, unless these SNPs 'split' hGTATA, each SNP will mark the effect of -5848 T>C and can therefore not be independently studied. One SNP that does appear to split hGTATA (when using haplotypes inferred using PHASE v2.1) is -1368 A>G, and this was therefore the one extra SNP that was needed, in later analysis, to mark all variation within *IL18* when using haplotypes inferred with PHASE

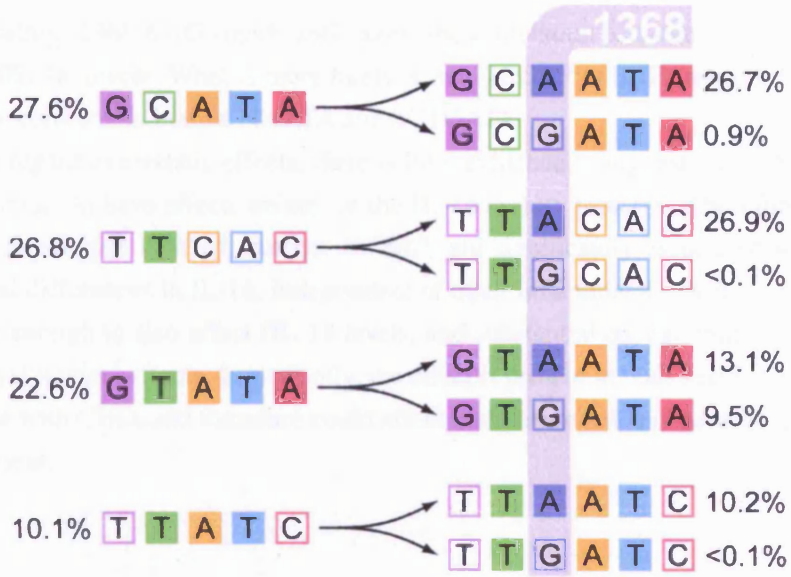

Figure 4.18: Haplotypes inferred using *IL18*-1368 A>G in addition to the tSNP set; ■ – common allele, □ – rare allele. Haplotypes are ordered -9731 G>T; -5848 T>C; (-1368 A>G); +105 A>C; +8855 T>A; +11015 A>C.

v2.1 (see section 3.2.6.1 on page 119). To assess their impact on the associations detailed within this chapter, both -1368 A>G and -11238 C>A (as a variant within the promoter) were genotyped in CABG. *IL18*-11238 C>A did not help to distinguish extra haplotypes (and is therefore not included in subsequent analysis) but by adding -1368 A>G, hGTATA, and hGTATA only, was split into two common haplotypes (see figure 4.18).

Inclusion of -1368 A>G also had an effect on the association between *IL18* haplotypes and IL-18 levels. The SNP itself was not associated with significant differences in either IL-18 or fIL-18 at baseline or 6 h, but was associated with significant differences in both IL-18 and fIL-18 at 24 h, with GG homozygotes having significantly lower levels than either heterozygotes or AA homozygotes (although there were only two GG individuals). In haplotype analysis, haplotypes were significantly associated with both IL-18 (see table 4.33 on page 182) and fIL-18 (see table 4.34 on page 182)at baseline, with hGTAATA being associated with significantly lower IL-18 and fIL-18. This haplotype was also borderline significantly associated with IL-18 and fIL-18 at 6 h in CABG. However, the 95% CI for the estimated mean IL-18 and fIL-18 levels for hGTAATA were largely similar to those seen for hGTATA (see table 4.17 on page 153 and table 4.19 on page 155). Furthermore given that the SNP itself is not associated with IL-18 levels at baseline or 6 h, strongly suggests that its inclusion does not clarify the association with hGTATA. Therefore, in conclusion, there is no evidence to suggest

that including -1368 A>G significantly alters the association between hGTATA and IL-18, and fIL-18, levels. What is more likely is that the SNP or SNPs responsible for the effect are common to both hGTAATA and hGTGATA.

With regard to epistatic effects, there is little evidence to suggest that tSNPs across genes interact to have effects on any of the IL-18 system proteins. Therefore, in conclusion, haplotypes in *IL18*, but not *IL18BP*, are significantly associated with inter-individual differences in IL-18, independent of other inflammatory factors. This effect is strong enough to also affect fIL-18 levels, and substantial enough that it could have pathophysiological effects. Importantly, the effect is present in both healthy individuals and those with CHD, and therefore could affect both future risk and severity of disease, once present.

Table 4.33: LnIL-18 levels by *IL18* haplotypes in CABG, using haplotypes inferred with the tSNP set and -1368 A>G. Haplotypes are ordered -9731;-5848;-1368;+105;+8855;+11015.

Haplotype		Freq. (%)	Haplotypic mean lnIL-18[95% CI] Baseline	p	6 h	p	24 h	p
hGCAATA	h121111	27.0	2.799[2.627–2.972]	Ref	3.144[2.989–3.299]	Ref	2.786[2.593–2.978]	Ref
hTTACAC	h211222	24.8	2.660[2.408–2.913]	0.41	2.931[2.775–3.087]	0.11	2.789[2.467–3.111]	0.99
hGTAATA	h111111	13.9	2.195[1.817–2.573]	0.006	2.866[2.634–3.099]	0.05	2.705[2.321–3.090]	0.72
hTTAATC	h211112	9.4	2.699[2.241–3.157]	0.69	3.125[2.861–3.389]	0.90	2.808[2.438–3.179]	0.92
hGTGATA	h112111	8.7	2.584[2.200–2.969]	0.37	2.924[2.630–3.219]	0.22	2.355[2.124–2.586]	0.01
hGCACAC	h121222	3.4	3.321[2.420–4.221]	0.27	3.200[2.364–4.036]	0.90	3.005[2.136–3.874]	0.63
hTTAAAC	h211122	3.3	1.698[0.893–2.503]	0.009	2.951[2.364–4.036]	0.54	2.686[2.135–3.238]	0.74
	Global p/R^2			0.004/13.0		0.40/4.4		0.70/3.0

Table 4.34: LnfIL-18 levels by *IL18* haplotypes in CABG, using haplotypes inferred with the tSNP set and -1368 A>G. Haplotypes are ordered -9731;-5848;-1368;+105;+8855;+11015.

Haplotype		Freq. (%)	Haplotypic mean lnfIL-18[95% CI] Baseline	p	6 h	p	24 h	p
hGCAATA	h121111	27.0	2.573[2.385–2.762]	Ref	2.991[2.832–3.149]	Ref	2.304[2.071–2.537]	Ref
hTTACAC	h211222	24.8	2.376[2.139–2.614]	0.25	2.754[2.592–2.916]	0.08	2.262[1.953–2.572]	0.84
hGTAATA	h111111	13.9	2.010[1.661–2.360]	0.009	2.723[2.485–2.961]	0.06	2.174[1.779–2.568]	0.60
hTTAATC	h211112	9.4	2.388[1.972–2.804]	0.43	2.979[2.713–3.246]	0.94	2.324[1.951–2.696]	0.94
hGTGATA	h112111	8.7	2.270[1.884–2.656]	0.21	2.784[2.464–3.475]	0.29	1.810[1.573–2.047]	0.007
hGCACAC	h121222	3.4	3.083[2.252–3.914]	0.24	3.066[2.342–3.790]	0.85	2.475[1.631–3.320]	0.70
hTTAAAC	h211122	3.3	1.474[0.700–2.248]	0.006	2.860[2.245–3.475]	0.69	2.166[1.634–2.697]	0.64
	Global p/R^2			0.005/12.6		0.42/4.4		0.65/3.4

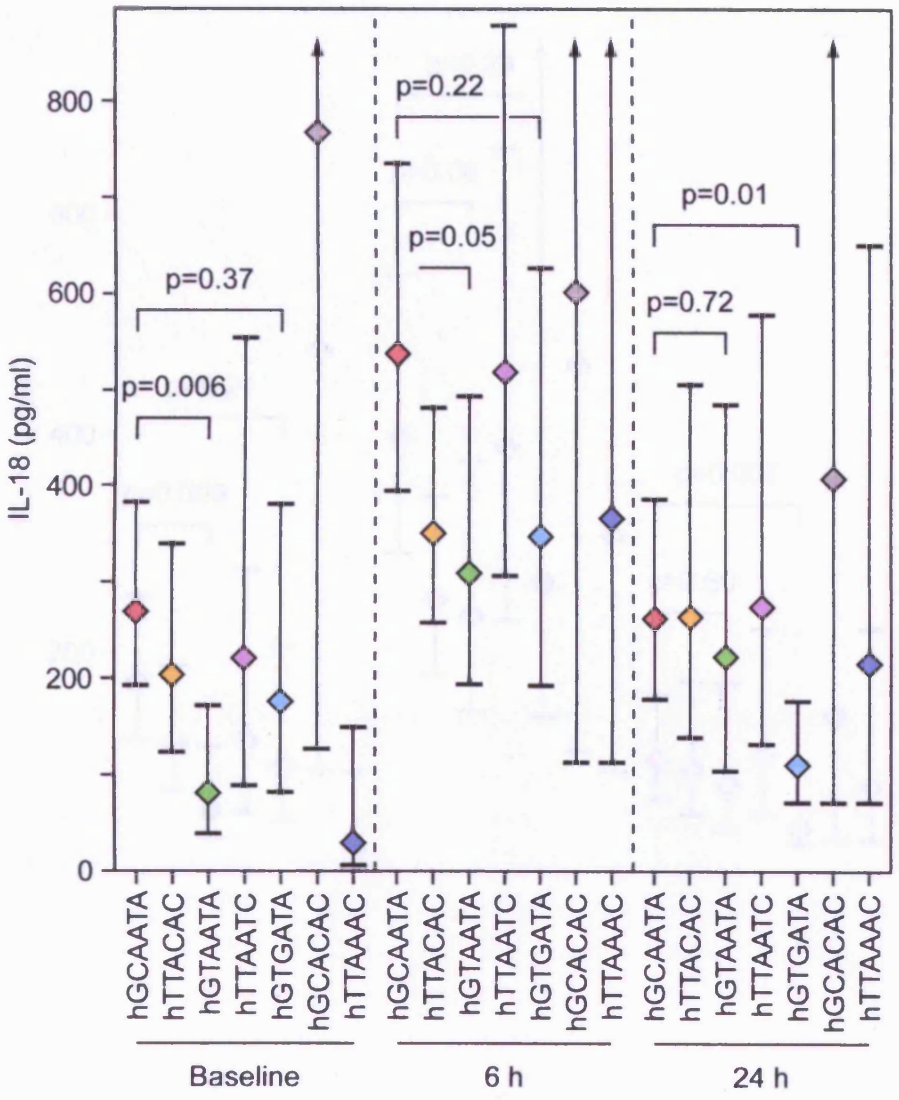

Figure 4.19: Estimated IL-18 levels for those homozygote for *IL18* haplotypes, that include -1368 A>G.

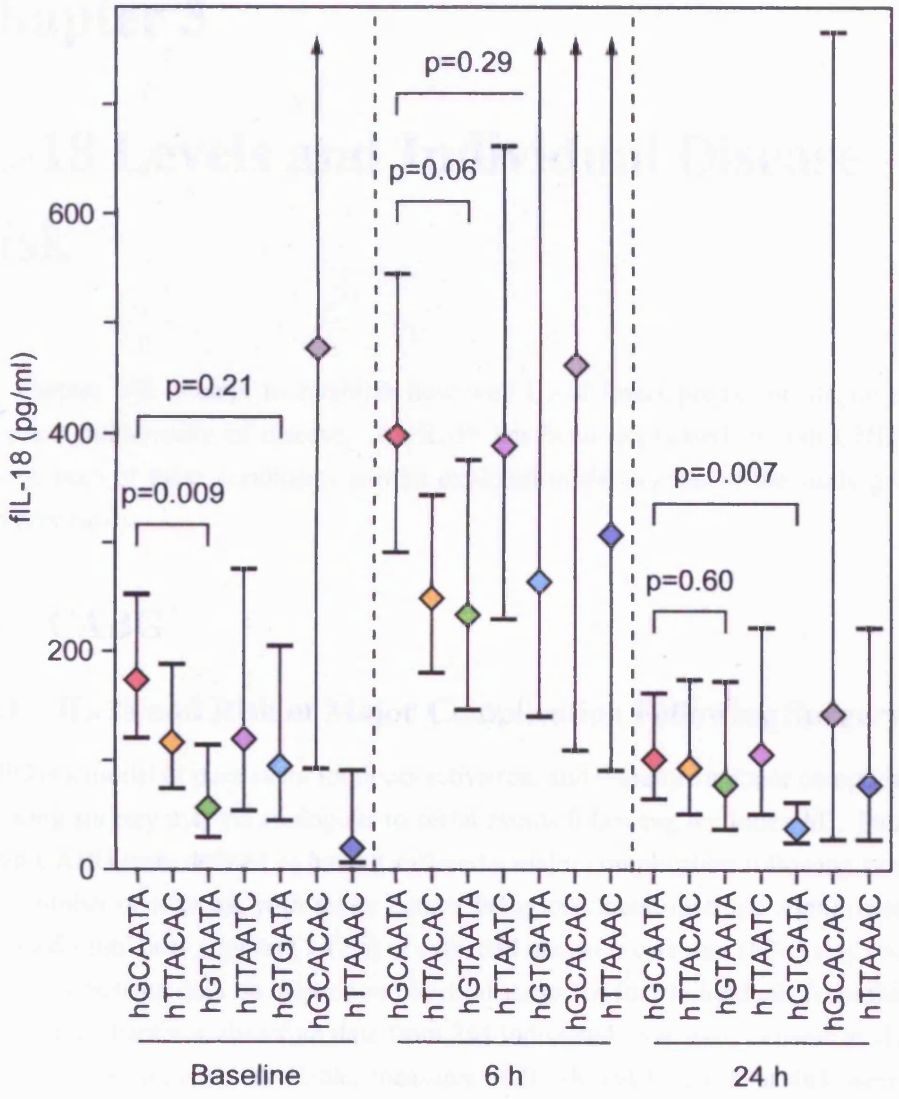

Figure 4.20: Estimated fIL-18 levels for those homozygote for *IL18* haplotypes, that include -1368 A>G.

Chapter 5

IL-18 Levels and Individual Disease Risk

This chapter will attempt to establish how well IL-18 levels predict or diagnose the existence and severity of disease. As IL-18 has been implicated in both CHD and obesity, both of these conditions will be explored in the context of the study groups used previously.

5.1 CABG

5.1.1 IL-18 and Risk of Major Complication Following Surgery

CABG is a model of post-event immuno-activation, and therefore a major complication following surgery may be analogous to serial events following the index MI. Patients within CABG were defined as having suffered a major complication following surgery for a number of reasons, with major causes being continued inotrope administration, increased ventilatory support (>12 h) or extended intensive care unit (ICU) stay (>2 d). There was missing data on major complication status for four individuals from the cohort used in chapter 4, therefore data from 244 individuals was used in these analyses. Due to the low numbers available, measures of IL-18 and IL-18BP at 48 h were not considered here.

5.1.1.1 Univariate Analysis

As can be seen in table 5.1 on the following page, baseline characteristics, and levels of inflammatory mediators following surgery, did not differ significantly between those who went on to suffer a major post-operative complication. However, both IL-18 and fIL-18 were significantly higher at 24 h in those who went on to suffer a major complication (p=0.001, and p=0.003, respectively, see figure 5.1 on page 188). IL-18 and

Table 5.1: Baseline characteristics for those who did or did not suffer a major complication in CABG. Data is presented as mean or geometric mean[95% CI].

Variable		No Major Complication (n=145)	Major Complication (n=99)	p
Male, %[n]		86.9[126]	78.8[78]	0.09
Age (yr)		64.4[63.0–65.9]	65.0[63.1–66.8]	0.64
Caucasian, %[n]		88.2[82]	84.6[115]	0.81
BMI (kg/m^2)		27.6[26.9–28.4]	28.4[27.4–29.3]	0.24
	0	66.2[96]	61.2[60]	
Past history of MI, %[n]	1	29.7[43]	26.5[26]	0.06
	2+	4.1[6]	12[12.2]	
Cholesterol-lowering medication, %[n]		76.8[109]	73.2[71]	0.53
Ever smoked, %[n]		77.8[112]	78.8[78]	0.57
Operation length (min)		198.8[191.4–206.2]	207.0[196.5–217.6]	0.19
Cardiopulmonary bypass (CPB) length (min)		68.2[65.1–71.3]	69.3[65.5–73.0]	0.66
Parsonnet score[1]		5.73[4.91–6.56]	6.98[5.71–8.25]	0.09
	Baseline	4.13[3.70–4.62]	4.35[3.78–5.01]	0.56
IL-6 (pg/ml)	6 h	190.76[164.19–221.85]	202.6[178.8–229.5]	0.57
	24 h	151.9[133.1–173.5]	188.5[158.7–223.9]	0.05
	Baseline	1.89[1.56–2.29]	1.96[1.55–2.48]	0.81
CRP (mg/l)	6 h	2.72[2.25–3.28]	2.10[1.63–2.71]	0.10
	24 h	74.9[68.5–82.0]	73.5[67.3–80.3]	0.78

[1]The Parsonnet score is pre-operative mortality risk score for those undergoing adult heart surgery, taking into account several risk factors.

Table 5.2: Geometric mean[95% CI] IL-18, IL-18BP, and fIL-18 levels in those who did, and those who did not, suffer a major complication following CABG surgery.

Variable		No Major Complication (n=145)	Major Complication (n=99)	p
IL-18	Baseline	184.3[147.5–230.3]	223.8[176.5–283.7]	0.24
	6 h	391.5[340.5–450.0]	474.7[415.3–542.5]	0.06
	24 h	202.6[163.9–250.5]	333.2[274.6–404.1]	0.001
IL-18BP	Baseline	4660[4223–5119]	5065[4547–5612]	0.25
	6 h	2813[2486–3161]	2730[2352–3136]	0.75
	24 h	12727[11968–13509]	13513[12657–14397]	0.19
fIL-18	Baseline	110.5[88.5–137.9]	130.7[103.7–164.7]	0.30
	6 h	285.7[248.7–328.2]	345.9[300.8–397.7]	0.06
	24 h	74.7[60.3–92.5]	116.8[96.2–141.7]	0.003

Table 5.3: RRs[95% CI] for a major post-operative complication following CABG surgery, by tertiles of IL-18 and fIL-18 at 6 h and 24 h.

		RR[95% CI]			
Tertile		6 h	p	24 h	p
IL-18	1	1	—	1	—
	2	1.60[1.16–2.21]	0.004	1.42[1.02–1.98]	0.04
	3	1.27[0.92–1.75]	0.16	1.75[1.23–2.51]	0.002
fIL-18	1	1	—	1	—
	2	1.33[0.97–1.82]	0.08	1.21[0.86–1.69]	0.29
	3	1.28[0.92–1.77]	0.15	1.56[1.10–2.22]	0.01

fIL-18 levels were also borderline significantly higher at 6 h in those who suffered a complication post-operatively (p=0.06 for both). At 6 h, those who did go on to suffer a major complication had IL-18 and fIL-18 levels 1.2-fold higher than those who did not (p=0.06 for both), whilst at 24 h, this difference was 1.6-fold (p=0.001 and p=0.003, respectively). The RRs for tertiles of IL-18 and fIL-18 associated with these associations are shown in table 5.3. The effect appeared strongest and most consistent at 24 h, with those in the upper tertile of IL-18 having a 1.8-fold increase in risk compared to the lowest tertile (p=0.002), whilst for fIL-18 the increase in risk was 1.6-fold (p=0.01).

5.1.1.2 Multivariate Analysis

As shown in table 5.1 on the previous page, there were few predictors of suffering a major complication following surgery. However both a past history of MI and IL-6

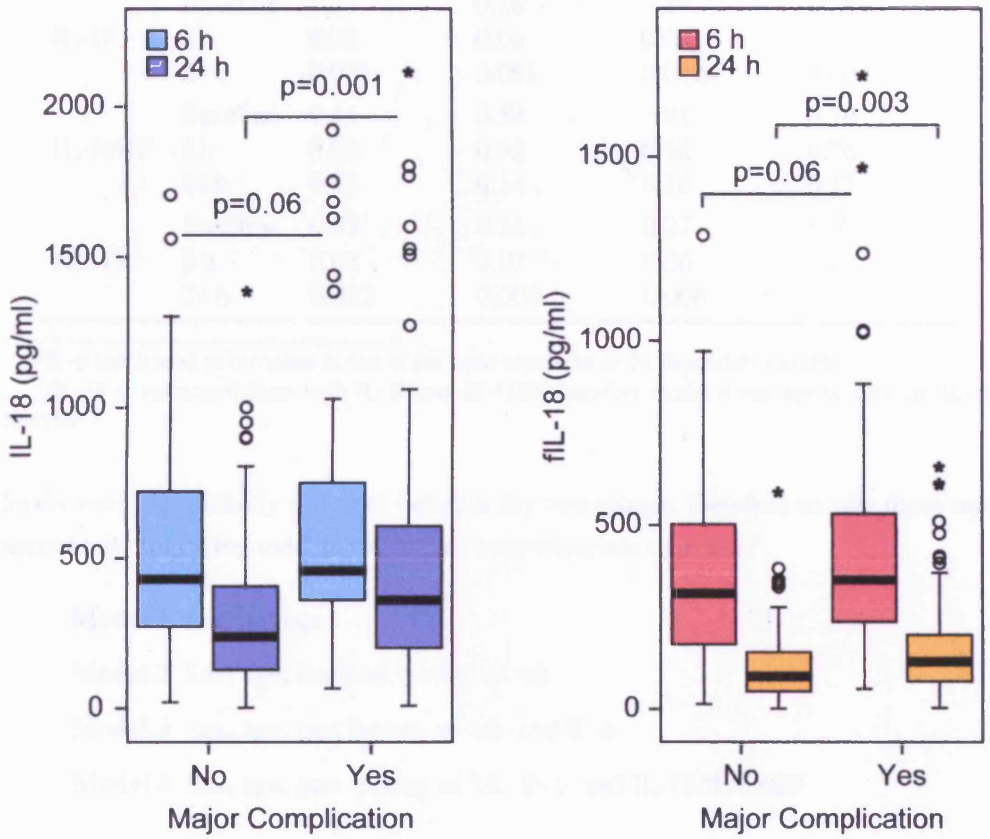

(a) IL-18 levels in those who did or did not suffer a major complication following CABG surgery

(b) fIL-18 levels in those who did or did not suffer a major complication following CABG surgery

Figure 5.1: Box plots of IL-18 and fIL-18 at both 6 h and 24 h in CABG. Data is divided into those who suffered a major complication and those who did not. Line – Median; Box – 75th to 25th percentile; ∘ – outlier (>1.5 box lengths out of box); ⋆ – extreme (>3 box lengths out of box); whisker – last value not an outlier.

Table 5.4: P values from multivariate analysis for IL-18, IL-18BP, and fIL-18 levels in those who suffered a major complication in CABG compared to those who did not.

Variable		Model 1 Sex and age	Model 2 Model 1 + Hx of MI	Model 3 Model 2 + IL-6[2]	Model 4 Model 3 + IL-18/IL-18BP
IL-18	Baseline	0.25	0.28	0.29	0.28
	6 h	0.08	0.06	0.06	0.07
	24 h	0.001	0.001	0.002	0.003
IL-18BP	Baseline	0.44	0.53	0.91	0.79
	6 h	0.62	0.62	0.58	0.76
	24 h	0.15	0.14	0.16	0.17
fIL-18	Baseline	0.29	0.31	0.27	—[3]
	6 h	0.08	0.07	0.06	—
	24 h	0.003	0.004	0.006	—

[2]IL-6 levels used as covariate is that of the same timepoint as the dependent variable

[3]fIL-18 is calculated from both IL-18 and IL-18BP therefore model 4 can not be used in fIL-18 analysis.

levels were significantly different between the two groups, therefore to take these into account the following models were used in multivariate analysis:

Model 1 Sex and age

Model 2 Sex, age, and past history of MI

Model 3 Sex, age, past history of MI, and IL-6

Model 4 Sex, age, past history of MI, IL-6, and IL-18/IL-18BP

As can be seen in table 5.4, the associations detailed above remained significant following adjustment for the various factors. Importantly, the associations also remained when adjusted for IL-6, another inflammatory mediator that differed between the two groups.

5.1.2 IL-18's Relation to BMI and BSA

As detailed in section 1.4.2.1 on page 56, IL-18 appears to have a role in metabolic control and obesity, and therefore could be an important link between obesity and inflammation, and therefore CHD.

Neither IL-18, IL-18BP, or fIL-18 levels differed between those individuals in CABG who were obese (BMI$\geq$30 kg/m^2), and those who were not (BMI$<$30 kg/m^2, see table 5.5 on the following page), or when the individuals were grouped according to tertiles of BMI or body surface area (BSA) (data not shown). However, peak IL-18

Table 5.5: Geometric mean[95% CI] IL-18, IL-18BP, and fIL-18 levels (pg/ml) by obesity status in CABG.

Variable		Non-obese (n=190)	Obese (n=58)	p
IL-18	Baseline	205.0[169.5–248.0]	172.1[127.4–232.5]	0.33
	6 h	430.4[386.3–479.5]	411.1[328.5–514.4]	0.70
	24 h	242.9[204.9–287.9]	300.4[225.6–400.0]	0.25
IL-18BP	Baseline	4969[4582–5373]	4466[3833–5148]	0.21
	6 h	2733[2462–3019]	3043[2465–3683]	0.32
	24 h	13034[12390–13694]	13176[12011–14396]	0.83
fIL-18	Baseline	121.0[100.1–146.3]	102.5[77.8–135.1]	0.32
	6 h	314.5[281.5–351.4]	292.5[235.1–363.8]	0.55
	24 h	88.3[74.4–104.8]	104.2[78.9–137.6]	0.37

and fIL-18 levels (ie. 6 h) were negatively correlated with BSA (IL-18 – Spearman's ρ=-0.16, p=0.04; fIL-18 – ρ=-0.16, p=0.05, see figure 5.2 on the next page).

5.2 NPHSII

NPHSII is a prospective study and therefore allows the study of the future impact of high/low IL-18 levels in otherwise healthy individuals. The study is ongoing and is presently in its 15th year of follow-up, with CHD events being recorded throughout this period and BMI being recorded at baseline and the following five years.

5.2.1 IL-18 as a Predictor of Future MI

5.2.1.1 Univariate Analysis

The sub-cohort from NPHSII in which IL-18, IL-18BP, and fIL-18 levels were measured was a nested case-control sample, with 167 individuals having a CHD event (stroke or MI) during follow-up. As shown in table 5.6 on page 192, those who suffered an event showed a risk factor profile consistent with increased risk. IL-18, IL-18BP, and fIL-18 levels were not significantly different between those who did, and those who did not suffer an event.

However, when only those who suffered an MI over 15 yr of follow-up were considered, both baseline IL-18 and fIL-18 were significantly higher in those who suffered an MI (n=95) than those who did not (n=330, see table 5.7 on page 192). For IL-18, levels in those who suffered an MI had geometric mean levels 1.2-fold higher than those who did not (p=0.008), whilst for fIL-18 levels, they were 1.1-fold higher (p=0.05, see figure 5.3 on page 193). The difference was such that those in the highest tertile of IL-18

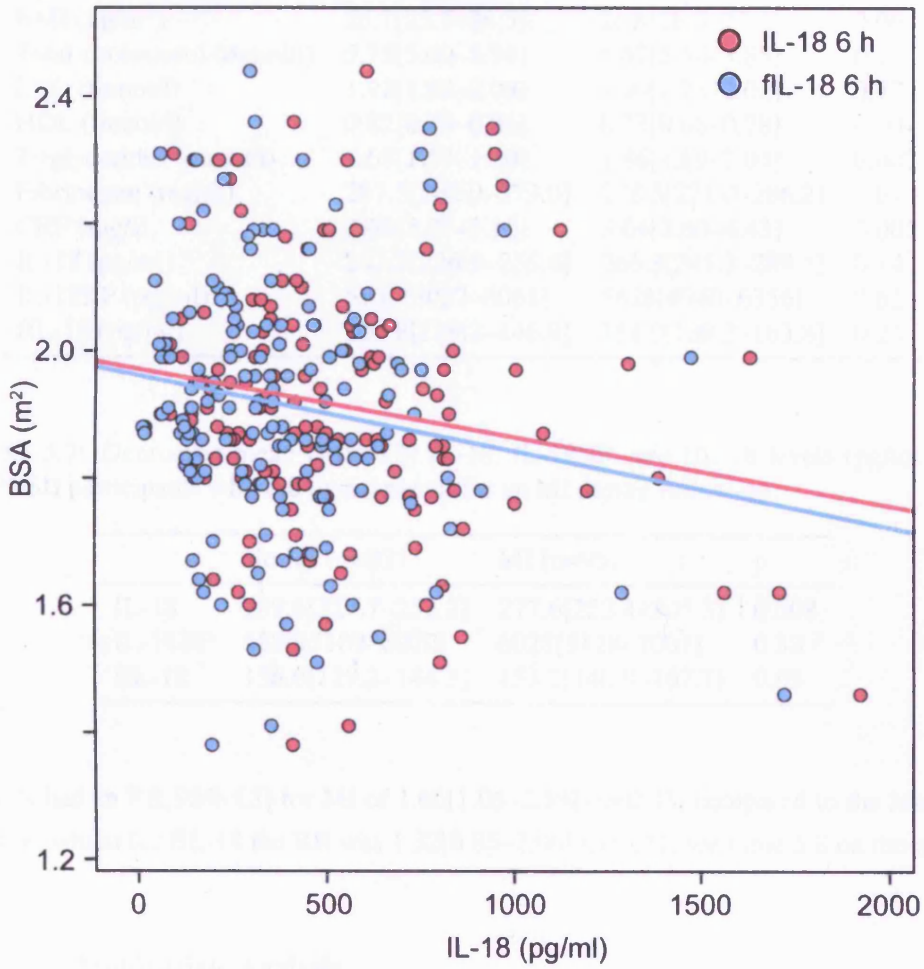

Figure 5.2: Scatter plot of both IL-18 and fIL-18 at 6 h with BSA, in CABG.

Table 5.6: Baseline characteristics of NPHSII participants (with IL-18 levels) who went on to develop any CHD event during follow-up.

Variable	No event (n=259)	Event (n=167)	p
Age	56.6[56.1–57.0]	56.4[55.9–57.0]	0.65
Ever smoked, %[n]	48.8[101]	65.4[70]	0.005
Hypertensive[4]	47.7[123]	59.3[99]	0.02
BMI (kg/m^2)	26.1[25.7–26.5]	26.8[26.3–27.3]	0.06
Total cholesterol (mmol/l)	5.75[5.60–5.90]	5.67[5.50–5.85]	0.21
LDL (mmol/l)	1.92[1.82–2.03]	1.90[1.78–2.02]	0.77
HDL (mmol/l)	0.82[0.79–0.86]	0.73[0.68–0.78]	0.004
Triglycerides (mmol/l)	1.68[1.57–1.80]	1.86[1.69–2.04]	0.007
Fibrinogen (mg/dl)	267.5[262.0–273.0]	278.5[271.0–286.2]	0.04
CRP (mg/l)	2.66[2.27–3.11]	3.64[3.00–4.43]	0.007
IL-18 (pg/ml)	241.2[226.9–256.4]	266.3[245.3–289.1]	0.14
IL-18BP (pg/ml)	5532[5027–6061]	5626[4940–6356]	0.62
fIL-18 (pg/ml)	137.8[129.2–146.9]	151.0[139.2–163.8]	0.24

Table 5.7: Geometric mean [95% CI] IL-18, IL-18BP, and fIL-18 levels (pg/ml) in NPHSII participants who did or did not suffer an MI during follow-up.

	No MI (n=331)	MI (n=95)	p
IL-18	239.6[227.7–252.2]	277.6[252.4–305.3]	0.008
IL-18BP	5580[5109–6072]	6028[5128–7001]	0.38
fIL-18	136.6[129.2–144.3]	153.2[140.0–167.7]	0.05

levels had an RR[95% CI] for MI of 1.66[1.06–2.59] (p=0.03) compared to the lowest tertile, whilst for fIL-18 the RR was 1.32[0.85–2.06] (p=0.21, see table 5.8 on the next page).

5.2.1.2 Multivariate Analysis

As shown in table 5.6, numerous factors were associated with an increased risk of CHD. The following models were used, concentrating on factors that may modulate the effect of IL-18 on MI risk:

Model 1 Age and ever smoked

Model 2 Age, ever smoked, and presence of hypertension

Model 3 Age, ever smoked, presence of hypertension, and CRP

Model 4 Age, ever smoked, presence of hypertension, CRP, and IL-18/IL-18BP (where appropriate)

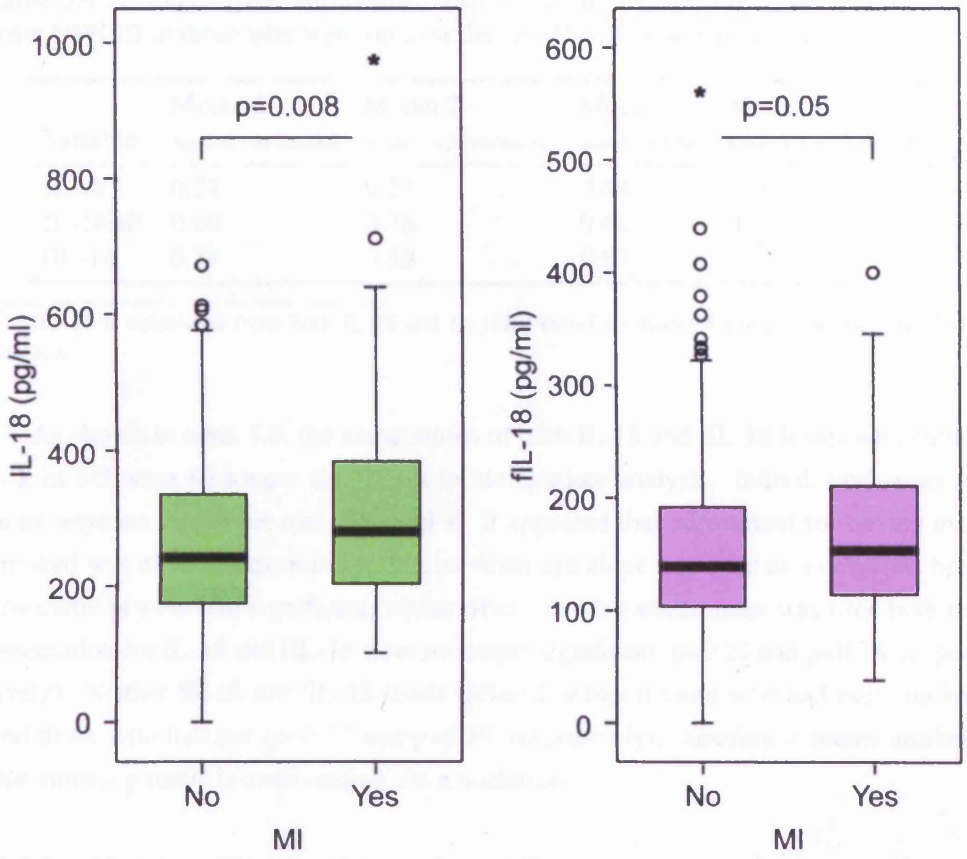

(a) IL-18 levels in those who suffered an MI compared to those who did not

(b) fIL-18 levels in those who suffered an MI compared to those who did not

Figure 5.3: Box plots for both IL-18 and fIL-18 levels in NPHSII showing significantly higher levels in those who suffered an MI during follow-up than those who did not.

Table 5.8: RRs[95% CI] for MI during follow-up by tertiles of IL-18 and fIL-18 in NPHSII

Tertile		RR[95% CI]	p
IL-18	1	1	—
	2	1.28[0.79–2.07]	0.31
	3	1.66[1.06–2.59]	0.03
fIL-18	1	1	—
	2	1.18[0.75–1.86]	0.48
	3	1.32[0.85–2.06]	0.21

Table 5.9: P values from multivariate analysis on IL-18, IL-18BP, and fIL-18 levels from NPHSII in those who went on to suffer an MI and those who did not.

Variable	Model 1 Age and ever smoked	Model 2 Model 1 + Hypertension	Model 3 Model 2 + CRP	Model 4 Model 3 + IL-18/IL-18BP
IL-18	0.21	0.25	0.48	0.60
IL-18BP	0.68	0.76	0.41	0.51
fIL-18	0.38	0.39	0.83	—[5]

[5]fIL-18 is calculated from both IL-18 and IL-18BP therefore model 4 can not be used in fIL-18 analysis.

As shown in table 5.9, the associations of both IL-18 and fIL-18 levels with future risk of MI were no longer significant in multivariate analysis. Indeed, both associations were no longer present in model 1. It appeared that adjustment for having ever smoked was most responsible for this, as when age alone was used as a covariate both associations were still significant, whilst when smoking status alone was used both the association for IL-18 and fIL-18 were no longer significant (p=0.21 and p=0.38, respectively). Neither IL-18 nor fIL-18 levels differed between those who had ever smoked and those who had not (p=0.78 and p=0.30, respectively), therefore it seems unlikely that smoking status is confounding the association.

5.2.2 IL-18 in Weight Control and Obesity

In NPHSII at baseline, 58 individuals from the subset with IL-18 and IL-18BP levels, were obese (BMI$\geq$30 kg/m^2). Obese individuals on average had higher triglycerides, and also had elevated plasma concentrations of CRP suggesting activation of the immune system in obesity (see table 5.10 on page 197). Neither IL-18 nor IL-18BP were significantly different between the two groups, however there was a trend for fIL-18 to be higher in obese than non-obese individuals (p=0.09). Plasma concentrations of all three proteins were significantly correlated with BMI (IL-18 – ρ=0.10, p=0.03; IL-18BP – ρ=-0.10, p=0.04; fIL-18 – ρ=0.15, p=0.003), with, overall, fIL-18 being positively correlated with increasing BMI.

Throughout the following five years of follow-up, BMI within the cohort increased marginally but significantly (see figure 5.5 on page 196), with an, on average, 0.35[0.19–0.52]kg/m^2 increase in BMI over this period (P<0.001). Neither baseline IL-18, IL-18BP, or fIL-18 differed between obese or non-obese individuals in any of these subsequent BMI measures. Furthermore, the correlation between baseline IL-18, IL-18BP, fIL-18, and BMI were diminished in these later measures, and they did not correlate with BMI increases/decreases over the six years (ρ=-0.04, p=0.45).

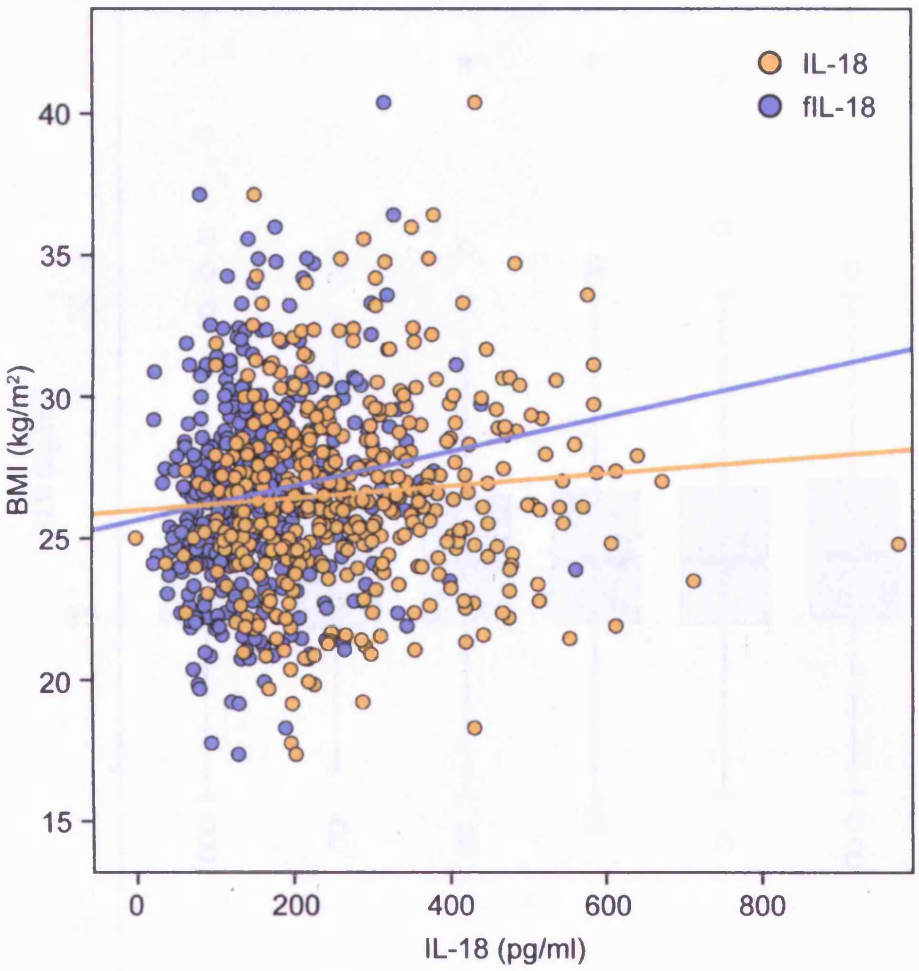

Figure 5.4: Scatter plot of both IL-18 and fIL-18 with BMI, in NPHSII.

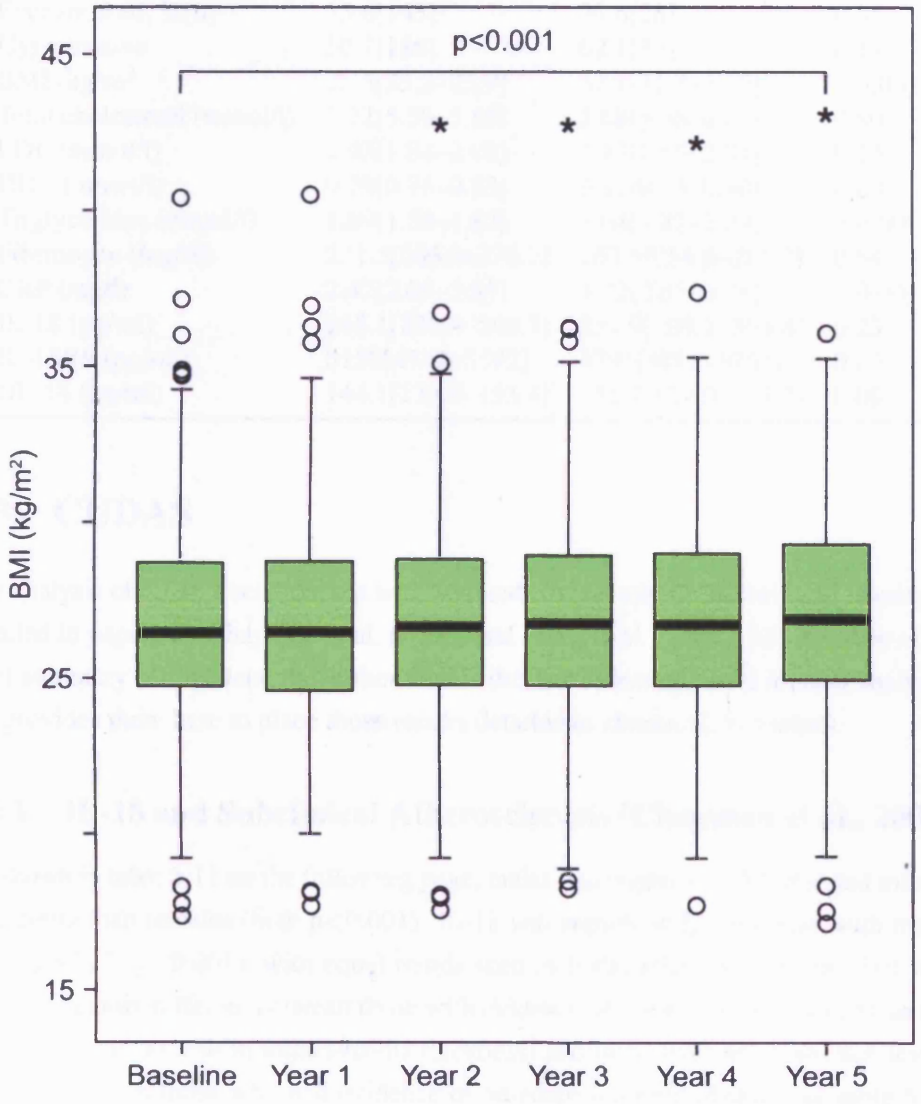

Figure 5.5: Box plots of BMI at baseline and over the five years of follow-up in NPHSII.

Table 5.10: Baseline Characteristics for those in NPHSII who were either obese or non-obese at baseline. Data is presented either as mean or geometric mean[95% CI].

Variable	Non-obese (n=368)	Obese (n=58)	p
Age	56.7[56.2–57.1]	56.7[55.3–57.8]	0.85
Ever smoked, %[n]	53.6[143]	59.6[28]	0.45
Hypertensive	50.7[186]	62.1[36]	0.11
BMI (kg/m^2	25.5[25.2–25.9]	32.1[31.3–32.9]	<0.001
Total cholesterol (mmol/l)	5.72[5.59–5.85]	5.68[5.36–6.03]	0.80
LDL (mmol/l)	1.93[1.84–2.02]	1.79[1.55–2.04]	0.25
HDL (mmol/l)	0.79[0.75–0.82]	0.81[0.73–0.90]	0.80
Triglycerides (mmol/l)	1.69[1.59–1.80]	2.08[1.81–2.39]	<0.001
Fibrinogen (mg/dl)	271.5[266.9–276.2]	267.6[254.6–281.2]	0.54
CRP (mg/l)	2.42[2.05–2.84]	4.22[2.83–6.28]	<0.001
IL-18 (pg/ml)	245.1[230.4–260.7]	251.9[209.1–303.4]	0.23
IL-18BP (pg/ml)	5158[4742–5592]	4791[3911–5761]	0.63
fIL-18 (pg/ml)	144.1[135.4–153.4]	151.7[127.0–181.2]	0.09

5.3 CUDAS

The analysis of IL-18's relationship with both subclinical atherosclerosis and obesity is detailed in papers by Chapman et al. [2006] and Hung et al. [2005]. What follows is a brief summary of this data, the author of this thesis was not involved in such analyses but provides them here to place those results detailed in chapter 4, in context.

5.3.1 IL-18 and Subclinical Atherosclerosis [Chapman et al., 2006]

As shown in table 5.11 on the following page, males had higher IL-18 levels and monocyte count than females (both $p<0.001$). IL-18 was significantly correlated with mean IMT ($\rho=0.17$, $p<0.001$), with equal trends seen in both males and females, but was not significantly different between those with evidence of carotid plaque (defined as focal increase of >1 mm in intima-media thickness) and those without. However, levels were elevated in those who had evidence of an atherosclerotic plaque (see table 5.12 on the next page), although IL-18 levels did not differ by tertiles of IMT. IL-18 did differ significantly when hypertensives were compared to non-hypertensives, with hypertensives having mean IL-18 levels 12% higher than non-hypertensives ($p<0.001$). A similar association was seen when comparing obese individuals to the non-obese, with those having a BMI$\geq$30 kg/m^2 having mean IL-18 levels 17% higher than those with BMI$<$30 kg/m^2.

Table 5.11: Baseline characteristics of males and females in the CUDAS sample. Data is mean or geometric mean[95% CI] [Chapman et al., 2006].

Variable	Females (n=550)	Males (n=557)	p
Age	53.2[52.1–54.3]	53.4[52.3–54.5]	NS
BMI (kg/m^2)	25.1[24.7–25.4]	26.5[26.2–26.8]	<0.001
WTHR	0.77[0.76–0.77]	0.90[0.90–0.90]	<0.001
SBP (mmHg)	127.1[125.4–128.8]	129.5[128.1–130.9]	0.03
HDL (mmol/l)	1.46[1.43–1.49]	1.13[1.11–1.15]	<0.001
LDL (mmol/l)	3.56[3.48–3.64]	3.70[3.63–3.77]	0.009
Triglycerides (mmol/l)	1.01[0.96–1.05]	1.28[1.23–1.34]	<0.001
Mean IMT (mm)	0.68[0.67–0.69]	0.72[0.70–0.73]	<0.001
IL-18 (pg/ml)	266.1[257.0–275.5]	340.4[329.1–352.0]	<0.001
CRP (mg/l)	1.84[1.67–2.02]	1.68[1.54–1.84]	NS
IL-6 (μg/l)	3.68[3.55–3.82]	3.61[3.47–3.76]	NS
Fibrinogen (g/l)	2.79[2.73–2.85]	2.70[2.65–2.75]	0.03
Monocyte count (10^9/l)	0.45[0.44–0.46]	0.53[0.52–0.55]	<0.001

Table 5.12: Geometric mean[95% CI] IL-18 levels (pg/ml) by hypertension, obesity, plaque, and past history of MI [Chapman et al., 2006].

	Geometric mean[95% CI] IL-18 (pg/ml)		
Variable	No	Yes	p
Hypertension	291.8[283.4–300.4]	327.7[311.4–344.8]	<0.001
Obesity	292.4[284.3–300.4]	342.7[322.8–363.9]	<0.001
Plaque	296.5[287.7–305.8]	311.1[295.0–328.3]	NS
History of MI and/or stroke	299.5[291.8–307.7]	309.5[283.2–338.3]	NS

5.3.2 IL-18 Levels and the Metabolic Syndrome [Hung et al., 2005]

IL-18 levels increased as the number of metabolic syndrome criteria increased, such that those with $\geq$3 criteria had levels 40% higher than those with no criteria (see table 5.13 on the following page). This association remained when adjusted for age, sex and BMI, such that individuals in the highest tertile of IL-18 had an OR[95% CI] of 2.28[1.33–3.91], p=0.007. Both IL-6 and CRP were associated with metabolic syndrome criteria, however these associations were attenuated when adjusted for age, sex and BMI.

5.4 SCARF

5.4.1 IL-18 Levels in Cases and Controls

A recently published paper by Hulthe et al. [2006] details levels of IL-18 in the SCARF cohort and related them to case/control status. The analysis presented below is separate from this paper and was carried out solely by the author of this thesis.

5.4.1.1 Univariate Analysis

As can be seen in table 5.14 on page 201, SCARF cases had a significantly worse risk factor profile than did controls, although both DBP and SBP were not significantly different between the two groups, a finding that is likely due to the large number of cases who were on anti-hypertensive treatment (95.3%). A treatment effect is also the most probable explanation for the significantly lower LDL concentrations seen in cases over controls, although there was no data available on statin treatment.

IL-18 levels were significantly higher in cases than controls (p=0.01), with cases having levels 7.1% higher than controls (see figure 5.6 on page 201). This translates into a 1.2-fold increase in risk for those in the highest tertile of IL-18 compared to those in the lowest tertile (p=0.05, see figure 5.7 on page 202). Within cases, IL-18 was significantly positively correlated with normalized plaque area (ρ=0.17, p=0.01, see figure 5.8 on page 202), but not with mean % stenosis (ρ=0.07, p=0.33).

5.4.1.2 Multivariate Analysis

Four models were used in multivariate analysis in assessing the difference in IL-18 levels between cases and controls. Covariates were selected that differed between cases and controls and that were likely to have biologically plausible effects on IL-18 levels:

Model 1 Age and ever smoked

Model 2 Age, ever smoked, and DBP

Model 3 Age, ever smoked, DBP, and CRP

Table 5.13: Baseline characteristics of the CUDAS cohort according to the number of National Cholesterol Education Program Third Adult Treatment Panel (NCEP-ATPIII) metabolic syndrome criteria. Data are mean or geometric mean[95% CI].

Variable	No. of metabolic syndrome criteria				
	0 (n=243)	1 (n=306)	2 (n=238)	≥3 (n=173)	p
Age	45.8[44.3–47.3]	54.5[53.1–55.8]	56.0[54.4–57.5]	57.1[55.3–58.9]	<0.001
Male, %[n]	37.0[90]	45.1[138]	56.7[135]	60.7[105]	<0.001
BMI (kg/m^2)	23.5[23.0–23.9]	25.1[24.7–25.4]	27.3[26.9–27.7]	29.9[29.3–30.3]	<0.001
Waist circumference (cm)	75.7[74.4–77.0]	81.6[80.5–82.8]	88.4[87.1–89.7]	96.4[94.8–97.9]	<0.001
Triglyceride (mmol/l)	0.9[0.8–0.9]	1.0[0.9–1.1]	1.4[1.3–1.5]	2.1[2.0–2.2]	<0.001
HDL (mmol/l)	1.56[1.52–1.60]	1.43[1.40–1.47]	1.24[1.19–1.28]	1.03[0.98–1.08]	<0.001
LDL (mmol/l)	3.4[3.3–3.5]	3.6[3.5–3.7]	3.8[3.6–3.9]	3.8[3.7–3.9]	<0.001
SBP (mmHg)	111[110–114]	130[126–132]	134[132–136]	139[136–141]	<0.001
DBP (mmHg)	72[71–73]	81[80–82]	83[81–84]	87[85–88]	<0.001
Smoking (pack years)	7.7[5.0–10.3]	10.4[8.0–12.8]	14.5[11.8–17.2]	18.1[15.0–21.3]	<0.001
Glucose (mmol/l)	5.2[5.1–5.3]	5.5[5.4–5.6]	5.7[5.6–5.8]	6.2[6.1–6.3]	<0.001
Insulin (mU/l)	4.2[3.5–4.8]	5.1[4.5–5.6]	7.0[6.3–7.6]	10.7[10.0–11.4]	<0.001
CRP (mg/l)	1.14[1.00–1.30]	1.57[1.39–1.77]	2.23[1.94–2.55]	2.70[2.30–3.17]	<0.001
IL-6 (µg/l)	3.08[2.92–3.26]	3.47[3.31–3.65]	3.93[3.71–4.15]	4.33[4.05–4.61]	<0.001
IL-18 (pg/ml)	255[243–268]	279[267–292]	315[300–331]	356[340–381]	<0.001

Table 5.14: Baseline characteristics of SCARF, by cases and controls. Data is either mean or geometric mean[95% CI].

Variable	Controls (n=387)	Cases (n=387)	p
Age	53.0[52.5–53.5]	52.5[51.9–53.0]	0.16
Ever smoked, %[n]	59.9[230]	75.3[290]	<0.001
BMI (kg/m^2)	25.7[25.4–26.0]	27.1[26.7–27.5]	<0.001
SBP (mmHg)	128.0[126.3–129.7]	128.8[127.0–130.6]	0.55
DBP (mmHg)	81.6[80.6–82.6]	80.3[79.3–81.3]	0.06
HDL (mmol/l)	1.35[1.31–1.39]	1.06[1.03–1.09]	<0.001
LDL (mmol/l)	3.47[3.38–3.55]	3.16[3.05–3.26]	<0.001
Triglycerides (mmol/l)	1.21[1.16–1.27]	1.67[1.59–1.76]	<0.001
Mean % stenosis	ND	32.1[31.0–33.3]	—
Normalised plaque area[6]	ND	0.21[0.20–0.22]	—
CRP (mg/l)	0.95[0.86–1.06]	1.59[1.41–1.79]	<0.001
IL-6 (pg/ml)	0.71[0.66–0.75]	0.95[0.88–1.02]	<0.001
IL-18 (pg/ml)	266.6[257.0–276.6]	285.6[274.2–297.4]	0.01

[6]Total plaque area normalised to segment length

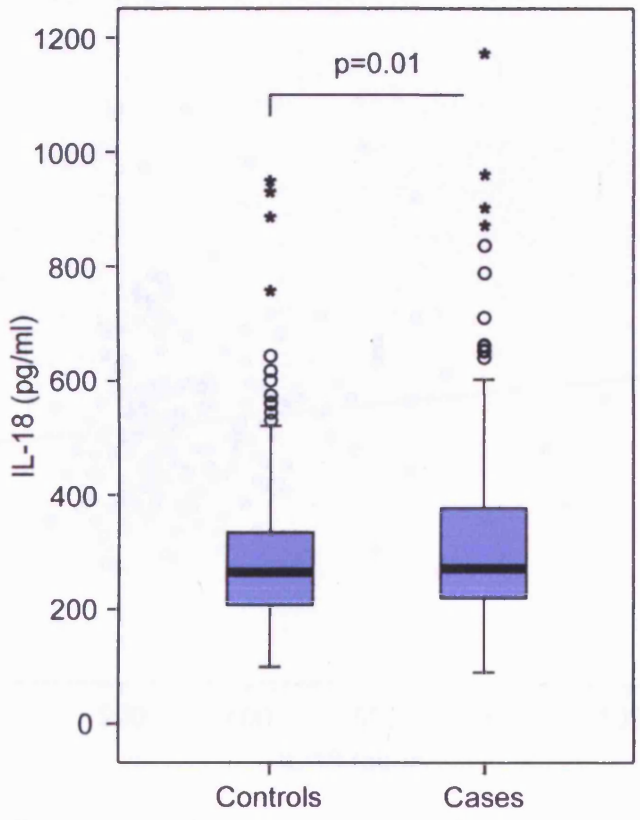

Figure 5.6: Box plots of IL-18 levels in SCARF by cases and controls.

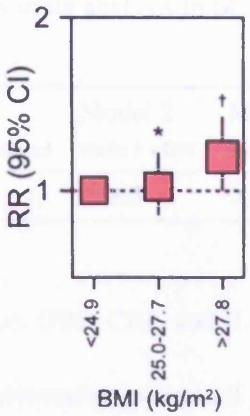

Figure 5.7: RRs[95% CI] for case vs, control in SCARF, across tertiles of IL-18. Size of box reflects number of cases; ⋆–p=0.81, †–p=0.05.

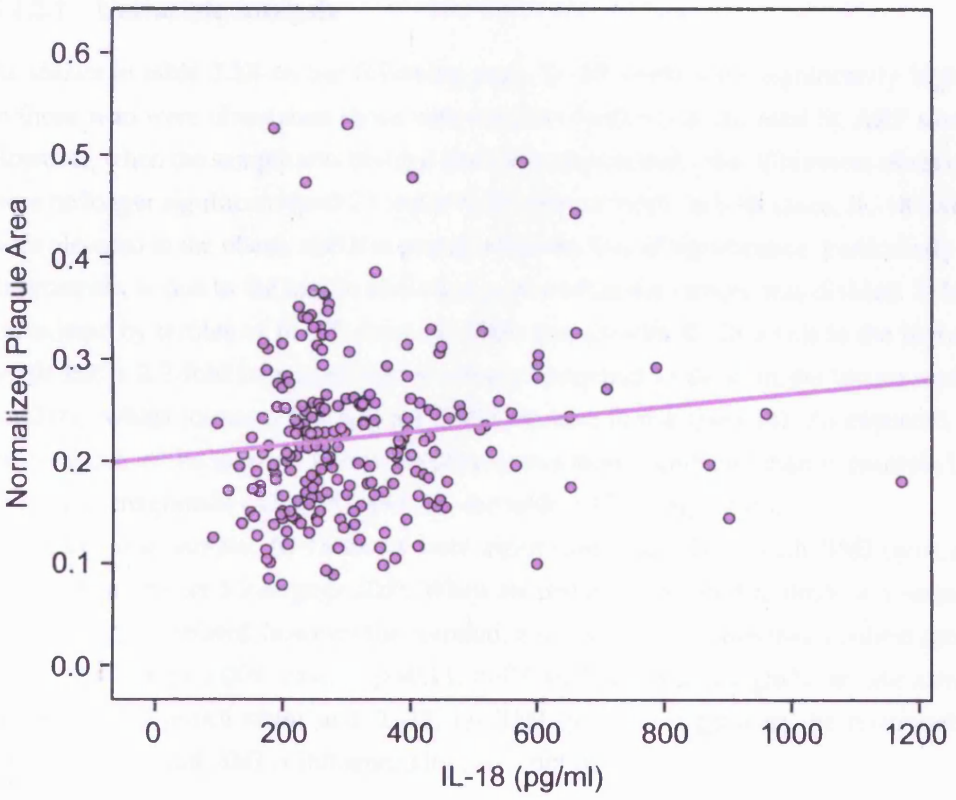

Figure 5.8: Scatter plot of IL-18 levels and normalized plaque area in SCARF cases.

Table 5.15: P values from multivariate analysis in SCARF comparing IL-18 levels between cases and controls.

Variable	Model 1 Age and ever smoked	Model 2 Model 1 + DBP	Model 3 Model 2 + CRP	Model 4 Model 3 + IL-6
IL-18	0.01	0.005	0.02	0.02

Model 4 Age, ever smoked, DBP, CRP, and IL-6

As shown in table 5.15, the association between IL-18 levels and case/control status remained statistically significant in all four models. Importantly, the association was still present following adjustment for both CRP and IL-6, showing the effect of IL-18 to be independent of these two inflammatory markers.

5.4.2 IL-18's Influence on Obesity

5.4.2.1 Univariate Analysis

As shown in table 5.16 on the following page, IL-18 levels were significantly higher in those who were obese than those who were not (p=0.02) in the total SCARF study. However, when the sample was divided into cases and controls, the differences observed were no longer significant (p=0.23 and p=0.08, respectively). In both cases, IL-18 levels were elevated in the obese, and it is possible that the loss of significance, particularly in the controls, is due to the loss in statistical power when the sample was divided. When considered by tertiles of IL-18, those SCARF controls with IL-18 levels in the highest tertile had a 2.2-fold increased risk of obesity compared to those in the lowest tertile (p=0.05), whilst for cases this was a 1.2-fold increase in risk (p=0.34). As expected, in the total cohort the increase in risk for obesity was more significant than in controls but of a lesser magnitude (RR=1.57, p=0.03, see table 5.17 on page 205).

In the total sample, IL-18 levels were significantly correlated with BMI (ρ=0.14, p<0.001, see figure 5.9 on page 205). When divided into cases and controls, it remained significantly correlated, however the correlation was weaker in cases than controls (controls – ρ=0.13, p=0.009; cases – ρ=0.11, p=0.04). There was a significant interaction between case/control status and IL-18, on BMI (p=0.03) suggesting the relationship between IL-18 and BMI is influenced by case/control status.

5.4.2.2 Multivariate Analysis

Four separate models were used in multivariate analysis with the following covariates used:

Table 5.16: IL-18 levels in obese and non-obese SCARF individuals within both cases and controls, and cases and controls individually.

Test Group	Geometric mean[95% CI] IL-18 (pg/ml) Within group %[n]	Non-obese	Within group %[n]	Obese	p
Total (n=774)	83.3[645]	271.7[263.7–279.9]	16.7[129]	297.6[278.0–318.6]	0.02
Controls (n=387)	89.7[347]	263.7[253.7–274.1]	10.3[40]	294.5[262.5–330.5]	0.08
Cases (n=387)	77.0[298]	281.7[268.9–295.0]	23.0[89]	299.0[274.4–325.7]	0.23

Table 5.17: RRs[95% CI] for obesity by tertiles of IL-18 in SCARF cases, controls, and cases and controls together.

	RR[95% CI] for obesity					
Tertile	Controls	p	Case	p	Total	p
1	1	—	1	—	1	—
2	1.75[0.76–4.03]	0.18	0.80[0.48–1.35]	0.41	1.04[0.67–1.62]	0.86
3	2.23[0.98–5.05]	0.05	1.23[0.79–1.92]	0.34	1.57[1.05–2.34]	0.03

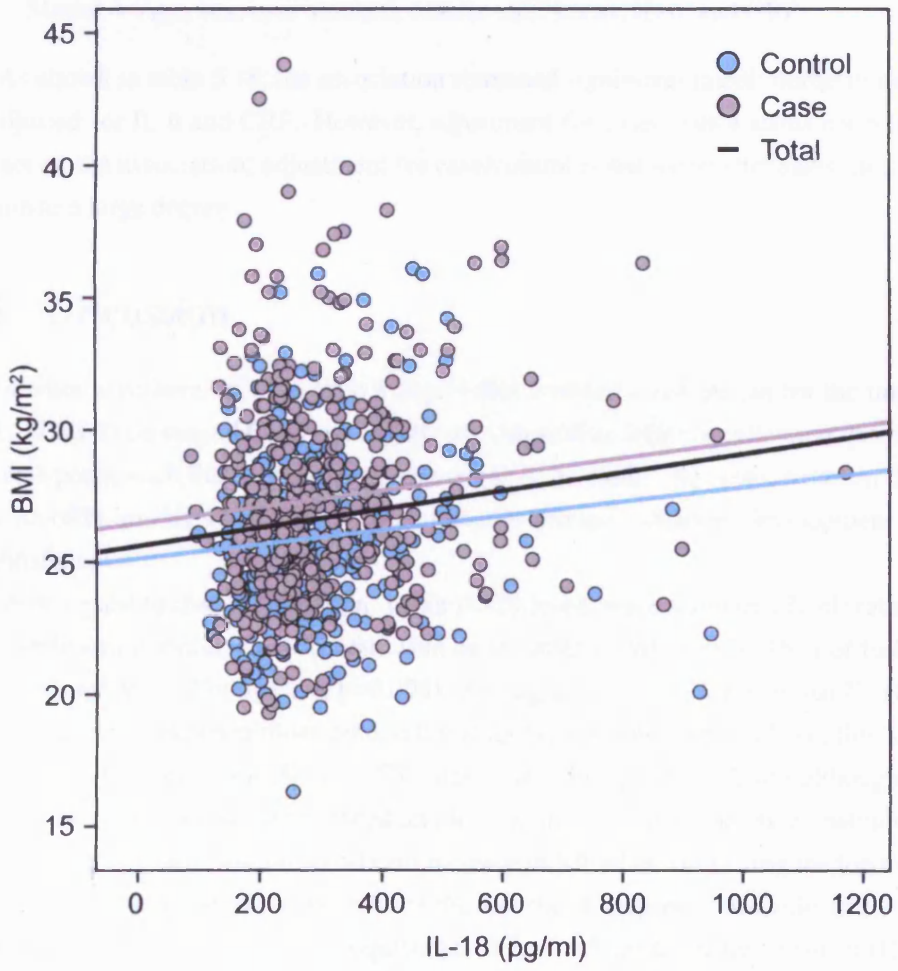

Figure 5.9: The correlation of IL-18 levels with BMI in SCARF cases, controls, and the total sample.

Table 5.18: Results (as p values) from multivariate analysis of differences in IL-18 levels by obesity status in SCARF.

Variable	Model 1 Age and smoking	Model 2 Model 1 + ever smoked	Model 3 Model 2 + case/control status	Model 4 Model 3 + IL-6 and CRP
IL-18	0.02	0.01	0.05	0.11

Model 1 Age and sex

Model 2 Age, sex, and ever smoked

Model 3 Age, sex, ever smoked, and case/control status

Model 4 Age, sex, ever smoked, case/control status, IL-6, and CRP

As shown in table 5.18, the association remained significant (albeit borderline) until adjusted for IL-6 and CRP. However, adjustment for case/control status has a large impact on the association; adjustment for case/control status alone attenuates the association to a large degree.

5.5 Discussion

The studies used here differ to such a degree that forming a conclusion for the impact of IL-18 levels on overall CHD risk is difficult. All studies differ in collection, purpose, and end-point, such that comparisons cannot easily be made. However, between them they do offer an insight into IL-18 production at disease initiation, development and establishment.

With regard to disease initiation, mean IL-18 levels were significantly elevated in those individuals within NPHSII who went on to suffer an MI over the 15 yr of follow-up (277.6 pg/ml vs. 239.6 pg/ml, p=0.008). As might be expected, given that IL-18BP was not different between those who suffered an MI and those who did not, this association was also seen with fIL-18 (153.2 pg/ml vs. 136.6 pg/ml, p=0.05) although the scale of the difference was diminished and less significant. As such, when analysed by tertiles of fIL-18 there was no significant increase in RR when comparing the top to the bottom tertile, but most likely this reflects the low statistical power available given only 95 incident MIs during follow-up, equating to 36 individuals in the top tertile of fIL-18 suffering an MI. Furthermore, fIL-18 is not strictly an observed variable but a calculated one, and as such, how well the calculated levels truly reflect *in vivo* fIL-18 levels is unknown. The use of a bioassay for fIL-18, such as that published by Konishi et al. [1997], would help to assess how well calculated fIL-18 correlates with IFNγ-inducing activity. However, these experiments have not been done.

Of significant interest is the observation that this predictive ability of IL-18 is specific to MI and was not seen when analysing all CHD end-points together (stroke, MI, and angina). Therefore those with the highest levels of IL-18 were more likely to suffer an MI as their first experience of disease, suggesting that the plaque responsible is significantly more prone to rupture than those for whom angina is the first sign of disease.

The study undertaken by Blankenberg et al. [2003] was comparable to the analyses undertaken here. The PRIME cohort was a prospective study composed of healthy middle-aged men collected from across Western Europe, with a combined end-point including hard coronary events (MI, and coronary death) and angina. As detailed in section 1.4.1.2 on page 47, IL-18 was significantly higher in those who suffered an event during the five-year follow-up than those who did not (p=0.005). However, contrary to the findings here, they found the effect to be weakest (though not significantly so) in those who suffered an actual MI over those who presented with angina (see figure 5.10 on the next page). The increase in RR, top tertile vs. bottom tertile, for angina was 1.79[1.23–1.61] (p for trend=0.003), whilst for MI/coronary death it was 1.38[0.98–1.93] (p for trend=0.06). However the difference between the two RRs was not statistically significant (p=0.31). There was substantial differences between RRs when those from France and Belfast were analysed separately, however the risk was consistently greater in those from Belfast, and therefore this geographic difference is not likely to be responsible for the difference seen between PRIME and NPHSII.

The ability of IL-18 to predict future MI was weak and did not survive multivariate analysis, indeed the association was lost with adjustment of smoking status alone. When separating the cohort into those who had ever smoked and those who had not, the association between IL-18 levels and future MI was not present in either subgroup, and IL-18 levels were not significantly different in those had smoked and those who had not. In logistic regression, with MI as the outcome variable, IL-18 was no longer a significant predictor of MI when smoking was included as a covariate, and there was no evidence for an interaction between smoking and IL-18 levels (p for interaction=0.42). Therefore the exact relationship between IL-18 and smoking status, and their relationship with future risk of MI, remains unclear.

The CUDAS study, as an asymptomatic cohort, is also able to give an insight into the impact of IL-18 on early disease development. In this study, Chapman et al. [2006] showed a significant correlation between IL-18 levels and IMT. However IL-18 levels did not differ significantly between those who had evidence of asymptomatic plaque and those who did not, suggesting that in this cohort IL-18 was more closely related to CHD *development* than initiation. However, these results are somewhat contradicted by those found in SCARF where IL-18 levels were significantly higher in cases than controls (285.6 pg/ml vs. 266.6 pg/ml, p=0.01). Most likely this disagreement was due

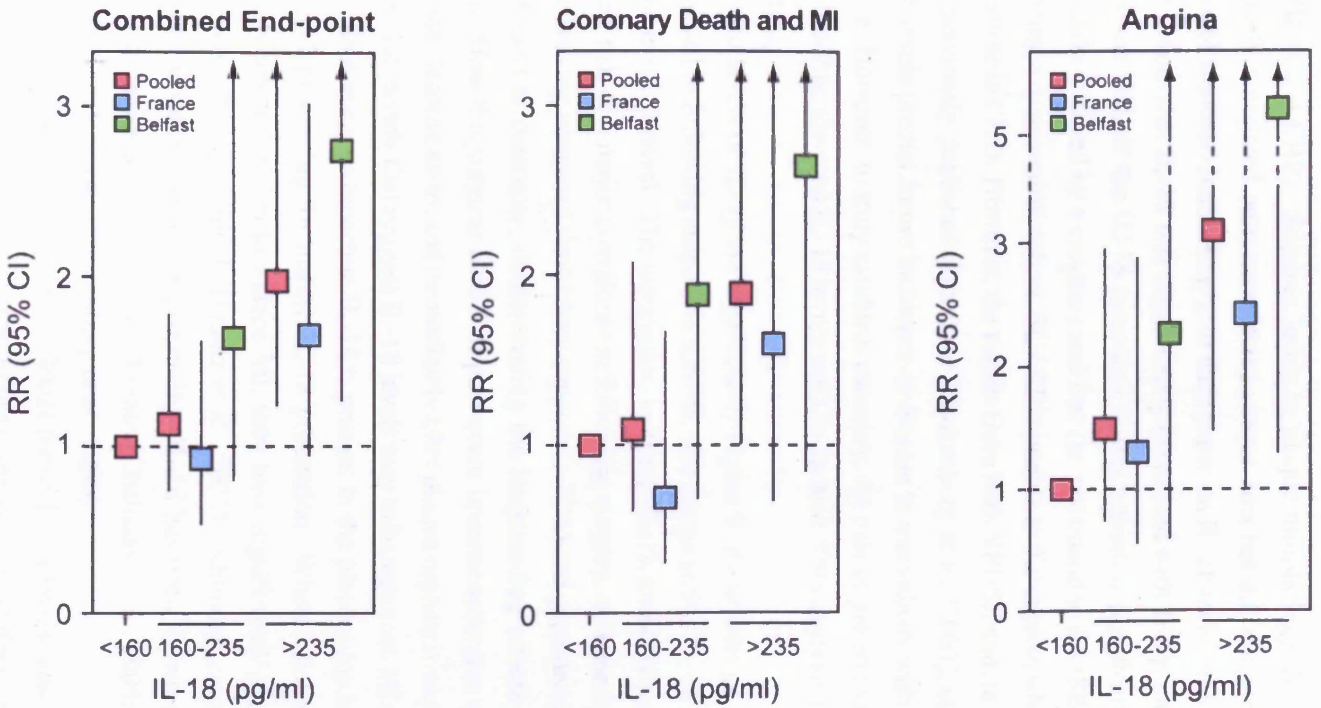

(a) RRs by IL-18 tertiles for combined end-point

(b) RRs by IL-18 tertiles for coronary death and MI end-point

(c) RRs by IL-18 tertiles for angina end-point

Figure 5.10: RRs[95% CI] for PRIME coronary events according to tertiles of IL-18, taken from Blankenberg et al. [2003]. Data is separated by country and end-point, and adjusted for BMI, smoking status, diabetes, hypertension, total cholesterol, HDL, triglycerides, and CRP.

to differences in the timeline of disease; CUDAS is an asymptomatic cohort, whilst SCARF cases had already suffered an MI prior to recruitment.

This difference in IL-18 levels between cases and controls in SCARF was robust, and was not significantly attenuated following adjustment for other inflammatory factors (IL-6 and CRP). Relating levels to plaque morphology, IL-18 was significantly positively correlated with normalized plaque area but did not appear to be related to degree of stenosis. Interestingly, in their paper on IL-18 levels in SCARF, Hulthe et al. [2006], note that IL-18 was significantly correlated with IFNγ and therefore it is safe to assume that, of the IL-18 measured in this cohort, a significant proportion is both mature (ie. cleaved by a caspase) and free (ie. not bound to IL-18BP).

Being a case/control cohort, SCARF is unable to distinguish whether IL-18 is causal or reactive in CHD. However, the results from both NPHSII and, in part, CUDAS, allied with previously published data from Blankenberg et al. [2003], strongly suggests that IL-18 levels predict future incidence of disease in individuals with no outward signs of disease. However, to truly establish causality, the role of genetic variants that associate with life-time elevated IL-18 levels must be studied. This analysis is detailed in the next chapter.

Since levels of IL-18 are significantly higher in those who go on to suffer a major complication following surgery in CABG, this suggests that IL-18 may also play a role in post-event survival. The association between IL-18 levels 24 h after surgery and increased risk of a major complication following surgery, remained significant in subset analysis using increased ventilatory support (>12 h) and extended ICU stay (>2 d, data not shown) as outcomes, demonstrating the longstanding effects of early IL-18 activation. How this surgical model of post-event immunoactivation used here equates to processes leading up to, and immediately after plaque rupture is unclear. However, there are animal models that suggest IL-18 levels may influence post-MI survival. In caspase-1 knockout mice no bioactive IL-18 is present in the plasma due to the requirement of caspase-1 processing for mature IL-18 production. When these animals undergo left coronary artery ligation to induce MI, they have significantly greater post-event survival than wild-type animals [Frantz et al., 2003]. Although caspase-1 has a number of functions other than IL-18 processing, IL-18 has been shown to predict long-term survival in patients with advanced disease [Chalikias et al., 2005; Blankenberg et al., 2002; Seta et al., 2000; Blankenberg et al., 2006].

In humans, Blankenberg et al. [2002] found IL-18 levels were significantly higher among those in the Athero*Gene* cohort (a prospective study of patients with documented CHD) who had a fatal cardiovascular event during follow-up than among those who did not (68.4 pg/ml vs. 58.7 pg/ml, $p<0.001$). Each quartile increase in baseline IL-18 concentration was associated with a 1.46[1.21–1.76] ($p<0.001$) increase in future cardiovascular death (see figure 5.11 on page 211). As in CABG, this association remained

significant following adjustment for other inflammatory mediators.

There is now a good deal of data to implicate the IL-18 system in determining plaque stability, and from the data here it appears that, within the IL-18 system, research should concentrate on IL-18 as IL-18BP did not show any significant associations. It has not been feasible to study the expression of the IL-18 receptor complex here, and it is possible that the relative expression of IL-18R differs between stable and unstable plaques (perhaps due to differences in cell content or state of activation/differentiation). Although IL-18R has been localized to atherosclerotic plaques [Mallat et al., 2001a], it's role in plaque stability has not been studied. Should a difference exist, then the effect of increased IL-18 expression in unstable vs. stable plaques could be exacerbated or reduced.

The realization that IL-18 may have effects beyond the immune system is a relatively recent discovery. As a pro-inflammatory cytokine it had been studied in the context of metabolic syndrome, but the observation that $il18^{-/-}$ mice were hyperphagic [Netea et al., 2006] suggested that IL-18 was closely involved in appetite regulation.

From the results presented here there is little evidence for an intimate relationship between plasma IL-18 and BMI. IL-18 levels did correlate with BMI and BSA however there was no real consensus between the studies, with CABG showing a negative correlation and both NPHSII and SCARF showing positive correlations. In any case, the degree of correlation, although significant, was not of a large degree with values of around $\rho = \pm 0.1$. In SCARF IL-18 levels were significantly higher in those who were obese than those who were not obese. However, there were substantially more obese individuals in the case group than the control (n=89 vs. n=40, $p<0.001$), and when analysed in cases and controls separately there was no difference between obese and non-obese. Furthermore, in multivariate analysis the association was borderline when adjusting for case/control status (p=0.05) and so it therefore seems likely that the association seen with obesity is simply reflecting the higher IL-18 levels seen in cases than controls.

Netea et al. [2006] suggested that because only intra-cerebral injection reversed the phenotype of the $il18^{-/-}$ mouse, the hypothalamus may be the target of IL-18. Therefore local, not systemic, production of IL-18 could be more important in appetite regulation. IL-18 mRNA expression has been observed in the bovine [Nagai et al., 2005] and rat pituitary gland (functionally connected to the hypothalamus by the median eminence), where it was significantly increased following stress [Wang et al., 2006]. It therefore seems possible that IL-18 production within the brain is more important in appetite regulation than systemic production.

In conclusion, IL-18 levels were a significant predictor of, specifically, incidence of future MI over a period of 15 yr. The association was seen with both total and free IL-18, but was not independent of other risk factors and seemed particularly related to

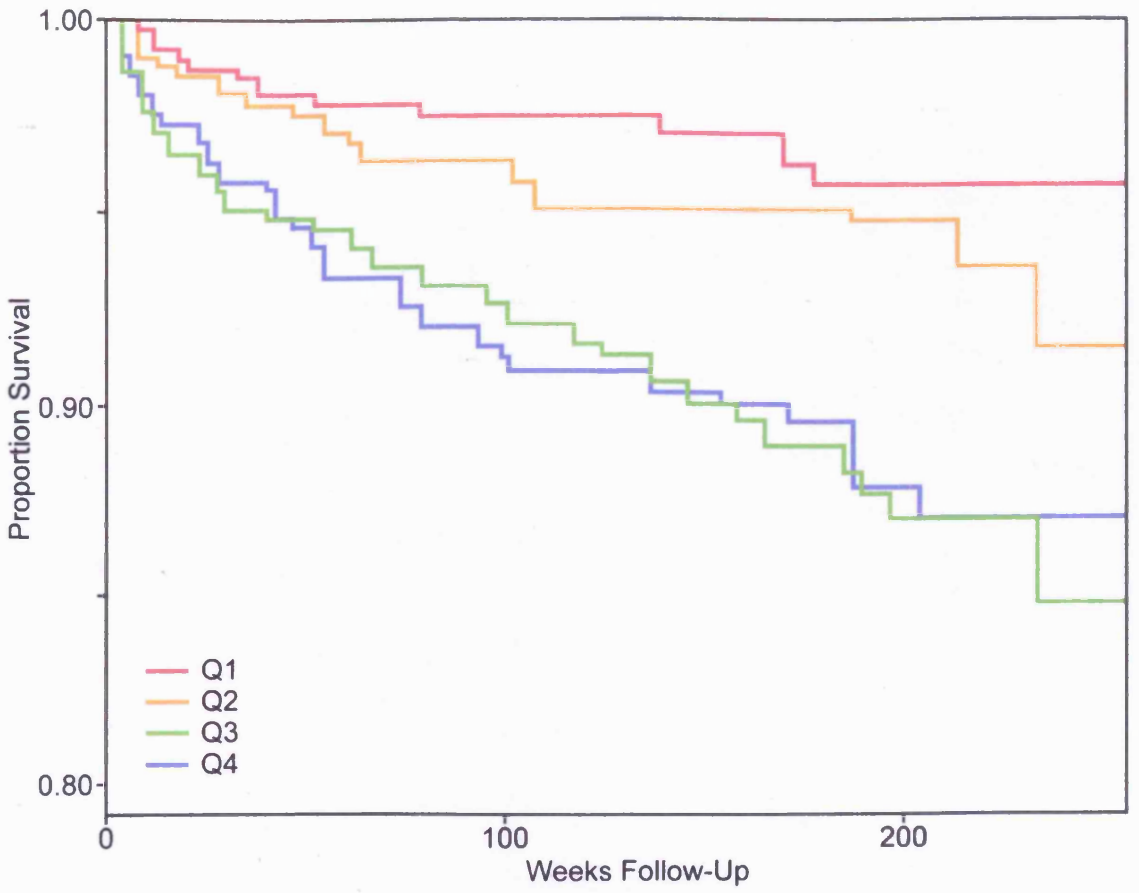

Figure 5.11: Kaplan-Meier curves for survival according to quartiles of IL-18; p(logrank test)<0.001 [Blankenberg et al., 2002]

smoking status. Furthermore both total and free IL-18 levels at 24 h following surgery were predictors of a major post-operative complication. There appeared little relevance of systemic IL-18 levels to BMI or future risk of obesity.

Chapter 6

The Influence of IL-18 System Genetic Variation on Disease Risk

The aim of this chapter is to relate the results from chapter 4 to those presented in chapter 5. If those individuals possessing particular genetic variation that predisposes them to elevated/decreased fIL-18 levels throughout their life, were also at an increased risk of disease, it would suggest that IL-18 was causal in such diseases. This is the basis of mendelian randomization [Davey Smith and Ebrahim, 2005; Little and Khoury, 2003], which has been shown to be of use in distinguishing between causality and reverse causality [Timpson et al., 2005; Herder et al., 2007; Casas et al., 2005]. CUDAS and CUPID data is not presented here as relevant data analysis was not possible.

6.1 CABG

6.1.1 Genetic Variation and Risk of Major Post-Operative Complication

6.1.1.1 Single SNP Analysis

As shown in table 6.1 on the next page, in the CABG study only *IL18*+8855 T>A genotype frequencies differed significantly between those who suffered a major complication and those who did not (p=0.007). The association was such that heterozygotes were more common in those who suffered a major complication, thus being heterozygote at +8855 was associated with a 1.3-fold increase in risk (p=0.007). Importantly *IL18*-5848 T>C (the tSNP associated with differences in IL-18 and fIL-18 levels) genotype frequencies did not differ significantly between the two groups (p=0.76). There was also no significant difference in the frequency of *IL18BP* tSNP genotype frequencies between the two groups (see table 6.2 on page 215).

Table 6.1: Allele frequencies and RRs[95% CI] for *IL18* tSNPs in those who suffered a major post-operative complication following CABG, and those who did not.

tSNP and completeness of genotyping (%)		Total HWE p	%[n] No Major Complication (n=218)	%[n] Major Complication (n=202)	χ^2 p	RR[95% CI]	p
	GG		35.0[76]	34.8[70]		1	—
-9731 (99.5)	GT	0.82	47.5[103]	50.2[101]	0.74	1.03[0.83–1.28]	0.77
	TT		17.5[38]	14.9[30]		0.92[0.67–1.26]	0.60
	TT		34.9[76]	38.1[77]		1	—
-5848 (100.0)	TC	0.45	50.9[111]	47.5[96]	0.76	0.92[0.74–1.14]	0.46
	CC		14.2[31]	14.4[29]		0.96[0.71–1.30]	0.79
	AA		51.4[112]	42.3[99]		1	—
+105 (99.8)	AC	0.95	37.6[82]	49.3[99]	0.06	1.27[1.03–1.56]	0.03
	CC		11.0[24]	8.5[17]		0.96[0.65–1.43]	0.84
	TT		49.5[108]	39.5[79]		1	—
+8855 (99.5)	TA	0.57	38.1[83]	53.0[106]	0.007	1.33[1.08–1.64]	0.007
	AA		12.4[27]	7.5[15]		0.85[0.55–1.31]	0.44
	AA		33.5[72]	28.4[57]		1	—
+11015 (99.0)	AC	0.28	47.4[102]	56.2[113]	0.20	1.19[0.94–1.50]	0.13
	CC		19.1[41]	15.4[31]		0.97[0.70–1.35]	0.88

Table 6.2: Allele frequencies and RRs[95% CI] for *IL18BP* tSNPs in those who suffered a major post-operative complication following CABG, and those who did not.

tSNP and completeness of genotyping (%)		Total HWE p	%[n] No Major Complication (n=218)	%[n] Major Complication (n=202)	χ^2 p	RR[95% CI]	p
	TT		86.1[186]	89.3[176]		1	—
-1765 (98.3)	TC	0.02	12.5[27]	9.6[19]	0.61	0.85[0.59–1.22]	0.35
	CC		1.4[3]	1.0[2]		0.82[0.28–2.42]	0.70
	TT		76.9[166]	84.3[166]		1	—
-559 (98.3)	TG	0.49	22.2[48]	15.2[30]	0.16	0.77[0.57–1.04]	0.07
	GG		0.9[2]	0.5[1]		0.67[0.13–3.31]	0.57
	CC		94.0[204]	94.5[189]		1	—
+3041 (99.3)	CT	0.55	6.0[13]	5.5[11]	0.83	0.95[0.61–1.49]	0.83
	TT		—	—		—	—

Table 6.3: Haplotype frequencies and ORs[95% CI] for *IL18* tSNP haplotypes in those who suffered a major post-operative complication following CABG, and those who did not.

Haplotype		Total	Frequency (%) No Major Complication (n=179)	Major Complication (n=168)	OR[95% CI]	p
hGCATA	h12111	27.9	28.1	27.7	1	—
hTTCAC	h21222	24.7	24.1	25.4	1.02[0.69–1.50]	0.93
hGTATA	h11111	22.4	22.1	22.7	0.99[0.65–1.50]	0.95
hTTATC	h21112	9.3	10.8	7.7	0.68[0.38–1.20]	0.18

Table 6.4: Haplotype frequencies and ORs[95% CI] for *IL18BP* tSNP haplotypes in those who suffered a major post-operative complication following CABG, and those who did not.

Haplotype		Total	Frequency (%) No Major Complication (n=179)	Major Complication (n=168)	OR[95% CI]	p
hTTC	h111	87.1	84.9	89.5	1	
hTGC	h121	8.0	9.7	6.2	0.60[0.34–1.06]	0.08
hCTT	h212	1.8	1.4	2.1	1.51[0.47–4.88]	0.49
hCTC	h211	1.4	1.5	1.3	0.86[0.20–3.59]	0.83

6.1.1.2 Haplotype Analysis

As shown in table 6.3, table 6.4, and figure 6.1 on the next page, no *IL18* or *IL18BP* haplotype was significantly associated with increased or decreased risk of a major complication following surgery.

6.1.1.3 MDR Analysis

There was no evidence for a significant epistatic effect between the *IL18* and *IL18BP* tSNP sets, when considering a major complication following surgery as the outcome (see figure 6.2 on page 218).

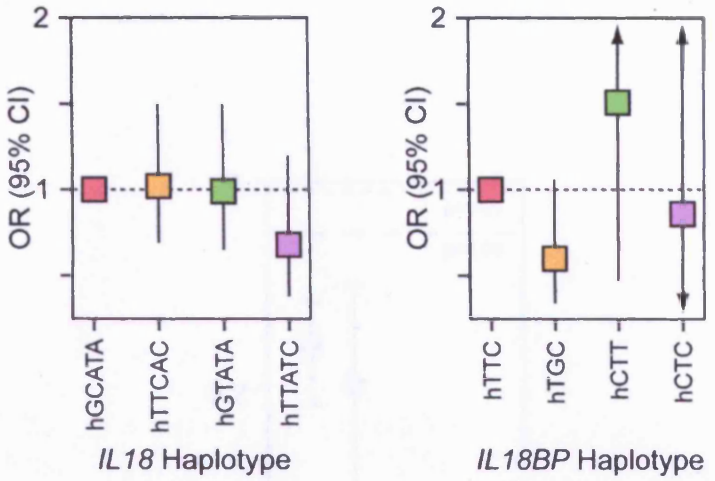

(a) OR for major complication by *IL18* haplotype.

(b) OR for major complication by *IL18BP* haplotype.

Figure 6.1: ORs[95% CI] associated with risk of major complication following CABG surgery for each *IL18* and *IL18BP* haplotype.

6.1.2 *IL18*'s Effect on Obesity and BMI

6.1.2.1 Single SNP Analysis

Univariate Analysis As shown in table 6.5 on page 219, only *IL18*-5848 T>C genotype frequency differed significantly between those who were obese and non-obese in CABG (p=0.01). This equated to a lower RR for C allele carriers. Heterozygotes had an RR[95% CI] of 0.57[0.40–0.83] (p=0.003), whilst for C homozygotes this was 0.68[0.40–1.15] although this was not significant (p=0.13). *IL18*-5848 was also associated with significant differences in BMI (p=0.008, see table 6.6 on page 220) although the pattern was not a straightforward additive pattern with heterozygotes having lower BMI than both homozygote groups. This effect was similar when analysis was restricted to the non-obese, but was only borderline significant (p=0.06). In the obese no significant differences were observed between the genotype groups (p=0.38, see figure 6.3 on page 221).

There were no significant associations between *IL18BP* tSNPs and risk of obesity or BMI (see table 6.7 on page 222 and table 6.8 on page 223).

Multivariate Analysis Four models were used in multivariate analysis to test the effect of covariates on the association between variation in *IL18* and BMI:

Model 1 Sex and age

Model 2 Sex, age, and smoking

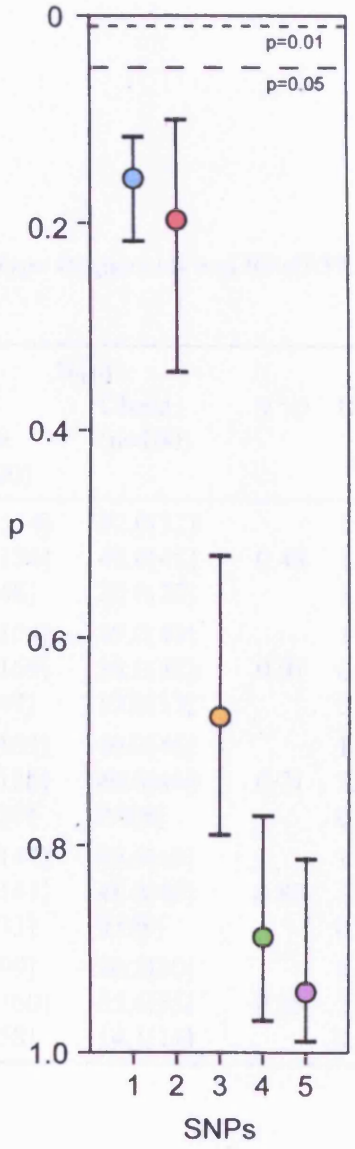

Figure 6.2: Mean p values[SD] from MDR analysis in CABG using major complication following surgery as outcome.

Table 6.5: *IL18* tSNP genotype frequencies and RRs[95% CI] in obese and non-obese individuals within CABG.

tSNP		%[n] Non-Obese (n=320)	%[n] Obese (n=100)	χ^2 p	RR[95% CI]	p
	GG	35.8[114]	32.0[32]		1	—
-9731	GT	49.1[156]	48.0[48]	0.48	1.07[0.72–1.59]	0.72
	TT	15.1[48]	20.0[20]		1.34[0.83–2.17]	0.23
	TT	32.5[104]	49.0[49]		1	—
-5848	TC	52.8[169]	38.0[38]	0.01	0.57[0.40–0.83]	0.003
	CC	14.7[47]	13.0[13]		0.68[0.40–1.15]	0.13
	AA	47.3[151]	46.0[46]		1	—
+105	AC	42.3[135]	46.0[46]	0.71	1.09[0.76–1.55]	0.64
	CC	10.3[33]	8.0[8]		0.84[0.43–1.63]	0.59
	TT	45.3[144]	43.0[43]		1	—
+8855	TA	44.3[141]	48.0[48]	0.80	1.10[0.77–1.58]	0.59
	AA	10.4[33]	9.0[9]		0.93[0.49–1.76]	0.83
	AA	31.2[99]	30.3[30]		1	—
+11015	AC	50.5[160]	55.6[55]	0.56	1.10[0.75–1.62]	0.63
	CC	18.3[58]	14.1[14]		0.84[0.48–1.47]	0.53

Table 6.6: Geometric mean[95% CI] BMI (kg/m^2) by *IL18* tSNP in both obese and non-obese individuals in CABG.

tSNP		Geometric mean BMI[95% CI] (kg/m^2) Total	p/R^2	Non-Obese (n=320)	p/R^2	Obese (n=100)	p/R^2
	GG	28.3[27.4–29.1]		26.2[25.5–26.9]		33.5[32.6–34.5]	
-9731	GT	27.9[27.1–28.6]	0.69/0.2	25.5[24.9–26.0]	0.26/1.4	33.3[32.4–34.2]	0.93/0.1
	TT	28.4[27.1–29.7]		25.7[24.8–26.6]		33.3[31.5–35.1]	
	TT	28.9[28.1–29.7]		26.2[25.6–26.8]		33.2[32.3–34.2]	
-5848	TC	27.3[26.5–28.0]	0.008/3.2	25.3[24.8–25.9]	0.06/2.8	33.2[32.4–34.1]	0.38/2.0
	CC	28.8[27.3–30.4]		26.4[25.3–27.6]		34.5[32.7–36.5]	
	AA	28.4[27.7–29.1]		26.2[25.6–26.8]		33.3[32.5–34.2]	
+105	AC	27.8[27.0–28.7]	0.59/0.4	25.1[24.5–25.7]	0.009/4.7	33.7[32.7–34.8]	0.20/3.3
	CC	28.3[27.1–29.5]		26.8[25.8–27.8]		31.7[30.8–32.6]	
	TT	28.3[27.6–29.0]		26.2[25.6–26.8]		33.4[32.5–34.2]	
+8855	TA	27.9[27.1–28.7]	0.72/0.2	25.2[24.6–25.8]	0.02/4.0	33.7[32.7–34.8]	0.17/3.6
	AA	28.2[27.1–29.4]		26.7[25.8–27.6]		31.7[30.9–32.4]	
	AA	28.4[27.6–29.2]		26.4[25.7–27.1]		33.1[32.4–34.0]	
+11015	AC	28.2[27.4–28.9]	0.52/0.4	25.5[25.0–26.0]	0.11/2.2	33.7[32.8–34.6]	0.49/1.5
	CC	27.5[26.3–28.7]		25.7[24.7–26.7]		32.7[30.7–34.9]	

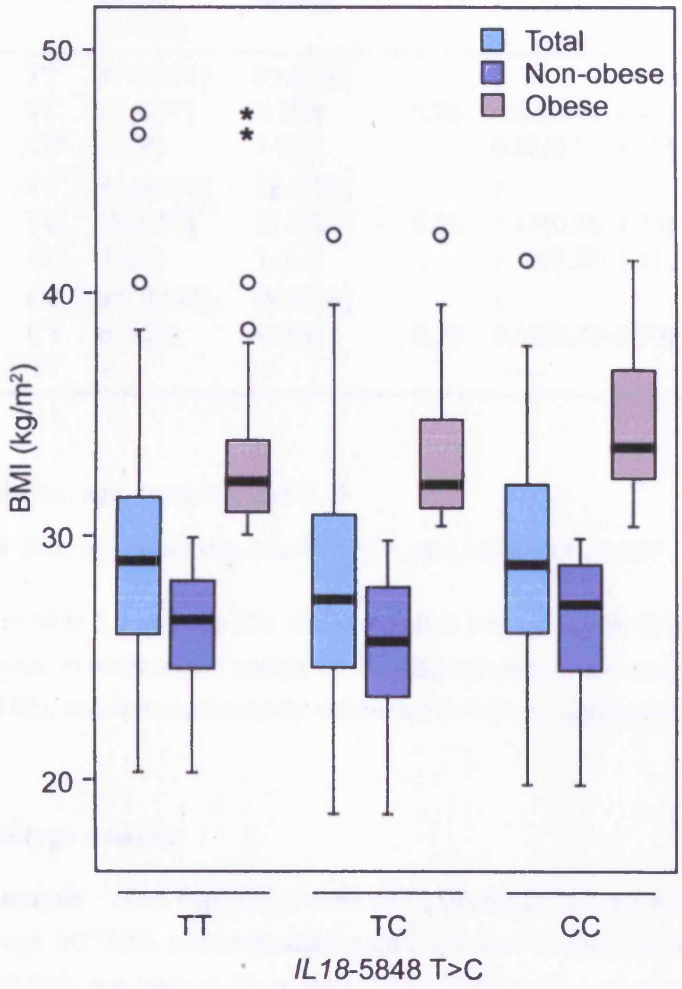

Figure 6.3: Box plots of BMI by *IL18* tSNP genotype in the total CABG cohort and the obese and non-obese within it. Line – Median; Box – 75th to 25th percentile; ∘ – outlier (>1.5 box lengths out of box); ⋆ – extreme (>3 box lengths out of box); whisker – last value not an outlier.

Table 6.7: *IL18BP* tSNP genotype frequencies and RRs[95% CI] in obese and non-obese individuals within CABG.

tSNP		%[n] Non-Obese (n=320)	Obese (n=100)	χ^2 p	RR[95% CI]	p
	TT	87.0[274]	89.8[88]		1	—
-1765	TC	11.7[37]	9.2[9]	0.76	0.80[0.44–1.49]	0.48
	CC	1.3[4]	1.0[1]		0.82[0.14–4.79]	0.82
	TT	81.2[254]	78.0[78]		1	—
-559	TG	18.2[57]	21.0[21]	0.76	1.15[0.76–1.73]	0.52
	GG	0.6[2]	1.0[1]		1.42[0.28–7.11]	0.69
	CC	93.7[297]	96.0[96]		1	—
+3041	CT	6.3[20]	4.0[4]	0.39	0.68[0.27–1.70]	0.39
	TT	—	—		—	—

Model 3 Sex, age, smoking, and IL-6

Model 4 Sex, age, smoking, baseline IL-6, and baseline IL-18BP

As shown in table 6.9 on page 224, the association between *IL18*-5848 and BMI remained significant in multivariate analysis following adjustment for sex, age, smoking, and IL-6 (p=0.02), but was significantly attenuated following adjustment for IL-18BP (p=0.24).

6.1.2.2 Haplotype Analysis

Univariate Analysis *IL18* haplotypes were not globally associated with differences in BMI, although hGTATA was associated with a 1.9-fold increase in risk of obesity in CABG (p=0.004, see table 6.10 on page 225 and figure 6.4 on page 224). This haplotype was also associated with significantly higher BMI with those homozygote for the haplotype estimated to have a BMI of 30.3 kg/m^2 compared to 27.5 kg/m^2 for the reference haplotype (hGCATA, see figure 6.5 on page 227). When analysing in both the obese and non-obese the effect of hGTATA on BMI was not significant in either group, although the estimated haplotypic mean lnBMI was higher for hGTATA in the non-obese only (see table 6.12 on page 226).

No *IL18BP* haplotype was seen to differ in frequency between the obese and non-obese groups, and none was significantly associated with differences in BMI (see table 6.11 on page 225 and table 6.13 on page 226).

Table 6.8: Geometric mean[95% CI] BMI (kg/m^2) by *IL18BP* tSNP in both obese and non-obese individuals in CABG.

tSNP		Geometric mean BMI[95% CI] (kg/m^2) Total	p/R^2	Non-Obese (n=320)	p/R^2	Obese (n=100)	p/R^2
	TT	28.0[27.5–28.6]		25.7[25.3–26.2]		33.3[32.7–33.9]	
-1765	TC	28.4[26.7–30.3]	0.61/0.3	26.1[24.7–27.7]	0.72/0.3	33.6[31.4–35.9]	0.77/0.2
	CC	26.3[20.6–33.6]		25.0[18.6–33.5]		—	
	TT	28.0[27.5–28.6]		25.7[25.2–26.1]		33.5[32.8–34.2]	
-559	TG	28.4[27.3–29.5]	0.71/0.2	26.1[25.3–27.1]	0.56/0.6	32.7[31.2–34.3]	0.30/2.8
	GG	30.0[18.3–49.0]		26.7[19.1–37.4]		—	
	CC	28.1[27.6–28.6]		25.8[25.4–26.2]		33.3[32.7–34.0]	
+3041	CT	27.7[24.4–31.4]	0.72/<0.1	25.0[22.2–28.3]	0.42/0.3	34.6[29.2–41.0]	0.43/0.6
	TT	—		—		—	

Table 6.9: Results from multivariate analysis of *IL18* tSNP's association with BMI in CABG.

IL18 SNP	Model 1 Sex and age	Model 2 Model 1 + smoking	Model 3 Model 2 + baseline IL-6	Model 4 Model 3 + baseline IL-18BP
-9731	0.73	0.79	0.92	0.42
-5848	0.002	0.002	0.02	0.24
+105	0.78	0.70	0.84	0.53
+8855	0.85	0.80	0.84	0.76
+11015	0.75	0.73	0.63	0.49

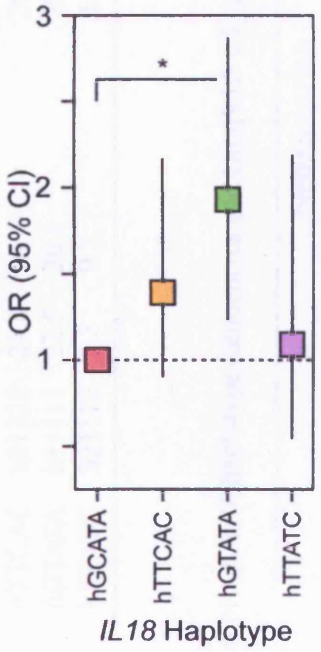

Figure 6.4: OR[95% CI] for obesity associated with each *IL18* haplotype in CABG; ⋆–p=0.004.

Table 6.10: *IL18* haplotype frequencies and ORs[95% CI] in obese and non-obese individuals within CABG

Haplotype		Frequency (%) Total	Non-obese (n=260)	Obese (n=87)	OR[95% CI]	p
hGCATA	h12111	27.8	28.7	24.9	1	—
hTTCAC	h21222	24.8	24.4	26.1	1.39[0.90–2.17]	0.14
hGTATA	h11111	22.5	20.1	29.6	1.93[1.23–3.05]	0.004
hTTATC	h21112	9.3	9.7	8.1	1.09[0.54–2.19]	0.81

Table 6.11: *IL18BP* haplotype frequencies and ORs[95% CI] in obese and non-obese individuals within CABG

Haplotype		Frequency (%) Total	Non-obese (n=260)	Obese (n=87)	OR[95% CI]	p
hTTC	h111	87.1	87.7	85.4	1	—
hTGC	h121	8.0	7.2	10.5	1.48[0.82–2.70]	0.20
hCTT	h212	1.7	2.0	1.1	0.55[0.12–2.48]	0.43
hCTC	h211	1.4	1.3	2.0	1.77[0.41–7.75]	0.45

Table 6.12: Haplotypic mean lnBMI[95% CI] by *IL18* haplotypes in the total CABG cohort, and in obese and non-obese individuals separately.

Haplotype		Haplotypic mean lnBMI[95% CI] Total	p/R^2	Non-obese (n=260)	p/R^2	Obese (n=87)	p/R^2
hGCATA	h12111	1.658[1.639–1.677]	—	1.623[1.606–1.640]	—	1.749[1.722–1.777]	—
hTTCAC	h21222	1.661[1.631–1.691]	0.95	1.618[1.592–1.645]	0.83	1.732[1.699–1.765]	0.16
hGTATA	h11111	1.706[1.677–1.735]	0.02	1.647[1.622–1.673]	0.16	1.766[1.743–1.788]	0.85
hTTATC	h21112	1.649[1.605–1.693]	0.81	1.609[1.572–1.647]	0.51	1.764[1.725–1.804]	0.94
	Global p/R^2		0.11/3.2		0.49/2.4		0.36/5.1

Table 6.13: Haplotypic mean lnBMI[95% CI] by *IL18BP* haplotypes in the total CABG cohort, and in obese and non-obese individuals separately.

Haplotype		Haplotypic mean lnBMI[95% CI] Total	p/R^2	Non-obese (n=260)	p/R^2	Obese (n=87)	p/R^2
hTTC	h111	1.668[1.657–1.679]	—	1.625[1.616–1.635]	—	1.752[1.741–1.763]	—
hTGC	h121	1.694[1.649–1.739]	0.29	1.636[1.587–1.685]	0.69	1.757[1.728–1.787]	0.76
hCTT	h212	1.636[1.556–1.717]	0.45	1.586[1.518–1.653]	0.26	1.862[1.753–1.967]	0.06
hCTC	h211	1.656[1.542–1.771]	0.85	1.563[1.408–1.718]	0.43	1.715[1.572–1.857]	0.61
	Global p/R^2		0.80/0.8		0.56/2.3		0.40/4.6

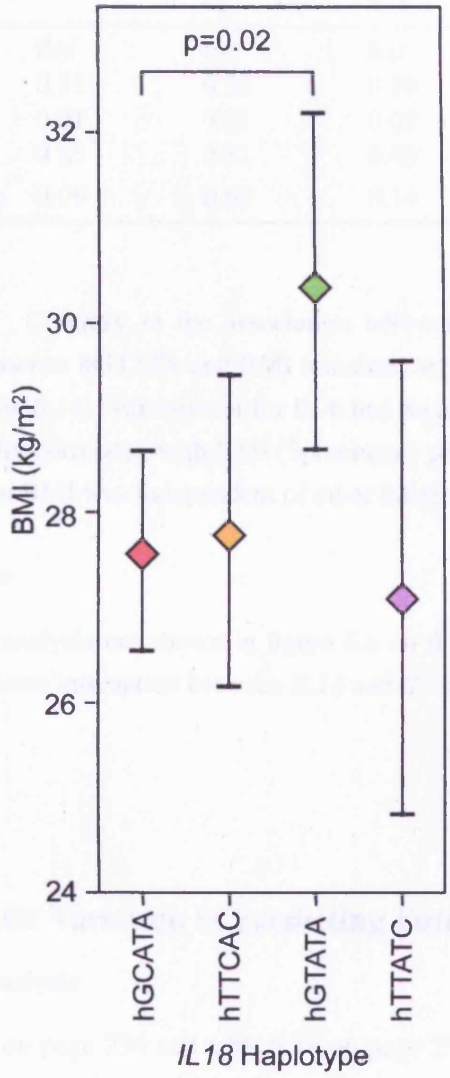

Figure 6.5: Estimated BMI[95% CI] for homozygotes of common *IL18* haplotypes in the total CABG cohort. P values refer to haplotypic mean analysis.

Table 6.14: Results from multivariate analysis of *IL18* haplotypes and their association with BMI in CABG.

IL18 haplotype		Model 1 Sex and age	Model 2 Model 1 + smoking	Model 3 Model 2 + baseline IL-6	Model 4 Model 3 + baseline IL-18BP
hGCATA	h12111	Ref	Ref	Ref	Ref
hTTCAC	h21222	0.31	0.30	0.39	0.90
hGTATA	h11111	0.01	0.01	0.02	0.02
hTTATC	h21112	0.85	0.81	0.93	0.97
	Global p	0.09	0.08	0.14	0.06

Multivariate Analysis Contrary to the association between *IL18*-5848 T>C and BMI, the association between hGTATA and BMI remained significant in all four multivariate models (see table 6.14). Adjustment for IL-6 had no effect on the association, despite being significantly correlated with BMI (Spearman's ρ=0.23, p<0.001), showing the effect of IL-18 on BMI was independent of other inflammatory mediators.

6.1.2.3 MDR Analysis

The results from MDR analysis are shown in figure 6.6 on the following page, there appeared to be no significant interaction between *IL18* and *IL18BP* tSNPs on obesity in CABG.

6.2 NPHSII

6.2.1 Use of Genetic Variation in Predicting Future Risk of MI

6.2.1.1 Single SNP Analysis

As shown in table 6.15 on page 230 and table 6.16 on page 231, none of the *IL18* or *IL18BP* tSNPs were present at significantly different frequencies in those who suffered an MI during follow-up and those who did not. Of particular note, the genotype frequencies of both *IL18BP*-1765 and +3041 differed significantly from that expected by HWE (p<0.001 and p=0.007, respectively). For -1765 T>C the observed[expected] genotype counts were: TT – 2443[2433]; TC – 230[249]; CC – 16[6], whilst for +3041 C>T they were: CC – 2577[2574]; CT – 103[109]; CC – 4[1]. Therefore in both cases the disequilibrium was due to an excess of rare allele homozygotes.

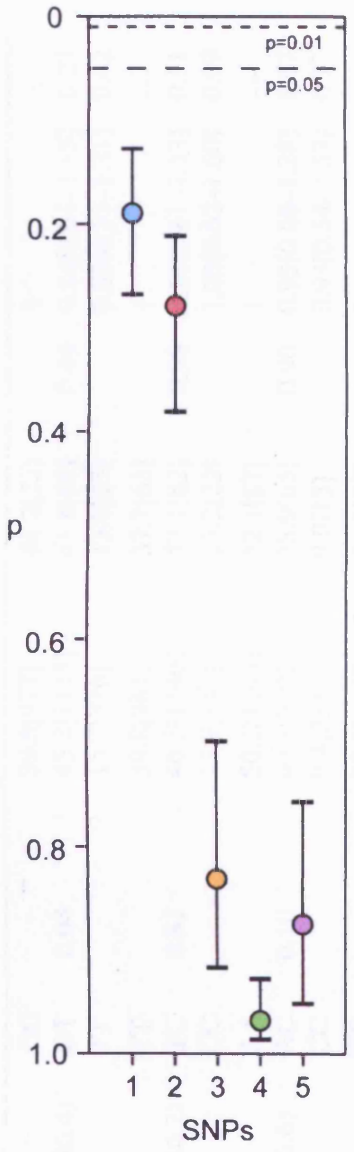

Figure 6.6: Results from MDR analysis in CABG using obesity as the outcome variable.

Table 6.15: Allele frequencies and RRs[95% CI] for *IL18* tSNPs in those who suffered an MI during follow-up in NPHSII, and those who did not.

tSNP and completeness of genotyping (%)		Total HWE p	%[n] No MI (n=2870)	MI (n=182)	χ^2 p	RR[95% CI]	p
	GG		39.5[977]	44.2[73]		1	—
-9731 (86.4)	GT	0.04	45.2[1118]	41.8[69]	0.49	0.84[0.61–1.15]	0.27
	TT		15.2[376]	13.9[23]		0.83[0.53–1.31]	0.42
	TT		39.8[981]	37.7[63]		1	—
-5848 (86.2)	TC	0.81	46.3[1140]	49.1[82]	0.78	1.11[0.81–1.53]	0.51
	CC		13.9[343]	13.2[22]		1.00[0.62–1.60]	0.99
	AA		50.2[1244]	52.1[87]		1	—
+105 (86.6)	AC	0.10	40.3[999]	38.9[65]	0.90	0.93[0.68–1.28]	0.67
	CC		9.4[233]	9.0[15]		0.93[0.54–1.57]	0.77
	TT		50.3[1202]	52.8[85]		1	—
+8855 (83.6)	TA	0.02	39.9[954]	37.9[61]	0.83	0.91[0.66–1.25]	0.56
	AA		9.8[233]	9.3[15]		0.92[0.54–1.56]	0.75
	AA		37.1[929]	38.9[65]		1	—
+11015 (87.4)	AC	0.07	46.3[1157]	45.5[76]	0.88	0.94[0.68–1.30]	0.72
	CC		16.6[415]	15.6[26]		0.90[0.58–1.40]	0.64

Table 6.16: Allele frequencies and RRs[95% CI] for *IL18BP* tSNPs in those who suffered an MI during follow-up and those who did not.

tSNP and completeness of genotyping (%)		Total HWE p	%[n] No MI (n=2870)	MI (n=182)	χ^2 p	RR[95% CI]	p
	TT		91.0[2295]	88.6[148]		1	—
-1765 (88.1)	TC	<0.001	8.4[212]	10.8[18]	0.57	1.29[0.81–2.07]	0.29
	CC		0.6[15]	0.6[1]		1.03[0.15–6.93]	0.97
	TT		77.4[1947]	77.2[129]		1	—
-559 (87.9)	TG	0.62	21.0[529]	21.6[36]	0.92	1.03[0.72–1.47]	0.89
	GG		1.6[40]	1.2[2]		0.77[0.20–2.99]	0.70
	CC		96.1[2416]	95.3[161]		1	—
+3041 (87.9)	CT	0.007	3.8[96]	4.1[7]	0.30	1.09[0.52–2.26]	0.82
	TT		0.1[3]	0.6[1]		4.00[0.73–21.99]	0.12

Table 6.17: Haplotype frequencies and ORs[95% CI] for *IL18* haplotypes in those who suffered an MI during follow-up and those who did not.

Haplotype		Total	Frequency (%) No MI (n=2870)	MI (n=182)	OR[95% CI]	p
hGCATA	h12111	31.6	31.6	32.1	1	—
hTTCAC	h21222	25.6	25.7	23.8	0.93[0.70–1.24]	0.63
hGTATA	h11111	26.6	26.4	28.4	1.07[0.81–1.42]	0.62
hTTATC	h21112	9.9	9.9	10.0	1.01[0.67–1.54]	0.95

Table 6.18: Haplotype frequencies and ORs[95% CI] for *IL18BP* haplotypes in those who suffered an MI during follow-up and those who did not.

Haplotype		Total	Frequency (%) No MI (n=2870)	MI (n=182)	OR[95% CI]	p
hTTC	h111	84.2	84.3	83.7	1	—
hTGC	h121	10.9	10.9	10.1	0.93[0.64–1.35]	0.70
hCTT	h212	2.1	2.0	2.7	1.31[0.69–2.48]	0.41
hCTC	h211	1.6	1.6	1.7	1.05[0.42–2.64]	0.92

6.2.1.2 Haplotype Analysis

Neither *IL18* nor *IL18BP* haplotype frequencies differed significantly between those who suffered an MI during follow-up and those who did not (see table 6.17 and table 6.18).

6.2.1.3 MDR Analysis

The results from MDR analysis in NPHSII using incidence of MI during follow-up as the outcome are shown in figure 6.7 on the next page. There was no evidence for a significant epistatic effect between *IL18* and *IL18BP* tSNPs, on MI risk.

6.2.2 Genetic Variation and Obesity

6.2.2.1 Single SNP Analysis

No *IL18* or *IL18BP* tSNP was seen at significantly different frequencies in those who were obese or non-obese in NPHSII at baseline (see table 6.19 on page 234 and table 6.20 on page 235). However, after five years of follow-up (during which a further 50 individuals became obese), the *IL18*-5848 C allele was significantly rarer in those who

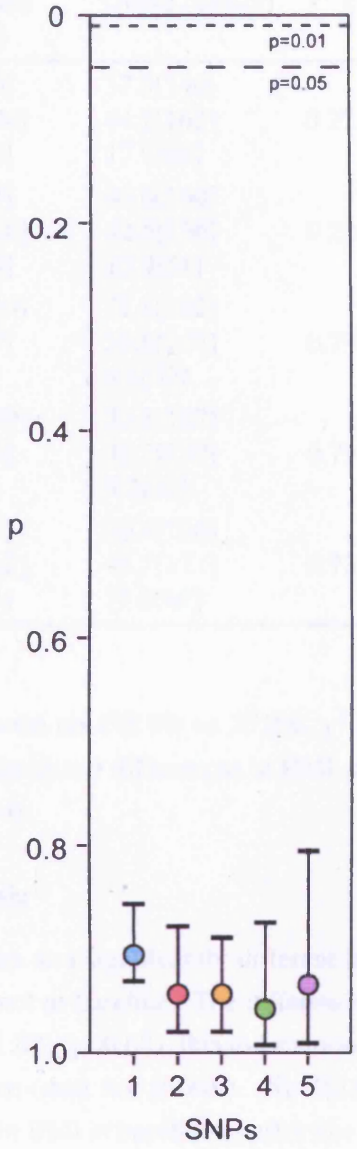

Figure 6.7: The results from MDR analysis in NPHSII using MI during follow-up as the outcome variable.

Table 6.19: Allele frequencies and RRs[95% CI] for *IL18* tSNPs in those who were obese or non-obese at baseline in NPHSII.

tSNP		%[n] Non-Obese (n=2623)	Obese (n=429)	χ^2 p	RR[95% CI]	p
	GG	40.1[910]	37.9[140]		1	—
-9731	GT	45.2[1024]	44.2[163]	0.27	1.03[0.83–1.27]	0.78
	TT	14.7[333]	17.9[66]		1.24[0.95–1.62]	0.12
	TT	39.0[884]	43.6[160]		1	—
-5848	TC	47.1[1066]	42.5[156]	0.22	0.83[0.68–1.02]	0.08
	CC	13.9[314]	13.9[51]		0.91[0.68–1.22]	0.53
	AA	50.1[1139]	51.8[192]		1	—
+105	AC	40.4[917]	39.6[147]	0.79	0.96[0.78–1.17]	0.67
	CC	9.5[216]	8.6[32]		0.89[0.63–1.27]	0.53
	TT	50.2[1100]	52.1[187]		1	—
+8855	TA	40.0[876]	38.7[139]	0.79	0.94[0.77–1.16]	0.57
	AA	9.8[215]	9.2[33]		0.92[0.65–1.29]	0.62
	AA	37.4[858]	36.4[136]		1	—
+11015	AC	46.3[1062]	45.7[171]	0.73	1.01[0.82–1.25]	0.90
	CC	16.3[374]	17.9[67]		1.11[0.85–1.45]	0.45

were obese than those who were not (33.9% vs. 37.8%, χ^2 p=0.04, data not shown). No SNP was associated with significant differences in BMI at baseline or after five years of follow-up (data not shown).

6.2.2.2 Haplotype Analysis

Only *IL18* hTTATC was seen at a significantly different frequency in those who were obese and those who were not at baseline. The difference in frequency equated to an OR[95% CI] of 1.39[1.06–1.82] (p=0.02), this association was also present using data from five years of follow-up (data not shown). No *IL18* or *IL18BP* haplotype was associated with differences in BMI at baseline or after five years of follow-up (data not shown).

6.2.2.3 MDR Analysis

As shown in figure 6.8 on page 236, there was no evidence for interaction between *IL18* and *IL18BP* SNPs in causing obesity inNPHSII at baseline, or five years.

Table 6.20: Allele frequencies and RRs[95% CI] for *IL18BP* tSNPs in those who were obese or non-obese at baseline in NPHSII.

tSNP		%[n] Non-Obese (n=2623)	Obese (n=429)	χ^2 p	RR[95% CI]	p
	TT	90.5[2093]	93.1[350]		1	—
-1765	TC	9.0[208]	5.9[22]	0.06	0.67[0.44–1.01]	0.05
	CC	0.5[12]	1.1[4]		1.75[0.74–4.10]	0.23
	TT	77.2[1782]	78.2[294]		1	—
-559	TG	21.1[486]	21.0[79]	0.43	0.99[0.78–1.24]	0.91
	GG	1.7[39]	0.8[3]		0.50[0.17–1.51]	0.20
	CC	96.1[2216]	95.8[361]		1	—
+3041	CT	3.8[88]	4.0[15]	0.81	1.04[0.64–1.68]	0.87
	TT	0.1[3]	0.3[1]		1.78[0.33–9.77]	0.53

Table 6.21: *IL18* haplotype frequencies and ORs[95% CI] in those who were obese or non-obese at baseline in NPHSII.

Haplotype		Total	Frequency (%) Non-Obese (n=2623)	Obese (n=429)	OR[95% CI]	p
hGCATA	h12111	31.5	31.9	29.2	1	—
hTTCAC	h21222	25.6	25.8	24.8	1.02[0.84–1.24]	0.82
hGTATA	h11111	26.6	26.5	27.0	1.08[0.89–1.32]	0.43
hTTATC	h21112	9.9	9.5	12.3	1.39[1.06–1.82]	0.02

Table 6.22: *IL18BP* haplotype frequencies and ORs[95% CI] in those who were obese or non-obese at baseline in NPHSII.

Haplotype		Total	Frequency (%) Non-Obese (n=2623)	Obese (n=429)	OR[95% CI]	p
hTTC	h111	84.2	84.0	85.3	1	—
hTGC	h121	10.9	10.9	10.6	0.96[0.74–1.24]	0.75
hCTT	h212	2.0	2.0	2.2	1.10[0.66–1.81]	0.72
hCTC	h211	1.7	1.7	1.1	0.66[0.30–1.45]	0.30

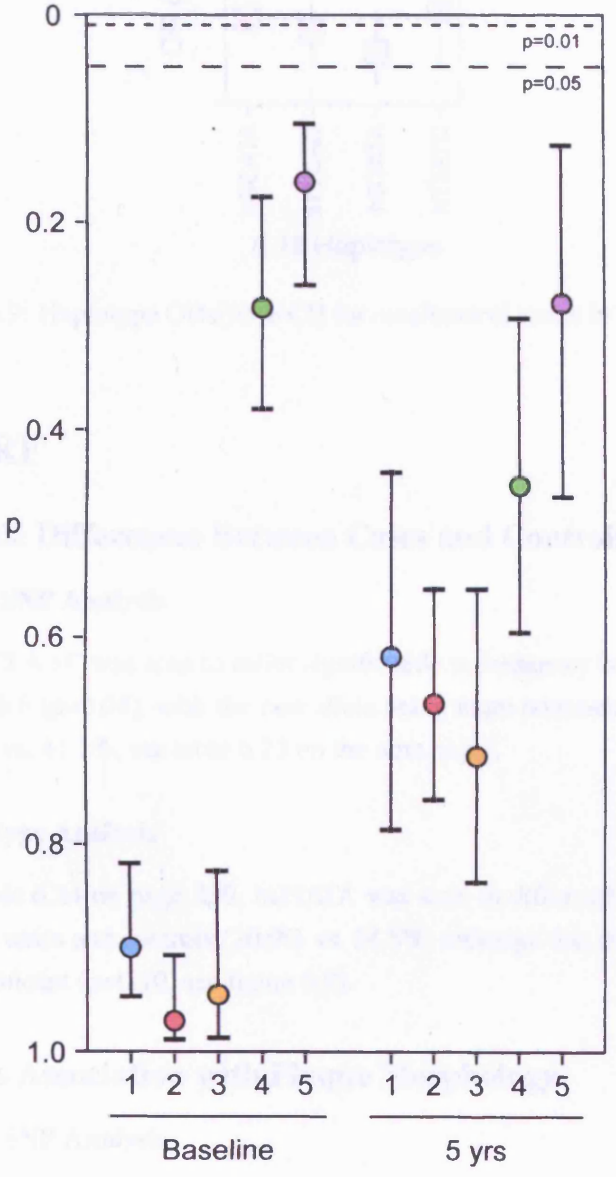

Figure 6.8: Results from MDR analysis in NPHSII using obesity at baseline as the outcome variable.

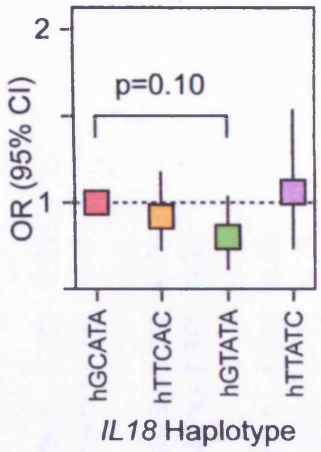

Figure 6.9: Haplotype ORs[95% CI] for case/control status in SCARF.

6.3 SCARF

6.3.1 Genetic Differences Between Cases and Controls

6.3.1.1 Single SNP Analysis

Only *IL18*+11015 A>C was seen to differ significantly in frequency between cases and controls in SCARF (p=0.04), with the rare allele being more common in cases than in controls (44.3% vs. 41.5%, see table 6.23 on the next page).

6.3.1.2 Haplotype Analysis

As shown in table 6.24 on page 239, hGTATA was seen to differ substantially in frequency between cases and controls (20.9% vs. 24.5%) although this difference was not statistically significant (p=0.10, see figure 6.9).

6.3.2 *IL18*'s Association with Plaque Morphology

6.3.2.1 Single SNP Analysis

Univariate Analysis *IL18*-9731 G>T, -5848 T>C, and +11015 A>C were all significantly associated with normalized (to segment length) plaque area (p=0.004, 0.05, and 0.01 respectively, see table 6.25 on page 239) and all showed additive genotype patterns (see figure 6.10 on page 240).

Multivariate Analysis Four separate models were used in multivariate analysis:

Model 1 Sex and age

Table 6.23: Allele frequencies for *IL18* tSNPs in cases and controls within SCARF, with resulting RRs[95% CI].

tSNP and completeness of genotyping (%)		Total HWE p	%[n] Controls (n=387)	Cases (n=387)	χ^2 p	RR[95% CI]	p
	GG		35.8[138]	35.9[135]		1	—
-9731 (98.4)	GT	0.71	49.7[192]	45.2[170]	0.22	0.95[0.81–1.12]	0.53
	TT		14.5[56]	18.9[71]		1.13[0.93–1.37]	0.23
	TT		39.5[152]	37.2[140]		1	—
-5848 (98.3)	TC	0.62	47.8[184]	47.9[180]	0.64	1.03[0.88–1.21]	0.70
	CC		12.7[49]	14.9[56]		1.11[0.90–1.38]	0.34
	AA		43.8[169]	44.8[169]		1	—
+105 (98.6)	AC	0.97	46.6[180]	42.4[160]	0.29	0.94[0.81–1.10]	0.44
	CC		9.6[37]	12.7[48]		1.13[0.91–1.40]	0.29
	TT		44.0[170]	44.8[169]		1	—
+8855 (98.6)	TA	0.90	46.4[179]	42.2[159]	0.25	0.94[0.81–1.10]	0.46
	AA		9.6[37]	13.0[49]		1.14[0.92–1.41]	0.24
	AA		33.3[129]	34.2[129]		1	—
+11015 (98.7)	AC	0.20	50.4[195]	43.0[162]	0.04	0.91[0.77–1.07]	0.26
	CC		16.3[63]	22.8[86]		1.15[0.96–1.39]	0.13

Table 6.24: Haplotype frequencies and ORs[95% CI] in cases and controls within SCARF.

Haplotype		Total	Frequency (%) Controls (n=387)	Cases (n=387)	OR[95% CI]	p
hGCATA	h12111	33.1	33.2	33.1	1	—
hTTCAC	h21222	29.9	29.9	29.8	0.92[0.72–1.18]	0.52
hGTATA	h11111	22.7	24.5	20.9	0.80[0.61–1.04]	0.10
hTTATC	h21112	9.1	8.5	9.7	1.06[0.73–1.54]	0.77

Table 6.25: Normalized plaque area and % stenosis of diseased vessel by *IL18* genotype in SCARF. Data available for cases only.

tSNP		Normalized plaque area Geometric mean[95% CI]	p/R^2 (%)	% stenosis Mean[95% CI]	p/R^2 (%)
	GG	0.192[0.178–0.207]		30.2[27.9–32.5]	
-9731	GT	0.220[0.206–0.235]	0.004/4.6	33.0[31.4–34.6]	0.06/2.4
	TT	0.230[0.211–0.252]		33.3[31.1–35.6]	
	TT	0.224[0.209–0.240]		32.7[31.1–34.4]	
-5848	TC	0.208[0.195–0.222]	0.05/2.5	31.9[30.1–33.6]	0.52/0.6
	CC	0.190[0.168–0.215]		30.6[26.4–34.9]	
	AA	0.201[0.187–0.215]		31.2[29.1–33.3]	
+105	AC	0.221[0.207–0.237]	0.10/2.0	32.4[30.9–34.0]	0.40/0.8
	CC	0.219[0.197–0.243]		33.6[30.8–36.3]	
	TT	0.201[0.187–0.215]		31.2[29.1–33.3]	
+8855	TA	0.222[0.208–0.237]	0.10/2.0	32.5[31.0–34.1]	0.44/0.7
	AA	0.217[0.195–0.241]		33.2[30.5–35.9]	
	AA	0.195[0.180–0.211]		30.5[28.1–33.0]	
+11015	AC	0.215[0.201–0.230]	0.01/3.9	32.7[31.0–34.4]	0.18/1.4
	CC	0.232[0.215–0.251]		33.1[31.1–35.1]	

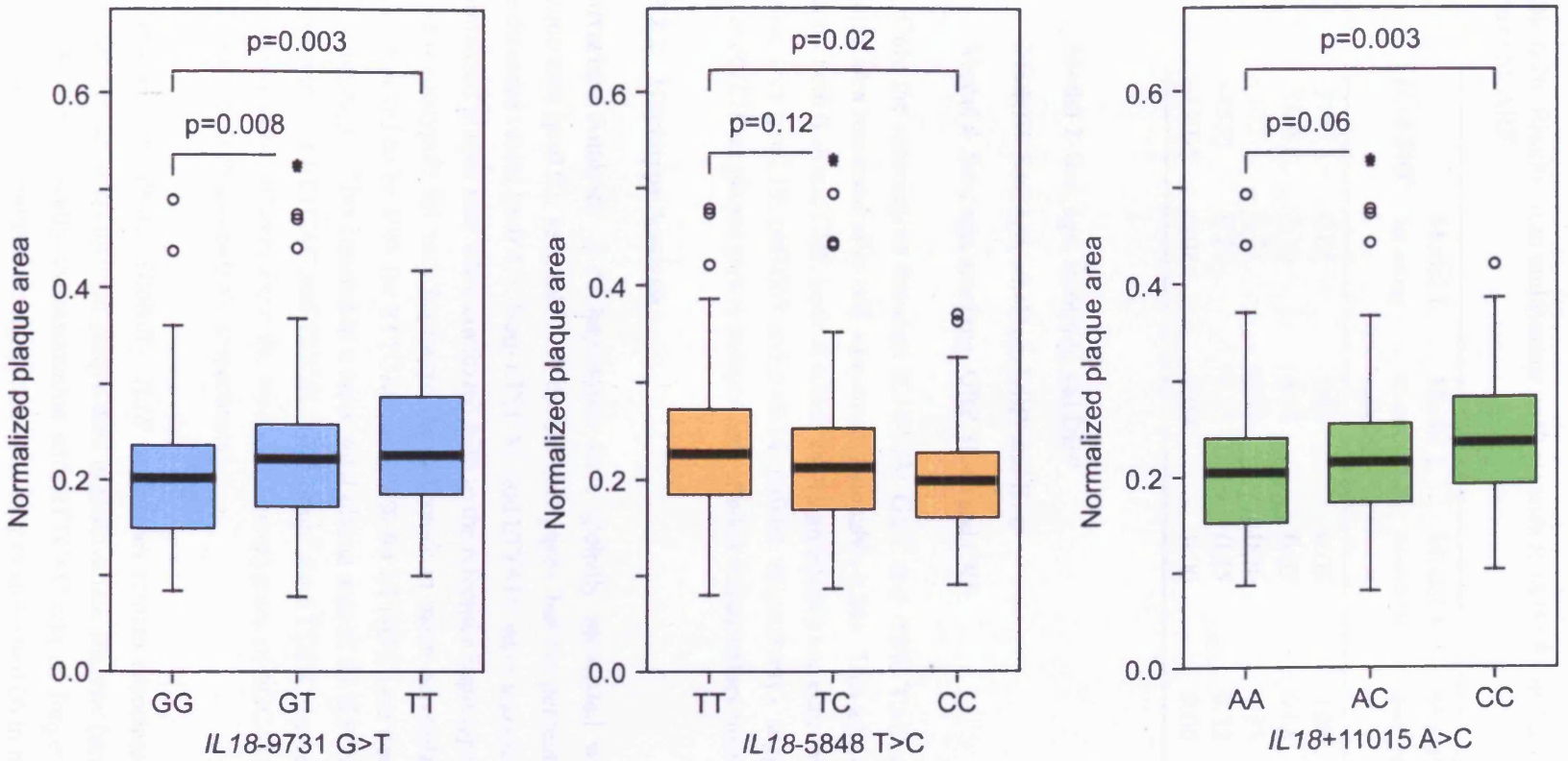

(a) Normalized plaque area by *IL18*-9731 G>T genotype

(b) Normalized plaque area by *IL18*-5848 T>C genotype

(c) Normalized plaque area by *IL18*+11015 A>C genotype

Figure 6.10: The association of *IL18* tSNPs and normalized plaque area in SCARF.

Table 6.26: Results from multivariate analysis with *IL18* tSNPs and normalized plaque area in SCARF.

IL18 SNP	Model 1 Sex and age	Model 2 Model 1 + smoking and DBP	Model 3 Model 2 + IL-6	Model 4 Model 3 + CRP
-9731	0.01	0.03	0.03	0.03
-5848	0.10	0.05	0.03	0.03
+105	0.21	0.38	0.36	0.33
+8855	0.20	0.37	0.35	0.32
+11015	0.04	0.09	0.06	0.06

Model 2 Sex, age, smoking, and DBP

Model 3 Sex, age, smoking, DBP, and IL-6

Model 4 Sex, age, smoking, DBP, IL-6, and CRP

Only the associations between *IL18*-9731 G>T and -5848 T>C, and normalized plaque area remained after full adjustment (see table 6.26). This adjustment included that for both IL-6 and CRP, both of which were significantly correlated with normalized plaque area (ρ=0.19, p=0.005 and ρ=0.14, p=0.03, respectively), suggesting that the effect of *IL18* on plaque area is independent of other inflammatory mediators.

6.3.2.2 Haplotype Analysis

Univariate Analysis *IL18* haplotypes were globally associated with normalized plaque area (p=0.02, see table 6.27 on the next page), but not percentage stenosis of the diseased vessel (p=0.47). Both hTTCAC and hTTATC were associated with higher normalized plaque area when compared with to the reference haplotype (hGCATA). In those homozygote for each haplotype the difference in mean normalized plaque area was estimated to be 19% for hTTCAC, and 38% for hTTATC (see figure 6.11 on the following page). This equated to a mean *total* plaque area of 66.2[57.6–74.7]mm^2 for homozygotes of hTTCAC and 72.8[56.7–88.9]mm^2 for hTTATC, however these were not significantly different from the mean for homozygotes of hGCATA – 59.0[51.2–66.7]mm^2 (p=0.28 and p=0.13, respectively).

Multivariate Analysis Globally, *IL18* haplotypes remain associated with significant differences in normalized plaque area in multivariate analysis (see table 6.28 on page 243). Specifically, the association with hTTCAC was no longer significant although it remained borderline significant in all four models (p=0.06 in model 4). However, the association between hTTATC and normalized plaque area was highly signifi-

Table 6.27: Normalized plaque area (ln transformed) and % stenosis of diseased vessel by *IL18* haplotypes in SCARF. Data available for cases only.

Haplotype		ln Normalized plaque area Geometric mean [95% CI]	p	% stenosis Mean[95% CI]	p
hGCATA	h12111	-0.82[-0.87– -0.78]	Ref	15.3[14.2–16.5]	Ref
hTTCAC	h21222	-0.74[-0.79– -0.68]	0.03	16.7[15.1–18.3]	0.19
hGTATA	h11111	-0.80[-0.86– -0.74]	0.60	15.6[13.9–17.3]	0.83
hTTATC	h21112	-0.66[-0.77– -0.54]	0.01	17.5[14.8–20.3]	0.17
Global p/R^2			0.02/5.0		0.47/1.5

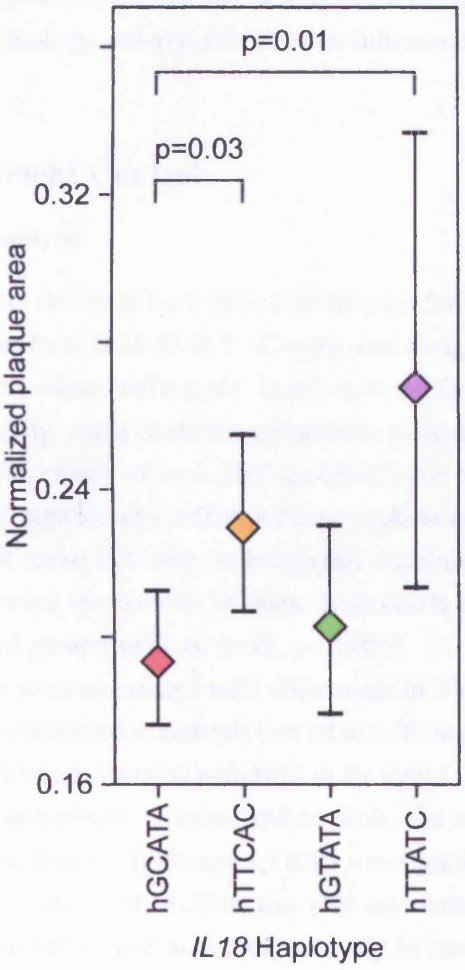

Figure 6.11: Estimated mean[95% CI] normalized plaque area for homozygotes of *IL18* haplotypes in SCARF.

Table 6.28: Results from multivariate analysis with *IL18* haplotypes and normalized plaque area in SCARF.

IL18 haplotype		Model 1 Sex and age	Model 2 Model 1 + smoking and DBP	Model 3 Model 2 + IL-6	Model 4 Model 3 + CRP
hGCATA	h12111	Ref	Ref	Ref	Ref
hTTCAC	h21222	0.06	0.06	0.08	0.06
hGTATA	h11111	0.56	0.37	0.38	0.39
hTTATC	h21112	0.006	0.004	0.004	0.005
	Global p	0.02	0.02	0.03	0.02

cant in all four models (p=0.005 in model 4), adding to the evidence of a role for IL-18 in dictating plaque morphology, independent of other inflammatory pathways and mediators.

6.3.3 *IL18* and Weight Control

6.3.3.1 Single SNP Analysis

Univariate Analysis As shown in both table 6.29 on page 245 and figure 6.12 on the next page, all tSNPs apart from *IL18*-5848 T>C were seen at significantly different frequencies in obese and non-obese individuals. In all cases the rare allele was associated with a higher risk of obesity, and a co-dominant/additive pattern between the genotype groups was observed. The effects of each SNP appeared to be exclusive to cases, with genotype frequencies not significantly different between obese and non-obese individuals in controls, but significantly different (or borderline significantly different) in cases (data not shown). However, the number of obese individuals in the case group were double that of the control group (n=89 vs. n=40, p<0.001).

Each of these tSNPs were associated with differences in BMI, with the effects appearing greatest in cases compared to controls (see table 6.30 on page 246 and table 6.31 on page 247). *IL18*-9731 was associated with BMI in the total SCARF cohort, but when divided into obese and non-obese, or cases and controls, the effect was only seen in cases, as was the case for +11015 (although +11015 was significantly associated with BMI in obese individuals also). *IL18*-5848 was also associated with significant differences in BMI, but this effect was also observed only in cases and not in the total cohort.

Multivariate Analysis The following four models were used in multivariate analysis:

Model 1 Sex and age

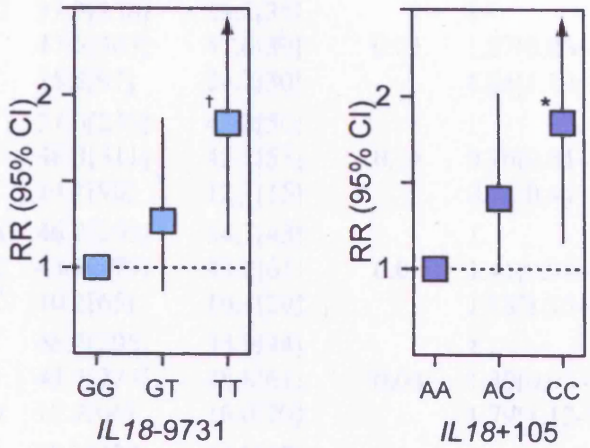

(a) Risk of obesity by *IL18* -9731 genotype

(b) Risk of obesity by *IL18* +105 genotype

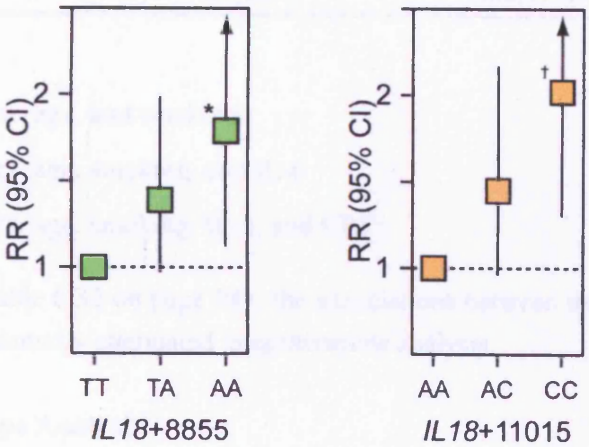

(c) Risk of obesity by *IL18* +8855 genotype

(d) Risk of obesity by *IL18* +11015 genotype

Figure 6.12: Obesity RR[95% CI] for *IL18* SNPs in SCARF; $\star$ – $p \leq 0.05$, † – $p < 0.01$.

Table 6.29: Genotype frequencies and RRs[95% CI] for *IL18* tSNPs in obese and non-obese individuals in SCARF

tSNP		%[n] Non-Obese (n=320)	Obese (n=100)	χ^2 p	RR[95% CI]	p
	GG	37.3[238]	28.2[35]		1	—
-9731	GT	47.5[303]	47.6[59]	0.03	1.27[0.86–1.87]	0.22
	TT	15.2[97]	24.2[30]		1.84[1.19–2.86]	0.006
	TT	37.0[236]	45.2[56]		1	—
-5848	TC	48.8[311]	42.7[53]	0.24	0.76[0.54–1.07]	0.11
	CC	14.1[90]	12.1[15]		0.74[0.44–1.26]	0.26
	AA	46.2[295]	34.7[43]		1	—
+105	AC	43.7[279]	49.2[61]	0.03	1.41[0.98–2.02]	0.06
	CC	10.2[65]	16.1[20]		1.85[1.15–2.97]	0.01
	TT	46.2[295]	35.2[44]		1	—
+8855	TA	43.4[277]	48.8[61]	0.04	1.39[0.97–1.99]	0.07
	AA	10.3[66]	16.0[20]		1.79[1.12–2.87]	0.02
	AA	35.7[228]	24.0[30]		1	—
+11015	AC	46.5[297]	48.0[60]	0.007	1.45[0.96–2.17]	0.07
	CC	17.8[114]	35[28.0]		2.02[1.30–3.15]	0.002

Model 2 Sex, age, and smoking

Model 3 Sex, age, smoking, and IL-6

Model 4 Sex, age, smoking, IL-6, and CRP

As shown in table 6.32 on page 247, the associations between the *IL18* tSNPs and BMI are not substantially attenuated in multivariate analysis.

6.3.3.2 Haplotype Analysis

Univariate Analysis *IL18* hTTCAC was associated with a 1.4-fold increase in risk of obesity (p=0.04, see table 6.33 on page 249). As shown in table 6.34 on page 249, *IL18* haplotypes were globally associated with significant differences in BMI in the total SCARF cohort and in cases, but not in controls alone. hTTCAC was associated with significant differences in BMI in the total SCARF cohort, but this effect was exclusively found in cases and not controls (see figure 6.13 on page 250). The effect was such that those homozygous for hTTCAC were estimated to have BMI 6.6% higher than those homozygous for hGCATA. hTTATC was also associated with significant differences in BMI but in cases alone. The difference was greater than that observed for hTTCAC,

Table 6.30: Geometric mean BMI[95% CI] (kg/m^2) by *IL18* genotype in obese and non-obese individuals in SCARF.

tSNP		Geometric mean BMI[95% CI] (kg/m^2) Total	p/R^2	Non-Obese (n=320)	p/R^2	Obese (n=100)	p/R^2
	GG	25.9[25.5–26.3]		25.0[24.7–25.3]		32.7[31.8–33.6]	
-9731	GT	26.4[26.0–26.8]	0.002/1.7	25.4[25.1–25.7]	0.08/0.8	32.2[31.7–32.8]	0.17/2.9
	TT	27.3[26.6–28.0]		25.7[25.2–26.2]		33.3[32.1–34.5]	
	TT	26.7[26.2–27.1]		25.3[25.0–25.7]		32.9[32.2–33.7]	
-5848	TC	26.2[25.8–26.5]	0.22/0.4	25.3[25.0–25.6]	0.95/<0.1	32.3[31.7–32.9]	0.40/1.5
	CC	26.2[25.6–26.9]		25.3[24.8–25.8]		32.6[31.4–33.8]	
	AA	26.0[25.7–26.4]		25.2[24.9–25.4]		33.0[32.2–33.9]	
+105	AC	26.5[26.2–26.9]	0.03/0.9	25.4[25.2–25.7]	0.36/0.3	32.2[31.6–32.8]	0.15/3.1
	CC	27.0[26.2–27.9]		25.4[24.7–26.1]		33.2[32.0–34.4]	
	TT	26.1[25.7–26.4]		25.2[24.9–25.4]		32.9[32.1–33.8]	
+8855	TA	26.5[26.2–26.9]	0.04/0.9	25.4[25.1–25.7]	0.38/0.3	32.2[31.6–32.8]	0.16/2.9
	AA	27.0[26.2–27.9]		25.4[24.7–26.1]		33.2[32.0–34.4]	
	AA	25.9[25.5–26.3]		25.1[24.8–25.4]		32.7[31.7–33.7]	
+11015	AC	26.4[26.0–26.8]	0.003/1.5	25.4[25.1–25.7]	0.36/0.3	32.0[31.5–32.5]	0.03/5.8
	CC	27.2[26.5–27.8]		25.5[25.0–26.0]		33.5[32.4–34.6]	

Table 6.31: Geometric mean BMI[95% CI] (kg/m^2) by *IL18* genotype in cases and controls in SCARF.

tSNP		Geometric mean BMI[95% CI] (kg/m^2) Controls (n=387)	p/R^2	Cases (n=387)	p/R^2
	GG	25.5[25.0–25.9]		26.4[25.8–27.0]	
-9731	GT	25.7[25.3–26.2]	0.33/0.6	27.2[26.7–27.7]	0.006/2.8
	TT	26.2[25.3–27.1]		28.2[27.2–29.2]	
	TT	25.6[25.1–26.2]		27.8[27.1–28.5]	
-5848	TC	25.7[25.3–26.2]	0.98/<0.1	26.7[26.2–27.2]	0.02/2.0
	CC	25.7[24.9–26.6]		26.6[25.7–27.6]	
	AA	25.5[25.0–25.9]		26.6[26.1–27.2]	
+105	AC	25.8[25.4–26.3]	0.39/0.5	27.3[26.8–27.9]	0.09/1.3
	CC	26.1[24.7–27.5]		27.8[26.7–29.0]	
	TT	25.5[25.0–25.9]		26.6[26.1–27.2]	
+8855	TA	25.8[25.4–26.3]	0.44/0.4	27.3[26.8–27.9]	0.09/1.3
	AA	26.1[24.7–27.5]		27.8[26.7–29.0]	
	AA	25.6[25.1–26.1]		26.2[25.6–26.8]	
+11015	AC	25.6[25.2–26.0]	0.24/0.8	27.4[26.9–28.0]	0.004/3.0
	CC	26.3[25.4–27.3]		27.8[26.9–28.7]	

Table 6.32: Results from multivariate analysis with *IL18* tSNPs and BMI in SCARF.

IL18 SNP	Model 1 Sex and age	Model 2 Model 1 + smoking	Model 3 Model 2 + IL-6	Model 4 Model 3 + CRP
-9731	0.001	0.003	0.001	0.003
-5848	0.22	0.27	0.13	0.09
+105	0.04	0.04	0.03	0.04
+8855	0.04	0.05	0.04	0.04
+11015	0.003	0.006	0.002	0.003

with those homozygous for hTTATC estimated to have a BMI 8.1% higher than those homozygous for hGCATA.

Multivariate Analysis *IL18* haplotypes remained globally associated with BMI in all multivariate models (p=0.02 in model 4, see table 6.35 on page 251). The association with hTTCAC remained in all four models (p=0.01 in model 4) whilst that with hTTATC is significantly attenuated in model 4 and was only borderline significantly associated with BMI (p=0.02). Therefore, despite IL-6 and CRP being strongly correlated with BMI (ρ=0.29, p<0.001 and ρ=0.33, p<0.001, respectively), variation in *IL18* remained associated with BMI, thereby suggesting a novel pathway independent of these inflammatory mediators.

6.4 UDACS

The University College London Diabetes and Cardiovascular Study (UDACS) consists of 1011 consecutive multiethnic patients recruited from the diabetes clinic at University College London Hospitals National Health Service Trust between the years 2001 and 2002 [Dhamrait et al., 2004; Stephens et al., 2004]. All participants had diabetes according to WHO criteria [Alberti and Zimmet, 1998]. Ethical approval was granted by the institutional ethical committee and written informed consent was obtained before recruitment. Data on BMI was collected for 994 individuals, and this cohort is the basis for data analysis in this section. IL-18 levels were not measured in UDACS and therefore the study was not suitable for previous chapters.

6.4.1 Baseline Characteristics

UDACS is a multiethnic cohort including individuals of African, Caucasian, Indian and Oriental origin. Numerous baseline characteristics, including BMI, differed between the ethnic groups (see table 6.36 on page 252). The genotype distribution of *IL18*-9731, -5848 and +11015 also differed significantly across the genotype ethnic groups (see table 6.37 on page 253), as did the frequency of common haplotypes (see figure 6.14 on page 251).

6.4.2 *IL18*'s Association with Obesity Risk

6.4.2.1 Single SNP Analysis

No *IL18* genotype was seen at significantly different frequencies between obese and non-obese individuals (see table 6.38 on page 254).

Table 6.33: *IL18* haplotype frequencies in obese and non-obese individuals within SCARF.

Haplotype		Total	Frequency (%) Non-obese (n=260)	Obese (n=87)	OR[95% CI]	p
hGCATA	h12111	33.1	34.3	27.4	1	—
hTTCAC	h21222	29.7	28.7	35.2	1.40[1.01–1.95]	0.04
hGTATA	h11111	22.7	23.4	19.4	0.96[0.65–1.41]	0.84
hTTATC	h21112	9.2	8.9	11.2	1.42[0.90–2.26]	0.13

Table 6.34: Geometric mean BMI[95% CI] (kg/m^2) by *IL18* haplotype in cases and controls in SCARF.

Haplotype		Total	p/R^2	Haplotypic mean lnBMI[95% CI] Controls (n=387)	p/R^2	Cases (n=387)	p/R^2
hGCATA	h12111	1.631[1.620–1.641]	Ref	1.624[1.611–1.637]	Ref	1.635[1.621–1.650]	Ref
hTTCAC	h21222	1.650[1.639–1.661]	0.02	1.631[1.617–1.646]	0.51	1.667[1.650–1.684]	0.01
hGTATA	h11111	1.622[1.609–1.635]	0.35	1.612[1.595–1.630]	0.34	1.638[1.619–1.657]	0.83
hTTATC	h21112	1.651[1.632–1.669]	0.07	1.624[1.598–1.651]	0.99	1.674[1.647–1.701]	0.01
	Global p/R^2		0.02/1.6		0.63/0.7		0.02/2.9

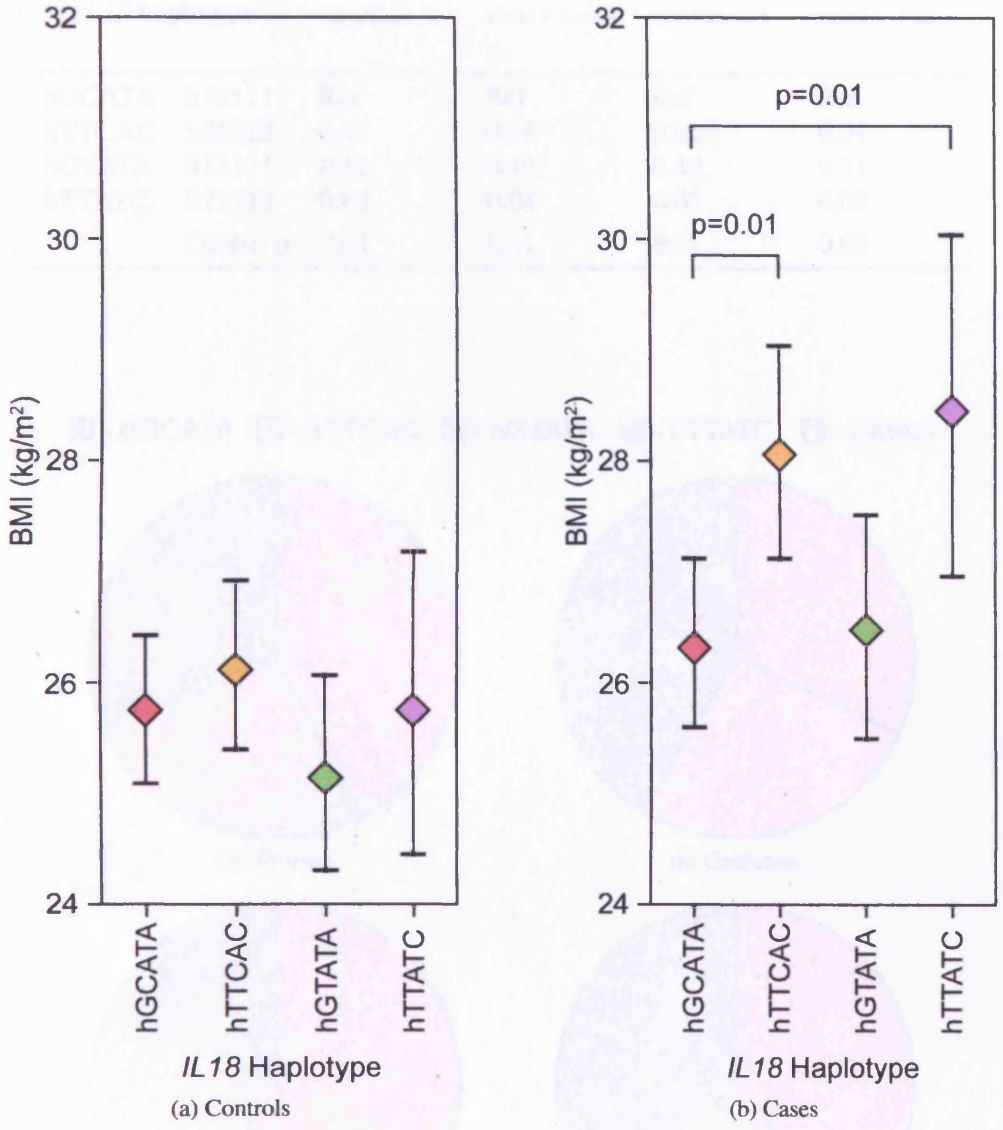

Figure 6.13: Estimated homozygote mean BMI[95% CI] by *IL18* haplotype in both cases and controls within SCARF.

Table 6.35: Results from multivariate analysis with *IL18* haplotypes and BMI in SCARF.

IL18 haplotype		Model 1 Sex and age	Model 2 Model 1 + smoking	Model 3 Model 2 + IL-6	Model 4 Model 3 + CRP
hGCATA	h12111	Ref	Ref	Ref	Ref
hTTCAC	h21222	0.01	0.01	0.01	0.01
hGTATA	h11111	0.52	0.49	0.49	0.71
hTTATC	h21112	0.04	0.04	0.05	0.07
	Global p	0.01	0.01	0.01	0.02

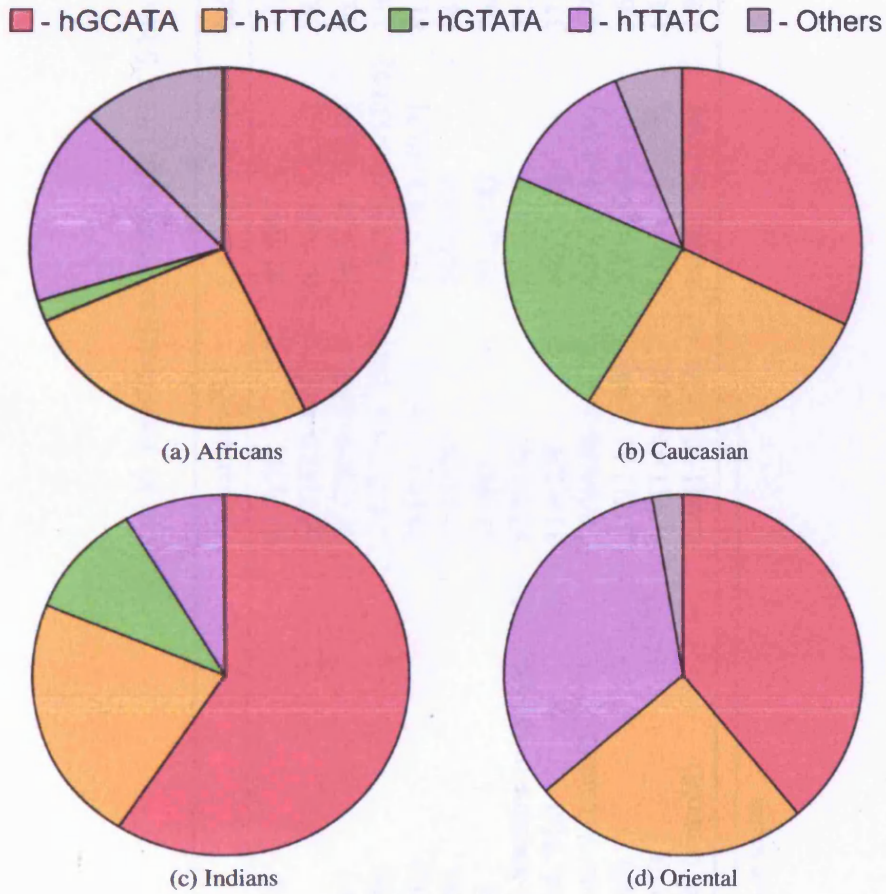

Figure 6.14: Common european *IL18* haplotype frequencies by ethnicity in UDACS.

Table 6.36: Baseline characteristics in UDACS by ethnic group

Variable	African (n=79)	Caucasian (n=786)	Indian (n=111)	Oriental (n=18)	p
Males, %[n]	63.3[50]	60.3[471]	73.9[82]	66.7[12]	0.05
Age (yr)	59.7[57.0–62.4]	62.5[61.5–63.4]	58.9[56.9–61.0]	58.8[55.0–62.6]	0.002
BMI (kg/m^2)	27.7[26.6–28.9]	28.5[28.1–28.9]	26.5[25.7–27.2]	26.3[24.5–28.2]	0.001
SBP (mmHg)	136.7[131.8–141.8]	138.5[137.1–139.9]	136.8[133.1–140.6]	131.1[125.0–137.6]	0.34
DBP (mmHg)	83.0[80.3–85.7]	79.5[78.7–80.3]	81.1[79.1–83.1]	75.2[70.9–79.7]	0.01
TIIDM, %[n]	91.1[72]	74.9[589]	94.6[105]	94.4[17]	<0.001
CHD[1] %[n]	11.4[9]	20.2[158]	26.4[29]	16.7[3]	0.09
Cholesterol-lowering medication, %[n]	17.9[14]	26.8[209]	27.3[30]	50.0[9]	0.04
Ever smoked, %[n]	31.6[25]	49.9[385]	37.0[40]	55.6[10]	0.002
Total cholesterol (mmol/l)	5.10[4.88–5.32]	5.01[4.94–5.09]	4.79[4.58–5.00]	4.88[4.46–5.32]	0.14
LDL (mmol/l)	2.75[2.55–2.97]	2.72[2.66–2.79]	2.65[2.44–2.87]	2.69[2.29–3.13]	0.87
HDL (mmol/l)	1.50[1.41–1.60]	1.36[1.33–1.39]	1.14[1.08–1.21]	1.18[1.07–1.30]	<0.001
Triglycerides (mmol/l)	2.28[1.72–3.02]	3.05[2.78–3.34]	4.20[3.37–5.25]	5.01[3.15–7.99]	0.001

[1]History of MI or angina

Table 6.37: *IL18* tSNP genotype frequencies across ethnic groups in UDACS.

tSNP an completeness of genotyping (%)		African (n=79) %[n]	HWE p	Caucasian (n=786) %[n]	HWE p	Indian (n=111) %[n]	HWE p	Oriental (n=18) %[n]	HWE p	χ^2 p
	GG	31.6[24]		32.9[251]		47.6[50]		11.1[2]		
-9731 (96.8)	GT	48.7[37]	0.91	50.3[384]	0.36	43.8[46]	0.73	55.6[10]	0.47	0.008
	TT	19.7[15]		16.8[128]		8.6[9]		33.3[6]		
	TT	32.9[25]		39.2[296]		17.0[18]		33.3[6]		
-5848 (96.2)	TC	39.5[30]	0.07	46.4[351]	0.76	48.1[51]	0.95	50.0[9]	0.90	<0.001
	CC	27.6[21]		14.4[109]		34.9[37]		16.7[3]		
	AA	55.3[42]		48.7[368]		61.7[66]		50.0[9]		
+105 (96.3)	AC	36.8[28]	0.66	41.9[317]	0.82	31.8[34]	0.37	50.0[9]	0.16	0.17
	CC	7.9[6]		9.4[71]		6.5[7]		—		
	TT	55.3[42]		48.7[370]		62.6[67]		50.0[9]		
+8855 (96.7)	TA	35.5[27]	0.39	42.1[320]	0.95	30.8[33]	0.30	50.0[9]	0.16	0.12
	AA	9.2[7]		9.2[70]		6.5[7]		—		
	AA	24.0[18]		31.5[240]		47.7[52]		16.7[3]		
+11015 (96.9)	AC	42.7[32]	0.23	50.7[386]	0.35	44.0[48]	0.65	50.0[9]	0.90	<0.001
	CC	33.3[25]		17.7[135]		8.3[9]		33.3[6]		

Table 6.38: *IL18* tSNP genotype frequencies in obese and non-obese individuals, and RR[95% CI] for obesity, in UDACS (all ethnic groups).

tSNP		%[n] Non-Obese (n=320)	Obese (n=100)	χ^2 p	RR[95% CI]	p
	GG	34.2[217]	33.5[110]		1	—
-9731	GT	49.7[315]	49.4[162]	0.92	1.01[0.83–1.23]	0.92
	TT	16.1[102]	17.1[56]		1.05[0.81–1.37]	0.70
	TT	34.3[216]	39.4[129]		1	—
-5848	TC	47.4[298]	43.7[143]	0.30	0.87[0.72–1.05]	0.15
	CC	18.3[115]	16.8[55]		0.87[0.67–1.12]	0.26
	AA	51.4[325]	49.2[160]		1	—
+105	AC	39.2[248]	43.1[140]	0.44	1.09[0.91–1.31]	0.34
	CC	9.3[59]	7.7[25]		0.90[0.63–1.28]	0.56
	TT	51.7[327]	49.1[161]		1	—
+8855	TA	39.0[247]	43.3[142]	0.37	1.11[0.92–1.33]	0.28
	AA	9.3[59]	7.6[25]		0.90[0.63–1.28]	0.56
	AA	32.8[208]	32.0[105]		1	—
+11015	AC	49.6[315]	48.8[160]	0.84	1.00[0.82–1.23]	0.97
	CC	17.6[112]	19.2[63]		1.07[0.83–1.38]	0.58

6.4.2.2 Haplotype Analysis

To avoid any confounding or bias caused by the substantial differences in haplotype frequency between the ethnic groups (see figure 6.14 on page 251), all haplotype analysis in UDACS was limited to Caucasians. *IL18* haplotype frequencies were not seen at significantly different frequencies between obese and non-obese individuals (see table 6.39 on the following page).

6.4.3 *IL18* Genetic Variation and BMI

6.4.3.1 Single SNP Analysis

Univariate Analysis As shown in table 6.40 on page 256, only *IL18*-9731 G>T was associated with significant differences in BMI, with the common allele being associated with higher BMI (p=0.007), however this association was seen only in the non-obese individuals.

As the effect of *IL18* variation on BMI appeared to be influenced by underlying disease, the association of the *IL18* tSNPs were also studied in those with and without TIIDM (see table 6.41 on page 257). *IL18*-5848 T>C was borderline significantly associated with differences in BMI (p=0.07) showing an additive effect.

Table 6.39: *IL18* tSNP haplotype frequencies in obese and non-obese individuals, and OR[95% CI] for obesity, in UDACS (Caucasians only).

Haplotype		Frequency (%) Total	Non-obese (n=260)	Obese (n=87)	OR[95% CI]	p
hGCATA	h12111	32.1	33.0	30.6	1	—
hTTCAC	h21222	26.8	27.0	26.5	1.06[0.81–1.38]	0.67
hGTATA	h11111	22.3	21.8	23.1	1.14[0.86–1.50]	0.37
hTTATC	h21112	12.5	11.8	13.8	1.24[0.89–1.73]	0.20

Table 6.40: Geometric mean BMI[95% CI] by *IL18* tSNP genotype in obese and non-obese individuals in UDACS (all ethnic groups).

tSNP		Geometric mean BMI[95% CI] (kg/m^2) Total	p/R^2	Non-Obese (n=320)	p/R^2	Obese (n=100)	p/R^2
	GG	28.2[27.7–28.8]		25.7[25.3–26.0]		34.1[33.3–35.0]	
-9731	GT	28.3[27.8–28.8]	0.29/0.3	25.5[25.1–25.8]	0.007/1.6	34.6[33.9–35.3]	0.51/0.4
	TT	27.5[26.7–28.4]		24.5[23.9–25.2]		34.0[33.0–35.0]	
	TT	28.4[27.8–28.9]		25.3[24.8–25.7]		34.4[33.8–35.1]	
-5848	TC	28.1[27.6–28.6]	0.55/0.1	25.4[25.0–25.8]	0.68/0.1	34.7[33.9–35.5]	0.09/1.5
	CC	27.8[27.1–28.5]		25.6[25.0–26.1]		33.2[32.1–34.4]	
	AA	28.2[27.7–28.6]		25.6[25.3–25.9]		34.2[33.5–34.9]	
+105	AC	28.3[27.7–28.8]	0.29/0.3	25.2[24.8–25.6]	0.15/0.6	34.7[33.9–35.5]	0.48/0.5
	CC	27.3[26.1–28.5]		25.0[24.0–26.0]		33.7[32.4–35.0]	
	TT	28.2[27.7–28.6]		25.6[25.3–25.9]		34.2[33.6–34.9]	
+8855	TA	28.3[27.7–28.9]	0.34/0.2	25.2[24.8–25.6]	0.16/0.6	34.7[33.9–35.4]	0.51/0.4
	AA	27.4[26.2–28.5]		25.1[24.1–26.1]		33.7[32.4–35.0]	
	AA	28.3[27.7–28.9]		25.6[25.2–26.0]		34.5[33.6–35.5]	
+11015	AC	28.2[27.7–28.6]	0.79/<0.1	25.4[25.1–25.8]	0.19/0.5	34.4[33.8–35.1]	0.91/0.1
	CC	27.9[27.1–28.8]		24.9[24.3–25.6]		34.2[33.2–35.2]	

Table 6.41: Geometric mean BMI[95% CI] by *IL18* tSNP genotype in in those with and without TIIDM in UDACS (all ethnic groups).

tSNP		Geometric mean BMI[95% CI] (kg/m^2) No TIIDM (n=211)	p/R^2	TIIDM (n=783)	p/R^2
	GG	26.5[25.3–27.8]		28.7[28.2–29.4]	
-9731	GT	25.8[25.0–26.8]	0.58/0.5	28.9[28.4–29.5]	0.46/0.2
	TT	25.6[24.1–27.2]		28.2[27.2–29.3]	
	TT	25.7[24.8–26.7]		29.2[28.6–29.9]	
-5848	TC	25.8[24.8–26.8]	0.31/1.2	28.7[28.2–29.3]	0.07/0.7
	CC	27.3[25.1–29.6]		27.9[27.2–28.7]	
	AA	26.7[25.7–27.7]		28.6[28.1–29.1]	
+105	AC	25.5[24.5–26.6]	0.10/2.3	29.0[28.4–29.7]	0.35/0.3
	CC	24.6[22.4–27.0]		28.2[26.9–29.5]	
	TT	26.7[25.7–27.7]		28.6[28.1–29.1]	
+8855	TA	25.6[24.6–26.6]	0.16/1.8	29.1[28.4–29.7]	0.30/0.3
	AA	24.8[22.5–27.3]		28.2[26.9–29.5]	
	AA	26.9[25.7–28.2]		28.7[28.0–29.3]	
+11015	AC	25.5[24.6–26.4]	0.17/1.8	28.9[28.3–29.4]	0.84/<0.1
	CC	25.7[24.1–27.4]		28.6[27.7–29.6]	

Multivariate Analysis Four different models were used in multivariate analysis:

Model 1 Sex and age

Model 2 Sex, age, and smoking

Model 3 Sex, age, smoking and IL-6

Model 4 Sex, age, smoking, IL-6, and CRP

Multivariate analysis was limited to those in UDACS who had TIIDM. As shown in table 6.42 on the next page, the association between *IL18*-5848 and BMI remained significant in both model 1 and 2, but was significantly attenuated when BMI was further adjusted for IL-6 and CRP.

6.4.3.2 Haplotype Analysis

Univariate Analysis *IL18* haplotypes were significantly associated with significant differences in BMI but in non-obese individuals only (see table 6.43 on page 259), with this effect most likely attributable to hTTCAC alone – the only haplotype significantly associated with differences in BMI (p=0.006). This association was such that those non-obese Caucasians homozygous for hTTCAC were estimated to have a mean BMI[95%

Table 6.42: Results from multivariate analysis of *IL18* tSNPs and BMI in those with TIIDM in UDACS.

IL18 SNP	Model 1 Sex and age	Model 2 Model 1 + smoking	Model 3 Model 2 + IL-6	Model 4 Model 3 + CRP
-9731	0.45	0.53	0.49	0.41
-5848	0.04	0.04	0.09	0.11
+105	0.28	0.33	0.25	0.27
+8855	0.25	0.29	0.23	0.26
+11015	0.76	0.79	0.86	0.84

CI] of 24.5[24.0–25.1]kg/m^2, which was 95% of that estimated for homozygotes of hGCATA (25.8[25.2–26.4]kg/m^2).

When UDACS was divided into those with and without TIIDM, *IL18* haplotypes were no longer globally associated with BMI (see table 6.44 on the next page). In this analysis, hTTCAC remained associated with lower BMI but only in those individuals who did not suffer from TIIDM (p=0.05). In those with TIIDM, hGTATA was associated with significantly higher BMI, such that those homozygote for hGTATA were estimated to have mean BMI of 31.0 kg/m^2 compared to 28.8 kg/m^2 for those homozygote for hGCATA (see figure 6.15 on page 260).

Multivariate Analysis The association between hGTATA and BMI was no longer significant in multivariate analysis (see table 6.45 on page 262). Adjustment for age alone was sufficient to significantly attenuate the association (p=0.11), despite not being significantly correlated with BMI (ρ=-0.04, p=0.33).

6.5 Discussion

The results from this chapter suggest that, although variation within *IL18* is not associated with CHD initiation, it appears to influence plaque development. The *IL18* tSNP set was also associated with significant differences in BMI and therefore implies a causal role for IL-18 in weight control. However, there was no evidence that *IL18BP* had any role in these conditions, and furthermore there was no evidence of interactions/epistasis between the two genes. A summary of the *IL18* results are shown in figure 6.16 on page 261, and it serves to illustrate the inconsistent nature of the associations found across all study groups.

Chapter 5, details an association between elevated IL-18 levels and risk of a major complication following CPB surgery. Despite genetic variants in *IL18* being associated

Table 6.43: Geometric mean lnBMI[95% CI] by *IL18* tSNP haplotype in obese and non-obese individuals in UDACS (Caucasians only).

Haplotype		Total	p/R^2	Haplotypic mean lnBMI[95% CI] Non-obese (n=260)	p/R^2	Obese (n=87)	p/R^2
hGCATA	h12111	1.672[1.657–1.687]	Ref	1.625[1.613–1.637]	Ref	1.766[1.749–1.782]	Ref
hTTCAC	h21222	1.662[1.646–1.679]	0.46	1.600[1.588–1.611]	0.006	1.775[1.753–1.797]	0.56
hGTATA	h11111	1.693[1.673–1.712]	0.14	1.632[1.614–1.651]	0.56	1.785[1.764–1.806]	0.19
hTTATC	h21112	1.678[1.651–1.705]	0.71	1.620[1.599–1.641]	0.68	1.749[1.715–1.783]	0.39
	Global p/R^2		0.32/0.6		0.04/2.0		0.38/1.5

Table 6.44: Geometric mean lnBMI[95% CI] by *IL18* tSNP haplotype in those with and without TIIDM in UDACS (Caucasians only).

Haplotype		Haplotypic mean lnBMI[95% CI] No TIIDM (n=197)	p/R^2	TIIDM (n=589)	p/R^2
hGCATA	h12111	1.646[1.622–1.669]	Ref	1.680[1.662–1.698]	Ref
hTTCAC	h21222	1.602[1.567–1.637]	0.05	1.682[1.663–1.700]	0.89
hGTATA	h11111	1.631[1.587–1.675]	0.59	1.717[1.694–1.740]	0.02
hTTATC	h21112	1.646[1.578–1.714]	0.99	1.686[1.658–1.714]	0.74
	Global p/R^2		0.42/2.1		0.12/1.3

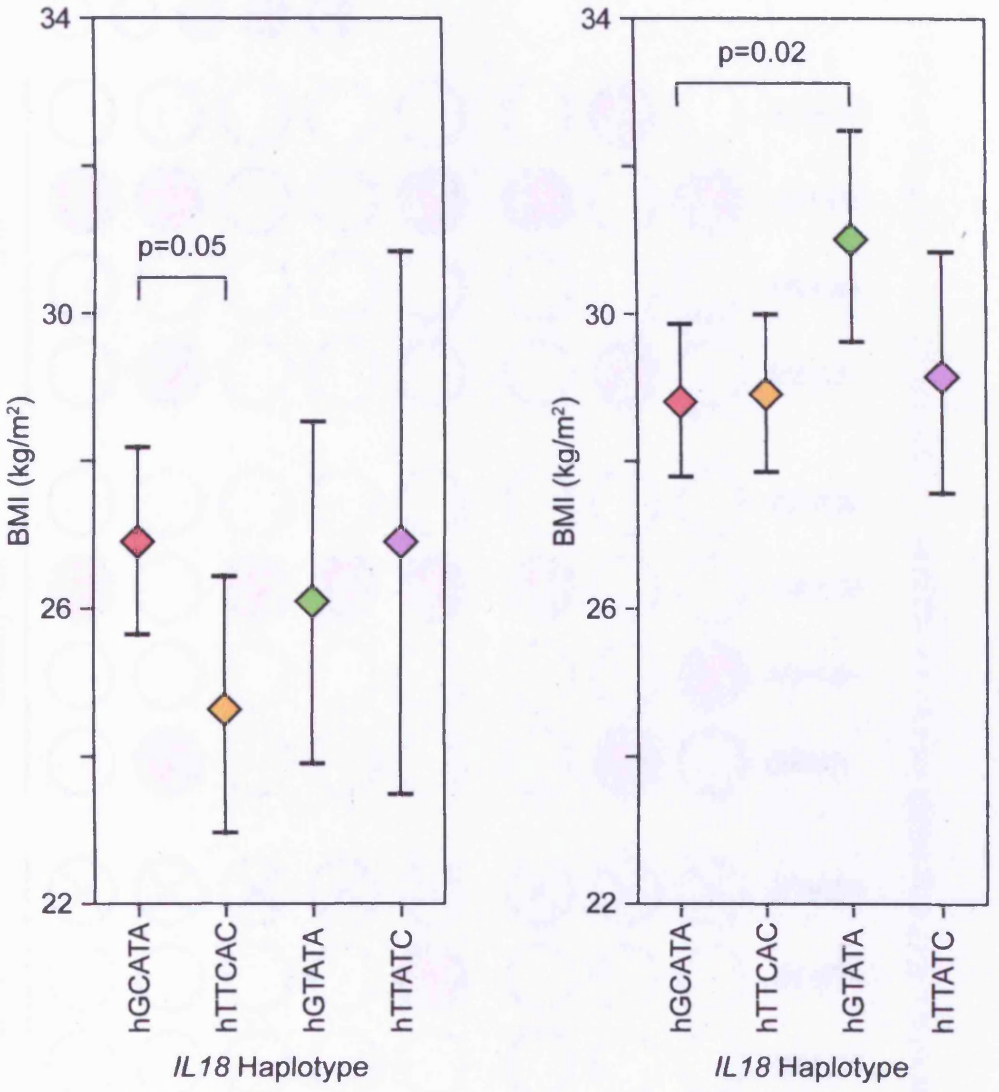

Figure 6.15: Estimated mean BMI[95% CI] for homozygotes of *IL18* haplotypes in those with and those without TIIDM in UDACS.

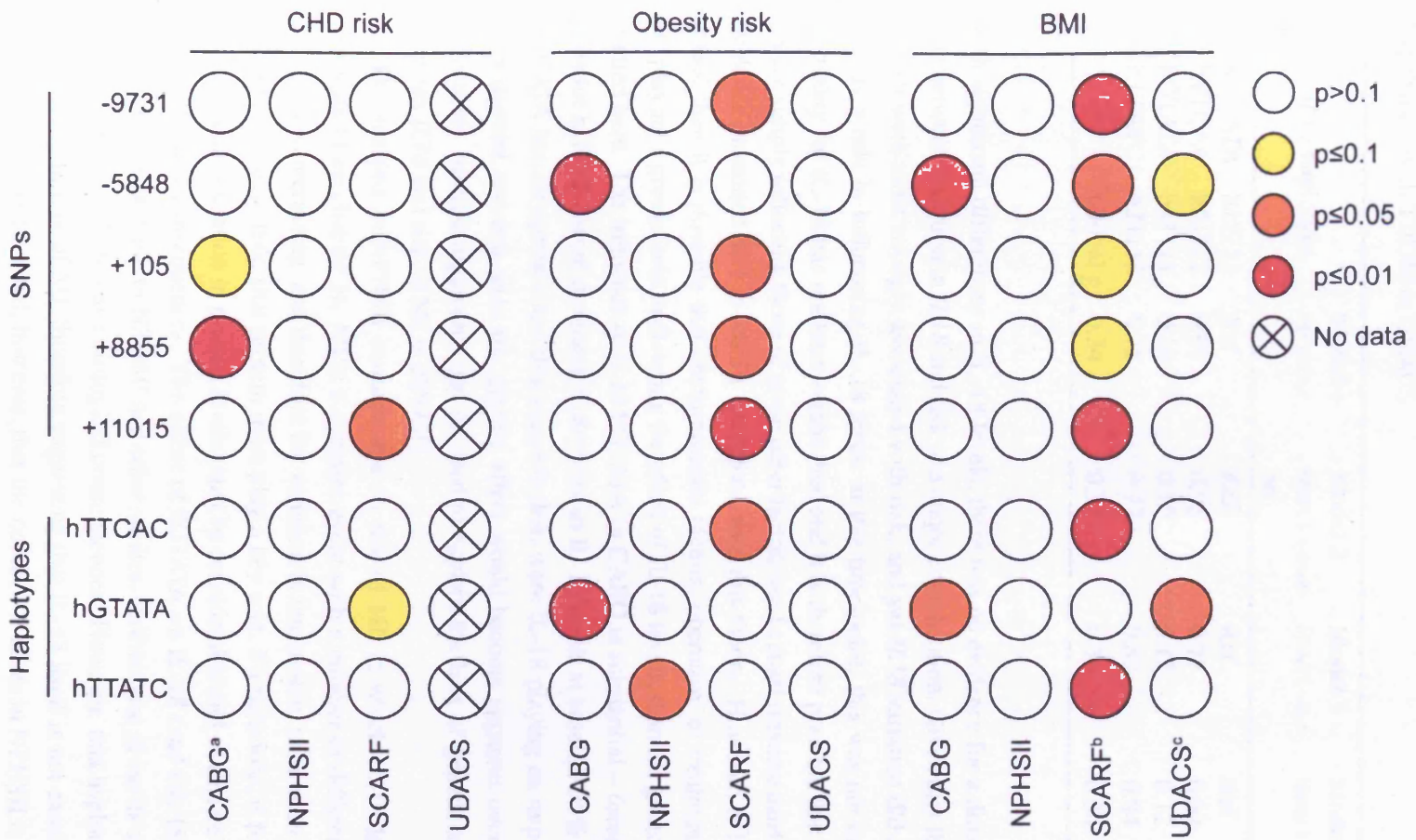

Figure 6.16: Graphical summary of the *IL18* association results; a – outcome is major complication following surgery; b – cases only; c – individuals with TIIDM only.

Table 6.45: Results from multivariate analysis with *IL18* haplotypes and BMI in those Caucasians with TIIDM in UDACS.

IL18 haplotype		Model 1 Sex and age	Model 2 Model 1 + smoking	Model 3 Model 2 + IL-6	Model 4 Model 3 + CRP
hGCATA	h12111	Ref	Ref	Ref	Ref
hTTCAC	h21222	0.90	0.92	0.77	0.69
hGTATA	h11111	0.10	0.10	0.12	0.12
hTTATC	h21112	0.75	0.77	0.89	0.84
	Global p	0.34	0.33	0.35	0.34

with significant differences in IL-18 levels, there was no evidence for a direct association between variation in *IL18* and risk of a major complication. Given that IL-18 levels at 24 h were most strongly associated with risk, and yet *IL18* variation did not appear to play a role in influencing IL-18 levels at this time-point, this was not unexpected. Causality for IL-18 has not been established and it is therefore possible that IL-18 levels are simply reflecting those of some other factor, itself causal (reverse causality). The evidence presented here is wholly compliant with this theory. However, if IL-18 were causal then it is possible that environmental factors, operative, or treatment regimen, are playing a greater role in dictating the effect of IL-18 levels, than the genetic variants studied here. The influence of *IL18* hGTATA in CABG is substantial – those homozygous for hGTATA were estimated to have mean IL-18 levels at baseline 35% of that for hGCATA homozygotes – and this suggests that, were IL-18 playing an important role in post-event survival, then the genetic effect would become apparent over the other influences. Similar arguments can be used to explain the lack of genetic association between *IL18* and risk of MI in NPHSII.

The analysis in NPHSII concentrated on risk of MI, in which IL-18 levels were implicated (see chapter 5). MI is a complex event with a number of different biological systems interacting, and therefore for variation in one protein to have an impact on individual disease risk, that protein must play a key role. Furthermore, it follows that the individual variation in protein levels must be considerable and of a scale that could have biological consequences. The effect of hGTATA on IL-18 (and fIL-18) does appear to be considerable in NPHSII and other studies, furthermore given its association with BMI it is likely to have biological consequences. However, this haplotype is not associated with risk of MI, therefore suggesting that IL-18 itself is not causal in CHD initiation. It must be noted, however, that the number of cases in NPHSII is relatively small and therefore any small increases/decreases in risk caused by genetic variants would not be detectable because of low power. Further analysis in a larger prospective

study with a greater number of events is required.

Analysis in SCARF revealed that, despite allele frequencies not differing between cases and controls, a number of SNPs were associated with significant differences in normalized plaque area. Most importantly, the only SNP found to be associated with differences in IL-18 levels (*IL18*-5848 T>C) was also associated with borderline significant differences in normalized plaque area (p=0.05). However, the association seems slightly counterintuitive, with the C allele, associated with higher IL-18 levels, being associated with smaller plaque area. With regard to haplotypes, both hTTCAC and hGTATA were associated with significant differences in IL-18 levels when compared to hGCATA. However, of these only hTTCAC was associated with significantly different normalized plaque area. The haplotype results match those of the single SNP analysis, with hTTCAC being associated with lower IL-18 levels, but higher normalized plaque area.

The extent of disease in SCARF was assessed by quantitative coronary angiography, a procedure that assesses the area of plaque that encroaches above the vessel line, a significant proportion of which will be made up of the fibrous cap. As detailed in section 1.4.1.2 on page 47, IL-18 has been implicated in plaque stability. IFNγ, the major downstream of IL-18 activation, has been shown to decrease collagen and ECM synthesis, as well as SMC proliferation [Amento et al., 1991; Yuan et al., 1999]. This, along with it's induction of MMP production [Schonbeck et al., 1997] and SMC apoptosis [Geng et al., 1996] leads to an overall thinning of the fibrous cap, a process that would lead to an decrease in plaque stability but perhaps also a decrease in plaque area, when assessed by coronary angiography. Therefore, in the context of the genetic effects described here, a decrease in IL-18 would also lead to a decrease in IFNγ, resulting in a thickening of the fibrous cap and therefore an overall increase in plaque area (when assessed by coronary angiography). That hGTATA, the haplotype most commonly associated with lower IL-18 levels, was not associated with plaque area may be due to a difference in the cells involved. The genetic effect of this haplotype is likely to differ between the different IL-18-producing cells, and it is possible that those cells responsible for systemic IL-18 production are either not the same type, or not in the same state, as those responsible for IL-18 production within the plaque. Indeed IL-18 expression has been observed in SMC within the plaque [Mallat et al., 2001a] and may be responsible for IL-18 production within the fibrous cap, and it is therefore likely that *IL18* is regulated differently in these cells and that the effect of hGTATA may not be present.

In multivariate analysis, with both IL-6 and CRP included as covariates, the effects of hTTCAC were significantly attenuated but remained borderline significant (p=0.06) in the full model (sex, age, smoking status, DBP, IL-6, and CRP as covariates), whilst the association with hTTATC remained highly significant (p=0.005). Indeed, *IL18* haplotypes remained globally associated with normalized plaque area, suggesting that this

Table 6.46: Results from WTCCC GWA study using CHD cohort and those SNPs occurring within the *IL18* region considered here. P values quoted are frequentist p-values for both an additive (add) and a general (gen) model. Data accessed through www.wtccc.org.uk in May 2008.

SNP	rs number	p (add)	p (gen)
-8963 G>T	rs360718	0.48	0.56
-927 C>T	rs360722	0.48	0.57
+1949 G>C	rs1834481	0.15	0.36
+8855 T>A	rs360729	0.89	0.90

effect of IL-18 is independent of other inflammatory processes and pathways. Therefore, from the data presented here, it appears that IL-18 is not causal in atherogenesis *per se*, but may be a factor that determines overall plaque stability. However, this is a hypothesis built on data from only one study and therefore needs replication and further investigation.

The increasing efficiency of large-scale genotyping has led to a rise in the number of genome-wide association (GWA) studies being conducted in recent years, and they have been shown to be a powerful approach in identifying genes involved in human disease. One recent study was carried out using the Wellcome Trust Case Control Consortium (WTCCC) population, representing 2000 cases and 3000 shared controls for seven complex human diseases of major public health importance, including CHD [WTCCC, 2007]. All data has been released freely through their website. In total, four SNPs within *IL18* were genotyped, none of which returned significant p values in case-control analysis using the CHD cohort (see table 6.46), or any of the other disease cohorts (data not shown). None of these SNPs were in sufficiently high LD with -5848 T>C to mark hGTATA, and therefore do not serve to represent the major genetic effect seen here.

GWA studies are of potentially great use in both identifying new potentially causal variants and replicating previous results, and it is likely that GWA will become the main genetic association analysis methodology replacing the single SNP/tSNP methods used here. However, much work remains to make the most of the available data. Establishing methodologies for assessing both epistatic and haplotypic effects will be important steps forward, as will be an agreed standardization of analysis to account for the intrinsic risk of type I error.

Publication of data from $il18^{-/-}$ mice has suggested that IL-18 may also play an important role in weight control [Netea et al., 2006]. Data presented here is the first to suggest a causal role for IL-18 in determining weight gain, possibly through influencing feeding behaviour. In CABG, SCARF cases, and those in UDACS with TIIDM, *IL18*-

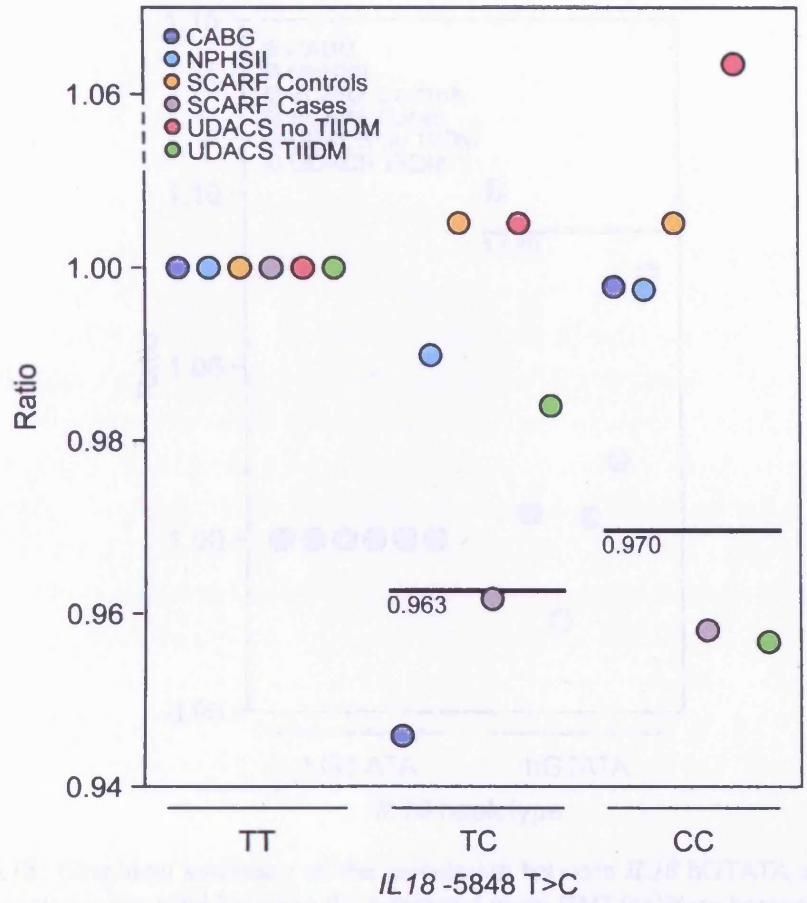

Figure 6.17: Graphical summary of the association between *IL18*-5848 T>C and BMI. Data is ratio of mean BMI of TT genotype group compared to TC and CC group. Line represents average ratio of those studies that showed significant results (CABG, SCARF cases, and UDACS individuals with TIIDM).

5848 T>C was associated with significant differences in BMI. However, as shown in figure 6.17, the pattern is not a straightforward additive/co-dominant effect. In these groups, those heterozygous at -5848 had, on average, 3.7% lower BMI, whilst those who were CC homozygous had 3.0% lower BMI, than TT homozygotes. This lack of additivity could be explained by a dominant or recessive effect, yet in each of the studies the genotype pattern was different. In SCARF cases, the genotype pattern appears dominant, with C allele carriers having similar BMI whether homozygous or heterozygous; in CABG both homozygote groups have similar BMI, and the heterozygote group had lower BMI; in those UDACS participants with TIIDM, the genotype pattern appeared additive.

The different pattern for -5848 could be due to chance fluctuations in the small samples available, and the CIs for the TC and TT groups, in general, overlap. However

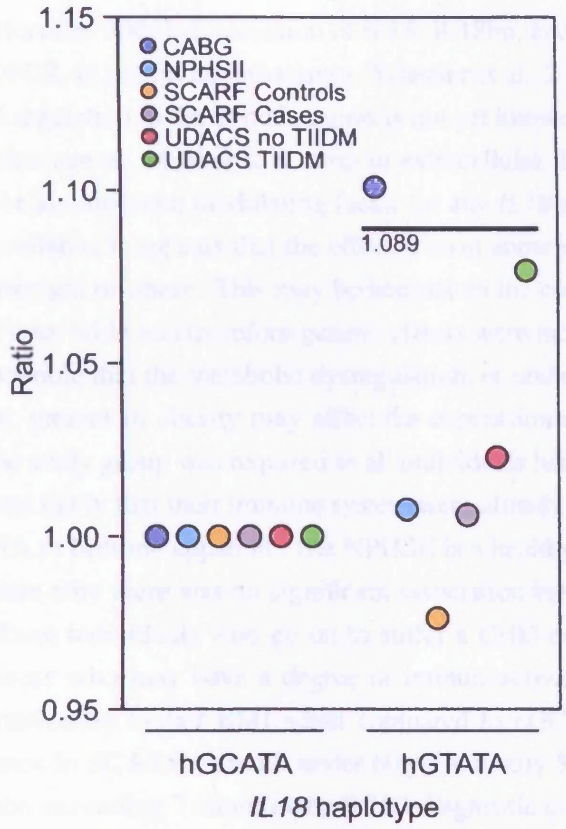

Figure 6.18: Graphical summary of the association between *IL18* hGTATA and BMI. Data presented is the ratio between the estimated mean BMI for those homozygote for both hGTATA and hGCATA, the reference haplotype. Line represents the average ratio for those studies in which the association was significant (CABG and those in UDACS who had TIIDM).

it could also be due to a more complex haplotypic effect; those homozygous for a single SNP are not necessarily homozygous for a haplotype. In both CABG and those in UDACS with TIIDM, *IL18* hGTATA was associated with significantly higher BMI when compared to hGCATA. As shown in figure 6.18 those homozygous for hGTATA within CABG and UDACS (Caucasians with TIIDM only), had, on average, BMI 9% higher than those homozygous for hGCATA. This equates to a 7 kg weight difference for an 1.75 m tall individual with a BMI of 25 kg/m^2.

The results presented in chapter 5 showed significant positive correlations between IL-18 (and fIL-18 in NPHSII) and BMI. However, there appeared no significant difference in IL-18 levels between those who were obese and those who were not. In the *il18*$^{-/-}$ mice, only intra-cerebral injection of IL-18 reversed the phenotype [Netea et al., 2006], therefore it can be assumed that local IL-18 production is most important, and also that the hypothalamus is the most likely target given its major role in regulating

hunger and thirst [Horvath, 2005]. Expression of il-18, il-18bp, and il-18 receptor has been detected, by QPCR, in the rat hypothalamus [Wheeler et al., 2000]. The nature of il-18 transcriptional regulation in the hypothalamus is not yet known, and neither is the nature of proil-18 cleavage ie. whether it is intra- or extracellular. Indeed, the activity of caspase-1 could be an important modulating factor for any *IL18*-associated effect.

From the data available, it appears that the effect is most apparent in those individuals who were overweight or obese. This may be because in the cohorts with a higher mean BMI, the CIs were wide and therefore genetic effects were more easily observed. Alternatively it is possible that the metabolic dysregulation, or underlying activation of the immune system, present in obesity may affect the expression of *IL18*. In CABG no subdivision of the study group was required as all individuals had advanced disease, and it therefore seems likely that their immune system were already activated, allowing the effect of hGTATA to become apparent. The NPHSII is a healthy cohort, and therefore this might explain why there was no significant association between hGTATA and BMI, although in those individuals who go on to suffer a CHD event during follow-up, and therefore those who may have a degree of immunoactivation, hGTATA was associated with significantly higher BMI when compared to hGCATA (p=0.02, data not shown). The cases in SCARF were all under 60 yr, and only 8.5% of these had a glucose concentration exceeding 7 mmol/l (the WHO diagnostic criteria for diabetes), whilst 15.9% of those in CABG were diabetic, and 12% had a glucose concentration exceeding 7 mmol/l. These observations, along with the substantial differences in BMI (SCARF cases – 26.4 kg/m^2 vs. CABG – 28.1 kg/m^2), suggests that there was greater metabolic dysregulation in CABG than in SCARF, and may explain why there was no observed effect of hGTATA on BMI.

In SCARF *IL18*-5848 T>C was associated with both normalized plaque area and BMI, but this did not translate into an association with hGTATA as it did in both CABG and UDACS. The T allele is carried by both hTTATC and hTTCAC, both of which are associated with significant differences in BMI and normalized plaque area (whilst only hTTCAC was associated with significant differences in IL-18 levels). This appears to suggest that the genetic effect in SCARF marked by -5848, is not the same as that in CABG and UDACS, but that it may mark a separate functional polymorphism that appears on the hTTCAC haplotype. The SCARF study group is a Swedish cohort, whilst the analysis in both CABG and UDACS was carried out in British Caucasians, therefore there could be genetic heterogeneity between the samples although this seems unlikely.

The associations seen between variation within *IL18* and BMI were largely unaffected by adjustment for numerous factors, including other inflammatory mediators, suggesting a degree of independence for IL-18's effect on weight control. However, the association between hGTATA and BMI in UDACS participants with TIIDM was no

longer significant following adjustment for age alone, the cause of this remains unclear as there appeared no obvious relationship between age and BMI, and age did not differ by *IL18* genotype (data not shown). In a minimal model with just IL-6 and CRP as covariates, hGTATA was borderline significantly associated (p=0.06) with BMI in UDACS participants with TIIDM.

Therefore, in summary, this data suggests that IL-18 does indeed play an important role in weight control in humans, independent of other inflammatory mediators. However, this effect does not become apparent until a degree of immunoactivation or metabolic dysregulation, is present. This effect requires further study to establish IL-18's exact role, its mode and site of action, and the nature of the requisite activation.

Chapter 7

The Frequency of *IL18* Haplotypes Across Africa

Data presented in chapter 6 showed there were considerable differences in SNP and haplotype frequency, between African and Caucasian groups (see figure 6.14 on page 251). The analysis in this chapter investigates the genotype distribution of the *IL18* tSNPs across Africa and attempts to establish the historic causes of any differences.

7.1 Introduction

7.1.1 EHH Test

Under neutral evolution, new variants require a long time to reach a high frequency in the population, and LD around the variants will decay substantially during this period owing to recombination. As a result, common alleles will most likely be old and only have short-range LD surrounding them. Rare variants will either be young or old and will therefore have short- or long-range LD surrounding them. A key characteristic of positive selection, however, is that it causes a rapid rise in frequency over a short time, so short that recombination does not substantially break down the haplotype on which the mutation occurred. This is the basis of the extended haplotype homozygosity (EHH) test. EHH is defined as the probability that two randomly chosen chromosomes carrying the core haplotype of interest are identical by descent (as shown by homozygosity at all SNPs) from the core region to point x. The EHH score can therefore be used to assess the degree of long-range LD on a specific allele [Sabeti et al., 2002].

Such a method has been implemented by Voight et al. [2006] in the web-based tool, Haplotter (http://hg-wen.uchicago.edu/selection/haplotter.htm), and this was used here to test for recent positive selection at each of the single SNPs. To test for recent positive selection at the haplotype level, scripts were developed by Krishna Veeramah at The UCL Centre for Genetic Anthropology, London.

7.1.2 Samples Used

The NPHSII study, with its samples collected from nine general practices across UK, was used as the European sample. Each practice was analysed as a sub-group in this chapter. DNA samples from males over 18 yr from locations in and around Africa (see table 7.1 on the following page and figure 7.1 on page 272) were grouped based on their cultural identity and, together with NPHSII, form the basis for the analyses presented here. All African samples were kindly provided by Drs Neil Bradman and Mark Thomas at The UCL Centre for Genetic Anthropology, London.

7.2 Sample Differentiation

7.2.1 Single SNP Analysis

Each of the *IL18* tSNPs were genotyped in the African samples with genotypes recorded for >88% of all samples (see table 7.2 on page 273). The number of samples that deviated from HWE (n=9, data not shown) were no more than that expected by chance alone.

To assess whether allele frequencies differed between the samples, an analysis of molecular variance (AMOVA) test was used, the results of which are shown in table 7.3 on page 275. Overall the amongst population variance decreased across all SNPs (except -9731) when analysis was restricted to sub-Saharan samples. An exact test for population differentiation (Raymond and Rousset's exact test [Raymond and Rousset, 1995]) was highly significant ($p<0.001$) for all single SNPs.

In each single SNP, principal co-ordinate analysis (PCO) (a representation of homogeneity between samples that uses F statistic matrices) showed few consistent patterns, although, as might be expected, the NPHSII samples were clustered tightly whilst the African samples were more diffusely scattered (see figure 7.2 on page 274).

7.2.2 Haplotype Analysis

The frequency of the four *IL18* haplotypes, studied in the previous chapters, in the African and NPHSII populations are shown in table 7.4 on page 276. There is considerable variation across the populations, with the most marked variations being in the frequency of hGTATA which ranges from 29% (in HARE, an NPHSII sub-sample), to <1% in 19 of the populations. Amongst-population variance in haplotype frequency was 2.56% when all samples were included and decreased to 2.28% when the NPHSII samples were excluded. Limiting analysis to sub-Saharan samples further reduced the variance to 1.36%. When using haplotype frequencies, Raymond and Rousset's exact test returned a p value <0.001, demonstrating that there is significant differentiation

Table 7.1: Summary of the African samples used, and the longitude and latitude of their collection point.

Population Code	Population	Place Collected	Longitude	Latitude
AF	Ethiopian Afar	Assaita (Asayita), Ethiopia	41°26′00″	11°34′00″
ALG-LN	Algerian Arabs	Port Say, Algeria	-2°14′00″	35°05′00″
ARB	Cameroonian Arabe	Kousseri, Cameroon	15°01′55″	12°04′33″
AT	Anatolian Turks	Ankara, Turkey	32°51′12″	39°55′45″
AYL	European	Aylesbury, England	-0°48′30″	51°48′57″
BAN	South African Bantu	Johannesburg, SA	28°03′01″	-26°08′39″
BBR	Moroccan Berbers	Ifrane, Morocco	-5°09′55″	33°35′17″
CAMB	European	Camberley, England	-0°44′34″	51°20′07″
CARN	European	Carnoustie, Scotland	-2°42′08″	56°30′11″
CHEST	European	Chesterfield, England	-1°25′18″	53°14′06″
EAM	Ethiopian Amhara	Mekane Selam, Ethiopia	38°09′00″	11°41′00″
EAN	Ethiopian Anuak	Gambela, Ethiopia	34°35′33″	8°14′36″
EOR	Ethiopian Oromo	Jimma, (Jima, Kefa), Ethiopia	36°49′51″	7°39′50″
GPN-BUL	Ghanaian Bulsa	Sandema, Ghana	-1°16′44″	10°43′34″
HALE	European	Halesworth, England	1°30′04″	52°20′35″
HARE	European	Harefield, England	-0°28′52″	51°36′10″
HAU	Cameroonian Hausa	Mayo Darle, Cameroon	11°33′05″	6°28′38″
IGB	Nigerian Igbo	Calabar, Nigeria	8°18′52″	4°57′26″
KAN	Cameroonian Kanuri	Waza, Cameroon	14°34′13″	11°24′06″
KOT	Cameroonian Kotoko	Makari, Cameroon	14°29′00″	12°35′00″
LBB	Zimbabwean Lemba	Mberengwa, Zim	29°54′50″	-20°28′48″
LOM	Malawian Lomwe	Lilongwe, Malawi	33°46′26″	-13°58′57″
MANJ	Senegalese Manjak	Dakar, Senegal	-17°27′07″	14°41′12″
MD	Cameroonian Fulbe	Mayo Darle, Cameroon	11°33′05″	6°28′38″
MLW	Malawian Chewa	Lilongwe, Malawi	33°46′26″	-13°58′57″
MP	Mozambican Mposi	Mposi, Zimbabwe	29°54′50″	-20°28′48″
NGO	Malawian Ngoni	Mangochi (Mangoche), Malawi	35°15′49″	-14°28′39″
NMY	European	North Mymms, England	-0°12′18″	51°43′16″
NSD	Northern Sudanese	Dunqulah, Sudan	30°28′27″	19°10′10″
PARK	European	Parkstone, England	-1°56′41″	50°43′13″
SA	Mozambican Sena	(Vila de) Sena, Mozambique	35°01′56″	-17°26′43″
SM	Mozambican Sena	(Vila de) Sena, Mozambique	35°01′56″	-17°26′43″
SOM	Cameroonian Mambila	Mayo Darle, Cameroon	11°33′05″	6°28′38″
SSD	Southern Sudanese	Bor, Sudan	31°34′02″	6°13′38″
STAN	European	St Andrews, Scotland	-2°47′51″	56°20′28″
TAN	Tanzanian Chagga	Dodoma, Tanzania	35°42′29″	-6°05′34″
TBK	Malawian Tumbuka	Mzuzu, Malawi	34°01′22″	-11°27′53″
UJW	Ugandan Ssese	Ssese Islands in Lake Victoria, Bujumba, Uganda used as focus	32°17′00″	-0°20′00″
YAM	Cameroonian Yamba	Mayo Darle, Cameroon	11°33′05″	6°28′38″
YAO	Malawian Yao	Mangochi (Mangoche), Malawi	35°15′49″	-14°28′39″
YMH	Yemeni	Al Mukalla, Yemen	49°07′38″	14°32′37″
YMS	Yemeni	Sena (Sanaa), Yemen	44°14′31″	15°24′31″
ZIM	Zimbabwean	Harare, Zimbabwe	31°03′14″	-17°49′45″

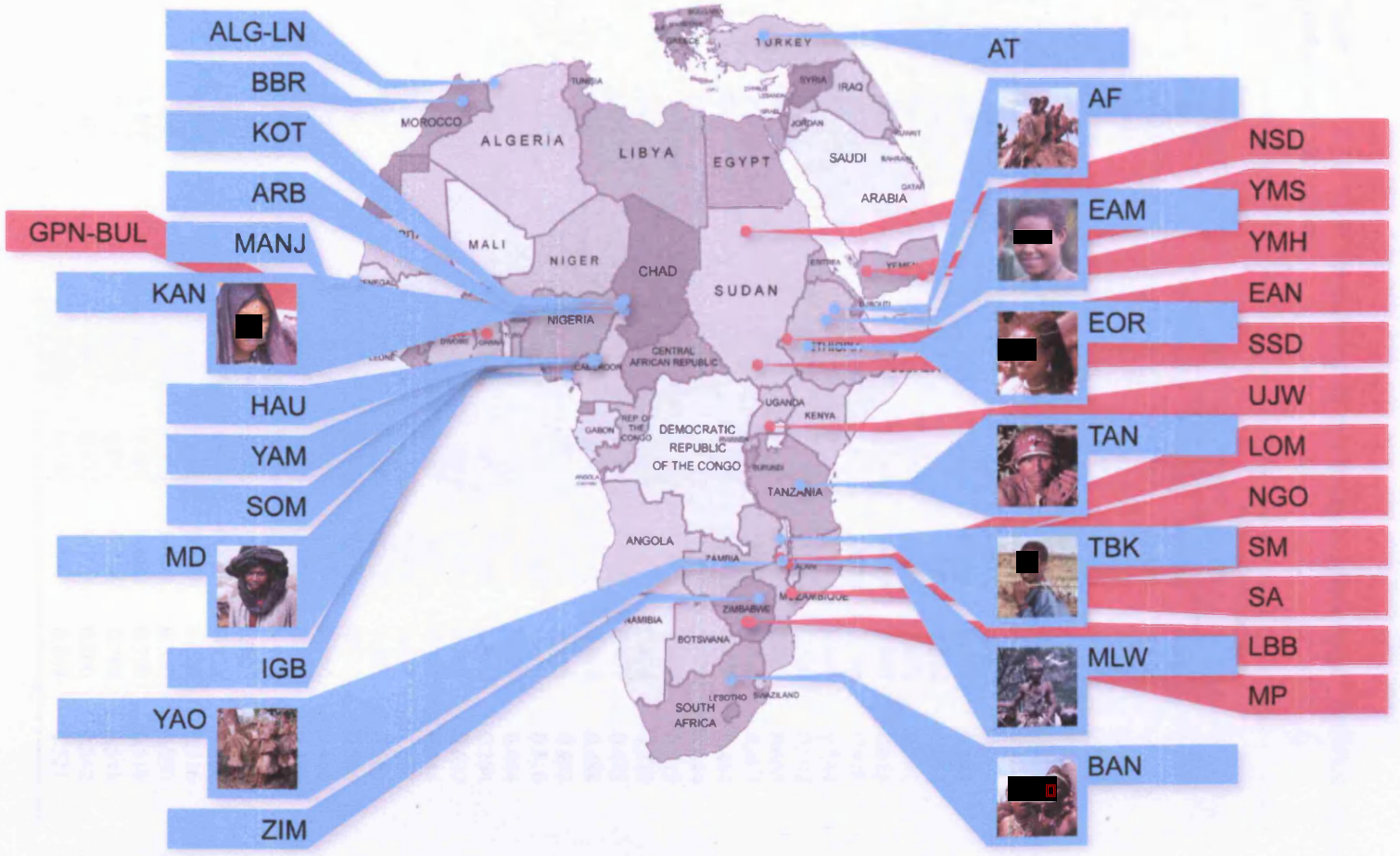

Figure 7.1: Location of African populations used.

Table 7.2: *IL18* SNP frequencies in the study samples used. NPHSII samples are marked with an asterisk.

		Allele Frequency				
Population Code	n	-9731 G	-5848 T	+105 A	+8855 T	+11015 A
AF	14	0.571	0.571	0.786	0.714	0.536
ALG-LN	162	0.522	0.581	0.681	0.678	0.513
ARB	91	0.626	0.450	0.862	0.828	0.500
AT	96	0.617	0.553	0.801	0.806	0.644
AYL*	114	0.619	0.649	0.690	0.689	0.597
BAN	101	0.672	0.450	0.931	0.882	0.505
BBR	108	0.495	0.575	0.639	0.638	0.481
CAMB*	432	0.587	0.659	0.690	0.688	0.577
CARN*	408	0.604	0.646	0.696	0.697	0.591
CHEST*	263	0.611	0.631	0.692	0.694	0.583
EAM	263	0.637	0.390	0.805	0.802	0.551
EAN	95	0.758	0.350	0.909	0.903	0.413
EOR	94	0.620	0.441	0.800	0.788	0.478
GPN-BUL	90	0.700	0.455	0.865	0.850	0.544
HALE*	435	0.618	0.634	0.705	0.704	0.592
HARE*	299	0.680	0.600	0.737	0.733	0.665
HAU	27	0.595	0.519	0.692	0.704	0.407
IGB	100	0.645	0.537	0.846	0.835	0.464
KAN	9	0.611	0.556	0.833	0.750	0.444
KOT	42	0.756	0.381	0.878	0.869	0.512
LBB	102	0.723	0.416	0.911	0.876	0.579
LOM	19	0.667	0.500	0.972	0.921	0.472
MANJ	85	0.706	0.494	0.776	0.768	0.488
MD	57	0.550	0.518	0.731	0.746	0.453
MLW	92	0.714	0.462	0.923	0.885	0.516
MP	18	0.500	0.618	0.875	0.853	0.444
NGO	17	0.529	0.676	0.900	0.900	0.294
NMY*	294	0.647	0.571	0.727	0.722	0.620
NSD	147	0.595	0.491	0.816	0.821	0.446
PARK*	419	0.624	0.635	0.674	0.673	0.587
SA	15	0.700	0.400	0.933	0.893	0.567
SM	69	0.709	0.396	0.932	0.912	0.566
SOM	96	0.633	0.526	0.797	0.786	0.464
SSD	129	0.780	0.373	0.920	0.919	0.384
STAN*	388	0.638	0.629	0.740	0.742	0.639
TAN	40	0.590	0.488	0.872	0.882	0.500
TBK	65	0.619	0.484	0.879	0.823	0.500
UJW	39	0.444	0.667	0.786	0.736	0.316
YAM	20	0.794	0.475	0.950	0.950	0.550
YAO	53	0.654	0.462	0.868	0.798	0.519
YMH	83	0.543	0.512	0.774	0.768	0.543
YMS	37	0.643	0.457	0.770	0.800	0.542
ZIM	56	0.620	0.514	0.883	0.869	0.521

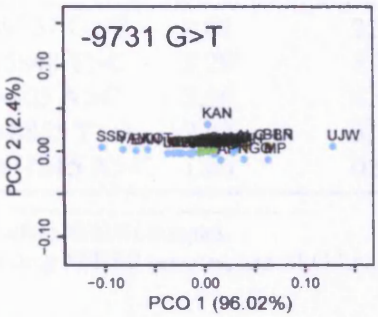

(a) PCO analysis in *IL18* -9731 G>T

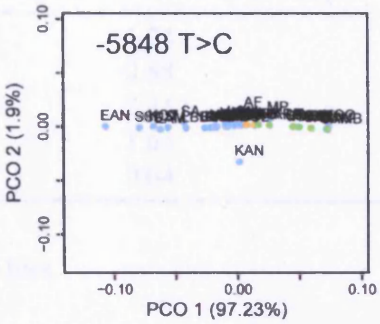

(b) PCO analysis in *IL18* -5848 T>C

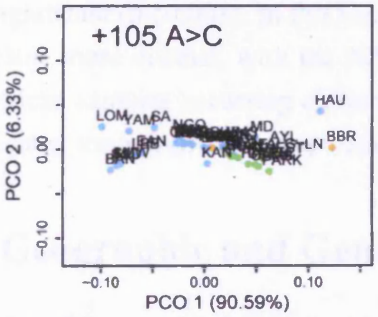

(c) PCO analysis in *IL18* +105 A>C

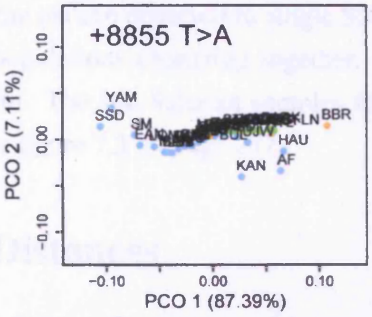

(d) PCO analysis in *IL18* +8855 T>A

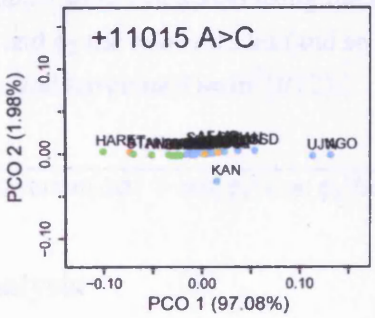

(e) PCO analysis in *IL18* +11015 A>C

Figure 7.2: Results from PCO analysis in the African and NPHSII populations. ● – sub-Saharan populations; ● – north African populations; ● – NPHSII populations.

Table 7.3: Amongst population variances of *IL18* tSNPs within the NPHSII and African samples.

	Amongst-population variance (%)		
SNP	All samples	African samples[1]	Sub-Saharan samples[2]
-9731 G>T	1.07	2.38	1.74
-5848 T>C	3.29	1.29	0.88
+105 A>C	3.66	4.58	2.41
+8855 T>A	2.92	3.39	1.63
+11015 A>C	1.66	0.91	0.64

[1]Excluding NPHSII samples.
[2]Excluding NPHSII samples, and ALG-LN, AT, and BBR.

among all samples. When only sub-Saharan samples were analysed the test remained highly significant ($p<0.001$). In PCO analysis the pattern observed in single SNP analysis became more distinct, with the NPHSII populations clustering together, and the north African samples occurring closest to them. The sub-Saharan samples formed a diffuse scatter away from these populations (see figure 7.3 on page 277).

7.3 Geographic and Genetic Distances

Geographic distances (d) between samples and from the most northern population (CARN – Carnoustie, Scotland) were calculated using the haversine formula where R is the radius of the earth, ϕ_1 and ϕ_2 the two latitudes (and so $\Delta\phi$ the latitude difference), $\Delta\lambda$ the longitude separation, and haversin(θ)=sin^2($\theta/2$):

$$d = 2R\arcsin\left(\sqrt{\text{haversin}(\Delta\phi) + \cos(\phi_1)\cos(\phi_2)\text{haversin}(\Delta\lambda)}\right) \quad (7.1)$$

7.3.1 Single SNP Analysis

All single SNP MAFs were significantly correlated with distance from Carnoustie except *IL18*-9731 G>T (R^2=-0.13, p=0.41; -5848 T>C R^2=0.58, $p<0.001$; +105 A>C R^2=-0.81, $p<0.001$; +8855 T>A R^2=-0.75, $p<0.001$; +11015 A>C R^2=0.52, $p<0.001$, see figure 7.4 on page 278). To test for a correlation between matrices of genetic distances (F statistic) and geographic distances, the Mantel test was used [Mantel, 1967]. All but -9731 G>T (p=0.93) showed significant correlations ($p<0.001$).

Table 7.4: Common European *IL18* haplotype frequencies in the study samples used. NPHSII samples are marked with an asterisk.

	Haplotype				
Population	hGCATA h12111	hTTCAC h21222	hGTATA h11111	hTTATC h21112	Other
AF	0.35	0.21	0.14	0.12	0.18
ALG-LN	0.40	0.31	0.09	0.15	0.05
ARB	0.48	0.14	0.02	0.20	0.17
AT	0.41	0.20	0.20	0.15	0.04
AYL*	0.31	0.27	0.27	0.09	0.07
BAN	0.49	0.10	0.01	0.20	0.20
BBR	0.41	0.35	0.06	0.14	0.05
CAMB*	0.29	0.27	0.26	0.11	0.06
CARN*	0.29	0.26	0.27	0.10	0.07
CHEST*	0.30	0.26	0.26	0.11	0.07
EAM	0.44	0.18	0.05	0.13	0.19
EAN	0.38	0.09	<0.01	0.11	0.41
EOR	0.45	0.21	<0.01	0.15	0.18
GPN-BUL	0.54	0.14	—	0.15	0.17
HALE*	0.32	0.26	0.26	0.11	0.05
HARE*	0.35	0.23	0.29	0.07	0.06
HAU	0.39	0.30	<0.01	0.08	0.23
IGB	0.47	0.16	—	0.18	0.18
KAN	0.39	0.13	<0.01	0.13	0.35
KOT	0.51	0.12	<0.01	0.12	0.25
LBB	0.57	0.09	<0.01	0.15	0.19
LOM	0.22	<0.01	0.09	0.11	0.58
MANJ	0.46	0.22	0.01	0.08	0.23
MD	0.42	0.25	<0.01	0.14	0.19
MLW	0.51	0.08	—	0.17	0.25
MP	0.40	0.14	0.03	0.33	0.10
NGO	0.29	0.10	—	0.36	0.25
NMY*	0.36	0.22	0.24	0.10	0.07
NSD	0.40	0.19	0.02	0.20	0.18
PARK*	0.32	0.28	0.25	0.08	0.07
SA	0.54	0.04	<0.01	0.18	0.23
SM	0.57	0.07	—	0.21	0.16
SOM	0.44	0.20	—	0.14	0.22
SSD	0.37	0.08	<0.01	0.12	0.43
STAN*	0.31	0.23	0.30	0.10	0.06
TAN	0.50	0.13	—	0.28	0.09
TBK	0.49	0.12	0.01	0.20	0.18
UJW	0.31	0.22	<0.01	0.28	0.18
YAM	0.47	0.03	0.02	0.12	0.37
YAO	0.51	0.13	—	0.13	0.23
YMH	0.46	0.22	0.05	0.20	0.06
YMS	0.51	0.20	0.02	0.16	0.11
ZIM	0.52	0.11	<0.01	0.26	0.11

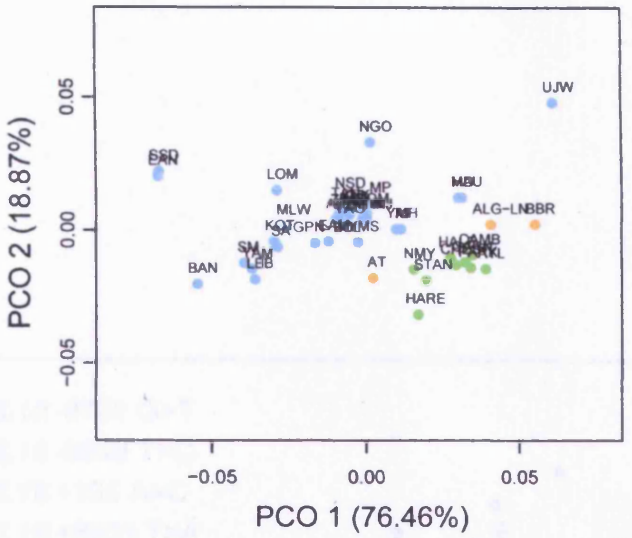

Figure 7.3: Results from PCO analysis of *IL18* haplotypes in the African and NPHSII samples. • – sub-Saharan populations; • – north African populations; • – NPHSII populations.

7.3.2 Haplotype Analysis

The Mantel test showed a highly significant correlation between genetic distance and geographic distance ($p<0.001$), however limiting analysis to sub-Saharan analysis gave no significant correlation ($p=0.56$). Each of the four common European haplotypes showed significant correlation between haplotype frequency and distance from Carnoustie (hGTATA R^2=-0.86, $p<0.001$; hGCATA R^2=0.60, $p<0.001$; hTTATC R^2=0.62, $p<0.001$; hTTCAC R^2=-0.74, $p<0.001$, see figure 7.5 on page 279 and figure 7.6 on page 280). The most striking results were that for hGTATA which was seen at frequencies <1% in the majority of the sub-Saharan Africa populations, 5–20% in north African samples, and 25–30% in the UK populations.

7.4 EHH Test

The above results suggested a significant cline in haplotype and single SNP frequency from southern Africa to northern Europe. As haplotypes, in particular hGTATA, have been shown to be associated with significant differences in IL-18 levels, it was possible this difference in haplotype frequency could be due to a positive selective pressure.

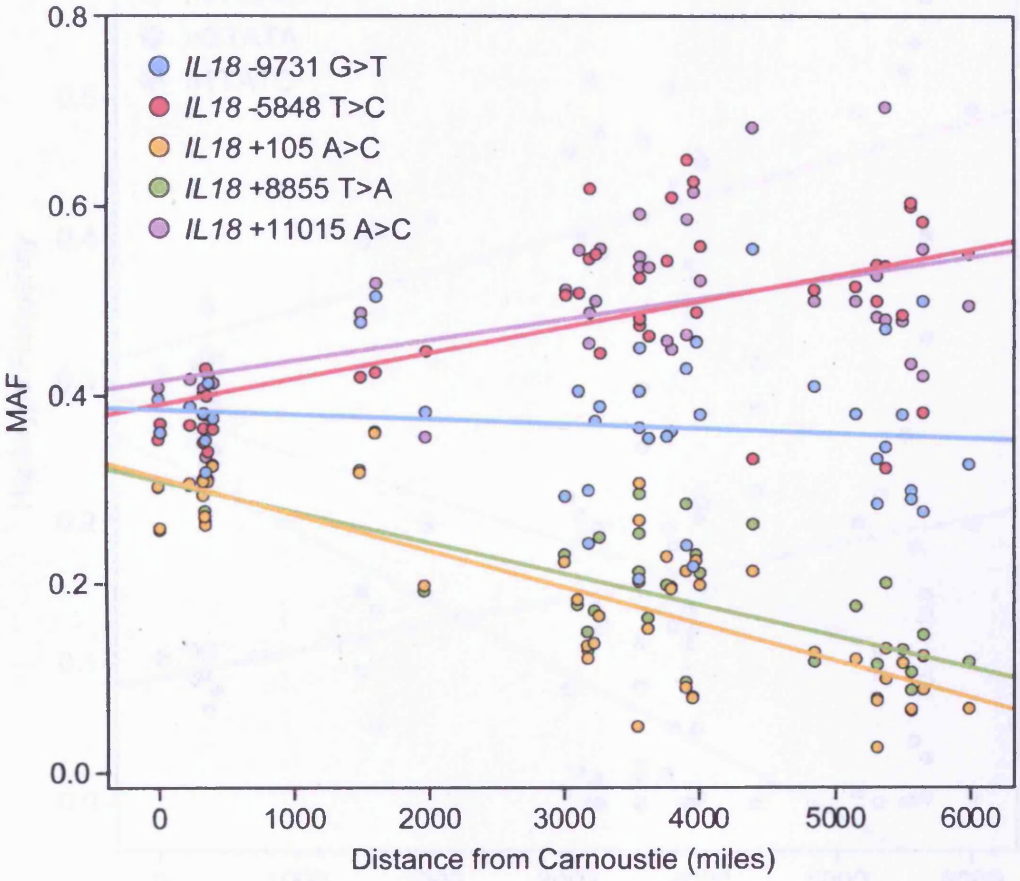

Figure 7.4: Scatter plot of *IL18* SNP MAF and distance from Carnoustie (miles).

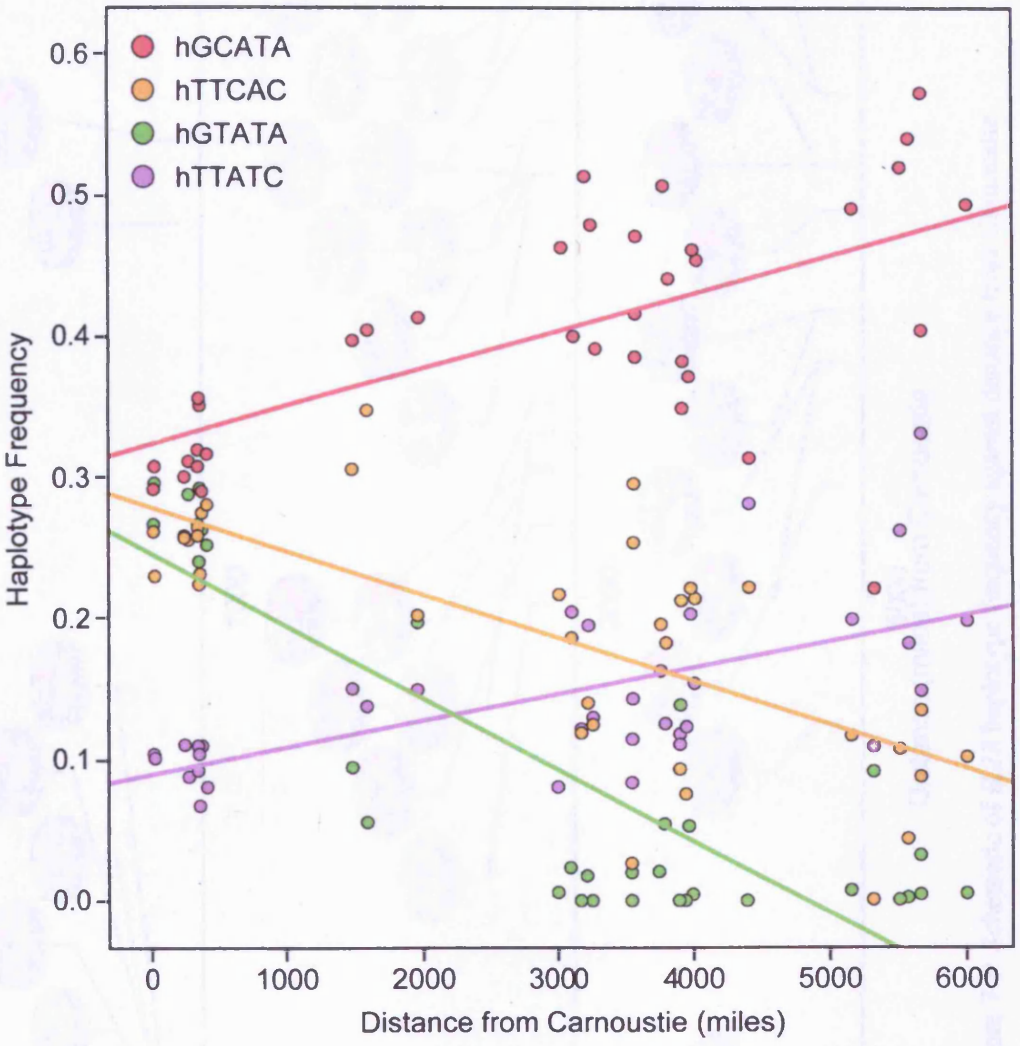

Figure 7.5: Scatter plots of common European *IL18* haplotype frequency and distance from Carnoustie (miles) in the African populations.

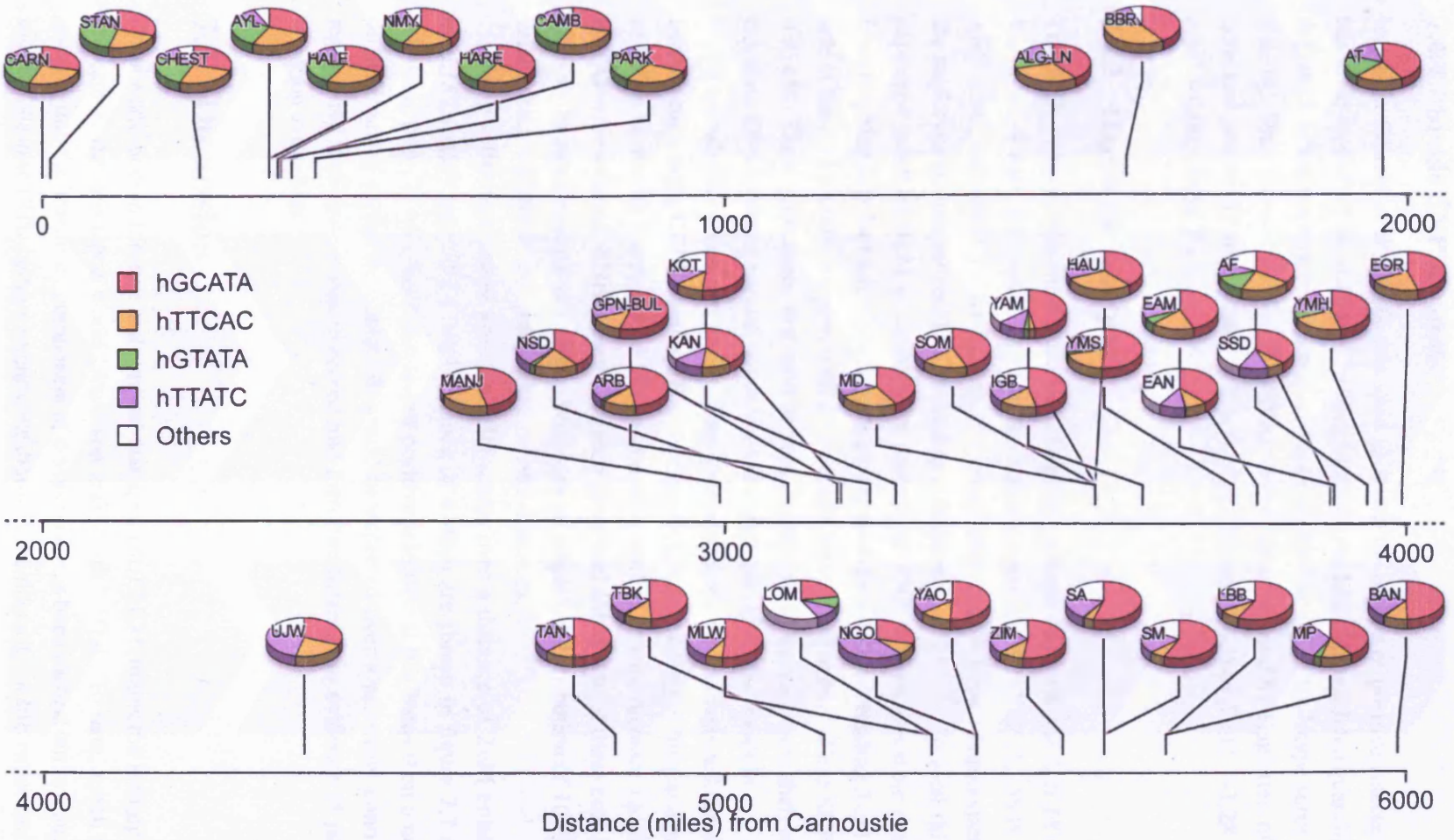

Figure 7.6: Schematic of *IL18* haplotype frequency against distance from Carnoustie.

7.4.1 Single SNP Analysis

Haplotter [Voight et al., 2006] was used to assess the degree of positive selection that has acted on each of the *IL18* tSNPs. This tool uses the EHH approach but quantifies the degree of recent positive selection at a locus with the integrated haplotype score (iHS) statistic. Only three of the five *IL18* tSNPs have been surveyed by Haplotter, of these none had potentially significant (> 2 or < -2) iHS scores (-5848 T>C – -1.28; +105 A>C – 0.99; +8855 T>A – 0.99).

7.4.2 Haplotype Analysis

The EHH analysis presented here uses HapMap release #21. Of the 5 *IL18* tSNPs used here, 4 were previously typed in the HapMap project (-9731 G>T, -5848 T>C, +105 A>C, and +8855 T>A). In the CEPH population they defined 7 haplotypes, with the haplotype of interest (hGTAT) found at a frequency of 21.7%. In total this core haplotype was 0.0033 cM in length from first to last SNP. Haplotypes were extracted from HapMap data for each of the three populations over a region extending 2 cM either side of the core haplotype region with SNP density maintained at around one SNP every 0.05 cM. Those haplotypes that held the core haplotype of interest were then used to calculate EHH scores at regular points 0.1 cM either side of *IL18* over 4 cM.

To test whether any of the EHH values generated from this analysis indicated positive selection in the CEPH dataset, 1000 core haplotypes consisting of the same number of SNPs, of similar frequency (±5%), and over a similar genetic distance (±20%) as hGTAT were selected. EHH scores were then generated either side of these core haplotypes in the same manner as above, resulting in an empirical distribution of 1000 EHH values at each of the twenty pre-defined genetic distances.

The p values associated with the EHH scores over a distance of 2 cM either side of *IL18* (roughly equalling a total distance of 4 Mbp) are shown in figure 7.7 on the following page. If there had been recent positive selection at this locus then a number of EHH values within the upper 5% would be expected over a relatively continuous region. No such pattern was observed and therefore there is no evidence of positive selection at this locus.

7.5 Discussion

Despite advances in lifestyle and medical management, CHD remains the leading cause of death in the developed world [Anderson and Smith, 2003]. To date, much of the research into the hereditary component of disease risk has been carried out in Caucasian subjects, despite CHD being a major contributor to the disparity in life expectancy and

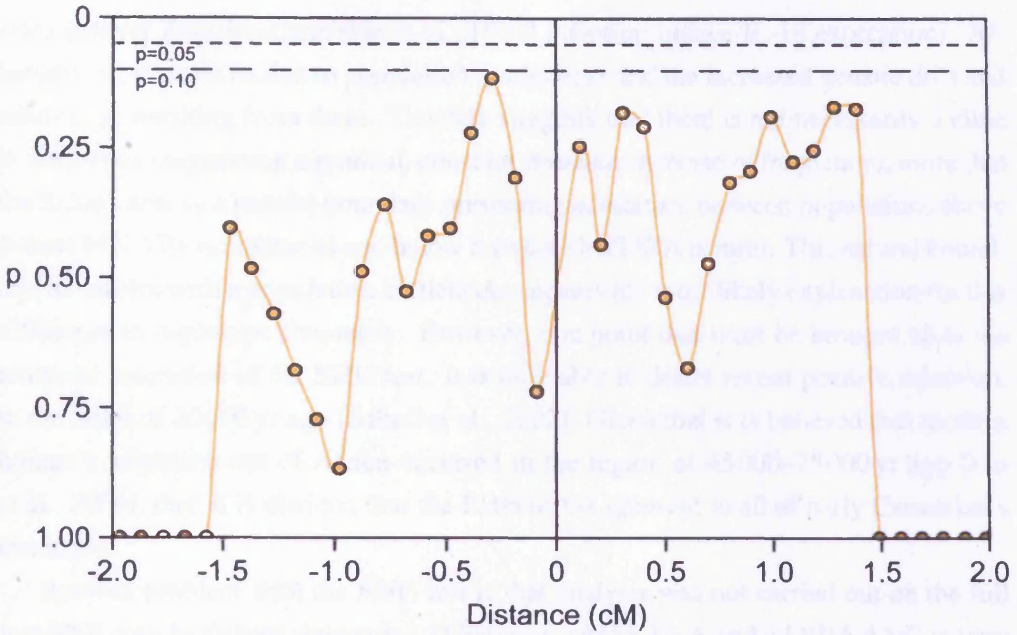

Figure 7.7: A graph of p-values and genetic distance showing the results of EHH analysis in individuals carrying hGTATA.

mortality rate between blacks and whites in US [Cooper et al., 2000; Geronimus et al., 1996]. Therefore the distribution across Africa of genetic variation within *IL18* was studied and a common haplotype, previously shown to be protective in Caucasians, was found to be non-existent in much of Africa.

The results from this study suggests that the genetic architecture and variation within *IL18*, is similar across much of sub-Saharan Africa; from AMOVA analyses combining all five SNPs, the amongst-population variance was 1.36%, substantially less than when all samples were included (2.56%). Observing the gradient in common UK haplotype frequencies from South Africa to north Scotland, the correlation between matrices of genetic and geographic distances were assessed using the Mantel test. When including only sub-Saharan samples no significant correlation was observed (p=0.56), however including all samples in the analysis returned a highly significant correlation (p>0.001).

Correlations of haplotype frequency with distance from Carnoustie (the most northern sample), showed all common UK haplotypes had significant correlations, with hGTATA being the strongest (R^2=-0.86). However the EHH test showed no evidence of recent positive selection on hGTATA. The differences in haplotype frequency between Europe and Africa could be due to negative selective pressure (for which there is currently no test) on hGTATA in sub-Saharan Africa; hGTATA is associated with lower production of IL-18 and therefore this selective pressure could be due to poor reaction to infection (eg. both *Plasmodium falciparum* [Kojima et al., 2004] and *Trypanosoma*

cruzi [Meyer Zum Buschenfelde et al., 1997] infection induce IL-18 expression). Alternatively, it could be due to population bottlenecks and the increased genetic drift and inbreeding resulting from them. The data suggests that there is not necessarily a cline in frequency (suggesting a gradual, constant decrease/increase in frequency), more that the Sahara acts as a natural boundary preventing admixture between populations above (where hGTATA is common) and below it (where hGTATA is rare). This natural boundary, in tandem with a population bottleneck, appears the most likely explanation for this difference in haplotype frequency. However, one point that must be brought up is the temporal resolution of the EHH test. It is only able to detect recent positive selection, in the order of 20000 yr ago [Sabeti et al., 2002]. Given that is is believed that modern human's migration out of Africa occurred in the region of 45000–75000 yr ago [Liu et al., 2006], then it is obvious that the EHH test is ignorant to all of early Caucasian's evolution.

Another problem with the EHH test is that analysis was not carried out on the full five-SNP core haplotype, however LD between +8855 T>A and +11015 A>C is very strong. In both IGB and GPN-BUL, the two closest populations to Ibadan, Nigeria (place of YRI collection), there was LD of D'=1 between +8855 and +11015, as it was for NPHSII. Therefore it is possible, with reasonable accuracy, to apply the HapMap four SNP haplotypes to the five SNP haplotypes described here. In doing so it is obvious that the Yoruba have a far higher hGTATA frequency than any other sub-Saharan population sampled here (17%). That the Yoruba seem genetically more similar to Caucasian populations than their geographic neighbours suggests that it may not be the correct population to test for positive selection at hGTATA (and indeed raises doubts as to its suitability as a 'representative' population of Africa), however there is no other African population available with the requisite genotype density.

The results in this thesis have not truly confirmed or refuted the association between hGTATA and protection from CHD risk, shown by Tiret et al. [2005]. The association was found in a prospective study of individuals with advanced disease, and given that the association between hGTATA and IL-18 levels appears especially strong in those with disease, it is likely that the effect of hGTATA on disease risk may not be sufficiently apparent in ostensibly healthy individuals. The only prospective study used here, NPHSII, recruited healthy middle-aged individuals.

However if hGTATA was found to be protective of CHD, then its complete absence in sub-Saharan Africa predisposes over 770 million people [World Bank, 2006] to an increased risk of death from cardiovascular disease. Potentially of greater importance, given the current low incidence of CHD in Africa, it may also predispose around 35 million US African-Americans to greater risk. The distribution of *IL18* haplotype frequencies in African-Americans was not studied directly here, but they are primarily descended from slaves sold during the Atlantic slave trade that occurred from 16th to

the 19th century. Most slaves were shipped from west and central Africa, and given the only recent (1970s) abolition of racial segregation in US (and the resultant rise in interracial marriage) it is highly unlikely that *IL18* haplotype frequencies deviate greatly from that seen in sub-Saharan Africa.

In conclusion, this chapter demonstrates the importance of studying genetic determinants of CHD in populations other than Caucasians. Data presented here shows a highly significant difference in SNP and haplotype frequency, between Caucasian and African populations. Given that hGTATA is a potentially protective factor in (Caucasian) CHD, further study of its effect in African-Americans is required.

Chapter 8

Assessing the Role of Genetic Variation on *IL18* Transcription *In Vitro*

This chapter aims to assess the impact of hGTATA on *IL18* transcription *in vitro* using QPCR. A number of carriers of *IL18* hGTATA and hGCATA were recruited and the concentration of *IL18* mRNA species assessed in their circulating monocytes. The Pfaffl method [Pfaffl, 2001] was then used to compare expression between the two groups and assess the significant of any differences.

8.1 Introduction

8.1.1 Potential Functional Variants

As there are no non-synonymous variants within *IL18*, the effect of hGTATA must derive from an effect on either promoter activity, splicing, or mRNA stability. If this effect derives from a single SNP, then this SNP must be in strong LD with *IL18*-5848, with the allele differing between hGCATA and hGTATA. As shown in figure 8.1 on the next page, within the region resequenced by IIPGA there are 18 SNPs whose allele differs between hGCATA and hGTATA, one of which is *IL18*-5848. One of these, *IL18*-11238 C>A, occurs within the proximal promoter and is therefore a good potentially functional proximal promoter variant.

As discussed in section 4.3 on page 175, *IL18*-11238 C>A was genotyped in 85 CABG individuals, and haplotypes (of -11238 C>A and the *IL18* tSNP set) were inferred. As shown in table 8.1 on page 287, haplotypes inferred from the CABG data confirm that -11238 A is only seen on hGTATA. There were two other haplotypes that also carry the A allele, however these were relatively rare and may simply be errors in haplotype inference. Therefore it is possible that -11238 C>A is the SNP responsible for the effect of hGTATA on IL-18 levels, however the SNP is not seen in a region of between-species conservation. Unfortunately -11238 C>A is outside of the re-

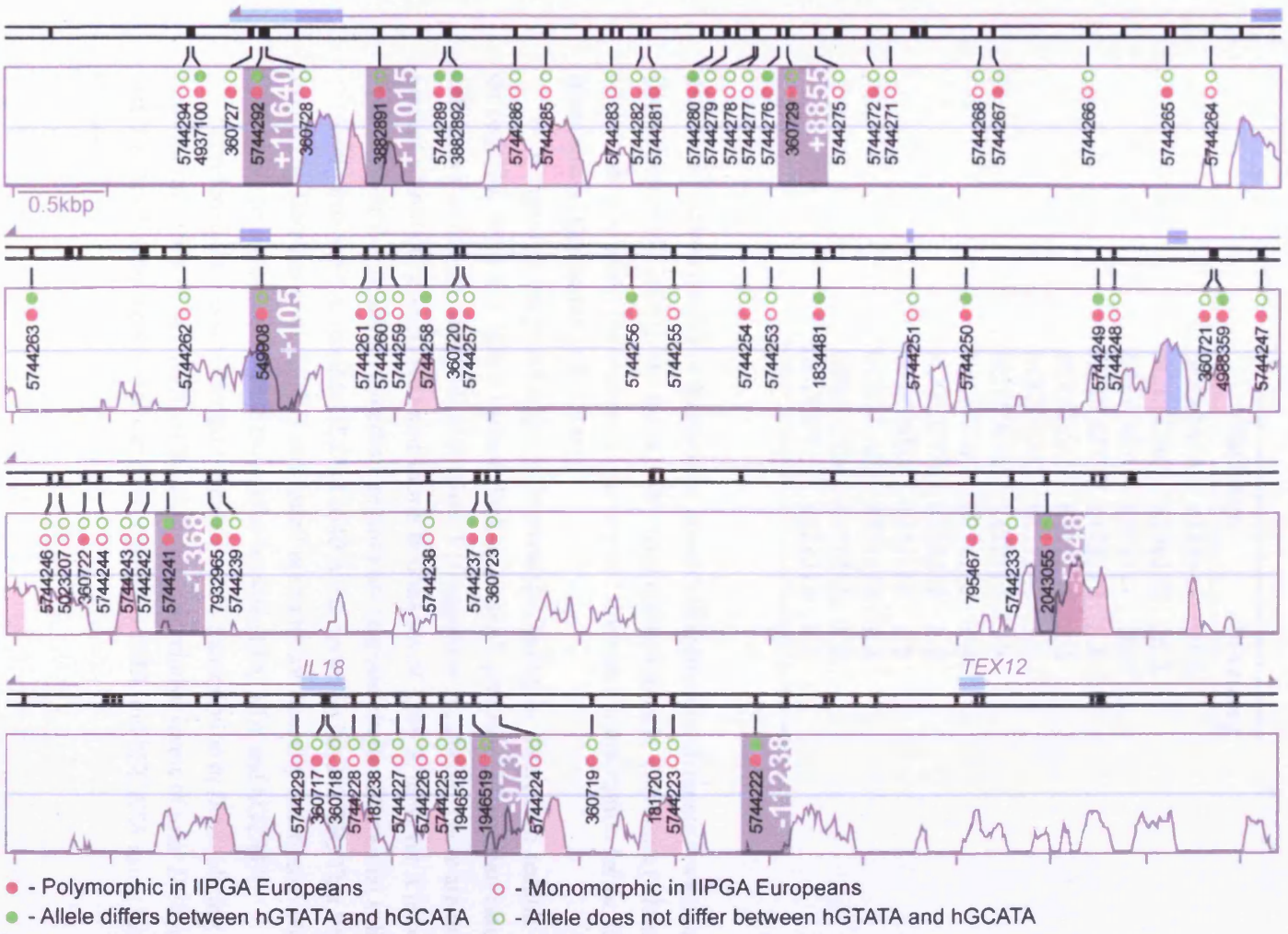

Figure 8.1: Schematic of SNPs within the *IL18* region showing those SNPs that might be responsible for the effect of hGTATA. Numbers are rs numbers, with the IIPGA offset (relative to transcription) shown for the *IL18* tSNPs, whilst the background VISTA plot is a human:mouse allignment taken from the VISTA genome browser (accessed November 2007).

Table 8.1: Frequencies for common (>1%) haplotypes inferred from the *IL18* tSNP set and *IL18*-11238 C>A. Haplotypes are ordered: -11238 C>A; -9731 G>T; -5848 T>C; +105 A>C; +8855 T>A; +11015 A>C.

Haplotype		Frequency
hCGCATA	h112111	27.5
hCTTCAC	h121222	25.5
hAGTATA	h211111	20.0
hCTTATC	h121112	8.3
hCGCCAC	h112222	4.0
hCGTCAC	h111222	3.0
hCTCATA	h122111	1.9
hAGTCAC	h211222	1.4
hCGCCTA	h112211	1.2
hCGTATC	h111112	1.2
hCTTAAC	h121122	1.2
hAGTCTA	h211211	1.2
hATTCTC	h221212	1.2

gion searched by cisRED (a database of conserved regulatory elements www.cisred.org [Robertson et al., 2006]), but the A allele does create a muscle TATA box (whilst the C allele does not) when the sequence is processed through a transcription factor database (Genomatix [Cartharius et al., 2005]).

With regard to the possibility of differential splicing, as detailed in section 1.3.1.1 on page 30, there is a splice variant, lacking exon 3, produced by ovarian carcinoma cell lines that is not processed by caspase-1 [Gaggero et al., 2004]. There are no SNPs present within the immediate exon-intron boundaries of exon 3, however it is possible that SNPs outside of these immediate regions are responsible for differential splicing.

As regards mRNA stability, *IL18*+11640 A>G occurs in the 3' UTR. This SNP was studied by Barbaux et al. [2007] and found not to be intrinsically functional. No other SNPs were found in the 3' UTR that differ between hGCATA and hGTATA.

Therefore to assess whether differences in *IL18* transcription or *IL18* splicing are the basis for the effect of hGTATA on IL-18 levels, the relative levels of total *IL18* mRNA, and *IL18*Δex3, were assessed in carriers of both hGTATA and hGCATA using the Pfaffl method.

8.1.2 Assessing Differences in Gene Expression

8.1.2.1 Traditional Method

Traditionally, the relative expression of control gene to target gene (ΔCt) was calculated by:

$$\Delta Ct = Ct_{Target} - Ct_{Control} \tag{8.1}$$

Assuming that levels of control gene mRNA remained consistent across samples and treatments, ΔCt values were compared, thereby assessing differences in target gene expression between samples. This was calculated by:

$$\Delta\Delta Ct = \Delta Ct_{Sample} - \Delta Ct_{Reference} \tag{8.2}$$

The fold-difference in target mRNA between sample and reference was then calculated by an assumption of 100% efficiency in the PCR reaction (ie. a doubling of PCR product at each cycle)[1]:

$$mRNA_{Sample-Reference} = 2^{-\Delta\Delta Ct} \tag{8.3}$$

However, this approach has a number of problems. Firstly, the assumption that the expression of the control gene remains constant across patients, treatments, and runs, is contentious; some studies show housekeeping genes remain stable across treatments and tissues [Marten et al., 1994; Foss et al., 1998; Thellin et al., 1999], whilst others show the opposite [Bhatia et al., 1994; Bereta and Bereta, 1995; Chang et al., 1998; Zhang and Snyder, 1992]. Differences in control gene expression will have a large impact on the resulting values of ΔΔCt, possibly leading to unrepresentative values. As there is no easy way to recognize or assess control gene instability (without relying on other potentially unstable control genes), this assumption can be dangerous.

Secondly, the efficiency of PCR (the fold-change in PCR products at each cycle) is not consistent across primer pairs. Again, any difference in assay efficiency could lead to unrepresentative values. As shown in equation (8.3), with a 100% efficiency we can assume that a ΔCt of two PCR cycles is equal to a four-fold difference in starting material. However, if the efficiency of that assay were 1.6, then a ΔCt of two would equal an $mRNA_{Sample-Reference}$ of 2.6. As ΔCt increases, the potential error grows exponentially (see figure 8.2 on the next page).

Thirdly, although the method provides a measure of the difference between samples and reference it gives no indication of the statistical significance of that difference.

[1]The sign of ΔΔCt is switched in equation (8.3) so that a negative ΔΔCt (equivalent to higher levels of mRNA than a positive ΔΔCt) gives rise to a correspondingly higher $mRNA_{Sample-Reference}$

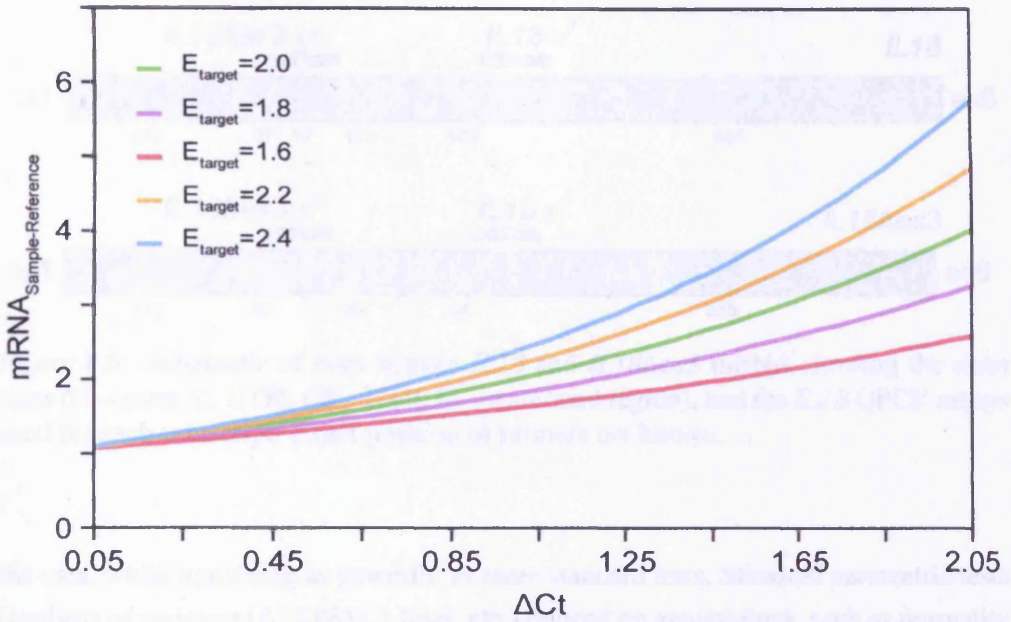

Figure 8.2: Chart showing the effect of differing PCR efficiency (E) on $\text{mRNA}_{Sample-Reference}$ over a range of ΔCt.

8.1.2.2 The Pfaffl Method

The Pfaffl method [Pfaffl, 2001] is an adaptation of the ΔΔCt method that calculates the relative expression ratio (RER), taking into account the efficiency of target and control assays. The key equation is:

$$RER = \frac{(E_{target})^{\Delta Ct_{target}(control-sample)}}{(E_{ref})^{\Delta Ct_{ref}(control-sample)}} \tag{8.4}$$

Both E_{target} and E_{ref} are calculated from a regression slope of Ct against cDNA input, using:

$$E = 10^{(-1/slope)} \tag{8.5}$$

Relative Expression Software Tool (REST) is a software package that adopts the Pfaffl approach and runs a simulated data exchange to assess statistical significance of any observed differences. The software is freely available at http://rest.gene-quantification.info/.

REST utilizes a pairwise fixed reallocation randomization test to assess differences in expression between control and treated sample group means. Permutation or randomization tests are a useful alternative to standard parametric tests for analysing experimental data. They have the advantage of making no distributional assumptions about

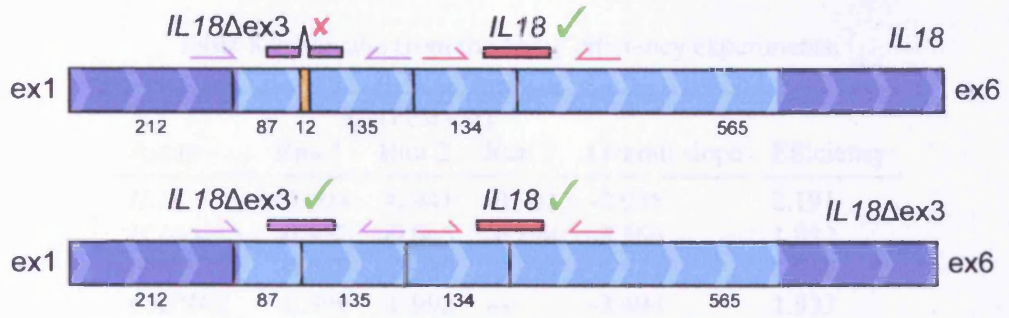

Figure 8.3: Schematic of both mature *IL18* and *IL18*Δex3 mRNA showing the exon sizes (■ – exon 3), UTRs (■ – UTR; ■ – translated region), and the *IL18* QPCR assays used for each transcript. Exact position of primers not known.

the data, while remaining as powerful as more standard tests. Standard parametric tests (analysis of variance (ANOVA), t-tests, etc.) depend on assumptions, such as normality of distributions, whose validity is doubtful. RER is a ratio, therefore its distribution is unlikely to be normal and it is difficult to see how a parametric test could be constructed [Pfaffl et al., 2002].

Standard statistical tests are based on the probability of an effect as large as that observed occurring under the null hypothesis of no treatment effect. If this hypothesis were true, the values in one treatment group were just as likely to have occurred in the other group. The randomization test repeatedly and randomly reallocates the observed values to the two groups, and notes the apparent effect each time. The proportion of these effects that are as large as those actually observed gives the p-value of the test [Pfaffl et al., 2002].

8.2 Results

8.2.1 QPCR Assays Used

Two *IL18* TaqMan assays were used so that the amount of total IL-18 and *IL18*Δex3 mRNA could be measured (see figure 8.3). As REST is able to normalize target gene expression to multiple control genes, three control genes were used – *GAPDH*, *BACT* and *UBC*. This reduces errors caused by differential expression of 'housekeeping' genes. Total *IFNγ* was also measured using a TaqMan probe that targeted the ex3-ex4 boundary.

Table 8.2: Results from the assay efficiency experiments.

	R^2 (Pearson)				
Assay	Run 1	Run 2	Run 3	Overall slope	Efficiency
IL18	-0.994	-0.941	-0.961	-2.935	2.191
*IL18*Δex3	-0.977	-0.965	-0.874	-3.366	1.982
IFNγ	-0.989	-0.980	-0.971	-3.537	1.917
GAPDH	-0.999	-0.998	—	-3.494	1.933
BACT	-0.999	-0.999	—	-3.639	1.883
UBC	-0.998	-0.987	—	-3.662	1.875

8.2.2 Control Selection

The cell line MDA-MB-231 (ECACC 92020424) is a human Caucasian breast adenocarcinoma cell line that is known to express the *IL18*Δex3 transcript (personal communication with Silvano Ferrini, Instituto Nazionale par la Ricerca sul Cancro, Genova, Italy, 2007, corresponding author on paper by Gaggero et al. [2004]). This cell line therefore served as the template for the *IL18*Δex3 assay efficiency experiments. A sample of MDA-MB-231 cells was kindly donated by Jonathan Abbott (UCL Centre for Cardiovascular Biology) and RNA aliquots were prepared as described in section 2.2.2 on page 85.

8.2.3 Assay Efficiencies

To calculate the efficiency of each QPCR assay, serial dilutions of cDNA were made and then used for each QPCR assay. Each experiment used triplicates for each cDNA concentration, and three experiments were carried out on separate days using separate aliquots of the same PBMC RNA sample (except for the control genes, for which only two experiments were carried out, see figure 8.4 on the following page). All assays gave an acceptable relationship between Ct and cDNA concentration. A regression line was drawn for each assay from the results of all experiments, and this figure gave the assay efficiency (see table 8.2).

8.2.4 Recruitment and Genotyping of Study Participants

The recruitment of hGTATA and hGCATA carriers was done in collaboration with the Cauldwell Xtreme Everest project (www.xtreme-everest.co.uk). Cauldwell Xtreme Everest is a research project coordinated by the UCL Centre for Altitude, Space and Extreme environment medicine. The group placed a research team on the summit of Mount Everest in May 2007 and made the first measurement of the level of oxygen

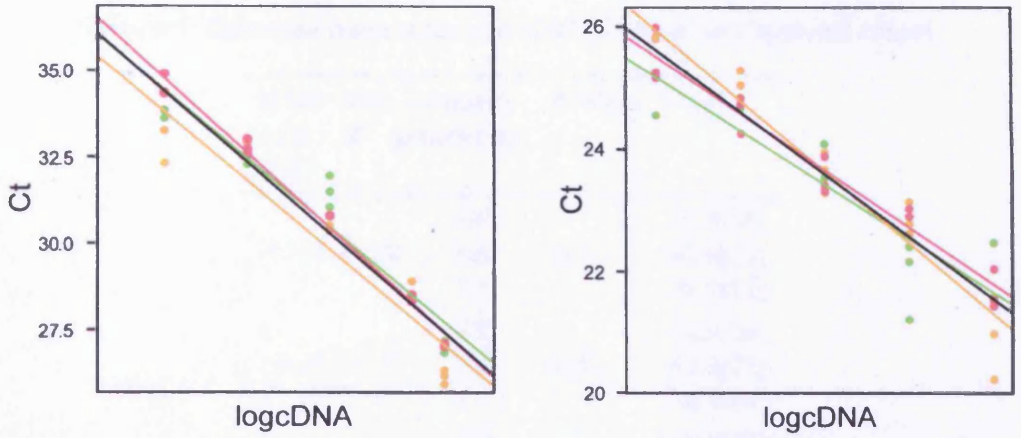

(a) *IL18*.

(b) *IL18*Δex3.

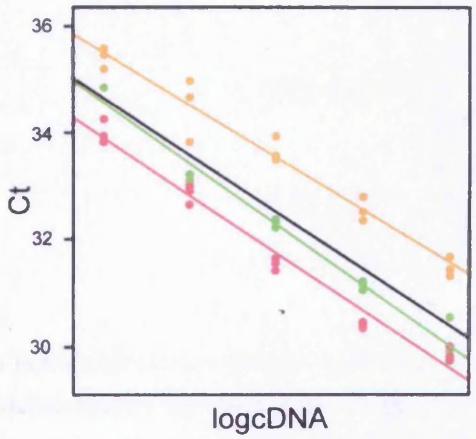

(c) *IFNγ*.

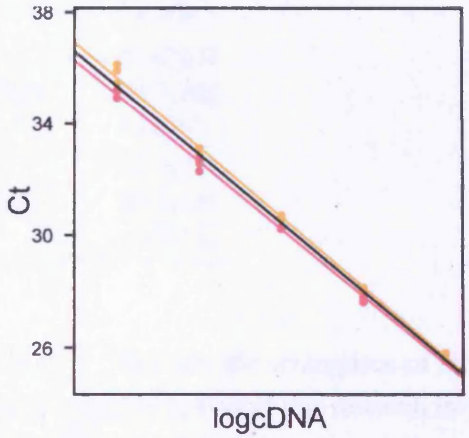

(d) *GAPDH*.

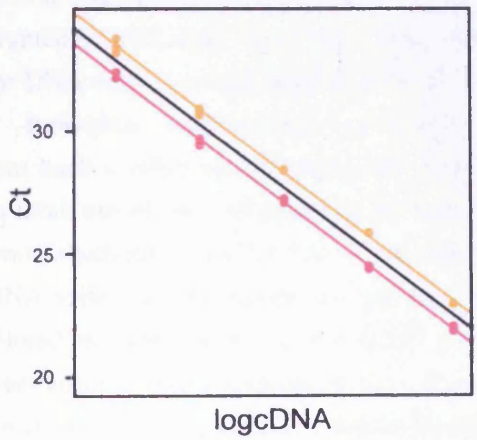

(e) *BACT*.

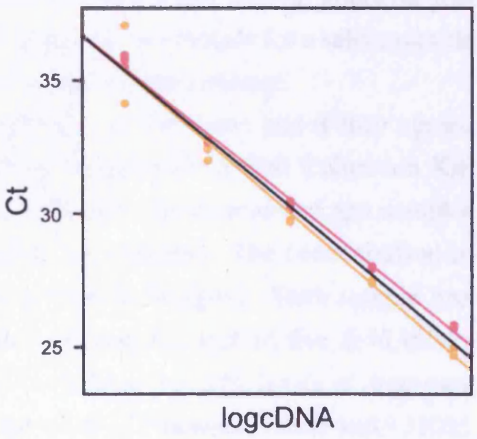

(f) *UBC*.

Figure 8.4: Graphs showing the decrease in Ct associated with decrease in cDNA concentrations for each QPCR assay. Data is triplicated for each cDNA concentration, over three separate experiments (• • •) for IL-18, IL-18Δex3, and IFNγ, and two separate experiments for the control genes (*GAPDH*, *BACT*, and *UBC*). The overall trend line is shown in black.

Table 8.3: Genotype frequencies and HWE p values for Cauldwell cohort.

tSNP and completeness of genotyping (%)		HWE p	%[n]
-9731 (98.2)	GG	0.31	33.3[18]
	GT		42.6[23]
	TT		24.1[13]
-5848 (98.2)	TT	0.41	38.9[21]
	TC		42.6[23]
	CC		18.5[10]
+105 (100.0)	AA	0.39	45.5[25]
	AC		40.0[22]
	CC		14.5[8]
+8855 (98.2)	TT	0.43	44.4[24]
	TA		40.7[22]
	AA		14.8[8]
+11015 (72.7)	AA	0.21	27.5[11]
	AC		40.0[16]
	CC		32.5[13]

in human blood at 8400 m, on the balcony of Everest. This was the centrepiece of an extensive and continuing programme of research into hypoxia. Part of this research involved the recruitment of a number of individuals for aerobic performance testing, as such a database of healthy London-based men was established. Ethical approval was granted by UCL Research Ethics Committee to approach individuals for a saliva sample for DNA extraction and potential later blood sampling and processing.

Individuals were approached by letter to take part in the study, and if they agreed sent back a saliva sample using the DNAgenotek Oragene DNA Self Collection Kit. In total, out of the 150 packs that were sent out, 55 individuals returned spit samples from which an aliquot of 500 µl was taken and DNA extracted. The concentration of DNA varied widely across the samples, ranging from 5–50 µg/ml. Each sample was diluted to a concentration of 5 ng/µl for TaqMan genotyping, and all five *IL18* tSNPs were successfully genotyped in the cohort, although there was a high rate of drop-outs for *IL18*+11015 A>C (27%). Given the high degree of LD between +8855 and +11015 this was unlikely to significantly affect the accuracy of haplotype inference. All SNPs had genotype distributions consistent with HWE (see table 8.3).

PHASE was used to infer the most likely haplotype pair for each individual (see table 8.4 on page 295). Those individuals who were homozygous for hGCATA were selected as the 'control' group, whilst those who were homozygous or heterozygous

for hGTATA (with hGCATA as the other haplotype) were recruited as the test group. Unfortunately, the only individual who was homozygous for hGTATA (#38) was not able to donate a blood sample.

8.2.5 QPCR of Selected Samples

In total, 10 individuals (five hGCATA/hGTATA heterozygotes and five hGCATA homozygotes) attended for blood-taking, where a 15–20 ml sample of venous blood was collected. Immediately following this, two aliquots of PBMCs were isolated and preserved in RNAlater before being stored at −80 °C (see section 2.2.1 on page 84). When all PBMC samples had been collected, RNA was extracted as detailed in section 2.2.2 on page 85. RNA extraction was successful in all samples, with concentrations ranging from 15–45 ng/µl with a high purity (A_{260}/A_{280} - 1.99–2.34; A_{260}/A_{230} - 0.07–1.02). The relative concentrations of *IL18* and *IFNγ* transcripts were then measured using QPCR in three separate repeat experiments on three consecutive days, using fresh cDNA prepared each day. On all three occasions 75 ng of RNA was used in cDNA synthesis, resulting in similar cDNA concentrations across each run (mean for all samples in run 1=961.7 ng/µl; run 2=966.9 ng/µl; run 3=892.1 ng/µl) with within-sample coefficient of variations (CVs) being 6.6% on average (range 0.9–12.5%).

Unfortunately sample 27 failed to produce any QPCR traces across all three runs and has therefore not been included in the following analysis. The first significant observation was that there is little evidence for significant expression of *IL18*Δex3 in the samples (see figure 8.5 on page 296). *IL18*Δex3 expression is evident in MDA-MB-231 cells but is substantially lower than that of *IL18*. The $\Delta Ct_{IL18\Delta ex3-IL18}$ for the MDA-MB-231 is, on average, 2.5. This therefore equates to a 5.7-fold excess of *IL18* to *IL18*Δex3. For the Cauldwell cohort, no consistent expression of *IL18*Δex3 was observed in any of the samples. In some cases a QPCR trace arose with a Ct of 35+ cycles. If a real finding and not due to contamination, this would suggest that *IL18*Δex3 represents <1% of *IL18* mRNA, and is therefore unlikely to be responsible for the association between hGTATA and IL-18 levels.

IL18 expression was observed at similar levels to *IFNγ* but at substantially lower levels compared to the reference genes (*GAPDH*, *UBC*, and *BACT*, see figure 8.6 on page 297). *IL18* mRNA levels were 2.4-fold higher in hGTATA/hGCATA heterozygotes compared to hGCATA homozygotes, although this difference was not significant (p=0.39). *IFNγ*'s expression was 1.2-fold higher in heterozygotes compared to homozygotes, but again this difference was not significant (p=0.83).

Only one of the individuals recruited for this study was involved in the ascent of Everest. To allow the effects of extreme altitude to subside, PBMC isolation from this individual was delayed by three months. There was no evidence that either *IFNγ* or *IL18*

Table 8.4: *IL18* haplotype pairs within Cauldwell cohort; prob. – probability given by PHASE that haplotype pair prediction is correct, selected samples are highlighted.

Ind.	Prob.	hGTATA	hGTATC	hGTCAC	hGCATA	hGCCAC	hTTATC	hTTCAC	hTCATA
1	0.997	■						■	
2	1.000						■	■	
3	0.997	■						■	
4	1.000				■■				
5	1.000			■				■	
6	1.000				■■				
7	1.000	■			■				
8	0.978				■		■		
9	0.993				■			■	
10	0.996				■				■
11	0.993				■			■	
12	0.978				■		■		
13	0.993				■			■	
14	0.978				■		■		
15	1.000							■■	
16	1.000							■■	
17	1.000				■■				
18	0.993				■			■	
19	1.000	■			■				
20	0.991	■					■		
21	1.000				■■				
22	1.000	■	■						
23	0.999							■	■
24	1.000							■■	
25	1.000	■			■				
26	1.000							■■	
27	1.000	■			■				
28	0.978				■		■		

Ind.	Prob.	hGTATA	hGTATC	hGTCAC	hGCATA	hGCCAC	hTTATC	hTTCAC	hTCATA
29	1.000						■	■	
30	1.000							■■	
31	0.993				■			■	
32	1.000						■	■	
33	1.000						■	■	
34	0.993				■			■	
35	1.000	■			■				
36	0.993				■			■	
37	0.531					■	■		
38	1.000	■■							
39	1.000							■■	
40	1.000						■	■	
41	0.942				■				■
42	0.994							■■	
43	0.962				■	■			
44	0.879	■			■				
45	0.848	■					■		
46	0.940				■■				
47	0.962				■			■	
48	0.877	■						■	
49	0.941				■			■	
50	0.877	■			■				
51	0.937				■■				
52	0.481				■			■	
53	0.876	■						■	
54	0.938				■■				
55	0.878	■			■				

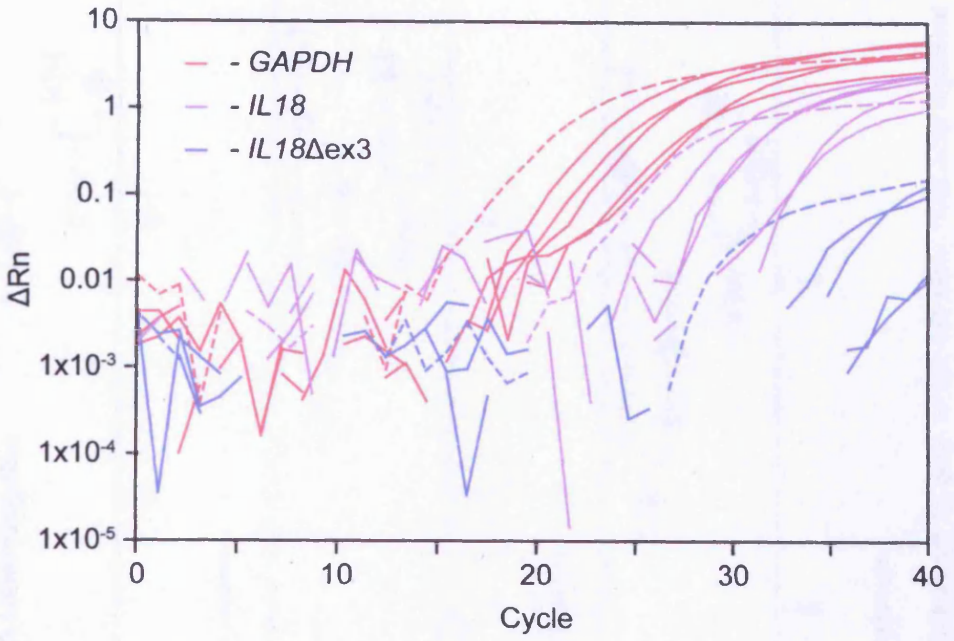

Figure 8.5: The difference in Rn (reporter dye fluorescence normalized to passive reference dye) by cycle number for *GAPDH*, *IL18* and *IL18*Δex3 assays. Those traces associated with RNA from MDA-MB-231 cells are shown as dotted lines. Data is a representative selection of traces from a single experiment and plotted on a logarithmic scale.

Table 8.5: Ct[95% CI] for all assays in those homozygous for hGCATA or heterozygous for hGTATA. Results presented are average of triplicates in three separate experiments, with p values derived from REST analysis.

	Ct[95% CI]		
Assay	hGCATA Homozygotes	hGCATA/hGTATA Heterozygotes	p
IL18	33.8[32.2–35.4]	32.1[30.5–33.7]	0.39
IFNγ	34.2[33.1–35.3]	33.2[31.9–34.5]	0.83
GAPDH	27.2[25.9–28.4]	26.2[24.9–27.5]	—
UBC	27.0[26.0–28.1]	26.4[25.3–27.4]	—
BACT	25.1[24.1–26.2]	24.5[23.4–25.6]	—

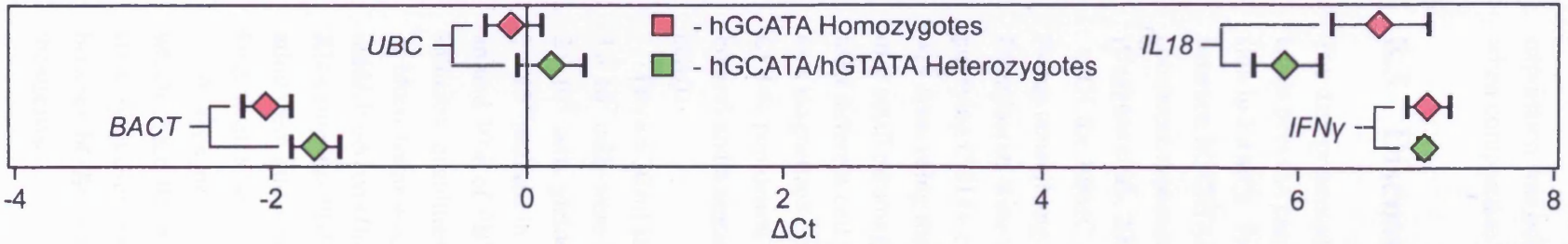

(a) ΔCt for each gene using *GAPDH* as reference.

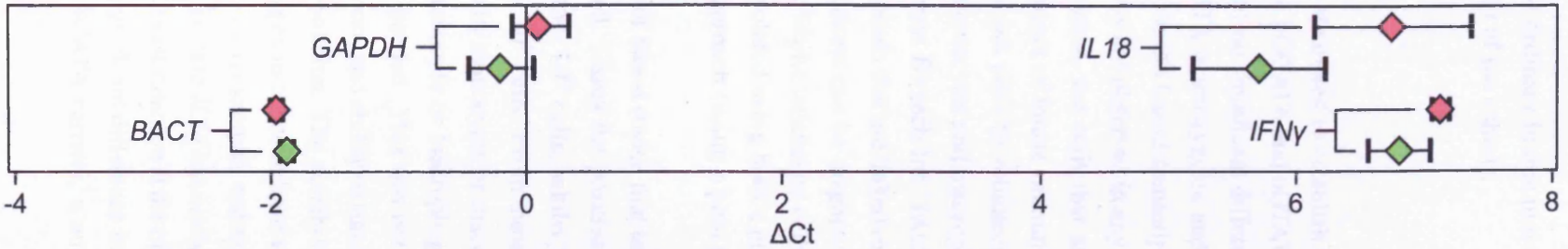

(b) ΔCt for each gene using *UBC* as reference.

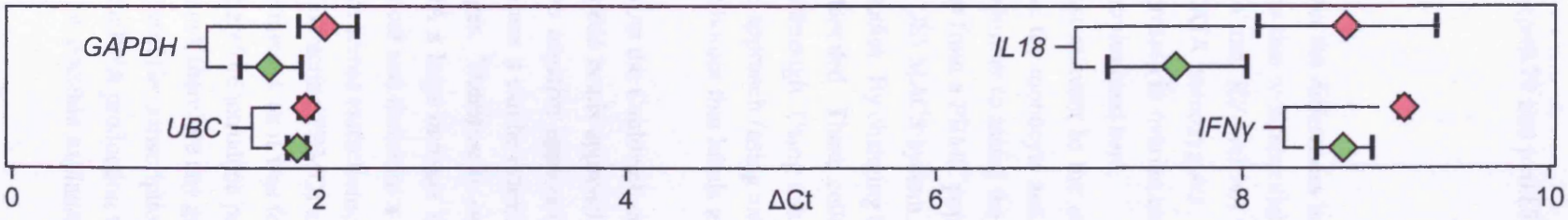

(c) ΔCt for each gene using *BACT* as reference.

Figure 8.6: ΔCt (Ct_{Target}-$Ct_{Reference}$) plots for the two haplotype groups, using each housekeeping gene as the reference. Whiskers represent 95% CIs derived from the raw Ct data, and do not take into account the base 2 nature of the scale.

expression was out of the ordinary in this individual (p=0.79 and p=0.88, respectively when compared to the rest of the cohort).

8.3 Discussion

The data presented here attempted to establish whether the differences in serum IL-18 levels between carriers of hGCATA and hGTATA, was due to differential gene expression in PBMCs. However, no significant difference in total *IL18* mRNA was observed between hGCATA/hGTATA heterozygotes and hGCATA homozygotes. Furthermore consistent expression of the *IL18*Δex3 transcript, expressed in ovarian carcinoma cells [Gaggero et al., 2004], was not observed in any of samples used here.

Of the PBMC population, the cells that are most relevant to the atherosclerosis (when considering the impact of innate immunity) are the monocyte and macrophage. Experiments were carried out prior to volunteer recruitment to assess the feasibility of purifying CD14+ cells (monocytes and macrophages) from a PBMC population. This was done using the Miltenyi Biotech Inc. (Auburn, US) MACS system. This system uses small paramagnetic beads that are linked to antibodies. By changing the antibodies used different cell populations can be magnetically labelled. Those cells are retained on a magnetized column, whilst unlabelled cells pass through. Using this approach the CD14+ population was isolated using both a positive approach (using anti-CD14 antibodies) and a negative approach (using a pool of antibodies that labels all but CD14+ cells).

From a 30 ml sample of blood (twice that taken from the Cauldwell cohort) around 3×10^7 cells were isolated. Using the positive magnetic beads approach, an input of 2×10^7 cells yielded 1.45×10^6 cells, whilst for the negative approach an input of 1×10^7 resulted in 1.29×10^6 cells. From these numbers it can be estimated that only around 10% of PBMCs are monocytes or macrophages. Therefore in order to obtain sufficient quantities of monocyte or macrophage RNA a large increase in the volume of blood taken would be needed. This was not practical and therefore a decision was made, based on efficacy, cost, and ability to standardize across extractions, to isolate the RNA from the PBMC population. The possibility of extracting PBMCs and differentiating them into macrophages in tissue culture was dismissed, as it was felt this would be difficult to standardize across samples and might therefore introduce potential error.

A non-synonymous variant in *IL18* has not been found, therefore any genetic variant which affects IL-18 levels must function at the mRNA level (ie. transcription, splicing or stability). Given that no significant difference in *IL18* mRNA production was observed between hGTATA and hGCATA carriers, a number of possible explanations present themselves:

1. PBMCs are not the cells responsible for the bulk of serum IL-18 production
2. The hypothesized difference in *IL18* transcription only becomes apparent upon cell activation/stress
3. The haplotype effect only becomes apparent in hGTATA homozygotes
4. The effect of hGTATA on IL-18 production is not simply through a difference in rate of transcription
5. The number of individuals used in the study was too few
6. The observed association between hGTATA and IL-18 serum levels was a chance finding, not a true biological phenomena

Which tissue is the major contributor to serum IL-18 concentrations is not known. The assumptions made in this work were that circulating PBMCs made a major contribution to serum IL-18 levels, and that even if this were not the case, the effect of hGTATA on *IL18* expression would be the same. The monocyte appears the best candidate for serum production of IL-18, but it is possible that an as yet unidentified other source of IL-18 has a greater contribution. Given the observation that adipocyte *IL18* mRNA levels correlate with IL-18 plasma levels [Leick et al., 2007], it is possible that adipose tissue is a major contributor to plasma IL-18 levels. All the associations presented here were between hGTATA and serum IL-18 levels, it is possible therefore that the regulation of IL-18 production, and therefore the effect of hGTATA, differs between the source of serum IL-18 and monocytes, and so no effect on monocytes would be observed.

What seems more likely is that the monocyte requires a degree of activation/stress, modifying *IL18* mRNA production or regulation, before the effect of hGTATA can be observed with the techniques used here. As detailed in section 4.3 on page 175 the association between hGTATA and serum IL-18 levels became especially apparent in those study groups that recruited individuals with advanced disease, and therefore activated immune systems. On the whole, the volunteers used here were very healthy. The initial recruitment involved a free VO_2 test of physical fitness that otherwise would cost around £200, and therefore attracted amateur sportsmen. None of the individuals recruited were overweight, and it is likely that they did not suffer from underlying cardiovascular disease that might serve to amplify any genetic effect. Despite their being healthy, this cohort was used as they had no underlying health issues and were not therefore on any medication. Medication is likely to have effects on IL-18 production (eg. Fluvastatin reduces serum IL-18 levels [Leu et al., 2005]), and it is probable that if subjects with disease had been recruited, differences in medication between individuals

would mask any actual differences in *IL18* mRNA concentration between the haplotype groups. As mentioned above, the process of individually isolating macrophages and then further activating them would have to be done sample by sample, and eliminating any variance caused by this process would be very difficult.

Despite successful PBMC extraction, mRNA extraction, and cDNA synthesis, sample 27 failed to produce any QPCR traces in all three runs. Why this was the case is not known, most likely it is due to contamination or degradation of the RNA or PBMC sample. However, sample 27 was one of the later samples to be collected (one and a half months before QPCR), and its RNA sample was sufficiently pure (30.0 ng/µl, A_{260}/A_{280}=1.92, A_{260}/A_{230}=0.45). What cannot be ascertained is the quality of this RNA, and this may be the cause of the failure. Due to the loss of sample 27, analysis was carried out in a cohort of 9 individuals, four heterozygous for hGCATA/hGTATA and five homozygous for hGCATA. It is difficult to say whether this is too few without a good estimate of the ΔCt between the two haplotype groups (if one exists).

The control group from SCARF is the most similar to the Cauldwell cohort in terms of health and age. Although significant (p=0.001) the difference in haplotypic mean IL-18 associated with hGTATA and hGCATA was only modest, such that those homozygous for hGTATA might be expected to have mean[95% CI] IL-18 levels (pg/ml) of 225.9[204.4–249.6] whilst for hGCATA this was 281.5[265.1–304.9] (see figure 4.13 on page 164). Assuming additivity of the haplotype effect, we can assume that hGCATA/hGTATA heterozygotes might have serum IL-18 levels ~250 pg/ml. Given this relatively minor decrease in IL-18 production (10%), it is unlikely that QPCR would have sufficient statistical power to identify such a difference when only a small number of individuals were recruited. The observed data suggest that a greater difference may occur but was not statistically significant in this small sample.

However, how well differences in mRNA concentration relate to serum IL-18 levels is not clear from the data here. Barbaux et al. [2007] carried out experiments to assess the difference in *IL18* transcription between carriers of three different haplotypes associated with IL-18 levels by Tiret et al. [2005]. Data presented by Tiret et al. [2005] show a similar magnitude of haplotypic effect when compared to that observed here in SCARF controls. Barbaux et al. [2007] showed that individuals (n=11) homozygous for the haplotype equivalent to hGTATA (see section 3.2.6.2 on page 120) had an approximately 2.5-fold lower expression of *IL18* than those homozygous for the haplotype equivalent to hGCATA (p=0.03). This amounts to a ΔCt of $\log_2(2.5)=1.3$[2]. Given that the effect of hGTATA is believed to operate in an additive manner, the ΔCt between those heterozygous for hGTATA/hGCATA and those homozygous for hGCATA, that might theoretically be observed in these experiments would be $\log_{2.191}\left(1+\frac{2.5-1}{2}\right)=0.7$.

[2]This assumes an efficiency of 2 for the *IL18* QPCR assay as Barbaux et al. [2007] did not perform any efficiency studies

The two haplotype groups analysed here show a fold-difference in expression (when normalized to control genes) of 2.36 (data not shown), and a ΔCt that ranges from 0.74–1.11 (depending on which control genes serves as the reference), yet it is not significant in the random reallocation test. Given that the effect of hGTATA would, presumably, be doubled in homozygotes this suggests that recruitment of hGTATA homozygotes in larger numbers (20+ individuals) should have reasonable power to detect such an effect with statistical certainty.

However, of more concern is that the difference observed between the two haplotype groups is contrary to that which one would expect given the results presented in chapter 4, with hGCATA/hGTATA heterozygotes having 2.4-fold *higher* expression than hGCATA homozygotes (although this was not significant). Assessing and presenting the error in these measures is difficult as the Ct scale itself is base 2, therefore the 95% CIs presented in figure 8.6 on page 297, are most likely misleading as these measures rely on normally distributed data. The expression ratio for *IL18* between the two haplotype groups is 2.36 (normalized to all three control genes), however if we consider that this figure has a standard error of ± 2.32 it becomes apparent that the difference observed is more than likely due to random error.

It is possible that the effect of hGTATA is not simply due to a difference in rate of transcription. As discussed above, Barbaux et al. [2007] demonstrated a significant difference in total *IL18* mRNA produced by Epstein-Barr virus-transformed lymphoblastoid cell lines. In an attempt to identify the underlying cause of this difference they carried out luciferase reporter assays, mRNA stability, and allelic imbalance assays using the 3' UTR (where their particular SNP [+11640] of interest was found). Despite an observed difference in *IL18* expression, the exact functional mechanism was not elucidated. The effect of hGTATA may also not lie simply in transcriptional activity. But without further experiments, assessing mRNA stability etc., no conclusions can be made.

Finally, it must be considered that the association between hGTATA and IL-18 is simply an anomalous statistical result and, in reality, no actual difference exists. Although plausible, this explanation becomes difficult to reconcile with the data from different studies and groups, which, on the whole, agree. Given that hGTATA does also appear to be associated with BMI, the data strongly suggests that genetic variation present on hGTATA has an effect on the production of IL-18.

In conclusion, the data presented in this chapter gives no evidence for differential expression of *IL18* between hGCATA homozygotes and hGCATA/hGTATA heterozygotes, in monocytes obtained from healthy individuals. However, the lack of any hGTATA homozygotes means that the expected deviations were most likely beyond the resolution of the technique given the measurement errors. This chapter also demonstrates that the *IL18*Δex3 transcript is not expressed in normal tissues, and therefore the

isoform identified by Gaggero et al. [2004] must be considered either pathological or produced as a result of pathology.

Chapter 9

Discussion

CHD remains the most serious health issue facing the Western world despite improvements in medical management, costing the UK in excess of £7 billion per year [Liu et al., 2002]. The epidemiological transition towards the end of the last century led to significant increase in life-expectancy, and, coupled with rises in population, has left the deaths due to CHD in the US fairly constant over the last quarter century. The incidence of global CVD deaths looks set to increase to 6.2–8.2 million per year by 2030 [Mathers and Loncar, 2006] as the developing world becomes industrialized, therefore knowledge of CHD risk factors in these countries (and associated ethnic groups) will be ever more important.

Numerous CHD risk biomarkers have been identified, but family history remains the strongest independent risk factor [Lusis et al., 2004]. Although social and behavioural factors inevitably play their part within this, it is highly likely that genetic variation within the biomarker genes, passed down from parents to offspring, significantly contribute to CHD risk. So far, identification of disease-causing variants has been slow, and to date the variants only explain a small fraction of disease heritability [Watkins and Farrall, 2006]. However, as genomic technologies progress and we gain ever greater insight into the 3.1 billion bps of the human genome, it is hoped that targeted genetic testing, studying genes collectively rather than in isolation, will become a powerful tool in risk stratification [Drenos et al., 2007].

This thesis has been concerned with assessing the impact of genetic variation within the IL-18 system, on both CHD risk and obesity. As an IFNγ-inducing factor, IL-18 promotes the T_H1 lineage of cells [Elhage et al., 2003], encouraging foam cell formation [Bjorkbacka et al., 2004], and potentially influencing the stability of the atherosclerotic plaque [Mallat et al., 2001a]. This cytokine also appears to have a role in weight control with knockout mice having higher fat mass, possibly caused by eating dysregulation and increased feed efficiency [Zorrilla et al., 2007]. The system comprises two secreted proteins (along with two receptor proteins), IL-18BP and IL-18, both of which were studied in tandem. In essence this work has loosely applied a Mendelian randomization

[Davey Smith and Ebrahim, 2005] approach. The impact of the gene on the protein, and the protein on the disease are assessed separately. If associations are found in both of these 'arms', then, if the protein is causal in the disease, a matching association between the gene and the disease should be found.

Initially this thesis was concerned with establishing an association between genetic variation with *IL18* and IL-18 serum levels. Consistently a single *IL18* haplotype, hGTATA (frequency of ~25%), was associated with roughly 30% lower IL-18 levels when compared to the most common haplotype (hGCATA). Importantly, this association was also observed when analysing fIL-18 levels. The relative difference between hGTATA and hGCATA was greater in individuals with established disease (mean IL-18 hGTATA/mean hGCATA IL-18=0.61) than in healthy individuals (mean IL-18 hGTATA/mean hGCATA IL-18=0.80). The difference was therefore considerable and of a magnitude that, given previous published data, could have pathological consequences.

On the basis of Mendelian randomization, from the work presented here, there does not appear to be strong support of a causal role for IL-18 in CHD. Despite capturing near total genetic variation within *IL18* and *IL18BP*, strong and consistent associations between *IL18* haplotypes and fIL-18 levels, and mild associations between IL-18 serum levels and future risk of MI/post-event survival, there was no consistent difference in the frequency of *IL18* haplotypes between cases and controls. This contradicts work from the Athero*Gene* investigators.

The Athero*Gene* study is a cohort of 1229 patients with at least one stenosis >30% in a major coronary artery, followed-up for death from cardiovascular causes. Blankenberg et al. [2002] demonstrated that in this cohort the risk of death from cardiovascular causes increased near-linearly with increasing quartiles of IL-18, an association that remained significant following adjustment for potential confounders including IL-6, CRP, and BMI. Using a set of SNPs that marked genetic variation throughout *IL18*, Tiret et al. [2005] then demonstrated that an *IL18* haplotype was associated with both IL-18 serum levels and cardiovascular mortality, although the association was most strong in those deaths occurring within 4 yr of follow-up.

The largest prospective study used here, NPHSII, recruited ostensibly healthy middle-aged men. However, with an average age of 56 yr it would be surprising if a significant number did not have some evidence of atherosclerosis; within CUDAS (a population-based sample with similar age distribution to NPHSII) 29% of males have an asymptomatic carotid plaque [Chapman et al., 2006]. In NPHSII, IL-18 was significantly higher in those who went on to suffer an MI during the 15 yr of follow-up (fIL-18 was also higher, but only marginally significant). Furthermore *IL18* hGTATA was also associated with significantly lower IL-18 levels in the sub-group with IL-18 measures. However, there was no significant difference in hGTATA frequency between those who suffered an MI (n=182) and those who did not (n=2870), in fact the frequency of hG-

TATA was marginally higher in those who suffered an MI (28.4% vs. 26.4%, p=0.62).

The number of cases are comparable between the studies (NPHSII – 182; Athero*Gene* – 142), but do differ in their nature. Athero*Gene* considers cardiovascular mortality, whilst NPHSII (in the analysis here) is concerned with MI incidence, therefore it is possible that the role of IL-18 may differ between the two end-points. NPHSII does record mortality data, however, at present only 42 fatal MI events have occurred within the cohort. As might be expected given the low number of cases, no significant difference in hGTATA frequency was observed (data not shown).

CHD is a complex disease and therefore no single genetic variant will be responsible. It is possible that the studies used here lack the statistical power necessary to identify what is likely to be a small effect of *IL18* on CHD risk. In total the studies used here (SCARF and NPHSII) represent 569 CHD cases. At present there is on-going work to genotype the European Prospective Investigation of Cancer (EPIC)-Norfolk cohort [Day et al., 1999], a prospective study that currently contains 1035 CHD cases [Arsenault et al., 2007]. Combined with SCARF and NPHSII, and potentially with published data, there should be sufficient cases for a well-powered meta-analysis that will give greater confidence to the estimate of *IL18*'s role in CHD.

Obesity is known to be a major CHD risk factor, with mortality rates over 30 yr estimated to be 3.9 times higher for overweight individuals than normal weight [Garrison and Castelli, 1985], a worrying observation considering that the global obesity epidemic continues apace with over half of adult Americans being overweight [National Task Force on the Prevention and Treatment of Obesity, 2000]. IL-18 has recently been assigned a role in weight control, appearing to act through regulation of eating cycle and feed efficiency [Zorrilla et al., 2007]. The data presented here is the first demonstration that genetic variation within *IL18* is associated with BMI, and therefore the first to suggest that IL-18 may be an important regulator of weight in humans.

To date, the data regarding IL-18 and obesity has largely concentrated on its behaviour either following weightloss [Esposito et al., 2002c, 2003b; Vilarrasa et al., 2007] or in isolated adipocytes cultured from biopsies [Leick et al., 2007; Skurk et al., 2005; Wood et al., 2005]. The results from such studies, although providing associative evidence, are not able to imply causality. Indeed, further studies showing IL-18 levels are modulated by food intake [Esposito et al., 2003a, 2002b] tends to suggest that elevated levels in obesity may simply be reactive and not causative. However, the demonstration that injection of IL-18 into $il18^{-/-}$ mice reverses the adipogenic phenotype, strongly suggested IL-18 plays a central, active role in murine weight control [Zorrilla et al., 2007]. That hGTATA is associated with significantly higher BMI further implicates IL-18 in human weight control, however this association was only found in UDACS and CABG. These studies had the highest average BMI and the widest 95%CIs (CABG – 28.1[27.6–28.6]kg/m^2; UDACS – 28.5[28.1–28.9]kg/m^2; NPHSII –

23.2[23.1–26.3]kg/m^2; SCARF – 26.4[26.1–26.7]kg/m^2) of all the studies in which this analysis was carried out, therefore they represent the studies in which the spread of data is greatest and so the effect of IL-18 would most likely be apparent. However, it is also possible that the regulation of IL-18 undergoes some change during disease that results in it participating to a greater degree in weight control. Given that IL-18 secretion by adipocytes from obese donors is greater than that from non-obese (5.5±4.2 pg/ml vs. 1.8±0.9 pg/ml, p=0.09 [Skurk et al., 2005]), it is possible that the adipocyte is the site of this dysregulation.

The exact method of action for IL-18 in this instance is not wholly clear and will require further study. From the mouse studies it appears that serum IL-18 *per se* does not play a role as only intra-cerebral and intra-peritoneal injection reversed the phenotype [Zorrilla et al., 2007; Netea et al., 2006], this may explain the lack of any consistent association between serum IL-18 levels and BMI in the study groups used here. Human intestinal epithelial cells express IL-18 [Takeuchi et al., 1997] whilst IL-18R and IL-18 is expressed in the hypothalamus of adult rats [Wheeler et al., 2000]. There is therefore the potential for a regulatory loop linking food intake (serum IL-18 levels are known to be modulated by familiar foodstuffs [Esposito et al., 2003a]) and feeding behaviour (the hypothalamus play a critical role in the regulation of food intake and weight) mediated by IL-18. In such circumstances the temporal dimension of IL-18 production, to which all studies used here were ignorant, will be important (ie. it may take longer for hG-TATA carriers' serum IL-18 levels to reach a threshold that activates the hypothalamus, therefore allowing greater food intake and subsequent weight gain).

The data regarding IL-18BP suggests that genetic variation within *IL18BP* has no effect on either IL-18BP or fIL-18 levels, and furthermore does not have any bearing on incidence of CHD or obesity. However, the studies here are only concerned with one of the isoforms – IL-18BPa. This is the most abundant isoform and is able to effectively inhibit IL-18, however, so is IL-18BPc (see section 1.3.1.2 on page 33, [Kim et al., 2000]). IL-18 is a cytokine with a pivotal role in determining immune reactions, and is therefore likely to be under very tight regulation. Given IL-18BP's key role in IL-18 regulation, and that it is potentially under the control of IFNγ [Paulukat et al., 2001], it is difficult to believe that it is not influenced by/influencing disease initiation or progression. It could be that IL-18BPc, or IL-1F7 (as an enhancer of IL-18BP function [Bufler et al., 2002]) become more important in disease.

As regards the genetic data, all of the *IL18BP* tSNPs used here are relatively rare (the most common has a MAF of 12% in NPHSII) and inevitably this leads to a number of rare haplotypes; one haplotype accounts for 84% of all haplotypes in NPHSII. This lack of diversity does not lend itself to identifying differentially expressing haplotypes as the rarer a haplotype the greater the effect needs to be for it to be identified.

Throughout this thesis both IL-18 and IL-18BP, and *IL18* and *IL18BP*, have been

considered together. For the serum measures this was done by calculating fIL-18, whilst for the two genes evidence of epistasis was searched for using the MDR approach. fIL-18 was calculated for each individual given their IL-18 and IL-18BP levels, and as a calculated value (albeit using well-established biological laws) it has potential for greater error. Exactly how well this calculated value reflects the true concentration of fIL-18 across individuals (especially when it only considers the influence of IL-18BPa) is not clear, as at present there remains no other suitable method for measuring fIL-18 within the plasma.

MDR is an attractive method for searching for epistasis as its intuitive approach lends itself well to straightforward analysis. However the problem remains with the interpretation of results; as the data are split in numerous dimensions the root of a positive result becomes harder and harder to identify. As high-throughput genotyping platforms have become cheaper and more efficient, population genetics has now reached a point whereby generation of data is no longer the bottleneck, rather its processing and analysis. There is no doubt that in multi-factorial diseases, such as CHD or obesity, gene-gene interactions will exist and must be considered. At present this field is in its infancy and will no doubt develop as computing resources and statistical techniques evolve.

The MDR data presented here shows no significant interaction between *IL18* and *IL18BP*, although it is difficult to assess the size of the dataset needed to identify any interactions. IL-18Rα and IL-18Rβ (possibly with SIGIRR also) bind together to form IL-18R and, given their proximity on chromosome 2, it is possible that there are significant interactions between both the proteins and the genes. A number of SNPs within *IL18R*α and *IL18R*β have been genotyped within HapMap and therefore both genes lend themselves well to the tSNP approach. Indeed tSNPs have been selected and genotyped in NPHSII and are awaiting analysis, both individually and together. Given that there is no way to assess the SNPs effect on protein production, analysis must rely on intermediate phenotypes.

A striking observation was the considerably lower frequency of hGTATA in the UDACS subjects of African origin when compared to the Caucasian subjects. Given that this haplotype was shown to have significant effects on IL-18 production, a collaboration with the UCL Centre for Gene Genetic Anthropology was established and the distribution of hGTATA across Africa was studied. The results showed a definite cline in frequency of hGTATA, with it being seen at very low frequencies in much of southern Africa, and only rising to prominence at the very north of Africa. One of the reasons for this distribution could be positive selection at this locus, however using the EHH approach revealed no evidence for this, although it would only be able to detect positive selection that occurred within roughly the last 20000 yr. More work to assess the role of IL-18 in disease within Africa is required, but it is possible for this differ-

ence in hGTATA frequency to account to some extent for the heterogeneity in disease susceptibility seen across Africa.

For example, a recent publication showed higher expression of *IL18* in an African population with low susceptibility to malaria. Torcia et al. [2008] assessed the relative expression of a panel of genes involved in the immune response, in PBMCs taken from two sympatric populations (Fulani and Mossi, living in Barkoundouba, Burkina Faso). Both populations are homogenously exposed to *P. falciparum*, yet the Mossi show higher *P. falciparum* parasite rates than Fulani, and have have higher incidence of clinical malaria. Despite similar percentages of the different T-cell subsets, *IL18* mRNA was around five-fold higher in the Fulani than Mossi (p=0.04, [Torcia et al., 2008]). Since *IL18* may be important in malaria susceptibility it would be interesting to investigate the frequency of hGTATA in the Fulani and Mossi, or conversely, to assess the relative *P. falciparum* parasite rates, along with the incidence of other common infectious diseases, in the African populations genotyped here.

The results from the previous chapter, detailing the expression of *IL18* in PBMCs isolated from hGTATA carriers, were disappointing. No significant difference was observed in the expression of *IL18* mRNA, between individuals heterozygous for hGTATA/hGCATA and those homozygous for hGCATA. If anything, the heterozygous group was seen to have slightly higher *IL18* expression, however the difference was within the bounds of experimental error. The comparable work by Barbaux et al. [2007] was done using homozygotes of both (comparable) haplotypes, and it is clear that this significantly added to their ability to observe any difference. Further work is needed to better characterize the effect of hGTATA on *IL18*. *In vitro* work using cells isolated from individuals with known haplotypes, rather than cell lines with promoter constructs would be preferable, as the functional SNP is not yet known and may lie some distance from *IL18*. In terms of cell types, PBMCs remain a valid choice, and are particularly suitable given the ease with which they can be collected and isolated. However adipose tissue biopsies are relatively easily isolated and are a good candidate for contributing to circulating IL-18. Most importantly, hGTATA homozygotes need to be included which therefore means establishing a cohort of >300 individuals. Such a study aimed also at understanding the reactivity of IL-18 to common foodstuffs would be particularly relevant, and could establish the point of regulation whether it be *IL18* transcription or mature IL-18 release.

Ultimately the SNP(s) responsible for the association between hGTATA and decreased serum IL-18 levels must be identified. Once identified the factors responsible can be isolated and assessed as potential drug targets. Within the small region resequenced there are few serious candidates and therefore the search must be broadened beyond this region. An *in silico* approach, identifying potential regulatory or enhancer sites, in tandem with targeted genotyping of SNPs within those sites could yield a

number of candidate SNPs. It is also possible that extended genotyping and IL-18 measurement within the African cohorts may yield associations with novel haplotypes, that, when compared to common European haplotypes, isolate potentially functional SNPs/regions.

In conclusion, this thesis presents novel data that suggests a role for IL-18 in weight control. A single common *IL18* haplotype was consistently associated with lower serum fIL-18 levels, whilst also being associated with higher BMI, findings in agreement with previously published data. IL-18 is therefore an attractive anti-obesity therapeutic strategy. With regard to CHD the data does not support the theory that IL-18 is causal in atherosclerosis.

Bibliography

N. M. Albert. Inflammation and infection in acute coronary syndrome. *J. Cardiovasc. Nurs.*, 15(1):13–26, 2000.

K. G. Alberti and P. Z. Zimmet. Definition, diagnosis and classification of diabetes mellitus and its complications. part 1: diagnosis and classification of diabetes mellitus provisional report of a who consultation. *Diabet. Med.*, 15(7):539–553, 1998.

C. A. Alper, C. E. Larsen, D. P. Dubey, Z. L. Awdeh, D. A. Fici, and E. J. Yunis. The haplotype structure of the human major histocompatibility complex. *Hum. Immunol.*, 67(1-2):73–84, 2006.

E. P. Amento, N. Ehsani, H. Palmer, and P. Libby. Cytokines and growth factors positively and negatively regulate interstitial collagen gene expression in human vascular smooth muscle cells. *Arterioscler. Thromb.*, 11(5):1223–1230, 1991.

American Heart Association. Heart disease and stroke statistics – 2003 update. Report, 2002.

S. S. Anand, S. Yusuf, V. Vuksan, S. Devanesen, K. K. Teo, P. A. Montague, L. Kelemen, C. Yi, E. Lonn, H. Gerstein, R. A. Hegele, and M. McQueen. Differences in risk factors, atherosclerosis, and cardiovascular disease between ethnic groups in canada: the study of health assessment and risk in ethnic groups (share). *Lancet*, 356(9226): 279–284, 2000.

R. N. Anderson and B. L. Smith. Deaths: leading causes for 2001. *Natl. Vital Stat. Rep.*, 52(9):1–85, 2003.

T. J. Anderson, I. T. Meredith, A. C. Yeung, B. Frei, A. P. Selwyn, and P. Ganz. The effect of cholesterol-lowering and antioxidant therapy on endothelium-dependent coronary vasomotion. *N. Engl. J. Med.*, 332(8):488–493, 1995.

W. P. Arend, M. Malyak, Jr. M. F. Smith, T. D. Whisenand, J. L. Slack, J. E. Sims, J. G. Giri, and S. K. Dower. Binding of il-1 alpha, il-1 beta, and il-1 receptor antagonist by soluble il-1 receptors and levels of soluble il-1 receptors in synovial fluids. *J. Immunol.*, 153(10):4766–4774, 1994.

B. J. Arsenault, I. Lemieux, J. P. Despres, N. J. Wareham, R. Luben, J. J. Kastelein, K. T. Khaw, and S. M. Boekholdt. Cholesterol levels in small ldl particles predict the risk of coronary heart disease in the epic-norfolk prospective population study. *Eur. Heart J.*, 28(22):2770–2777, 2007.

S. M. Artaud-Wild, S. L. Connor, G. Sexton, and W. E. Connor. Differences in coronary mortality can be explained by differences in cholesterol and saturated fat intakes in 40 countries but not in france and finland. a paradox. *Circulation*, 88(6):2771–2779, 1993.

S. Asthana, S. Schmidt, and S. Sunyaev. A limited role for balancing selection. *Trends Genet.*, 21(1):30–32, 2005.

R. Balarajan. Ethnic differences in mortality from ischaemic heart disease and cerebrovascular disease in england and wales. *BMJ*, 302(6776):560–564, 1991.

R. Balarajan, P. Yuen, and V Raleigh Soni. Ethnic differences in general practitioner consultations. *BMJ*, 299(6705):958–960, 1989.

S. Barbaux, O. Poirier, T. Godefroy, H. Kleinert, S. Blankenberg, F. Cambien, and L. Tiret. Differential haplotypic expression of the interleukin-18 gene. *Eur. J. Hum. Genet.*, 15(8):856–863, 2007.

C. Bardel, V. Danjean, J. P. Hugot, P. Darlu, and E. Genin. On the use of haplotype phylogeny to detect disease susceptibility loci. *BMC. Genet.*, 6(1):24, 2005.

G. Barillari, L. Albonici, S. Incerpi, L. Bogetto, G. Pistritto, A. Volpi, B. Ensoli, and V. Manzari. Inflammatory cytokines stimulate vascular smooth muscle cells locomotion and growth by enhancing alpha5beta1 integrin expression and function. *Atherosclerosis*, 154(2):377–385, 2001.

J. C. Barrett, B. Fry, J. Maller, and M. J. Daly. Haploview: analysis and visualization of ld and haplotype maps. *Bioinformatics.*, 21(2):263–265, 2005.

S. Batzoglou, L. Pachter, J. P. Mesirov, B. Berger, and E. S. Lander. Human and mouse gene structure: comparative analysis and application to exon prediction. *Genome Res.*, 10(7):950–958, 2000.

G. S. Berenson, B. Radhakrishnamurthy, S. R. Srinivasan, P. Vijayagopal, E. R. Dalferes Jr, and C. Sharma. Recent advances in molecular pathology. carbohydrate-protein macromolecules and arterial wall integrity–a role in atherogenesis. *Exp. Mol. Pathol.*, 41(2):267–287, 1984.

J. Bereta and M. Bereta. Stimulation of glyceraldehyde-3-phosphate dehydrogenase mrna levels by endogenous nitric oxide in cytokine-activated endothelium. *Biochem. Biophys. Res. Commun.*, 217(1):363–369, 1995.

J. A. Berliner, M. Navab, A. M. Fogelman, J. S. Frank, L. L. Demer, P. A. Edwards, A. D. Watson, and A. J. Lusis. Atherosclerosis: basic mechanisms. oxidation, inflammation, and genetics. *Circulation*, 91(9):2488–2496, 1995.

X. Berrios, T. Koponen, T. Huiguang, N. Khaltaev, P. Puska, and A. Nissinen. Distribution and prevalence of major risk factors of noncommunicable diseases in selected countries: the who inter-health programme. *Bull. World Health Organ*, 75(2):99–108, 1997a.

X. Berrios, T. Koponen, T. Huiguang, N. Khaltaev, P. Puska, and A. Nissinen. Distribution and prevalence of major risk factors of noncommunicable diseases in selected countries: the who inter-health programme. *Bull. World Health Organ*, 75(2):99–108, 1997b.

P. Bhatia, W. R. Taylor, A. H. Greenberg, and J. A. Wright. Comparison of glyceraldehyde-3-phosphate dehydrogenase and 28s-ribosomal rna gene expression as rna loading controls for northern blot analysis of cell lines of varying malignant potential. *Anal. Biochem.*, 216(1):223–226, 1994.

H. Bjorkbacka, V. V. Kunjathoor, K. J. Moore, S. Koehn, C. M. Ordija, M. A. Lee, T. Means, K. Halmen, A. D. Luster, D. T. Golenbock, and M. W. Freeman. Reduced atherosclerosis in myd88-null mice links elevated serum cholesterol levels to activation of innate immunity signaling pathways. *Nat. Med.*, 10(4):416–421, 2004.

S. Blankenberg, H. J. Rupprecht, C. Bickel, C. Espinola-Klein, G. Rippin, G. Hafner, M. Ossendorf, K. Steinhagen, and J. Meyer. Cytomegalovirus infection with interleukin-6 response predicts cardiac mortality in patients with coronary artery disease. *Circulation*, 103(24):2915–2921, 2001.

S. Blankenberg, L. Tiret, C. Bickel, D. Peetz, F. Cambien, J. Meyer, and H. J. Rupprecht. Interleukin-18 is a strong predictor of cardiovascular death in stable and unstable angina. *Circulation*, 106(1):24–30, 2002.

S. Blankenberg, G. Luc, P. Ducimetiere, D. Arveiler, J. Ferrieres, P. Amouyel, A. Evans, F. Cambien, and L. Tiret. Interleukin-18 and the risk of coronary heart disease in european men: the prospective epidemiological study of myocardial infarction (prime). *Circulation*, 108(20):2453–2459, 2003.

S. Blankenberg, M. J. McQueen, M. Smieja, J. Pogue, C. Balion, E. Lonn, H. J. Rupprecht, C. Bickel, L. Tiret, F. Cambien, H. Gerstein, T. Munzel, and S. Yusuf. Comparative impact of multiple biomarkers and n-terminal pro-brain natriuretic peptide in the context of conventional risk factors for the prediction of recurrent cardiovascular events in the heart outcomes prevention evaluation (hope) study. *Circulation*, 114 (3):201–208, 2006.

U. Boehm, T. Klamp, M. Groot, and J. C. Howard. Cellular responses to interferon-gamma. *Annu. Rev. Immunol.*, 15:749–795, 1997.

G. Bondjers, O. Wiklund, G. Fager, E. H. Camejo, and G. Camejo. Transfer of lipoproteins from plasma to the cell populations of the normal and atherosclerotic arterial tissue. *Eur. Heart J.*, 11 Suppl E:158–163, 1990.

D. Boraschi and C. A. Dinarello. Il-18 in autoimmunity: review. *Eur. Cytokine Netw.*, 17(4):224–252, 2006.

T. L. Born, E. Thomassen, T. A. Bird, and J. E. Sims. Cloning of a novel receptor subunit, acpl, required for interleukin-18 signaling. *J. Biol. Chem.*, 273(45):29445–29450, 1998.

A. Bowie and L. A. O'Neill. The interleukin-1 receptor/toll-like receptor superfamily: signal generators for pro-inflammatory interleukins and microbial products. *J. Leukoc. Biol.*, 67(4):508–514, 2000.

K. Brand, C. L. Banka, N. Mackman, R. A. Terkeltaub, S. T. Fan, and L. K. Curtiss. Oxidized ldl enhances lipopolysaccharide-induced tissue factor expression in human adherent monocytes. *Arterioscler. Thromb.*, 14(5):790–797, 1994.

E. Braunwald. Shattuck lecture–cardiovascular medicine at the turn of the millennium: triumphs, concerns, and opportunities. *N. Engl. J. Med.*, 337(19):1360–1369, 1997.

N. Bray, I. Dubchak, and L. Pachter. Avid: A global alignment program. *Genome Res.*, 13(1):97–102, 2003.

J. L. Breslow. Cardiovascular disease burden increases, nih funding decreases. *Nat. Med.*, 3(6):600–601, 1997.

British Heart Foundation. Coronary heart disease statistics. British Heart Foundation, 1999.

M. S. Brown and J. L. Goldstein. A receptor-mediated pathway for cholesterol homeostasis. *Science*, 232(4746):34–47, 1986.

M. Brudno, C. B. Do, G. M. Cooper, M. F. Kim, E. Davydov, E. D. Green, A. Sidow, and S. Batzoglou. Lagan and multi-lagan: efficient tools for large-scale multiple alignment of genomic dna. *Genome Res.*, 13(4):721–731, 2003a.

M. Brudno, S. Malde, A. Poliakov, C. B. Do, O. Couronne, I. Dubchak, and S. Batzoglou. Glocal alignment: finding rearrangements during alignment. *Bioinformatics.*, 19 Suppl 1:i54–i62, 2003b.

D. J. Brull, H. E. Montgomery, J. Sanders, S. Dhamrait, L. Luong, A. Rumley, G. D. Lowe, and S. E. Humphries. Interleukin-6 gene -174g¿c and -572g¿c promoter polymorphisms are strong predictors of plasma interleukin-6 levels after coronary artery bypass surgery. *Arterioscler. Thromb. Vasc. Biol.*, 21(9):1458–1463, 2001.

P. Bufler, T. Azam, F. Gamboni-Robertson, L. L. Reznikov, S. Kumar, C. A. Dinarello, and S. H. Kim. A complex of the il-1 homologue il-1f7b and il-18-binding protein reduces il-18 activity. *Proc. Natl. Acad. Sci. U. S. A*, 99(21):13723–13728, 2002.

C. Buono, C. E. Come, G. Stavrakis, G. F. Maguire, P. W. Connelly, and A. H. Lichtman. Influence of interferon-gamma on the extent and phenotype of diet-induced atherosclerosis in the ldlr-deficient mouse. *Arterioscler. Thromb. Vasc. Biol.*, 23(3): 454–460, 2003.

E. C. Butcher. Leukocyte-endothelial cell recognition: three (or more) steps to specificity and diversity. *Cell*, 67(6):1033–1036, 1991.

F. Calara, P. Dimayuga, A. Niemann, J. Thyberg, U. Diczfalusy, J. L. Witztum, W. Palinski, P. K. Shah, B. Cercek, J. Nilsson, and J. Regnstrom. An animal model to study local oxidation of ldl and its biological effects in the arterial wall. *Arterioscler. Thromb. Vasc. Biol.*, 18(6):884–893, 1998.

A. D. Callow. Cardiovascular disease 2005–the global picture. *Vascul. Pharmacol.*, 45 (5):302–307, 2006.

L. R. Cardon and G. R. Abecasis. Using haplotype blocks to map human complex trait loci. *Trends Genet.*, 19(3):135–140, 2003.

S. M. Cardoso, T. E. DeFor, L. A. Tilley, J. L. Bidwell, D. J. Weisdorf, and M. L. MacMillan. Patient interleukin-18 gcg haplotype associates with improved survival and decreased transplant-related mortality after unrelated-donor bone marrow transplantation. *Br. J. Haematol.*, 126(5):704–710, 2004.

K. Cartharius, K. Frech, K. Grote, B. Klocke, M. Haltmeier, A. Klingenhoff, M. Frisch, M. Bayerlein, and T. Werner. Matinspector and beyond: promoter analysis based on transcription factor binding sites. *Bioinformatics.*, 21(13):2933–2942, 2005.

J. P. Casas, L. E. Bautista, L. Smeeth, P. Sharma, and A. D. Hingorani. Homocysteine and stroke: evidence on a causal link from mendelian randomisation. *Lancet*, 365 (9455):224–232, 2005.

Census of Population and Housing. Population and housing characteristics for census tracts and block numbering areas, los angeles - anaheim - riverside, ca. Report, 1990.

G. K. Chalikias, D. N. Tziakas, J. C. Kaski, E. I. Hatzinikolaou, D. A. Stakos, I. K. Tentes, A. Kortsaris, and D. I. Hatseras. Interleukin-18: interleukin-10 ratio and in-hospital adverse events in patients with acute coronary syndrome. *Atherosclerosis*, 182(1):135–143, 2005.

J. R. Chan, S. J. Hyduk, and M. I. Cybulsky. Detecting rapid and transient upregulation of leukocyte integrin affinity induced by chemokines and chemoattractants. *J. Immunol. Methods*, 273(1-2):43–52, 2003.

T. J. Chang, C. C. Juan, P. H. Yin, C. W. Chi, and H. J. Tsay. Up-regulation of beta-actin, cyclophilin and gapdh in n1s1 rat hepatoma. *Oncol. Rep.*, 5(2):469–471, 1998.

C. M. Chapman, B. M. McQuillan, J. P. Beilby, P. L. Thompson, and J. Hung. Interleukin-18 levels are not associated with subclinical carotid atherosclerosis in a community population the perth carotid ultrasound disease assessment study (cudas). *Atherosclerosis*, 189:414–419, 2006.

I. F. Charo and M. B. Taubman. Chemokines in the pathogenesis of vascular disease. *Circ. Res.*, 95(9):858–866, 2004.

N. Chaturvedi, P. M. McKeigue, and M. G. Marmot. Resting and ambulatory blood pressure differences in afro-caribbeans and europeans. *Hypertension*, 22(1):90–96, 1993.

Z. Chen, R. Peto, R. Collins, S. MacMahon, J. Lu, and W. Li. Serum cholesterol concentration and coronary heart disease in population with low cholesterol concentrations. *BMJ*, 303(6797):276–282, 1991.

G. M. Chisolm III, S. L. Hazen, P. L. Fox, and M. K. Cathcart. The oxidation of lipoproteins by monocytes-macrophages. biochemical and biological mechanisms. *J. Biol. Chem.*, 274(37):25959–25962, 1999.

H. K. Chung, I. K. Lee, H. Kang, J. M. Suh, H. Kim, K. C. Park, D. W. Kim, Y. K. Kim, H. K. Ro, and M. Shong. Statin inhibits interferon-gamma-induced expression of intercellular adhesion molecule-1 (icam-1) in vascular endothelial and smooth muscle cells. *Exp. Mol. Med.*, 34(6):451–461, 2002.

M. Clarke and M. Bennett. The emerging role of vascular smooth muscle cell apoptosis in atherosclerosis and plaque stability. *Am. J. Nephrol.*, 26(6):531–535, 2006.

M. C. Clarke, N. Figg, J. J. Maguire, A. P. Davenport, M. Goddard, T. D. Littlewood, and M. R. Bennett. Apoptosis of vascular smooth muscle cells induces features of plaque vulnerability in atherosclerosis. *Nat. Med.*, 12(9):1075–1080, 2006.

R. Cooper and C. Rotimi. Hypertension in populations of west african origin: is there a genetic predisposition? *J. Hypertens.*, 12(3):215–227, 1994.

R. Cooper, C. Rotimi, S. Ataman, D. McGee, B. Osotimehin, S. Kadiri, W. Muna, S. Kingue, H. Fraser, T. Forrester, F. Bennett, and R. Wilks. The prevalence of hypertension in seven populations of west african origin. *Am. J. Public Health*, 87 (2):160–168, 1997.

R. Cooper, J. Cutler, P. Desvigne-Nickens, S. P. Fortmann, L. Friedman, R. Havlik, G. Hogelin, J. Marler, P. McGovern, G. Morosco, L. Mosca, T. Pearson, J. Stamler, D. Stryer, and T. Thom. Trends and disparities in coronary heart disease, stroke, and other cardiovascular diseases in the united states - findings of the national conference on cardiovascular disease prevention. *Circulation*, 102(25):3137–3147, 2000.

R. S. Cooper. Health and the social status of blacks in the united states. *Ann. Epidemiol.*, 3(2):137–144, 1993.

M. H. Criqui and B. L. Ringel. Does diet or alcohol explain the french paradox? *Lancet*, 344(8939-8940):1719–1723, 1994.

A. Daugherty, N. R. Webb, D. L. Rateri, and V. L. King. Thematic review series: The immune system and atherogenesis. cytokine regulation of macrophage functions in atherogenesis. *J. Lipid Res.*, 46(9):1812–1822, 2005.

G. Davey Smith and S. Ebrahim. What can mendelian randomisation tell us about modifiable behavioural and environmental exposures? *BMJ*, 330(7499):1076–1079, 2005.

M. J. Davies. Glagovian remodelling, plaque composition, and stenosis generation. *Heart*, 84(5):461–462, 2000.

M. J. Davies and N. Woolf. Atherosclerosis: what is it and why does it occur? *Br. Heart J.*, 69(1 Suppl):S3–11, 1993.

M. J. Davies, P. D. Richardson, N. Woolf, D. R. Katz, and J. Mann. Risk of thrombosis in human atherosclerotic plaques: role of extracellular lipid, macrophage, and smooth muscle cell content. *Br. Heart J.*, 69(5):377–381, 1993.

P. F. Davies, M. A. Reidy, T. B. Goode, and D. E. Bowyer. Scanning electron microscopy in the evaluation of endothelial integrity of the fatty lesion in atherosclerosis. *Atherosclerosis*, 25(1):125–130, 1976.

P. F. Davies, J. A. Spaan, and R. Krams. Shear stress biology of the endothelium. *Ann. Biomed. Eng*, 33(12):1714–1718, 2005.

J. Davignon and P. Ganz. Role of endothelial dysfunction in atherosclerosis. *Circulation*, 109(23 Suppl 1):III27–III32, 2004.

I. N. Day and S. E. Humphries. Electrophoresis for genotyping: microtiter array diagonal gel electrophoresis on horizontal polyacrylamide gels, hydrolink, or agarose. *Anal. Biochem.*, 222(2):389–395, 1994.

N. Day, S. Oakes, R. Luben, K. T. Khaw, S. Bingham, A. Welch, and N. Wareham. Epic-norfolk: study design and characteristics of the cohort. european prospective investigation of cancer. *Br. J. Cancer*, 80 Suppl 1:95–103, 1999.

P. I. de Bakker, R. Yelensky, I. Pe'er, S. B. Gabriel, M. J. Daly, and D. Altshuler. Efficiency and power in genetic association studies. *Nat. Genet.*, 37(11):1217–1223, 2005.

J. H. der Thusen, J. Kuiper, T. J. van Berkel, and E. A. Biessen. Interleukins in atherosclerosis: molecular pathways and therapeutic potential. *Pharmacol. Rev.*, 55 (1):133–166, 2003.

S. S. Dhamrait, J. W. Stephens, J. A. Cooper, J. Acharya, A. R. Mani, K. Moore, G. J. Miller, S. E. Humphries, S. J. Hurel, and H. E. Montgomery. Cardiovascular risk in healthy men and markers of oxidative stress in diabetic men are associated with common variation in the gene for uncoupling protein 2. *Eur. Heart J.*, 25(6):468–475, 2004.

S. P. Donnan, S. C. Ho, J. Woo, S. L. Wong, K. S. Woo, C. Y. Tse, K. K. Chan, C. S. Kay, K. O. Cheung, and K. H. Mak. Risk factors for acute myocardial infarction in a southern chinese population. *Ann. Epidemiol.*, 4(1):46–58, 1994.

F. Drenos, J. C. Whittaker, and S. E. Humphries. The use of meta-analysis risk estimates for candidate genes in combination to predict coronary heart disease risk. *Ann. Hum. Genet.*, 71(Pt 5):611–619, 2007.

I. Dubchak, M. Brudno, G. G. Loots, L. Pachter, C. Mayor, E. M. Rubin, and K. A. Frazer. Active conservation of noncoding sequences revealed by three-way species comparisons. *Genome Res.*, 10(9):1304–1306, 2000.

J. B. Duguid. Thrombosis as a factor in the pathogenesis of coronary atherosclerosis. *Journal of Pathology and Bacteriology*, 58(2):207, 1946.

L. V. d'Uscio, S. Milstien, D. Richardson, L. Smith, and Z. S. Katusic. Long-term vitamin c treatment increases vascular tetrahydrobiopterin levels and nitric oxide synthase activity. *Circ. Res.*, 92(1):88–95, 2003.

C. Ehnholm, J. K. Huttunen, P. Pietinen, U. Leino, M. Mutanen, E. Kostiainen, J. Pikkarainen, R. Dougherty, J. Iacono, and P. Puska. Effect of diet on serum lipoproteins in a population with a high risk of coronary heart disease. *N. Engl. J. Med.*, 307 (14):850–855, 1982.

S. Ehrt, D. Schnappinger, S. Bekiranov, J. Drenkow, S. Shi, T. R. Gingeras, T. Gaasterland, G. Schoolnik, and C. Nathan. Reprogramming of the macrophage transcriptome in response to interferon-gamma and mycobacterium tuberculosis: signaling roles of nitric oxide synthase-2 and phagocyte oxidase. *J. Exp. Med.*, 194(8):1123–1140, 2001.

R. Elhage, J. Jawien, M. Rudling, H. G. Ljunggren, K. Takeda, S. Akira, F. Bayard, and G. K. Hansson. Reduced atherosclerosis in interleukin-18 deficient apolipoprotein e-knockout mice. *Cardiovasc. Res.*, 59(1):234–240, 2003.

E. A. Enas, S. Yusuf, and J. L. Mehta. Prevalence of coronary artery disease in asian indians. *Am. J. Cardiol.*, 70(9):945–949, 1992.

M. Endres, U. Laufs, Z. Huang, T. Nakamura, P. Huang, M. A. Moskowitz, and J. K. Liao. Stroke protection by 3-hydroxy-3-methylglutaryl (hmg)-coa reductase inhibitors mediated by endothelial nitric oxide synthase. *Proc. Natl. Acad. Sci. U. S. A*, 95(15):8880–8885, 1998.

P. Eriksson, H. Deguchi, A. Samnegard, P. Lundman, S. Boquist, P. Tornvall, C. G. Ericsson, L. Bergstrand, L. O. Hansson, S. Ye, and A. Hamsten. Human evidence that the cystatin c gene is implicated in focal progression of coronary artery disease. *Arterioscler. Thromb. Vasc. Biol.*, 24(3):551–557, 2004.

K. Esposito, F. Nappo, R. Marfella, G. Giugliano, F. Giugliano, M. Ciotola, L. Quagliaro, A. Ceriello, and D. Giugliano. Inflammatory cytokine concentrations are acutely increased by hyperglycemia in humans: role of oxidative stress. *Circulation*, 106(16):2067–2072, 2002a.

K. Esposito, F. Nappo, R. Marfella, G. Giugliano, F. Giugliano, M. Ciotola, L. Quagliaro, A. Ceriello, and D. Giugliano. Inflammatory cytokine concentrations are acutely increased by hyperglycemia in humans: role of oxidative stress. *Circulation*, 106(16):2067–2072, 2002b.

K. Esposito, A. Pontillo, M. Ciotola, C. Di Palo, E. Grella, G. Nicoletti, and D. Giugliano. Weight loss reduces interleukin-18 levels in obese women. *J. Clin. Endocrinol. Metab*, 87(8):3864–3866, 2002c.

K. Esposito, F. Nappo, F. Giugliano, C. Di Palo, M. Ciotola, M. Barbieri, G. Paolisso, and D. Giugliano. Meal modulation of circulating interleukin 18 and adiponectin concentrations in healthy subjects and in patients with type 2 diabetes mellitus. *Am. J. Clin. Nutr.*, 78(6):1135–1140, 2003a.

K. Esposito, A. Pontillo, C. Di Palo, G. Giugliano, M. Masella, R. Marfella, and D. Giugliano. Effect of weight loss and lifestyle changes on vascular inflammatory markers in obese women: a randomized trial. *JAMA*, 289(14):1799–1804, 2003b.

L. Excoffier and M. Slatkin. Maximum-likelihood estimation of molecular haplotype frequencies in a diploid population. *Mol. Biol. Evol.*, 12(5):921–927, 1995.

L. Excoffier, P. E. Smouse, and J. M. Quattro. Analysis of molecular variance inferred from metric distances among dna haplotypes: application to human mitochondrial dna restriction data. *Genetics*, 131(2):479–491, 1992.

A. Ferro-Luzzi, P. Strazzullo, C. Scaccini, A. Siani, S. Sette, M. A. Mariani, P. Mastranzo, R. M. Dougherty, J. M. Iacono, and M. Mancini. Changing the mediterranean diet: effects on blood lipids. *Am. J. Clin. Nutr.*, 40(5):1027–1037, 1984.

C. P. Fischer, L. B. Perstrup, A. Berntsen, P. Eskildsen, and B. K. Pedersen. Elevated plasma interleukin-18 is a marker of insulin-resistance in type 2 diabetic and non-diabetic humans. *Clin. Immunol.*, 117(2):152–160, 2005.

V. A. Folcik, R. Aamir, and M. K. Cathcart. Cytokine modulation of ldl oxidation by activated human monocytes. *Arterioscler. Thromb. Vasc. Biol.*, 17(10):1954–1961, 1997.

L. G. Fong, T. S. Albert, and S. E. Hom. Inhibition of the macrophage-induced oxidation of low density lipoprotein by interferon-gamma. *J. Lipid Res.*, 35(5):893–904, 1994.

D. L. Foss, M. J. Baarsch, and M. P. Murtaugh. Regulation of hypoxanthine phosphoribosyltransferase, glyceraldehyde-3-phosphate dehydrogenase and beta-actin mrna expression in porcine immune cells and tissues. *Anim Biotechnol.*, 9(1):67–78, 1998.

C. K. Francis. Research in coronary heart disease in blacks: issues and challenges. *J. Health Care Poor Underserved*, 8(3):250–269, 1997.

S. Frantz, A. Ducharme, D. Sawyer, L. E. Rohde, L. Kobzik, R. Fukazawa, D. Tracey, H. Allen, R. T. Lee, and R. A. Kelly. Targeted deletion of caspase-1 reduces early mortality and left ventricular dilatation following myocardial infarction. *J. Mol. Cell Cardiol.*, 35(6):685–694, 2003.

K. A. Frazer, L. Pachter, A. Poliakov, E. M. Rubin, and I. Dubchak. Vista: computational tools for comparative genomics. *Nucleic Acids Res.*, 32(Web Server issue): W273–W279, 2004.

J. Frostegard, A. K. Ulfgren, P. Nyberg, U. Hedin, J. Swedenborg, U. Andersson, and G. K. Hansson. Cytokine expression in advanced human atherosclerotic plaques: dominance of pro-inflammatory (th1) and macrophage-stimulating cytokines. *Atherosclerosis*, 145(1):33–43, 1999.

A. Gaggero, A. De Ambrosis, D. Mezzanzanica, T. Piazza, A. Rubartelli, M. Figini, S. Canevari, and S. Ferrini. A novel isoform of pro-interleukin-18 expressed in ovarian tumors is resistant to caspase-1 and -4 processing. *Oncogene*, 23(45):7552–7560, 2004.

Z. S. Galis, G. K. Sukhova, M. W. Lark, and P. Libby. Increased expression of matrix metalloproteinases and matrix degrading activity in vulnerable regions of human atherosclerotic plaques. *J. Clin. Invest*, 94(6):2493–2503, 1994.

R. J. Garrison and W. P. Castelli. Weight and thirty-year mortality of men in the framingham study. *Ann. Intern. Med.*, 103(6 (Pt 2)):1006–1009, 1985.

Y. J. Geng and G. K. Hansson. Interferon-gamma inhibits scavenger receptor expression and foam cell formation in human monocyte-derived macrophages. *J. Clin. Invest*, 89(4):1322–1330, 1992.

Y. J. Geng, Q. Wu, M. Muszynski, G. K. Hansson, and P. Libby. Apoptosis of vascular smooth muscle cells induced by in vitro stimulation with interferon-gamma, tumor necrosis factor-alpha, and interleukin-1 beta. *Arterioscler. Thromb. Vasc. Biol.*, 16 (1):19–27, 1996.

A. T. Geronimus, J. Bound, T. A. Waidmann, M. M. Hillemeier, and P. B. Burns. Excess mortality among blacks and whites in the united states. *N. Engl. J. Med.*, 335(21): 1552–1558, 1996.

V. Giedraitis, B. He, W. X. Huang, and J. Hillert. Cloning and mutation analysis of the human il-18 promoter: a possible role of polymorphisms in expression regulation. *J. Neuroimmunol.*, 112(1-2):146–152, 2001.

R. F. Gillum. The epidemiology of cardiovascular disease in black americans. *N. Engl. J. Med.*, 335(21):1597–1599, 1996.

S. Glagov, C. Zarins, D. P. Giddens, and D. N. Ku. Hemodynamics and atherosclerosis. insights and perspectives gained from studies of human arteries. *Arch. Pathol. Lab Med.*, 112(10):1018–1031, 1988.

J. Glas, H. P. Torok, L. Tonenchi, J. Kapser, U. Schiemann, B. Muller-Myhsok, M. Folwaczny, and C. Folwaczny. Association of polymorphisms in the interleukin-18 gene in patients with crohn's disease depending on the card15/nod2 genotype. *Inflamm. Bowel. Dis.*, 11(12):1031–1037, 2005.

E. Groszek and S. M. Grundy. The possible role of the arterial microcirculation in the pathogenesis of atherosclerosis. *J. Chronic. Dis.*, 33(11-12):679–684, 1980.

S. M. Grundy. Metabolic syndrome: a multiplex cardiovascular risk factor. *J. Clin. Endocrinol. Metab*, 92(2):399–404, 2007.

L. Gu, S. C. Tseng, and B. J. Rollins. Monocyte chemoattractant protein-1. *Chem. Immunol.*, 72:7–29, 1999.

R. Gupta and V. P. Gupta. Meta-analysis of coronary heart disease prevalence in india. *Indian Heart J.*, 48(3):241–245, 1996.

S. Gupta, A. M. Pablo, X. Jiang, N. Wang, A. R. Tall, and C. Schindler. Ifn-gamma potentiates atherosclerosis in apoe knock-out mice. *J. Clin. Invest*, 99(11):2752–2761, 1997.

J. R. Guyton and K. F. Klemp. Early extracellular and cellular lipid deposits in aorta of cholesterol-fed rabbits. *Am. J. Pathol.*, 141(4):925–936, 1992.

J. R. Guyton, T. M. Bocan, and T. A. Schifani. Quantitative ultrastructural analysis of perifibrous lipid and its association with elastin in nonatherosclerotic human aorta. *Arteriosclerosis*, 5(6):644–652, 1985.

C. G. Hames, K. Rose, M. Knowles, C. E. Davis, and H. A. Tyroler. Black-white comparisons of 20-year coronary heart disease mortality in the evans county heart study. *Cardiology*, 82(2-3):122–136, 1993.

R. A. Hand and A. B. Chandler. Atherosclerotic metamorphosis of autologous pulmonary thromboemboli in rabbit. *American Journal of Pathology*, 40(4):469, 1962.

G. K. Hansson. Immune mechanisms in atherosclerosis. *Arterioscler. Thromb. Vasc. Biol.*, 21(12):1876–1890, 2001.

G. K. Hansson, J. Holm, and L. Jonasson. Detection of activated t lymphocytes in the human atherosclerotic plaque. *Am. J. Pathol.*, 135(1):169–175, 1989.

HapMap. The international hapmap project. *Nature*, 426(6968):789–796, 2003.

E. J. Harvey and D. P. Ramji. Interferon-gamma and atherosclerosis: pro- or anti-atherogenic? *Cardiovasc. Res.*, 67(1):11–20, 2005.

W. H. Hauss, G. Junge-Huelsing, and H. J. Hollander. Changes in metabolism of connective tissue associated with ageing and arterio- or atherosclerosis. *J. Atheroscler. Res.*, 2:50–61, 1962.

M. E. Hawley and K. K. Kidd. Haplo: a program using the em algorithm to estimate the frequencies of multi-site haplotypes. *J. Hered.*, 86(5):409–411, 1995.

A. Heinzmann, K. Gerhold, K. Ganter, T. Kurz, L. Schuchmann, R. Keitzer, R. Berner, and K. A. Deichmann. Association study of polymorphisms within interleukin-18 in juvenile idiopathic arthritis and bronchial asthma. *Allergy*, 59(8):845–849, 2004.

S. O. Henderson, G. A. Coetzee, R. K. Ross, M. C. Yu, and B. E. Henderson. Elevated mortality rates from circulatory disease in african american men and women of los angeles county, california–a possible genetic susceptibility? *Am. J. Med. Sci.*, 320 (1):18–23, 2000.

M. G. Hennerici. The unstable plaque. *Cerebrovasc. Dis.*, 17 Suppl 3:17–22, 2004.

T. Henriksen, E. M. Mahoney, and D. Steinberg. Enhanced macrophage degradation of low density lipoprotein previously incubated with cultured endothelial cells: recognition by receptors for acetylated low density lipoproteins. *Proc. Natl. Acad. Sci. U. S. A*, 78(10):6499–6503, 1981.

C. Herder, N. Klopp, J. Baumert, M. Muller, N. Khuseyinova, C. Meisinger, S. Martin, T. Illig, W. Koenig, and B. Thorand. Effect of macrophage migration inhibitory factor (mif) gene variants and mif serum concentrations on the risk of type 2 diabetes: results from the monica/kora augsburg case-cohort study, 1984-2002. *Diabetologia*, 2007.

S. Higa, T. Hirano, M. Mayumi, M. Hiraoka, Y. Ohshima, M. Nambu, E. Yamaguchi, N. Hizawa, N. Kondo, E. Matsui, Y. Katada, A. Miyatake, I. Kawase, and T. Tanaka. Association between interleukin-18 gene polymorphism 105a/c and asthma. *Clin. Exp. Allergy*, 33(8):1097–1102, 2003.

H. F. Hoff and J. O'Neil. Lesion-derived low density lipoprotein and oxidized low density lipoprotein share a lability for aggregation, leading to enhanced macrophage degradation. *Arterioscler. Thromb.*, 11(5):1209–1222, 1991.

T. L. Horvath. The hardship of obesity: a soft-wired hypothalamus. *Nat. Neurosci.*, 8 (5):561–565, 2005.

K. Hoshino, H. Tsutsui, T. Kawai, K. Takeda, K. Nakanishi, Y. Takeda, and S. Akira. Cutting edge: generation of il-18 receptor-deficient mice: evidence for il-1 receptor-related protein as an essential il-18 binding receptor. *J. Immunol.*, 162(9):5041–5044, 1999.

B. N. Howie, C. S. Carlson, M. J. Rieder, and D. A. Nickerson. Efficient selection of tagging single-nucleotide polymorphisms in multiple populations. *Hum. Genet.*, 120 (1):58–68, 2006.

T. K. Hsiai, S. K. Cho, P. K. Wong, M. Ing, A. Salazar, A. Sevanian, M. Navab, L. L. Demer, and C. M. Ho. Monocyte recruitment to endothelial cells in response to oscillatory shear stress. *FASEB J.*, 17(12):1648–1657, 2003.

T. R. Hughes, T. S. Tengku-Muhammad, S. A. Irvine, and D. P. Ramji. A novel role of sp1 and sp3 in the interferon-gamma -mediated suppression of macrophage lipoprotein lipase gene transcription. *J. Biol. Chem.*, 277(13):11097–11106, 2002.

J. Hulthe, W. McPheat, A. Samnegard, P. Tornvall, A. Hamsten, and P. Eriksson. Plasma interleukin (il)-18 concentrations is elevated in patients with previous myocardial infarction and related to severity of coronary atherosclerosis independently of c-reactive protein and il-6. *Atherosclerosis*, 188(2):450–454, 2006.

J. Hung, B. M. McQuillan, C. M. Chapman, P. L. Thompson, and J. P. Beilby. Elevated interleukin-18 levels are associated with the metabolic syndrome independent of obesity and insulin resistance. *Arterioscler. Thromb. Vasc. Biol.*, 25(6):1268–1273, 2005.

G. W. Hunninghake, B. G. Monks, L. J. Geist, M. M. Monick, M. A. Monroy, M. F. Stinski, A. C. Webb, J. M. Dayer, P. E. Auron, and M. J. Fenton. The functional importance of a cap site-proximal region of the human prointerleukin 1 beta gene is defined by viral protein trans-activation. *Mol. Cell Biol.*, 12(8):3439–3448, 1992.

V. Hurgin, D. Novick, and M. Rubinstein. The promoter of il-18 binding protein: activation by an ifn-gamma -induced complex of ifn regulatory factor 1 and ccaat/enhancer binding protein beta. *Proc. Natl. Acad. Sci. U. S. A*, 99(26):16957–16962, 2002.

I. G. Huttner and G. Gabbiani. Vascular endothelium in hypertension. In Genest J, Kuchel O, Hamet P, and Cantin M, editors, *Hypertension*, pages 473–488. McGraw-Hill, 1983.

A. Ide, E. Kawasaki, N. Abiru, F. Sun, M. Kobayashi, T. Fukushima, R. Takahashi, H. Kuwahara, A. Kita, K. Oshima, S. Uotani, H. Yamasaki, Y. Yamaguchi, and K. Eguchi. Association between il-18 gene promoter polymorphisms and ctla-4 gene 49a/g polymorphism in japanese patients with type 1 diabetes. *J. Autoimmun.*, 22(1): 73–78, 2004.

M. Imboden, L. Nicod, A. Nieters, E. Glaus, G. Matyas, A. J. Bircher, U. Ackermann-Liebrich, W. Berger, and N. M. Probst-Hensch. The common g-allele of interleukin-18 single-nucleotide polymorphism is a genetic risk factor for atopic asthma. the sapaldia cohort study. *Clin. Exp. Allergy*, 36(2):211–218, 2006.

Y. Inagaki, S. Yamagishi, S. Amano, T. Okamoto, K. Koga, and Z. Makita. Interferon-gamma-induced apoptosis and activation of thp-1 macrophages. *Life Sci.*, 71(21): 2499–2508, 2002.

W. Jessup, L. Kritharides, and R. Stocker. Lipid oxidation in atherogenesis: an overview. *Biochem. Soc. Trans.*, 32(Pt 1):134–138, 2004.

G. C. Johnson, L. Esposito, B. J. Barratt, A. N. Smith, J. Heward, G. Di Genova, H. Ueda, H. J. Cordell, I. A. Eaves, F. Dudbridge, R. C. Twells, F. Payne, W. Hughes, S. Nutland, H. Stevens, P. Carr, E. Tuomilehto-Wolf, J. Tuomilehto, S. C. Gough, D. G. Clayton, and J. A. Todd. Haplotype tagging for the identification of common disease genes. *Nat. Genet.*, 29(2):233–237, 2001.

B. Johnston and E. C. Butcher. Chemokines in rapid leukocyte adhesion triggering and migration. *Semin. Immunol.*, 14(2):83–92, 2002.

Joint National Committee. The sixth report of the joint national committee on prevention, detection, evaluation, and treatment of high blood pressure. Report, 1997.

D. W. Jones, L. E. Chambless, A. R. Folsom, G. Heiss, R. G. Hutchinson, A. R. Sharrett, M. Szklo, and H. A. Taylor Jr. Risk factors for coronary heart disease in african americans: the atherosclerosis risk in communities study, 1987-1997. *Arch. Intern. Med.*, 162(22):2565–2571, 2002.

U. Kalina, K. Ballas, N. Koyama, D. Kauschat, C. Miething, J. Arnemann, H. Martin, D. Hoelzer, and O. G. Ottmann. Genomic organization and regulation of the human interleukin-18 gene. *Scand. J. Immunol.*, 52(6):525–530, 2000.

M. B. Katan, P. L. Zock, and R. P. Mensink. Dietary oils, serum lipoproteins, and coronary heart disease. *Am. J. Clin. Nutr.*, 61(6 Suppl):1368S–1373S, 1995.

Z. Kato, J. Jee, H. Shikano, M. Mishima, I. Ohki, H. Ohnishi, A. Li, K. Hashimoto, E. Matsukuma, K. Omoya, Y. Yamamoto, T. Yoneda, T. Hara, N. Kondo, and M. Shirakawa. The structure and binding mode of interleukin-18. *Nat. Struct. Biol.*, 10(11): 966–971, 2003.

J. S. Kaufman, E. E. Owoaje, S. A. James, C. N. Rotimi, and R. S. Cooper. Determinants of hypertension in west africa: contribution of anthropometric and dietary factors to urban-rural and socioeconomic gradients. *Am. J. Epidemiol.*, 143(12):1203–1218, 1996.

D. Kawasaki, T. Tsujino, S. Morimoto, Y. Fujioka, Y. Naito, T. Okumura, M. Masutani, H. Shimizu, M. Yuba, A. Ueda, M. Ohyanagi, S. Kashiwamura, H. Okamura, and T. Iwasaki. Usefulness of circulating interleukin-18 concentration in acute myocardial infarction as a risk factor for late restenosis after emergency coronary angioplasty. *Am. J. Cardiol.*, 91(10):1258–1261, 2003.

J. E. Keil, S. E. Sutherland, R. G. Knapp, and H. A. Tyroler. Does equal socioeconomic status in black and white men mean equal risk of mortality? *Am. J. Public Health*, 82(8):1133–1136, 1992.

J. E. Keil, S. E. Sutherland, R. G. Knapp, D. T. Lackland, P. C. Gazes, and H. A. Tyroler. Mortality rates and risk factors for coronary disease in black as compared with white men and women. *N. Engl. J. Med.*, 329(2):73–78, 1993.

J. E. Keil, S. E. Sutherland, C. G. Hames, D. T. Lackland, P. C. Gazes, R. G. Knapp, and H. A. Tyroler. Coronary disease mortality and risk factors in black and white men. results from the combined charleston, sc, and evans county, georgia, heart studies. *Arch. Intern. Med.*, 155(14):1521–1527, 1995.

W. J. Kent. Blat–the blast-like alignment tool. *Genome Res.*, 12(4):656–664, 2002.

W. J. Kent, C. W. Sugnet, T. S. Furey, K. M. Roskin, T. H. Pringle, A. M. Zahler, and D. Haussler. The human genome browser at ucsc. *Genome Res.*, 12(6):996–1006, 2002.

A Keys. *Seven Countries - A multivariate Analysis of Death and Coronary Heart Disease*. Harvard University Press, Cambridge, Mass., 1980.

S. H. Kim, M. Eisenstein, L. Reznikov, G. Fantuzzi, D. Novick, M. Rubinstein, and C. A. Dinarello. Structural requirements of six naturally occurring isoforms of the il-18 binding protein to inhibit il-18. *Proc. Natl. Acad. Sci. U. S. A*, 97(3):1190–1195, 2000.

S. H. Kim, L. L. Reznikov, R. J. Stuyt, C. H. Selzman, G. Fantuzzi, T. Hoshino, H. A. Young, and C. A. Dinarello. Functional reconstitution and regulation of il-18 activity by the il-18r beta chain. *J. Immunol.*, 166(1):148–154, 2001.

S. Kinlay, P. Libby, and P. Ganz. Endothelial function and coronary artery disease. *Curr. Opin. Lipidol.*, 12(4):383–389, 2001.

W. Koenig, N. Khuseyinova, J. Baumert, B. Thorand, H. Loewel, L. Chambless, C. Meisinger, A. Schneider, S. Martin, H. Kolb, and C. Herder. Increased concentrations of c-reactive protein and il-6 but not il-18 are independently associated with incident coronary events in middle-aged men and women. results from the monica/kora augsburg case-cohort study, 1984-2002. *Arterioscler. Thromb. Vasc. Biol.*, 26(12):2745–2751, 2006.

S. Kojima, Y. Nagamine, M. Hayano, S. Looareesuwan, and K. Nakanishi. A potential role of interleukin 18 in severe falciparum malaria. *Acta Trop.*, 89(3):279–284, 2004.

K. Konishi, F. Tanabe, M. Taniguchi, H. Yamauchi, T. Tanimoto, M. Ikeda, K. Orita, and M. Kurimoto. A simple and sensitive bioassay for the detection of human interleukin-18/interferon-gamma-inducing factor using human myelomonocytic kg-1 cells. *J. Immunol. Methods*, 209(2):187–191, 1997.

N. Koyama, D. Hoelzer, and O. G. Ottmann. Regulation of human il-18 gene expression: interaction of pu.1 with gc-box binding protein is involved in human il-18 expression in myeloid cells. *Eur. J. Immunol.*, 34(3):817–826, 2004.

A. Kretowski, K. Mironczuk, A. Karpinska, U. Bojaryn, M. Kinalski, Z. Puchalski, and I. Kinalska. Interleukin-18 promoter polymorphisms in type 1 diabetes. *Diabetes*, 51 (11):3347–3349, 2002.

S. Kumar, C. R. Hanning, M. R. Brigham-Burke, D. J. Rieman, R. Lehr, S. Khandekar, R. B. Kirkpatrick, G. F. Scott, J. C. Lee, F. J. Lynch, W. Gao, A. Gambotto, and M. T. Lotze. Interleukin-1f7b (il-1h4/il-1f7) is processed by caspase-1 and mature il-1f7b binds to the il-18 receptor but does not induce ifn-gamma production. *Cytokine*, 18 (2):61–71, 2002.

M. Laakso. Hyperglycemia and cardiovascular disease in type 2 diabetes. *Diabetes*, 48 (5):937–942, 1999.

M. Law and N. Wald. Why heart disease mortality is low in france: the time lag explanation. *BMJ*, 318(7196):1471–1476, 1999.

S. Leeder, S. Raymond, H. Greenberg, H. Lui, and K. Esson. *A Race Against Time. The Challenge of Cardiovascular Disease in Developing Countries.* Columbia University, New York, NY, 2004.

L. Leick, B. Lindegaard, D. Stensvold, P. Plomgaard, B. Saltin, and H. Pilegaard. Adipose tissue interleukin-18 mrna and plasma interleukin-18: effect of obesity and exercise. *Obesity. (Silver. Spring)*, 15(2):356–363, 2007.

H. B. Leu, J. W. Chen, T. C. Wu, Y. A. Ding, S. J. Lin, and M. J. Charng. Effects of fluvastatin, an hmg-coa reductase inhibitor, on serum levels of interleukin-18 and matrix metalloproteinase-9 in patients with hypercholesterolemia. *Clin. Cardiol.*, 28 (9):423–428, 2005.

H. Li, M. I. Cybulsky, M. A. Gimbrone Jr, and P. Libby. Inducible expression of vascular cell adhesion molecule-1 by vascular smooth muscle cells in vitro and within rabbit atheroma. *Am. J. Pathol.*, 143(6):1551–1559, 1993.

M. F. Linton and S. Fazio. Macrophages, inflammation, and atherosclerosis. *Int. J. Obes. Relat Metab Disord.*, 27 Suppl 3:S35–S40, 2003.

G. Y. Lip, A. H. Barnett, A. Bradbury, F. P. Cappuccio, P. S. Gill, E. Hughes, C. Imray, K. Jolly, and K. Patel. Ethnicity and cardiovascular disease prevention in the united kingdom: a practical approach to management. *J. Hum. Hypertens.*, 21(3):183–211, 2007.

J. Little and M. J. Khoury. Mendelian randomisation: a new spin or real progress? *Lancet*, 362(9388):930–931, 2003.

H. Liu, F. Prugnolle, A. Manica, and F. Balloux. A geographically explicit genetic model of worldwide human-settlement history. *Am. J. Hum. Genet.*, 79(2):230–237, 2006.

J. L. Liu, N. Maniadakis, A. Gray, and M. Rayner. The economic burden of coronary heart disease in the uk. *Heart*, 88(6):597–603, 2002.

D. M. Lloyd-Jones, M. G. Larson, A. Beiser, and D. Levy. Lifetime risk of developing coronary heart disease. *Lancet*, 353(9147):89–92, 1999.

J. C. Long, R. C. Williams, and M. Urbanek. An e-m algorithm and testing strategy for multiple-locus haplotypes. *Am. J. Hum. Genet.*, 56(3):799–810, 1995.

M. Loock, K. Steyn, P. Becker, and J. Fourie. Coronary heart disease and risk factors in black south africans: a case-control study. *Ethn. Dis.*, 16(4):872–879, 2006.

G. G. Loots, R. M. Locksley, C. M. Blankespoor, Z. E. Wang, W. Miller, E. M. Rubin, and K. A. Frazer. Identification of a coordinate regulator of interleukins 4, 13, and 5 by cross-species sequence comparisons. *Science*, 288(5463):136–140, 2000.

T. F. Luscher and M. Barton. Biology of the endothelium. *Clin. Cardiol.*, 20(11 Suppl 2):II–10, 1997.

A. J. Lusis. Atherosclerosis. *Nature*, 407(6801):233–241, 2000.

A. J. Lusis, R. Mar, and P. Pajukanta. Genetics of atherosclerosis. *Annu. Rev. Genomics Hum. Genet.*, 5:189–218, 2004.

Z. Mallat, A. Corbaz, A. Scoazec, S. Besnard, G. Leseche, Y. Chvatchko, and A. Tedgui. Expression of interleukin-18 in human atherosclerotic plaques and relation to plaque instability. *Circulation*, 104(14):1598–1603, 2001a.

Z. Mallat, A. Corbaz, A. Scoazec, P. Graber, S. Alouani, B. Esposito, Y. Humbert, Y. Chvatchko, and A. Tedgui. Interleukin-18/interleukin-18 binding protein signaling modulates atherosclerotic lesion development and stability. *Circ. Res.*, 89(7):E41–E45, 2001b.

N. Mantel. The detection of disease clustering and a generalized regression approach. *Cancer Res.*, 27(2):209–220, 1967.

M. Manuguerra, G. Matullo, F. Veglia, H. Autrup, A. M. Dunning, S. Garte, E. Gormally, C. Malaveille, S. Guarrera, S. Polidoro, F. Saletta, M. Peluso, L. Airoldi, K. Overvad, O. Raaschou-Nielsen, F. Clavel-Chapelon, J. Linseisen, H. Boeing, D. Trichopoulos, A. Kalandidi, D. Palli, V. Krogh, R. Tumino, S. Panico, H. B. Bueno-De-Mesquita, P. H. Peeters, E. Lund, G. Pera, C. Martinez, P. Amiano, A. Barricarte, M. J. Tormo, J. R. Quiros, G. Berglund, L. Janzon, B. Jarvholm, N. E. Day, N. E. Allen, R. Saracci, R. Kaaks, P. Ferrari, E. Riboli, and P. Vineis. Multi-factor dimensionality reduction applied to a large prospective investigation on gene-gene and gene-environment interactions. *Carcinogenesis*, 28(2):414–422, 2007.

M. G. Marmot. Coronary heart disease: rise and fall of a modern epidemic. In M. G. Marmot and Elliot P, editors, *Coronary Heart Disease Epidemiology*, pages 3–19. Oxford University Press, 1995.

M. G. Marmot. Understanding social inequalities in health. *Perspect. Biol. Med.*, 46(3 Suppl):S9–23, 2003.

N. W. Marten, E. J. Burke, J. M. Hayden, and D. S. Straus. Effect of amino acid limitation on the expression of 19 genes in rat hepatoma cells. *FASEB J.*, 8(8):538–544, 1994.

J. O. Mason. Understanding the disparities in morbidity and mortality among racial and ethnic groups in the united states. *Ann. Epidemiol.*, 3(2):120–124, 1993.

C. D. Mathers and D. Loncar. Projections of global mortality and burden of disease from 2002 to 2030. *PLoS. Med.*, 3(11):e442, 2006.

P. A. McCaskie, G. Cadby, J. Hung, B. M. McQuillan, C. M. Chapman, K. W. Carter, P. L. Thompson, L. J. Palmer, and J. P. Beilby. The c-480t hepatic lipase polymorphism is associated with hdl-c but not with risk of coronary heart disease. *Clin. Genet.*, 70(2):114–121, 2006.

C. McCord and H. P. Freeman. Excess mortality in harlem. *N. Engl. J. Med.*, 322(3): 173–177, 1990.

H. C. McGill Jr. Fatty streaks in the coronary arteries and aorta. *Lab Invest*, 18(5): 560–564, 1968.

P. M. McKeigue, B. Shah, and M. G. Marmot. Relation of central obesity and insulin resistance with high diabetes prevalence and cardiovascular risk in south asians. *Lancet*, 337(8738):382–386, 1991.

P. M. McKeigue, J. E. Ferrie, T. Pierpoint, and M. G. Marmot. Association of early-onset coronary heart disease in south asian men with glucose intolerance and hyperinsulinemia. *Circulation*, 87(1):152–161, 1993.

B. M. McQuillan, J. P. Beilby, M. Nidorf, P. L. Thompson, and J. Hung. Hyperhomocysteinemia but not the c677t mutation of methylenetetrahydrofolate reductase is an independent risk determinant of carotid wall thickening. the perth carotid ultrasound disease assessment study (cudas). *Circulation*, 99(18):2383–2388, 1999.

G. A. McVean, S. R. Myers, S. Hunt, P. Deloukas, D. R. Bentley, and P. Donnelly. The fine-scale structure of recombination rate variation in the human genome. *Science*, 304(5670):581–584, 2004.

J. R. Mead and D. P. Ramji. The pivotal role of lipoprotein lipase in atherosclerosis. *Cardiovasc. Res.*, 55(2):261–269, 2002.

C. Meyer Zum Buschenfelde, S. Cramer, C. Trumpfheller, B. Fleischer, and S. Frosch. Trypanosoma cruzi induces strong il-12 and il-18 gene expression in vivo: correlation with interferon-gamma (ifn-gamma) production. *Clin. Exp. Immunol.*, 110(3):378–385, 1997.

G. J. Miller, K. A. Bauer, S. Barzegar, J. A. Cooper, and R. D. Rosenberg. Increased activation of the haemostatic system in men at high risk of fatal coronary heart disease. *Thromb. Haemost.*, 75(5):767–771, 1996.

S. A. Miller, D. D. Dykes, and H. F. Polesky. A simple salting out procedure for extracting dna from human nucleated cells. *Nucleic Acids Res.*, 16(3):1215, 1988.

Z. Mojtahedi, S. Naeimi, S. Farjadian, G. R. Omrani, and A. Ghaderi. Association of il-18 promoter polymorphisms with predisposition to type 1 diabetes. *Diabet. Med.*, 23(3):235–239, 2006.

J. H. Moore. The ubiquitous nature of epistasis in determining susceptibility to common human diseases. *Hum. Hered.*, 56(1-3):73–82, 2003.

J. H. Moore and S. M. Williams. Traversing the conceptual divide between biological and statistical epistasis: systems biology and a more modern synthesis. *Bioessays*, 27(6):637–646, 2005.

J. H. Moore, J. C. Gilbert, C. T. Tsai, F. T. Chiang, T. Holden, N. Barney, and B. C. White. A flexible computational framework for detecting, characterizing, and interpreting statistical patterns of epistasis in genetic studies of human disease susceptibility. *J. Theor. Biol.*, 241(2):252–261, 2006.

K. Mullis, F. Faloona, S. Scharf, R. Saiki, G. Horn, and H. Erlich. Specific enzymatic amplification of dna in vitro: the polymerase chain reaction. *Cold Spring Harb. Symp. Quant. Biol.*, 51 Pt 1:263–273, 1986.

C. J. L. Murray and A. D. Lopez. *The Global Burden of Disease: A Comprehensive Assessment of Mortality and Disability From Diseases, Injuries, and Risk Factors in 1990 and Projected to 2020.* Harvard University Press, Cambridge, Mass., 1996.

Y. Nagai, T. Nochi, K. Watanabe, K. Watanabe, H. Aso, H. Kitazawa, M. Matsuzaki, S. Ohwada, and T. Yamaguchi. Localization of interleukin-18 and its receptor in somatotrophs of the bovine anterior pituitary gland. *Cell Tissue Res.*, 322(3):455–462, 2005.

K. Nakanishi, T. Yoshimoto, H. Tsutsui, and H. Okamura. Interleukin-18 regulates both th1 and th2 responses. *Annu. Rev. Immunol.*, 19:423–474, 2001a.

K. Nakanishi, T. Yoshimoto, H. Tsutsui, and H. Okamura. Interleukin-18 is a unique cytokine that stimulates both th1 and th2 responses depending on its cytokine milieu. *Cytokine Growth Factor Rev.*, 12(1):53–72, 2001b.

C. Napoli, F. P. D'Armiento, F. P. Mancini, A. Postiglione, J. L. Witztum, G. Palumbo, and W. Palinski. Fatty streak formation occurs in human fetal aortas and is greatly enhanced by maternal hypercholesterolemia. intimal accumulation of low density lipoprotein and its oxidation precede monocyte recruitment into early atherosclerotic lesions. *J. Clin. Invest*, 100(11):2680–2690, 1997.

National Center for Health Statistics. *Vital statistics of the United States, 1990-1995.*, volume 2, mortality pt. A. Government Printing Office, Washington, D.C., 1995.

National Task Force on the Prevention and Treatment of Obesity. Overweight, obesity, and health risk. *Arch. Intern. Med.*, 160(7):898–904, 2000.

M. G. Netea, L. A. Joosten, E. Lewis, D. R. Jensen, P. J. Voshol, B. J. Kullberg, C. J. Tack, H. van Krieken, S. H. Kim, A. F. Stalenhoef, F. A. van De Loo, I. Verschueren, L. Pulawa, S. Akira, R. H. Eckel, C. A. Dinarello, Berg W. van den, and J. W. van der Meer. Deficiency of interleukin-18 in mice leads to hyperphagia, obesity and insulin resistance. *Nat. Med.*, 12(6):650–656, 2006.

P. J. Nietert, S. E. Sutherland, J. E. Keil, and D. L. Bachman. Demographic and biologic influences on survival in whites and blacks: 40 years of follow-up in the charleston heart study. *Int. J. Equity. Health*, 5:8, 2006.

T. Niwa, H. Wada, H. Ohashi, N. Iwamoto, H. Ohta, H. Kirii, H. Fujii, K. Saito, and M. Seishima. Interferon-gamma produced by bone marrow-derived cells attenuates atherosclerotic lesion formation in ldlr-deficient mice. *J. Atheroscler. Thromb.*, 11 (2):79–87, 2004.

D. Novick, S. H. Kim, G. Fantuzzi, L. L. Reznikov, C. A. Dinarello, and M. Rubinstein. Interleukin-18 binding protein: a novel modulator of the th1 cytokine response. *Immunity.*, 10(1):127–136, 1999.

D. Novick, B. Schwartsburd, R. Pinkus, D. Suissa, I. Belzer, Z. Sthoeger, W. F. Keane, Y. Chvatchko, S. H. Kim, G. Fantuzzi, C. A. Dinarello, and M. Rubinstein. A novel il-18bp elisa shows elevated serum il-18bp in sepsis and extensive decrease of free il-18. *Cytokine*, 14(6):334–342, 2001.

Office for National Statistics. Uk census, april 2001. Report, 2001.

H. Okamura, K. Nagata, T. Komatsu, T. Tanimoto, Y. Nukata, F. Tanabe, K. Akita, K. Torigoe, T. Okura, S. Fukuda, and . A novel costimulatory factor for gamma interferon induction found in the livers of mice causes endotoxic shock. *Infect. Immun.*, 63(10):3966–3972, 1995a.

H. Okamura, H. Tsutsi, T. Komatsu, M. Yutsudo, A. Hakura, T. Tanimoto, K. Torigoe, T. Okura, Y. Nukada, and K. Hattori. Cloning of a new cytokine that induces ifn-gamma production by t cells. *Nature*, 378(6552):88–91, 1995b.

B. Osterud and E. Bjorklid. Role of monocytes in atherogenesis. *Physiol Rev.*, 83(4): 1069–1112, 2003.

P. Pais, J. Pogue, H. Gerstein, E. Zachariah, D. Savitha, S. Jayprakash, P. R. Nayak, and S. Yusuf. Risk factors for acute myocardial infarction in indians: a case-control study. *Lancet*, 348(9024):358–363, 1996.

W. Palinski, M. E. Rosenfeld, S. Yla-Herttuala, G. C. Gurtner, S. S. Socher, S. W. Butler, S. Parthasarathy, T. E. Carew, D. Steinberg, and J. L. Witztum. Low density lipoprotein undergoes oxidative modification in vivo. *Proc. Natl. Acad. Sci. U. S. A*, 86(4):1372–1376, 1989.

C. G. Panousis and S. H. Zuckerman. Interferon-gamma induces downregulation of tangier disease gene (atp-binding-cassette transporter 1) in macrophage-derived foam cells. *Arterioscler. Thromb. Vasc. Biol.*, 20(6):1565–1571, 2000.

P. Parnet, K. E. Garka, T. P. Bonnert, S. K. Dower, and J. E. Sims. Il-1rrp is a novel receptor-like molecule similar to the type i interleukin-1 receptor and its homologues t1/st2 and il-1r acp. *J. Biol. Chem.*, 271(8):3967–3970, 1996.

J. Paulukat, M. Bosmann, M. Nold, S. Garkisch, H. Kampfer, S. Frank, J. Raedle, S. Zeuzem, J. Pfeilschifter, and H. Muhl. Expression and release of il-18 binding protein in response to ifn-gamma. *J. Immunol.*, 167(12):7038–7043, 2001.

A. Pawlik, M. Kurzawski, B. Czerny, B. Gawronska-Szklarz, M. Drozdzik, and M. Herczynska. Interleukin-18 promoter polymorphism in patients with rheumatoid arthritis. *Tissue Antigens*, 67(5):415–418, 2006.

M. O. Pentikainen, K. Oorni, M. Ala-Korpela, and P. T. Kovanen. Modified ldl- trigger of atherosclerosis and inflammation in the arterial intima. *J. Intern. Med.*, 247(3): 359–370, 2000.

M. W. Pfaffl. A new mathematical model for relative quantification in real-time rt-pcr. *Nucleic Acids Res.*, 29(9):e45, 2001.

M. W. Pfaffl, G. W. Horgan, and L. Dempfle. Relative expression software tool (rest) for group-wise comparison and statistical analysis of relative expression results in real-time pcr. *Nucleic Acids Res.*, 30(9):e36, 2002.

P. Puska, J. M. Iacono, A. Nissinen, H. J. Korhonen, E. Vartianinen, P. Pietinen, R. Dougherty, U. Leino, M. Mutanen, S. Moisio, and J. Huttunen. Controlled, randomised trial of the effect of dietary fat on blood pressure. *Lancet*, 1(8314-5):1–5, 1983.

O. Quehenberger. Thematic review series: the immune system and atherogenesis. molecular mechanisms regulating monocyte recruitment in atherosclerosis. *J. Lipid Res.*, 46(8):1582–1590, 2005.

M. Raymond and F. Rousset. An exact test for population differentiation. *Evolution*, 49 (6):1280–1283, 1995.

D. E. Reich, M. Cargill, S. Bolk, J. Ireland, P. C. Sabeti, D. J. Richter, T. Lavery, R. Kouyoumjian, S. F. Farhadian, R. Ward, and E. S. Lander. Linkage disequilibrium in the human genome. *Nature*, 411(6834):199–204, 2001.

A. B. Reiss, C. A. Patel, M. M. Rahman, E. S. Chan, K. Hasneen, M. C. Montesinos, J. D. Trachman, and B. N. Cronstein. Interferon-gamma impedes reverse cholesterol transport and promotes foam cell transformation in thp-1 human monocytes/macrophages. *Med. Sci. Monit.*, 10(11):BR420–BR425, 2004.

S. Renaud, M. de Lorgeril, J. Delaye, J. Guidollet, F. Jacquard, N. Mamelle, J. L. Martin, I. Monjaud, P. Salen, and P. Toubol. Cretan mediterranean diet for prevention of coronary heart disease. *Am. J. Clin. Nutr.*, 61(6 Suppl):1360S–1367S, 1995.

N. Resnick, H. Yahav, L. M. Khachigian, T. Collins, K. R. Anderson, F. C. Dewey, and M. A. Gimbrone Jr. Endothelial gene regulation by laminar shear stress. *Adv. Exp. Med. Biol.*, 430:155–164, 1997.

A. K. Robertson and G. K. Hansson. T cells in atherogenesis: for better or for worse? *Arterioscler. Thromb. Vasc. Biol.*, 26(11):2421–2432, 2006.

G. Robertson, M. Bilenky, K. Lin, A. He, W. Yuen, M. Dagpinar, R. Varhol, K. Teague, O. L. Griffith, X. Zhang, Y. Pan, M. Hassel, M. C. Sleumer, W. Pan, E. D. Pleasance, M. Chuang, H. Hao, Y. Y. Li, N. Robertson, C. Fjell, B. Li, S. B. Montgomery, T. Astakhova, J. Zhou, J. Sander, A. S. Siddiqui, and S. J. Jones. cisred: a database system for genome-scale computational discovery of regulatory elements. *Nucleic Acids Res.*, 34(Database issue):D68–D73, 2006.

M. Romano, E. Romano, S. Bjorkerud, and E. Hurt-Camejo. Ultrastructural localization of secretory type ii phospholipase a2 in atherosclerotic and nonatherosclerotic regions of human arteries. *Arterioscler. Thromb. Vasc. Biol.*, 18(4):519–525, 1998.

A. Rosengren, S. Hawken, S. Ounpuu, K. Sliwa, M. Zubaid, W. A. Almahmeed, K. N. Blackett, C. Sitthi-amorn, H. Sato, and S. Yusuf. Association of psychosocial risk factors with risk of acute myocardial infarction in 11119 cases and 13648 controls from 52 countries (the interheart study): case-control study. *Lancet*, 364(9438):953–962, 2004.

R. Ross. Atherosclerosis–an inflammatory disease. *N. Engl. J. Med.*, 340(2):115–126, 1999.

R. Ross. The pathogenesis of atherosclerosis–an update. *N. Engl. J. Med.*, 314(8): 488–500, 1986.

R. Ross and J. A. Glomset. The pathogenesis of atherosclerosis (second of two parts). *N. Engl. J. Med.*, 295(8):420–425, 1976a.

R. Ross and J. A. Glomset. The pathogenesis of atherosclerosis (first of two parts). *N. Engl. J. Med.*, 295(7):369–377, 1976b.

S. Rozen and H. Skaletsky. Primer3 on the www for general users and for biologist programmers. *Methods Mol. Biol.*, 132:365–386, 2000.

P. C. Sabeti, D. E. Reich, J. M. Higgins, H. Z. Levine, D. J. Richter, S. F. Schaffner, S. B. Gabriel, J. V. Platko, N. J. Patterson, G. J. McDonald, H. C. Ackerman, S. J. Campbell, D. Altshuler, R. Cooper, D. Kwiatkowski, R. Ward, and E. S. Lander. Detecting recent positive selection in the human genome from haplotype structure. *Nature*, 419(6909):832–837, 2002.

F. Sanger and A. R. Coulson. A rapid method for determining sequences in dna by primed synthesis with dna polymerase. *J. Mol. Biol.*, 94(3):441–448, 1975.

U. Schonbeck, F. Mach, G. K. Sukhova, C. Murphy, J. Y. Bonnefoy, R. P. Fabunmi, and P. Libby. Regulation of matrix metalloproteinase expression in human vascular smooth muscle cells by t lymphocytes: a role for cd40 signaling in plaque rupture? *Circ. Res.*, 81(3):448–454, 1997.

K. Schroder, P. J. Hertzog, T. Ravasi, and D. A. Hume. Interferon-gamma: an overview of signals, mechanisms and functions. *J. Leukoc. Biol.*, 75(2):163–189, 2004.

P. Sebastiani, R. Lazarus, S. T. Weiss, L. M. Kunkel, I. S. Kohane, and M. F. Ramoni. Minimal haplotype tagging. *Proc. Natl. Acad. Sci. U. S. A*, 100(17):9900–9905, 2003.

Y. K. Seedat. Ethnicity, hypertension, coronary heart disease and renal diseases in south africa. *Ethn. Health*, 1(4):349–357, 1996.

K. Sen and R. Bonita. Global health status: two steps forward, one step back. *Lancet*, 356(9229):577–582, 2000.

Y. Seta, T. Kanda, T. Tanaka, M. Arai, K. Sekiguchi, T. Yokoyama, M. Kurimoto, J. Tamura, and M. Kurabayashi. Interleukin 18 in acute myocardial infarction. *Heart*, 84(6):668, 2000.

P. K. Shah. Mechanisms of plaque vulnerability and rupture. *J. Am. Coll. Cardiol.*, 41 (4 Suppl S):15S–22S, 2003.

T. Sheth, C. Nair, M. Nargundkar, S. Anand, and S. Yusuf. Cardiovascular and cancer mortality among canadians of european, south asian and chinese origin from 1979 to 1993: an analysis of 1.2 million deaths. *CMAJ.*, 161(2):132–138, 1999.

H. D. Shin, L. H. Kim, B. L. Park, Y. H. Choi, H. S. Park, S. J. Hong, B. W. Choi, J. H. Lee, and C. S. Park. Association of interleukin 18 (il18) polymorphisms with specific ige levels to mite allergens among asthmatic patients. *Allergy*, 60(7):900–906, 2005.

S. P. Sivalingam, K. H. Yoon, D. R. Koh, and K. Y. Fong. Single-nucleotide polymorphisms of the interleukin-18 gene promoter region in rheumatoid arthritis patients: protective effect of aa genotype. *Tissue Antigens*, 62(6):498–504, 2003.

T. Skurk, H. Kolb, S. Muller-Scholze, K. Rohrig, H. Hauner, and C. Herder. The proatherogenic cytokine interleukin-18 is secreted by human adipocytes. *Eur. J. Endocrinol.*, 152(6):863–868, 2005.

E. B. Smith. Transport, interactions and retention of plasma proteins in the intima: the barrier function of the internal elastic lamina. *Eur. Heart J.*, 11 Suppl E:72–81, 1990.

E. B. Smith and R. S. Slater. Relationship between low-density lipoprotein in aortic intima and serum-lipid levels. *Lancet*, 1(7748):463–469, 1972.

E. Sobel and K. Lange. Descent graphs in pedigree analysis: applications to haplotyping, location scores, and marker-sharing statistics. *Am. J. Hum. Genet.*, 58(6): 1323–1337, 1996.

Y. I. Son, R. M. Dallal, R. B. Mailliard, S. Egawa, Z. L. Jonak, and M. T. Lotze. Interleukin-18 (il-18) synergizes with il-2 to enhance cytotoxicity, interferon-gamma production, and expansion of natural killer cells. *Cancer Res.*, 61(3):884–888, 2001.

H. C. Stary, A. B. Chandler, R. E. Dinsmore, V. Fuster, S. Glagov, W. Insull Jr, M. E. Rosenfeld, C. J. Schwartz, W. D. Wagner, and R. W. Wissler. A definition of advanced types of atherosclerotic lesions and a histological classification of atherosclerosis. a report from the committee on vascular lesions of the council on arteriosclerosis, american heart association. *Arterioscler. Thromb. Vasc. Biol.*, 15(9):1512–1531, 1995.

D. Steinberg. Low density lipoprotein oxidation and its pathobiological significance. *J. Biol. Chem.*, 272(34):20963–20966, 1997a.

D. Steinberg. Lewis a. conner memorial lecture. oxidative modification of ldl and atherogenesis. *Circulation*, 95(4):1062–1071, 1997b.

J. W. Stephens, S. J. Hurel, J. Acharya, and S. E. Humphries. An interaction between the interleukin-6 -174 gene variant and urinary protein excretion influences plasma oxidative stress in subjects with type 2 diabetes. *Cardiovasc. Diabetol.*, 3:2, 2004.

M. Stephens, N. J. Smith, and P. Donnelly. A new statistical method for haplotype reconstruction from population data. *Am. J. Hum. Genet.*, 68(4):978–989, 2001.

K. Steyn, K. Sliwa, S. Hawken, P. Commerford, C. Onen, A. Damasceno, S. Ounpuu, and S. Yusuf. Risk factors associated with myocardial infarction in africa: the interheart africa study. *Circulation*, 112(23):3554–3561, 2005.

B. Stockinger and M. Veldhoen. Differentiation and function of th17 t cells. *Curr. Opin. Immunol.*, 19(3):281–286, 2007.

M. Straczkowski, I. Kowalska, A. Nikolajuk, E. Otziomek, A. Adamska, M. Karolczuk-Zarachowicz, and M. Gorska. Increased serum interleukin-18 concentration is associated with hypoadiponectinemia in obesity, independently of insulin resistance. *Int. J. Obes. (Lond)*, 31(2):221–225, 2007.

M. C. Stuhlinger and P. S. Tsao. Etiology and pathogenesis of atherosclerosis. In J. D. Coffman and R. T. Eberhardt, editors, *Peripheral Artery Disease*, book chapter 1, pages 1–19. Humana Press, 2003.

T. Sugiura, N. Maeno, Y. Kawaguchi, S. Takei, H. Imanaka, Y. Kawano, H. Terajima-Ichida, M. Hara, and N. Kamatani. A promoter haplotype of the interleukin-18 gene is associated with juvenile idiopathic arthritis in the japanese population. *Arthritis Res. Ther.*, 8(3):R60, 2006.

J. S. Szeszko, J. M. Howson, J. D. Cooper, N. M. Walker, R. C. Twells, H. E. Stevens, S. L. Nutland, and J. A. Todd. Analysis of polymorphisms of the interleukin-18 gene in type 1 diabetes and hardy-weinberg equilibrium testing. *Diabetes*, 55(2):559–562, 2006.

S. Takashiba, T. E. Van Dyke, S. Amar, Y. Murayama, A. W. Soskolne, and L. Shapira. Differentiation of monocytes to macrophages primes cells for lipopolysaccharide stimulation via accumulation of cytoplasmic nuclear factor kappab. *Infect. Immun.*, 67(11):5573–5578, 1999.

M. Takeuchi, Y. Nishizaki, O. Sano, T. Ohta, M. Ikeda, and M. Kurimoto. Immunohistochemical and immuno-electron-microscopic detection of interferon-gamma-inducing factor ("interleukin-18") in mouse intestinal epithelial cells. *Cell Tissue Res.*, 289(3): 499–503, 1997.

M. Tamminen, G. Mottino, J. H. Qiao, J. L. Breslow, and J. S. Frank. Ultrastructure of early lipid accumulation in apoe-deficient mice. *Arterioscler. Thromb. Vasc. Biol.*, 19 (4):847–853, 1999.

K. Tamura, Y. Fukuda, H. Sashio, N. Takeda, H. Bamba, T. Kosaka, S. Fukui, K. Sawada, K. Tamura, M. Satomi, T. Yamada, T. Yamamura, Y. Yamamoto, J. Furuyama, H. Okamura, and T. Shimoyama. Il18 polymorphism is associated with an increased risk of crohn's disease. *J. Gastroenterol.*, 37 Suppl 14:111–116, 2002.

S. C. Tao, Z. D. Huang, X. G. Wu, B. F. Zhou, Z. K. Xiao, J. S. Hao, Y. H. Li, R. C. Cen, and X. X. Rao. Chd and its risk factors in the people's republic of china. *Int. J. Epidemiol.*, 18(3 Suppl 1):S159–S163, 1989.

A. Tedgui and Z. Mallat. Cytokines in atherosclerosis: pathogenic and regulatory pathways. *Physiol Rev.*, 86(2):515–581, 2006.

T. J. Tegos, E. Kalodiki, M. M. Sabetai, and A. N. Nicolaides. The genesis of atherosclerosis and risk factors: a review. *Angiology*, 52(2):89–98, 2001.

D. G. Tenen, R. Hromas, J. D. Licht, and D. E. Zhang. Transcription factors, normal myeloid development, and leukemia. *Blood*, 90(2):489–519, 1997.

A. Tenesa and M. G. Dunlop. Validity of tagging snps across populations for association studies. *Eur. J. Hum. Genet.*, 14(3):357–363, 2006.

O. Thellin, W. Zorzi, B. Lakaye, B. De Borman, B. Coumans, G. Hennen, T. Grisar, A. Igout, and E. Heinen. Housekeeping genes as internal standards: use and limits. *J. Biotechnol.*, 75(2-3):291–295, 1999.

B. Thorand, H. Kolb, J. Baumert, W. Koenig, L. Chambless, C. Meisinger, T. Illig, S. Martin, and C. Herder. Elevated levels of interleukin-18 predict the development of type 2 diabetes: results from the monica/kora augsburg study, 1984-2002. *Diabetes*, 54(10):2932–2938, 2005.

N. J. Timpson, D. A. Lawlor, R. M. Harbord, T. R. Gaunt, I. N. Day, L. J. Palmer, A. T. Hattersley, S. Ebrahim, G. D. Lowe, A. Rumley, and G. Davey Smith. C-reactive protein and its role in metabolic syndrome: mendelian randomisation study. *Lancet*, 366(9501):1954–1959, 2005.

L. Tiret, T. Godefroy, E. Lubos, V. Nicaud, D. A. Tregouet, S. Barbaux, R. Schnabel, C. Bickel, C. Espinola-Klein, O. Poirier, C. Perret, T. Munzel, H. J. Rupprecht, K. Lackner, F. Cambien, and S. Blankenberg. Genetic analysis of the interleukin-18 system highlights the role of the interleukin-18 gene in cardiovascular disease. *Circulation*, 112(5):643–650, 2005.

M. Tone, S. A. Thompson, Y. Tone, P. J. Fairchild, and H. Waldmann. Regulation of il-18 (ifn-gamma-inducing factor) gene expression. *J. Immunol.*, 159(12):6156–6163, 1997.

M. G. Torcia, V. Santarlasci, L. Cosmi, A. Clemente, L. Maggi, V. D. Mangano, F. Verra, G. Bancone, I. Nebie, B. S. Sirima, F. Liotta, F. Frosali, R. Angeli, C. Severini, A. R. Sannella, P. Bonini, M. Lucibello, E. Maggi, E. Garaci, M. Coluzzi, F. Cozzolino, F. Annunziato, S. Romagnani, and D. Modiano. Functional deficit of t regulatory cells in fulani, an ethnic group with low susceptibility to plasmodium falciparum malaria. *Proc. Natl. Acad. Sci. U. S. A*, 2008.

K. Torigoe, S. Ushio, T. Okura, S. Kobayashi, M. Taniai, T. Kunikata, T. Murakami, O. Sanou, H. Kojima, M. Fujii, T. Ohta, M. Ikeda, H. Ikegami, and M. Kurimoto. Purification and characterization of the human interleukin-18 receptor. *J. Biol. Chem.*, 272(41):25737–25742, 1997.

D. A. Tregouet, S. Barbaux, S. Escolano, N. Tahri, J. L. Golmard, L. Tiret, and F. Cambien. Specific haplotypes of the p-selectin gene are associated with myocardial infarction. *Hum. Mol. Genet.*, 11(17):2015–2023, 2002.

D. A. Tregouet, S. Escolano, L. Tiret, A. Mallet, and J. L. Golmard. A new algorithm for haplotype-based association analysis: the stochastic-em algorithm. *Ann. Hum. Genet.*, 68(Pt 2):165–177, 2004.

E. Tremoli, M. Camera, V. Toschi, and S. Colli. Tissue factor in atherosclerosis. *Atherosclerosis*, 144(2):273–283, 1999.

A. Trichopoulou and P. Lagiou. Healthy traditional mediterranean diet: an expression of culture, history, and lifestyle. *Nutr. Rev.*, 55(11 Pt 1):383–389, 1997.

US Census Bureau. 2005 american community survey. Report, 2005.

USCEPR and PRC. An epidemiological study of cardiovascular and cardiopulmonary disease risk factors in four populations in the people's republic of china. baseline report from the p.r.c.-u.s.a. collaborative study. people's republic of china–united states cardiovascular and cardiopulmonary epidemiology research group (uscepr). *Circulation*, 85(3):1083–1096, 1992.

S. Ushio, M. Namba, T. Okura, K. Hattori, Y. Nukada, K. Akita, F. Tanabe, K. Konishi, M. Micallef, M. Fujii, K. Torigoe, T. Tanimoto, S. Fukuda, M. Ikeda, H. Okamura, and M. Kurimoto. Cloning of the cdna for human ifn-gamma-inducing factor, expression in escherichia coli, and studies on the biologic activities of the protein. *J. Immunol.*, 156(11):4274–4279, 1996.

A. J. Valente, J. F. Xie, M. A. Abramova, U. O. Wenzel, H. E. Abboud, and D. T. Graves. A complex element regulates ifn-gamma-stimulated monocyte chemoattractant protein-1 gene transcription. *J. Immunol.*, 161(7):3719–3728, 1998.

A. Varnava. Coronary artery remodelling. *Heart*, 79(2):109–110, 1998.

N. Vilarrasa, J. Vendrell, J. Maravall, M. Broch, A. Estepa, A. Megia, J. Soler, I. Simon, C. Richart, and J. M. Gomez. Il-18: Relationship with anthropometry, body composition parameters, leptin and arterial hypertension. *Horm. Metab Res.*, 38(8): 507–512, 2006.

N. Vilarrasa, J. Vendrell, R. Sanchez-Santos, M. Broch, A. Megia, C. Masdevall, N. Gomez, J. Soler, J. Pujol, C. Bettonica, H. Aranda, and J. M. Gomez. Effect of weight loss induced by gastric bypass on proinflammatory interleukin-18, soluble tumour necrosis factor-alpha receptors, c-reactive protein and adiponectin in morbidly obese patients. *Clin. Endocrinol. (Oxf)*, 67(5):679–686, 2007.

R. Virmani, F. D. Kolodgie, A. P. Burke, A. Farb, and S. M. Schwartz. Lessons from sudden coronary death: a comprehensive morphological classification scheme for atherosclerotic lesions. *Arterioscler. Thromb. Vasc. Biol.*, 20(5):1262–1275, 2000.

M. N. Vissers, P. L. Zock, S. A. Wiseman, S. Meyboom, and M. B. Katan. Effect of phenol-rich extra virgin olive oil on markers of oxidation in healthy volunteers. *Eur. J. Clin. Nutr.*, 55(5):334–341, 2001.

B. F. Voight, S. Kudaravalli, X. Wen, and J. K. Pritchard. A map of recent positive selection in the human genome. *PLoS. Biol.*, 4(3):e72, 2006.

M. Wada, H. Okamura, K. Nagata, T. Shimoyama, and Y. Kawade. Cellular mechanisms in in vivo production of gamma interferon induced by lipopolysaccharide in mice infected with mycobacterium bovis bcg. *J. Interferon Res.*, 5(3):431–443, 1985.

N. Wang, S. Sugama, B. Conti, A. Teramoto, and T. Shibasaki. Interleukin-18 mrna expression in the rat pituitary gland. *J. Neuroimmunol.*, 173(1-2):117–125, 2006.

Z. Y. Wang, A. Gaggero, A. Rubartelli, O. Rosso, S. Miotti, D. Mezzanzanica, S. Canevari, and S. Ferrini. Expression of interleukin-18 in human ovarian carcinoma and normal ovarian epithelium: evidence for defective processing in tumor cells. *Int. J. Cancer*, 98(6):873–878, 2002.

H. Watkins and M. Farrall. Genetic susceptibility to coronary artery disease: from promise to progress. *Nat. Rev. Genet.*, 7(3):163–173, 2006.

C. Weber, W. Erl, K. S. Weber, and P. C. Weber. Hmg-coa reductase inhibitors decrease cd11b expression and cd11b-dependent adhesion of monocytes to endothelium and reduce increased adhesiveness of monocytes isolated from patients with hypercholesterolemia. *J. Am. Coll. Cardiol.*, 30(5):1212–1217, 1997.

R. D. Wheeler, A. C. Culhane, M. D. Hall, S. Pickering-Brown, N. J. Rothwell, and G. N. Luheshi. Detection of the interleukin 18 family in rat brain by rt-pcr. *Brain Res. Mol. Brain Res.*, 77(2):290–293, 2000.

S. C. Whitman, P. Ravisankar, H. Elam, and A. Daugherty. Exogenous interferon-gamma enhances atherosclerosis in apolipoprotein e-/- mice. *Am. J. Pathol.*, 157(6): 1819–1824, 2000.

S. C. Whitman, P. Ravisankar, and A. Daugherty. Interleukin-18 enhances atherosclerosis in apolipoprotein e(-/-) mice through release of interferon-gamma. *Circ. Res.*, 90(2):E34–E38, 2002.

S. Wild and P. McKeigue. Cross sectional analysis of mortality by country of birth in england and wales, 1970-92. *BMJ*, 314(7082):705–710, 1997.

J. L. Witztum and D. Steinberg. Role of oxidized low density lipoprotein in atherogenesis. *J. Clin. Invest*, 88(6):1785–1792, 1991.

K. S. Woo and S. P. Donnan. Epidemiology of coronary arterial disease in the chinese. *Int. J. Cardiol.*, 24(1):83–93, 1989.

I. S. Wood, B. Wang, J. R. Jenkins, and P. Trayhurn. The pro-inflammatory cytokine il-18 is expressed in human adipose tissue and strongly upregulated by tnfalpha in human adipocytes. *Biochem. Biophys. Res. Commun.*, 337(2):422–429, 2005.

N. Woolf. Pathology of atherosclerosis. *Br. Med. Bull.*, 46(4):960–985, 1990.

World Bank. Key development data and statistics. Data File, 2006.

P. Worth Longest and C. Kleinstreuer. Comparison of blood particle deposition models for non-parallel flow domains. *J. Biomech.*, 36(3):421–430, 2003.

WTCCC. Genome-wide association study of 14,000 cases of seven common diseases and 3,000 shared controls. *Nature*, 447(7145):661–678, 2007.

T. H. Wyman, C. A. Dinarello, A. Banerjee, F. Gamboni-Robertson, A. A. Hiester, K. M. England, M. Kelher, and C. C. Silliman. Physiological levels of interleukin-18 stimulate multiple neutrophil functions through p38 map kinase activation. *J. Leukoc. Biol.*, 72(2):401–409, 2002.

H. Yamagami, K. Kitagawa, T. Hoshi, S. Furukado, H. Hougaku, Y. Nagai, and M. Hori. Associations of serum il-18 levels with carotid intima-media thickness. *Arterioscler. Thromb. Vasc. Biol.*, 25(7):1458–1462, 2005.

G. Yang, L. Fan, J. Tan, G. Qi, Y. Zhang, J. M. Samet, C. E. Taylor, K. Becker, and J. Xu. Smoking in china: findings of the 1996 national prevalence survey. *JAMA*, 282(13):1247–1253, 1999.

S. Yla-Herttuala, W. Palinski, M. E. Rosenfeld, S. Parthasarathy, T. E. Carew, S. Butler, J. L. Witztum, and D. Steinberg. Evidence for the presence of oxidatively modified low density lipoprotein in atherosclerotic lesions of rabbit and man. *J. Clin. Invest*, 84(4):1086–1095, 1989.

M. Yokoyama, K. Hirata, S. Kawashima, and Y. Kawahara. Regulation of nitric oxide synthase gene expression by cytokines. *J. Card Fail.*, 2(4 Suppl):S179–S185, 1996.

T. Yoshimoto, K. Takeda, T. Tanaka, K. Ohkusu, S. Kashiwamura, H. Okamura, S. Akira, and K. Nakanishi. Il-12 up-regulates il-18 receptor expression on t cells, th1 cells, and b cells: synergism with il-18 for ifn-gamma production. *J. Immunol.*, 161(7):3400–3407, 1998.

J. L. Young, P. Libby, and U. Schonbeck. Cytokines in the pathogenesis of atherosclerosis. *Thromb. Haemost.*, 88(4):554–567, 2002.

W. Yuan, T. Yufit, L. Li, Y. Mori, S. J. Chen, and J. Varga. Negative modulation of alpha1(i) procollagen gene expression in human skin fibroblasts: transcriptional inhibition by interferon-gamma. *J. Cell Physiol*, 179(1):97–108, 1999.

S. Yusuf, S. Reddy, S. Ounpuu, and S. Anand. Global burden of cardiovascular diseases: Part ii: variations in cardiovascular disease by specific ethnic groups and geographic regions and prevention strategies. *Circulation*, 104(23):2855–2864, 2001a.

S. Yusuf, S. Reddy, S. Ounpuu, and S. Anand. Global burden of cardiovascular diseases: part i: general considerations, the epidemiologic transition, risk factors, and impact of urbanization. *Circulation*, 104(22):2746–2753, 2001b.

S. Yusuf, S. Hawken, S. Ounpuu, T. Dans, A. Avezum, F. Lanas, M. McQueen, A. Budaj, P. Pais, J. Varigos, and L. Lisheng. Effect of potentially modifiable risk factors associated with myocardial infarction in 52 countries (the interheart study): case-control study. *Lancet*, 364(9438):937–952, 2004.

J. Zhang and S. H. Snyder. Nitric oxide stimulates auto-adp-ribosylation of glyceraldehyde-3-phosphate dehydrogenase. *Proc. Natl. Acad. Sci. U. S. A*, 89(20): 9382–9385, 1992.

Y. Zhang, W. J. Cliff, G. I. Schoefl, and G. Higgins. Plasma protein insudation as an index of early coronary atherogenesis. *Am. J. Pathol.*, 143(2):496–506, 1993.

A. Zirlik, S. M. Abdullah, N. Gerdes, L. Macfarlane, U. Schonbeck, A. Khera, D. K. McGuire, G. L. Vega, S. Grundy, P. Libby, and J. A. de Lemos. Interleukin-18, the metabolic syndrome, and subclinical atherosclerosis. results from the dallas heart study. *Arterioscler. Thromb. Vasc. Biol.*, 27(9):2043–2049, 2007.

E. P. Zorrilla, M. Sanchez-Alavez, S. Sugama, M. Brennan, R. Fernandez, T. Bartfai, and B. Conti. Interleukin-18 controls energy homeostasis by suppressing appetite and feed efficiency. *Proc. Natl. Acad. Sci. U. S. A*, 104(26):11097–11102, 2007.

Papers Resulting From This Thesis

Original Research

S. R. Thompson, J. Sanders, J. W. Stephens, G. J. Miller, S. E. Humphries SE. A common *IL18* haplotype is associated with higher BMI in subjects with diabetes and CHD. *Metabolism*, 56(5):662-9, 2007.

S. R. Thompson, P. A. McCaskie, J. P. Beilby, J. Hung, M. Jennens, C. Chapman, P. Thompson, S. E. Humphries. *IL18* haplotypes are associated with serum IL-18 concentrations in a population-based study and a cohort of individuals with premature CHD. *Clin Chem.*, 2007, *in press.*

S. R. Thompson, D. Novick, C. J. Stock, J. Sanders, D. Brull, J. Cooper, P. Woo, G. Miller, M. Rubinstein, S. E. Humphries. fIL-18 levels, and the impact of *IL18* and *IL18BP* genetic variation, in CHD patients and healthy men. *Arterioscler Thromb Vasc Biol.*, 27(12):2743-9, 2007.

Review Article

S. R. Thompson, S. E. Humphries. IL-18 genetics and inflammatory disease susceptibility. *Genes Immun.*, 8(2):91-9, 2007.